

cancers

The Shaping of Cancer by the Tumour Microenvironment and Its Relevance for Cancer Therapy

Edited by

Patrícia Alexandra Saraiva Madureira

Printed Edition of the Special Issue Published in *Cancers*

The Shaping of Cancer by the Tumour Microenvironment and Its Relevance for Cancer Therapy

The Shaping of Cancer by the Tumour Microenvironment and Its Relevance for Cancer Therapy

Editor

Patrícia Alexandra Saraiva Madureira

MDPI • Basel • Beijing • Wuhan • Barcelona • Belgrade • Manchester • Tokyo • Cluj • Tianjin



Editor

Patrícia Alexandra Saraiva Madureira
Centre for Biomedical Research
University of Algarve
Faro
Portugal

Editorial Office

MDPI
St. Alban-Anlage 66
4052 Basel, Switzerland

This is a reprint of articles from the Special Issue published online in the open access journal *Cancers* (ISSN 2072-6694) (available at: www.mdpi.com/journal/cancers/special_issues/Tumour_Microenvironment).

For citation purposes, cite each article independently as indicated on the article page online and as indicated below:

LastName, A.A.; LastName, B.B.; LastName, C.C. Article Title. <i>Journal Name</i> Year , <i>Volume Number</i> , Page Range.
--

ISBN 978-3-0365-1608-0 (Hbk)

ISBN 978-3-0365-1607-3 (PDF)

© 2021 by the authors. Articles in this book are Open Access and distributed under the Creative Commons Attribution (CC BY) license, which allows users to download, copy and build upon published articles, as long as the author and publisher are properly credited, which ensures maximum dissemination and a wider impact of our publications.

The book as a whole is distributed by MDPI under the terms and conditions of the Creative Commons license CC BY-NC-ND.

Contents

About the Editor	vii
Preface to "The Shaping of Cancer by the Tumour Microenvironment and Its Relevance for Cancer Therapy"	ix
Agathe L. Chédeville and Patricia A. Madureira The Role of Hypoxia in Glioblastoma Radiotherapy Resistance Reprinted from: <i>Cancers</i> 2021 , <i>13</i> , 542, doi:10.3390/cancers13030542	1
Varintra E. Krisnawan, Jennifer A. Stanley, Julie K. Schwarz and David G. DeNardo Tumor Microenvironment as a Regulator of Radiation Therapy: New Insights into Stromal-Mediated Radioresistance Reprinted from: <i>Cancers</i> 2020 , <i>12</i> , 2916, doi:10.3390/cancers12102916	17
Shuhui Cheng, Eleanor J. Cheadle and Timothy M. Illidge Understanding the Effects of Radiotherapy on the Tumour Immune Microenvironment to Identify Potential Prognostic and Predictive Biomarkers of Radiotherapy Response Reprinted from: <i>Cancers</i> 2020 , <i>12</i> , 2835, doi:10.3390/cancers12102835	43
Nada S. Aboeella, Caitlin Brandle, Timothy Kim, Zhi-Chun Ding and Gang Zhou Oxidative Stress in the Tumor Microenvironment and Its Relevance to Cancer Immunotherapy Reprinted from: <i>Cancers</i> 2021 , <i>13</i> , 986, doi:10.3390/cancers13050986	63
Ru Li, Annie Wen and Jun Lin Pro-Inflammatory Cytokines in the Formation of the Pre-Metastatic Niche Reprinted from: <i>Cancers</i> 2020 , <i>12</i> , 3752, doi:10.3390/cancers12123752	87
Bryce Ordway, Michal Tomaszewski, Samantha Byrne, Dominique Abrahams, Pawel Swietach, Robert J. Gillies and Mehdi Damaghi Targeting of Evolutionarily Acquired Cancer Cell Phenotype by Exploiting pHi-Metabolic Vulnerabilities Reprinted from: <i>Cancers</i> 2020 , <i>13</i> , 64, doi:10.3390/cancers13010064	103
Javier Martinez-Useros, Mario Martin-Galan and Jesus Garcia-Foncillas The Match between Molecular Subtypes, Histology and Microenvironment of Pancreatic Cancer and Its Relevance for Chemoresistance Reprinted from: <i>Cancers</i> 2021 , <i>13</i> , 322, doi:10.3390/cancers13020322	119
Marcin Domagala, Chloé Laplagne, Edouard Leveque, Camille Laurent, Jean-Jacques Fournié, Eric Espinosa and Mary Poupot Cancer Cells Resistance Shaping by Tumor Infiltrating Myeloid Cells Reprinted from: <i>Cancers</i> 2021 , <i>13</i> , 165, doi:10.3390/cancers13020165	137
Alamelu G. Bharadwaj, Ryan W. Holloway, Victoria A. Miller and David M. Waisman Plasmin and Plasminogen System in the Tumor Microenvironment: Implications for Cancer Diagnosis, Prognosis, and Therapy Reprinted from: <i>Cancers</i> 2021 , <i>13</i> , 1838, doi:10.3390/cancers13081838	167

Alamelu G. Bharadwaj, Margaret L. Dahn, Rong-Zong Liu, Patricia Colp, Lynn N. Thomas, Ryan W. Holloway, Paola A. Marignani, Catherine K. L. Too, Penelope J. Barnes, Roseline Godbout, Paola Marcato and David M. Waisman S100A10 Has a Critical Regulatory Function in Mammary Tumor Growth and Metastasis: Insights Using MMTV-PyMT Oncomice and Clinical Patient Sample Analysis Reprinted from: <i>Cancers</i> 2020, 12, 3673, doi:10.3390/cancers12123673	201
Charles M. Haughey, Debayan Mukherjee, Rebecca E. Steele, Amy Popple, Lara Dura-Perez, Adam Pickard, Mehjabin Patel, Suneil Jain, Paul B. Mullan, Rich Williams, Pedro Oliveira, Niamh E. Buckley, Jamie Honeychurch, Simon S. McDade, Timothy Illidge, Ian G. Mills and Sharon L. Eddie Investigating Radiotherapy Response in a Novel Syngeneic Model of Prostate Cancer Reprinted from: <i>Cancers</i> 2020, 12, 2804, doi:10.3390/cancers12102804	223
Sven Burgdorf, Stefan Porubsky, Alexander Marx and Zoran V. Popovic Cancer Acidity and Hypertonicity Contribute to Dysfunction of Tumor-Associated Dendritic Cells: Potential Impact on Antigen Cross-Presentation Machinery Reprinted from: <i>Cancers</i> 2020, 12, 2403, doi:10.3390/cancers12092403	243
Anmi Jose, Gautham G. Shenoy, Gabriel Sunil Rodrigues, Naveena A. N. Kumar, Murali Munisamy, Levin Thomas, Jill Kolesar, Ganesha Rai, Praveen P. N. Rao and Mahadev Rao Histone Demethylase KDM5B as a Therapeutic Target for Cancer Therapy Reprinted from: <i>Cancers</i> 2020, 12, 2121, doi:10.3390/cancers12082121	257
Catarina Nascimento, Ana Catarina Urbano, Andreia Gameiro, João Ferreira, Jorge Correia and Fernando Ferreira Serum PD-1/PD-L1 Levels, Tumor Expression and PD-L1 Somatic Mutations in HER2-Positive and Triple Negative Normal-Like Feline Mammary Carcinoma Subtypes Reprinted from: <i>Cancers</i> 2020, 12, 1386, doi:10.3390/cancers12061386	273
Flávia Martins, Rosa Oliveira, Bruno Cavadas, Filipe Pinto, Ana Patrícia Cardoso, Flávia Castro, Bárbara Sousa, Marta Laranjeiro Pinto, Ana João Silva, Diogo Adão, José Pedro Loureiro, Nicole Pedro, Rui Manuel Reis, Luísa Pereira, Maria José Oliveira and Angela Margarida Costa Hypoxia and Macrophages Act in Concert Towards a Beneficial Outcome in Colon Cancer Reprinted from: <i>Cancers</i> 2020, 12, 818, doi:10.3390/cancers12040818	289

About the Editor

Patrícia Alexandra Saraiva Madureira

Patrícia Alexandra Saraiva Madureira obtained her licenciatura degree in biochemistry from the Faculty of Sciences, University of Lisbon in 1998 and completed a PhD (supported by an FCT fellowship) in biomedical sciences with distinction from the Faculty of Medicine, University of Lisbon in 2005. She continued her scientific career as a postdoc at Imperial College London, U.K., where she gained expertise in cancer cell signalling with a postdoctoral fellowship from FCT. To broaden her expertise in cancer research, she became a senior postdoc at Dalhousie University, Canada, funded by a CRTP postdoctoral fellowship. In March 2012 she was awarded a prestigious WELCOME II principal investigator contract, co-funded by the FCT and Marie Curie actions/FP7 Program that allowed her to establish her laboratory and initiate a number of research projects. Currently, she is a principal investigator at the Centre for Biomedical Research (CBMR), Univ Algarve, supported by a prestigious FCT Investigator award from the FCT.

Preface to “The Shaping of Cancer by the Tumour Microenvironment and Its Relevance for Cancer Therapy”

The simplistic view of a tumour as the sole result of the uncontrolled proliferation of transformed cells has long been refuted. It is well established that cancer is not an independent entity, and that the tumour microenvironment plays a pivotal role in shaping the evolution of cancer cells and consequently the progression of the tumour. To survive and spread/metastasize, cancer cells need to adapt to the pressures imposed by their microenvironments. These include high oxidative stress conditions, reduced oxygen (hypoxia), immune system surveillance and exposure to chemo- and radiotherapy. It is crucial to understand the interplay between the cancer cells and the tumour microenvironment to develop efficient therapies against primary and, importantly, recurrent cancers that have evolved in response to treatment.

Patrícia Alexandra Saraiva Madureira

Editor

Review

The Role of Hypoxia in Glioblastoma Radiotherapy Resistance

Agathe L. Chédeville ^{1,2,3} and Patricia A. Madureira ^{4,*} 

¹ INSERM, UMR 1287, Gustave Roussy, CEDEX 94805 Villejuif, France; Agathe.CHEDEVILLE@gustaveroussy.fr

² Université Paris-Saclay, UMR 1287, Gustave Roussy, CEDEX 94805 Villejuif, France

³ Gustave Roussy, UMR 1287, 114, Rue Edouard-Vaillant, CEDEX 94805 Villejuif, France

⁴ Centre for Biomedical Research (CBMR), University of Algarve, Gambelas Campus, Building 8, Room 2.22, 9005-139 Faro, Portugal

* Correspondence: patricia.madureira75@gmail.com or pamadureira@ualg.pt

Simple Summary: Glioblastoma (GB) is the deadliest type of primary brain tumor. Following diagnosis the patient's median survival is only 16 months. There are currently around 450 clinical trials focused on the development of more effective therapies for GB. Nevertheless, radiotherapy remains the most clinically relevant and effective treatment for this devastating disease. Unfortunately, radiotherapy resistance (radioresistance) is frequently observed in GB patients. As a consequence tumor regrowth (recurrence) occurs and eventually the patient succumbs to the disease. It is crucial to fully understand the mechanisms by which GB cells become resistant to radiation in order to improve the sensitivity of these cells to radiotherapy and develop novel strategies to overcome this issue. In this review, we examined how low tumor oxygenation (known as hypoxia) which is a main feature of GB contributes to radioresistance to better understand the implications of this tumor microenvironment in GB treatment and recurrence.

Abstract: Glioblastoma (GB) (grade IV astrocytoma) is the most malignant type of primary brain tumor with a 16 months median survival time following diagnosis. Despite increasing attention regarding the development of targeted therapies for GB that resulted in around 450 clinical trials currently undergoing, radiotherapy still remains the most clinically effective treatment for these patients. Nevertheless, radiotherapy resistance (radioresistance) is commonly observed in GB patients leading to tumor recurrence and eventually patient death. It is therefore essential to unravel the molecular mechanisms underpinning GB cell radioresistance in order to develop novel strategies and combinational therapies focused on enhancing tumor cell sensitivity to radiotherapy. In this review, we present a comprehensive examination of the current literature regarding the role of hypoxia (O_2 partial pressure less than 10 mmHg), a main GB microenvironmental factor, in radioresistance with the ultimate goal of identifying potential molecular markers and therapeutic targets to overcome this issue in the future.

Keywords: glioblastoma (GB); hypoxia; radiotherapy; Hypoxia Inducible Factor (HIF); radioresistance; glioma stem cells (GSC)



Citation: Chédeville, A.L.; Madureira, P.A. The Role of Hypoxia in Glioblastoma Radiotherapy Resistance. *Cancers* **2021**, *13*, 542. <https://doi.org/10.3390/cancers13030542>

Academic Editor: David Wong
Received: 28 December 2020
Accepted: 29 January 2021
Published: 1 February 2021

Publisher's Note: MDPI stays neutral with regard to jurisdictional claims in published maps and institutional affiliations.



Copyright: © 2021 by the authors. Licensee MDPI, Basel, Switzerland. This article is an open access article distributed under the terms and conditions of the Creative Commons Attribution (CC BY) license (<https://creativecommons.org/licenses/by/4.0/>).

1. Introduction

Glioblastoma (GB) is classified by the World Health Organization (WHO) as a grade IV astrocytoma. It is the deadliest primary malignant brain tumor; the median patient survival time being only 16 months [1–3].

The current classification of the Central Nervous System (CNS) tumors by the WHO combines both their histopathological name followed by the characteristic genetic signature [4]. In accordance to this, GB is classified as GB, IDH-wildtype which is the most prevalent type, corresponding to approximately 90% of all cases, and GB, IDH-mutant. Over 90% of GB develop de novo, called primary GB. However, a minority of GB develop

slowly from low-grade astrocytomas (secondary GB). Mutations in *IDH* are more frequently observed in secondary GB. There are three Isocitrate Dehydrogenase (*IDH*) enzymes (*IDH1*, *IDH2* and *IDH3*), but only *IDH1* and *IDH2* enzymes have been shown to be mutated in GB. *IDH*s are responsible for the conversion of isocitrate to α -ketoglutarate. This process results in the production of the reducing agent Nicotinamide Adenine Dinucleotide Phosphate (NADPH). *IDH*-mutant enzymes have approximately 50% less activity compared to *IDH* wild-type (WT) proteins. This results in impaired production of bioenergy (NADPH) and intermediates and the production of the onco-metabolite 2-hydroxyglutarate (2-HG) which causes epigenetic changes. 2-HG via hyper-methylation leads to the loss of differentiation of GB cells. These changes caused by *IDH* mutation lead to reduced GB, *IDH*-mutant tumor growth compared to GB, *IDH*-WT. This consequently translates to a better overall prognosis for patients with GB, *IDH*-mutant [5].

GB has been further sub-classified into classical, proneural, neural and mesenchymal sub-types based on specific genetic signatures [6,7]. In this way, the classical sub-type is characterized by *Epidermal Growth Factor Receptor (EGFR)* gene amplification or mutation (leading to a constitutively active receptor) as well as by over-expression of neural stem cell genes. These include *Sonic hedgehog*, *Notch* and *NES* [7]. The proneural sub-type shows a gene signature characterized by over-expression of many proneural genes (e.g., *DCX*, *SOX*, *TCF4*, *ASCL1* and *DLL3*), amplification of the *Platelet-Derived Growth Factor Receptor A (PDGFRA)* gene and inactivation or loss of *TP53* [7,8]. In addition, *IDH* mutations are more common within the proneural subtype [9]. The expression of neuron gene markers, such as *NEFL*, *GABRA1*, *SYT1* and *SLC12A5* is a hallmark of the neural sub-type [7]. Lastly, the mesenchymal sub-type signature includes the expression of mesenchymal genes (e.g., *CHI3L1* and *MET*) [8] as well as inactivating mutations or deletion of the *Neurofibromin 1 (NF1)* gene [7,10,11].

The current standard treatment for GB was established in 2005 by Roger Stupp and colleagues [12]. The so called “Stupp protocol” encompasses GB resection surgery (when possible as evaluated by MRI imaging) after what concurrent radiotherapy and chemotherapy with temozolomide (TMZ) are implemented. This is followed by additional 6 cycles of TMZ administration [12]. Radiotherapy alone can considerably increase patient survival. However, beneficial effects of chemotherapy with TMZ are most commonly observed in a sub-set of patients whose tumors contain *O6-methylguanine DNA methyltransferase (MGMT)* promoter methylation [1,9]. *MGMT* promoter methylation is also a prognostic factor associated with longer survival irrespective of TMZ treatment as well as longer post-progression survival (3–4 months) in patients with recurrent GB [13]. *MGMT* is a DNA repair enzyme that fixes damaged guanine nucleotides (O6-methylguanine) via transferring the methyl group at the O6 site of guanine to its cysteine residues. This reverts the gene mutation and subsequently avoids cell death induced by alkylating agents such as TMZ [14]. Several studies have demonstrated that regulation of *MGMT* expression in GB occurs mainly via epigenetic modification, namely through the methylation of CpG islands within the *MGMT* promoter. This leads to heterochromatinization which is accompanied by rearrangement and random localization of nucleosomes. Consequently, binding of transcription factors to the *MGMT* promoter becomes impaired [14].

The current standard radiotherapy dosage is a total of 60 Grays (Gy) in fractions of 2 Gy, administered 5 days a week for 6 weeks [12]. TMZ is concurrently administered at a dose of 75 mg/m² daily for 6 weeks. After a rest period of one month, TMZ chemotherapy is restarted at a dose of 150 mg/m² daily for 5 days in the first month cycle. If this dose is tolerated, it can be increased up to 200 mg/m² for 5 days per month. TMZ is administered for 6 months after radiotherapy, but many physicians continue TMZ administration for 12–18 months even though it has not been proved to increase overall survival [12,15]. Worryingly, almost all GB patients develop resistance to current therapy and eventually succumb to the disease.

Despite the development of a large number of studies and hundreds of ongoing clinical trials, GB treatment has not changed since 2005 [9,12]. Understanding the complex

biology of GB and the role of the tumor microenvironment is therefore crucial to develop novel and effective treatments in GB.

GB pathological features include hypoxic foci (where O_2 partial pressure is less than 10 mmHg) containing necrotic cores. The hypoxic areas are surrounded by cell pseudopalisades and microvascular hyperplasia [9]. Research suggests that cellular pseudopalisades constitute invasive fronts of the tumor that likely originated from GB cells migrating away from the hypoxic regions. These cells over-secrete proangiogenic factors leading to an intensified form of angiogenesis which is known as microvascular hyperplasia [9].

The GB hypoxic microenvironment has been shown to be highly associated with tumor invasion and resistance to chemo- and radiotherapy which are the main causes of death in GB patients [16,17]. Importantly, dynamic contrast enhanced MRI analyses have indicated that Hypoxia Inducible Factor 1 (HIF-1) (hypoxia marker) and Vascular Endothelial Growth Factor A (VEGFA) staining and tumor vascularity significantly correlate with worse progression-free and overall GB patient survival [18,19].

In this review article, we examined the existing literature regarding the role of hypoxia in supporting radiotherapy resistance in GB with the aim to better understand the implications of this tumor microenvironment in GB treatment and recurrence.

2. Basic Principles of Cancer Radiotherapy

Radiotherapy is currently the major and most effective treatment modality for GB patients. Nevertheless, radioresistance remains a major clinical problem for these patients.

Ionizing radiation (IR) was discovered just before the turn of the 20th century by Marie and Pierre Curie and Wilhelm Conrad Roentgen [20]. It was during the 1920s that cancer radiotherapy was piloted and significantly evolved [20] due to several technologic and research advances. These included the invention by Coolidge et al. of a sealed-off vacuum x-ray tube which could be operated at 180,000 to 200,000 volts which introduced the kilovoltage era in radiotherapy. Another important advancement that contributed to the effectiveness of radiotherapy at that time was the development of the first quantitative methods for the measurement of radiation dose and of the first physical unit of dose, the roentgen (later replaced by the rad). Lastly, the experimental and clinical radiobiology research work led by Claude Regaud at the Fondation Curie in Paris pioneered the procedure and development of fractionated radiotherapy which is still currently in use [20].

The ability of IR to kill tumor cells relies mainly on its DNA damaging effects. This damage can occur either directly on the DNA molecules (accounting for 30–40% of lesions), or indirectly through the generation of free radicals such as reactive oxygen species (ROS) or reactive nitrogen species (RNS) that in turn damage the DNA molecules (responsible for 60–70% of lesions) [21,22].

Water radiolysis is a main process in the formation of free radicals (ROS) by IR, resulting in the formation of electrons, H^\bullet atoms, OH^\bullet radicals, H_3O^+ , OH^- ions and dihydrogen (H_2) and hydrogen peroxide (H_2O_2) molecules [23].

IR produces a spectrum of DNA base lesions, the most prevalent being 8-oxo-guanine (8-oxoG), thymine glycol (5,6-dihydroxy-5,6-dihydrothymine) and formamidopyrimidines [4,6-diamino-5-formamidopyrimidine (FapyAde) and 2,6-diamino-4-hydroxy-5-formamidopyrimidine (FapyGua)] [24]. In addition, IR produces DNA Single Strand Breaks (SSBs) that have a unique signature, generating 3' phosphate or 3'-phosphoglycolate ends rather than 3'-OH ends. Particularly important IR induced lesions are double strand breaks (DSBs) which occur due to multiple damaged sites closely located on both strands of the DNA molecule [24]. DSBs are more difficult to repair compared to SSBs leading to cancer cell death [25]. DSBs typically trigger DNA-damage responses (DDR). However, when DSBs cannot be efficiently repaired by the cellular DDR mechanisms, irradiated cells undergo the so-called mitotic catastrophe which is a major cell death mechanism caused by IR-induced DNA damage [26].

Typically, a dose of 1Gy of X-ray radiation produces around 3000 damaged bases, 1000 SSBs and 40 DSBs [22].

The decreased oxygen levels observed in hypoxic GB cells, lead to resistance to IR due to the reduced availability of oxygen which is needed to stabilize the DNA strand breaks caused by radiotherapy [27]. Under normoxic conditions (physiological or normal oxygen levels, where tissue oxygenation is around 40 mmHg), cells are vulnerable to IR due to oxygen fixation leading to irreversible DNA damage. However, under hypoxic conditions (where O₂ partial pressure (pO₂) is below 10 mmHg), there is diminished production of DNA radicals due to the low levels of oxygen and subsequently cells become more resistant to radiotherapy [28]. Consequently, the radiation dose required to achieve the same biological effect is about three times higher in the absence of oxygen as compared to physiological oxygen levels [27].

3. Hypoxia in GB

Tumor hypoxia is a hallmark of GB and mainly occurs due to the abnormal neo-vascularization observed within these tumors [29]. The blood vessels that feed the GB are typically highly permeable and easily collapsible due to the excessive recruitment and proliferation of endothelial cells (caused by excessive secretion of VEGFA by the tumor cells) and lack of pericyte coverage (which are cells that provide support to the blood vessels) [30–32]. In addition, these vessels exhibit larger diameters and possess thicker basement membranes when compared to physiological brain blood vessels [33]. As a consequence, the occurrence of microvascular thromboses and vessel occlusions are frequently observed in GB [34] which significantly impede blood flow leading to a heterogeneous microenvironment regarding tumor oxygenation [35]. Moreover, the anarchic organization and instability of the vascular system within the tumor can lead to dynamic phases of hypoxia and then reoxygenation within the different tumor fractions, known as “cycling hypoxia” [36].

3.1. Regulation of HIF Transcription Factors

The cellular response to hypoxic stress is largely orchestrated by the HIF transcription factors. HIFs are heterodimers composed of an α subunit (e.g., HIF-1 α , EPAS1/HIF-2 α , or HIF-3 α) which is negatively regulated by oxygen (O₂) and a β subunit, HIF-1 β , also known as aryl hydrocarbon receptor nuclear translocator (ARNT), which is expressed constitutively in cells [37,38]. Regarding protein domain structures, HIF-1 α , HIF-2 α , and HIF-1 β subunits all have a Per-Arnt-Sim (PAS) and a basic Helix-Loop-Helix (bHLH) domains which are involved in the heterodimer assembly and binding to Hypoxia Responsive Elements (HRE) within HIF target gene promoters and a characteristic C-Terminal Domain (C-TAD) (Figure 1). Each HIF- α subunit also contain an Oxygen-Dependent Degradation Domain (ODDD) that is involved in the degradation of these proteins in the presence of normal levels of oxygen, and a specific N-Terminal Domain (N-TAD) (Figure 1). N-TAD and C-TAD domains are able to interact with p300/CBP HIF transcriptional coactivators [39–41]. Different variants of the HIF-3 α subunit containing diverse deletions of the domains described above have been shown to exist (reviewed in [42]).

HIF transcriptional activity is highly dependent on the degradation (negative regulation) or stabilization (positive regulation) of the HIF- α subunit which is regulated by intracellular levels of oxygen. In normoxic cells, the Prolyl Hydroxylases 1-3 (PHD1-3) hydroxylate two prolyl residues within the HIF- α subunit. This enables the binding of the Von Hippel-Lindau (VHL) protein to the HIF- α subunit and the subsequent recruitment of E3 ubiquitin ligases that target HIF- α for degradation via the proteasome (Figure 2) [43–45]. Hypoxia inhibits PHD activity and consequently leads to HIF- α stabilization and translocation to the nucleus where it binds to the HIF-1 β subunit and p300/CBP cofactors. HIFs bind to HRE within their target gene promoters orchestrating the hypoxic response [46–48]. The hydroxylase, Factor-Inhibiting HIF (FIH) has also been shown to regulate HIF activity in an oxygen dependent manner. In normoxic cells, FIH hydroxylates an asparagine residue within the HIF- α subunit which impairs the interaction between HIF and the transcrip-

tional activators, p300/CBP subsequently negatively impacting on HIF transcriptional activity (Figure 2) [49,50].

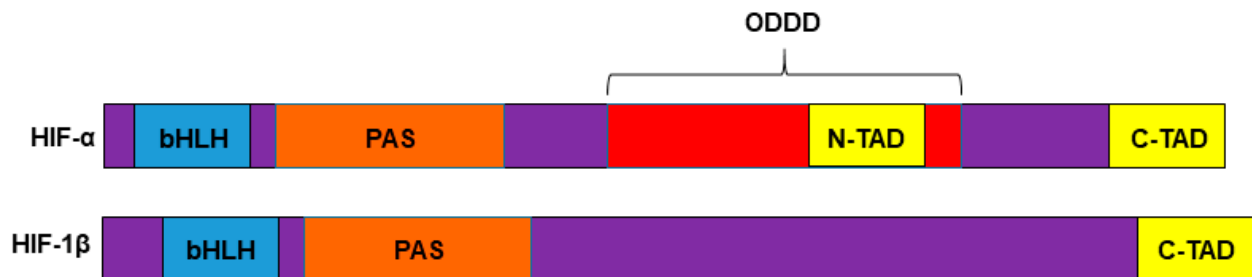


Figure 1. HIF protein domain structures. HIF-1 α , HIF-2 α , and HIF-1 β subunits contain a bHLH domain (blue box), a PAS domain (orange box) and a C-TAD domain (yellow box). In addition, HIF-1 α and HIF-2 α subunits contain an ODDD (red box) and N-TAD (yellow box) domains. Different variants of the HIF-3 α subunit containing diverse deletions of the domains shown in the figure have been shown to exist.

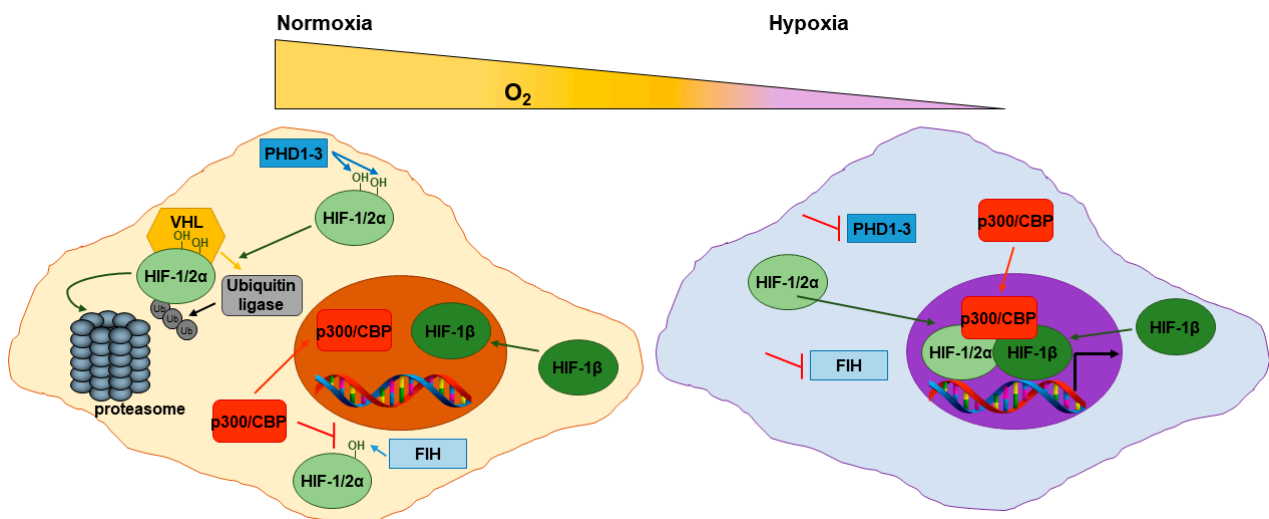


Figure 2. Regulation of HIF transcription factors. In normoxic cells, the PHD1-3 hydroxylate two prolyl residues within the HIF- α subunit enabling the binding of the VHL protein to the HIF- α subunit. VHL recruits E3 ubiquitin ligases that target HIF- α for degradation via the proteasome. In hypoxic cells, PHD1-3 activity (which is oxygen dependent) is inhibited. This leads to HIF- α stabilization and translocation to the nucleus where it binds to the HIF-1 β subunit and p300/CBP cofactors. HIFs bind to HRE within their target gene promoters. In normoxic cells, FIH hydroxylates an asparagine residue within the HIF- α subunit. This blocks the interaction between HIF and the transcriptional activators, p300/CBP.

HIF-1 and HIF-2 are considered the main regulators of the hypoxia response [37,38], while the existence of multiple variants of HIF-3 α has highlighted that HIF-3 can function in some cases as a transcriptional activator whereas certain variants can act as dominant negative regulators of HIF-1 and/or HIF-2 transcriptional functions [42,51].

3.2. Hypoxia Independent HIF Activation in GB

Several genetic alterations leading to HIF activation, even in the absence of hypoxia, have been reported in GB (Figure 3). These include the activation of the EGFR (either by amplification or mutation of the *EGFR* gene) and the loss of the tumor suppressor genes *TP53* and Phosphatase and Tensin homolog (*PTEN*) [52–54]. The most common *EGFR* mutation observed in GB is the deletion of exons 2–7 (*EGFRvIII*) resulting in the expression of a constitutively active and ligand independent *EGFRvIII* receptor [55]. *EGFR* signaling leads to the up-regulation of HIF-1 α levels via the activation of the PI3K/AKT/mTOR pathway [56,57]. Depletion of *PTEN* has been reported in about 20–40% of GB [53]. *PTEN* constitutes the main negative regulator of the PI3K/AKT signaling pathway. Therefore, loss of *PTEN*

promotes the up-regulation of HIF-1 α due to enhanced activity of the PI3K/AKT/mTOR pathway which is observed in the absence of PTEN protein. Loss of the *TP53* gene has been linked to HIF-1 α stabilization due to down-regulation of *MDM2* transcription and subsequent inhibition of MDM2 mediated ubiquitination and degradation of HIF-1 α (Figure 3) [54].

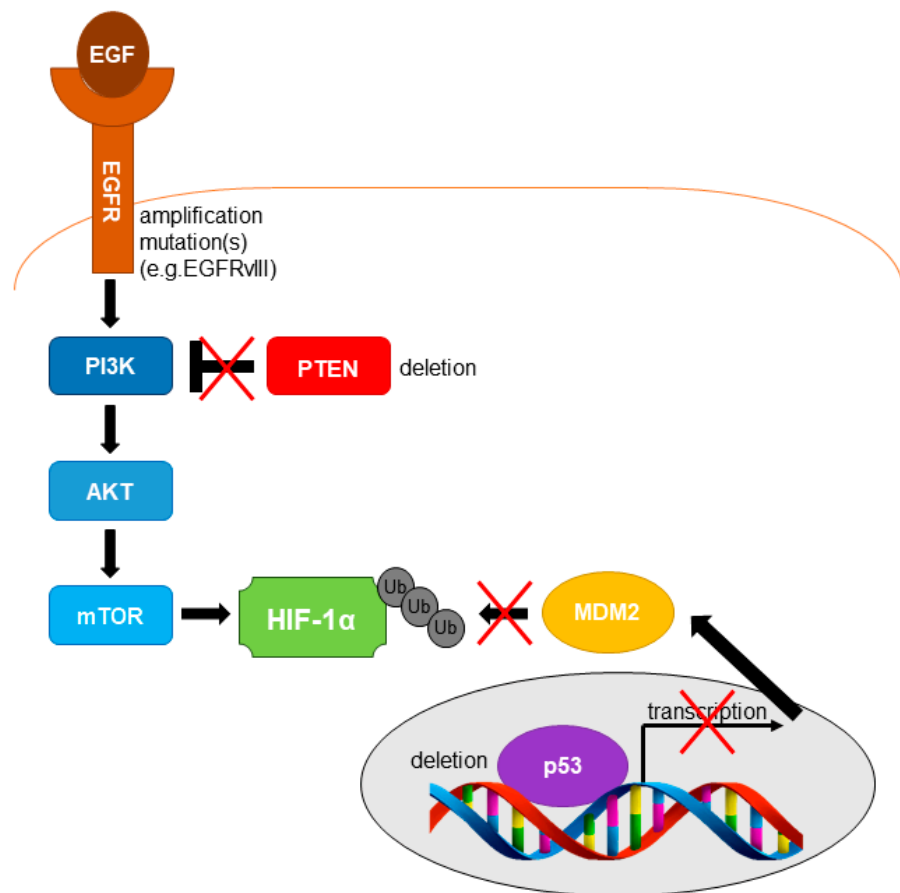


Figure 3. Genetic alterations leading to HIF activation in GB. Activation of the Epidermal Growth Factor Receptor (EGFR) by *EGFR* gene mutation (e.g., EGFRvIII) and/or amplification frequently occurs in GB cells resulting in activation of the PI3K/AKT/mTOR pathway with the subsequent accumulation of HIF-1 α levels. The tumor suppressor Phosphatase and Tensin homolog (*PTEN*) gene is deleted in 20–40% of GBs. *PTEN* is the main inhibitor of the PI3K/AKT signaling pathway. Consequently, loss of *PTEN* will also lead to accumulation of HIF-1 α via the PI3K/AKT/mTOR pathway. Loss of p53 inhibits MDM2-mediated ubiquitination of HIF-1 α leading to its accumulation and increased HIF activity in GB cells.

3.3. HIF Transcriptional Targets in GB

HIFs induce the transcription of hundreds of genes involved in the regulation of main cellular processes including angiogenesis, glycolysis, autophagy, motility and invasion, chemo- and radioresistance [58,59].

Several studies using GB cell lines and/or clinical samples support a hypoxia triggered metabolic switch towards glycolysis including the up-regulation of HK2, PFKFB3, PFKFB4, PFKFBP, LDHA, PDK1, SLC2A1/GLUT-1, CA9/CA IX, PGAM1, ENO1, ENO2, ALDOA and SLC16A3/ MCT-4 genes and proteins (Figure 4) [9,59,60]. Hypoxic up-regulation of many pro-angiogenic genes and proteins is also commonly observed in GB. These include VEGFA, VEGFC, VEGFD, PGF/PlGF, ADM and ANGPTL4 (Figure 4) [32,59,61,62]. GB is a highly invasive tumor and hypoxia has been shown to induce proteins of the plasminogen system. These include the plasminogen receptor, S100A10, the receptor for the urokinase

Plasminogen Activator (uPA), uPAR and the Plasminogen Activator Inhibitor-1 (PAI-1) (Figure 4) [59,63,64]. The co-localization of S100A10 with uPAR at the outer cell membrane has been shown to promote the generation of the serine protease, plasmin by putting plasminogen (inactive form of plasmin) and its activator, uPA into close proximity. This leads to the subsequent degradation of the Extra-Cellular Matrix (ECM) by plasmin which is a critical step in GB cell invasion. Importantly, plasmin also has the capacity to cleave and activate many pro-MMPs, further accelerating ECM degradation [65,66]. The GB hypoxic environment has also been shown to promote the up-regulation of autophagy genes including *BNIP-3* and *DDIT4* (Figure 4) [59,67,68]. Several studies support that during hypoxic stress autophagy allows the recycling of cellular components which is critical for cell survival under oxygen and nutrients limiting conditions. Association of GB hypoxia with chemoresistance has also been demonstrated. Several reports have shown that hypoxic induction of *ANGPTL4*, *DDIT4* and *NDRG1* lead to resistance to chemotherapy (Figure 4) [59,69–73].

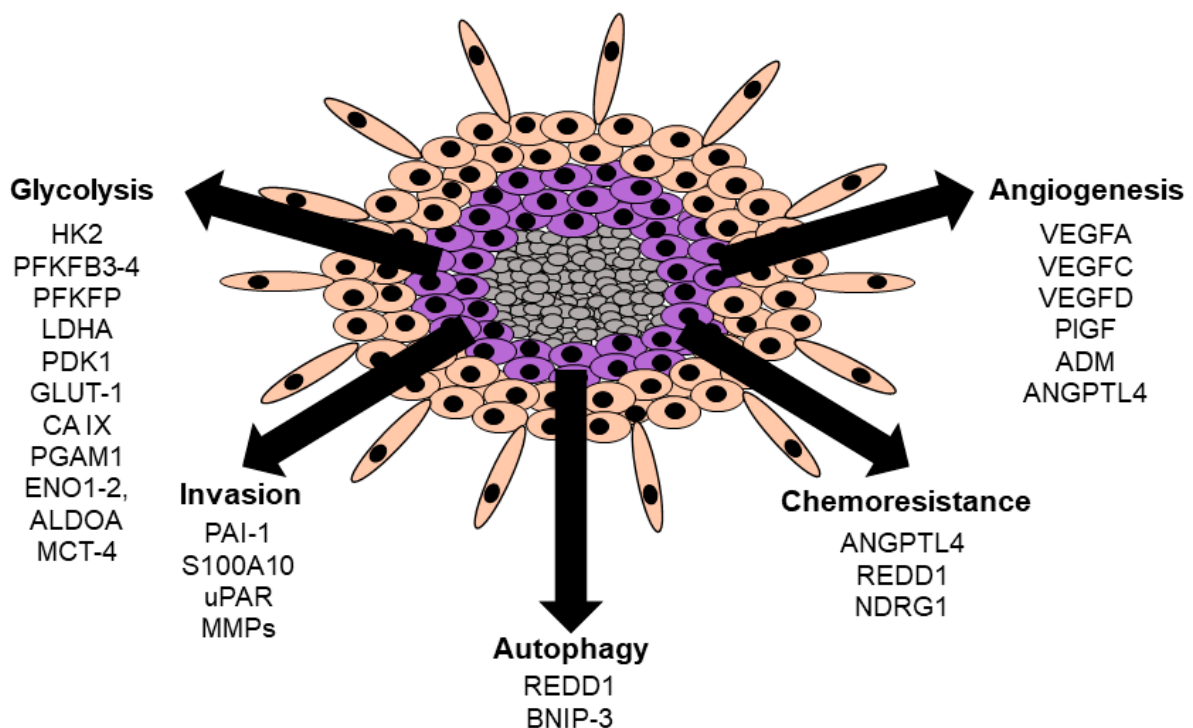


Figure 4. Hypoxia induced gene/protein expression in GB cells. Necrotic cells are represented in grey, hypoxic cells are represented in purple, and normoxic cells are represented in peach color.

4. The Role of Hypoxia in GB Radioresistance

The molecular mechanisms by which GB becomes resistant to radiotherapy are still not fully understood. However, it has been shown that radioresistance can at least in part be due to the presence of hypoxic regions within the tumor [74].

Hypoxia contributes to radioresistance by controlling several cellular processes including regulation of the cell cycle, inhibition of apoptosis and senescence, regulation of autophagy and antioxidant/redox activity, promoting invasion and cancer cell stemness. In addition, radiotherapy is more efficient in rapidly proliferating cells as compared to slow-proliferating, quiescent and stem-like cells that are localized in the most hypoxic regions of the tumor [28].

4.1. The Role of Cell Cycle Regulation Proteins in Hypoxia Induced Radioresistance

Several molecular mechanisms involved in cell cycle regulation have been shown to play a role in hypoxia induced radioresistance in GB (Figures 5 and 6). A study showed

that MEK/ERK inhibition either by treatment with the drug, U0126 or downregulation of ERK by siRNA significantly enhanced the radiosensitivity of hypoxic T98G, U87MG and U138MG GB cells [75]. Using a combination of siRNA approaches and chemical inhibitors these authors further mapped the MEK/ERK/DNA-PKc/HIF-1 α functional interplay in hypoxia dependent GB radioresistance.

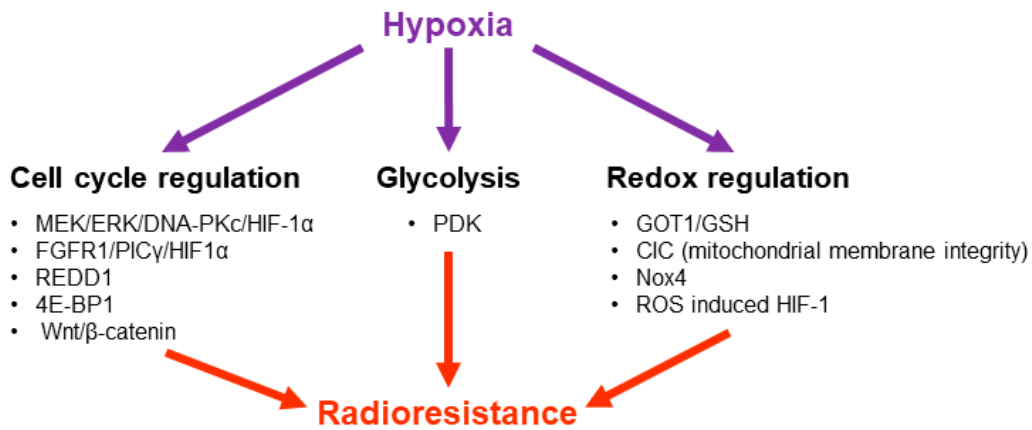


Figure 5. The role of hypoxia in GB radioresistance. Cell cycle regulation, glycolysis and Redox/ROS regulatory mechanisms have been shown to support hypoxia dependent radioresistance in GB cells.

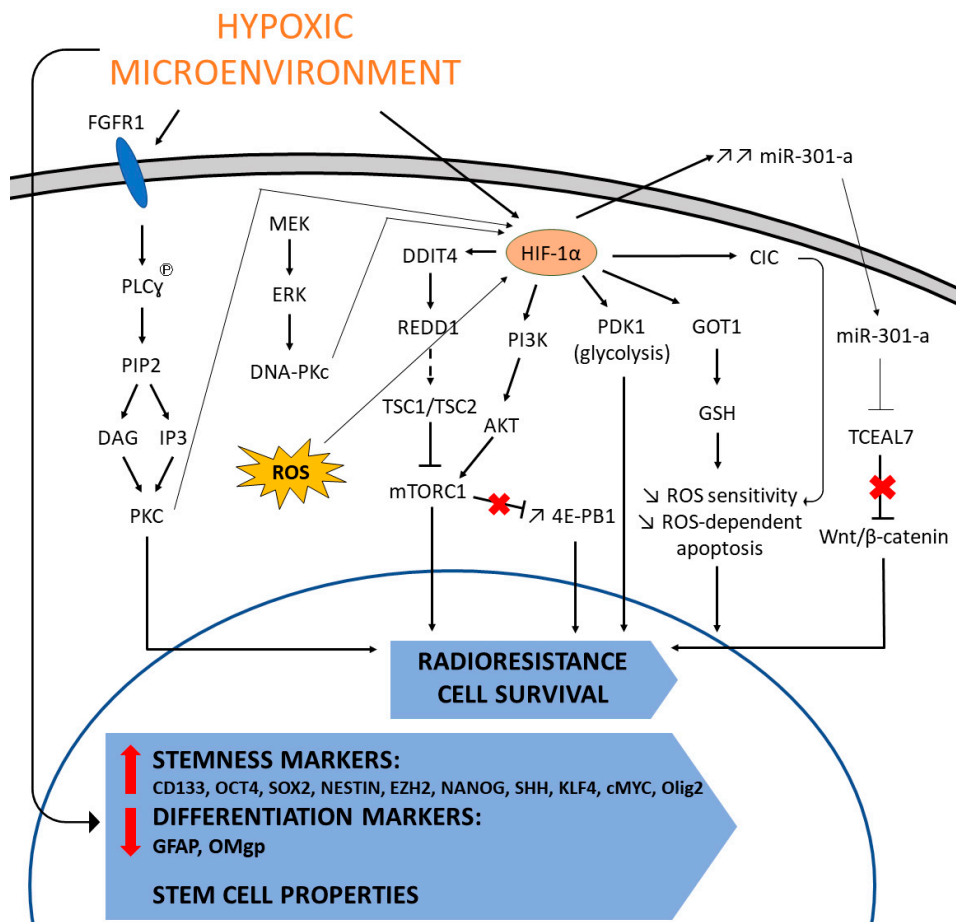


Figure 6. Hypoxia induced mechanisms leading to radioresistance in GB. The hypoxic environment induces several mechanisms involved in radioresistance including mechanisms involved in cell cycle regulation, Redox regulation, glycolysis and the maintenance of GSCs.

Another report highlighted the role of the Fibroblast Growth Factor Receptor 1 (FGFR1) in Phospholipase C Gamma (PIC γ)/HIF1 α -dependent GB radioresistance [76]. FGFR signalling is involved in the regulation of cell proliferation, differentiation, migration, angiogenesis and tissue injury repair. PIC γ binds through its SH2 domain to a phosphotyrosine residue within the C-terminal tail of FGFRs and is phosphorylated at the tyrosine residues by the activated receptor tyrosine kinase. This phosphorylation activates PIC γ which then hydrolyzes phosphatidylinositol 4,5-bisphosphate (PIP2) to generate inositol1,4,5-trisphosphate (IP3) and 1,2-diacylglycerol (DAG) leading to Protein Kinase C (PKC) activation. Using in vitro and in vivo knockdown approaches, the authors were able to demonstrate that FGFR1/PIC γ /HIF1 α signalling pathway confers radioresistance to GB cells (e.g., U87, LN18) and derived tumor mouse xenografts via controlling radiation-induced centrosome overduplication and radiation-induced mitotic cell death.

We recently observed a significant increase in *DDIT4* expression in hypoxic GB cells (e.g., U87, SEBTA-003, SEBTA-023, UP-007, UP-029) as compared to their normoxic counterpart control cells [59]. These data supported a previous report using U87 cells [67]. We also observed high expression of *DDIT4* in GB patient clinical samples, particularly in GB hypoxic core region as compared to normal brain specimens [59]. *DDIT4* gene product is the protein, REDD1 which is involved in the activation of the Tuberous Sclerosis 1/2 (TSC1/TSC2) complex, a main negative regulator of mTORC1 [77]. Even though overexpression of REDD1 in GB has been linked to chemo- and radioresistance the molecular mechanisms involved in these outcomes are still not fully understood [70,78].

Phosphorylation of 4E-BP1 occurs after activation of mTORC1, which functions downstream of the PI3K/AKT and AMPK kinase signaling pathways [79]. As previously mentioned, the PI3K/AKT signaling pathway is frequently activated in GB. Consequently, this leads to increased rates of cap-dependent translation in an mTORC1/4E-BP1-dependent manner. Using a mouse U87 GB xenograft model, a study has shown that 4E-BP1 promotes hypoxia dependent radioresistance [80]. These authors found that loss of 4E-BP1 expression by siRNA did not significantly affect in vitro growth of U87 GB cells, but significantly enhanced the growth of U87 tumor xenografts. Furthermore, 4E-BP1 knockdown U87 cells were significantly more sensitive to hypoxia-induced in vitro cell death. Most importantly, 4E-BP1 knockdown cells produced tumors with reduced fractions of radioresistant hypoxic cells.

The exosomal secretion of micro-RNA-301-a (miR-301-a) by hypoxic GB cells (e.g., U87, LN229, U251) has also been shown to lead to radioresistance [81]. Importantly, clinical analysis revealed higher levels of miR-301a expression in glioma samples with high HIF-1 α levels and the percentage of serum exosomal miR-301a (low versus high) was distributed according to the HIF-1 α immunohistochemistry score. In vitro studies demonstrated that miR-301a expression is regulated by HIF-1 α . Furthermore, miR-301a directly repressed the promoter of the tumor suppressor gene, *TCEAL7* whose encoded protein binds to β -catenin inhibiting its translocation from the cytoplasm to the nucleus. Therefore, negatively regulating the Wnt/ β -catenin signaling pathway. In summary, targeting of *TCEAL7* gene expression by miR-301a secreted by hypoxic GB cells induced enhanced activation of the Wnt/ β -catenin signaling axis leading to radioresistance.

4.2. The Role of Glycolysis in Hypoxia Induced Radioresistance

As aforementioned, hypoxia induces a metabolic reprogramming towards glycolysis in GB cells. Interestingly, a research study has shown that modulation of the glucose metabolism can sensitize GB cells to IR (Figures 5 and 6) [82]. Treatment of GB cells (e.g., U87, U251, LN229, DBTRG) with dichloroacetate, a PDK inhibitor, in combination with radiotherapy reversed the radiotherapy-induced glycolytic shift in these cells and inhibited their clonogenicity in vitro. Investigation into the molecular mechanism of action revealed that dichloroacetate sensitized GB cells to radiotherapy by inducing G2-M phase cell-cycle arrest, reducing mitochondrial reserve capacity, and increasing oxidative stress and DNA damage in these cells [82]. In vivo studies using a mouse xenograft model showed that

radiotherapy in combination with dichloroacetate improved the survival of orthotopic GB-bearing mice [82]. Taking into account that hypoxia constitutes a major microenvironmental factor that triggers glycolysis in GB (including the specific up-regulation of PDK1 [59]) this report provides encouraging data regarding targeting the glycolytic metabolism in order to sensitize hypoxic GB cells to radiotherapy.

4.3. The Role of ROS Regulatory Systems in Hypoxia Induced Radioresistance

Several studies have shown that the regulation of intracellular ROS levels plays a key role in hypoxic GB radioresistance (Figures 5 and 6). ROS are radical and non-radical oxygen-containing chemical molecules with different degrees of reactivity, including biologically relevant molecules such as superoxide anion (O_2^-), hydroxyl radical ($\cdot OH$) and hydrogen peroxide (H_2O_2) [58]. Of note, H_2O_2 constitutes a key second messenger in many cell signaling pathways [58,83]. However, due to their reactive properties ROS contribute to protein oxidation, lipid peroxidation and/or DNA damage that can ultimately result in either cell death or tumorigenesis (due to DNA mutagenesis) [58]. To overcome this issue, cells possess several antioxidant systems that inactivate ROS and recycle oxidized molecules (reviewed in [58]). A study showed that exposure of T98G GB cells to cycling hypoxia induced the up-regulation of the aspartate-aminotransferase Glutamic-Oxaloacetic Transaminase 1 (GOT1) protein, leading to increased levels of the antioxidant protein, glutathione (GSH), decreased intracellular ROS levels and enhanced radioresistance [84]. Most importantly, targeting glutamine-dependent antioxidant capacity or glutathione metabolism reversed the cycling hypoxia induced GB cells radioresistance. Exposure to either acute or cycling hypoxia was shown to trigger the up-regulation of the mitochondrial Citrate Carrier (CIC) and IDH2 in T98G GB cells in vitro [85]. CIC protein belongs to the large family of mitochondrial metabolite carriers. It is a mitochondrial transmembrane protein whose main function is to mediate the exchange of mitochondrial citrate for cytosolic malate. This process is accompanied with the transport of one proton and therefore can influence the mitochondrial membrane potential [86]. In fact, the tumorigenic activity of CIC has been shown to be linked to its role in mitochondrial membrane integrity [87] which is crucial to inhibit ROS induced apoptosis.

NADPH oxidase subunit 4 (Nox4) has been shown to mediate cycling (intermittent) hypoxia induced radioresistance in GB cells [88]. In this report, the GBM8401 and U251 cell lines were stably transfected with a dual hypoxia HIF-1 signaling reporter construct. The mouse tumor xenograft studies showed that Nox4 was highly expressed in the cycling hypoxic areas within the tumor microenvironment. In addition, when compared to the normoxic or acutely hypoxic GB cells, the cycling hypoxic GB cells derived from tumor xenografts showed significantly higher expression of Nox4, enhanced ROS levels and increased radioresistance which was reversed by Nox4 suppression in intracerebral GB bearing mice [88].

Another report revealed that hypoxia increased U87 GB cell radioresistance in vitro and in vivo via long-term induction of HIF-1 signaling transduction in a ROS dependent-manner [89]. These authors performed clonogenic survival assays to show that hypoxia pretreatment of U87 cells significantly increased GB cell resistance to IR compared with normoxic U87 control cells. To determine whether HIF-1 was a crucial mediator of hypoxia-induced radioresistance in U87 cells, they used a HIF-1 siRNA approach. Hypoxic HIF-1 knockdown U87 cells showed similar sensitivity to IR as compared to normoxic HIF-1 knockdown U87 control cells, indicating that the increased radioresistance observed in hypoxic U87 cells was mediated by HIF-1. The authors further confirmed these results in vivo using a mouse xenograft model [89].

4.4. The Role of Glioma Stem Cells in Radioresistance

As early as 1997, Bonnet and Dick described for the first-time leukemic cells that could transplant leukaemia in vivo into immunodeficient mice [90]. These cells were called “cancer stem cells” (CSCs) and were later identified in different types of cancer including

breast, colon, lung, as well as in CNS cancers such as GB [91]. CSCs are slow-dividing small subpopulations of tumor cells that have the ability to undergo asymmetric cell division for self-renewal and multilineage differentiation giving rise to more mature cancer cells that constitute the bulk of the tumor [92,93]. The CSC hypothesis states that these cells have the ability to generate the cellular heterogeneity which is commonly observed within tumors. CSCs, called Glioma Stem Cells (GSCs) in GB, are suspected of being a main cause of tumor recurrence after treatment.

GSCs have been shown to have similar properties to Neural Stem Cells (NSCs). In addition to self-renewal capacity and multilineage differentiation potential, GSCs also express stemness markers involved in the regulation of specific signaling pathways, telomerase activity, expression of ABC transporter proteins, migration, secretion of cytokines, growth and pro-angiogenic factors [93].

It has been shown that hypoxia treatment of GB cells (e.g., SJ-1, U87) promoted CD133 expression (marker for GSC) and increased OCT4 and SOX2 mRNA levels, while promoting the loss of the glial differentiation marker, GFAP [94]. These data indicate that hypoxia promotes a GSC phenotype in GB. Another report took a broader approach by screening cell lines of different cancer types alongside human embryonic stem cells for overlapping changes of common genes when grown under hypoxic conditions [95]. The authors showed that OCT4, NANOG, SOX2, KLF4, cMYC, and miRNA-302 were all induced under hypoxic conditions in 11 different cancer cell lines from prostate, brain (U251 GB cell line), kidney, cervix, lung, colon, liver and breast tumors [95]. This report further supported a link between hypoxia and the stem cell phenotype by showing a correlation between the expression of HIFs and OCT4 [95].

Whether HIF-1 α , HIF-2 α or both transcription factors play a main role in hypoxia induced GSC phenotype is still a theme up for debate, with many studies showing differing results [29,95–98].

It has been well established that CSCs are significantly more radioresistant as compared to non-CSCs [26]. This is due to their enhanced DNA-repair capability, antioxidant defenses (in particular ROS scavenging systems) and self-renewal potential [99]. Interestingly, GSCs are found within a particular hypoxic environment, called a “niche”. This hypoxic niche forces the GSCs to develop mechanisms of survival and resistance to this harmful environment and also keeps the GSCs in a state of quiescence making them less vulnerable to the effects of radiotherapy [93]. Upon radiotherapy, the GSC populations containing advantageous genomic alterations that protect them against IR are selected and continue to sustain the tumor leading to recurrence.

Hypoxia has been shown to promote the undifferentiated state of GSCs through the activation of the Notch signaling pathway in a HIF dependent manner, contributing in this manner to GB radioresistance [100]. In summary, hypoxia is able of inducing the dedifferentiation of GB cells towards a GSCs phenotype, thus conferring aggressiveness and increased resistance to radiotherapy.

Interestingly, Dahan et al. demonstrated that IR itself is capable of inducing dedifferentiation of GB cells leading to overexpression of stem cell markers (SOX2, Nestin, SHH, Nanog, EZH2, Olig2) and a decrease in glial and neuronal differentiation markers (GFAP and OMgp, respectively) which resulted in increased tumorigenicity in vivo [101]. In addition, this team observed overexpression of survivin (a protein with anti-apoptotic properties that is expressed during neurogenesis) after irradiation of GB cells. Inhibition of this protein prevented the dedifferentiation of GB cells into GSCs [101]. This highlights a potential signaling pathway involved in the dedifferentiation of GB cells and a prospective therapeutic target which would make it possible to inhibit the acquisition of this stem-like phenotype highly linked to GB recurrence.

5. Conclusions

Targeting hypoxia-mediated radioresistance is considered an attractive approach to improve therapy outcome in GB. However, clinical trials evaluating the use of hypoxia-

targeting agents have failed to reveal a benefit for GB patients, reviewed in [102]. This emphasizes the need for more effective and mechanism-based therapies to overcome hypoxia-induced radioresistance and the co-development of predictive biomarkers and improved imaging of heterogeneous GB hypoxia to guide radiotherapy protocols. As previously described, hypoxic areas of the tumor are more resistant to IR compared to normoxic areas. For this reason, increased radiation doses or number of radiation cycles within the GB hypoxic areas could be considered. Here we performed a review of the current literature, regarding the molecular mechanisms which are activated by hypoxia and that can potentially be targeted in the future to improve radiotherapy efficiency in GB patients. We revealed that several signaling pathways involved in cell cycle regulation were shown to provide radioresistance in hypoxic GB cells. These included the MEK/ERK/DNA-PKc/HIF-1 α ; PI3K/AKT/mTORC1/4E-BP1; and inhibition of *TCEAL7* transcription by miR-301-a leading to activation of the Wnt/ β -catenin signaling pathway. The glycolytic metabolism which is triggered by hypoxia in GB cells was also shown to be involved in radioresistance and its inhibition showed promising in vivo results using a mouse xenograft model, providing radiosensitivity in the GB-bearing mice. These results are encouraging regarding the development of glycolytic inhibiting therapy approaches in combination with IR treatment. In addition, several ROS-dependent and Redox regulatory mechanisms were shown to play a role in hypoxic GB radioresistance. These included enhanced expression of GOT1 leading to increased levels of the antioxidant protein, GSH; up-regulation of CIC which has been linked to mitochondrial membrane integrity and inhibition of ROS-induced apoptosis; up-regulation of Nox4 and ROS-dependent up-regulation of HIF-1. Taken together these data highlight that targeting key Redox systems in combination with IR treatment might constitute a promising approach in GB therapy. Finally, the hypoxic microenvironment has been shown to play a role in GSC maintenance and quiescence which are associated with GB radioresistance. This occurs via inhibition of differentiation markers (e.g., GFAP, OMgp) and induction of stemness markers (e.g., CD133, OCT4, SOX2, NANOG, NESTIN, EZH2, SHH, KLF4, cMYC, Olig2).

In conclusion, targeting key cellular proteins/mechanisms involved in cell cycle regulation, glycolytic metabolism, Redox regulation and/or GSC maintenance in combination with IR treatment may potentially lead to the development of novel and effective therapies for GB patients.

Funding: P.A.M. was funded by an FCT Investigator contract from the Foundation for Science and Technology (Fundação para a Ciência e a Tecnologia, FCT), Portugal (ref: IF/00614/2014) and FCT exploratory grant, ref:IF/00614/2014/CP12340006. CBMR was financed by an FCT Research Center Grant ref: UID/BIM/04773/2013CBMR1334. A.L.C. is supported by a PhD fellowship from the University Paris Diderot.

Conflicts of Interest: The authors declare no conflict of interest.

References

1. Gilbert, M.R.; Wang, M.; Aldape, K.D.; Stupp, R.; Hegi, M.E.; Jaeckle, K.A.; Armstrong, T.S.; Wefel, J.S.; Won, M.; Blumenthal, D.T.; et al. Dose-dense temozolomide for newly diagnosed glioblastoma: A randomized phase III clinical trial. *J. Clin. Oncol.* **2013**, *31*, 4085–4091. [[CrossRef](#)] [[PubMed](#)]
2. Stupp, R.; Hegi, M.E.; Mason, W.P.; van den Bent, M.J.; Taphoorn, M.J.; Janzer, R.C.; Ludwin, S.K.; Allgeier, A.; Fisher, B.; Belanger, K.; et al. European Organisation for Research and Treatment of Cancer Brain Tumour and Radiation Oncology Groups; National Cancer Institute of Canada Clinical Trials Group Effects of radiotherapy with concomitant and adjuvant temozolomide versus radiotherapy alone on survival in glioblastoma in a randomised phase III study: 5-year analysis of the EORTC-NCIC trial. *Lancet Oncol.* **2009**, *10*, 459–466. [[CrossRef](#)] [[PubMed](#)]
3. Wang, M.; Dignam, J.J.; Won, M.; Curran, W.; Mehta, M.; Gilbert, M.R. Variation over time and interdependence between disease progression and death among patients with glioblastoma on RTOG 0525. *Neuro-Oncology* **2015**, *17*, 999–1006. [[CrossRef](#)] [[PubMed](#)]
4. Louis, D.N.; Ohgaki, H.; Wiestler, O.D.; Cavenee, W.K.; Ellison, D.W. (Eds.) *WHO Classification of Tumours of the Central Nervous System WHO Classification of Tumours*, 4th ed.; IARC Publications: Lyon, France, 2016. Available online: <https://www.iarc.who.int/news-events/iarc-publications-who-classification-of-tumours-of-the-central-nervous-system/> (accessed on 21 January 2021).

5. Nørøxe, D.S.; Poulsen, H.S.; Lassen, U. Hallmarks of glioblastoma: A systematic review. *ESMO Open* **2016**, *1*, e000144. [[CrossRef](#)] [[PubMed](#)]
6. McLendon, R.; Friedman, A.; Bigner, D.; Van Meir, E.G.; Brat, D.J.; Mastrogianakis, G.M.; Olson, J.J.; Mikkelsen, T.; Lehman, N.; Aldape, K.; et al. Comprehensive genomic characterization defines human glioblastoma genes and core pathways. *Nature* **2008**, *455*, 1061–1068. [[CrossRef](#)]
7. Verhaak, R.G.W.; Hoadley, K.A.; Purdom, E.; Wang, V.; Qi, Y.; Wilkerson, M.D.; Miller, C.R.; Ding, L.; Golub, T.; Mesirov, J.P.; et al. Cancer Genome Atlas Research Network Integrated genomic analysis identifies clinically relevant subtypes of glioblastoma characterized by abnormalities in PDGFRA, IDH1, EGFR, and NF1. *Cancer Cell* **2010**, *17*, 98–110. [[CrossRef](#)]
8. Phillips, H.S.; Kharbanda, S.; Chen, R.; Forrester, W.F.; Soriano, R.H.; Wu, T.D.; Misra, A.; Nigro, J.M.; Colman, H.; Soroceanu, L.; et al. Molecular subclasses of high-grade glioma predict prognosis, delineate a pattern of disease progression, and resemble stages in neurogenesis. *Cancer Cell* **2006**, *9*, 157–173. [[CrossRef](#)]
9. Monteiro, A.R.; Hill, R.; Pilkington, G.J.; Madureira, P.A. The Role of Hypoxia in Glioblastoma Invasion. *Cells* **2017**, *6*, 45. [[CrossRef](#)]
10. Brennan, C.W.; Verhaak, R.G.W.; McKenna, A.; Campos, B.; Nounshmehr, H.; Salama, S.R.; Zheng, S.; Chakravarty, D.; Sanborn, J.Z.; Berman, S.H.; et al. The somatic genomic landscape of glioblastoma. *Cell* **2013**, *155*, 462–477. [[CrossRef](#)]
11. Nounshmehr, H.; Weisenberger, D.J.; Diefes, K.; Phillips, H.S.; Pujara, K.; Berman, B.P.; Pan, F.; Pelloski, C.E.; Sulman, E.P.; Bhat, K.P.; et al. Cancer Genome Atlas Research Network Identification of a CpG island methylator phenotype that defines a distinct subgroup of glioma. *Cancer Cell* **2010**, *17*, 510–522. [[CrossRef](#)]
12. Stupp, R.; Mason, W.P.; van den Bent, M.J.; Weller, M.; Fisher, B.; Taphoorn, M.J.B.; Belanger, K.; Brandes, A.A.; Marosi, C.; Bogdahn, U.; et al. European Organisation for Research and Treatment of Cancer Brain Tumor and Radiotherapy Groups; National Cancer Institute of Canada Clinical Trials Group Radiotherapy plus concomitant and adjuvant temozolomide for glioblastoma. *N. Engl. J. Med.* **2005**, *352*, 987–996. [[CrossRef](#)] [[PubMed](#)]
13. Birzu, C.; French, P.; Caccese, M.; Cerretti, G.; Idbaih, A.; Zagonel, V.; Lombardi, G. Recurrent Glioblastoma: From Molecular Landscape to New Treatment Perspectives. *Cancers* **2020**, *13*, 47. [[CrossRef](#)] [[PubMed](#)]
14. Yu, W.; Zhang, L.; Wei, Q.; Shao, A. O6-Methylguanine-DNA Methyltransferase (MGMT): Challenges and New Opportunities in Glioma Chemotherapy. *Front. Oncol.* **2020**, *9*, 1547. [[CrossRef](#)] [[PubMed](#)]
15. Rajaratnam, V.; Islam, M.M.; Yang, M.; Slaby, R.; Ramirez, H.M.; Mirza, S.P. Glioblastoma: Pathogenesis and current status of chemotherapy and other novel treatments. *Cancers* **2020**, *12*, 937. [[CrossRef](#)]
16. Yang, L.; Lin, C.; Wang, L.; Guo, H.; Wang, X. Hypoxia and hypoxia-inducible factors in glioblastoma multiforme progression and therapeutic implications. *Exp. Cell Res.* **2012**, *318*, 2417–2426. [[CrossRef](#)]
17. Kaur, B.; Khwaja, F.W.; Severson, E.A.; Matheny, S.L.; Brat, D.J.; Van Meir, E.G. Hypoxia and the hypoxia-inducible-factor pathway in glioma growth and angiogenesis. *Neuro-Oncology* **2005**, *7*, 134–153. [[CrossRef](#)]
18. Clara, C.A.; Marie, S.K.N.; de Almeida, J.R.W.; Wakamatsu, A.; Oba-Shinjo, S.M.; Uno, M.; Neville, M.; Rosemberg, S. Angiogenesis and expression of PDGF-C, VEGF, CD105 and HIF-1 α in human glioblastoma. *Neuropathology* **2014**, *34*, 343–352. [[CrossRef](#)]
19. Jensen, R.L.; Mumert, M.L.; Gillespie, D.L.; Kinney, A.Y.; Schabel, M.C.; Salzman, K.L. Preoperative dynamic contrast-enhanced MRI correlates with molecular markers of hypoxia and vascularity in specific areas of intratumoral microenvironment and is predictive of patient outcome. *Neuro-Oncology* **2014**, *16*, 280–291. [[CrossRef](#)]
20. Kaplan, Y.S. Basic principles in radiation oncology. *Cancer* **1977**, *39* (Suppl. 2), 689–693. [[CrossRef](#)]
21. Santivasi, W.L.; Xia, F. Ionizing Radiation-Induced DNA Damage, Response, and Repair. *Antioxid. Redox Signal.* **2014**, *21*, 251–259. [[CrossRef](#)]
22. Nickoloff, J.A.; Sharma, N.; Taylor, L. Clustered DNA Double-Strand Breaks: Biological Effects and Relevance to Cancer Radiotherapy. *Genes* **2020**, *15*, 99. [[CrossRef](#)] [[PubMed](#)]
23. Le Caë, S. Water Radiolysis: Influence of Oxide Surfaces on H₂ Production under Ionizing Radiation. *Water* **2011**, *3*, 235–253. [[CrossRef](#)]
24. Chatterjee, N.; Walker, G.C. Mechanisms of DNA damage, repair and mutagenesis. *Environ. Mol. Mutagen.* **2017**, *58*, 235–263. [[CrossRef](#)] [[PubMed](#)]
25. Hill, R.; Leidal, A.M.; Madureira, P.A.; Gillis, L.D.; Waisman, D.M.; Chiu, A.; Lee, P.W.K. Chromium-mediated apoptosis: Involvement of DNA-dependent protein kinase (DNA-PK) and differential induction of p53 target genes. *DNA Repair* **2008**, *7*, 1484–1499. [[CrossRef](#)] [[PubMed](#)]
26. Rycaj, K.; Tang, D.G. Cancer stem cells and radioresistance. *Int. J. Radiat. Biol.* **2014**, *90*, 615–621. [[CrossRef](#)] [[PubMed](#)]
27. Jordan, B.F.; Sonveaux, P. Targeting tumor perfusion and oxygenation to improve the outcome of anticancer therapy. *Front. Pharmacol.* **2012**, *3*, 94. [[CrossRef](#)] [[PubMed](#)]
28. Pawlik, T.M.; Keyomarsi, K. Role of cell cycle in mediating sensitivity to radiotherapy. *Int. J. Radiat. Oncol. Biol. Phys.* **2004**, *59*, 928–942. [[CrossRef](#)]
29. Bar, E.E.; Lin, A.; Mahairaki, V.; Matsui, W.; Eberhart, C.G. Hypoxia increases the expression of stem-cell markers and promotes clonogenicity in glioblastoma neurospheres. *Am. J. Pathol.* **2010**, *177*, 1491–1502. [[CrossRef](#)]
30. Winkler, F.; Kozin, S.V.; Tong, R.T.; Chae, S.-S.; Booth, M.F.; Garkavtsev, I.; Xu, L.; Hicklin, D.J.; Fukumura, D.; di Tomaso, E.; et al. Kinetics of vascular normalization by VEGFR2 blockade governs brain tumor response to radiation: Role of oxygenation, angiopoietin-1, and matrix metalloproteinases. *Cancer Cell* **2004**, *6*, 553–563. [[CrossRef](#)]




31. Yuan, F.; Salehi, H.A.; Boucher, Y.; Vasthare, U.S.; Tuma, R.F.; Jain, R.K. Vascular permeability and microcirculation of gliomas and mammary carcinomas transplanted in rat and mouse cranial windows. *Cancer Res.* **1994**, *54*, 4564–4568.
32. Plate, K.H.; Mennel, H.D. Vascular morphology and angiogenesis in glial tumors. *Exp. Toxicol. Pathol.* **1995**, *47*, 89–94. [[CrossRef](#)]
33. Bullitt, E.; Zeng, D.; Gerig, G.; Aylward, S.; Joshi, S.; Smith, J.K.; Lin, W.; Ewend, M.G. Vessel tortuosity and brain tumor malignancy: A blinded study. *Acad. Radiol.* **2005**, *12*, 1232–1240. [[CrossRef](#)] [[PubMed](#)]
34. Rong, Y.; Durden, D.L.; Van Meir, E.G.; Brat, D.J. “Pseudopalisading” necrosis in glioblastoma: A familial morphologic feature that links vascular pathology, hypoxia, and angiogenesis. *J. Neuropathol. Exp. Neurol.* **2006**, *65*, 529–539. [[CrossRef](#)] [[PubMed](#)]
35. Jain, R.K.; di Tomaso, E.; Duda, D.G.; Loeffler, J.S.; Sorensen, A.G.; Batchelor, T.T. Angiogenesis in brain tumours. *Nat. Rev. Neurosci.* **2007**, *8*, 610–622. [[CrossRef](#)] [[PubMed](#)]
36. Saxena, K.; Jolly, M.K. Acute vs. Chronic vs. cyclic hypoxia: Their differential dynamics, molecular mechanisms, and effects on tumor progression. *Biomolecules* **2019**, *9*, 339. [[CrossRef](#)]
37. Majmundar, A.J.; Wong, W.J.; Simon, M.C. Hypoxia-Inducible Factors and the Response to Hypoxic Stress. *Mol. Cell* **2010**, *40*, 294–309. [[CrossRef](#)]
38. Keith, B.; Johnson, R.S.; Simon, M.C. HIF1 α and HIF2 α : Sibling rivalry in hypoxic tumour growth and progression. *Nat. Rev. Cancer* **2011**, *12*, 9–22. [[CrossRef](#)]
39. Huang, L.E.; Bunn, H.F. Hypoxia-inducible factor and its biomedical relevance. *J. Biol. Chem.* **2003**, *278*, 19575–19578. [[CrossRef](#)]
40. Schofield, C.J.; Ratcliffe, P.J. Oxygen sensing by HIF hydroxylases. *Nat. Rev. Mol. Cell Biol.* **2004**, *5*, 343–354. [[CrossRef](#)]
41. Semenza, G.L. Regulation of mammalian O₂ homeostasis by hypoxia-inducible factor 1. *Annu. Rev. Cell Dev. Biol.* **1999**, *15*, 551–578. [[CrossRef](#)]
42. Duan, C. Hypoxia-inducible factor 3 biology: Complexities and emerging themes. *Am. J. Physiol. Cell Physiol.* **2016**, *310*, C260–C269. [[CrossRef](#)] [[PubMed](#)]
43. Cockman, M.E.; Masson, N.; Mole, D.R.; Jaakkola, P.; Chang, G.-W.; Clifford, S.C.; Maher, E.R.; Pugh, C.W.; Ratcliffe, P.J.; Maxwell, P.H. Hypoxia Inducible Factor- α Binding and Ubiquitylation by the von Hippel-Lindau Tumor Suppressor Protein. *J. Biol. Chem.* **2000**, *275*, 25733–25741. [[CrossRef](#)] [[PubMed](#)]
44. Maxwell, P.H.; Wiesener, M.S.; Chang, G.W.; Clifford, S.C.; Vaux, E.C.; Cockman, M.E.; Wyckoff, C.C.; Pugh, C.W.; Maher, E.R.; Ratcliffe, P.J. The tumour suppressor protein VHL targets hypoxia-inducible factors for oxygen-dependent proteolysis. *Nature* **1999**, *399*, 271–275. [[CrossRef](#)] [[PubMed](#)]
45. Srinivas, V.; Zhang, L.P.; Zhu, X.H.; Caro, J. Characterization of an oxygen/redox-dependent degradation domain of hypoxia-inducible factor alpha (HIF-alpha) proteins. *Biochem. Biophys. Res. Commun.* **1999**, *260*, 557–561. [[CrossRef](#)]
46. Ebert, B.L.; Bunn, H.F. Regulation of transcription by hypoxia requires a multiprotein complex that includes hypoxia-inducible factor 1, an adjacent transcription factor, and p300/CREB binding protein. *Mol. Cell. Biol.* **1998**, *18*, 4089–4096. [[CrossRef](#)]
47. Huang, L.E.; Arany, Z.; Livingston, D.M.; Bunn, H.F. Activation of hypoxia-inducible transcription factor depends primarily upon redox-sensitive stabilization of its alpha subunit. *J. Biol. Chem.* **1996**, *271*, 32253–32259. [[CrossRef](#)]
48. Kallio, P.J.; Pongratz, I.; Gradin, K.; McGuire, J.; Poellinger, L. Activation of hypoxia-inducible factor 1alpha: Posttranscriptional regulation and conformational change by recruitment of the Arnt transcription factor. *Proc. Natl. Acad. Sci. USA* **1997**, *94*, 5667–5672. [[CrossRef](#)]
49. Mahon, P.C.; Hirota, K.; Semenza, G.L. FIH-1: A novel protein that interacts with HIF-1alpha and VHL to mediate repression of HIF-1 transcriptional activity. *Genes Dev.* **2001**, *15*, 2675–2686. [[CrossRef](#)]
50. Lando, D.; Peet, D.J.; Gorman, J.J.; Whelan, D.A.; Whitelaw, M.L.; Bruick, R.K. FIH-1 is an asparaginyl hydroxylase enzyme that regulates the transcriptional activity of hypoxia-inducible factor. *Genes Dev.* **2002**, *16*, 1466–1471. [[CrossRef](#)]
51. Zhang, P.; Yao, Q.; Lu, L.; Li, Y.; Chen, P.-J.; Duan, C. Hypoxia-inducible factor 3 is an oxygen-dependent transcription activator and regulates a distinct transcriptional response to hypoxia. *Cell Rep.* **2014**, *6*, 1110–1121. [[CrossRef](#)]
52. Frederick, L.; Wang, X.Y.; Eley, G.; James, C.D. Diversity and frequency of epidermal growth factor receptor mutations in human glioblastomas. *Cancer Res.* **2000**, *60*, 1383–1387. [[PubMed](#)]
53. Sansal, I.; Sellers, W.R. The biology and clinical relevance of the PTEN tumor suppressor pathway. *J. Clin. Oncol.* **2004**, *22*, 2954–2963. [[CrossRef](#)] [[PubMed](#)]
54. Ravi, R.; Mookerjee, B.; Bhujwala, Z.M.; Sutter, C.H.; Artemov, D.; Zeng, Q.; Dillehay, L.E.; Madan, A.; Semenza, G.L.; Bedi, A. Regulation of tumor angiogenesis by p53-induced degradation of hypoxia-inducible factor 1alpha. *Genes Dev.* **2000**, *14*, 34–44. [[PubMed](#)]
55. Holland, E.C.; Hively, W.P.; DePinho, R.A.; Varmus, H.E. A constitutively active epidermal growth factor receptor cooperates with disruption of G1 cell-cycle arrest pathways to induce glioma-like lesions in mice. *Genes Dev.* **1998**, *12*, 3675–3685. [[CrossRef](#)]
56. Clarke, K.; Smith, K.; Gullick, W.J.; Harris, A.L. Mutant epidermal growth factor receptor enhances induction of vascular endothelial growth factor by hypoxia and insulin-like growth factor-1 via a PI3 kinase dependent pathway. *Br. J. Cancer* **2001**, *84*, 1322–1329. [[CrossRef](#)]
57. Zhong, H.; Chiles, K.; Feldser, D.; Laughner, E.; Hanrahan, C.; Georgescu, M.M.; Simons, J.W.; Semenza, G.L. Modulation of hypoxia-inducible factor 1alpha expression by the epidermal growth factor/phosphatidylinositol 3-kinase/PTEN/AKT/FRAP pathway in human prostate cancer cells: Implications for tumor angiogenesis and therapeutics. *Cancer Res.* **2000**, *60*, 1541–1545.
58. Castaldo, S.A.; Freitas, J.R.; Conchinha, N.V.; Madureira, P.A. The Tumorigenic Roles of the Cellular REDOX Regulatory Systems. *Oxid. Med. Cell. Longev.* **2016**, *2016*, 8413032. [[CrossRef](#)]

59. Chédeville, A.L.; Lourdasamy, A.; Monteiro, A.R.; Hill, R.; Madureira, P.A. Investigating glioblastoma response to hypoxia. *Biomedicines* **2020**, *8*, 310. [[CrossRef](#)]
60. Sanzey, M.; Abdul Rahim, S.A.; Oudin, A.; Dirkse, A.; Kaoma, T.; Vallar, L.; Herold-Mende, C.; Bjerkvig, R.; Golebiewska, A.; Niclou, S.P. Comprehensive analysis of glycolytic enzymes as therapeutic targets in the treatment of glioblastoma. *PLoS ONE* **2015**, *10*, e0123544. [[CrossRef](#)]
61. Plate, K.H.; Breier, G.; Weich, H.A.; Risau, W. Vascular endothelial growth factor is a potential tumour angiogenesis factor in human gliomas in vivo. *Nature* **1992**, *359*, 845–848. [[CrossRef](#)]
62. Shweiki, D.; Itin, A.; Soffer, D.; Keshet, E. Vascular endothelial growth factor induced by hypoxia may mediate hypoxia-initiated angiogenesis. *Nature* **1992**, *359*, 843–845. [[CrossRef](#)]
63. Arai, Y.; Kubota, T.; Nakagawa, T.; Kabuto, M.; Sato, K.; Kobayashi, H. Production of urokinase-type plasminogen activator (u-PA) and plasminogen activator inhibitor-1 (PAI-1) in human brain tumours. *Acta Neurochir.* **1998**, *140*, 377–386. [[CrossRef](#)] [[PubMed](#)]
64. Kubala, M.H.; DeClerck, Y.A. The plasminogen activator inhibitor-1 paradox in cancer: A mechanistic understanding. *Cancer Metastasis Rev.* **2019**, *38*, 483–492. [[CrossRef](#)] [[PubMed](#)]
65. Madureira, P.A.; Surette, A.P.; Phipps, K.D.; Taboski, M.A.S.; Miller, V.A.; Waisman, D.M. The role of the annexin A2 heterotetramer in vascular fibrinolysis. *Blood* **2011**, *118*, 4789–4797. [[CrossRef](#)] [[PubMed](#)]
66. Madureira, P.A.; O’Connell, P.A.; Surette, A.P.; Miller, V.A.; Waisman, D.M. The biochemistry and regulation of S100A10: A multifunctional plasminogen receptor involved in oncogenesis. *J. Biomed. Biotechnol.* **2012**, *2012*, 353687. [[CrossRef](#)] [[PubMed](#)]
67. Mongiardi, M.P.; Savino, M.; Falchetti, M.L.; Illi, B.; Bozzo, F.; Valle, C.; Helmer-Citterich, M.; Ferrè, F.; Nasi, S.; Levi, A. c-MYC inhibition impairs hypoxia response in glioblastoma multiforme. *Oncotarget* **2016**, *7*, 33257–33271. [[CrossRef](#)]
68. Hu, Y.L.; DeLay, M.; Jahangiri, A.; Molinaro, A.M.; Rose, S.D.; Carbonell, W.S.; Aghi, M.K. Hypoxia-induced autophagy promotes tumor cell survival and adaptation to antiangiogenic treatment in glioblastoma. *Cancer Res.* **2012**, *72*, 1773–1783. [[CrossRef](#)]
69. Tsai, Y.-T.; Wu, A.-C.; Yang, W.-B.; Kao, T.-J.; Chuang, J.-Y.; Chang, W.-C.; Hsu, T.-I. ANGPTL4 Induces TMZ Resistance of Glioblastoma by Promoting Cancer Stemness Enrichment via the EGFR/AKT/4E-BP1 Cascade. *Int. J. Mol. Sci.* **2019**, *20*, 5625. [[CrossRef](#)]
70. Foltyn, M.; Luger, A.-L.; Lorenz, N.I.; Sauer, B.; Mittelbronn, M.; Harter, P.N.; Steinbach, J.P.; Ronellenfitsch, M.W. The physiological mTOR complex 1 inhibitor DDIT4 mediates therapy resistance in glioblastoma. *Br. J. Cancer* **2019**, *120*, 481–487. [[CrossRef](#)]
71. Said, H.M.; Stein, S.; Hagemann, C.; Polat, B.; Staab, A.; Anacker, J.; Schoemig, B.; Theobald, M.; Flentje, M.; Vordermark, D. Oxygen-dependent regulation of NDRG1 in human glioblastoma cells in vitro and in vivo. *Oncol. Rep.* **2009**, *21*, 237–246. [[CrossRef](#)]
72. Said, H.M.; Safari, R.; Al-Kafaji, G.; Ernestus, R.I.; Löhr, M.; Katzer, A.; Flentje, M.; Hagemann, C. Time- and oxygen-dependent expression and regulation of NDRG1 in human brain cancer cells. *Oncol. Rep.* **2017**, *37*, 3625–3634. [[CrossRef](#)] [[PubMed](#)]
73. Weiler, M.; Blaes, J.; Pusch, S.; Sahm, F.; Czabanka, M.; Luger, S.; Bunse, L.; Solecki, G.; Eichwald, V.; Jugold, M.; et al. mTOR target NDRG1 confers MGMT-dependent resistance to alkylating chemotherapy. *Proc. Natl. Acad. Sci. USA* **2014**, *111*, 409–414. [[CrossRef](#)] [[PubMed](#)]
74. Luo, W.; Wang, Y. Hypoxia mediates tumor malignancy and therapy resistance. In *Advances in Experimental Medicine and Biology*; Springer: New York, NY, USA, 2019; Volume 1136, pp. 1–18.
75. Marampon, F.; Gravina, G.L.; Zani, B.M.; Popov, V.M.; Fratticci, A.; Cerasani, M.; Di Genova, D.; Mancini, M.; Ciccarelli, C.; Ficorella, C.; et al. Hypoxia sustains glioblastoma radioresistance through ERKs/DNA-PKcs/HIF-1 α functional interplay. *Int. J. Oncol.* **2014**, *45*, 2121–2131. [[CrossRef](#)] [[PubMed](#)]
76. Gouazé-Andersson, V.; Delmas, C.; Taurand, M.; Martinez-Gala, J.; Ene Evrard, S.; Mazoyer, S.; Toulas, C.; Cohen-Jonathan-Moyal, E. Therapeutics, Targets, and Chemical Biology FGFR1 Induces Glioblastoma Radioresistance through the PLCg/Hif1 α Pathway. *Cancer Res.* **2016**, *76*, 3036–3044. [[CrossRef](#)]
77. De Young, M.P.; Horak, P.; Sofer, A.; Sgroi, D.; Ellisen, L.W. Hypoxia regulates TSC1/2-mTOR signaling and tumor suppression through REDD1-mediated 14-3-3 shuttling. *Genes Dev.* **2008**, *22*, 239–251. [[CrossRef](#)]
78. Pinto, J.A.; Rolfo, C.; Raez, L.E.; Prado, A.; Araujo, J.M.; Bravo, L.; Fajardo, W.; Morante, Z.D.; Aguilar, A.; Neciosup, S.P.; et al. In silico evaluation of DNA Damage Inducible Transcript 4 gene (DDIT4) as prognostic biomarker in several malignancies. *Sci. Rep.* **2017**, *7*, 1526. [[CrossRef](#)]
79. Richter, J.D.; Sonenberg, N. Regulation of cap-dependent translation by eIF4E inhibitory proteins. *Nature* **2005**, *433*, 477–480. [[CrossRef](#)]
80. Dubois, L.; Magagnin, M.G.; Cleven, A.H.G.; Weppler, S.A.; Grenacher, B.; Landuyt, W.; Lieuwes, N.; Lambin, P.; Gorr, T.A.; Koritzinsky, M.; et al. Inhibition of 4E-BP1 Sensitizes U87 Glioblastoma Xenograft Tumors to Irradiation by Decreasing Hypoxia Tolerance. *Int. J. Radiat. Oncol. Biol. Phys.* **2009**, *73*, 1219–1227. [[CrossRef](#)]
81. Yue, X.; Lan, F.; Xia, T. Hypoxic Glioma Cell-Secreted Exosomal miR-301a Activates Wnt/ β -catenin Signaling and Promotes Radiation Resistance by Targeting TCEAL7. *Mol. Ther.* **2019**, *27*, 1939–1949. [[CrossRef](#)]
82. Shen, H.; Hau, E.; Joshi, S.; Dilda, P.J.; McDonald, K.L. Sensitization of Glioblastoma Cells to Irradiation by Modulating the Glucose Metabolism. *Mol. Cancer Ther.* **2015**, *14*, 1794–1804. [[CrossRef](#)]

83. Castaldo, S.A.; Ajime, T.; Serrão, G.; Anastácio, F.; Rosa, J.T.; Giacomantonio, C.A.; Howarth, A.; Hill, R.; Madureira, P.A. Annexin A2 regulates akt upon h2o2-dependent signaling activation in cancer cells. *Cancers* **2019**, *11*, 492. [[CrossRef](#)] [[PubMed](#)]
84. Matschke, J.; Riffkin, H.; Klein, D.; Handrick, R.; Lüdemann, L.; Metzen, E.; Shlomi, T.; Stuschke, M.; Jendrossek, V. Targeted Inhibition of Glutamine-Dependent Glutathione Metabolism Overcomes Death Resistance Induced by Chronic Cycling Hypoxia. *Antioxid. Redox Signal.* **2016**, *25*, 89–107. [[CrossRef](#)] [[PubMed](#)]
85. Hlouschek, J.; Hansel, C.; Jendrossek, V.; Matschke, J. The mitochondrial citrate carrier (SLC25A1) sustains redox homeostasis and mitochondrial metabolism supporting radioresistance of cancer cells with tolerance to cycling severe hypoxia. *Front. Oncol.* **2018**, *8*, 170. [[CrossRef](#)] [[PubMed](#)]
86. Peng, R.; Zhang, M.; Wang, H.; Lin, J.; Wang, H.; Wang, F.; Liu, L.; Zhao, Q.; Liu, J. Advances into Understanding the Vital Role of the Mitochondrial Citrate Carrier (CIC) in Metabolic Diseases. *Pharmacol. Res.* **2020**, *161*, 105132. [[CrossRef](#)] [[PubMed](#)]
87. Catalina-Rodriguez, O.; Kolukula, V.K.; Tomita, Y.; Preet, A.; Palmieri, F.; Wellstein, A.; Byers, S.; Giaccia, A.J.; Glasgow, E.; Albanese, C.; et al. The mitochondrial citrate transporter, CIC, is essential for mitochondrial homeostasis. *Oncotarget* **2012**, *3*, 1220–1235. [[CrossRef](#)] [[PubMed](#)]
88. Hsieh, C.H.; Wu, C.P.; Lee, H.T.; Liang, J.A.; Yu, C.Y.; Lin, Y.J. NADPH oxidase subunit 4 mediates cycling hypoxia-promoted radiation resistance in glioblastoma multiforme. *Free Radic. Biol. Med.* **2012**, *53*, 649–658. [[CrossRef](#)]
89. Hsieh, C.H.; Lee, C.H.; Liang, J.A.; Yu, C.Y.; Shyu, W.C. Cycling hypoxia increases U87 glioma cell radioresistance via ROS induced higher and long-term HIF-1 signal transduction activity. *Oncol. Rep.* **2010**, *24*, 1629–1636. [[CrossRef](#)]
90. Bonnet, D.; Dick, J.E. Human acute myeloid leukemia is organized as a hierarchy that originates from a primitive hematopoietic cell. *Nat. Med.* **1997**, *3*, 730–737. [[CrossRef](#)]
91. Crowder, S.W.; Balikov, D.A.; Hwang, Y.-S.; Sung, H.-J. Cancer Stem Cells Under Hypoxia as a Chemoresistance Factor in the Breast and Brain. *Curr. Pathobiol. Rep.* **2014**, *2*, 33–40. [[CrossRef](#)]
92. Jordan, C.T.; Guzman, M.L.; Noble, M. Cancer Stem Cells. *N. Engl. J. Med.* **2006**, *355*, 1253–1261. [[CrossRef](#)]
93. Fidoamore, A.; Cristiano, L.; Antonosante, A.; D’Angelo, M.; Di Giacomo, E.; Astarita, C.; Giordano, A.; Ippoliti, R.; Benedetti, E.; Cimini, A. Glioblastoma Stem Cells Microenvironment: The Paracrine Roles of the Niche in Drug and Radioresistance. *Stem Cells Int.* **2016**, *2016*, 1–17. [[CrossRef](#)] [[PubMed](#)]
94. Kolenda, J.; Jensen, S.S.; Aaberg-Jessen, C.; Christensen, K.; Andersen, C.; Brüner, N.; Kristensen, B.W. Effects of hypoxia on expression of a panel of stem cell and chemoresistance markers in glioblastoma-derived spheroids. *J. Neurooncol.* **2011**, *103*, 43–58. [[CrossRef](#)] [[PubMed](#)]
95. Mathieu, J.; Zhang, Z.; Zhou, W.; Wang, A.J.; Heddleston, J.M.; Pinna, C.M.A.; Hubaud, A.; Stadler, B.; Choi, M.; Bar, M.; et al. HIF induces human embryonic stem cell markers in cancer cells. *Cancer Res.* **2011**, *71*, 4640–4652. [[CrossRef](#)] [[PubMed](#)]
96. Seidel, S.; Garvalov, B.K.; Wirta, V.; Von Stechow, L.; Schänzer, A.; Meletis, K.; Wolter, M.; Sommerlad, D.; Henze, A.T.; Nistér, M.; et al. A hypoxic niche regulates glioblastoma stem cells through hypoxia inducible factor 2 α . *Brain* **2010**, *133*, 983–995. [[CrossRef](#)] [[PubMed](#)]
97. Méndez, O.; Zavadil, J.; Esencay, M.; Lukyanov, Y.; Santovasi, D.; Wang, S.-C.C.; Newcomb, E.W.; Zagzag, D. Knock down of HIF-1 α in glioma cells reduces migration in vitro and invasion in vivo and impairs their ability to form tumor spheres. *Mol. Cancer* **2010**, *9*, 133. [[CrossRef](#)]
98. Heddleston, J.M.; Wu, Q.; Rivera, M.; Minhas, S.; Lathia, J.D.; Sloan, A.E.; Iliopoulos, O.; Hjelmeland, A.B.; Rich, J.N. Hypoxia-induced mixed-lineage leukemia 1 regulates glioma stem cell tumorigenic potential. *Cell Death Differ.* **2012**, *19*, 428–439. [[CrossRef](#)]
99. Bao, S.; Wu, Q.; McLendon, R.E.; Hao, Y.; Shi, Q.; Hjelmeland, A.B.; Dewhirst, M.W.; Bigner, D.D.; Rich, J.N. Glioma stem cells promote radioresistance by preferential activation of the DNA damage response. *Nature* **2006**, *444*, 756–760. [[CrossRef](#)]
100. Rankin, E.B.; Giaccia, A.J. The role of hypoxia-inducible factors in tumorigenesis. *Cell Death Differ.* **2008**, *15*, 678–685. [[CrossRef](#)]
101. Dahan, P.; Martinez Gala, J.; Delmas, C.; Monferran, S.; Malric, L.; Zentkowski, D.; Lubrano, V.; Toulas, C.; Cohen-Jonathan Moyal, E.; Lemarie, A. Ionizing radiations sustain glioblastoma cell dedifferentiation to a stem-like phenotype through survivin: Possible involvement in radioresistance. *Cell Death Dis.* **2014**, *5*, e1543. [[CrossRef](#)]
102. Bindra, R.S.; Chalmers, A.J.; Evans, S.; Dewhirst, M. GBM radiosensitizers: Dead in the water ... or just the beginning? *J. Neurooncol.* **2017**, *134*, 513–521. [[CrossRef](#)]

Review

Tumor Microenvironment as a Regulator of Radiation Therapy: New Insights into Stromal-Mediated Radioresistance

Varintra E. Krisnawan ^{1,2} , Jennifer A. Stanley ^{3,4}, Julie K. Schwarz ^{3,4,5}  and David G. DeNardo ^{1,2,4,*} 

¹ Department of Medicine, Washington University School of Medicine, St. Louis, MO 63110, USA; varintra@wustl.edu

² Department of Pathology and Immunology, Washington University School of Medicine, St. Louis, MO 63110, USA

³ Department of Radiation Oncology, Washington University School of Medicine, St. Louis, MO 63110, USA; jastanley@wustl.edu (J.A.S.); jschwarz@wustl.edu (J.K.S.)

⁴ Siteman Cancer Center, Washington University School of Medicine, St. Louis, MO 63110, USA

⁵ Department of Cell Biology and Physiology, Washington University School of Medicine, St. Louis, MO 63110, USA

* Correspondence: ddenardo@wustl.edu

Received: 21 September 2020; Accepted: 9 October 2020; Published: 11 October 2020



Simple Summary: Cancer is multifaceted and consists of more than just a collection of mutated cells. These cancerous cells reside along with other non-mutated cells in an extracellular matrix which together make up the tumor microenvironment or tumor stroma. The composition of the tumor microenvironment plays an integral role in cancer initiation, progression, and response to treatments. In this review, we discuss how the tumor microenvironment regulates the response and resistance to radiation therapy and what targeted agents have been used to combat stromal-mediated radiation resistance.

Abstract: A tumor is a complex “organ” composed of malignant cancer cells harboring genetic aberrations surrounded by a stroma comprised of non-malignant cells and an extracellular matrix. Considerable evidence has demonstrated that components of the genetically “normal” tumor stroma contribute to tumor progression and resistance to a wide array of treatment modalities, including radiotherapy. Cancer-associated fibroblasts can promote radioresistance through their secreted factors, contact-mediated signaling, downstream pro-survival signaling pathways, immunomodulatory effects, and cancer stem cell-generating role. The extracellular matrix can govern radiation responsiveness by influencing oxygen availability and controlling the stability and bioavailability of growth factors and cytokines. Immune status regarding the presence of pro- and anti-tumor immune cells can regulate how tumors respond to radiation therapy. Furthermore, stromal cells including endothelial cells and adipocytes can modulate radiosensitivity through their roles in angiogenesis and vasculogenesis, and their secreted adipokines, respectively. Thus, to successfully eradicate cancers, it is important to consider how tumor stroma components interact with and regulate the response to radiation. Detailed knowledge of these interactions will help build a preclinical rationale to support the use of stromal-targeting agents in combination with radiotherapy to increase radiosensitivity.

Keywords: stroma; cancer-associated fibroblast (CAF); extracellular matrix (ECM); cytokine/chemokine; growth factors; pro- and anti-tumor immune cells; immunomodulatory roles; radiotherapy dose fractionation; radioresistance; radiosensitivity

1. Introduction

The field of oncology has evolved from a malignant mutated cancer cell-centered view to the understanding of cancer as a complex “organ” composed of both malignant cells and diverse nonmalignant cellular and non-cellular components termed the tumor stroma or tumor microenvironment (TME) [1–5]. The concept of cancer as a disease focusing only on malignant tumor cells has been deemed inaccurate; in some cancers, stromal cells represent the majority of cell types, as is frequently seen in pancreatic and breast cancers [6]. These cellular stromal components often include activated cancer-associated fibroblasts (CAFs), leukocytes, and vascular cells, but they also sometimes include other adjacent normal tissue/cells such as non-transformed epithelia, adipose tissue, or neurons [1–5]. The non-cellular compartment of the tumor stroma comprises extracellular matrix (ECM) components like collagens, laminins, fibrinogen, elastin, and proteoglycan, and secreted factors such as cytokines, chemokines, and sequestered growth factors [1–11]. Accumulating evidence highly suggests that malignant cancer cells and the tumor stroma reciprocally communicate with and influence one another, but this relationship is complex and remains poorly understood. To treat cancer as a disease, we cannot single-mindedly focus on cancer cells with their autonomous genetic mutations; we need to simultaneously consider the TME because its interactions with tumor cells often contribute to disease initiation, progression, and treatment response [2–4,6,12].

Radiation therapy (RT) is a powerful anti-cancer therapeutic used to treat up to 50–60% of cancer patients [12,13]. The goal of RT is to target highly proliferative cancer cells while sparing normal tissue. The concept of dose fractionation—delivering small daily RT doses over several days—is designed to exploit cancer cells’ vulnerabilities in repairing DNA damage, leading to their demise, while giving normal healthy cells a chance to activate their DNA repair and cell cycle mechanisms [13–16]. Historically, radiobiology has utilized linear quadratic modeling to estimate the therapeutic treatment ratio, with increasing radiation toxicity to cancer cells while avoiding surrounding normal tissue. This “therapeutic ratio” is based on differences between the DNA damage and repair kinetics of cancer and normal cells. The linear-quadratic model utilizes the α and β parameters to describe the linear and quadratic portions of the cell survival curve, respectively, and experimental evidence suggests that these parameters and the $\alpha:\beta$ ratio differ widely across and even within some tumor types [17,18]. Classical modeling predicts that delivering small doses of radiation over the course of multiple treatments (i.e., conventional dose fractionation) can increase the therapeutic ratio compared to single-dose delivery, and early studies using small and large animal models confirmed these effects [17–19]. However, recent evidence has called into question whether small doses of radiation delivered over a protracted treatment course (conventional fractionation) are required to achieve these effects.

Standard of care for the majority of solid tumors requires 50 to 70 Gy total radiation dose delivered with conventionally fractionated schedules, most commonly utilizing 1.8 to 2 Gy per fraction. Over the past decade significant technologic advances in image-guided radiation, tumor tracking, beam intensity modulation, and beam shaping have facilitated the capacity to precisely deliver higher dose per fraction to the tumor while sparing larger volumes of surrounding normal structures. This concept of hypofractionation, or higher fractional doses of radiation over fewer total fractions and commonly delivered with stereotactic guidance via stereotactic body radiotherapy (SBRT) or stereotactic radiosurgery (SRS), has demonstrated safety and efficacy in many tumor types [20–23]. However, data also suggest that the clinical effects of hypofractionation are not solely due to differences in tumor and normal tissue DNA repair kinetics but also to the effects of radiotherapy on the TME. Although largely anecdotal, TME alterations can be demonstrated through the observation of “out-of-field” or abscopal responses to focused radiation as first described in the early 1950s [24]. Since then, additional work has demonstrated that the abscopal response is dependent on alterations in the immune system and the surrounding stromal tissue. Radiation can result in immune cell priming, neoantigen and cytokine release, modification of tumor vasculature, and alteration of the ECM, all of which have the potential to be optimized to enhance RT efficacy [25–29].

Despite RT designed to target malignant tumor cells, and the knowledge that RT can be used to prime the immune system, the complex interaction between malignant tumor cells and other cells within the TME is important because the stroma can impact malignant cells' response and contribute to treatment resistance [12]. Additionally, there are reports that RT can cause numerous changes in stromal cells within the TME that further promote undesirable tumor growth, invasion, and treatment resistance [12]. To successfully eradicate cancers, these reciprocal interactions between the tumor cells and tumor stroma must be characterized in detail. Moreover, the use of stromal-targeting agents in combination with RT is a largely unaddressed therapeutic option. These topics deserve more attention to broaden our knowledge to design better treatment strategies to combat cancers, particularly those characterized by a high density of stromal cells and other stromal components within the TME. In this review, we summarize the roles of stromal components and the TME that contribute to cancer cell radioresistance (Figure 1) and discuss how they may be targeted for possible therapeutic benefit (Figure 2).

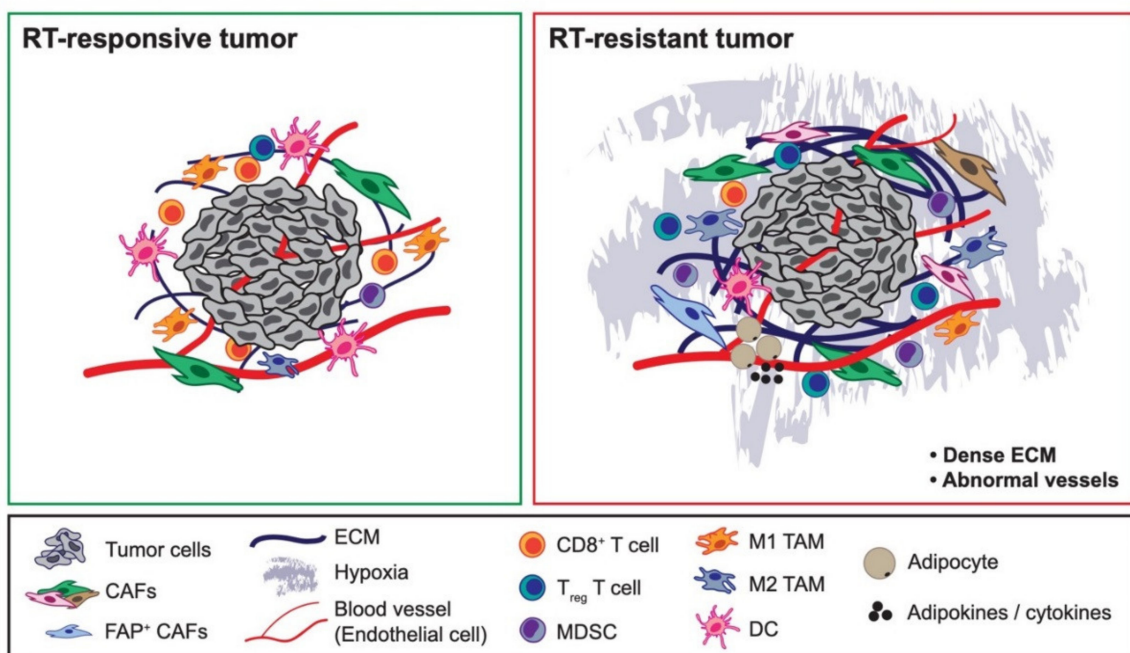


Figure 1. Components of the tumor microenvironment governing radiotherapy responsiveness. Components of the tumor stroma differentially dictate whether tumor cells are radiotherapy (RT)-responsive (Left) vs. RT-resistant (Right). Some tumor-promoting cancer-associated fibroblast (CAF) populations can cause tumors to be resistant to RT, such as fibroblast activated protein (FAP)⁺ CAFs. While immune cells such as CD8⁺ T cells, dendritic cells, and M1-like tumor-associated macrophages (TAMs) have been linked with RT-responsive tumors, pro-tumorigenic immune cells such as CD4⁺ T regulatory (T_{reg}) cells, myeloid-derived suppressor cells, and M2-like TAMs have been associated with RT-resistant tumors. Dense extracellular matrix and abnormal endothelial cells and vessel formation, which contribute to tumor hypoxia, have been associated with RT-resistant tumors. Likewise, adipokines secreted by cancer-associated adipocytes can similarly cause tumors to be resistant to RT.

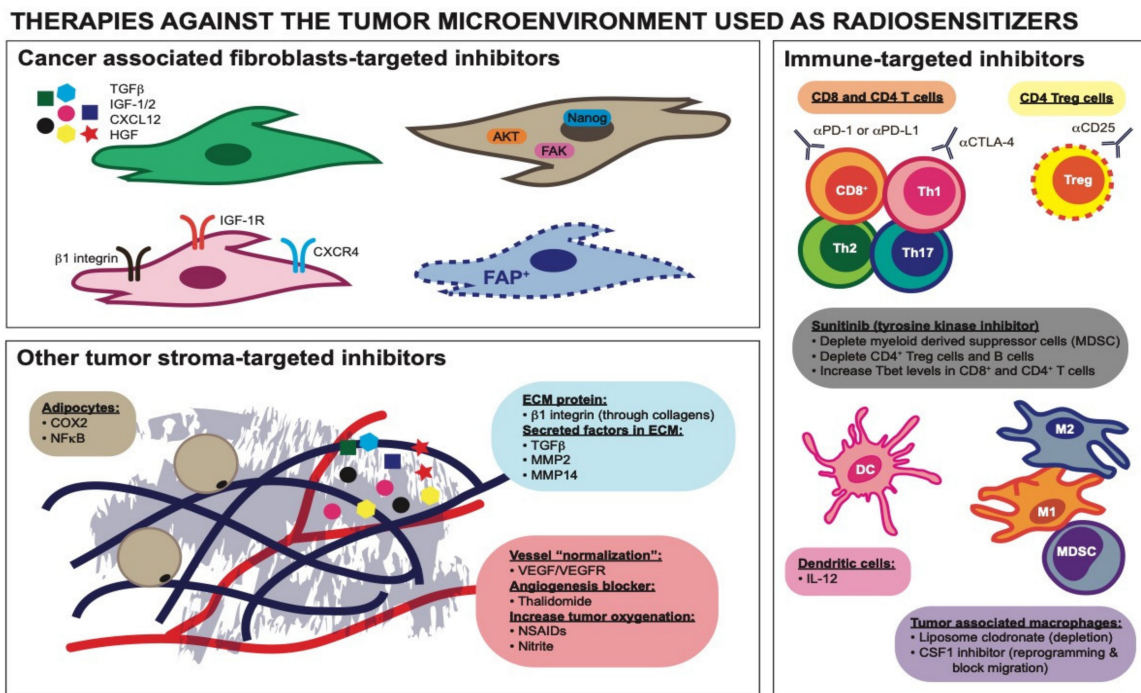


Figure 2. Therapies directed against distinct tumor stromal components used as radiosensitizers. Targeted inhibitors against CAFs' secretory molecules, CAFs' downstream cytosolic and nuclear signaling pathways, and CAFs' receptors can increase RT efficacy. Targeting a unique population of CAFs, FAP⁺ CAFs, specifically for depletion can also radiosensitize tumors. Components of the ECM can activate β1 integrin receptor on CAFs and targeting β1 integrin can reverse tumor radioresistance. Targeted inhibitors against secreted factors reserved in the ECM have been shown to be radiosensitizing agents. "Normalizing" tumor vessels using VEGF/VEGFR inhibitors and Thalidomide can reverse tumor radioresistance. NSAIDs and nitrite have also been used as radiosensitizers due to their ability to increase tumor oxygenation. Inhibitors of COX-2 and NFκB targeted against cancer-associated adipocytes can reverse the radioresistance in tumors. Immune checkpoint inhibitors (αPD-1 or αPD-L1 and αCTLA-4 antibodies) can rescue "dysfunctional" CD8⁺ and/or CD4⁺ T cells and are beneficial when combined with RT. Depletion antibody αCD25 targeted against CD4⁺ T regulatory cells (T_{regs}) can render tumor cells more radiosensitive. Interleukin-12 capable of enhancing the function of dendritic cells can increase the efficacy of RT. TAMs depletion agent, liposome clodronate, and CSF1 inhibitor can increase RT sensitivity. CSF1 inhibitor can also reprogram/polarize TAMs into having a more anti-tumorigenic phenotype. The tyrosine kinase inhibitor, sunitinib, has been used as a radiosensitizer due to its immunomodulatory ability.

2. The Impact of RT on the Tumor Stroma

RT seeks to exploit DNA repair deficiencies in malignant tumor cells, but even in perfect scenarios, it invariably affects stromal cells within the tumor mass or at its boundaries [30]. Although many RT-mediated stromal changes are beneficial, such as the revival of or polarization toward tumor-suppressing immunity, RT can act as a double-edged sword in tumors [13]. Specifically, deleterious side effects could facilitate cancer progression and treatment resistance. These are the byproducts of RT we hope to avoid by carefully designing and planning RT dose regimens and combinatorial treatments.

One impact of RT on the tumor stroma is chronic inflammation that drives RT-induced fibrosis marked by an increased number of stromal cells and ECM components, through several mechanisms that have been reviewed elsewhere [31]. RT-induced fibrosis is a well-known side effect that can arise in some patients [1,31,32]. RT can completely transform the TME by inducing rapid and

chronic loss of hyaluronic acid [33] and collagen remodeling [34] by altering how CAFs regulate their collagen production [10,35]. Furthermore, RT-treated CAF populations can undergo modifications and alterations in terms of their diversity, secretome, and phenotype [36]. Additionally, RT enhances activation of proliferating machinery involving the RAS and mitogen-activated protein kinase (MAPK) cascades; the invasion pathways, which involve matrix metalloproteins (MMPs), laminin 5, and filamin A; transforming growth factor beta (TGF β) signaling, which is involved in tumor progression, resistance, and metastasis [2,7,37]. Likewise, RT to the stroma can increase tumor invasiveness due to increased hepatocyte growth factor (HGF)/c-Met (HGF receptor) signaling and MAPK activity, which enhances tumor mobility and can be deleterious [38]. Taken together, these reports suggest that RT can activate stromal features indicative of potential stromal-mediated treatment resistance.

It is still unclear how different fractionated RT regimens alter the stromal components of the TME and how these changes affect subsequent responses of cancer cells to RT. Similarly, the attempts to combine stromal-disrupting agents with RT to overcome stromal-mediated radioresistance remain unclear and merit further study.

3. The Impact of CAFs on RT Efficacy

CAFs are heterogeneous and the major contributors to the tumor stroma [3,4]. CAFs have been shown to control tumor phenotype at all stages of tumor progression. Their roles have been reviewed elsewhere and include the ability to shape the ECM; modulate innate and adaptive immune microenvironments; recruit and regulate leukocyte migration and inflammation via cytokines, chemokines, and growth factors; provide metabolic support (amino acids, lipids, and tricarboxylic acid cycle intermediates); and contribute to paracrine activation of mitogenic and pro-survival cellular signaling via cell surface receptor-ligand interaction and secreted proteins or exosomes [3,4,39]. The mechanisms by which CAFs contribute to radioresistance are likely mediated through their secreted factors, contact-mediated signaling, immunomodulatory effects, and ECM alterations [40].

CAFs secrete a number of different active factors that have diverse effects on tumor phenotype [3,4]. For example, through their active secretory function, tumor stromal fibroblasts can transfer RNA within exosomes to cancer cells. This exosome transfer mechanism has been implicated in paracrine anti-viral RIG-I and juxtacrine NOTCH (NOTCH3-JAG1) signaling pathways, which both contributed to the expansion of therapy-resistant tumor-initiating cells. Stromal cells, which include CAFs and some bone marrow cells, protected breast cancer cells by inducing an interferon (IFN)-related DNA damage resistance signature in a STAT1-dependent manner and caused the tumors to be chemo- and radio-resistant [41]. In another model, conditioned media (CM) from pancreatic stellate cells (PSCs), which are the central mediator of desmoplasia and major contributors of pancreatic CAFs, dose-dependently enhanced pancreatic tumor cell proliferation, migration, invasion, and colony formation and caused resistance to gemcitabine and RT. The CM was found to activate the MAPK AKT pathways in tumor cells, and the authors postulated that factors such as interleukin-1 β (IL-1 β) and TGF β were responsible [42]. The TME of glioblastoma is known to produce abundant TGF β , a pleiotropic cytokine that promotes an effective DNA damage response. Glioma-initiating cells were protected from RT-induced cell death by this increase in TGF β production, which promoted an effective DNA damage response and self-renewal via C-X-C chemokine receptor type 4 (CXCR4) and NOTCH1. TGF β inhibition prevented tumor cell DNA repair and enhanced RT efficacy in this glioblastoma model [43]. Furthermore, CAFs can promote irradiated cancer cell recovery and tumor relapse after RT by producing insulin-like growth factor-1/2 (IGF-1/2), C-X-C motif chemokine ligand 12 (CXCL12), and β -hydroxybutyrate. These secreted factors increase reactive oxygen species (ROS) levels post-RT, which enhanced protein phosphatase 2A activity and repressed the mammalian target of rapamycin activation, therefore inducing autophagy in cancer cells to promote cancer cell recovery. It was argued that blocking IGF-2 and autophagy can reduce CAF-promoted tumor relapse in mice after RT and could be a promising RT sensitization therapeutic strategy (Figure 2) [44].

CAF-secreted factors trigger many downstream autocrine and/or paracrine signaling pathways that regulate treatment response. A network of paracrine signaling among cancer cells, myeloid cells, and stromal cells such as endothelial cells can drive the processes of treatment resistance and metastasis [45]. CXCL1 signaling is an example of paracrine signaling that contributes to radioresistance. Along with cancer cells, CAFs highly express and secrete CXCL1, which inhibits expression of the ROS-scavenging enzyme superoxide dismutase 1, leading to ROS accumulation following RT [46]. In this scenario, tumor cells take advantage of ROS accumulation to enhance DNA damage repair mechanisms and ultimately cause radioresistance. This radioresistance is also mediated by activation of the mitogen-activated protein kinase ERK kinase/extracellular-signal-regulated kinase (MEK/ERK) signaling pathway important for malignant transformation [47,48]. Crosstalk between CAFs and tumor cells through CXCL1 expression in an autocrine/paracrine signaling loop is responsible for the radioresistance phenotype [46]. Together, these studies showed that through their secreted active factors, CAFs can confer radioresistance to tumor cells.

CAFs are embedded in the tumor stroma, allowing them to actively communicate with other cells present in their surrounding environment through various mechanisms [3,4]. Besides acting through their secreted factors, CAFs also induce radioresistance through direct contact-mediated signaling between cancer cells and CAFs [3]. In pancreatic cancer, PSCs promote radioprotection and stimulate the proliferation of pancreatic cancer cells through β 1 integrin signaling. β 1 integrin is known to modulate the cellular response to genotoxic stress including RT [49]. It was found that this effect is independent of phosphoinositide 3-kinase (PI3K) but depends on focal adhesion kinase (FAK). β 1 integrin inhibition or FAK knockout can abolish PSC-mediated radioprotection in pancreatic cancer cells to single-dose and fractionated RT [50]. These findings indicate that downstream cellular signaling pathways activated due to direct interactions between CAFs and tumor cells can mediate radioresistance.

Additionally, CAFs can work through paracrine networking to enrich cancer stem cells (CSCs), which have been implicated in chemo- and radioresistance. In pancreatic cancer, the presence of PSCs can induce CSC characteristics by increasing the epithelial-mesenchymal transition (EMT) phenotype. A proteomic screen revealed that TGF β is involved in the radioresistance phenotype, and TGF β neutralizing antibody can inhibit the EMT and CSC phenotype, thus sensitizing tumor cells to RT and reducing tumorigenicity in vivo [51]. In another setting, IGF-1 receptor (IGF-1R) signaling activation in cancer cells in the presence of CAFs expressing IGF-2 induced Oct3/4, Nanog, and Sox2 expression and promoted stemness pathways related to IGF-1R, EMT, PI3K, TGF β , WNT, and Hedgehog signaling. This group showed that CAF-derived HGF, IGF-2, basic fibroblast growth factor (bFGF), WNT, and oncostatin M regulated CSC-like characteristics in a paracrine manner through counterpart receptor signaling components and stemness factors. They found that blocking IGF-2/IGF-1R/AKT/Nanog signaling reduced CSC stemness and concluded that there were potential clinical applications of targeted therapy to improve chemo- and radioresistance (Figure 2) [52]. Furthermore, CSCs play an important role in disease recurrence after RT as a result of their high DNA repair and antioxidative capabilities. Fractionated RT can enhance IGF-1 secretion and subsequent upregulation of IGF-1R in CSCs. IGF-1R upregulation exerts a dual radioprotective effect by inducing upregulation of AKT/ERK survival signaling and FoxO3 activation, which results in radiation protection. Additionally, they showed that inhibition of IGF-1R signaling reverses CSC radioresistance [53]. Collectively, these findings showed that CAFs can trigger radioresistance through their CSC-promoting roles.

In addition to CAFs' de novo roles in mediating radioresistance, changes in CAFs due to RT can mediate further treatment resistance. This is important because most anti-cancer treatment regimens, including RT, are given in multiple treatment cycles with gaps to allow for normal cell recovery [32]. These gaps between treatment cycles can be exploited by both the tumor and stromal cells to take advantage of survival mechanisms. Thus, changes in the TME in between treatment cycles are important to consider with regard to the subsequent treatment response and resistance [32]. CAFs are not usually killed by RT; they are highly radioresistant due to the defective p53/p21 response pathway

and high expression of the cancer marker Survivin [54]. Irradiated fibroblasts can promote the invasive growth of squamous cell carcinoma through the induction of c-Met, RAS, MAPK cascade (Raf-1, MEK1, ERK-1/2), MMP-1, MMP-9, laminin 5, and filamin A. Irradiated fibroblasts also express high levels of TGF β 1 [37]. The effects these irradiated fibroblasts can have on non-irradiated neighboring cells are referred to as radiation-induced bystander effects [55], and there is evidence that many of these factors can promote radioresistance.

There are several examples by which RT-induced changes in CAFs contribute to radioresistance. After genotoxic stress, CAFs can secrete WNT16B to the TME and promote prostate cancer therapy resistance. WNT16B, a secreted protein that is activated in fibroblasts through the nuclear factor (NF) κ B pathway after DNA damage, subsequently activates the canonical WNT program and promotes EMT in neoplastic cells through paracrine signaling. This process attenuates the effects of both chemo- and radiotherapies and promotes tumor cell survival and disease progression [56]. Moreover, exposure to low-dose RT (<20 cGy) can induce premature senescence in stromal fibroblasts. In one setting, these senescent CAFs are responsible for stimulating enhanced proliferation of breast carcinoma cells and are correlated with radioresistance, which is partly mediated by the AKT pathway [57]. In addition, senescent CAFs can induce a senescence-associated secretory phenotype that includes the production of IL-6, IL-8, and osteopontin that are considered to be pro-tumorigenic factors and have been associated with immunosuppression and stromal-mediated therapeutic resistance [3,6,58]. RT can also promote EMT transition and invasion of pancreatic cancer cells by activating CAFs. CAF-derived CXCL12 directly promoted tumor cell EMT and invasion by acting through CXCR4 on tumor cells and downstream activation of the P38 pathway. Blocking CXCL12/CXCR4 signaling between pancreatic cancer cells and CAFs could attenuate RT-induced tumor cell invasion [59]. Indeed, HGF secretion by irradiated CAFs can increase phosphorylation of c-Met and MAPK activity in pancreatic tumor cells, which translates into enhanced invasion. This unwanted byproduct of RT can be overcome by blocking HGF signaling with an HGF antagonist [38]. Finally, exposure of CAFs to 18 Gy RT resulted in potent induction of multiple DNA damage response (DDR) foci; induced premature cellular senescence; and inhibited proliferative, migrative, and invasive capacity of CAFs. This RT dose increased the expression of integrins α 2, β 1, and α 5 and dramatically augmented and redistributed focal contacts [60]. The increase in β 1 integrin has been correlated with radioresistance [50]. All of these examples point to RT-induced changes in CAFs that can promote further radioresistance. This should encourage us to find therapeutic regimens that target both the tumor and stroma to successfully deliver anti-cancer treatment.

CAF-secreted factors, contact-mediated signaling, downstream pro-survival signaling pathways, CSC-generating role, and changes due to RT all comprise intricate crosstalk between CAFs and cancer cells to render tumor cells radioresistant. While we understand that CAFs play a critical role in shaping responses to RT, there are several areas where we do not fully understand their impact. First, CAFs in tumors are a diverse heterogeneous population that can have opposing roles [3,4,39]. While an abundance of literature supports the tumor-supporting roles of CAFs, some studies also suggest that certain CAF subsets may have tumor-restraining abilities [61,62]. These diverse CAF subsets may have differential effects on radioresistance and, in turn, be shaped differently by RT. Second, the plasticity, diverse origins, and spatial location of CAFs [40,63–65] may complicate things further in terms of their contributions to radioresistance. RT may alter CAF phenotypes temporally and spatially, and this will also affect cancer cells' responses to RT. Lastly, RT dose fractionation may differentially impact CAF diversification. Our understanding of CAF diversity and plasticity is still limited, but it is logical to assume that CAF-mediated radioresistance is a problem in RT success and needs further study.

4. The Impact of ECM on RT Efficacy

The ECM plays an essential role in regulating cancer progression and radiosensitivity. Tumor ECMs are dynamic structures that are remodeled during tumor progression and/or treatment [8]. Among the approximately 300 proteins present in the ECM that are known to regulate tissue homeostasis,

inflammation, and disease, collagen is the most abundant, constituting up to 90% of the tumor ECM. In addition to collagens, other prominent fibrous proteins are elastins, fibronectins, and laminins, which are also involved in controlling tumor phenotype [8]. Tumor ECM is typically denser and mechanically stiffer than normal ECM, due to the quantity of ECM as well as structural changes in molecular architecture such as the extent of crosslinking [66]. These changes in ECM density, composition, and stiffness significantly impact malignant cell invasion, survival, and proliferation [67,68]. Variations in ECM stiffness and density have been correlated with disease aggressiveness, progression-free survival, and in some cases, resistance to different treatment modalities [8].

The ability of tumor-promoting ECM to drive treatment resistance is particularly applicable to RT. Tumor cells can interact with the ECM through direct interaction (cell-protein contact), and one major way is through the engagement with integrins [49]. ECM stiffness can facilitate integrin clustering, which can lead to activation of downstream FAK activation and MAP/ERK kinase signaling pathways leading to cell survival, proliferation, migration, and invasion. Integrin-mediated adhesions can also activate transcription factors NF κ B, inositol lipid metabolism, and MMP activity [49], in addition to the activation of PI3K/AKT and RAS/MAPK pathways. Integrin activation is important in regulating tumor phenotypes and has been associated with processes such as angiogenesis, survival, invasion, metastasis, and treatment resistance [2,4]. Further complicating this is the fact that RT can increase the expression of integrins α 2, α 5, β 1, and β 6; therefore, we need to consider how RT fractionation controls subsequent treatment resistance [60,69,70]. For example, it was found that β 1 integrin controls radioresistance by resisting cellular apoptosis from RT through the activation of AKT signaling. Inhibition of β 1 integrin can resensitize tumor cells to RT by decreasing proliferation and increasing apoptosis (Figure 2) [71,72]. Another group also found that β 1 integrin-mediated adhesion confers RT resistance through downstream FAK-interacting proteins (p130Cas and paxillin) and PI3K/AKT-mediated pro-survival signaling pathways [73]. Together, these examples showed that contact-mediated signaling between tumor cells and ECM proteins in cancers can contribute to radioresistance.

The ECM also contains secreted soluble signaling molecules from tumor and stromal cells. The ECM acts as a reservoir for these cytokines, chemokines, and growth factors. Two prominent examples of these secreted factors that control tumor phenotype are TGF β and various members of the MMP family. Besides interacting directly with the stromal cells and surface proteins in the ECM, tumor cells are constantly and sophisticatedly communicating with these secreted regulatory molecules [10]. Many of these proteins are already known to be capable of inducing radioresistance, such as TGF β [42,43,51]. Moreover, RT can further increase TGF β levels, which can accelerate tumor progression. Inhibition with TGF β neutralizing antibodies has been shown to prevent radiation-induced metastatic progression [74]. Another class of secreted proteins that are highly abundant in the ECM and mediate tumor progression are the different MMPs [2,8,75]. MMP2 is known to degrade collagen IV and plays a role in RT-induced lung injury. MMP2 inhibition prior to RT abrogated the induction of FoxM1 expression, reduced p53 and p21 expression, decreased expression of DNA repair genes XRCC1 and Chk2/1, and abrogated G2 cell cycle arrest, leading to apoptosis and enhanced radiosensitivity [76]. These examples showed that the ECM serves as a tumor growth factor and cytokine sink, which contributes to tumor radioresistance and worthy of consideration in future therapeutic planning.

Besides controlling the stability and bioavailability of numerous growth factors and cytokines, ECM structure and integrity also influence oxygen availability, acidity, and interstitial fluid pressure in tumors, through its regulation of the tumor vascular system, so it has important effects in terms of controlling treatment response (Figure 1) [8,66]. Oxygen availability is critical for RT response as hypoxic cells are generally 2.5–3 times less radiosensitive than normoxic cells [77–80]. The indirect effects of RT produce ROS through the hydrolysis of water, which then propagate and modify lipids, membranes, and proteins [10]. Using nitric oxide-dependent arteriole vasorelaxation as a way to increase the partial pressure of oxygen in tumors, multiple groups found that low-dose nitrite can sensitize tumors to RT, leading to a significant tumor growth delay and longer survival [81,82].

Antiangiogenic therapy such as vascular endothelial growth factor (VEGF) receptor 2 blockade, which can create a “normalization window” that increases tumor oxygenation, has also been shown to enhance the RT response (Figure 2). This effect is dependent on the increased pericyte coverage of tumor vessels via the upregulation of angiopoietin 1 and degradation of the pathologically thick basement membrane via MMP activation [83]. Thalidomide, an angiogenesis inhibitor, can also increase tumor reoxygenation correlated with reduced interstitial fluid pressure and increased perfusion, sufficient to radiosensitize tumors [84]. Non-steroidal anti-inflammatory drugs (NSAIDs) are another radiosensitizing drug class that works through increasing tumor oxygenation via either a decrease in macrophage recruitment or inhibiting mitochondrial respiration. Using four different NSAIDs (diclofenac, indomethacin, piroxicam, and NS-398), radiation sensitivity in tumor cells can be increased by enhancing radioinduced apoptosis and inhibiting repair of sublethal RT damage [85]. These studies showed that tumor ECM governs oxygen bioavailability in cancers, controls radiosensitivity, and that RT requires sufficient tumor oxygenation to avoid radioresistance (Figure 1).

In most cancers, tumor cells are embedded in stromal cells with abundant ECM components, that, as described above, govern radioresistance through direct interaction with tumor cells and the ECM's roles as protein reservoirs and a major controller of tumor oxygen bioavailability. Even though many of these factors negatively impact RT efficacy, there are known inhibitors that can successfully reverse ECM-mediated radioresistance. As with CAFs, our current knowledge is still lacking on how RT dose fractionation may differentially impact ECM alterations and how they contribute to radioresistance.

5. The Impact of Immune Cells on RT Efficacy

RT is a powerful therapeutic approach used in many patients due to its numerous beneficial effects leading to tumor cell eradication. Besides the direct killing of highly proliferating tumor cells by mitotic catastrophe or apoptosis or necrosis, RT is increasingly appreciated to have immunomodulatory effects, which can take advantage of the fact that our immune cells can target and kill abnormal cancerous cells [11,13,30,32,86]. RT modulates the immunogenicity and adjuvanticity of tumors by increasing the expression and release of tumor-associated antigens, increasing the expression of major histocompatibility complex I (MHC-I), inducing immunogenic cell death (ICD) and its downstream anti-tumor pathways, and releasing danger signals and chemokines that recruit inflammatory anti-tumor immune cells to the TME, including antigen-presenting cells that can activate cytolytic T cells [75,87,88]. RT can also enhance tumor killing by increasing the number of tumor-infiltrating immunostimulatory cells and neoantigen expression [89–91]. However, there are reports that RT can induce immunosuppression on top of anti-tumor immune promoting effects [12,32]. The balance between the two variables predicts the treatment response. Due to its double-edged sword effects on immune modulation, precise dosing regimens and combinatorial treatments of RT must be carefully considered to avoid unwanted immunosuppressive effects [7,9–11,13,30,32,86,87].

As we have discussed with CAFs and ECM, radiosensitivity depends on the complex interaction of malignant cancer cells with their immune TME [86]. Notably, the host immune status also determines the efficacy of treatments, including RT (Figure 1). The presence and activation status of dendritic cells (DCs) and CD8⁺ T cells and anti-tumor cytokines such as IFN γ determine the responsiveness to RT [92–95]. IFN-related DNA damage resistance signature (IRDS) genes including STAT1, IFN-stimulated genes 15 (ISG15), and IFN-induced protein with tetratricopeptide repeats 1 (IFIT1) are associated with resistance to chemotherapy and/or RT across different tumor cell lines [69]. Additionally, the intratumoral immune response after RT also determines the therapeutic response. RT success is dependent on the antigen-specific nature of immune activation, which can be enhanced by combining RT with immune checkpoint blockade therapies like α PD-1 and α CTLA-4 [26,87,96,97]. Increases in intratumoral anti-tumor immune cells and IFN γ were found to imbue CD8⁺ T cells with lytic activity against tumor cells, and the addition of IL-12 as immunotherapy can augment this RT-induced anti-tumor immunity [94,98]. Radiation can upregulate the expression of programmed death ligand 1 (PD-L1) on

tumor cells in numerous *in vivo* models, which binds with immune checkpoint receptor PD-1 expressed by CTLs and thereby promotes their dysfunction. The combination of radiation and inhibition of this immune checkpoint has been shown to improve the radiation-induced anti-tumor response through activation of cytotoxic T cells and diminished the influx of myeloid-derived suppressive cells (MDSCs) into the TME [99–101]. Interestingly, several studies in mice and humans have demonstrated abscopal effects, with response of both the primary tumor and distant disease to combination therapy of RT and immune checkpoint blockade [102]. Although most of these studies were conducted utilizing hypofractionated or single-dose ablative radiation schemes, the optimal dose, fractionation, and timing to achieve this effect are unknown [103]. *In vivo* studies have demonstrated that PD-L1 expression peaks at 3 days post-irradiation, and that concurrent but not sequential treatment with checkpoint inhibitors is necessary for a T cell-mediated tumor response [93,101]. Interestingly, in the KEYNOTE-001 trial, patients who received radiation at any time prior to immune checkpoint therapy had significantly increased progression-free survival, with median time ranging from 9.5 to 11.5 months [104,105]. Despite these appealing data, larger studies demonstrating sufficient survival benefits to lead to approval of regimens containing RT in combination with immune checkpoints have not been published. However, these findings showed the importance of the host's immune status as one major contributor that can predict radiosensitivity.

Like CAFs, immune cells in the TME are very diverse and have different roles. Tumor-associated macrophages (TAMs), MDSCs, and CD4⁺ regulatory T cells (T_{regs}) are known to be immune suppressive and pro-tumorigenic; on the other hand, immune cells such as DCs, CD8⁺ T cells, and NK cells are anti-tumorigenic [12]. Likewise, these immune cells also differentially regulate radiosensitivity in cancers (Figure 1). The presence of TAMs correlates with increased radioresistance in many different tumors [106]. Radiation plays a role in the recruitment and phenotype modulation of TAMs in the TME. Recruitment of TAMs occurs irrespective of dose and fractionation [107]. Conventional fractionation leads to transcription of colony-stimulating factor 1 (CSF1), which when blocked in prostate cancer models reduces TAM recruitment. Conversely, hypofractionated regimens promote TAM recruitment in hypoxic conditions, where in glioma models radiation-induced hypoxia-inducible factor 1 (HIF-1) expression leads to the increased density of TAMs [108,109]. Co-implantation of tumor cells with bone marrow-derived macrophages increased tumor radioresistance, so depletion of TAMs using a systemic or local injection of macrophage-depleting liposomal clodronate before RT can increase anti-tumor effects in different RT dosing regimens. Radioresistance coming from TAMs is mediated by the tumor necrosis factor (TNF) signaling-dependent upregulation of VEGF, and anti-VEGF or anti-TNF therapy can reverse this radioresistance (Figure 2) [110]. The effect of the radiation-induced influx of TAMs in the TME depends on the exact phenotype they acquire once infiltrated. The decision tree for macrophage polarization, unlike recruitment, does appear to be dependent on the radiation dose and fraction. Anti-tumor phenotypes may be favored in conventionally fractionated dosing, which can in turn enhance T cell-mediated tumor control [111,112]. Importantly, this effect may be lost in hypofractionated and single-dose ablative regimens. One reason may be that hypoxia which results from vascular impairment by RT promotes macrophage immunosuppressive and pro-tumorigenic tissue remodeling functions [113–115]. However, this is likely an oversimplification, and the true impact of TAMs may depend on the organ- and cancer-specific context in which radiation is employed. RT itself can cause an influx of MDSCs into tumors that eventually polarize the TME into an immune-suppressive environment. This polarization is dependent on transcriptional regulation by the NFκB p50 subunit, as mice lacking NFκB p50 are much more sensitive to RT [116]. Additionally, MDSCs can be recruited further into the TME from RT in a fractionated RT regimen due to the recruitment of DNA damage-induced kinase ABL1 into cell nuclei where it binds the CSF1 gene promoter and enhances its transcription. Hence, blocking macrophage migration with a CSF1 inhibitor radiosensitizes tumors [46]. Another group also found that a neutralizing antibody to CSF1 or a small molecular inhibitor to the CSF1 receptor kinase efficiently depletes macrophages and delays tumor regrowth following RT (Figure 2). This delay is a reflection of the increased presence of CD8⁺

T cells and reduced presence of CD4⁺ T cells, the main source of T helper 2 (Th2) cytokines IL-4 and IL-13. The authors proposed that the response to RT could be enhanced by reducing TAMs in tumors or blocking their induction of Th2 polarization [117]. Moreover, treatment with the small tyrosine kinase inhibitor sunitinib resulted in a significant reduction of MDSCs and phospho-STAT3 and increased T cell proliferative activity in cancer patients. Sunitinib's ability to increase RT efficacy in tumors is mediated through the reduction in the number and function of immunosuppressive MDSCs and is significantly correlated with lower CD4⁺ T_{reg} and B cell numbers and augmentation of Tbet expression in primary CD4⁺ and CD8⁺ T cells [118,119]. Finally, due to the intrinsic radioresistant nature of CD4⁺ T_{regs} and its immunosuppressive roles, CD4⁺ T_{reg} presence in tumors has also been correlated with radioresistance [120,121]. T_{regs} are essential to generating immune tolerance, are radioresistant compared to other T cell subtypes, and demonstrate a relative increase in the TME after irradiation. T_{regs} are known to increase in mice receiving whole-body radiation [122], and studies of human cervical cancers treated with 10-30 Gy demonstrate decreased CD8⁺ and CD4⁺ T cells, without any effect on T_{reg} numbers [123]. In vivo tumor models with systemically depleted T_{regs} demonstrate significant detriment of primary and metastatic tumor progression. When these tumors are irradiated, these models demonstrate significantly reduced tumor burden post-RT and improved overall survival [124–129]. Dose and fractionation have also been demonstrated to play a role in the balance of immune priming and immunosuppression post-RT. A B16 murine model receiving a single 5 Gy dose of irradiation showed a relative increase in the T_{reg} population compared to cytotoxic T cells. However, a single 10 Gy dose resulted in a relative decrease of T_{regs}, while a single 15 Gy dose increased both T_{reg} and effector T cells [130]. Systemic elimination of CD4⁺ T_{regs} using anti-CD25 monoclonal antibody enhances radiotherapeutic benefits via immune modulation (Figure 2) [122]. Collectively, these studies showed that pro-tumorigenic immune cells can modulate radioresistance in many cancers.

While initially thought to create an immunosuppressive TME, radiation has recently gained momentum clinically as a means to prime the immune system to recognize and remove tumor cells. To achieve this end, cross-presentation of tumor antigen by DCs to cytotoxic T cells must be upregulated. Radiation has been shown to increase IFN-I signaling, leading to expansion and activation of DCs, through induction of the stimulator of IFN genes (STING) pathway [26,93,131,132]. Additionally, tumor cell removal requires the induction of cell death pathways, which can be variable, and include apoptosis, necrosis, autophagy, and mitotic catastrophe. Immunogenic cell death upregulation is frequently observed following irradiation. This involves three key molecular signals: calreticulin, which undergoes translocation from the endoplasmic reticulum to the plasma membrane to signal uptake of dying tumor cells by DCs; high-mobility group protein B1 (HMGB1), which is released from the dying cells to bind Toll-like receptor 4 on DCs promoting antigen cross-presentation; and adenosine triphosphate (ATP), which activates cytotoxic T cells through inflammasome activation via the P2XR7 pathway [86,132–135]. In vitro experiments have demonstrated that the generation of these three key signaling molecules is dependent on irradiation dose [88]. However, the optimal dose and fractionation of irradiation required to induce ICD in vivo is influenced by the TME [75,86,133]. Utilizing a B16 melanoma mouse model expressing ovalbumin antigen, several groups have demonstrated that single-dose, 15-20 Gy irradiation was more effective in generating activated cytotoxic T cells than more conventional fractionated schedules of 15 Gy in 5 daily fractions and 20 Gy in 4 bi-weekly fractions. This indicated that the prescribed dose per fraction and also the specific timing of individual dose delivery are important to elicit RT-induced immune responses [26,131]. Clinical investigations of this mechanism in patients with colorectal and prostate cancer demonstrated a detectable increase in circulating cytotoxic T cells (Survivin- and/or prostate-specific antigen-specific) in post-irradiation blood samples [136,137]. Additionally, early-stage non-small cell lung cancer patients treated with SBRT, 48 Gy in 6-8 fractions, showed increased circulating cytotoxic T cells [138]. Many studies have indicated that ablative radiation doses are required for activation of T cell immunity, and this is corroborated by clinical evidence suggesting that conventional fractionation can have a detrimental effect on the

TME as a result of the death of infiltrating anti-tumor lymphocytes [32,139–141]. In preclinical studies, mice bearing bilateral flank implants of CT26 colon carcinoma treated with conventional fractionation (10 Gy in 5 fractions) initially demonstrated T cell reductions after each dose of radiation; however, this regimen at 7 days post-therapy led to an expansion of local polyclonal T cells responses and infiltrating T cells, revealing a treatment duration effect in this model system [142]. Several groups have moved away from flank models, due to the prevailing theory that to initiate tumor growth you create a wound stimulating a subsequent acute immune response. Instead, several groups have adopted genetically-engineered mouse models (GEMMs) that spontaneously form tumors. Recent publications utilizing GEMMs of pancreatic cancer and sarcoma have demonstrated that reprogramming the TME can induce T cell immunity and sensitize tumors to radiation [143–145] from both single high-dose and hypofractionated RT schemes.

Radiation also plays an important role in overcoming T cell exclusion from the TME. One barrier is the dampened homing of effector T cells, which is modulated by cytokines released from tumor cells and the surrounding stroma. Irradiation can significantly enhance the secretion of CXCL16 by mouse and human breast cancer cells; this chemokine binds to CXCR6 on activated cytotoxic T cells and plays an important role in their recruitment to inflammation sites. CXCL16 can be induced in vitro by a single fraction dose of 5 Gy; while in vivo induction was found to be dose-dependent, reaching a plateau at 12 Gy [146,147]. In another study, mice deficient in IFN γ , a cytokine that is critical for innate and adaptive immunity, received tumor-localized irradiation and demonstrated decreased expression of MHC-I and CXCL9/CXCL10, which are important chemoattractants for cytotoxic T cells [147,148]. TNF α can also be induced by single-fraction irradiation in tumor cell lines [149]. Radiation also leads to upregulation of anti-inflammatory cytokines, like TGF β , which will suppress the function of DCs and cytotoxic T cells and promote maturation of T_{regs}. Single fraction radiation from 5–10 Gy in mouse mammary tumors upregulated TGF β in both tumor cells and the surrounding adipose stroma [34,150]. In irradiated tissues, there is a relative increase in ROS, leading to activation of TGF β . Mouse models of mammary carcinoma demonstrate that activation of DCs and priming of cytotoxic T cells during RT can be improved by administering TGF β -neutralizing antibodies [99,150].

Tumors counteract this influx of activated cytotoxic T cells through the downregulation of antigen-presenting MHC-I proteins. Historical studies revealed that radiation increases MHC-I protein expression on tumor cells, leading to restored antigen recognition by cytotoxic T cells. In primary glioblastoma lines, increasing doses of radiation up to 12 Gy led to increased MHC-I expression, and a similar effect was demonstrated in ovarian and cervical cancer cell lines with doses of 25 to 100 Gy [151–154]. Conventionally fractionated radiation also can induce MHC-I expression, where conditioned media from breast cancer lines treated with 6–10 Gy delivered in 3–5 fractions was able to stimulate expression of total cellular and surface MHC-I in recipient cells [155].

The interactions between tumor cells and their immune microenvironment is very complex due to their abundance, diversity, and varying roles. Evidence showing the presence of anti-tumor immune cells and IRDS genes being important to determine RT efficacy and the roles of pro-tumor immune cells to promote radioresistance should inspire us to design therapeutic regimens with different immune-modulating drugs to synergize with RT. However, it is still unclear how different RT fractions affect immune TME. Additionally, it was recently discovered that distinct immune cell origins (bone marrow or embryonic) have different roles in controlling tumor phenotype [156]. How the immune cell origin contributes to immune-mediated radioresistance is still a largely unaddressed question in the field and needs to be studied [157,158].

6. Immunomodulatory Roles of CAFs and the ECM and How Their Interactions Regulate RT Efficacy

With recent discoveries, it is increasingly appreciated that malignant tumor cells interact with their TME in a complex and reciprocal manner to regulate tumor progression and treatment response [1–5]. In addition to the ability of the individual stromal components to directly control tumor cell phenotype,

interactions among the components of the TME themselves can also exert the same effects [6,66]. Immune cells in the TME are regulated by their microenvironment, including the CAFs and ECM in addition to the tumor cells. These communal interactions in the TME are important to consider because they can inadvertently affect treatment response [11,32,86].

CAFs have various pro-tumorigenic roles by regulating tumor immunity, ECM, and hypoxia, among many other factors [66]. One group reported that fibroblast activation protein (FAP)⁺ CAFs, one subtype of CAFs, are responsible for suppressing anti-tumor immunity and thus contribute to uncontrollable tumor growth. Depleting FAP-expressing cells provides some tumor growth control through a process involving IFN γ and TNF α [159]. In a cervical cancer model, mesenchymal stromal cells were responsible for immunosuppression through their ability to dampen CD8⁺ T cell proliferation, activation, and effector functions. This was found to be mediated by the expression of CD39 and CD73 ectonucleotidases and the generation of adenosine by the stromal cells [160]. Lastly, CAFs can support tumorigenesis and mediate tumor-enhancing inflammation by enhancing tumor angiogenesis, proliferation, and invasion. These tumor-promoting characteristics are mediated by NF κ B pathways [161]. These tumor-promoting roles of CAFs, through their modulation of tumor immunity, may apply to the mechanisms of stromal-mediated radioresistance.

CAFs can control tumor immunity through multiple mechanisms [66,162]. CAFs regulate both adaptive and innate immune cell functions, including T cell and immunosuppressive myeloid cells. CAFs can negatively impair the function of CD8⁺ T cells including cytolytic activity and cytokine production through the production of soluble factors, such as TGF β and VEGF, metabolic reprogramming via indoleamine 2,3-dioxygenase and arginase, and expression of checkpoint inhibitors like PD-L1 [66,163]. Many of these factors were discussed previously in the other sections as they are implicated in radioresistance [42,43,51,110]. CAFs can also affect myeloid cell and DC maturation status and function [164–167]. These immune cells are essential mediators of radiosensitivity [92–95,106]. More importantly, many recent discoveries have shown how targeting the stroma can reawaken anti-tumor immunity and synergize with immunotherapy [168–170], as reviewed elsewhere [66]. The concept of how stromal interactions with the immune microenvironment affect immunotherapy response may also hold true for RT responses.

One way by which CAFs regulate the immune TME is through their secreted factors. CAFs secrete many active factors to the TME which are eventually stored in the ECM reservoir, including the various MMPs [2,8,10,75]. MMP14 mediates tumor progression through vascular and immune-modulatory effects. The anti-MMP14 inhibitory antibody can inhibit tumor growth, reduce tissue hypoxia, increase macrophage number, and shift cell phenotype towards the more anti-tumor M1-like phenotype due to reduced active TGF β and SMAD2/3 signaling, hence synergistically enhancing RT effects (Figure 2) [171]. This example demonstrates that CAF interactions with the ECM and the immune microenvironment can regulate tumor cell radiosensitivity.

CAFs and the ECM have many immunomodulatory functions, which can control tumor cells' treatment response, including RT efficacy. Even on their own, CAFs, ECM, and immune cells can directly confer a radioresistance phenotype to tumor cells, and their interactions among themselves also affect how tumor cells respond to RT. It is presently unclear how these relationships among the tumor stroma components are affected by host immune status and vice versa. Similarly, it is not known how different RT doses and fractionations change these complex interactions and their ensuing tumor-regulating phenotype. It will be fascinating to see how new technologies such as single-cell RNA sequencing will help us discover novel stromal and immune cells and shape our understanding of the immunomodulatory functions of stromal cells in cancers.

7. The Impact of Other Stromal Cells on RT Efficacy

The TME contains other stromal cells present besides CAFs: blood endothelial cells, lymphatic endothelial cells, adipocytes, mesenchymal stem cells, fibrocytes, pericytes, neurons, etc. Although

their contribution is small in terms of their numbers in the TME, they still play important roles in tumor progression, treatment response, treatment resistance, and cancer metastasis [1,7].

Endothelial cells are important players in many different types of cancer. They supply nutrients for tumor growth, provide routes for metastatic dissemination, and contribute to chemo- and radioresistance [80,172,173]. Hence, it is important to understand the tumor vasculature to comprehend endothelial cell-mediated radioresistance. Tumors have two main ways to develop vasculature: angiogenesis and vasculogenesis. Angiogenesis is the process in which vessels are developed from nearby endothelial cells, while vasculogenesis is the formation of blood vessels from circulating cells postulated to come from the bone marrow [80]. It is clear that angiogenesis is an important process fundamental to treatment refractoriness, but vasculogenesis is especially imperative in RT resistance due to the fact that local RT abrogates local angiogenesis, forcing tumors to rely heavily on the vasculogenesis pathway for blood vessel regrowth post-RT. This mechanism poses another barrier to T cell infiltration. Dysfunctional tumor-associated vasculature has endothelial cells lining the vessels that suppress T cell activity, target them for destruction, and block entry into the TME [174]. Studies of ablative doses of radiation as high as 25 Gy led to the infiltration of TAMs expressing immunosuppressive enzymes [175]. Notably, single-fraction ablative doses also induce significant endothelial cell death, causing reduced vascular flow, hampering T cell recruitment, and inducing a hypoxic and immunosuppressive TME [176,177]. These ablative doses have been evaluated by bioinformatic studies, demonstrating that alteration of tumor vasculature post-irradiation accounts for 20–30% of the radiographic response of brain metastases in stereotactic radiosurgery cases [178]. In contrast, radiation doses <10 Gy have been shown to promote vascular relaxation and increase tumor oxygenation, with fractionated schedules providing the maximal benefit on tumor growth delay due to tumor reoxygenation [179,180]. Low-dose radiation also plays a role in the reprogramming of macrophages, which are important during the angiogenesis process, allowing increased T cell extravasation in vivo through inducible nitric oxide synthetase [112]. There is an influx of CD11b⁺ myeloid cells following tumor irradiation, and increased tumor hypoxia increases HIF-1 levels and subsequently upregulates stromal cell-derived factor 1 (SDF1, also known as CXCL12) to initiate vasculogenesis [80]. Many angiogenic inhibitors have been used in the clinic and have proven efficacy as radiosensitizing agents because of multiple different mechanisms related to the “normalization” of tumor vessels and their subsequent oxygen content and acidity (Figure 2) [2,6,32]. One group claims that the use of the VEGF receptor inhibitor axitinib radiosensitized tumor endothelium and enabled tumor control [181]. Another group found that angiogenesis-promoting factors that protect against endothelial damage can diminish the RT response. Reversing this effect with a VEGF inhibitor promotes RT-induced endothelial injury through the generation of the second messenger ceramide through acid sphingomyelinase trafficking to the plasma membrane. This tumor endothelial cell RT resensitization was shown to mediate tumor control [181]. These studies demonstrated that endothelial cells are important mediators of tumor radioresistance due to their ability to form vessels and control tumor oxygen content.

Adipocytes are also active players in the TME that control cancer development, progression, metastasis, and treatment response, especially in cancers that interact closely with adipose tissue-like breast cancers [182]. Cancer-associated adipocytes (CAAs) are energetic cells capable of secreting a heterogeneous group of molecules known as adipokines that include hormones, growth factors, and cytokines. Some examples of adipokines are leptin, adiponectin, autotaxin, IL-6, TNF α , IGF-1, and HGF. In addition, CAAs actively participate in metabolic remodeling that supports cancer cell growth by regulating the fatty acid reservoir to increase mitochondrial β -oxidation. They also interact closely with CAFs and ECM molecules through ECM remodeling. More importantly, they act as obstacles to various anti-cancer therapies as they are involved in diverse resistance mechanisms [1,7].

One mechanism of adipocyte-mediated radioresistance is through their secreted adipokines. Some of these adipokines such as TNF α , IGF-1, and HGF were discussed earlier with regard to their contributions to stromal-mediated radioresistance (Figure 1) [38,52,110,159]. Another group reported

that these adipokines can increase the gene expression of NF κ B and cyclin D to induce anti-apoptotic transcription and stabilize pro-oncogenic factors such as β -catenin and cyclin-dependent kinases [182]. It was also found that breast cancer cells co-cultured with adipocytes are radioresistant, and the mechanism is through adipocyte secretion of IL-6 resulting in the phosphorylation of Chk1 associated with decreased cancer cell death [182,183]. Another mechanism of adipocyte-mediated radioresistance is the initiation of autotaxin (ATX)–lysophosphatidic acid (LPA) signaling. This group found that CAAs, which closely interact with adjacent tumor cells, can become inflamed from tumor-derived cytokines, which results in the stimulation of adipocytes' ATX secretion and subsequent LPA production. This further promotes inflammatory cytokine production in a vicious feed-forward cycle. RT-induced adipocyte injury triggers increased levels of ATX, cyclooxygenase-2 (COX-2), IL-1 β , IL-6, IL-10, TNF α , and LPA1 and LPA2 receptors. This inflammatory response depends on the DNA damage response pathways ATM, ATR, and PARP-1 and inflammatory mediators COX-2 and NF κ B, which can potentially be inhibited to reverse radioresistance. Induction of LPA signaling enhances lymphocyte invasion and cytokine and VEGF production to stimulate angiogenesis required for tumor growth [184]. As detailed earlier, angiogenesis is one factor that contributes to tumor cell radioresistance [8]. These studies showed that adipocytes are not dormant “fat” cells; they are active contributors to tumor phenotype through their active metabolism and secreted factors.

Even though endothelial cells and adipocytes do not make up a significant portion of the tumor stroma, they contribute to tumor radioresistance. Multiple groups have shown that we should not negate their roles in controlling RT response to prevent the formation of radioresistant cancer cells. However, the complexity of different RT doses and fractionation regimens has left the field with an unanswered question regarding their effect on stromal cells present in cancers.

8. Forward Looking Conclusions

Malignant tumor cells that harbor genetic aberrations are in close proximity with the tumor stroma composed of diverse cellular and non-cellular entities including CAFs, ECM components, immune cells, endothelial cells, adipocytes, and secreted bioactive molecules. At every step of the tumor lifecycle, there is reciprocal communication between these malignant cancer cells and their neighbors. Their highly dynamic interactions control tumor initiation, progression, invasion, metastasis, and treatment resistance, which complicates cancer therapeutic planning [1–6,8,10–13,185]. Here, we reviewed how the tumor stroma can contribute to cancer radioresistance; many of which are mediated through secreted factors, cell surface receptors, and downstream pro-survival and/or anti-apoptotic signaling pathways. The tumor stroma is very diverse, and our current knowledge of distinct cell types is still lacking. It will be interesting to see how new technologies to discover novel CAFs and immune cell types will broaden our knowledge of tumor-stromal interactions.

Further complicating the concept of stromal-mediated radioresistance is the fact that with successive treatments tumor and stromal cells can become more resistant, which could be a problem for many anti-cancer treatment regimens given in cycles, such as chemo- and radiotherapies. Based on the potential of these tumor stroma to induce radioresistance, it seems plausible to include stromal-targeted agents in combination with RT for therapeutic benefit. Multi-directed treatments toward both the tumor cells and the tumor stroma could help eradicate cancers and prevent therapeutic resistance and tumor relapse.

Lastly, RT is a rapidly evolving field. Ultra-high dose rate of RT (FLASH-RT) is a new technology that enables the ultra-fast delivery of doses while sparing normal tissues [186,187]. It will be important to see how FLASH-RT influences tumor-stroma communications and stromal-mediated radioresistance. Despite many recent discoveries, there are still many remaining questions in the field to be addressed, such as how CAF diversity affects radioresistance and how the tumor stroma changes with different RT dosing and fractionation regimens. Future discoveries about these mechanisms can be used for the design of novel RT and drug combinations to target stromal-mediated RT resistance.

Author Contributions: V.E.K., J.A.S., J.K.S., and D.G.D. wrote the manuscript; V.E.K. and D.G.D. prepared the figures. All authors contributed to the writing of the manuscript. All authors have read and agreed to the published version of the manuscript.

Funding: V.E.K. was supported by NCI predoctoral fellowship F30CA243233. J.A.S. was supported by RSNA Research Resident/Fellow Grant RR2062. J.K.S. was supported by NIH R01CA248917, Siteman Investment Program, and AACR/Bristol Meyers Squibb Female Investigator Award. D.G.D. was supported by NCI R01CA177670, R01CA244938, R01CA203890, R01CA248917, P50CA196510, and U2CCA223303.

Conflicts of Interest: The authors declare no conflict of interest.

References

1. Valkenburg, K.C.; De Groot, A.E.; Pienta, K.J. Targeting the tumour stroma to improve cancer therapy. *Nat. Rev. Clin. Oncol.* **2018**, *15*, 366–381. [[CrossRef](#)] [[PubMed](#)]
2. Mueller, M.M.; Fusenig, N.E. Friends or foes—Bipolar effects of the tumour stroma in cancer. *Nat. Rev. Cancer* **2004**, *4*, 839–849. [[CrossRef](#)] [[PubMed](#)]
3. Kalluri, R. The biology and function of fibroblasts in cancer. *Nat. Rev. Cancer* **2016**, *16*, 582–598. [[CrossRef](#)] [[PubMed](#)]
4. Kalluri, R.; Zeisberg, M. Fibroblasts in cancer. *Nat. Rev. Cancer* **2006**, *6*, 392–401. [[CrossRef](#)]
5. D’Arcangelo, E.; Wu, N.C.; Cadavid, J.L.; McGuigan, A.P. The life cycle of cancer-associated fibroblasts within the tumour stroma and its importance in disease outcome. *Br. J. Cancer* **2020**. [[CrossRef](#)]
6. Junttila, M.R.; De Sauvage, F.J. Influence of tumour micro-environment heterogeneity on therapeutic response. *Nature* **2013**, *501*, 346–354. [[CrossRef](#)]
7. Turley, S.J.; Cremasco, V.; Astarita, J.L. Immunological hallmarks of stromal cells in the tumour microenvironment. *Nat. Rev. Immunol.* **2015**, *15*, 669–682. [[CrossRef](#)]
8. Gilkes, D.M.; Semenza, G.L.; Wirtz, D. Hypoxia and the extracellular matrix: Drivers of tumour metastasis. *Nat. Rev. Cancer* **2014**, *14*, 430–439. [[CrossRef](#)]
9. Iyer, S.P.; Hunt, C.R.; Pandita, T.K. Cross Talk between Radiation and Immunotherapy: The Twain Shall Meet. *Radiat. Res.* **2018**, *189*, 219–224. [[CrossRef](#)]
10. Barcellos-Hoff, M.H.; Park, C.; Wright, E.G. Radiation and the microenvironment—Tumorigenesis and therapy. *Nat. Rev. Cancer* **2005**, *5*, 867–875. [[CrossRef](#)]
11. McLaughlin, M.; Patin, E.C.; Pedersen, M.; Wilkins, A.; Dillon, M.T.; Melcher, A.A.; Harrington, K.J. Inflammatory microenvironment remodelling by tumour cells after radiotherapy. *Nat. Rev. Cancer* **2020**. [[CrossRef](#)] [[PubMed](#)]
12. Barker, H.E.; Paget, J.T.E.; Khan, A.A.; Harrington, K.J. The tumour microenvironment after radiotherapy: Mechanisms of resistance and recurrence. *Nat. Rev. Cancer* **2015**, *15*, 409–425. [[CrossRef](#)] [[PubMed](#)]
13. Weichselbaum, R.R.; Liang, H.; Deng, L.; Fu, Y.X. Radiotherapy and immunotherapy: A beneficial liaison? *Nat. Rev. Clin. Oncol.* **2017**, *14*, 365–379. [[CrossRef](#)] [[PubMed](#)]
14. Hwang, W.L.; Pike, L.R.G.; Royce, T.J.; Mahal, B.A.; Loeffler, J.S. Safety of combining radiotherapy with immune-checkpoint inhibition. *Nat. Rev. Clin. Oncol.* **2018**, *15*, 477–494. [[CrossRef](#)]
15. Schae, D.; McBride, W.H. Opportunities and challenges of radiotherapy for treating cancer. *Nat. Rev. Clin. Oncol.* **2015**, *12*, 527–540. [[CrossRef](#)]
16. Grassberger, C.; Ellsworth, S.G.; Wilks, M.Q.; Keane, F.K.; Loeffler, J.S. Assessing the interactions between radiotherapy and antitumour immunity. *Nat. Rev. Clin. Oncol.* **2019**, *16*, 729–745. [[CrossRef](#)]
17. Van Leeuwen, C.M.; Oei, A.L.; Crezee, J.; Bel, A.; Franken, N.A.P.; Stalpers, L.J.A.; Kok, H.P. The alfa and beta of tumours: A review of parameters of the linear-quadratic model, derived from clinical radiotherapy studies. *Radiat. Oncol.* **2018**, *13*, 96. [[CrossRef](#)]
18. Hall, E.; Giaccia, A. Cell survival curves. In *Radiobiology for the Radiologist*, 7th ed.; Lippincott Williams & Wilkins: Philadelphia, PA, USA, 2012; pp. 35–53.
19. Papiez, L.; Timmerman, R. Hypofractionation in radiation therapy and its impact. *Med. Phys.* **2008**, *35*, 112–118. [[CrossRef](#)]
20. Mahajan, A.; Ahmed, S.; McAleer, M.F.; Weinberg, J.S.; Li, J.; Brown, P.; Settle, S.; Prabhu, S.S.; Lang, F.F.; Levine, N.; et al. Post-operative stereotactic radiosurgery versus observation for completely resected brain metastases: A single-centre, randomised, controlled, phase 3 trial. *Lancet Oncol.* **2017**, *18*, 1040–1048. [[CrossRef](#)]

21. Qiu, H.; Moravan, M.J.; Milano, M.T.; Usuki, K.Y.; Katz, A.W. SBRT for Hepatocellular Carcinoma: 8-Year Experience from a Regional Transplant Center. *J. Gastrointest. Cancer* **2018**, *49*, 463–469. [[CrossRef](#)]
22. Kishan, A.U.; King, C.R. Stereotactic Body Radiotherapy for Low- and Intermediate-Risk Prostate Cancer. *Semin. Radiat. Oncol.* **2017**, *27*, 268–278. [[CrossRef](#)] [[PubMed](#)]
23. Aridgides, P.; Bogart, J. Stereotactic Body Radiation Therapy for Stage I Non-Small Cell Lung Cancer. *Thorac. Surg. Clin.* **2016**, *26*, 261–269. [[CrossRef](#)] [[PubMed](#)]
24. Mole, R.H. Whole body irradiation; radiobiology or medicine? *Br. J. Radiol.* **1953**, *26*, 234–241. [[CrossRef](#)] [[PubMed](#)]
25. Dewan, M.Z.; Galloway, A.E.; Kawashima, N.; Dewyngaert, J.K.; Babb, J.S.; Formenti, S.C.; Demaria, S. Fractionated but not single-dose radiotherapy induces an immune-mediated abscopal effect when combined with anti-CTLA-4 antibody. *Clin. Cancer Res.* **2009**, *15*, 5379–5388. [[CrossRef](#)] [[PubMed](#)]
26. Lee, Y.; Auh, S.L.; Wang, Y.; Burnette, B.; Wang, Y.; Meng, Y.; Beckett, M.; Sharma, R.; Chin, R.; Tu, T.; et al. Therapeutic effects of ablative radiation on local tumor require CD8+ T cells: Changing strategies for cancer treatment. *Blood* **2009**, *114*, 589–595. [[CrossRef](#)]
27. Reits, E.A.; Hodge, J.W.; Herberths, C.A.; Groothuis, T.A.; Chakraborty, M.; Wansley, E.K.; Camphausen, K.; Luiten, R.M.; de Ru, A.H.; Neijssen, J.; et al. Radiation modulates the peptide repertoire, enhances MHC class I expression, and induces successful antitumor immunotherapy. *J. Exp. Med.* **2006**, *203*, 1259–1271. [[CrossRef](#)]
28. Reynders, K.; Illidge, T.; Siva, S.; Chang, J.Y.; De Ruyscher, D. The abscopal effect of local radiotherapy: Using immunotherapy to make a rare event clinically relevant. *Cancer Treat. Rev.* **2015**, *41*, 503–510. [[CrossRef](#)]
29. Riaz, N.; Morris, L.; Havel, J.J.; Makarov, V.; Desrichard, A.; Chan, T.A. The role of neoantigens in response to immune checkpoint blockade. *Int. Immunol.* **2016**, *28*, 411–419. [[CrossRef](#)]
30. Leroi, N.; Lallemand, F.; Coucke, P.; Noel, A.; Martinive, P. Impacts of ionizing radiation on the different compartments of the tumor microenvironment. *Front. Pharmacol.* **2016**, *7*, 1–9. [[CrossRef](#)]
31. Straub, J.M.; New, J.; Hamilton, C.D.; Lominska, C.; Shnyder, Y.; Thomas, S.M. Radiation-induced fibrosis: Mechanisms and implications for therapy. *J. Cancer Res. Clin. Oncol.* **2015**, *141*, 1985–1994. [[CrossRef](#)]
32. Arnold, K.M.; Flynn, N.J.; Raben, A.; Romak, L.; Yu, Y.; Dicker, A.P.; Mourtada, F.; Sims-Mourtada, J. The Impact of Radiation on the Tumor Microenvironment: Effect of Dose and Fractionation Schedules. *Cancer Growth Metastasis* **2018**, *11*. [[CrossRef](#)] [[PubMed](#)]
33. Penney, D.P.; Wayne, A.; Rosenkrans, J. Cell-Cell Matrix Interactions in Induced Lung Injury: I. The Effects of X-Irradiation on Basal Laminar Proteoglycans. *Radiat. Res.* **1984**, *99*, 410–419. [[CrossRef](#)] [[PubMed](#)]
34. Barcellos-Hoff, M.H. Radiation-induced Transforming Growth Factor β and Subsequent Extracellular Matrix Reorganization in Murine Mammary Gland. *Cancer Res.* **1993**, *53*, 3880–3886. [[PubMed](#)]
35. Remy, J.; Wegrowski, J.; Crechet, F.; Martin, M.; Daburon, F. Long-Term Overproduction of Collagen in Radiation-Induced Fibrosis. *Radiat. Res.* **1991**, *125*, 14–19. [[CrossRef](#)]
36. Chargari, C.; Clemenson, C.; Martins, I.; Perfettini, J.-L.; Deutsch, E. Understanding the functions of tumor stroma in resistance to ionizing radiation: Emerging targets for pharmacological modulation. *Drug Resist. Updat.* **2013**, *16*, 10–21. [[CrossRef](#)]
37. Kamochi, N.; Nakashima, M.; Aoki, S.; Uchihashi, K.; Sugihara, H.; Toda, S.; Kudo, S. Irradiated fibroblast-induced bystander effects on invasive growth of squamous cell carcinoma under cancer-stromal cell interaction. *Cancer Sci.* **2008**, *99*, 2417–2427. [[CrossRef](#)]
38. Ohuchida, K.; Mizumoto, K.; Murakami, M.; Qian, L.W.; Sato, N.; Nagai, E.; Matsumoto, K.; Nakamura, T.; Tanaka, M. Radiation to Stromal Fibroblasts Increases Invasiveness of Pancreatic Cancer Cells through Tumor-Stromal Interactions. *Cancer Res.* **2004**, *64*, 3215–3222. [[CrossRef](#)]
39. Tommelein, J.; Verset, L.; Boterberg, T.; Demetter, P.; Bracke, M.; De Wever, O. Cancer-Associated Fibroblasts Connect Metastasis-Promoting Communication in Colorectal Cancer. *Front. Oncol.* **2015**, *5*, 1–11. [[CrossRef](#)]
40. Wang, Z.; Tang, Y.; Tan, Y.; Wei, Q.; Yu, W. Cancer-associated fibroblasts in radiotherapy: Challenges and new opportunities. *Cell Commun. Signal.* **2019**, *17*, 1–12. [[CrossRef](#)]
41. Boelens, M.C.; Wu, T.J.; Nabet, B.Y.; Xu, B.; Qiu, Y.; Yoon, T.; Azzam, D.J.; Twyman-Saint Victor, C.; Wiemann, B.Z.; Ishwaran, H.; et al. Exosome transfer from stromal to breast cancer cells regulates therapy resistance pathways. *Cell* **2014**, *159*, 499–513. [[CrossRef](#)]

42. Hwang, R.F.; Moore, T.; Arumugam, T.; Ramachandran, V.; Amos, K.D.; Rivera, A.; Ji, B.; Evans, D.B.; Logsdon, C.D. Cancer-associated stromal fibroblasts promote pancreatic tumor progression. *Cancer Res.* **2008**, *68*, 918–926. [[CrossRef](#)] [[PubMed](#)]
43. Hardee, M.E.; Marciscano, A.E.; Medina-Ramirez, C.M.; Zagzag, D.; Narayana, A.; Lonning, S.M.; Barcellos-Hoff, M.H. Resistance of glioblastoma-initiating cells to radiation mediated by the tumor microenvironment can be abolished by inhibiting transforming growth factor- β . *Cancer Res.* **2012**, *72*, 4119–4129. [[CrossRef](#)] [[PubMed](#)]
44. Wang, Y.; Gan, G.; Wang, B.; Wu, J.; Cao, Y.; Zhu, D.; Xu, Y.; Wang, X.; Han, H.; Li, X.; et al. Cancer-associated Fibroblasts Promote Irradiated Cancer Cell Recovery Through Autophagy. *EBioMedicine* **2017**, *17*, 45–56. [[CrossRef](#)] [[PubMed](#)]
45. Acharyya, S.; Oskarsson, T.; Vanharanta, S.; Malladi, S.; Kim, J.; Morris, P.G.; Manova-Todorova, K.; Leversha, M.; Hogg, N.; Seshan, V.E.; et al. A CXCL1 paracrine network links cancer chemoresistance and metastasis. *Cell* **2012**, *150*, 165–178. [[CrossRef](#)]
46. Zhang, H.; Yue, J.; Jiang, Z.; Zhou, R.; Xie, R.; Xu, Y.; Wu, S. CAF-secreted CXCL1 conferred radioresistance by regulating DNA damage response in a ROS-dependent manner in esophageal squamous cell carcinoma. *Cell Death Dis.* **2017**, *8*, e2790. [[CrossRef](#)]
47. Downward, J. Targeting RAS signalling pathways in cancer therapy. *Nat. Rev. Cancer* **2003**, *3*, 11–22. [[CrossRef](#)]
48. Dhillon, A.S.; Hagan, S.; Rath, O.; Kolch, W. MAP kinase signalling pathways in cancer. *Oncogene* **2007**, *26*, 3279–3290. [[CrossRef](#)]
49. Cordes, N. Integrin-mediated cell-matrix interactions for prosurvival and antiapoptotic signaling after genotoxic injury. *Cancer Lett.* **2006**, *242*, 11–19. [[CrossRef](#)]
50. Mantoni, T.S.; Lunardi, S.; Al-Assar, O.; Masamune, A.; Brunner, T.B. Pancreatic stellate cells radioprotect pancreatic cancer cells through β 1-integrin signaling. *Cancer Res.* **2011**, *71*, 3453–3458. [[CrossRef](#)]
51. Al-Assar, O.; Demiciorglu, F.; Lunardi, S.; Gaspar-Carvalho, M.M.; McKenna, W.G.; Muschel, R.M.; Brunner, T.B. Contextual regulation of pancreatic cancer stem cell phenotype and radioresistance by pancreatic stellate cells. *Radiother. Oncol.* **2014**, *111*, 243–251. [[CrossRef](#)]
52. Chen, W.J.; Ho, C.C.; Chang, Y.L.; Chen, H.Y.; Lin, C.A.; Ling, T.Y.; Yu, S.L.; Yuan, S.S.; Louisa Chen, Y.J.; Lin, C.Y.; et al. Cancer-associated fibroblasts regulate the plasticity of lung cancer stemness via paracrine signalling. *Nat. Commun* **2014**, *5*. [[CrossRef](#)] [[PubMed](#)]
53. Osuka, S.; Sampetean, O.; Shimizu, T.; Saga, I.; Onishi, N.; Sugihara, E.; Okubo, J.; Fujita, S.; Takano, S.; Matsumura, A.; et al. IGF1 receptor signaling regulates adaptive radioprotection in glioma stem cells. *Stem Cells* **2013**, *31*, 627–640. [[CrossRef](#)] [[PubMed](#)]
54. Hawsawi, N.M.; Ghebeh, H.; Hendrayani, S.F.; Tulbah, A.; Al-Eid, M.; Al-Tweigeri, T.; Ajarim, D.; Alaiya, A.; Dermime, S.; Aboussekhra, A. Breast carcinoma-associated fibroblasts and their counterparts display neoplastic-specific changes. *Cancer Res.* **2008**, *68*, 2717–2725. [[CrossRef](#)] [[PubMed](#)]
55. Tang, F.R.; Loke, W.K. Molecular mechanisms of low dose ionizing radiation-induced hormesis, adaptive responses, radioresistance, bystander effects, and genomic instability. *Int. J. Radiat. Biol.* **2015**, *91*, 13–27. [[CrossRef](#)]
56. Sun, Y.; Campisi, J.; Higano, C.; Beer, T.M.; Porter, P.; Coleman, I.; True, L.; Nelson, P.S. Treatment-induced damage to the tumor microenvironment promotes prostate cancer therapy resistance through WNT16B. *Nat. Med.* **2012**, *18*, 1359–1368. [[CrossRef](#)]
57. Tsai, K.K.C.; Stuart, J.; Chuang, Y.-Y.E.; Little, J.B.; Yuan, Z.-M. Low-Dose Radiation-Induced Senescent Stromal Fibroblasts Render Nearby Breast Cancer Cells Radioresistant. *Radiat. Res.* **2009**, *172*, 306–313. [[CrossRef](#)]
58. Pazolli, E.; Alspach, E.; Milczarek, A.; Prior, J.; Piwnica-Worms, D.; Stewart, S.A. Chromatin remodeling underlies the senescence-associated secretory phenotype of tumor stromal fibroblasts that supports cancer progression. *Cancer Res.* **2012**, *72*, 2251–2261. [[CrossRef](#)]
59. Li, D.; Qu, C.; Ning, Z.; Wang, H.; Zang, K.; Zhuang, L.; Chen, L.; Wang, P.; Meng, Z. Radiation promotes epithelial-to-mesenchymal transition and invasion of pancreatic cancer cell by activating carcinoma-associated fibroblasts. *Am. J. Cancer Res.* **2016**, *6*, 2192–2206.

60. Hellevik, T.; Pettersen, I.; Berg, V.; Winberg, J.O.; Moe, B.T.; Bartnes, K.; Paulssen, R.H.; Busund, L.T.; Bremnes, R.; Chalmers, A.; et al. Cancer-associated fibroblasts from human NSCLC survive ablative doses of radiation but their invasive capacity is reduced. *Radiat. Oncol.* **2012**, *7*. [[CrossRef](#)]
61. Özdemir, B.C.; Pentcheva-Hoang, T.; Carstens, J.L.; Zheng, X.; Wu, C.C.; Simpson, T.R.; Laklai, H.; Sugimoto, H.; Kahlert, C.; Novitskiy, S.V.; et al. Depletion of carcinoma-associated fibroblasts and fibrosis induces immunosuppression and accelerates pancreas cancer with reduced survival. *Cancer Cell* **2014**, *25*, 719–734. [[CrossRef](#)]
62. Rhim, A.D.; Oberstein, P.E.; Thomas, D.H.; Mirek, E.T.; Palermo, C.F.; Sastra, S.A.; Dekleva, E.N.; Saunders, T.; Becerra, C.P.; Tattersall, I.W.; et al. Stromal elements act to restrain, rather than support, pancreatic ductal adenocarcinoma. *Cancer Cell* **2014**, *25*, 735–747. [[CrossRef](#)] [[PubMed](#)]
63. Biffi, G.; Oni, T.E.; Spielman, B.; Hao, Y.; Elyada, E.; Park, Y.; Preall, J.; Tuveson, D.A. IL1-Induced JAK/STAT Signaling Is Antagonized by TGF β to Shape CAF Heterogeneity in Pancreatic Ductal Adenocarcinoma. *Cancer Discov.* **2019**, *9*, 282. [[CrossRef](#)] [[PubMed](#)]
64. Elyada, E.; Bolisetty, M.; Laise, P.; Flynn, W.F.; Courtois, E.T.; Burkhart, R.A.; Teinor, J.A.; Belleau, P.; Biffi, G.; Lucito, M.S.; et al. Cross-species single-cell analysis of pancreatic ductal adenocarcinoma reveals antigen-presenting cancer-associated fibroblasts. *Cancer Discov.* **2019**. [[CrossRef](#)] [[PubMed](#)]
65. Öhlund, D.; Handly-Santana, A.; Biffi, G.; Elyada, E.; Almeida, A.S.; Ponz-Sarvisé, M.; Corbo, V.; Oni, T.E.; Hearn, S.A.; Lee, E.J.; et al. Distinct populations of inflammatory fibroblasts and myofibroblasts in pancreatic cancer. *J. Exp. Med.* **2017**, *214*, 579–596. [[CrossRef](#)]
66. Jiang, H.; Hegde, S.; DeNardo, D.G. Tumor-associated fibrosis as a regulator of tumor immunity and response to immunotherapy. *Cancer Immunol. Immunother.* **2017**, *66*, 1037–1048. [[CrossRef](#)]
67. Lu, P.; Weaver, V.M.; Werb, Z. The extracellular matrix: A dynamic niche in cancer progression. *J. Cell Biol.* **2012**, *196*, 395–406. [[CrossRef](#)]
68. Poltavets, V.; Kochetkova, M.; Pitson, S.M.; Samuel, M.S. The Role of the Extracellular Matrix and Its Molecular and Cellular Regulators in Cancer Cell Plasticity. *Front. Oncol.* **2018**, *8*, 431. [[CrossRef](#)]
69. Weichselbaum, R.R.; Ishwaran, H.; Yoon, T.; Nuyten, D.S.A.; Baker, S.W.; Khodarev, N.; Su, A.W.; Shaikh, A.Y.; Roach, P.; Kreike, B.; et al. An interferon-related gene signature for DNA damage resistance is a predictive marker for chemotherapy and radiation for breast cancer. *Proc. Natl. Acad. Sci. USA* **2008**, *105*, 18490–18495. [[CrossRef](#)]
70. Puthawala, K.; Hadjiangelis, N.; Jacoby, S.C.; Bayongan, E.; Zhao, Z.; Yang, Z.; Devitt, M.L.; Horan, G.S.; Weinreb, P.H.; Lukashev, M.E.; et al. Inhibition of integrin $\alpha\beta 6$, an activator of latent transforming growth factor- β , prevents radiation-induced lung fibrosis. *Am. J. Respir. Crit. Care Med.* **2008**, *177*, 82–90. [[CrossRef](#)]
71. Park, C.C.; Zhang, H.; Pallavicini, M.; Gray, J.W.; Baehner, F.; Park, C.J.; Bissell, M.J. B1 Integrin Inhibitory Antibody Induces Apoptosis of Breast Cancer Cells, Inhibits Growth, and Distinguishes Malignant from Normal Phenotype in Three Dimensional Cultures and in Vivo. *Cancer Res.* **2006**, *66*, 1526–1535. [[CrossRef](#)]
72. Park, C.C.; Zhang, H.J.; Yao, E.S.; Park, C.J.; Bissell, M.J. B1 Integrin Inhibition Dramatically Enhances Radiotherapy Efficacy in Human Breast Cancer Xenografts. *Cancer Res.* **2008**, *68*, 4398–4405. [[CrossRef](#)] [[PubMed](#)]
73. Cordes, N.; Seidler, J.; Durzok, R.; Geinitz, H.; Brakebusch, C. B1-Integrin-Mediated Signaling Essentially Contributes to Cell Survival After Radiation-Induced Genotoxic Injury. *Oncogene* **2006**, *25*, 1378–1390. [[CrossRef](#)] [[PubMed](#)]
74. Biswas, S.; Freeman, M.L.; Arteaga, C.L.; Biswas, S.; Guix, M.; Rinehart, C.; Dugger, T.C.; Chytil, A.; Moses, H.L.; Freeman, M.L.; et al. Inhibition of TGF Beta with neutralizing antibodies prevents radiation-induced acceleration of metastatic cancer progression Find the latest version: Inhibition of TGF- β with neutralizing antibodies prevents radiation-induced acceleration of metastatic. *J. Clin. Investig.* **2007**, *117*, 1305–1313. [[CrossRef](#)] [[PubMed](#)]
75. Hellevik, T.; Martinez-Zubiaurre, I. Radiotherapy and the tumor stroma: The importance of dose and fractionation. *Front. Oncol.* **2014**, *4*, 1–12. [[CrossRef](#)]
76. Chetty, C.; Bhoopathi, P.; Rao, J.S.; Lakka, S.S. Inhibition of matrix metalloproteinase-2 enhances radiosensitivity by abrogating radiation-induced FoxM1-mediated G2/M arrest in A549 lung cancer cells. *Int. J. Cancer* **2009**, *124*, 2468–2477. [[CrossRef](#)]
77. Bertout, J.A.; Patel, S.A.; Simon, M.C. The impact of O₂ availability on human cancer. *Nat. Rev. Cancer* **2008**, *8*, 967–975. [[CrossRef](#)]

78. Gray, L.H.; Conger, A.D.; Ebert, M.; Hornsey, S.; Scott, O.C.A. The Concentration of Oxygen Dissolved in Tissues at the Time of Irradiation as a Factor in Radiotherapy. *Br. J. Radiol.* **1953**, *26*, 638–648. [[CrossRef](#)]
79. Brown, J.M. The hypoxic cell: A target for selective cancer therapy—Eighteenth Bruce F. Cain Memorial Award Lecture. *Cancer Res.* **1999**, *59*, 5863–5870.
80. Brown, J.M. Vasculogenesis: A crucial player in the resistance of solid tumours to radiotherapy. *Br. J. Radiol.* **2014**, *87*. [[CrossRef](#)]
81. Frérart, F.; Sonveaux, P.; Rath, G.; Smoos, A.; Meqor, A.; Charlier, N.; Jordan, B.F.; Saliez, J.; Noel, A.; Dessy, C.; et al. The acidic tumor microenvironment promotes the reconversion of nitrite into nitric oxide: Towards a new and safe radiosensitizing strategy. *Clin. Cancer Res.* **2008**, *14*, 2768–2774. [[CrossRef](#)]
82. Mitchell, J.B.; Wink, D.A.; DeGraff, W.; Gamson, J.; Keefer, L.K.; Krishna, M.C. Hypoxic mammalian cell radiosensitization by nitric oxide. *Cancer Res.* **1993**, *53*, 5845–5848. [[PubMed](#)]
83. Winkler, F.; Kozin, S.V.; Tong, R.T.; Chae, S.-S.; Booth, M.F.; Garkavtsev, I.; Xu, L.; Hicklin, D.J.; Fukumura, D.; di Tomaso, E.; et al. Kinetics of vascular normalization by VEGFR2 blockade governs brain tumor response to radiation. *Cancer Cell* **2004**, *6*, 553–563. [[CrossRef](#)] [[PubMed](#)]
84. Ansiaux, R.; Baudelet, C.; Jordan, B.F.; Beghein, N.; Sonveaux, P.; De Wever, J.; Martinive, P.; Grégoire, V.; Feron, O.; Gallez, B. Thalidomide radiosensitizes tumors through early changes in the tumor microenvironment. *Clin. Cancer Res.* **2005**, *11*, 743–750.
85. Crockart, N.; Radermacher, K.; Jordan, B.F.; Baudelet, C.; Cron, G.O.; Grégoire, V.; Beghein, N.; Bouzin, C.; Feron, O.; Gallez, B. Tumor radiosensitization by antiinflammatory drugs: Evidence for a new mechanism involving the oxygen effect. *Cancer Res.* **2005**, *65*, 7911–7916. [[CrossRef](#)] [[PubMed](#)]
86. Demaria, S.; Formenti, S.C. Radiation as an immunological adjuvant: Current evidence on dose and fractionation. *Front. Oncol.* **2012**, *2*, 1–7. [[CrossRef](#)]
87. Formenti, S.C.; Rudqvist, N.P.; Golden, E.; Cooper, B.; Wennerberg, E.; Lhuillier, C.; Vanpouille-Box, C.; Friedman, K.; Ferrari de Andrade, L.; Wucherpfennig, K.W.; et al. Radiotherapy induces responses of lung cancer to CTLA-4 blockade. *Nat. Med.* **2018**, *24*, 1845–1851. [[CrossRef](#)]
88. Golden, E.B.; Frances, D.; Pellicciotta, I.; Demaria, S.; Helen Barcellos-Hoff, M.; Formenti, S.C. Radiation fosters dose-dependent and chemotherapy-induced immunogenic cell death. *Oncoimmunology* **2014**, *3*, e28518. [[CrossRef](#)]
89. Harding, S.M.; Benci, J.L.; Irianto, J.; Discher, D.E.; Minn, A.J.; Greenberg, R.A. Mitotic progression following DNA damage enables pattern recognition within micronuclei. *Nature* **2017**, *548*, 466–470. [[CrossRef](#)]
90. Dillon, M.T.; Bergerhoff, K.F.; Pedersen, M.; Whittock, H.; Crespo-Rodriguez, E.; Patin, E.C.; Pearson, A.; Smith, H.G.; Paget, J.T.E.; Patel, R.R.; et al. ATR Inhibition Potentiates the Radiation-induced Inflammatory Tumor Microenvironment. *Clin. Cancer Res.* **2019**, *25*, 3392–3403. [[CrossRef](#)]
91. Mackenzie, K.J.; Carroll, P.; Martin, C.A.; Murina, O.; Fluteau, A.; Simpson, D.J.; Olova, N.; Sutcliffe, H.; Rainger, J.K.; Leitch, A.; et al. cGAS surveillance of micronuclei links genome instability to innate immunity. *Nature* **2017**, *548*, 461–465. [[CrossRef](#)]
92. Blair, T.C.; Bambina, S.; Alice, A.F.; Kramer, F.; Medler, T.R.; Baird, J.R.; Broz, M.L.; Tormoen, G.W.; Troesch, V.; Crittenden, M.R.; et al. Dendritic Cell Maturation Defines Immunological Responsiveness of Tumors to Radiation Therapy. *J. Immunol.* **2020**, *204*. [[CrossRef](#)] [[PubMed](#)]
93. Gupta, A.; Probst, H.C.; Vuong, V.; Landshammer, A.; Muth, S.; Yagita, H.; Schwendener, R.; Pruschy, M.; Knuth, A.; van den Broek, M. Radiotherapy Promotes Tumor-Specific Effector CD8 + T Cells via Dendritic Cell Activation. *J. Immunol.* **2012**, *189*, 558–566. [[CrossRef](#)] [[PubMed](#)]
94. Gerber, S.A.; Sedlacek, A.L.; Cron, K.R.; Murphy, S.P.; Frelinger, J.G.; Lord, E.M. IFN- γ mediates the antitumor effects of radiation therapy in a murine colon tumor. *Am. J. Pathol.* **2013**, *182*, 2345–2354. [[CrossRef](#)] [[PubMed](#)]
95. Filatenkov, A.; Baker, J.; Mueller, A.M.S.; Kenkel, J.; Ahn, G.O.; Dutt, S.; Zhang, N.; Kohrt, H.; Jensen, K.; Dejbakhsh-Jones, S.; et al. Ablative tumor radiation can change the tumor immune cell microenvironment to induce durable complete remissions. *Clin. Cancer Res.* **2015**, *21*, 3727–3739. [[CrossRef](#)]
96. Sharabi, A.B.; Nirschl, C.J.; Kochel, C.M.; Nirschl, T.R.; Francica, B.J.; Velarde, E.; Deweese, T.L.; Drake, C.G. Stereotactic radiation therapy augments antigen-specific PD-1-mediated antitumor immune responses via cross-presentation of tumor antigen. *Cancer Immunol. Res.* **2015**, *3*, 345–355. [[CrossRef](#)]

97. Yoshimoto, Y.; Suzuki, Y.; Mimura, K.; Ando, K.; Oike, T.; Sato, H.; Okonogi, N.; Maruyama, T.; Izawa, S.; Noda, S.E.; et al. Radiotherapy-induced anti-tumor immunity contributes to the therapeutic efficacy of irradiation and can be augmented by CTLA-4 blockade in a mouse model. *PLoS ONE* **2014**, *9*, e92572. [[CrossRef](#)]
98. Gerber, S.A.; Lim, J.Y.H.; Connolly, K.A.; Sedlacek, A.L.; Barlow, M.L.; Murphy, S.P.; Egilmez, N.K.; Lord, E.M. Radio-responsive tumors exhibit greater intratumoral immune activity than nonresponsive tumors. *Int. J. Cancer* **2014**, *134*, 2383–2392. [[CrossRef](#)]
99. Vanpouille-Box, C.; Diamond, J.M.; Pilonis, K.A.; Zavadil, J.; Babb, J.S.; Formenti, S.C.; Barcellos-Hoff, M.H.; Demaria, S. TGF β Is a Master Regulator of Radiation Therapy-Induced Antitumor Immunity. *Cancer Res.* **2015**, *75*, 2232–2242. [[CrossRef](#)]
100. Deng, L.; Liang, H.; Burnette, B.; Beckett, M.; Darga, T.; Weichselbaum, R.R.; Fu, Y.X. Irradiation and anti-PD-L1 treatment synergistically promote antitumor immunity in mice. *J. Clin. Investig.* **2014**, *124*, 687–695. [[CrossRef](#)]
101. Dovedi, S.J.; Adlard, A.L.; Lipowska-Bhalla, G.; McKenna, C.; Jones, S.; Cheadle, E.J.; Stratford, I.J.; Poon, E.; Morrow, M.; Stewart, R.; et al. Acquired resistance to fractionated radiotherapy can be overcome by concurrent PD-L1 blockade. *Cancer Res.* **2014**, *74*, 5458–5468. [[CrossRef](#)]
102. Park, S.S.; Dong, H.; Liu, X.; Harrington, S.M.; Krco, C.J.; Grams, M.P.; Mansfield, A.S.; Furutani, K.M.; Olivier, K.R.; Kwon, E.D. PD-1 Restrains Radiotherapy-Induced Abscopal Effect. *Cancer Immunol. Res.* **2015**, *3*, 610–619. [[CrossRef](#)] [[PubMed](#)]
103. Formenti, S.C.; Demaria, S. Systemic effects of local radiotherapy. *Lancet Oncol.* **2009**, *10*, 718–726. [[CrossRef](#)]
104. Shaverdian, N.; Lisberg, A.E.; Bornazyan, K.; Veruttipong, D.; Goldman, J.W.; Formenti, S.C.; Garon, E.B.; Lee, P. Previous radiotherapy and the clinical activity and toxicity of pembrolizumab in the treatment of non-small-cell lung cancer: A secondary analysis of the KEYNOTE-001 phase 1 trial. *Lancet Oncol.* **2017**, *18*, 895–903. [[CrossRef](#)]
105. Kang, J.; Demaria, S.; Formenti, S. Current clinical trials testing the combination of immunotherapy with radiotherapy. *J. Immunother. Cancer* **2016**, *4*, 51. [[CrossRef](#)] [[PubMed](#)]
106. Milas, L. Tumor Bed Effect in Murine Tumors: Relationship to Tumor Take and Tumor Macrophage Content. *Radiat. Res.* **1990**, *123*, 232. [[CrossRef](#)] [[PubMed](#)]
107. Vatner, R.E.; Formenti, S.C. Myeloid-derived cells in tumors: Effects of radiation. *Semin. Radiat. Oncol.* **2015**, *25*, 18–27. [[CrossRef](#)] [[PubMed](#)]
108. Xu, J.; Escamilla, J.; Mok, S.; David, J.; Priceman, S.; West, B.; Bollag, G.; McBride, W.; Wu, L. CSF1R signaling blockade stanches tumor-infiltrating myeloid cells and improves the efficacy of radiotherapy in prostate cancer. *Cancer Res.* **2013**, *73*, 2782–2794. [[CrossRef](#)]
109. Ceradini, D.J.; Kulkarni, A.R.; Callaghan, M.J.; Tepper, O.M.; Bastidas, N.; Kleinman, M.E.; Capla, J.M.; Galiano, R.D.; Levine, J.P.; Gurtner, G.C. Progenitor cell trafficking is regulated by hypoxic gradients through HIF-1 induction of SDF-1. *Nat. Med.* **2004**, *10*, 858–864. [[CrossRef](#)]
110. Meng, Y.; Beckett, M.A.; Liang, H.; Mauceri, H.J.; Van Rooijen, N.; Cohen, K.S.; Weichselbaum, R.R. Blockade of tumor necrosis factor α signaling in tumor-associated macrophages as a radiosensitizing strategy. *Cancer Res.* **2010**, *70*, 1534–1543. [[CrossRef](#)]
111. Prakash, H.; Klug, F.; Nadella, V.; Mazumdar, V.; Schmitz-Winnenthal, H.; Umansky, L. Low doses of gamma irradiation potentially modifies immunosuppressive tumor microenvironment by retuning tumor-associated macrophages: Lesson from insulinoma. *Carcinogenesis* **2016**, *37*, 301–313. [[CrossRef](#)]
112. Klug, F.; Prakash, H.; Huber, P.E.; Seibel, T.; Bender, N.; Halama, N.; Pfirschke, C.; Voss, R.H.; Timke, C.; Umansky, L.; et al. Low-dose irradiation programs macrophage differentiation to an iNOS⁺/M1 phenotype that orchestrates effective T cell immunotherapy. *Cancer Cell* **2013**, *24*, 589–602. [[CrossRef](#)] [[PubMed](#)]
113. Chiang, C.S.; Fu, S.Y.; Wang, S.C.; Yu, C.F.; Chen, F.H.; Lin, C.M.; Hong, J.H. Irradiation promotes an m2 macrophage phenotype in tumor hypoxia. *Front. Oncol.* **2012**, *2*, 89. [[CrossRef](#)] [[PubMed](#)]
114. Okubo, M.; Kioi, M.; Nakashima, H.; Sugiura, K.; Mitsudo, K.; Aoki, I.; Taniguchi, H.; Tohno, I. M2-polarized macrophages contribute to neovasculogenesis, leading to relapse of oral cancer following radiation. *Sci. Rep.* **2016**, *6*, 27548. [[CrossRef](#)] [[PubMed](#)]
115. Seifert, L.; Werba, G.; Tiwari, S.; Giao Ly, N.N.; Nguy, S.; Alothman, S.; Alqunaibit, D.; Avanzi, A.; Daley, D.; Barilla, R.; et al. Radiation Therapy Induces Macrophages to Suppress T-Cell Responses Against Pancreatic Tumors in Mice. *Gastroenterology* **2016**, *150*, 1659–1672. [[CrossRef](#)] [[PubMed](#)]

116. Crittenden, M.R.; Cottam, B.; Savage, T.; Nguyen, C.; Newell, P.; Gough, M.J. Expression of NF- κ B p50 in tumor stroma limits the control of tumors by radiation therapy. *PLoS ONE* **2012**, *7*, e39295. [[CrossRef](#)] [[PubMed](#)]
117. Shiao, S.L.; Ruffell, B.; DeNardo, D.G.; Faddegon, B.A.; Park, C.C.; Coussens, L.M. TH2-polarized CD4+ T Cells and macrophages limit efficacy of radiotherapy. *Cancer Immunol. Res.* **2015**, *3*, 518–525. [[CrossRef](#)]
118. Chen, H.M.; Ma, G.; Gildener-Leapman, N.; Eisenstein, S.; Coakley, B.A.; Ozao, J.; Mandeli, J.; Divino, C.; Schwartz, M.; Sung, M.; et al. Myeloid-derived suppressor cells as an immune parameter in patients with concurrent sunitinib and stereotactic body radiotherapy. *Clin. Cancer Res.* **2015**, *21*, 4073–4085. [[CrossRef](#)] [[PubMed](#)]
119. Ko, J.S.; Zea, A.H.; Rini, B.I.; Ireland, J.L.; Elson, P.; Cohen, P.; Golshayan, A.; Rayman, P.A.; Wood, L.; Garcia, J.; et al. Sunitinib mediates reversal of myeloid-derived suppressor cell accumulation in renal cell carcinoma patients. *Clin. Cancer Res.* **2009**, *15*, 2148–2157. [[CrossRef](#)]
120. Persa, E.; Balogh, A.; Sáfrány, G.; Lumniczky, K. The effect of ionizing radiation on regulatory T cells in health and disease. *Cancer Lett.* **2015**, *368*, 252–261. [[CrossRef](#)]
121. Facciabene, A.; Motz, G.T.; Coukos, G. T-Regulatory cells: Key players in tumor immune escape and angiogenesis. *Cancer Res.* **2012**, *72*, 2162–2171. [[CrossRef](#)]
122. Kachikwu, E.L.; Iwamoto, K.S.; Liao, Y.P.; Demarco, J.J.; Agazaryan, N.; Economou, J.S.; McBride, W.H.; Schaeue, D. Radiation enhances regulatory T cell representation. *Int. J. Radiat. Oncol. Biol. Phys.* **2011**, *81*, 1128–1135. [[CrossRef](#)] [[PubMed](#)]
123. Qinfeng, S.; Depu, W.; Xiaofeng, Y.; Shah, W.; Hongwei, C.; Yili, W. In situ observation of the effects of local irradiation on cytotoxic and regulatory T lymphocytes in cervical cancer tissue. *Radiat. Res.* **2013**, *179*, 584–589. [[CrossRef](#)] [[PubMed](#)]
124. Komatsu, N.; Hori, S. Full restoration of peripheral Foxp3+ regulatory T cell pool by radioresistant host cells in scurfy bone marrow chimeras. *Proc. Natl. Acad. Sci. USA* **2007**, *104*, 8959–8964. [[CrossRef](#)] [[PubMed](#)]
125. Schaeue, D.; Xie, M.W.; Ratikan, J.A.; McBride, W.H. Regulatory T cells in radiotherapeutic responses. *Front. Oncol.* **2012**, *2*, 90. [[CrossRef](#)] [[PubMed](#)]
126. Bos, P.D.; Plitas, G.; Rudra, D.; Lee, S.Y.; Rudensky, A.Y. Transient regulatory T cell ablation deters oncogene-driven breast cancer and enhances radiotherapy. *J. Exp. Med.* **2013**, *210*, 2435–2466. [[CrossRef](#)] [[PubMed](#)]
127. Oweida, A.J.; Darragh, L.; Phan, A.; Binder, D.; Bhatia, S.; Mueller, A.; Court, B.V.; Milner, D.; Raben, D.; Woessner, R.; et al. STAT3 Modulation of Regulatory T Cells in Response to Radiation Therapy in Head and Neck Cancer. *J. Natl. Cancer Inst.* **2019**, *111*, 1339–1349. [[CrossRef](#)] [[PubMed](#)]
128. Oweida, A.; Hararah, M.K.; Phan, A.; Binder, D.; Bhatia, S.; Lennon, S.; Bukkapatnam, S.; Van Court, B.; Uyanga, N.; Darragh, L.; et al. Resistance to Radiotherapy and PD-L1 Blockade Is Mediated by TIM-3 Upregulation and Regulatory T-Cell Infiltration. *Clin. Cancer Res.* **2018**, *24*, 5368–5380. [[CrossRef](#)] [[PubMed](#)]
129. Bhatia, S.; Oweida, A.; Lennon, S.; Darragh, L.B.; Milner, D.; Phan, A.V.; Mueller, A.C.; Van Court, B.; Raben, D.; Serkova, N.J.; et al. Inhibition of EphB4-Ephrin-B2 Signaling Reprograms the Tumor Immune Microenvironment in Head and Neck Cancers. *Cancer Res.* **2019**, *79*, 2722–2735. [[CrossRef](#)]
130. Schaeue, D.; Ratikan, J.A.; Iwamoto, K.S.; McBride, W.H. Maximizing tumor immunity with fractionated radiation. *Int. J. Radiat. Oncol. Biol. Phys.* **2012**, *83*, 1306–1310. [[CrossRef](#)]
131. Lugade, A.A.; Moran, J.P.; Gerber, S.A.; Rose, R.C.; Frelinger, J.G.; Lord, E.M. Local radiation therapy of B16 melanoma tumors increases the generation of tumor antigen-specific effector cells that traffic to the tumor. *J. Immunol.* **2005**, *174*, 7516–7523. [[CrossRef](#)]
132. Apetoh, L.; Ghiringhelli, F.; Tesniere, A.; Obeid, M.; Ortiz, C.; Criollo, A.; Mignot, G.; Maiuri, M.C.; Ullrich, E.; Saulnier, P.; et al. Toll-like receptor 4-dependent contribution of the immune system to anticancer chemotherapy and radiotherapy. *Nat. Med.* **2007**, *13*, 1050–1059. [[CrossRef](#)] [[PubMed](#)]
133. Demaria, S.; Golden, E.B.; Formenti, S.C. Role of Local Radiation Therapy in Cancer Immunotherapy. *JAMA Oncol.* **2015**, *1*, 1325–1332. [[CrossRef](#)] [[PubMed](#)]
134. Obeid, M.; Tesniere, A.; Ghiringhelli, F.; Fimia, G.M.; Apetoh, L.; Perfettini, J.L.; Castedo, M.; Mignot, G.; Panaretakis, T.; Casares, N.; et al. Calreticulin exposure dictates the immunogenicity of cancer cell death. *Nat. Med.* **2007**, *13*, 54–61. [[CrossRef](#)]

135. Ghiringhelli, F.; Apetoh, L.; Tesniere, A.; Aymeric, L.; Ma, Y.; Ortiz, C.; Vermaelen, K.; Panaretakis, T.; Mignot, G.; Ullrich, E.; et al. Activation of the NLRP3 inflammasome in dendritic cells induces IL-1beta-dependent adaptive immunity against tumors. *Nat. Med.* **2009**, *15*, 1170–1178. [[CrossRef](#)] [[PubMed](#)]
136. Gulley, J.L.; Arlen, P.M.; Bastian, A.; Morin, S.; Marte, J.; Beetham, P.; Tsang, K.Y.; Yokokawa, J.; Hodge, J.W.; Ménard, C.; et al. Combining a recombinant cancer vaccine with standard definitive radiotherapy in patients with localized prostate cancer. *Clin. Cancer Res.* **2005**, *11*, 3353–3362. [[CrossRef](#)]
137. Schaeue, D.; Comin-Anduix, B.; Ribas, A.; Zhang, L.; Goodglick, L.; Sayre, J.W.; Debucquoy, A.; Haustermans, K.; McBride, W.H. T-cell responses to survivin in cancer patients undergoing radiation therapy. *Clin. Cancer Res.* **2008**, *14*, 4883–4890. [[CrossRef](#)]
138. Rutkowski, J.; Ślebioda, T.; Kmiec, Z.; Zaucha, R. Changes in systemic immune response after stereotactic ablative radiotherapy. Preliminary results of a prospective study in patients with early lung cancer. *Pol. Arch. Intern. Med.* **2017**, *127*, 245–253. [[CrossRef](#)]
139. Wasserman, J.; Blomgren, H.; Rotstein, S.; Petrini, B.; Hammarström, S. Immunosuppression in irradiated breast cancer patients: In vitro effect of cyclooxygenase inhibitors. *Bull. N. Y. Acad. Med.* **1989**, *65*, 36–44.
140. Rödel, F.; Frey, B.; Manda, K.; Hildebrandt, G.; Hehlhans, S.; Keilholz, L.; Seegenschmiedt, M.H.; Gaipl, U.S.; Rödel, C. Immunomodulatory properties and molecular effects in inflammatory diseases of low-dose x-irradiation. *Front. Oncol.* **2012**, *2*, 120. [[CrossRef](#)]
141. Trowell, O.A. The sensitivity of lymphocytes to ionising radiation. *J. Pathol. Bacteriol.* **1952**, *64*, 687–704. [[CrossRef](#)]
142. Frey, B.; Rückert, M.; Weber, J.; Mayr, X.; Derer, A.; Lotter, M.; Bert, C.; Rödel, F.; Fietkau, R.; Gaipl, U.S. Hypofractionated Irradiation Has Immune Stimulatory Potential and Induces a Timely Restricted Infiltration of Immune Cells in Colon Cancer Tumors. *Front. Immunol.* **2017**, *8*, 231. [[CrossRef](#)] [[PubMed](#)]
143. Panni, R.Z.; Herndon, J.M.; Zuo, C.; Hegde, S.; Hogg, G.D.; Knolhoff, B.L.; Breden, M.A.; Li, X.; Krisnawan, V.E.; Khan, S.Q.; et al. Agonism of CD11b reprograms innate immunity to sensitize pancreatic cancer to immunotherapies. *Sci. Transl. Med.* **2019**, *11*. [[CrossRef](#)] [[PubMed](#)]
144. Hegde, S.; Krisnawan, V.E.; Herzog, B.H.; Zuo, C.; Breden, M.A.; Knolhoff, B.L.; Hogg, G.D.; Tang, J.P.; Baer, J.M.; Mpyoy, C.; et al. Dendritic Cell Paucity Leads to Dysfunctional Immune Surveillance in Pancreatic Cancer. *Cancer Cell* **2020**, *37*, 289–307. [[CrossRef](#)] [[PubMed](#)]
145. Wisdom, A.J.; Hong, C.S.; Lin, A.J.; Xiang, Y.; Cooper, D.E.; Zhang, J.; Xu, E.S.; Kuo, H.C.; Mowery, Y.M.; Carpenter, D.J.; et al. Neutrophils promote tumor resistance to radiation therapy. *Proc. Natl. Acad. Sci. USA* **2019**, *116*, 18584–18589. [[CrossRef](#)] [[PubMed](#)]
146. Matsumura, S.; Demaria, S. Up-regulation of the pro-inflammatory chemokine CXCL16 is a common response of tumor cells to ionizing radiation. *Radiat. Res.* **2010**, *173*, 418–425. [[CrossRef](#)]
147. Matsumura, S.; Wang, B.; Kawashima, N.; Braunstein, S.; Badura, M.; Cameron, T.O.; Babb, J.S.; Schneider, R.J.; Formenti, S.C.; Dustin, M.L.; et al. Radiation-induced CXCL16 release by breast cancer cells attracts effector T cells. *J. Immunol.* **2008**, *181*, 3099–3107. [[CrossRef](#)]
148. Lugade, A.A.; Sorensen, E.W.; Gerber, S.A.; Moran, J.P.; Frelinger, J.G.; Lord, E.M. Radiation-induced IFN-gamma production within the tumor microenvironment influences antitumor immunity. *J. Immunol.* **2008**, *180*, 3132–3139. [[CrossRef](#)]
149. Hallahan, D.E.; Spriggs, D.R.; Beckett, M.A.; Kufe, D.W.; Weichselbaum, R.R. Increased tumor necrosis factor alpha mRNA after cellular exposure to ionizing radiation. *Proc. Natl. Acad. Sci. USA* **1989**, *86*, 10104–10107. [[CrossRef](#)]
150. Barcellos-Hoff, M.H.; Derynck, R.; Tsang, M.L.; Weatherbee, J.A. Transforming growth factor-beta activation in irradiated murine mammary gland. *J. Clin. Invest.* **1994**, *93*, 892–899. [[CrossRef](#)]
151. Marincola, F.M.; Jaffee, E.M.; Hicklin, D.J.; Ferrone, S. Escape of human solid tumors from T-cell recognition: Molecular mechanisms and functional significance. *Adv. Immunol.* **2000**, *74*, 181–273. [[CrossRef](#)]
152. Klein, B.; Loven, D.; Lurie, H.; Rakowsky, E.; Nyska, A.; Levin, I.; Klein, T. The effect of irradiation on expression of HLA class I antigens in human brain tumors in culture. *J. Neurosurg.* **1994**, *80*, 1074–1077. [[CrossRef](#)] [[PubMed](#)]

153. Santin, A.D.; Hermonat, P.L.; Hiserodt, J.C.; Chiriva-Internati, M.; Woodliff, J.; Theus, J.W.; Barclay, D.; Pecorelli, S.; Parham, G.P. Effects of irradiation on the expression of major histocompatibility complex class I antigen and adhesion costimulation molecules ICAM-1 in human cervical cancer. *Int. J. Radiat. Oncol. Biol. Phys.* **1997**, *39*, 737–742. [[CrossRef](#)]
154. Santin, A.D.; Hiserodt, J.C.; Fruehauf, J.; DiSaia, P.J.; Pecorelli, S.; Granger, G.A. Effects of irradiation on the expression of surface antigens in human ovarian cancer. *Gynecol. Oncol.* **1996**, *60*, 468–474. [[CrossRef](#)] [[PubMed](#)]
155. Wan, S.; Pestka, S.; Jubin, R.G.; Lyu, Y.L.; Tsai, Y.C.; Liu, L.F. Chemotherapeutics and radiation stimulate MHC class I expression through elevated interferon-beta signaling in breast cancer cells. *PLoS ONE* **2012**, *7*, e32542. [[CrossRef](#)]
156. Zhu, Y.; Herndon, J.M.; Sojka, D.K.; Kim, K.W.; Knolhoff, B.L.; Zuo, C.; Cullinan, D.R.; Luo, J.; Bearden, A.R.; Lavine, K.J.; et al. Tissue-Resident Macrophages in Pancreatic Ductal Adenocarcinoma Originate from Embryonic Hematopoiesis and Promote Tumor Progression. *Immunity* **2017**, *47*, 323–338. [[CrossRef](#)]
157. Wynn, T.A.; Chawla, A.; Pollard, J.W. Macrophage biology in development, homeostasis and disease. *Nature* **2013**, *496*, 445–455. [[CrossRef](#)]
158. DeNardo, D.G.; Ruffell, B. Macrophages as regulators of tumour immunity and immunotherapy. *Nat. Rev. Immunol.* **2019**, *19*, 369–382. [[CrossRef](#)]
159. Kraman, M.; Bambrough, P.J.; Arnold, J.N.; Roberts, E.W.; Magiera, L.; Jones, J.O.; Gopinathan, A.; Tuveson, D.A.; Fearon, D.T. Suppression of Antitumor. *Science* **2010**, *330*, 827–830. [[CrossRef](#)]
160. Lourdes Mora-García, M.; García-Rocha, R.; Morales-Ramírez, O.; Montesinos, J.J.; Weiss-Steider, B.; Hernández-Montes, J.; Ávila-Ibarra, L.R.; Don-López, C.A.; Velasco-Velázquez, M.A.; Gutiérrez-Serrano, V.; et al. Mesenchymal stromal cells derived from cervical cancer produce high amounts of adenosine to suppress cytotoxic T lymphocyte functions. *J. Transl. Med.* **2016**, *14*, 1–14. [[CrossRef](#)]
161. Erez, N.; Truitt, M.; Olson, P.; Hanahan, D. Cancer-Associated Fibroblasts Are Activated in Incipient Neoplasia to Orchestrate Tumor-Promoting Inflammation in an NF- κ B-Dependent Manner. *Cancer Cell* **2010**, *17*, 135–147. [[CrossRef](#)]
162. Liu, T.; Han, C.; Wang, S.; Fang, P.; Ma, Z.; Xu, L.; Yin, R. Cancer-associated fibroblasts: An emerging target of anti-cancer immunotherapy. *J. Hematol. Oncol.* **2019**, *12*, 86. [[CrossRef](#)] [[PubMed](#)]
163. Wynn, T.A.; Ramalingam, T.R. Mechanisms of fibrosis: Therapeutic translation for fibrotic disease. *Nat. Med.* **2012**, *18*, 1028–1040. [[CrossRef](#)] [[PubMed](#)]
164. Cheng, J.t.; Deng, Y.n.; Yi, H.m.; Wang, G.y.; Fu, B.s.; Chen, W.j.; Liu, W.; Tai, Y.; Peng, Y.w.; Zhang, Q. Hepatic carcinoma-associated fibroblasts induce IDO-producing regulatory dendritic cells through IL-6-mediated STAT3 activation. *Oncogenesis* **2016**, *5*, e198. [[CrossRef](#)]
165. Khosravi-Maharlooei, M.; Pakyari, M.; Jalili, R.B.; Salimi-Elizei, S.; Lai, J.C.Y.; Poormasjedi-Meibod, M.; Kilani, R.T.; Dutz, J.; Ghahary, A. Tolerogenic effect of mouse fibroblasts on dendritic cells. *Immunology* **2016**, *148*, 22–33. [[CrossRef](#)] [[PubMed](#)]
166. Mace, T.A.; Ameen, Z.; Collins, A.; Wojcik, S.; Mair, M.; Young, G.S.; Fuchs, J.R.; Eubank, T.D.; Frankel, W.L.; Bekaii-Saab, T.; et al. Pancreatic Cancer-Associated Stellate Cells Promote Differentiation of Myeloid-Derived Suppressor Cells in a STAT3-Dependent Manner. *Cancer Res.* **2013**, *73*, 3007. [[CrossRef](#)]
167. Kim, J.H.; Oh, S.-H.; Kim, E.-J.; Park, S.J.; Hong, S.P.; Cheon, J.H.; Kim, T.I.; Kim, W.H. The role of myofibroblasts in upregulation of S100A8 and S100A9 and the differentiation of myeloid cells in the colorectal cancer microenvironment. *Biochem. Biophys. Res. Commun.* **2012**, *423*, 60–66. [[CrossRef](#)]
168. Feig, C.; Jones, J.O.; Kraman, M.; Wells, R.J.B.; Deonaraine, A.; Chan, D.S.; Connell, C.M.; Roberts, E.W.; Zhao, Q.; Caballero, O.L.; et al. Targeting CXCL12 from FAP-expressing carcinoma-associated fibroblasts synergizes with anti-PD-L1 immunotherapy in pancreatic cancer. *PNAS* **2013**, *110*, 20212. [[CrossRef](#)]
169. Jiang, H.; Hegde, S.; Knolhoff, B.L.; Zhu, Y.; Herndon, J.M.; Meyer, M.A.; Nywening, T.M.; Hawkins, W.G.; Shapiro, I.M.; Weaver, D.T.; et al. Targeting focal adhesion kinase renders pancreatic cancers responsive to checkpoint immunotherapy. *Nat. Med.* **2016**, *22*, 851–860. [[CrossRef](#)]
170. Serrels, A.; Lund, T.; Serrels, B.; Byron, A.; McPherson, R.C.; von Kriegsheim, A.; Gómez-Cuadrado, L.; Canel, M.; Muir, M.; Ring, J.; et al. Nuclear FAK Controls Chemokine Transcription, Tregs, and Evasion of Anti-tumor Immunity. *Cell* **2015**, *163*, 160–173. [[CrossRef](#)]

171. Ager, E.I.; Kozin, S.V.; Kirkpatrick, N.D.; Seano, G.; Kodack, D.P.; Askoxylakis, V.; Huang, Y.; Goel, S.; Snuderl, M.; Muzikansky, A.; et al. Blockade of MMP14 activity in murine breast carcinomas: Implications for macrophages, vessels, and radiotherapy. *J. Natl. Cancer Inst.* **2015**, *107*, 1–12. [[CrossRef](#)]
172. Shibuya, M. Vascular endothelial growth factor and its receptor system: Physiological functions in angiogenesis and pathological roles in various diseases. *J. Biochem.* **2013**, *153*, 13–19. [[CrossRef](#)] [[PubMed](#)]
173. Kibria, G.; Hatakeyama, H.; Harashima, H. Cancer multidrug resistance: Mechanisms involved and strategies for circumvention using a drug delivery system. *Arch. Pharm. Res.* **2014**, *37*, 4–15. [[CrossRef](#)] [[PubMed](#)]
174. Lanitis, E.; Irving, M.; Coukos, G. Targeting the tumor vasculature to enhance T cell activity. *Curr. Opin. Immunol.* **2015**, *33*, 55–63. [[CrossRef](#)] [[PubMed](#)]
175. Tsai, C.S.; Chen, F.H.; Wang, C.C.; Huang, H.L.; Jung, S.M.; Wu, C.J.; Lee, C.C.; McBride, W.H.; Chiang, C.S.; Hong, J.H. Macrophages from irradiated tumors express higher levels of iNOS, arginase-I and COX-2, and promote tumor growth. *Int. J. Radiat. Oncol. Biol. Phys.* **2007**, *68*, 499–507. [[CrossRef](#)] [[PubMed](#)]
176. Park, H.J.; Griffin, R.J.; Hui, S.; Levitt, S.H.; Song, C.W. Radiation-induced vascular damage in tumors: Implications of vascular damage in ablative hypofractionated radiotherapy (SBRT and SRS). *Radiat. Res.* **2012**, *177*, 311–327. [[CrossRef](#)]
177. Hasmim, M.; Noman, M.Z.; Messai, Y.; Bordereaux, D.; Gros, G.; Baud, V.; Chouaib, S. Cutting edge: Hypoxia-induced Nanog favors the intratumoral infiltration of regulatory T cells and macrophages via direct regulation of TGF- β 1. *J. Immunol.* **2013**, *191*, 5802–5806. [[CrossRef](#)]
178. Kocher, M.; Treuer, H.; Voges, J.; Hoevels, M.; Sturm, V.; Müller, R.P. Computer simulation of cytotoxic and vascular effects of radiosurgery in solid and necrotic brain metastases. *Radiother. Oncol.* **2000**, *54*, 149–156. [[CrossRef](#)]
179. Sonveaux, P.; Dessy, C.; Brouet, A.; Jordan, B.F.; Grégoire, V.; Gallez, B.; Balligand, J.L.; Feron, O. Modulation of the tumor vasculature functionality by ionizing radiation accounts for tumor radiosensitization and promotes gene delivery. *FASEB J.* **2002**, *16*, 1979–1981. [[CrossRef](#)]
180. Crockart, N.; Jordan, B.F.; Baudalet, C.; Ansiaux, R.; Sonveaux, P.; Grégoire, V.; Beghein, N.; DeWever, J.; Bouzin, C.; Feron, O.; et al. Early reoxygenation in tumors after irradiation: Determining factors and consequences for radiotherapy regimens using daily multiple fractions. *Int. J. Radiat. Oncol. Biol. Phys.* **2005**, *63*, 901–910. [[CrossRef](#)]
181. Rao, S.S.; Thompson, C.; Cheng, J.; Haimovitz-Friedman, A.; Powell, S.N.; Fuks, Z.; Kolesnick, R.N. Axitinib sensitization of high Single Dose Radiotherapy. *Radiother. Oncol.* **2014**, *111*, 88–93. [[CrossRef](#)]
182. Choi, J.; Cha, Y.J.; Koo, J.S. Adipocyte biology in breast cancer: From silent bystander to active facilitator. *Prog. Lipid Res.* **2018**, *69*, 11–20. [[CrossRef](#)] [[PubMed](#)]
183. Bochet, L.; Meulle, A.; Imbert, S.; Salles, B.; Valet, P.; Muller, C. Cancer-associated adipocytes promotes breast tumor radioresistance. *Biochem. Biophys. Res. Commun.* **2011**, *411*, 102–106. [[CrossRef](#)] [[PubMed](#)]
184. Meng, G.; Tang, X.; Yang, Z.; Benesch, M.G.K.; Marshall, A.; Murray, D.; Hemmings, D.G.; Wuest, F.; McMullen, T.P.W.; Brindley, D.N. Implications for breast cancer treatment from increased autotaxin production in adipose tissue after radiotherapy. *FASEB J.* **2017**, *31*, 4064–4077. [[CrossRef](#)] [[PubMed](#)]
185. Begg, A.C.; Stewart, F.A.; Vens, C. Strategies to improve radiotherapy with targeted drugs. *Nat. Rev. Cancer* **2011**, *11*, 239–253. [[CrossRef](#)] [[PubMed](#)]
186. Vozenin, M.C.; Hendry, J.H.; Limoli, C.L. Biological Benefits of Ultra-high Dose Rate FLASH Radiotherapy: Sleeping Beauty Awoken. *Clin. Oncol.* **2019**, *31*, 407–415. [[CrossRef](#)]
187. Harrington, K.J. Ultrahigh dose-rate radiotherapy: Next steps for FLASH-RT. *Clin. Cancer Res.* **2019**, *25*, 3–5. [[CrossRef](#)]



Review

Understanding the Effects of Radiotherapy on the Tumour Immune Microenvironment to Identify Potential Prognostic and Predictive Biomarkers of Radiotherapy Response

Shuhui Cheng ¹ , Eleanor J. Cheadle ¹ and Timothy M. Illidge ^{1,2,*}

¹ Manchester Academic Health Science Centre, Manchester NIHR Biomedical Research Centre, Division of Cancer Sciences, Faculty of Biology, Medicine and Health, University of Manchester, Manchester M13 9PL, UK; shuhui.cheng@postgrad.manchester.ac.uk (S.C.); Eleanor.J.Cheadle@manchester.ac.uk (E.J.C.)

² The Christie NHS Foundation Trust, Manchester M20 4BX, UK

* Correspondence: tim.illidge@manchester.ac.uk

Received: 17 July 2020; Accepted: 23 September 2020; Published: 30 September 2020



Simple Summary: Around 50% of all cancer patients receive radiotherapy as part of their treatment. Recently immunotherapy has shown promising results and become established as an effective treatment for some cancers. Combining radiotherapy and immunotherapy is a novel approach to further increase the number of patients responding to immunotherapy. Biological markers of response (biomarkers) are urgently required to hasten the clinical translation and improve outcomes further. Radiotherapy can both stimulate and inhibit the immune system and understanding the immune effects of radiotherapy on the tumour and surrounding cells may lead to the identification of predictive and prognostic biomarkers to help make more individualized treatment decisions, when combining radiotherapy with immunotherapy. This review summarizes the immune effects of radiotherapy and biomarkers of response identified to date; providing new perspectives for future research which may facilitate the development of novel radiotherapy immunotherapy combinations based on tumour immunology and biomarker identification.

Abstract: Radiotherapy (RT) is a highly effective anti-cancer treatment. Immunotherapy using immune checkpoint blockade (ICI) has emerged as a new and robust pillar in cancer therapy; however, the response rate to single agent ICI is low whilst toxicity remains. Radiotherapy has been shown to have local and systemic immunomodulatory effects. Therefore, combining RT and immunotherapy is a rational approach to enhance anti-tumour immune responses. However, the immunomodulatory effects of RT can be both immunostimulatory or immunosuppressive and may be different across different tumour types and patients. Therefore, there is an urgent medical need to establish biomarkers to guide clinical decision making in predicting responses or in patient selection for RT-based combination treatments. In this review, we summarize the immunological effects of RT on the tumour microenvironment and emerging biomarkers to help better understand the implications of these immunological changes, and we provide new insights into the potential for combination therapies with RT and immunotherapy.

Keywords: radiotherapy; immunotherapy; tumour microenvironment; biomarker

1. Introduction

Radiotherapy (RT) is a highly effective anti-cancer treatment delivered to between 50% and 60% of all cancer patients as part of either curative treatment or for palliation of their disease [1].

Following the breakthrough of immune checkpoint inhibitors (ICI), immunotherapy has now become established as an important component of cancer therapy. However, the response rate to single agent ICI in most solid tumours is low, at approximately 20% to 30%, and further developments are ongoing to improve response rates and outcomes further. RT has long since been known to be highly effective at inducing DNA damage and in recent years has been shown to have local and systemic immunomodulatory effects. Therefore, combining RT and immunotherapy is a logical approach to enhance anti-tumour immune responses. However, the immunomodulatory effects of RT can be both immunostimulatory and immunosuppressive, which may be different across different tumour types and patients. This potential diversity in the immune response to RT adds complexity to the interpretation of how the immune landscape in the tumour microenvironment (TME) might respond in patients receiving RT. The nature of the immune response to RT and whether this is immunostimulatory or immunosuppressive further highlights the importance of identifying immunological biomarkers to assess treatment responses in patients undergoing RT. In this review, the effects of RT on the tumour microenvironment, candidate immune targets, emerging biomarkers and the related cutting-edge technologies for analysis of immune biomarkers will be outlined. Finally, the implications of these immunological consequences on the potential for combination therapy with RT and immunotherapy will be discussed.

2. The Tumour Immune Microenvironment

2.1. The Components and Classification of TME

The term “tumour microenvironment” (TME) refers to an “ecological niche” which affects tumour growth and progression and is characterized by complex biological interactions between the tumour and the stroma [2,3]. The TME encompasses cancer cells, stromal cells (such as fibroblasts), a diversity of resident and infiltrating immune cells and soluble messengers [2]. The constituent cell types in the TME vary from T cells, dendritic cells (DCs), tumour-associated macrophages (TAMs), myeloid-derived suppressor cells (MDSCs), mast cells, to natural killer (NK) cells, which secrete a variety of factors (chemokines, cytokines and enzymes) that directly or indirectly participate in immune responses. The composition and the interplay of the components within the TME may have a critical role in the outcome of tumour evolution and treatment response [2].

There are certain cell types in the TME that play an essential role in immune surveillance, such as DCs, cytotoxic T cells and NK cells. Among these, the T cell infiltrates are potentially some of the most important immune effector cells populations which have been investigated extensively. One such investigation is the immunoscore, which refers to the density of two different lymphocyte populations (CD3+, CD8+ or CD45RO+ cells) quantified in the tumour core and the invasive margin, which was first shown to correlate with outcome in colorectal cancer (CRC) [4]. The prognostic power of the immunoscore is also being investigated and validated in other cancer types including melanoma and breast cancer [5].

The TME can however become highly immunosuppressive as a result of the infiltration and interaction of a multitude of immune effector cells which act to suppress immune responses, including MDSCs, regulatory T cells (Tregs) and TAMs. Tregs play a significant role in facilitating immune escape and promoting tumour progression. A low number of Tregs before treatment was found to be correlated with active immune responses and favourable clinical outcome in breast cancer patients following surgery and RT [6]. In terms of TAM, the TME encourages the switch from a tumour-killing M1-TAM to a tumour-promoting M2-TAM type. MDSCs are a heterogeneous population of myeloid cells [7] and have been demonstrated to be associated with a poor prognosis in pancreatic, oesophageal and gastric cancers, which suggests their potential as an important prognostic biomarker [7].

It is increasingly recognized that tumour responses to treatments to some extent depend on the microenvironment. Therefore, it is important to understand how immunostimulatory and suppressive

effects are reflected and balanced in the TME, thereby hopefully tailoring the treatment according to the TME landscape.

2.2. The Effects of RT on the Tumour Microenvironment

RT has been widely used to eradicate cancer with its direct tumour-killing effects [8]; however, increasing evidence shows that RT can cause tumour rejection by enhancing local anti-tumour immune responses that can lead to a distant systemic immune response called the “abscopal effect”, where the tumour regresses outside the irradiated site [9]. However, it is increasingly understood that RT has both immunostimulatory and immunosuppressive effects. In order to utilize RT to enhance the immunostimulatory effects and overcome intrinsic immunosuppression within the TME, a greater understanding of RT-induced immune effects is required.

2.2.1. RT-Induced Immunostimulation

RT is well documented to initiate tumour rejection by enhancing anti-tumour immune responses, although mostly in murine tumours [10–16]. The phenomenon “abscopal effect”, which refers to a tumour in a non-irradiated site regressing after RT [17], offers further evidence of the ability of RT to induce immunological responses. RT can mediate these effects in several ways including immunogenic effects on tumour cells and immunostimulatory effects on the immune system.

RT can increase the antigenicity of tumour cells by inducing or upregulating the release of tumour-associated antigen (TAA) through induction of tumour cell death and increasing the expression of MHC class I molecules that are expressed on the surface of tumour cells. RT can also greatly alter the repertoire of MHC class I restricted peptides [18].

It has been shown that RT is able to induce immunogenic cell death (ICD), whereby tumour cells dying after RT undergo a form of cellular death induced by a cascade of complex reactions which can elicit immune responses [19] (Figure 1).

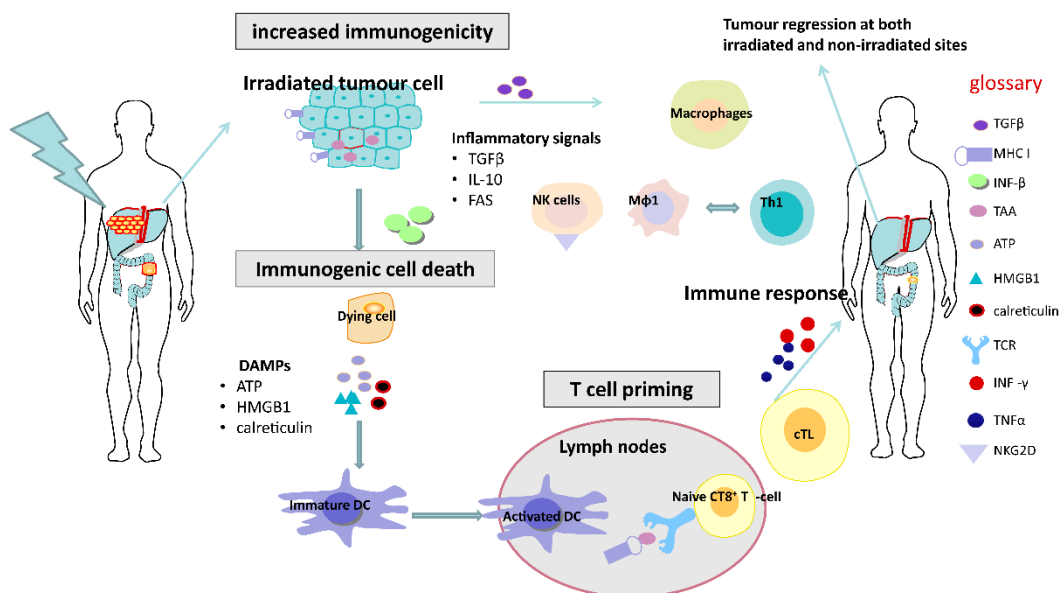


Figure 1. Immunostimulatory effects of radiotherapy. Radiotherapy can enhance the antigenicity of tumour cells by stimulating the induction of immunogenic cell death mediated by damage-associated molecular pattern molecules (DAMPs), which contributes to DC maturation and T cell priming. Activated cytotoxic T cells (cTL) in the blood can cause systemic immune responses, potentially resulting in tumour regression outside the irradiated field. DC, dendritic cell; Mφ1 cells, macrophage type-1 cell; Th1 cell, T helper type 1 cell.

After irradiation, tumour cells can undergo a form of cell death known as immunogenic cell death and express damage-associated molecule patterns (DAMP) or “danger signals”, which includes exposure of calreticulin, the extracellular release of ATP and high mobility group box 1 (HMGB1) and uric acid. Calreticulin is a protein that can serve as an “eat me” signal, stimulating the engulfment of dying tumour cells and their apoptotic debris by macrophages and immature DCs [19,20]. ATP can be a potent signal for activating myeloid cells including monocytes/macrophages and immature DCs. HMGB1 is a factor that can be released by dead cells and can interact with several distinct pattern recognition receptors, including toll-like receptor 4 (TLR4). These DAMPs, induced by RT, may potentially play an important role in promoting the recruitment, differentiation and effective acquisition, processing and presentation of TAA by stimulating dendritic cell (DC) maturation within TME [21].

Additionally, there are other potential immunological mechanisms through which RT can increase the susceptibility to anti-tumour immune surveillance. These include the multiple death receptors induced by RT expressed on the surface of tumour cells, including FAS (also known as CD95) and tumour necrosis factor-related apoptosis-inducing ligand (TRAIL) receptors 1 and 2 (TRAIL-R1 and TRAIL-R2), which can render the tumour cells more vulnerable to apoptosis [20].

In addition to these immunogenic and phenotypic changes, RT can stimulate immune responses via interactions with the immune system. Whilst the direct contribution of infiltrating versus resident T cells to overall tumour control remains to be clarified, the number and function of TILs have been shown to increase following single, ablative doses of RT. Likewise, both high single-dose and fractionated RT have been shown to increase T cell receptor (TCR) diversity and clonality, predominantly leading to the enrichment of T cell clones already resident within the TME [12,22].

RT can also upregulate MHC class I molecules, leading to enhanced recognition of tumour cells by cytotoxic T cells, and increased NKG2D expression may result in greater NK cell-mediated eradication of tumours [21,23].

Production of type I interferons due to RT-induced accumulation of cytosolic DNA and activation of the STING pathway [24] can also lead to increased expansion of tumour-specific T cells, as a consequence of enhanced cross-presentation of tumour antigens by dendritic cells. RT can trigger the production of pro-inflammatory chemokines including CXCL9, CXCL10 and CXCL16, resulting in the chemotactic recruitment of effector CD8+ T cells into the TME. Macrophages are another immune effector cell population in the TME which may have a potentially important role in dictating the response of the tumour to radiotherapy. Macrophages have been characterised into M1 and M2 phenotypes, although it is understood that there can be “plasticity” between such phenotypes. M1 macrophages mediate vascular normalization, promoting T cell recruitment and subsequent rejection of tumours. In contrast, the M2 phenotype is considered to promote immunosuppression. Interestingly, conventional lower doses of RT (2 Gy) frequently used in routine clinical practice have also been found to transform an immunosuppressive M2 TAM into a tumour-killing iNOS producing M1 TAM [25].

2.2.2. RT-Induced Immunosuppression

In contrast to the potential immunostimulatory effects, RT can have several immunosuppressive effects that may negatively impact or suppress the development of anti-cancer immunity. These negative effects of RT can be imposed directly on the TME, such as the RT-induced death of immune cells, or indirectly through modulation of stromal cells and tumour vasculature (Figure 2).

In addition to direct cytotoxic effects on immune cells, RT can lead to the production of pro-inflammatory cytokines and chemokines (such as TNF, interleukin and TGF- β) and the subsequent recruitment of suppressive immune cells such as MDSCs, TAMs and Tregs [26]. TGF- β is a potent immunosuppressive cytokine that inhibits cross-priming of T cells by damaging the antigen-presenting function of dendritic cells and the functional differentiation of T cells into effectors [27]. Infiltration of Tregs can lead to cytotoxic CD8+ T cell inactivation by expression of the checkpoint inhibitor

molecule CTLA-4. Interestingly, on some occasions, these immunosuppressive reactions can be overcome by RT-induced immune stimulation, which is characterised by ICD induced antigen exposure, DC maturation, T cell recruitment and activation.

Irradiated normal tissue adjacent to tumour undergoes a process of inflammation, wound healing and fibrosis. This process involves the expansion of cancer-associated fibroblasts (CAFs) and extracellular matrix modelling, which leads to post-radiation tumour hardening and shrinkage, and ultimately facilitates tumour spread or recurrence [26]. CAFs are a heterogeneous cell population that constitute the majority of cells within the stroma in many carcinomas [28]. RT activates CAFs by causing DNA damage and production of ROS [29]. Irradiated CAFs can contribute to cancer progression via the transforming growth factor beta (TGF- β)-CXCL12 dependent pathway. However, whether CAFs play a tumour-killing or tumour-promoting role may vary depending on the type of signal [30]. RT-induced vascular damage is aggravated by tumour hypoxia through CXCL-12 and HIF-1 α -mediated MDSC recruitment [31].

In hypoxic environments, RT-induced free radical production is reduced and consequently RT causes less DNA damage in hypoxic areas. A further potentially important mechanism for RT to induce immunosuppression in hypoxic areas may be increases in the production of vascular endothelial growth factor (VEGF), reactive oxygen species (ROS) and hypoxia-inducible factor-1 α (HIF-1 α) [26]. HIF-1 α participates in several specific processes resulting in tumour vascularization and reoxygenation. Furthermore, it was found to be an independent predictor of poor prognosis after RT [26].

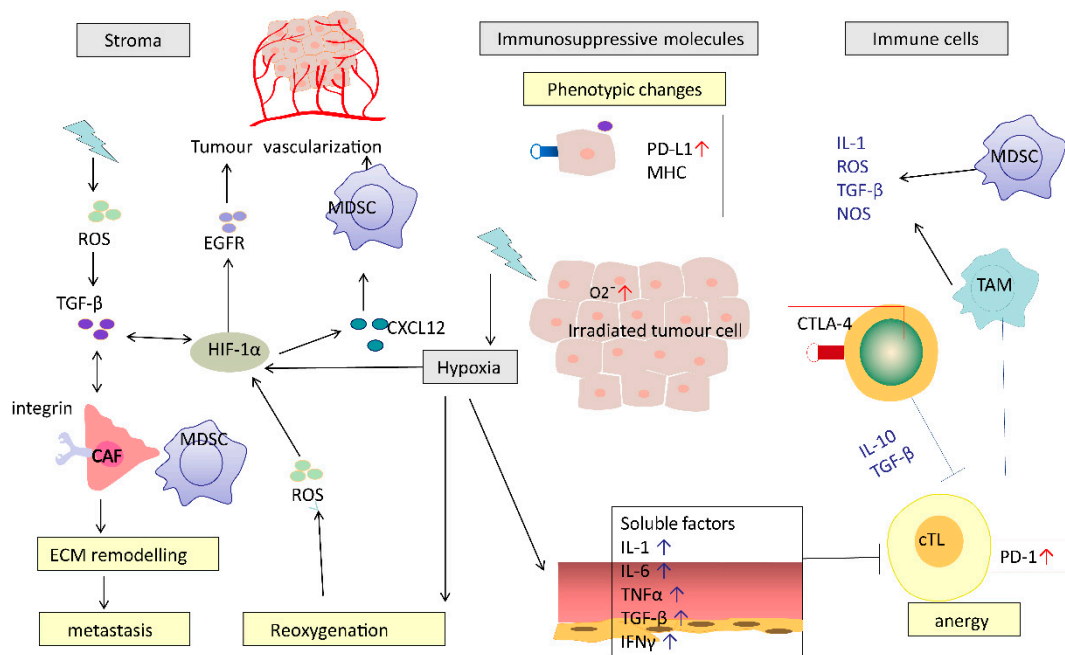


Figure 2. Potential mechanisms of RT-induced immunosuppression. RT causes a series of immunosuppressive processes: modifying tumour stromal environment, production of immunosuppressive molecules, recruiting immunosuppressive cells and impairing effective T cells. RT causes hypoxia, which induces HIF-1 α and TGF- β . HIF-1 α -activated CAFs mediated by TGF- β or directly by RT promote ECM re-modelling. These effects work in concert to promote cancer metastasis. CAF, cancer-associated fibroblasts; MDSC, myeloid-derived suppressor cell; cTL, cytotoxic T lymphocyte; TAM, tumour-associated macrophages; ECM, extracellular matrix; HIF-1 α , hypoxia-inducible factor-1 α ; TGF- β , transforming growth factor beta.

2.2.3. RT and Cell Death

Tumour cells usually evolve to escape death by inactivating the cell death pathways commonly used to eliminate damaged and harmful cells [32]. This ability to avoid cell death may lead to resistance

during treatment [33]. Therefore, it is necessary to have an overall understanding of the mechanisms of cell death induced by RT in order to develop new anti-tumour treatments.

For many years, apoptosis has been proposed as the principal cell death pathway induced by radiotherapy. Recently, non-apoptotic cell death morphologies or alternative death mechanisms have been discovered during radiation, including autophagy, necrosis, programmed necroptosis and ferroptosis, all of which will be summarised below. The mode of cell death induced by RT is of particular importance as certain modes of cell death will lead to the release of tumour antigens which are subsequently processed and presented on antigen-presenting cells [21].

Among all these cell death types, one particularly distinct type of “cell death” is radiation necrosis. Radiation necrosis is unprogrammed cell death and, for example, can occur as a rare late side effect following high-dose radiation (typically > 55 Gy) of both intracranial and extracranial tumours, such as nasopharyngeal carcinoma [34]. Unlike all other cell deaths, it has not been often reported to be associated with tumour suppression, but it presents similar imaging findings and symptoms to tumour recurrence, which can pose a challenge to differential diagnosis [35]. The aetiology of radiation necrosis is not yet clear. Possible histopathological changes might be radiation-induced vascular damage and the resultant ischemic necrosis, radiation-induced damage to oligodendrocytes and their precursors or impaired neurogenesis, implicating the vascular cells and/or oligodendrocytes as the targets of radiation injury [34].

Autophagy is a catabolic process whose activation acts as a pro-survival mechanism and can induce autophagic cell death in some circumstances [36]. Targeting autophagy has been proposed as a novel anti-tumour treatment [37]; however, it is still controversial as to whether autophagy stimulation or inhibition is better [38]. Autophagy has also been identified to play a dual role in the response of cancer cells to RT, with preclinical models showing that autophagy inhibition increases radiosensitivity *in vitro* yet reduces efficacy of radiotherapy *in vivo* due to deficient immunogenic signalling [39,40]. Inhibiting autophagy with chloroquine or hydroxychloroquine might improve the efficacy of several anticancer therapies in patients, and exploratory clinical studies are ongoing [41]. However, the results of trials using these drugs have been generally disappointing, with limited clinical efficacy [42,43]. In addition, some researchers have proposed that whether autophagy should be enhanced or inhibited is context-dependent [37,44].

Necroptosis is a caspase-independent form of regulated cell death executed by the receptor-interacting protein kinase 1 (RIP1), RIP3, and mixed lineage kinase domain-like protein (MLKL) [45], which can lead to DAMP release [46] and chronic inflammation associated with aging. Much of the tumour radioresistance and recurrence results from tumour cell repopulation after radiotherapy. A preclinical study showed that necroptosis-associated tumour repopulation after radiotherapy depended on activation of the RIP1/RIP3/MLKL/JNK/IL-8 pathway and this novel pathway could be a promising target for blocking tumour repopulation to enhance the efficacy of colorectal cancer radiotherapy [47]. However, there is still a long way to go for necroptosis-based cancer therapy to be developed as many questions are still unclear—for instance, the intrinsic or acquired defects of necroptotic machinery observed in many cancer cells [45].

Ferroptosis is a form of regulated cell death characterised by lipid peroxidation and was recently identified to be potentially tumour-suppressive. Ferroptotic cancer cells have modulatory effects on tumour immunity at many steps [48]; however, various putative signals released by ferroptotic cancer cells may lead to the stimulation or suppression of different immune cells. Triggering ferroptosis may be a novel approach in cancer therapy; several strategies to target ferroptosis have been investigated [48]. Although the link between RT and ferroptosis has not been experimentally addressed or widely proven, recent evidence suggests that radiotherapy induces ferroptosis in cancer patients [49], and increased ferroptosis was demonstrated to be associated with improved response to radiotherapy and better survival in oesophageal tumour samples [50].

3. Biomarkers

To date, there have been limited clinical studies addressing the RT-induced immunological changes in humans. Further preclinical and clinical investigations are needed to identify potential biomarkers of RT-induced immunological changes to guide decision-making in clinical practice, particularly when considering RT–IO agent combination therapies.

There is growing demand to develop predictive biomarkers which guide the development and delivery of tailored therapies, i.e., “right drug to the right patients”, by predicting benefit to a medical intervention and prognostic biomarkers which are used to identify likelihood of a clinical event, disease recurrence or progression. Several diagnostic tumour markers are now included in routine clinical practice, such as PSA, CA125, β -HCG and AFP [51], but few biomarkers are currently validated for clinical practice in RT and none to guide RT in combination with IO agents. In addition to static biomarkers, dynamic biomarkers are proposed to investigate how treatments may influence key transitions and potentially identify responders and non-responders in a more timely fashion, sparing patients’ toxicities from ineffective treatments and potentially guiding therapy decisions to more effective approaches. Such dynamic tumour biomarkers requiring serial sampling would facilitate real-time decision-making that has not been previously possible with pre-treatment biomarkers [52]. The process of developing biomarkers for patients undergoing RT is outlined below (Figure 3).

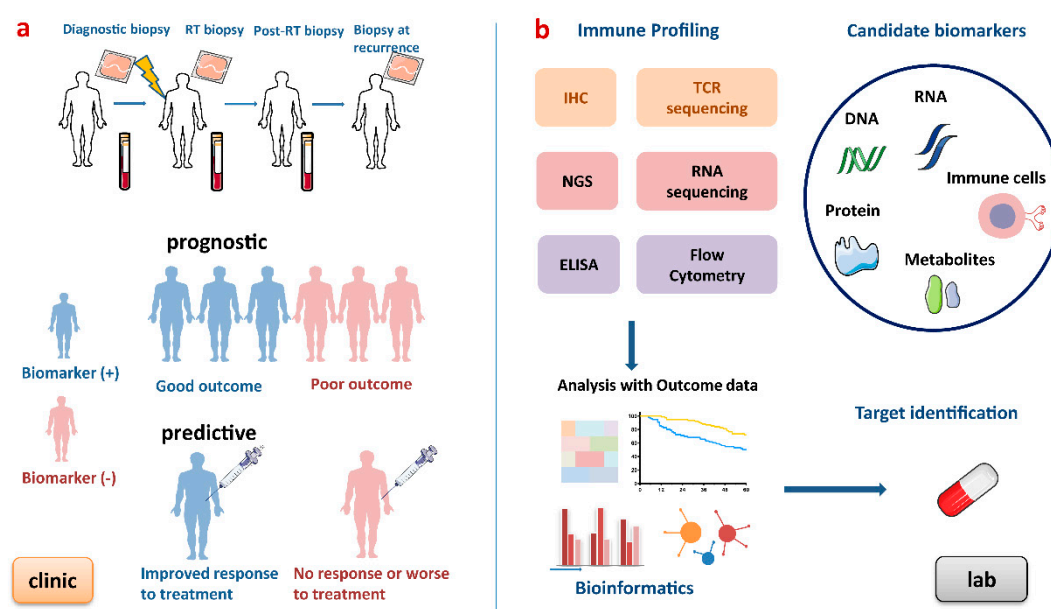


Figure 3. Process of developing biomarkers for patients undergoing radiotherapy. (a) Blood and tumour biopsies are taken at baseline, during RT, after RT and at recurrence to obtain dynamic immune profiling. This figure shows an ideal example of prognostic and predictive biomarkers. Prognostic biomarkers provide information on disease progression and outcomes, and predictive biomarkers indicate the response to a medical intervention. (b) In the lab, these biomarkers can be discovered by high-throughput gene technologies, immune-based technologies and analysed by bioinformatic approaches. RT, radiotherapy; IHC, immunohistochemistry; NGS, next-generation sequencing; TCR, T cell receptor; ELISA, enzyme-linked immunosorbent assay.

3.1. Radiotherapy-Related Biomarkers

It is important to note that the TME is dependent on many factors, such as patient age [53], treatment (chemotherapy, radiotherapy and immunotherapy), tumour type (e.g., solid or haematological) and whether the tumour is virally or hormonally driven. For virally driven tumours such as HNSCC, a recent study demonstrated that HPV-positivity correlated with increased immune cytolytic activity and a T-cell-inflamed gene expression profile, suggesting that HPV status can be

used to predict the effectiveness of PD-1 inhibitors in HNSCC, independently of PD-L1 expression and TMB, and probably results from an inflamed TME induced by HPV infection and anti-tumour activity of HPV antigen-specific T cells [54]. For hormone dependent tumours such as breast cancer or prostate cancer, the TME may be affected by more complex regulation, such as oestrogen or testosterone signalling pathways [55,56]. Furthermore, it is difficult to delineate whether changes to the TME as a result of RT are due to a specific effect of RT or the change in tumour size as a result of RT, and serial biopsies allowing a thorough investigation into the dynamics and kinetics of changes are only possible in preclinical models. Here, we focus on the impact of RT on the TME, and some of the potential immune-related biomarkers of response to RT which have been identified to date are summarized below (Table 1). Whilst numerous biomarkers during RT are under investigation, there are few available to guide clinical decision-making in predicting responses or in patient selection for radiotherapy-based treatments. Furthermore, biomarker identification is in its infancy and it will be important to consider that any identified biomarker will need to be validated across factors such as different tumour types, age of patients and hormone or viral dependency of the tumour.

Table 1. Clinical studies on immune-related biomarkers in radiotherapy-based treatment.

Category	Sample Origin	Biomarker	Cancer Type	Treatment	Clinical Response	Reference
Circulating cells	Peripheral blood mononuclear cell	Lymphopenia	Cervical cancer	Definitive CRT	↓ OS, DFS	[57]
	Whole blood	↑ Myeloid-derived suppressor cell	HCC	RT	↓ OS	[58]
	Whole blood	↑ MDSCs + Tregs	Rectal cancer	Short-term pCRT + surgery	Early marker of response	[59]
Circulating cytokine	Plasma	VEGF, PIGF and IL-6	CRC	Neoadjuvant bevacizumab + CRT + surgery	Predictive of response	[60]
Immune Infiltrates	FFPE tissue	↑ CD3+, CD8+ TILs	HNSCC	Definitive CRT	↑ OS, PFS Predictive of CRT	[61]
	FFPE tissue, surgical specimens	↑ CD3+, CD8+ TILs	CRC	pCRT	Predictive of pathological downstaging	[62]
	FFPE tissue	↑ Ratio of PD-1+/CD8+ TILs	Extrahepatic cholangiocarcinoma	Adjuvant CRT	↓ OS	[63]
	FFPE tissue, surgical specimens	Immunoscore	CRC	pCRT	Predictive of downstaging after pCRT	[62]
T-cell-related	Surgical specimens	Immunoscore	Brain metastasis	Surgery + whole brain RT	Prognostic to OS	[62]
	FFPE tissue	PD-L1 (+) post RT	Cervical carcinoma	Carbon-ion	↑ PFS	[64]
	Plasma	↑ PD-L1	HCC	RT	↓ OS	[65]
Gene expression profiling	Plasma	T cell receptor repertoire and ↑ serum IFN β	Lung cancer	RT + ipilimumab	Predictive of response to combination therapy	[66]
	FFPE tissue	High tumour mutational burden	HNSCC	Definitive CRT	↓ OS	[67]
	FFPE tissue	↑ IFN- γ signature	Bladder cancer	pCRT + surgery + CRT	↑ Disease-specific survival	[68]

CRT, chemoradiotherapy; RT, radiotherapy; HCC, hepatocellular carcinoma; pCRT, preoperative chemoradiotherapy; CRC, colorectal cancer; FFPE, formalin-fixed paraffin-embedded; HNSCC, head and neck squamous cell carcinoma; PD-L1, programmed death-ligand 1; OS, overall survival; PFS, progression-free survival; DFS, disease-free survival; ↑ increased; ↓ decreased.

3.1.1. PD-1/PD-L1 Expression

Engagement of PD-L1 with its receptor PD-1 results in the inactivation of T cells and NK cells, ultimately contributing to immune evasion [69]. Since Toplian and his colleagues first revealed that tumour PD-L1 expression reflects an immune-active microenvironment [70], several clinical trials have demonstrated that clinical responses to PD-1 blockade are correlated with PD-L1 expression in many cancer types [71–74].

The role of PD-L1 as a potential biomarker in patients treated with RT has emerged recently [64,75]. The PD-L1 expression after 12 Gy carbon-ion irradiation correlated with better progression-free survival in human uterine cervical adeno/adenosquamous carcinoma [64], while soluble PD-L1 was found to be correlated with worse survival in hepatocellular carcinoma [65]. Interestingly, both studies demonstrated that RT results in increased PD-L1 expression in vivo through interferon gamma production by T cells and that this appears to be an adaptive resistance pathway [10] that can be overcome by PD-L1-blockade [76]. Haematological malignancies such as Hodgkin lymphoma also show upregulation of PD-L1/PD-1 after chemotherapy/radiotherapy [77] and are known to be highly responsive to PD-1 blockade [78], and RT in combination with PD-1 blockade can induce abscopal responses [79]. The Pacific study showed that the addition of durvalumab (anti PD-L1) after consolidated chemoradiotherapy (CRT) enhanced both progression free survival (PFS) and overall survival (OS) of phase III unresectable non-small-cell lung carcinoma (NSCLC) patients; subgroup analysis showed that survival benefit was achieved in both PD-L1 positive and negative patients [76]. Long-term follow-up showed that the survival benefit of durvalumab was observed in subgroups with different PD-L1 levels, except patients with PD-L1 < 1% [80]. The findings from this study were disappointing regarding the potential utility of PD-L1 as a predictive biomarker, but since baseline PD-L1 level before CRT was not mandated and only measured where samples were available, it is currently unknown whether CRT changed the PD-L1 expression level and how it affected the results. Furthermore, durvalumab was given 2–42 days after CRT, which is a quite broad timespan; the optimal time for drug administration should be explored as well as how PD-L1 was affected by CRT dynamically.

In short, the level of PD-L1 within tumours has been suggested to be a promising prognostic biomarker in patients undergoing RT, but the role of PD-L1 as a predictive biomarker still needs further investigation. Ultimately, being able to clearly measure the number of cells expressing PD-L1 (reported as a percentage of stained cells) is critical. This issue is confounded by multiple unresolved problems: variable detection antibodies, differing IHC cut-off values, tissue preparation, processing variabilities, primary versus metastatic biopsies, oncogenic versus induced PD-L1 expression and staining of tumour versus immune cells [81,82]. The cut-off value constituting a positive or negative test result varies by both tumour type and by the antibody clone used to test the sample [83]. Moreover, there are several commercially available IHC assays to measure PD-L1 [83]. The measurement of PD-L1 requires standardization because the PD-L1 can be expressed on both lymphocytes and cancer cells, on both the cell membrane or in the cytoplasm. Recently, an IHC approach was approved by the US FDA as a companion diagnostic to make treatment recommendations for NSCLC patients using the anti-PD-1 agent pembrolizumab [83]. Three additional IHC assays have been approved as complementary diagnostics [84].

3.1.2. Immune Infiltrates

Immune infiltrates were proposed to be reflective of an adaptive anti-tumour response in the TME and may indicate a favourable response to RT. Data on the role of TILs in the context of RT are limited, with mixed findings. A retrospective single centre study examined pre-treatment specimens from 101 neck squamous cell carcinoma (HNSCC) patients before definitive CRT and reported that TILs are associated with favourable survival and are an independent prognostic factor to response to CRT [61]. However, the amount of CD8+ TIL infiltration alone is not always correlated with better clinical outcome. In patients with extrahepatic cholangiocarcinoma treated with adjuvant CRT, high expression of PD-1 on CD8+ TILs was strongly associated with inferior OS and the density of CD8+ TILs alone was not an independent prognostic factor for OS [63].

The presence of TILs can be measured by IHC, flow cytometry and droplet digital PCR technology. Moreover, there is an emerging novel technique of “immuno-positron emission tomography”, which enables identification of CD8+ cells non-invasively and has been used in murine models of melanoma and breast cancer [85]. Whilst flow cytometry may enable quantification of a greater number

of immune cells, issues around the requirement for fresh tumours mean that IHC of formalin-fixed tissue biopsies is currently the preferred method of choice for researchers.

3.1.3. Immunoscore

Given that the effect of TILs might be tumour-type-dependent, it is rational to develop combination analysis of different cell populations in immune infiltrates when exploring biomarkers for different cancers. For example, in a retrospective study of 166 CRC cancers with or without preoperative chemoradiation (pCRT), classification into one of five immunoscore groups significantly correlated with differences in disease free survival (DFS) and OS (all $p < 0.005$), with high infiltration of CD3+ and CD8+ lymphocytes in tumour biopsies associated with downstaging of the tumour after pCRT [62]. Currently, immune changes in the TME after CRT, including the value of immunoscore in response to chemoradiation, are mostly found in CRC patients [86]. This is possibly because the immunoscore was first validated and is most studied in CRC, perhaps due to the relatively easy opportunity to obtain biopsies to investigate the effects on the TME after RT and pCRT.

Another study took pre-treatment and post-treatment biopsies from 136 rectal cancer patients who underwent neoadjuvant RT, CT or CRT before radical resection and demonstrated that high levels of CD3+ and CD8+ TILs at baseline were correlated with better pathological responses (TRG ≥ 3) to neoadjuvant CRT and a favourable DFS and OS; in addition, CRT can enhance local immune response by increasing TIL infiltration [87]. One of the difficulties in the interpretation of this study is the diversity of treatment regimens used and the lack of matched immune blood markers to provide correlations with changes in TME. However, despite these caveats, changes in TILs after treatment were not associated with prognosis. Furthermore, Hagland et al. found a correlation between circulating T cells in pre-operative blood with intratumoural density and location of CD3+ and CD8+ T cells in colorectal cancer, suggestive of the potential for a liquid biopsy immunoscore [88]. However, this remains to be investigated for RT responses.

Brain metastases have also proven to be another good opportunity to study the effect of RT after whole brain radiotherapy (WBRT). Berghoff and colleagues investigated the influence of TIL and immunoscore on brain metastases [89]. Interestingly, despite the common preconception that the brain is an immune-privileged site, TIL infiltrates were detected in 115/116 (99.1%) brain metastasis biopsies. The density of CD3+, CD8+ and CD45RO+ TILs showed a significant correlation with favourable median OS. The immunoscore showed significant correlation with survival (27 vs. 10 mo; $p < 0.001$) and was established by multivariable analysis to be an independent prognostic factor (HR 0.612, $p < 0.001$). Interestingly, both the immunoscore and post-surgical WBRT showed an independent additive effect on OS. Considering that WBRT was delivered after surgery, the biopsy could not reflect the impact of RT on the TME; however, the immune infiltrates can serve as baseline data and may aid in patient selection for RT.

3.1.4. Gene Expression Profiling

Genetic mutation is one of the most significant hallmarks of cancer [2] and exists in metastatic settings across many cancer types, particularly frequently in cancers such as bladder cancer, melanoma, NSCLC, CRC and HNSCC [90]. Tumour mutational burden (TMB), which refers to the number of DNA mutations per megabase in a cancer cell, has previously been established as a prognostic biomarker and predictive factor of response to ICI across multiple tumour types [91,92]. The predictive value of gene expression profiling to evaluate the efficacy of RT currently remains unclear. A multicentre retrospective study from Germany developed a 327-gene panel to define TMB and then performed TMB analysis in 101 archival tumour samples from HNSCC patients treated with definitive CRT, aiming to assess the impact of TMB on prognosis. High TMB was demonstrated to be correlated with poor survival, which suggests that it may predict patients who might potentially benefit from CRT-ICI combinations [67]. Further research is needed to determine the value of TMB in response to RT alone.

Another retrospective study performed transcriptome-wide gene expression profiling of primary tumours from 136 muscle-invasive bladder cancer (MIBC) patients treated with bladder-sparing trimodality therapy (TMT) and compared to another cohort of 223 MIBC patients treated with neoadjuvant chemotherapy (NAC) and radical cystectomy (RC) in patients who had not received CRT. Results showed that signatures of T cell activation and IFN- γ signalling were associated with improved disease-specific survival (DSS) in the TMT cohort, but not in the NAC and RC cohort, whereas higher stromal infiltration was associated with shorter DSS after NAC and RC [68]. This suggests that gene expression profiling may be useful in developing predictive biomarkers to CRT but, given the limitations of this retrospective study, additional validation in larger prospective studies is required.

Currently, there is no uniform definition of a high TMB [93]. Standardization of the process of measuring TMB is required, including the method used, the ideal timing of TMB analysis (e.g., diagnostic biopsy or pre-treatment) and the ideal specimen (e.g., primary tumour versus metastasis). DNA next-generation sequencing approaches determining TMB include whole-exome sequencing (WES) and whole-genome sequencing (WGS). WES is considered to be the gold standard test as it generates a large amount of data and gives an overview of the gene mutation landscape; however, the fact that it is costly and requires more DNA may hinder its wider application. Targeted gene panels are unable to cover all the tumour mutations but offer reduced cost and requires less DNA, which enables easier integration into hospital labs.

3.1.5. Neoantigens

Neoantigens, as downstream products of TMB, are small peptide epitopes arising from tumour-specific mutations which are processed and presented on MHC molecules [94,95]. Unlike tumour-associated antigens (TAA) which are commonly shared by patients with the same tumour type, neoantigens are tumour-specific and are generally patient-specific. Recognition of neoantigens may be an important driver of the anti-immune responses to T cell targeting therapy including ICI [95–98]. One study demonstrated that clinical responses to ICIs mostly occur in patients with pre-existing neoantigen-specific T cells in tumours [99].

There is great interest in developing neoantigens as vaccines to induce immune responses [100]. Although it has been reported that neoantigens were generated in treatment with ICI alone [98] or combined with RT and may be a biomarker of response [66,79], there are some barriers even at the experimental stage. For example, approximately only 1% of all tumour mutations generate a neoantigen with sufficient affinity for MHC to prime T cell responses; therefore, determining how to define a high-quality neoantigen which can trigger robust immune responses still presents a significant challenge. With the development of bioinformatics tools, several findings have emerged. Łuksza and colleagues proposed a neoantigen fitness model based on two main factors: the likelihood of neoantigen presentation on MHC and subsequent recognition by T cells [101]. Another study found that T cells targeting clonal mutations expressed by all tumour cells (trunk mutations) can achieve better anti-tumour immune responses than T cells targeting mutations expressed only in a proportion of tumour cells (subclonal branch mutations) in patients receiving ICI [98]. More work is needed to determine if the number of neoantigens or the frequency of neoantigen-specific T cells may be biomarkers of response to RT with or without ICI.

3.2. Imaging Biomarkers

In addition to the above blood-based biomarkers or tissue-based biomarkers, in recent years, non-invasive and clinically useful image-based techniques such as SPE-CT, PET-CT and MRI have been developed to evaluate the immune response to radiotherapy and/or immunotherapy [102]. These advanced imaging techniques may address the dilemma of patients unsuitable for biopsies or with multiple disease sites. A retrospective, European, multicentre cohort study examined tissue samples collected at diagnosis from 208 classical Hodgkin's lymphoma patients treated with two ABVD (doxorubicin, bleomycin, vinblastine and dacarbazine) courses with fluorodeoxyglucose (FDG)-PET

and analysed baseline staging and interim restaging. They found that early-interim FDG-PET scan after two ABVD chemotherapy courses (PET-2) was the only factor able to predict both progression-free survival and overall survival. In PET-2 negative patients, expression of CD68 ($\geq 25\%$) and PD1 (diffuse or rosetting pattern) in microenvironmental cells, and STAT1 negativity in Hodgkin Reed Sternberg cells, identified a subset of PET-2 negative patients with a 3-year progression-free survival significantly lower than that of the remaining PET-2 negative population [103]. This revealed the combined role of biomarkers and interim PET scan in prediction of treatment outcome and provided a new insight into developing immune cancer biomarkers.

Despite its role in staging being increasingly recognized in lymphoma and non-small cell lung cancer [104], ^{18}F -FDG-PET has several major drawbacks for use in immune imaging. This is a particular problem when it comes to the phenomenon of pseudoprogression, where the increased immune activity in response to successful therapy is difficult to distinguish from increased tumour metabolism in response to therapeutic failure [105]. Additionally, other limitations of PET imaging are that it is costly and exposes patients to radiation, and these have hindered its wider application in the clinic.

3.3. Biomarkers for RT and ICI Combination Therapies

Since the emergence of ICIs as delivering durable anti-tumour responses in a range of cancer types, albeit in the minority of patients treated, the number of clinical trials evaluating immunotherapy alone or combined with conventional oncology treatments such as RT or chemotherapy has greatly increased, with thousands of clinical trials in progress or being developed [106]. Whilst a detailed list of the clinical trials combining RT with immuno-oncology agents is beyond the scope of this review, the synergistic anti-tumour effects of RT and ICI has been investigated in many clinical studies and there are significant numbers of RT and ICI combination trials registered on clinicaltrials.gov [107].

One prospective trial investigated the efficacy of RT plus the anti-CTLA-4 ICI Ipilimumab in relapsed non-small-cell lung cancer. Twenty one of thirty nine enrolled patients completed the treatment protocol, with an overall objective response rate of 18%. Of the 20 evaluable patients, an increased serum IFN- β after RT and early dynamic changes in T cell clones appeared to be the strongest predictive biomarkers of response. Interestingly, T cells targeting a neoantigen controlled by a gene upregulated by RT were identified in one responding patient whose samples were analysed in more detail [66], but this “in-depth analysis” was only performed in one responding patient. Similarly, another study analysed three patients with refractory Hodgkin’s lymphoma treated with a combination of radiation and nivolumab; results showed that all three patients achieved durable complete local and abscopal responses. Further analysis found high PD-L1 expression in all three patient tumours, a mutation in the STAT6 gene, amplification of a “neoantigen” Erb-B2 receptor tyrosine kinase 2 (ERBB2) along with DNA damage response in patient 2 and an intermediate tumour mutation burden (TMB) with 8.15 mutations per megabase in patient 3. This suggested that the expression of PD-L1, DNA damage response and TMB might be potential biomarkers of response [79]. Due to the limitation of a small sample size and the retrospective nature of the study, these findings require validation in larger patient groups.

4. Conclusions and Future Directions

Tumours have been broadly divided into immunologically “hot”, characterised by high numbers of tumour-infiltrating T cells, and “cold”, characterised by low numbers of T cells [108]. What is currently less well characterised is how RT interacts with such “hot” or “cold” tumours to induce immune changes in human tumours. RT may well be immunostimulatory and potentially further enhance “hot” tumours and increase the number and diversity of T cell clones or potentially convert a “cold” tumour to a “hot” tumour with an increase in T cell infiltration. In contrast, RT could be immunosuppressive and convert a “hot” tumour to a “cold” tumour or make the tumour microenvironment of an already “cold” tumour even more immunosuppressive by inducing the cytokines that lead to infiltration of immunosuppressive immune effector cells. An enhanced understanding of how RT affects the TME in

“real time” as the patient is receiving RT will be extremely informative but requires a huge effort for serial tumour biopsies with the development of dynamic tumour biomarkers. Only when such data are available can we realistically begin to potentially implement different strategies to potentially enhance or modulate the RT-induced immune response and move towards a more personalized treatment approach for patients.

Currently, preclinical data are emerging which suggest that such a strategy of selecting an IO agent to combine with RT to improve outcomes may be possible at least for the “hot” tumours. In some murine tumours, anti-PD1 (ICI) combined with RT may lead to the generation of systemic immunity and long-term tumour control [10,22]. In contrast, for “cold” tumours, which are normally poorly infiltrated by T cells and contain increased numbers of immunosuppressive myeloid cells, anti-PD1 and RT may be less effective. Therefore, combining RT with IO or immune-stimulatory agents which act to reprogramme myeloid cells and drive increased T cell infiltration into tumours (e.g., TLR agonists, anti-CD40 mAb, anti-OX40 mAb) may be required to overcome this immunosuppressive TME and improve tumour control and survival [109,110].

However, to date, there are still many unanswered questions and future work in both the preclinical and clinical settings is required to establish the optimal RT regimen and any potential biomarkers which may inform IO agent choice when trying to further enhance the synergy of RT in combination with different immunotherapy modalities. Firstly, current data on immune infiltrates and tumour cell PD-L1 expression come from pre-treatment biopsies or surgery specimens, which mainly reflect the immune status at baseline, and there is limited information on changes in TME during or post-treatment. Additionally, few data exist on systemic immune biomarkers post-RT [57–59,111]. Therefore, there is an urgent unmet clinical need to collect tumour samples and matching bloods pre- and post-RT from patients undergoing routine RT to further understand the potentially diverse impact of RT between patients and tumour types.

Whilst changes in the TME are likely to be most reflective of immune changes induced by RT, investigations in peripheral blood may provide additional information to enable biomarker detection and surveillance during and after RT with less invasive sampling.

In addition, to identify whether a human tumour is immunologically “hot” or “cold”, there are now many technologies available to analyse immunological markers in tumour and blood. IHC is often used to identify tumour immune contexture by analysing FFPE samples and platforms now exist to multiplex up to 40 different cell markers. RNA gene expression arrays can be used to profile changes in immune genes in greater depth and possible immune gene signatures may arise as potential biomarkers [112,113]. Systemic immune changes can be monitored by profiling of PBMC populations through flow cytometry or mass spectrometry, TCR sequencing to investigate T cell clonality and analysis of serum cytokines and chemokines through multiplex bead-based assays or ELISAs. A thorough investigation of RT-induced changes in the immune TME and in the systemic circulation is the first step to identifying potential biomarkers of immune responses post-RT and determining if these biomarkers are predictive, prognostic or dynamic.

There is still much work to be done to enhance our understanding in the development of biomarkers for RT and RT + immunotherapy combinations in the clinic. Although there are currently thousands of clinical trials evaluating IO agents alone or combined with conventional oncology treatments such as RT or chemotherapy [58], only the minority have translational immunological research that may provide mechanistic insights and help the development of immunological biomarkers. For RT and RT in combination with IO agents, this field is still in its infancy and requires the coordinated efforts of the pioneers to incorporate biomarker-driven research into their design. Only with this focus on translational research will progress be made and provide us with the possibility that tumours may be stratified for treatment according to immune biomarkers identified in the TME and/or the peripheral blood that will predict immune responses post-RT and may inform RT/IO combinations.

Author Contributions: All authors equally contributed to this review. All authors have read and agreed to the published version of the manuscript.

Funding: Timothy M. Illidge and Eleanor J. Cheadle were supported by NIHR Manchester Biomedical Research Centre. This work was supported by Cancer Research UK via funding to the Cancer Research Manchester Centre.

Conflicts of Interest: The authors declare no conflict of interest.

References

1. Herrera, F.G.; Bourhis, J.; Coukos, G. Radiotherapy combination opportunities leveraging immunity for the next oncology practice. *CA A Cancer J. Clin.* **2016**, *67*, 65–85. [[CrossRef](#)]
2. Hanahan, D.; Weinberg, R.A. Hallmarks of Cancer: The Next Generation. *Cell* **2011**, *144*, 646–674. [[CrossRef](#)] [[PubMed](#)]
3. Mantovani, A.; Ponzetta, A.; Inforzato, A.; Jaillon, S. Innate immunity, inflammation and tumour progression: Double-edged swords. *J. Intern. Med.* **2019**, *285*, 524–532. [[CrossRef](#)] [[PubMed](#)]
4. Pagès, F.; Kirilovsky, A.; Mlecnik, B.; Asslaber, M.; Tosolini, M.; Bindea, G.; Lagorce, C.; Wind, P.; Marliot, F.; Bruneval, P.; et al. In Situ Cytotoxic and Memory T Cells Predict Outcome in Patients With Early-Stage Colorectal Cancer. *J. Clin. Oncol.* **2009**, *27*, 5944–5951. [[CrossRef](#)]
5. Galon, J.; Pagès, F.; Marincola, F.M.; Angell, H.K.; Thurin, M.; Lugli, A.; Zlobec, I.; Berger, A.; Bifulco, C.B.; Botti, G.; et al. Cancer classification using the Immunoscore: A worldwide task force. *J. Transl. Med.* **2012**, *10*, 205. [[CrossRef](#)] [[PubMed](#)]
6. Chaudhary, B.; Elkord, E. Regulatory T Cells in the Tumor Microenvironment and Cancer Progression: Role and Therapeutic Targeting. *Vaccines* **2016**, *4*, 28. [[CrossRef](#)] [[PubMed](#)]
7. Lindau, D.; Gielen, P.; Kroesen, M.; Wesseling, P.; Adema, G.J. The immunosuppressive tumour network: Myeloid-derived suppressor cells, regulatory T cells and natural killer T cells. *Immunol.* **2013**, *138*, 105–115. [[CrossRef](#)]
8. Kim, W.; Lee, S.; Seo, D.; Kim, D.; Kim, K.; Kim, E.; Kang, J.; Seong, K.M.; Youn, H.; Youn, B. Cellular Stress Responses in Radiotherapy. *Cells* **2019**, *8*, 1105. [[CrossRef](#)]
9. Mole, R.H. Whole Body Irradiation—Radiobiology or Medicine? *Br. J. Radiol.* **1953**, *26*, 234–241. [[CrossRef](#)]
10. Dovedi, S.J.; Adlard, A.; Lipowska-Bhalla, G.; McKenna, C.; Jones, S.; Cheadle, E.J.; Stratford, I.J.; Poon, E.; Morrow, M.; Stewart, R.; et al. Acquired Resistance to Fractionated Radiotherapy Can Be Overcome by Concurrent PD-L1 Blockade. *Cancer Res.* **2014**, *74*, 5458–5468. [[CrossRef](#)]
11. Sharabi, A.B.; Nirschl, C.J.; Kochel, C.M.; Nirschl, T.R.; Francica, B.J.; Velarde, E.; Deweese, T.L.; Drake, C.G.; Francisca, B.J. Stereotactic Radiation Therapy Augments Antigen-Specific PD-1-Mediated Antitumor Immune Responses via Cross-Presentation of Tumor Antigen. *Cancer Immunol. Res.* **2014**, *3*, 345–355. [[CrossRef](#)] [[PubMed](#)]
12. Victor, C.T.-S.; Rech, A.J.; Maity, A.; Rengan, R.; Pauken, K.E.; Stelekati, E.; Benci, J.L.; Xu, B.; Dada, H.; Odorizzi, P.M.; et al. Radiation and dual checkpoint blockade activate non-redundant immune mechanisms in cancer. *Nature* **2015**, *520*, 373–377. [[CrossRef](#)] [[PubMed](#)]
13. Formenti, S.C.; DeMaria, S. Systemic effects of local radiotherapy. *Lancet Oncol.* **2009**, *10*, 718–726. [[CrossRef](#)]
14. Nesslinger, N.J.; Sahota, R.A.; Stone, B.; Johnson, K.; Chima, N.; King, C.; Rasmussen, D.; Bishop, D.; Rennie, P.S.; Gleave, M.; et al. Standard Treatments Induce Antigen-Specific Immune Responses in Prostate Cancer. *Clin. Cancer Res.* **2007**, *13*, 1493–1502. [[CrossRef](#)]
15. Schaeue, D.; Comin-Anduix, B.; Ribas, A.; Zhang, L.; Goodglick, L.; Sayre, J.W.; Debucquoy, A.; Haustermans, K.; McBride, W.H. T-cell responses to survivin in cancer patients undergoing radiation therapy. *Clin. Cancer Res.* **2008**, *14*, 4883–4890. [[CrossRef](#)]
16. Reynders, K.; Illidge, T.; Siva, S.; Chang, J.Y.; De Ruyscher, D. The abscopal effect of local radiotherapy: Using immunotherapy to make a rare event clinically relevant. *Cancer Treat. Rev.* **2015**, *41*, 503–510. [[CrossRef](#)]
17. Postow, M.A.; Callahan, M.K.; Barker, C.A.; Yamada, Y.; Yuan, J.; Kitano, S.; Mu, Z.; Rasalan, T.; Adamow, M.; Ritter, E.; et al. Immunologic Correlates of the Abscopal Effect in a Patient with Melanoma. *N. Engl. J. Med.* **2012**, *366*, 925–931. [[CrossRef](#)]

18. Reits, E.A.; Hodge, J.W.; Herberts, C.A.; Groothuis, T.A.; Chakraborty, M.; K.Wansley, E.; Camphausen, K.; Luiten, R.M.; De Ru, A.H.; Neijssen, J.; et al. Radiation modulates the peptide repertoire, enhances MHC class I expression, and induces successful antitumor immunotherapy. *J. Exp. Med.* **2006**, *203*, 1259–1271. [[CrossRef](#)]
19. Obeid, M.; Tesniere, A.; Ghiringhelli, F.; Fimia, G.M.; Apetoh, L.; Perfettini, J.-L.; Castedo, M.; Mignot, G.; Panaretakis, T.; Casares, N.; et al. Calreticulin exposure dictates the immunogenicity of cancer cell death. *Nat. Med.* **2006**, *13*, 54–61. [[CrossRef](#)]
20. Kroemer, G.; Galluzzi, L.; Kepp, O.; Zitvogel, L. Immunogenic Cell Death in Cancer Therapy. *Annu. Rev. Immunol.* **2013**, *31*, 51–72. [[CrossRef](#)]
21. Honeychurch, J.; Illidge, T.M. The influence of radiation in the context of developing combination immunotherapies in cancer. *Ther. Adv. Vaccines Immunother.* **2018**, *5*, 115–122. [[CrossRef](#)] [[PubMed](#)]
22. Dovedi, S.J.; Cheadle, E.J.; Popple, A.; Poon, E.; Morrow, M.; Stewart, R.; Yusko, E.C.; Sanders, C.M.; Vignali, M.; Emerson, R.O.; et al. Fractionated Radiation Therapy Stimulates Antitumor Immunity Mediated by Both Resident and Infiltrating Polyclonal T-cell Populations when Combined with PD-1 Blockade. *Clin. Cancer Res.* **2017**, *23*, 5514–5526. [[CrossRef](#)] [[PubMed](#)]
23. Gasser, S.; Orsulic, S.; Brown, E.J.; Raulet, D.H. The DNA damage pathway regulates innate immune system ligands of the NKG2D receptor. *Nature* **2005**, *436*, 1186–1190. [[CrossRef](#)] [[PubMed](#)]
24. Durante, M.; Formenti, S.C. Radiation-Induced Chromosomal Aberrations and Immunotherapy: Micronuclei, Cytosolic DNA, and Interferon-Production Pathway. *Front. Oncol.* **2018**, *8*, 192. [[CrossRef](#)] [[PubMed](#)]
25. Klug, F.; Prakash, H.; Huber, P.E.; Seibel, T.; Bender, N.; Halama, N.; Pfirschke, C.; Voss, R.H.; Timke, C.; Umansky, L.; et al. Low-Dose Irradiation Programs Macrophage Differentiation to an iNOS+/M1 Phenotype that Orchestrates Effective T Cell Immunotherapy. *Cancer Cell* **2013**, *24*, 589–602. [[CrossRef](#)] [[PubMed](#)]
26. Barker, H.E.; Paget, J.T.E.; Khan, A.A.; Harrington, K.J. The tumour microenvironment after radiotherapy: Mechanisms of resistance and recurrence. *Nat. Rev. Cancer* **2015**, *15*, 409–425. [[CrossRef](#)]
27. Vanpouille-Box, C.; Diamond, J.M.; Pilonis, K.A.; Zavadil, J.; Babb, J.S.; Formenti, S.C.; Barcellos-Hoff, M.H.; DeMaria, S. TGF β Is a Master Regulator of Radiation Therapy-Induced Antitumor Immunity. *Cancer Res.* **2015**, *75*, 2232–2242. [[CrossRef](#)]
28. Yan, Y.; Chen, X.; Wang, X.; Zhao, Z.; Hu, W.; Zeng, S.; Wei, J.; Yang, X.; Qian, L.; Zhou, S.; et al. The effects and the mechanisms of autophagy on the cancer-associated fibroblasts in cancer. *J. Exp. Clin. Cancer Res.* **2019**, *38*, 171. [[CrossRef](#)]
29. Wang, Z.; Tang, Y.; Tan, Y.; Wei, Q.; Yu, W. Cancer-associated fibroblasts in radiotherapy: Challenges and new opportunities. *Cell Commun. Signal.* **2019**, *17*, 47. [[CrossRef](#)]
30. Augsten, M. Cancer-Associated Fibroblasts as Another Polarized Cell Type of the Tumor Microenvironment. *Front. Oncol.* **2014**, *4*, 62. [[CrossRef](#)]
31. Kioi, M.; Vogel, H.; Schultz, G.; Hoffman, R.M.; Harsh, G.R.; Brown, J.M. Inhibition of vasculogenesis, but not angiogenesis, prevents the recurrence of glioblastoma after irradiation in mice. *J. Clin. Investig.* **2010**, *120*, 694–705. [[CrossRef](#)]
32. Jäättelä, M. Multiple cell death pathways as regulators of tumour initiation and progression. *Oncogene* **2004**, *23*, 2746–2756. [[CrossRef](#)]
33. Long, J.S.; Ryan, K.M. New frontiers in promoting tumour cell death: Targeting apoptosis, necroptosis and autophagy. *Oncogene* **2012**, *31*, 5045–5060. [[CrossRef](#)]
34. Arrillaga-Romany, I.; Monje, M.; Wen, P.Y. Chapter 15—Neurologic Complications of Oncologic Therapy. In *Handbook of Neuro-Oncology Neuroimaging*, 2nd ed.; Newton, H.B., Ed.; Academic Press: San Diego, CA, USA, 2016; pp. 125–142.
35. Omay, S.B.; Atsina, K.K.; Baehring, J.M. Chapter 53—Nonneoplastic Mass Lesions of the Central Nervous System. In *Handbook of Neuro-Oncology Neuroimaging*, 2nd ed.; Newton, H.B., Ed.; Academic Press: San Diego, CA, USA, 2016; pp. 653–665.
36. Klionsky, D.J. Autophagy: From phenomenology to molecular understanding in less than a decade. *Nat. Rev. Mol. Cell Biol.* **2007**, *8*, 931–937. [[CrossRef](#)] [[PubMed](#)]
37. Levy, J.M.M.; Towers, C.G.; Thorburn, A. Targeting autophagy in cancer. *Nat. Rev. Cancer* **2017**, *17*, 528–542. [[CrossRef](#)] [[PubMed](#)]

38. Cirone, M.; Montani, M.S.G.; Granato, M.; Garufi, A.; Faggioni, A.; D’Orazi, G. Autophagy manipulation as a strategy for efficient anticancer therapies: Possible consequences. *J. Exp. Clin. Cancer Res.* **2019**, *38*, 262. [[CrossRef](#)] [[PubMed](#)]
39. Ko, A.; Kanehisa, A.; Martins, I.; Senovilla, L.; Chargari, C.; Dugue, D.; Mariño, G.; Kepp, O.; Michaud, M.; Perfettini, J.-L.; et al. Autophagy inhibition radiosensitizes in vitro, yet reduces radioresponses in vivo due to deficient immunogenic signalling. *Cell Death Differ.* **2013**, *21*, 92–99. [[CrossRef](#)] [[PubMed](#)]
40. Valkenburg, K.C.; De Groot, A.E.; Pienta, K.J. Targeting the tumour stroma to improve cancer therapy. *Nat. Rev. Clin. Oncol.* **2018**, *15*, 366–381. [[CrossRef](#)] [[PubMed](#)]
41. Chude, C.I.; Amaravadi, R.K. Targeting Autophagy in Cancer: Update on Clinical Trials and Novel Inhibitors. *Int. J. Mol. Sci.* **2017**, *18*, 1279. [[CrossRef](#)]
42. Rosenfeld, M.R.; Ye, X.; Supko, J.G.; Desideri, S.; Grossman, S.A.; Brem, S.; Mikkelsen, T.; Wang, D.; Chang, Y.C.; Hu, J.; et al. A phase I/II trial of hydroxychloroquine in conjunction with radiation therapy and concurrent and adjuvant temozolomide in patients with newly diagnosed glioblastoma multiforme. *Autophagy* **2014**, *10*, 1359–1368. [[CrossRef](#)]
43. Rojas-Puentes, L.L.; González-Pinedo, M.; Crismatt, A.; Gómez, A.O.; Gamboa-Vignolle, C.; Núñez-Gómez, R.; Dorantes-Gallareta, Y.; Arce-Salinas, C.; Arrieta, O. Phase II randomized, double-blind, placebo-controlled study of whole-brain irradiation with concomitant chloroquine for brain metastases. *Radiat. Oncol.* **2013**, *8*, 209. [[CrossRef](#)] [[PubMed](#)]
44. Rubinsztein, D.C.; Codogno, P.; Levine, B. Autophagy modulation as a potential therapeutic target for diverse diseases. *Nat. Rev. Drug Discov.* **2012**, *11*, 709–730. [[CrossRef](#)] [[PubMed](#)]
45. Su, Z.; Yang, Z.; Xie, L.; DeWitt, J.P.; Chen, Y. Cancer therapy in the necroptosis era. *Cell Death Differ.* **2016**, *23*, 748–756. [[CrossRef](#)] [[PubMed](#)]
46. Royce, G.H.; Brown-Borg, H.M.; Deepa, S.S. The potential role of necroptosis in inflammaging and aging. *GeroScience* **2019**, *41*, 795–811. [[CrossRef](#)] [[PubMed](#)]
47. Wang, Y.; Zhao, M.; He, S.; Luo, Y.; Zhao, Y.; Cheng, J.; Gong, Y.; Xie, J.; Wang, Y.; Hu, B.; et al. Necroptosis regulates tumor repopulation after radiotherapy via RIP1/RIP3/MLKL/JNK/IL8 pathway. *J. Exp. Clin. Cancer Res.* **2019**, *38*, 1–16. [[CrossRef](#)]
48. Angeli, J.P.F.; Krysko, D.V.; Conrad, M. Ferroptosis at the crossroads of cancer-acquired drug resistance and immune evasion. *Nat. Rev. Cancer* **2019**, *19*, 405–414. [[CrossRef](#)]
49. Lang, X.; Green, M.D.; Wang, W.; Yu, J.; Choi, J.E.; Jiang, L.; Liao, P.; Zhou, J.; Zhang, Q.; Dow, A.; et al. Radiotherapy and Immunotherapy Promote Tumoral Lipid Oxidation and Ferroptosis via Synergistic Repression of SLC7A11. *Cancer Discov.* **2019**, *9*, 1673–1685. [[CrossRef](#)]
50. Lei, G.; Zhang, Y.; Koppula, P.; Liu, X.; Zhang, J.; Lin, S.H.; Ajani, J.A.; Xiao, Q.; Liao, Z.; Wang, H.; et al. The role of ferroptosis in ionizing radiation-induced cell death and tumor suppression. *Cell Res.* **2020**, *30*, 146–162. [[CrossRef](#)]
51. Gutman, S.; Kessler, L.G. The US Food and Drug Administration perspective on cancer biomarker development. *Nat. Rev. Cancer* **2006**, *6*, 565–571. [[CrossRef](#)]
52. Lesterhuis, W.J.; Bosco, A.; Millward, M.J.; Small, M.; Nowak, A.K.; Lake, R.A. Dynamic versus static biomarkers in cancer immune checkpoint blockade: Unravelling complexity. *Nat. Rev. Drug Discov.* **2017**, *16*, 264–272. [[CrossRef](#)]
53. Fane, M.; Weeraratna, A.T. How the ageing microenvironment influences tumour progression. *Nat. Rev. Cancer* **2019**, *20*, 89–106. [[CrossRef](#)] [[PubMed](#)]
54. Wang, J.; Sun, H.; Zeng, Q.; Guo, X.-J.; Wang, H.; Liu, H.-H.; Dong, Z.-Y. HPV-positive status associated with inflamed immune microenvironment and improved response to anti-PD-1 therapy in head and neck squamous cell carcinoma. *Sci. Rep.* **2019**, *9*, 13404. [[CrossRef](#)] [[PubMed](#)]
55. Stewart, G.D.; Ross, J.A.; McLaren, D.; Parker, C.C.; Habib, F.K.; Riddick, A.C. The relevance of a hypoxic tumour microenvironment in prostate cancer. *BJU Int.* **2010**, *105*, 8–13. [[CrossRef](#)]
56. Rothenberger, N.J.; Somasundaram, A.; Stabile, L.P. The Role of the Estrogen Pathway in the Tumor Microenvironment. *Int. J. Mol. Sci.* **2018**, *19*, 611. [[CrossRef](#)]
57. Onal, C.; Yildirim, B.A.; Guler, O.C.; Mertsoylu, H. The Utility of Pretreatment and Posttreatment Lymphopenia in Cervical Squamous Cell Carcinoma Patients Treated with Definitive Chemoradiotherapy. *Int. J. Gynecol. Cancer* **2018**, *28*, 1553–1559. [[CrossRef](#)] [[PubMed](#)]

58. Wang, N.; An, G.; Xie, S.; Yao, Y.; Feng, G. The clinical and prognostic significance of CD14+HLA-DR⁻/low myeloid-derived suppressor cells in hepatocellular carcinoma patients receiving radiotherapy. *Tumor Biol.* **2016**, *37*, 10427–10433. [[CrossRef](#)]
59. Napolitano, M.; D'Alterio, C.; Cardone, E.; Trotta, A.; Pecori, B.; Rega, D.; Pace, U.; Scala, D.; Scognamiglio, G.; Tatangelo, F.; et al. Peripheral myeloid-derived suppressor and T regulatory PD-1 positive cells predict response to neoadjuvant short-course radiotherapy in rectal cancer patients. *Oncotarget* **2015**, *6*, 8261–8270. [[CrossRef](#)]
60. Willett, C.G.; Duda, D.G.; Di Tomaso, E.; Boucher, Y.; Ancukiewicz, M.; Sahani, D.V.; Lahdenranta, J.; Chung, D.C.; Fischman, A.J.; Lauwers, G.Y.; et al. Efficacy, Safety, and Biomarkers of Neoadjuvant Bevacizumab, Radiation Therapy, and Fluorouracil in Rectal Cancer: A Multidisciplinary Phase II Study. *J. Clin. Oncol.* **2009**, *27*, 3020–3026. [[CrossRef](#)]
61. Balermipas, P.; Michel, Y.; Wagenblast, J.; Seitz, O.; Weiss, C.; Rödel, F.; Rödel, C.; Fokas, E. Tumour-infiltrating lymphocytes predict response to definitive chemoradiotherapy in head and neck cancer. *Br. J. Cancer* **2013**, *110*, 501–509. [[CrossRef](#)]
62. Anitei, M.-G.; Zeitoun, G.; Mlecnik, B.; Marliot, F.; Haicheur, N.; Todosi, A.M.; Kirilovsky, A.; Lagorce, C.; Bindea, G.; Ferariu, D.; et al. Prognostic and Predictive Values of the Immunoscore in Patients with Rectal Cancer. *Clin. Cancer Res.* **2014**, *20*, 1891–1899. [[CrossRef](#)]
63. Lim, Y.J.; Koh, J.; Kim, K.; Chie, E.K.; Kim, B.; Lee, K.; Jang, J.-Y.; Kim, S.-W.; Oh, -Y.; Bang, Y.-J.; et al. High ratio of programmed cell death protein 1 (PD-1)+/CD8+ tumor-infiltrating lymphocytes identifies a poor prognostic subset of extrahepatic bile duct cancer undergoing surgery plus adjuvant chemoradiotherapy. *Radiother. Oncol.* **2015**, *117*, 165–170. [[CrossRef](#)] [[PubMed](#)]
64. Iijima, M.; Okonogi, N.; Nakajima, N.I.; Morokoshi, Y.; Kanda, H.; Yamada, T.; Kobayashi, Y.; Banno, K.; Wakatsuki, M.; Yamada, S.; et al. Significance of PD-L1 expression in carbon-ion radiotherapy for uterine cervical adeno/adenosquamous carcinoma. *J. Gynecol. Oncol.* **2020**, *31*, 19. [[CrossRef](#)] [[PubMed](#)]
65. Kim, H.J.; Park, S.; Kim, K.-J.; Seong, J. Clinical significance of soluble programmed cell death ligand-1 (sPD-L1) in hepatocellular carcinoma patients treated with radiotherapy. *Radiother. Oncol.* **2018**, *129*, 130–135. [[CrossRef](#)] [[PubMed](#)]
66. Formenti, S.C.; Rudqvist, N.-P.; Golden, E.; Cooper, B.T.; Wennerberg, E.; Lhuillier, C.; Vanpouille-Box, C.; Friedman, K.; De Andrade, L.F.; Wucherpfennig, K.W.; et al. Radiotherapy induces responses of lung cancer to CTLA-4 blockade. *Nat. Med.* **2018**, *24*, 1845–1851. [[CrossRef](#)]
67. Eder, T.; Hess, A.; Kunschak, R.; Stromberger, C.; Jöhrens, K.; Fleischer, V.; Hummel, M.; Balermipas, P.; Von Der Grün, J.; Linge, A.; et al. Interference of tumour mutational burden with outcome of patients with head and neck cancer treated with definitive chemoradiation: A multicentre retrospective study of the German Cancer Consortium Radiation Oncology Group. *Eur. J. Cancer* **2019**, *116*, 67–76. [[CrossRef](#)]
68. Efstathiou, J.A.; Mouw, K.W.; Gibb, E.A.; Liu, Y.; Wu, C.-L.; Drumm, M.R.; Da Costa, J.B.; Du Plessis, M.; Wang, N.Q.; Davicioni, E.; et al. Impact of Immune and Stromal Infiltration on Outcomes Following Bladder-Sparing Trimodality Therapy for Muscle-Invasive Bladder Cancer. *Eur. Urol.* **2019**, *76*, 59–68. [[CrossRef](#)]
69. Pardoll, D.M. The blockade of immune checkpoints in cancer immunotherapy. *Nat. Rev. Cancer* **2012**, *12*, 252–264. [[CrossRef](#)]
70. Topalian, S.L.; Hodi, F.S.; Brahmer, J.R.; Gettinger, S.N.; Smith, D.C.; McDermott, D.F.; Powderly, J.D.; Carvajal, R.D.; Sosman, J.A.; Atkins, M.B.; et al. Safety, Activity, and Immune Correlates of Anti-PD-1 Antibody in Cancer. *N. Engl. J. Med.* **2012**, *366*, 2443–2454. [[CrossRef](#)]
71. Robert, C.; Long, G.; Brady, B.; Dutriaux, C.; Maio, M.; Mortier, L.; Hassel, J.C.; Rutkowski, P.; McNeil, C.; Kalinka-Warzocha, E.; et al. Nivolumab in Previously Untreated Melanoma without BRAF Mutation. *N. Engl. J. Med.* **2015**, *372*, 320–330. [[CrossRef](#)]
72. Larkin, J.; Hodi, F.S.; Wolchok, J.D.; E Valsecchi, M. Combined Nivolumab and Ipilimumab or Monotherapy in Untreated Melanoma. *N. Engl. J. Med.* **2015**, *373*, 23–34. [[CrossRef](#)]
73. Do, H.B.; Paz-Ares, L.; Horn, L.; Spigel, D.R.; Steins, M.; Ready, N.E.; Chow, L.Q.; Vokes, E.E.; Felip, E.; Holgado, E.; et al. Nivolumab versus Docetaxel in Advanced Nonsquamous Non-Small-Cell Lung Cancer. *N. Engl. J. Med.* **2015**, *373*, 1627–1639. [[CrossRef](#)]

74. Taube, J.M.; Klein, A.; Brahmer, J.R.; Xu, H.; Pan, X.; Kim, J.H.; Chen, L.; Pardoll, E.M.; Topalian, S.L.; Anders, R.A. Association of PD-1, PD-1 ligands, and other features of the tumor immune microenvironment with response to anti-PD-1 therapy. *Clin. Cancer Res.* **2014**, *20*, 5064–5074. [[CrossRef](#)] [[PubMed](#)]
75. Lee, V.H.F.; Lo, A.W.; Leung, C.-Y.; Shek, W.-H.; Kwong, R.L.W.; Lam, K.-O.; Tong, C.-C.; Sze, C.-K.; Leung, T.-W. Correlation of PD-L1 Expression of Tumor Cells with Survival Outcomes after Radical Intensity-Modulated Radiation Therapy for Non-Metastatic Nasopharyngeal Carcinoma. *PLoS ONE* **2016**, *11*, e0157969. [[CrossRef](#)] [[PubMed](#)]
76. Antonia, S.J.; Villegas, A.; Daniel, D.; Vicente, D.; Murakami, S.; Hui, R.; Yokoi, T.; Chiappori, A.; Lee, K.H.; de Wit, M.; et al. Durvalumab after Chemoradiotherapy in Stage III Non-Small-Cell Lung Cancer. *N. Engl. J. Med.* **2017**, *377*, 1919–1929. [[CrossRef](#)]
77. Hollander, P.; Amini, R.-M.; Ginman, B.; Molin, D.; Enblad, G.; Glimelius, I. Expression of PD-1 and PD-L1 increase in consecutive biopsies in patients with classical Hodgkin lymphoma. *PLoS ONE* **2018**, *13*, e0204870. [[CrossRef](#)]
78. De Re, V.; Caggiari, L.; Repetto, O.; Mussolin, L.; Mascarini, M.; Re, D. Classical Hodgkin's Lymphoma in the Era of Immune Checkpoint Inhibition. *J. Clin. Med.* **2019**, *8*, 1596. [[CrossRef](#)]
79. Qin, Q.; Nan, X.; Miller, T.; Fisher, R.; Teh, B.; Pandita, S.; Farach, A.M.; Pingali, S.R.; Pandita, R.K.; Butler, E.B.; et al. Complete Local and Abscopal Responses from a Combination of Radiation and Nivolumab in Refractory Hodgkin's Lymphoma. *Radiat. Res.* **2018**, *190*, 322–329. [[CrossRef](#)]
80. Antonia, S.J.; Villegas, A.; Daniel, D.; Vicente, D.; Murakami, S.; Hui, R.; Kurata, T.; Chiappori, A.; Lee, K.H.; De Wit, M.; et al. Overall Survival with Durvalumab after Chemoradiotherapy in Stage III NSCLC. *N. Engl. J. Med.* **2018**, *379*, 2342–2350. [[CrossRef](#)]
81. Popple, A.; Illidge, T. Harmonization of programmed cell death ligand-1 diagnostic assays in non-small cell lung cancer. *Transl. Cancer Res.* **2017**, *6*, S553–S556. [[CrossRef](#)]
82. Patel, S.P.; Kurzrock, R. PD-L1 Expression as a Predictive Biomarker in Cancer Immunotherapy. *Mol. Cancer Ther.* **2015**, *14*, 847–856. [[CrossRef](#)]
83. Rimm, D.L.; Han, G.; Taube, J.M.; Yi, E.S.; Bridge, J.A.; Flieder, U.B.; Homer, R.; West, W.W.; Wu, H.; Roden, A.C.; et al. A Prospective, Multi-institutional, Pathologist-Based Assessment of 4 Immunohistochemistry Assays for PD-L1 Expression in Non-Small Cell Lung Cancer. *JAMA Oncol.* **2017**, *3*, 1051–1058. [[CrossRef](#)] [[PubMed](#)]
84. FDA Nods for Atezolizumab and Nivolumab. *Cancer Discov.* **2016**, *6*, 811. [[CrossRef](#)] [[PubMed](#)]
85. Rashidian, M.; Ingram, J.R.; Dougan, M.; Dongre, A.; Whang, K.A.; Le Gall, C.; Cragnolini, J.J.; Bierie, B.; Gostissa, M.; Gorman, J.; et al. Predicting the response to CTLA-4 blockade by longitudinal noninvasive monitoring of CD8 T cells. *J. Exp. Med.* **2017**, *214*, 2243–2255. [[CrossRef](#)] [[PubMed](#)]
86. Huang, A.; Xiao, Y.; Peng, C.; Liu, T.; Lin, Z.; Yang, Q.; Zhang, T.; Liu, J.; Ma, H. 53BP1 expression and immunoscore are associated with the efficacy of neoadjuvant chemoradiotherapy for rectal cancer. *Strahlenther. Onkol.* **2019**, *196*, 465–473. [[CrossRef](#)]
87. Teng, F.; Mu, D.; Meng, X.; Kong, L.; Zhu, H.; Liu, S.; Zhang, J.; Yu, J. Tumor infiltrating lymphocytes (TILs) before and after neoadjuvant chemoradiotherapy and its clinical utility for rectal cancer. *Am. J. Cancer Res.* **2015**, *5*, 2064–2074.
88. Hagland, H.; Lea, D.; Watson, M.; Søreide, K. Correlation of circulating T-cells in pre-operative blood to intratumoral density and location of CD3+ and CD8+ T-cells in colorectal cancer: A potential for an immunoscore by liquid biopsy? *Eur. J. Cancer* **2017**, *72*, S49–S50. [[CrossRef](#)]
89. Berghoff, A.S.; Fuchs, E.; Ricken, G.; Mlecnik, B.; Bindea, G.; Spanberger, T.; Hackl, M.; Widhalm, G.; Dieckmann, K.; Prayer, D.; et al. Density of tumor-infiltrating lymphocytes correlates with extent of brain edema and overall survival time in patients with brain metastases. *OncolImmunology* **2015**, *5*, e1057388. [[CrossRef](#)]
90. Zehir, A.; Benayed, R.; Shah, R.; Syed, A.; Middha, S.; Kim, H.R.; Srinivasan, P.; Gao, J.; Chakravarty, D.; Devlin, S.M.; et al. Mutational landscape of metastatic cancer revealed from prospective clinical sequencing of 10,000 patients. *Nat. Med.* **2017**, *23*, 703–713. [[CrossRef](#)]
91. Snyder, A.; Makarov, V.; Merghoub, T.; Yuan, J.; Zaretsky, J.M.; Desrichard, A.; Walsh, L.A.; Postow, M.A.; Wong, P.; Ho, T.S.; et al. Genetic Basis for Clinical Response to CTLA-4 Blockade in Melanoma. *N. Engl. J. Med.* **2014**, *371*, 2189–2199. [[CrossRef](#)]

92. Rizvi, N.A.; Hellmann, M.D.; Snyder, A.; Kvistborg, P.; Makarov, V.; Havel, J.J.; Lee, W.; Yuan, J.; Wong, P.; Ho, T.S.; et al. Mutational landscape determines sensitivity to PD-1 blockade in non-small cell lung cancer. *Science* **2015**, *348*, 124–128. [[CrossRef](#)]
93. Samstein, R.M.; Lee, C.-H.; Shoushtari, A.; Hellmann, M.D.; Shen, R.; Janjigian, Y.Y.; Barron, D.A.; Zehir, A.; Jordan, E.J.; Omuro, A.; et al. Tumor mutational load predicts survival after immunotherapy across multiple cancer types. *Nat. Genet.* **2019**, *51*, 202–206. [[CrossRef](#)] [[PubMed](#)]
94. Efremova, M.; Finotello, F.; Rieder, D.; Trajanoski, Z. Neoantigens Generated by Individual Mutations and Their Role in Cancer Immunity and Immunotherapy. *Front. Immunol.* **2017**, *8*, 1679. [[CrossRef](#)] [[PubMed](#)]
95. Schumacher, T.N.; Scheper, W.; Kvistborg, P. Cancer Neoantigens. *Annu. Rev. Immunol.* **2019**, *37*, 173–200. [[CrossRef](#)] [[PubMed](#)]
96. Yarchoan, M.; Johnson, B.A.; Lutz, E.R.; Laheru, D.A.; Jaffee, E.M. Targeting neoantigens to augment antitumour immunity. *Nat. Rev. Cancer* **2017**, *17*, 209–222. [[CrossRef](#)]
97. Schumacher, T.N.; Schreiber, R.D. Neoantigens in cancer immunotherapy. *Science* **2015**, *348*, 69–74. [[CrossRef](#)]
98. McGranahan, N.; Furness, A.J.S.; Rosenthal, R.; Ramskov, S.; Lyngaa, R.; Saini, S.K.; Jamal-Hanjani, M.; Wilson, G.A.; Birkbak, N.J.; Hiley, C.; et al. Clonal neoantigens elicit T cell immunoreactivity and sensitivity to immune checkpoint blockade. *Science* **2016**, *351*, 1463–1469. [[CrossRef](#)]
99. Tumei, P.C.; Harview, C.L.; Yearley, J.H.; Shintaku, I.P.; Taylor, E.J.M.; Robert, L.; Chmielowski, B.; Spasić, M.; Henry, G.; Ciobanu, V.; et al. PD-1 blockade induces responses by inhibiting adaptive immune resistance. *Nature* **2014**, *515*, 568–571. [[CrossRef](#)]
100. Peng, M.; Mo, Y.; Wang, Y.; Wu, P.; Zhang, Y.; Xiong, F.; Guo, C.; Wu, X.; Li, Y.; Li, X.; et al. Neoantigen vaccine: An emerging tumor immunotherapy. *Mol. Cancer* **2019**, *18*, 1–14. [[CrossRef](#)]
101. Łuksza, M.; Riaz, N.; Makarov, V.; Balachandran, V.P.; Hellmann, M.D.; Solovyov, A.; Rizvi, N.A.; Merghoub, T.; Levine, A.J.; Chan, T.A.; et al. A neoantigen fitness model predicts tumour response to checkpoint blockade immunotherapy. *Nature* **2017**, *551*, 517–520. [[CrossRef](#)]
102. Grassberger, C.; Ellsworth, S.G.; Wilks, M.Q.; Keane, F.K.; Loeffler, J.S. Assessing the interactions between radiotherapy and antitumour immunity. *Nat. Rev. Clin. Oncol.* **2019**, *16*, 729–745. [[CrossRef](#)]
103. Agostinelli, C.; Gallamini, A.; Stracqualursi, L.; Agati, P.; Tripodo, C.; Fuligni, F.; Sista, M.T.; Fanti, S.; Biggi, A.; Vitolo, U.; et al. The combined role of biomarkers and interim PET scan in prediction of treatment outcome in classical Hodgkin's lymphoma: A retrospective, European, multicentre cohort study. *Lancet Haematol.* **2016**, *3*, e467–e479. [[CrossRef](#)]
104. Fischer, B.M.; Lassen, U.; Mortensen, J.; Larsen, S.; Loft, A.; Bertelsen, A.; Ravn, J.; Clementsen, P.; Høgholm, A.; Larsen, K.; et al. Preoperative Staging of Lung Cancer with Combined PET–CT. *N. Engl. J. Med.* **2009**, *361*, 32–39. [[CrossRef](#)] [[PubMed](#)]
105. Chiou, V.L.; Burotto, M. Pseudoprogression and Immune-Related Response in Solid Tumors. *J. Clin. Oncol.* **2015**, *33*, 3541–3543. [[CrossRef](#)] [[PubMed](#)]
106. Kang, J.; DeMaria, S.; Formenti, S.C. Current clinical trials testing the combination of immunotherapy with radiotherapy. *J. Immunother. Cancer* **2016**, *4*, 51. [[CrossRef](#)]
107. Liu, Y.; Dong, Y.; Kong, L.; Shi, F.; Zhu, H.; Yu, J. Abscopal effect of radiotherapy combined with immune checkpoint inhibitors. *J. Hematol. Oncol.* **2018**, *11*, 104. [[CrossRef](#)] [[PubMed](#)]
108. Galon, J.; Bruni, D. Approaches to treat immune hot, altered and cold tumours with combination immunotherapies. *Nat. Rev. Drug Discov.* **2019**, *18*, 197–218. [[CrossRef](#)]
109. Aguilera, T.; Elghonaimy, E.A.; Shehade, H.; Rafat, M.; Castellini, L.; Jiang, D.; Kariolis, M.; Koong, A.C.; Le, Q.-T.; Ellies, L.G.; et al. Induced Tumor Heterogeneity Reveals Factors Informing Radiation and Immunotherapy Combinations. *Clin. Cancer Res.* **2020**, *26*, 2972–2985. [[CrossRef](#)]
110. Schölch, S.; Rauber, C.; Tietz, A.; Rahbari, N.N.; Bork, U.; Schmidt, T.; Kahlert, C.; Haberkorn, U.; Tomai, M.A.; Lipson, K.E.; et al. Radiotherapy combined with TLR7/8 activation induces strong immune responses against gastrointestinal tumors. *Oncotarget* **2014**, *6*, 4663–4676. [[CrossRef](#)]
111. Brøndum, L.; Eriksen, J.G.; Sørensen, B.S.; Mortensen, L.S.; Toustrup, K.; Overgaard, J.; Alsner, J. Plasma proteins as prognostic biomarkers in radiotherapy treated head and neck cancer patients. *Clin. Transl. Radiat. Oncol.* **2017**, *2*, 46–52. [[CrossRef](#)]

112. Ayers, M.; Luceford, J.K.; Nebozhyn, M.V.; Murphy, E.; Loboda, A.; Kaufman, D.R.; Albright, A.; Cheng, J.D.; Kang, S.P.; Shankaran, V.; et al. IFN- γ -related mRNA profile predicts clinical response to PD-1 blockade. *J. Clin. Investig.* **2017**, *127*, 2930–2940. [[CrossRef](#)]
113. Karachaliou, N.; González-Cao, M.; Crespo, G.; Drozdowskyj, A.; Aldeguer, E.; Giménez-Capitán, A.; Teixido, C.; Molina-Vila, M.Á.; Viteri, S.; De Los Llanos Gil, M.; et al. Interferon gamma, an important marker of response to immune checkpoint blockade in non-small cell lung cancer and melanoma patients. *Ther. Adv. Med. Oncol.* **2018**, *10*. [[CrossRef](#)] [[PubMed](#)]



© 2020 by the authors. Licensee MDPI, Basel, Switzerland. This article is an open access article distributed under the terms and conditions of the Creative Commons Attribution (CC BY) license (<http://creativecommons.org/licenses/by/4.0/>).

Review

Oxidative Stress in the Tumor Microenvironment and Its Relevance to Cancer Immunotherapy

Nada S. Aboeella ^{1,2} , Caitlin Brandle ¹, Timothy Kim ³, Zhi-Chun Ding ^{1,4}  and Gang Zhou ^{1,2,4,5,*}

¹ Georgia Cancer Center, Medical College of Georgia, Augusta University, Augusta, GA 30912, USA; naboellella@augusta.edu (N.S.A.); cbrandle@augusta.edu (C.B.); zding@augusta.edu (Z.-C.D.)

² The Graduate School, Augusta University, Augusta, GA 30912, USA

³ The Center for Undergraduate Research and Scholarship, Augusta University, Augusta, GA 30912, USA; timkim@augusta.edu

⁴ Department of Biochemistry and Molecular Biology, Medical College of Georgia, Augusta University, Augusta, GA 30912, USA

⁵ Department of Medicine, Medical College of Georgia, Augusta University, Augusta, GA 30912, USA

* Correspondence: GZHOU@augusta.edu; Tel.: +1-706-721-4472

Simple Summary: Cancer cells are consistently under oxidative stress, as reflected by elevated basal level of reactive oxygen species (ROS), due to increased metabolism driven by aberrant cell growth. This feature has been exploited to develop therapeutic strategies that control tumor growth by modulating the oxidative stress in tumor cells. This review provides an overview of recent advances in cancer therapies targeting tumor oxidative stress, and highlights the emerging evidence implicating the effectiveness of cancer immunotherapies in intensifying tumor oxidative stress. The promises and challenges of combining ROS-inducing agents with cancer immunotherapy are also discussed.

Abstract: It has been well-established that cancer cells are under constant oxidative stress, as reflected by elevated basal level of reactive oxygen species (ROS), due to increased metabolism driven by aberrant cell growth. Cancer cells can adapt to maintain redox homeostasis through a variety of mechanisms. The prevalent perception about ROS is that they are one of the key drivers promoting tumor initiation, progression, metastasis, and drug resistance. Based on this notion, numerous antioxidants that aim to mitigate tumor oxidative stress have been tested for cancer prevention or treatment, although the effectiveness of this strategy has yet to be established. In recent years, it has been increasingly appreciated that ROS have a complex, multifaceted role in the tumor microenvironment (TME), and that tumor redox can be targeted to amplify oxidative stress inside the tumor to cause tumor destruction. Accumulating evidence indicates that cancer immunotherapies can alter tumor redox to intensify tumor oxidative stress, resulting in ROS-dependent tumor rejection. Herein we review the recent progresses regarding the impact of ROS on cancer cells and various immune cells in the TME, and discuss the emerging ROS-modulating strategies that can be used in combination with cancer immunotherapies to achieve enhanced antitumor effects.

Keywords: oxidative stress; reactive oxygen species; immunotherapy; tumor microenvironment



Citation: Aboeella, N.S.; Brandle, C.; Kim, T.; Ding, Z.-C.; Zhou, G. Oxidative Stress in the Tumor Microenvironment and Its Relevance to Cancer Immunotherapy. *Cancers* **2021**, *13*, 986. <https://doi.org/10.3390/cancers13050986>

Academic Editor: Alberto Anel

Received: 27 January 2021

Accepted: 23 February 2021

Published: 27 February 2021

Publisher's Note: MDPI stays neutral with regard to jurisdictional claims in published maps and institutional affiliations.



Copyright: © 2021 by the authors. Licensee MDPI, Basel, Switzerland. This article is an open access article distributed under the terms and conditions of the Creative Commons Attribution (CC BY) license (<https://creativecommons.org/licenses/by/4.0/>).

1. Introduction

Reactive oxygen species (ROS) are a group of highly reactive oxygen-containing molecules, including free radicals such as hydroxyl (HO[•]), superoxide (O₂[•]), peroxides (RO[•]) and oxides of nitrogen (NO[•]) and the non-radical hydrogen peroxide (H₂O₂). ROS are physiologically generated as a byproduct of cellular respiration and aerobic metabolism, pathologically elevated in diseases like inflammation and cancer, and exogenously formulated after exposure to xenobiotics such as chemotherapy, radiotherapy, or UV. At low to medium levels, ROS can act as cellular signaling messengers, involved in regulating a variety of cellular functions including gene expression, cell proliferation and differentiation, and

immunity against diseases. At high levels, ROS cause oxidative damage to DNA, proteins, and lipids, and become detrimental to cells. Due to the multifaceted role of ROS in cell survival and function, the cellular levels of ROS have to be tightly controlled to maintain the redox homeostasis, i.e., the balance between ROS production and scavenging, through multi-layer mechanisms. Oxidative stress occurs when this balance is disrupted in cells. The ontogeny, regulation, and biological function of oxidative stress in cancer biology have been extensively reviewed by others [1–4]. In this review, we mainly discuss the impact of oxidative stress on the tumor microenvironment (TME), including cancer cells and various immune cells. By focusing on how the interplays between cancer cells and immune cells influence the redox status of both populations, we highlight the therapeutic potential of rational combination of ROS-modulating agents with cancer immunotherapies.

2. The Impact of Oxidative Stress on Cancer Cells

It has been well-established that cancer cells are under higher degree of basal level oxidative stress than normal cells, reflected by an increased presence of ROS. Mitochondria are the major cellular source of ROS production. Mitochondria produce ROS during respiration as a natural by-product of electron transport chain (ETC) activity. Incomplete electron transfer and leakage of electrons through ETC complexes I, II, and III results in superoxide production [5]. Membrane-bound NADPH oxidases (NOXs) are another important source of ROS. NOXs are a family of hetero-oligomeric enzymes that catalyze the production of superoxide from O₂ and NADPH. In most mammals, there are seven NOX isoforms: NOX1, NOX2, NOX3, NOX4, NOX5, dual oxidase (DUOX) 1, and DUOX2 [3,6]. Deregulated ROS generation in cancer cells may occur due to cell-intrinsic events such as oncogene activation, tumor suppressor gene inactivation, increased metabolism, and adaptation to hypoxia (i.e., low oxygen levels), or exogenous insults such as chemotherapy and ionizing radiation [2,3,7–9].

2.1. ROS in Tumor Initiation, Progression, and Survival

Mildly increased levels of ROS are known to contribute to tumor progression by promoting cell transformation [10], proliferation [11], and survival [12–14]. It has been well-documented that growth factor signaling and oncogenic mutations can result in increased ROS production, which is tightly associated with the incidence of various cancers. For example, platelet-derived growth factor (PDGF), epidermal growth factor (EGF), tumor necrosis factor α (TNF α), interleukin-1 (IL-1), transforming growth factor β (TGF β), etc. can stimulate ROS production and promote tumor progression [15–19]. Oncogenic mutations in RAS have been shown to cause increased generation of superoxide [20–23]. The oncogene-induced ROS can hyperactivate two important pathways: PI3K/Akt/mTOR and MAPK/ERK signaling cascades [20,24,25]. The PI3K/Akt/mTOR pathway critically regulates cell survival. ROS can activate this pathway by oxidizing and inactivating its negative phosphatase regulators, including phosphatase and tensin homolog (PTEN), protein-tyrosine phosphatase 1B (PTP1B), and protein phosphatase 2 (PP2A), or by the direct oxidation of kinases [26,27]. Many solid tumors, including glioblastoma, melanoma, prostate, and breast cancer, are frequently marked by inactivation of PTEN [28–30], suggesting that ROS-induced hyperactivation of the PI3K/Akt survival pathway is critical to the development of these cancers. MAPK signaling pathways are involved in cell growth, differentiation, and survival. Similar to PI3K/Akt/mTOR pathway hyperactivation, ROS induce MAPK/ERK-mediated proliferative signaling through oxidizing and inactivating MAPK phosphatases [31,32]. It is also worth mentioning that ROS can induce nuclear translocation of NF- κ B through oxidation and degradation of I κ B, the phosphatase inhibitor of NF- κ B [33–35]. NF- κ B is a transcription factor that regulates the genes responsible for inflammation, cell proliferation, differentiation, and survival and is known to promote tumorigenesis, angiogenesis, and metastasis [36,37]. Altogether these studies underscore the correlation between the aberrant cell signaling events and the deregulated ROS generation in cancers [38].

2.2. ROS in Tumor Angiogenesis, Metastasis, and Chemoresistance

Increased ROS also facilitate cancer cell angiogenesis [39], metastasis [40,41], and chemoresistance [12]. To meet the increased metabolic needs of proliferating cancer cells, new blood vessels are established to enhance oxygen and nutrient supplies. It is well-known that ROS promote blood vessel formation and angiogenesis [39,42,43]. Tumor hypoxia, a condition in which tumor cells are deprived of oxygen, occurs when tumor growth outpaces blood supply. Hypoxia stimulates the production of mitochondrial ROS (mROS) via the transfer of electrons from ubiquinone to molecular oxygen at the Q_o site of complex III of the mitochondrial electron transport chain [44,45]. Increased mROS induce and stabilize hypoxia-inducible factor-1 (HIF1a) [44,46,47], a transcription factor that enhances the survival and progression of tumors by upregulating genes regulating tumor angiogenesis, metabolism, metastasis, and chemoresistance [48,49].

Metastasis involves the spread of cancer cells from the primary tumor to the surrounding tissues and to distant organs. Epithelial to mesenchymal transition (EMT) is the process of epithelial cell transition into mesenchymal cell, which is the major cause of tumor metastasis. It has been shown that ROS promote EMT by inducing the expression and activity of certain matrix metalloproteinases (MMPs) that mediate proteolytic degradation of extracellular matrix (ECM) components [50,51]. Cancer stem cells (CSCs) represent a less differentiated but highly tumorigenic subpopulation of cancer cells that contribute to chemoresistance [52]. CSCs are marked by a heightened antioxidant capacity, which allows them to self-renew, differentiate, and importantly, to resist ROS-mediated oxidative damage and cell death induced by radiation or chemotherapy [53,54].

Excessive induction of ROS above a certain threshold can be lethal to the cancer cells [1–3]. Cancer cells have an increased antioxidant capacity, mediated by enzymatic and nonenzymatic antioxidants, to adapt to their high oxidative stress status. The main endogenous antioxidant enzymes include superoxide dismutase (SOD), catalase, glutathione peroxidase, glutathione reductase, thioredoxins, peroxiredoxins, etc. The natural nonenzymatic antioxidants include glutathione (GSH), carotenoids, vitamins, etc. One of the vital transcription factors that regulate redox homeostasis in cancer cells is nuclear factor erythroid 2-related factor 2 (NRF2) [55,56]. High levels of ROS prevent the proteasomal degradation of NRF2, thus promoting its nuclear translocation and initiation of the transcription of a multitude of antioxidant genes, including GSH peroxidases (GPXs), and GSH S-transferases (GSTs) [57], glutathione reductase, thioredoxin, thioredoxin reductase, peroxiredoxin and sulfiredoxin. Of note, NRF2 regulates the expression of glutamate-cysteine ligase catalytic (GCLC) and modifier (GCLM) subunits, which combine to form a heterodimer to catalyze the rate-limiting step in GSH biosynthesis. In addition, NRF2 regulates NADPH regeneration enzymes and NAD(P)H:quinone oxidoreductase 1 (NQO1), which inhibits the formation of free radicals by the redox-cycling of quinones [58,59]. NRF2 is therefore considered to be a stress alleviator, supporting cancer cell survival, growth, and escape from the deleterious effects of elevated ROS by maintaining a high but balanced redox status within TME. Moreover, it has been reported that mutations in genes encoding the NRF2 transcription factor and its negative regulator (KEAP1) are frequently detected in cancer [59–61]. These mutations may lead to aberrant NRF2 activation, which is associated with poor prognosis and correlates with chemoresistance and tumor recurrence [62,63]. Some recent studies reported that cancer cells can produce neuroglobin (NGB), a monomeric globin, in response to oxidative stress [64]. NGB can act as an oxidative stress sensor and compensatory protein that intersects with the NRF2 pathway to enable tumor cells to resist oxidative stress and acquire chemoresistance [65,66]. Due to its essential role in tumorigenesis, cancer cell proliferation and drug resistance, NRF2 represents a plausible target for anticancer therapy [61,63].

3. The Impact of Oxidative Stress on Immune Cells in the TME

The TME is a dynamic environment in which tumor cells reside and interact with the surrounding vasculature, various immune cells, fibroblasts, and ECM. On the one hand,

immunosurveillance mediated by T cells and natural killer (NK) cells can detect and attack transformed cells. ROS are important signal mediators involved in the activation of T cells and NK cells. ROS are also used by neutrophils and macrophages to destroy cancer cells. On the other hand, cancer cells possess the ability to induce tumor-promoting immune cells, including regulatory T cells (Tregs), myeloid-derived suppressor cells (MDSCs), tumor-associated macrophages (TAMs), and tumor-associated neutrophils (TANs). The presence of increased ROS and various types of myeloid cells in the TME is characteristic of chronic inflammation, which is intimately intertwined with cancer development and progression [67]. The crosstalk between inflammatory and oxidative stress mediators may form a positive feed-back loop termed “oxinflammation”, shaping the outcome of antitumor immune responses [68]. ROS in the TME, along with other mechanisms, are used by cancer cells and immunosuppressive cells to create immune tolerance to tumors [69–76]. Here, we focus on the impact of ROS on several types of immune cells with relevance to cancer immunotherapy.

3.1. The Impact of ROS on T Cells and NK Cells

T cell and NK cell activation leads to an increase in ROS production. It has been well-documented that a mild ROS elevation is required for proper T cell activation and differentiation. ROS act as a secondary messenger participating in the activation of nuclear factor of activated T cells (NFAT) and inhibition of negative regulatory phosphatases to ensure appropriate signaling [77,78]. ROS also contribute to activation induced cell death for T cells to maintain immune homeostasis. Kappler and Marrack reported that activation-induced ROS upregulate Fas expression and downregulate antiapoptotic Bcl2 expression to facilitate T cell apoptosis [79]. The levels of ROS in T and NK cells need to be delicately controlled to avoid the detrimental effects of high levels of ROS. Excessive ROS in T and NK cells can decrease TCR ζ - and CD16 ζ -chain levels, block NF- κ B activation, resulting in deficient IFN- γ , TNF- α , and IL-2 production [80–82]. The antioxidative GSH pathway plays a critical role in controlling the redox status in T cells. Mak et al. demonstrated that GSH deficiency in T cells has compromised activation of mammalian target of rapamycin-1 (mTOR) and reduces expression of NFAT and Myc transcription factors, resulting in impaired metabolic integration and reprogramming during inflammatory T cell responses [83]. Tumor-specific T cells treated with the antioxidant N-acetyl cysteine (NAC) during activation significantly reduce DNA damage and cell death, and show improved persistence and antitumor effects upon adoptive transfer into tumor-bearing mice [84–87]. T cells engineered to co-express a chimeric antigen receptor (CAR) and catalase not only reduce oxidative stress in themselves and exert superior antitumor activity, but also protect bystander NK cells from ROS-mediated repression [88]. Likewise, NK cells primed by IL-15 acquire resistance against oxidative stress through the thioredoxin system, and can aid in protecting other lymphocytes from ROS within the TME [89].

3.2. Oxidative Stress and Antigen Presentation

Appropriate levels of ROS are needed for the proper function of antigen-presenting cells. It has been reported that NOX2-mediated phagosomal ROS production in macrophages and dendritic cells (DCs) regulates antigen cross-presentation [90]. Extracellular ROS can also modify the immunogenicity of antigenic peptides, altering T cell priming [91,92]. It has been well-established that induction of oxidative stress in the endoplasmic reticulum (ER) can cause immunogenic death of cancer cells [93–95]. Immunogenic cell death (ICD) leads to exhibition and secretion of alarmins, i.e., damage-associated molecular patterns (DAMPs), including adenosine triphosphate (ATP), ER protein calreticulin (CRT) and nuclear heat-shock protein high mobility group box 1 (HMGB1). These DAMPs interact with their receptors (CD91 for CRT, TLR4 for HMGB1, P2RX7 for ATP) on DCs, leading to DC activation, antigen cross-presentation, and ultimately antitumor CD8⁺ T cell responses. It has been shown that scavenging ROS by antioxidants such as GSH and NAC diminishes ICD [96], whereas strategies that amplify ROS in the ER enhance ICD and augment antitu-

mor immunity [97]. However, there is also evidence that ROS can oxidize the danger signal HMGB1 released from dying cells and thereby neutralize its alarmin activity [98]. A recent study reported that targeted scavenging of extracellular ROS using a tumor ECM targeting nanomaterial can maintain the stimulatory activity of HMGB1 and restore ICD-induced antitumor immunity [99]. These studies suggest that the level and duration of ROS may determine whether or not ICD can occur and lead to effective antitumor immunity.

3.3. Oxidative Stress and Immunosuppressor Cells

ROS are not only involved in the induction of Tregs [100], but are also used by Tregs to suppress other immune cells [101–103]. Increased numbers of Tregs are often present at tumor sites, indicating that Tregs can persist in this environment despite increased oxidative stress in the TME. Previous studies have shown that Tregs exhibit resistance to oxidative stress, a phenomenon that may be attributed to their increased antioxidative capacity [104,105]. This is further supported by a report showing that GSH-deficiency in Tregs leads to increased serine metabolism, mTOR activation, and proliferation but downregulated FoxP3, resulting in diminished Treg suppressive function *in vitro* and *in vivo* [106]. Intriguingly, Tregs sensitive to oxidative stress have recently been described. Maj et al. reported that tumor-infiltrating Tregs tend to undergo apoptosis due to a weak NRF2-associated antioxidant system and resultant vulnerability to oxidative stress in the TME. The apoptotic Tregs convert a large amount of ATP to immunosuppressive adenosine, which antagonizes spontaneous and immune checkpoint blockade (ICB)-induced antitumor T cell immunity [107].

Myeloid cells, including neutrophils, macrophages and MDSCs, are known to produce high amounts of ROS. ROS released by phagocytic cells, mainly neutrophils and macrophages, contribute to tumor killing after chemoimmunotherapy in animal models [108]. However, neutrophils can also use ROS to suppress T cells [109,110]. MDSCs mediate immune suppression via production of ROS and reactive nitrogen species (RNS) [111]. MDSC-derived ROS and RNS reduce T cell responses by inhibiting T cell receptor (TCR) recognition of its ligand, the MHC-peptide complex on target cells [109,112,113]. It is worth mentioning that high levels of ROS in TME promote the maintenance of MDSCs in an immature and immunosuppressive state, while lacking NOX2 [114] or scavenging H₂O₂ with catalase [115] promotes immature myeloid cell differentiation into macrophages, resulting in loss of immune suppressive activity of MDSCs. MDSCs are resistant to increased oxidative stress due to an upregulated NRF2-mediated antioxidative system [116], allowing them to exert immunosuppression upon other immune cells through ROS [112,114,117–120], while protecting themselves from the detrimental effects of ROS.

4. Cancer Therapies Targeting Tumor Redox

At different levels, oxidative stress can exert either pro-tumor or anti-tumor effects, presenting as a double-edged sword to cancer cells. Two opposite strategies have been attempted to modulate tumor redox as a way to prevent or treat cancer. One approach is to reduce the tumor-promoting effects of ROS by attenuating oxidative stress using antioxidants. The other approach is to augment cancer cell death by intensifying the levels of ROS in cancer cells. Here we briefly summarize the current status of the two strategies in cancer therapy. More detailed reviews on this subject can be found elsewhere [7–9,121–125].

4.1. The Use of Antioxidants for Cancer Prevention

Given the role of ROS in promoting tumorigenesis, angiogenesis, and metastasis, various antioxidants have been tested as chemopreventive agents based on the rationale that ROS scavenging can reduce the incidence of cancer and/or delay cancer progression [126]. Gao et al. demonstrated that administration of the antioxidant NAC inhibits tumor incidence in mice by suppressing HIF1 α -driven tumor growth [127]. Along the same line, other studies showed that overexpression or targeted delivery of SOD, catalase, or glutathione peroxidase can inhibit tumor growth [128–132]. Although encouraging results

were observed in some pre-clinical studies, several large-scale clinical trials with dietary antioxidant supplementation such as vitamin A, vitamin E, and β -carotene failed to demonstrate measurable antitumor benefits [133,134]. Paradoxically, in some cases, antioxidant supplementation has been linked with increased rates of certain cancers [135–137]. Possible reasons behind the unexpected failure of the antioxidant approach include inefficient scavenging of tumor-promoting ROS in the relevant cellular compartment such as mitochondria, and/or interference with the antitumor roles of ROS in cancer cells [138–142].

4.2. The Use of Pro-Oxidants in Cancer Therapy

Although cancer cells can activate their antioxidant systems to allow them to thrive in the face of increased oxidative stress, they also become more sensitive to further redox disruption. The vulnerability of cancer cells to redox imbalance becomes the Achilles' heel for cancer. Breaking redox homeostasis in cancer cells can be achieved either by intensifying ROS production or decreasing ROS scavenging through suppressing the antioxidant systems. It is now clear that numerous chemotherapeutic agents exert tumor killing effects through the production of free radicals that cause irreversible cell injury [123,124,143]. Cisplatin, a widely used platinum-based chemotherapy, is known to induce tumor cell apoptosis through generating high levels of cellular superoxide, an effect that can be abolished by the superoxide scavenger Tiron or the antioxidant NAC [144]. 5-fluorouracil (5-FU), an antimetabolite used to treat colon, head, and neck cancers, and other solid tumors, induces tumor cell apoptosis via induction of mitochondrial ROS, and this effect can be blocked by the addition of mitoQ, a mitochondrial-selective antioxidant [145]. Doxorubicin, an anthracycline and topoisomerase inhibitor, induces cancer cell apoptosis as well as cardiotoxicity via direct oxidative DNA damage and indirect induction of H_2O_2 [146,147]. Chemotherapeutic agents such as taxanes (paclitaxel and docetaxel) and vinca alkaloids (vincristine and vinblastine) promote the release of cytochrome c from the mitochondria and interfere with the electron transport chain, resulting in the production of superoxide radicals and inducing cell death [148–150]. ROS induction also contributes to arsenic trioxide's potent inhibitory effect on acute promyelocytic leukemia [151]. Buthionine sulfoximine (BSO), an inhibitor of glutamate-cysteine ligase (GCL), the enzyme required for GSH synthesis, exhibits anticancer activity by depleting GSH [152,153]. Some tyrosine kinase inhibitors (TKI) widely used as targeted therapy for cancer, including erlotinib, imatinib, and dasatinib, have been found to induce oxidative stress, which contributes to cancer cell apoptosis, TKI resistance, and cardiac toxicity [154,155]. In addition to these well-established drugs, increasing number of novel compounds, such as beta-phenylethyl isothiocyanate (PEITC) [156], leinamycin [157], and lanperisone (LP) [158], that can act as pro-oxidants or antioxidant inhibitors, have been developed and tested for their anti-cancer effects. It should be noted that the application of oxidative stress-inducing drugs for cancer treatment also faces many challenges. For example, the use of pro-oxidants may encounter limited tumor-selectivity, dose-limiting toxicity, acquired resistance, and difficulty in effective drug delivery. Besides chemotherapeutic agents, ionizing radiation can also trigger tumor cell apoptosis via ROS induction and the release of mitochondrial cytochrome c [159,160]. Comprehensive summarization of the progress and status of oxidative stress-inducing cancer therapy can be found in other reviews [7–9,123–125,143].

5. The Impact of Cancer Immunotherapies on Oxidative Stress in the TME

In recent years, immune-based therapies, exemplified by ICB therapy and CAR-T cell therapy, have increasingly become a viable treatment option for patients with cancer. Durable and curative outcomes have been observed in a fraction of patients with certain types of cancer after receiving immunotherapies. For example, ICB with aPD1 (nivolumab) and aCTLA4 (ipilimumab) antibodies led to durable responses in ~20% of patients with metastatic melanoma [161], and complete responses were achieved in nearly 80% patients with advanced B-cell acute lymphoblastic leukemia (B-ALL) who received CD19-targeting CAR-T cell therapy [162]. ICB treatment leads to better T cell activation and function

by blocking the inhibitory signals transmitted by co-inhibitory molecules such as PD1 and CTLA4. CAR-T cells mediate antitumor effects by specifically recognizing the target molecules on cancer cells and subsequently destroying the cells through cytotoxic granules such as perforin and granzymes, along with inflammatory cytokines such as IFN- γ and TNF- α . Despite their distinct mechanisms of action, emerging evidence from preclinical studies indicates that ICB therapy and CAR-T therapy can both modulate oxidative stress in the TME, and that alteration of tumor oxidative stress contributes to the efficacy of immunotherapy [163,164].

Wang et al. reported that tumor stromal cells, such as fibroblasts, can facilitate tumor chemoresistance by modulating ROS in the TME [165]. GSH and cysteine released by fibroblasts can be used by ovarian cancer cells to diminish nuclear accumulation of platinum, resulting in resistance to platinum-based chemotherapy. The authors showed that tumor-infiltrating CD8 T cells can abolish fibroblast-mediated chemoresistance. Mechanistically, CD8+ T cell-derived IFN- γ reduces extracellular source of GSH and cysteine by upregulating gamma-glutamyl transferases, which break down extracellular GSH, and meanwhile repressing the expression of the cystine and glutamate antiporter system x c^- (xCT), which imports extracellular cystine to facilitate GSH synthesis [165]. The same research team further demonstrated that the combination of cyst(e)inase, an engineered enzyme which degrades both cystine and cysteine, and ICB therapy synergistically impairs cystine uptake via xCT in tumor cells, resulting in GSH deficiency, ROS accumulation, lipid peroxidation, and ferroptosis of cancer cells in preclinical models [164]. These studies imply that ROS-driven tumor ferroptosis is an exploitable anti-tumor mechanism, and targeting this pathway in the context of immunotherapy represents a promising therapeutic strategy.

Using mouse tumor models, we reported that adoptive T cell therapy (ACT) can profoundly alter tumor metabolism, resulting in GSH depletion and consequential ROS accumulation in tumor cells [163]. We found that T cell-derived TNF α can synergize with chemotherapy to intensify oxidative stress in cancer cells in a NOX-dependent manner. Reduction of oxidative stress, by preventing TNF α -signaling in tumor cells or scavenging ROS with NAC, antagonizes the therapeutic effects of ACT. Depletion of GSH is one of the mechanisms by which many anticancer drugs elicit ROS-induced tumor cell death [153,156,166]. Our study provides evidence that GSH depletion can be achieved by T cell-based immunotherapy. Unlike most small compound inhibitors, T cell-mediated GSH depletion does not impair the function of the rate-limiting GSH-synthesizing enzyme GCL. However, tumor-specific CD4+ effector T cells can simultaneously disrupt multiple metabolic pathways to cause deficits in several intermediate metabolites involved in GSH synthesis, including homocysteine, cystathionine, and glycine [163]. The overall collapse of the redox-related pathways driven by T cells may block potential compensatory mechanisms, thereby overcoming tumor resistance. These findings imply that the ability of T cells to tilt tumor redox balance toward oxidative destruction is integral to the efficacy of ACT.

The impact of therapeutic antibodies on tumor oxidative stress is examined in a study in which mice bearing implanted lung adenocarcinoma tumors were treated with a cocktail of immunomodulators (anti-PD1, anti-CTLA-4, anti-CD137, and anti-CD19 monoclonal antibodies). Treatment-induced reduction in tumor burden is associated with decreased tumor proliferation but increased oxidative stress, apoptosis, autophagy, and T cell infiltration. The data suggest that treatment with therapeutic antibodies may induce oxidative stress that drives cell cycle arrest and tumor cell death [167].

Taken together, accumulating studies start to reveal the cellular and molecular mechanisms by which the dynamic interplay among cancer cells, immune cells, and stromal cells in the TME alters the redox status of each cell population. It is increasingly clear that antitumor T cells possess the ability to induce oxidative stress in tumor cells, and meanwhile they are susceptible to suppression imposed by ROS derived from the surrounding immunosuppressive cells such as Tregs and MDSCs (Figure 1). Therefore, therapeutic strategies should be directed to amplify T cell-induced oxidative stress in cancer cells while relieving effector T cells from the elevated oxidative stress in the TME.

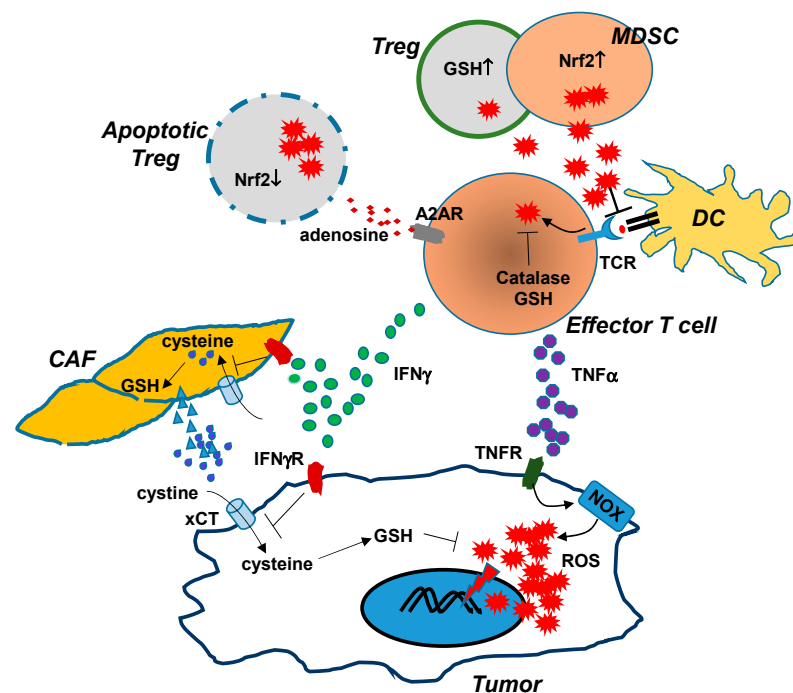


Figure 1. Interactions between cells in the TME lead to changes in redox status. Tumor-reactive effector T cells (CD4+ and CD8+) can induce increased levels of ROS in cancer cells via the actions of IFN γ and TNF α . TNF α signaling in tumor cells activates NADPH oxidases, which lead to increased production of ROS. IFN γ signaling in tumor cells diminishes xCT expression through transcriptional inhibition, reducing tumor uptake of extracellular cystine and subsequent GSH synthesis. IFN γ signaling in cancer-associated fibroblasts (CAF) blocks the release of GSH and cysteine, further depleting the extracellular pool of cystine and cysteine available to cancer cells. The severe redox imbalance in cancer cells, caused by TNF α -driven ROS production and IFN γ -induced GSH deficiency, leads to extensive oxidative damages and eventual tumor cell death. However, effector T cells are also susceptible to oxidative stress in the TME. ROS induced upon TCR engagement are counterbalanced by increased antioxidant systems such as GSH and catalase. T cell dysfunction may occur when effector T cells are exposed to ROS produced by MDSCs and Tregs, which are more resistant to oxidative stress due to their increased antioxidant systems. High levels of extracellular ROS can disrupt antigen-presentation between T cells and DCs, and can affect tumor antigen recognition by T cells. Some apoptosis-prone Tregs can increase the presence of adenosine in the TME, which suppresses the function of effector T cells in an A2AR-dependent manner. Therapeutic interventions should be directed to enhance T cell-induced tumor oxidative stress while enabling T cells to resist the elevated oxidative stress in the TME.

6. Emerging ROS-Modulating Agents with the Potential to Enhance the Efficacy of Cancer Immunotherapy

So far, extensive efforts have been focused on developing small molecule compounds or biologics to target certain redox pathways in cancer cells. Although promising results have been observed in some cases, the use of these pro-oxidants for cancer treatment often encounters challenges related to tumor selectivity, toxicity to normal tissues, and development of chemoresistance [7,8,123,124]. We postulate that these issues can be addressed by combining pro-oxidants with immunotherapy in a synergistic manner to achieve durable antitumor effects while minimizing unwanted side-effects. Indeed, the recent findings that increased tumor oxidative stress correlates with the efficacy of ICB and ACT in preclinical models imply that pro-oxidants can be employed to intensify tumor oxidative stress so as to sensitize tumor cells to T cell-based immunotherapy [163,164]. Given that T cells are also sensitive to oxidative stress, it is unlikely any type of pro-oxidant is suitable for combination with immunotherapy. We consider that an immunotherapy-compatible pro-oxidant should

meet the following criteria: (1) No obvious toxicity to tumor-reactive T cells at the doses needed to induce oxidative stress in tumor cells; (2) Easy administration to tumor-bearing hosts; (3) Good safety profiles that allow rapid translational studies. Many compounds may satisfy these criteria; here, we only highlight several representative agents which have shown the promise of being able to enhance the efficacy of T cell-based immunotherapy.

6.1. High Dose Ascorbate (Vitamin C)

Ascorbate, aka ascorbic acid (AA or vitamin C), at physiological dose functions as an antioxidant. However, mounting evidence indicates that ascorbate used at pharmacological doses (millimolar range) can act as a pro-oxidant that induces extracellular hydrogen peroxide (H_2O_2), which can freely diffuse into cells to cause damages in DNA, lipids, and proteins [168–170]. Since the uptake of oral ascorbate in humans is tightly controlled by the gut and kidney filtration, pharmacologic concentrations of ascorbate cannot be obtained by oral administration. Intravenous administration of ascorbate bypasses the tight control of the gut and renal excretion, resulting in high levels of ascorbate in plasma. Ascorbate undergoes autoxidation to generate a high flux of extracellular H_2O_2 . It has been shown that high-dose ascorbate can be tumoricidal in vitro and can inhibit tumor growth in a variety of preclinical models [171–176]. Although early randomized clinical trials concluded that oral administration of high-dose ascorbate to patients with advanced cancers does not afford any therapeutic benefits [177,178], this conclusion was later challenged based on the discovery that parenteral (i.v. or i.p.) injection, not oral administration, of ascorbate is required to achieve plasma concentration high enough (20 mM) to damage cancer cells [175,176,179–181]. Currently, there are more than 30 completed, recruiting and active clinical trials investigating the usefulness of high-dose ascorbate in cancer treatment, either as monotherapy or in combination with other chemotherapeutic agents (<https://clinicaltrials.gov>, accessed on 11 February 2021). Completed clinical trials demonstrated that high-dose intravenous ascorbate is well tolerated in cancer patients with normal renal function, and in some cases can alleviate the severity of side-effects caused by chemotherapy [171,175].

The mechanisms underlying the preferential toxicity of ascorbate toward cancer cells over normal cells are not fully understood. One apparent explanation is that the antioxidant systems in cancer cells, which are already overstretched due to increased basal level of ROS, are overwhelmed by the influx of ascorbate-induced H_2O_2 , while normal cells still have the capacity to mitigate the threat of the H_2O_2 burst. Additional mechanisms for ascorbate's tumorigenic toxicity have also been described [176]. It has been shown that high dose ascorbate can selectively kill human colorectal cancers (CRCs) carrying KRAS or BRAF mutations [173]. This effect is due to increased uptake of the oxidized form of ascorbate, dehydroascorbate (DHA), via the glucose transporter GLUT1. Intracellular DHA is reduced to ascorbate at the expense of intracellular GSH, causing increased oxidative stress in cancer cells. Accumulated ROS inactivate glyceraldehyde 3-phosphate dehydrogenase (GAPDH), an enzyme critically involved in regulating glycolysis, causing an energetic crisis and cell death in highly glycolytic KRAS or BRAF mutant CRC cells but not normal cells. However, another study reported that the selective tumor toxicity by ascorbate is not dependent on DHA uptake. Instead, ascorbate's toxicity on non-small-cell lung cancer (NSCLC) and glioblastoma (GBM) cells is dependent on the intracellular reactions of H_2O_2 and redox-active labile iron [182]. Cancer cells have increased basal levels of $O_2^{\cdot-}$ and H_2O_2 [183,184] and increased labile iron [185–187]. The increased labile iron in cancer cells leads to increased oxidation of ascorbate to generate more H_2O_2 capable of further exacerbating the differences in labile iron in cancer versus normal cells. This self-amplifying labile iron- H_2O_2 cycle results in increased Fenton chemistry to generate hydroxyl radicals ($\bullet OH$) that cause irreversible oxidative damages to cancer cells [182].

It should be noted that ascorbate may also mediate tumoricidal effects through ROS-independent mechanisms. It has been shown that ascorbate is a cofactor for the Ten-Eleven Translocation (TET) enzymes, which mediate DNA demethylation by converting 5-methylcytosine (5 mC) to 5-hydroxymethylcytosine (5 hmC) and other oxidized methyl-

cytosines. Shenoy et al. reported that ascorbate treatment of diffuse large B-cell (DLBCL) and peripheral T-cell (PTCL) lymphomas increases TET activities, which lead to increased demethylation in cancer cells [188]. This epigenetic effect of ascorbate results in reactivation of SMAD1, a tumor suppressor gene, which sensitizes cancer cells to chemotherapy. Along the same line, a subsequent study showed that high dose ascorbate reduces methylation and restores genome-wide 5 hmC levels in clear cell renal cell carcinoma (ccRCC) cell lines via TET activation [189]. Pharmacologic dose ascorbate treatment leads to increased intratumoral 5 hmC and reduced growth of ccRCC in vitro and in vivo. Furthermore, ascorbate treatment has been shown to mimic TET2 activities and suppress human leukemic colony formation and leukemia progression of primary human leukemia PDXs [190]. Of note, the TET-inducing effect of ascorbate is independent of hydrogen peroxide. These data indicate that in addition to its pro-oxidative effect, ascorbate-mediated epigenetic regulation may also contribute to tumor suppression.

It is important to note that two recent reports demonstrated that high dose ascorbate synergizes with anti-PD1 ICB therapy in mouse tumor models [191,192]. The two studies showed that administration of high dose ascorbate augments the efficacy of anti-PD1 therapy against several types of cancer in immunocompetent mice. The beneficial effects of ascorbate are associated with enhanced tumor infiltration by CD8+ T cells, granzyme B production by CD8+ T and NK cells, and IL-12 production by antigen-presenting cells. Interestingly, the immunopotentiating effects of high dose ascorbate appear to be independent of its pro-oxidant property. Instead, increased levels of 5 hmC are observed in both cancer and CD8+ T cells, suggesting the involvement of ascorbate-induced TET activities. Importantly, these studies demonstrated that high dose ascorbate does not harm effector T cells, but rather enhances T cell functionality through TET-mediated epigenetic modifications. It is worth noting that in these studies the assumption that the immunopotentiating effects of ascorbate are ROS-independent is based on the observation that provision of antioxidant NAC does not diminish the beneficial effect of ascorbate [192]. Future studies should employ more mechanism-based genetic and/or epigenetic approaches to further determine whether the pro-oxidant effects of ascorbate act in parallel to its epigenetic-modification effects. The possible mechanisms of action of ascorbate and potential combination with immunotherapy are illustrated in Figure 2A.

6.2. Non-Steroid Anti-Inflammatory Drugs (NSAIDs)

NSAIDs commonly used for relief of pain, fever, and inflammation act by inhibiting cyclooxygenases (COXs), COX1 and COX2, to suppress prostaglandin synthesis [193]. Some FDA-approved NSAIDs have also been shown to inhibit tumorigenesis in multiple rodent models, and epidemiological studies reported reduced incidence of various cancers in humans, especially colorectal cancer [194–196]. Their mechanisms in anticancer activities are not fully understood, but both COX-dependent and -independent pathways play a role. COX2-derived prostaglandin E2 (PGE2) can bind to its receptors on cancer cells and promote tumor cell proliferation, migration, angiogenesis, and chemoresistance [197,198]. Although the anticancer effects of many NSAIDs are attributable to inhibition of the COX2/PGE2 axis, additional mechanisms of action of NSAIDs have been characterized. NSAIDs can inhibit β -catenin transcriptional activity in cancer cells, resulting in reduced tumor growth [199,200]. In addition, suppression of tumor cell growth by some NSAIDs correlates with inhibition of cGMP degrading phosphodiesterase (PDE) activity [201,202]. Furthermore, it has been well-established that NSAIDs can induce oxidative and ER stresses that cause cancer cell apoptosis [203–209]. A number of commonly used NSAIDs, including sulindac, celecoxib, indomethacin, etc., have been found to induce ROS in various cancer cell lines and can inhibit tumor cell growth independent of COX2 inhibition [210–214]. It has been shown that NSAID treatment destabilizes the redox balance and antioxidant defense mechanisms of the thioredoxin and glutathione systems, resulting in GSH depletion and increased ROS production in tumor cells [215–217]. These events lead to a decline in mitochondrial membrane potential, release of cytochrome c, degradation of pro-survival

molecules BCL-XL and BCL-2, and activation of the caspase cascade that leads to cancer cell apoptosis [209].

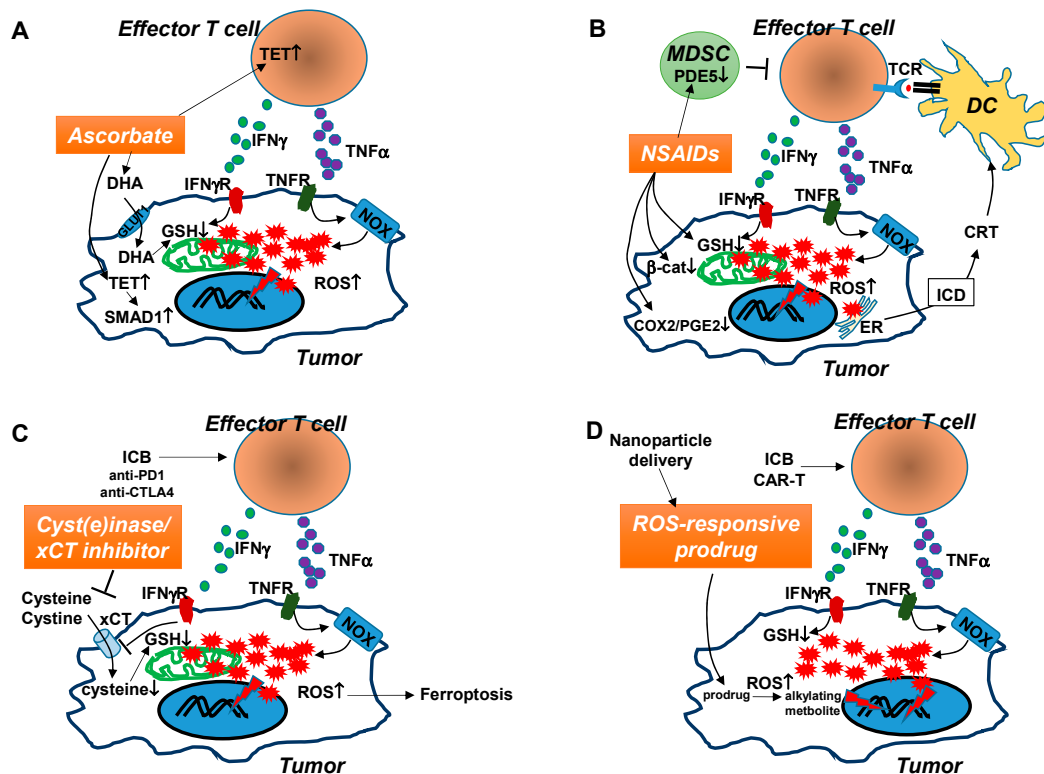


Figure 2. Hypothetical mechanisms by which certain pro-oxidants enhance the efficacy of cancer immunotherapies. Tumor-reactive effector T cells, emerging in the TME after either ICB therapy or adoptive transfer, can mediate tumor killing via well-characterized mechanisms involving cytolytic granules such as perforin and granzymes, and apoptosis-inducing ligands such as FASL and TRAIL. Increasing evidence reveals that inflammatory cytokines produced by effector T cells, including $\text{TNF}\alpha$ and $\text{IFN}\gamma$, can exert antitumor effect by modulating tumor redox. $\text{TNF}\alpha$ signaling in cancer cells activates NOX-dependent ROS production, while $\text{IFN}\gamma$ signaling exacerbates GSH deficiency by suppressing the cysteine/glutamate transporter xCT. The combined effects of $\text{TNF}\alpha$ and $\text{IFN}\gamma$ lead to substantial ROS accumulation in tumor cells, rendering them vulnerable to further redox disruption which can be incited by a pro-oxidant. A suitable pro-oxidant should preferentially induce oxidative stress in cancer cells without harming antitumor T cells. The potential mechanisms of action of four immunotherapy-compatible pro-oxidants are illustrated. (A). Pharmacological dose of ascorbate, in its oxidized form DHA, can be preferentially taken into cancer cells via the glucose transporter (GLUT1). Intracellular DHA is reduced to ascorbate at the expense of GSH. The GSH shortage aggravates ROS accumulation, which damages DNA/protein/lipid and derails cell metabolism, leading to tumor cell death. Meanwhile, ascorbate may induce TET activities in antitumor T cells and tumor cells. TET activation in T cells leads to enhanced function of T cells through epigenetic modifications. TET activation in tumor cells results in demethylation and activation of SMAD1, which increases tumor chemosensitivity. (B). NSAIDs can act as pro-oxidants to reduce GSH and thereby increase the levels of ROS in tumor cells. NSAID-induced ER stress may lead to release of calreticulin (CRT), a DAMP molecule characteristic of ICD, which can attract and activate DCs, which in turn elicit antitumor CD8^+ T cell responses. In addition, NSAIDs can suppress tumor cell growth by its inhibitory effect on β -catenin, COX2, and PGE2. Some NSAIDs may reduce MDSC activity by inhibiting PDE5 function in MDSCs. (C). Cyst(e)inase or xCT inhibitors can reduce the presence or block the uptake of extracellular cystine and cysteine, which tumor cells rely on to synthesize GSH, respectively. Cyst(e)inase can act in concert with ICB-induced antitumor T cells to drive tumor cell ferroptosis. (D). ROS-responsive prodrugs can be effectively delivered to tumor loci by nanoparticles. The increased levels of ROS in the TME can activate these prodrugs, which give rise to alkylating metabolites to cause further DNA damage and intensify oxidative stress in tumor cells. These prodrugs may synergize with antitumor T cells because ROS accumulated in tumor cells after immunotherapies such as ICB or CAR-T therapy can effectively activate prodrugs, which in turn further amplify ROS in tumor cells to drive apoptosis.

Published studies indicate that the antineoplastic activities of NSAIDs can also provoke antitumor immune responses. Inhibition of PGE₂, a potent immunosuppressive factor enriched in the TME, leads to improved antitumor immunity [198,218]. Inhibition of phosphodiesterase 5 (PDE5) activity can abrogate MDSC-mediated immune suppression [219,220]. Suppression of β -catenin can turn immunologic “cold” tumors into “hot” tumors by activating dendritic cells and recruiting T cells into tumors [221,222]. Moreover, NSAID-induced ER stress was reported to correlate with ICD and tumor immunosurveillance [223]. Moreover, tumor antigen-specific T cells stimulated in the presence of a NSAID indomethacin have been shown to acquire stem-like property and can mediate strong antitumor effects upon adoptive transfer in mouse models [224]. These data collectively suggest that certain NSAIDs are compatible with T cell-based immunotherapy. This is supported by the results from an elegant study in which administration of NSAIDs, including celecoxib and aspirin, augments the efficacy of anti-PD1 therapy in multiple mouse tumor models [225]. The beneficial effects of NSAIDs are largely attributed to inhibition of COX2 and PGE₂ in this study. It remains to be determined whether the pro-oxidant effect of NSAIDs can enhance immunotherapy for cancers that do not rely heavily on the COX2-PGE₂ axis for survival and progression. The development of non-COX inhibitory NSAIDs can also avoid GI and cardiovascular toxicities associated with long-term NSAID administration, reducing potential complications when used in combination with immunotherapy. The possible mechanisms of action of NSAIDs and potential combination with immunotherapy are illustrated in Figure 2B.

6.3. xCT Inhibitors and Cyst(e)inase

Cancer cells have a higher demand for GSH to counter balance increased levels of ROS to maintain redox homeostasis for survival and proliferation. Cysteine is the rate-limiting amino acid necessary for GSH biosynthesis. However, under the condition of increased oxidative stress, the production of cysteine in cancer cells is often insufficient to meet the requirements of GSH synthesis, causing cancer cells to rely on uptake of extracellular source of cysteine in its disulfide form cystine via the cystine-glutamate antiporter xCT [226]. Various approaches have been developed to target this pathway as an anticancer strategy [226–231]. xCT inhibitors, such as sulfasalazine [232–234] and erastin [235–239], can reduce GSH and increase ROS in cancer cells, propagating iron-dependent lipid peroxidation that leads to tumor ferroptosis. Since inhibition of xCT alone may force cancer cells to import cysteine via other amino acid transporters such as alanine/serine/cysteine/threonine transporters (ASCT1 and ASCT2), xCT inhibitors are often used in combination with other chemotherapeutic agents or radiotherapy to overcome drug resistance. An engineered protein cyst(e)inase has been developed to enzymatically degrade both cysteine and cystine [166]. Administration of cyst(e)inase mediates sustained depletion of the extracellular cysteine and cystine pool in mice and non-human primates. Cyst(e)inase selectively causes cell cycle arrest and death in cancer cells due to depletion of intracellular GSH and ensuing elevated ROS. Cyst(e)inase suppresses the growth of multiple types of cancer in mice, including prostate, breast, leukemia, and pancreatic cancer, yet no apparent toxicities are observed in mice after prolonged treatment [166,240]. These data implicate cyst(e)inase as a safe and effective therapeutic modality for inactivating antioxidant cellular responses in a wide range of malignancies.

Accumulating evidence suggests that xCT inhibitors and cyst(e)inase can be used in combination with immunotherapy to achieve a synergistic antitumor effect. Using genetic approaches, Arensman et al. demonstrated that while xCT is essential for tumor cell growth, it is dispensable for T cell proliferation in vivo and for the generation of primary and memory immune responses to tumors [241]. This study also showed that anti-CTLA4 therapy is more effective in treating xCT-deficient tumors in mouse models, providing proof of concept that administration of xCT inhibitors may augment the antitumor efficacy of ICB. Recent studies from Weiping Zou’s group demonstrated that antitumor CD8⁺ T cells can drive tumor ferroptosis through IFN- γ -mediated inhibition of xCT, and the combination of cyst(e)inase and ICB therapy synergistically suppresses tumor growth

in preclinical models [164,242]. The possible mechanisms of action of cyst(e)inase/xCT inhibitors and potential combination with immunotherapy are illustrated in Figure 2C.

6.4. ROS-Responsive Prodrugs

The feature that cancer cells have elevated levels of ROS compared to normal cells has been employed to develop a class of prodrugs that only become cytotoxic in the presence of ROS. Prodrugs that are specifically activated by ROS in tumor cells have the potential to improve tumor selectivity and reduce toxicity to normal tissues. Therapeutic molecules, including chemotherapeutics and anti-PDL1 antibody, can be delivered to and released within tumor cells or TME by ROS-responsive prodrugs or nanoparticles [243–248], resulting in significant inhibition of tumor cell growth both *in vitro* and *in vivo*. In recent years, several research groups have developed novel prodrugs that act as DNA cross-linking or alkylating agents upon activation by ROS. Leinamycin (LNM) is a potent antitumor antibiotic produced by *Streptomyces atroolivaceus* S-140. LNM E1 as a prodrug can be oxidatively activated by cellular ROS to generate an intermediate with DNA alkylating activity, exhibiting potent cytotoxicity to prostate cancer cell lines with increased levels of ROS [157]. Peng's group has developed a series of aromatic nitrogen mustards that are released from prodrugs upon a specific reaction between boronates and H₂O₂ in cancer cells [249,250]. These agents show potent DNA cross-linking abilities when coupled with H₂O₂, whereas little DNA cross-linking is detected in the absence of H₂O₂. These prodrugs can selectively kill leukemia and breast cancer cells, which have inherently high levels of ROS [251]. Interestingly, these prodrugs are not toxic to normal lymphocytes at the doses needed to kill cancer cells [252], suggesting their potential usage in combination with T cell-based immunotherapy. Prodrugs activated via ferrocene-mediated oxidation have also been developed to improve the selectivity of anticancer drugs [253–256]. These prodrugs show selective toxicity to a variety of cancer cell lines *in vitro* and *in vivo*, but remain weakly toxic to nonmalignant cells. Importantly, a recent study demonstrated that one such ROS-responsive prodrug, *N*-(3-(piperidin-1-ylmethyl)benzyl)-4-(ferrocenylcarbamate methyl)phenyl boronic acid pinacol ester (PipFcB), can sensitize human lymphoma cell lines and primary chronic lymphocytic leukemia cells to CD19CAR-T cells [257]. It is noteworthy that exposure of CAR-T cells to PipFcB does not influence T cell exhaustion, viability, or T cell subpopulations. The T cell-friendly feature of the prodrugs, together with the findings by our group and others that antitumor T cells intensify ROS accumulation in tumor cells, suggest potential synergistic anticancer effects when combining ROS-responsive prodrugs with T cell-based immunotherapies. One possible scenario is that antitumor T cells arising after ICB or CAR-T therapy cause ROS accumulation in cancer cells, which activates prodrugs to release alkylating intermediates, which in turn further amplifies ROS in tumor (Figure 2D). This mutually reinforcing and self-amplifying ROS-inducing loop may lead to specific and complete tumor rejection with minimal toxicities to normal tissues.

7. Conclusions and Perspectives

An increasing number of studies indicate that ROS accumulated in tumor cells after immunotherapies are not merely metabolic byproducts but actively contribute to the treatment efficacy. Since these studies were mostly conducted in preclinical models, it remains to be determined in clinical samples whether various forms of cancer immunotherapy, including cancer vaccines, ICB and CAR-T therapy, lead to increased oxidative stress in cancer cells, and whether the levels of tumor oxidative stress correlate with the treatment outcomes. Rational combination of ROS-modulating agents and cancer immunotherapy is emerging as a promising treatment strategy (Figure 2). Given the availability of a multitude of pro-oxidants developed in recent decades, it is possible to identify and utilize a number of novel T cell-compatible agents, such as cyst(e)inase and ROS-responsive prodrugs, to enhance the efficacy of ICB or CAR-T therapy. There are also existing drugs (some are FDA-approved), such as ascorbate and NSAIDs, that can be repurposed as pro-oxidants and used in combination with immunotherapy. Future studies should address the sequence

and timing of pro-oxidant administration in relation to immunotherapy, and determine the efficacy and toxicity of the combination therapy in preclinical models with the goal of translating this strategy for the betterment of cancer treatment.

Author Contributions: N.S.A. wrote/edited the manuscript, C.B., T.K., and Z.-C.D. reviewed/edited the manuscript, G.Z. wrote/edited the manuscript and prepared the figures. All authors have read and agreed to the published version of the manuscript.

Funding: G.Z. is supported in part by funds from the National Institutes of Health (1R01CA215523 and 1R01CA238514).

Conflicts of Interest: The authors declare no conflict of interest.

References

- Schumacker, P.T. Reactive oxygen species in cancer cells: Live by the sword, die by the sword. *Cancer Cell* **2006**, *10*, 175–176. [[CrossRef](#)]
- Liou, G.Y.; Storz, P. Reactive oxygen species in cancer. *Free Radic. Res.* **2010**, *44*, 479–496. [[CrossRef](#)]
- Chio, I.I.C.; Tuveson, D.A. ROS in Cancer: The Burning Question. *Trends Mol. Med.* **2017**, *23*, 411–429. [[CrossRef](#)]
- Reczek, C.R.; Chandel, N.S. The Two Faces of Reactive Oxygen Species in Cancer. *Annu. Rev. Cancer Biol.* **2017**, *1*, 79–98. [[CrossRef](#)]
- Murphy, M.P. How mitochondria produce reactive oxygen species. *Biochem. J.* **2009**, *417*, 1–13. [[CrossRef](#)]
- Bae, Y.S.; Oh, H.; Rhee, S.G.; Yoo, Y.D. Regulation of reactive oxygen species generation in cell signaling. *Mol. Cells* **2011**, *32*, 491–509. [[CrossRef](#)] [[PubMed](#)]
- Trachootham, D.; Alexandre, J.; Huang, P. Targeting cancer cells by ROS-mediated mechanisms: A radical therapeutic approach? *Nat. Rev. Drug Discov.* **2009**, *8*, 579–591. [[CrossRef](#)] [[PubMed](#)]
- Gorrini, C.; Harris, I.S.; Mak, T.W. Modulation of oxidative stress as an anticancer strategy. *Nat. Rev. Drug Discov.* **2013**, *12*, 931–947. [[CrossRef](#)]
- Nogueira, V.; Hay, N. Molecular pathways: Reactive oxygen species homeostasis in cancer cells and implications for cancer therapy. *Clin. Cancer Res.* **2013**, *19*, 4309–4314. [[CrossRef](#)] [[PubMed](#)]
- Behrend, L.; Henderson, G.; Zwacka, R.M. Reactive oxygen species in oncogenic transformation. *Biochem. Soc. Trans.* **2003**, *31*, 1441–1444. [[CrossRef](#)]
- Hu, Y.; Rosen, D.G.; Zhou, Y.; Feng, L.; Yang, G.; Liu, J.; Huang, P. Mitochondrial manganese-superoxide dismutase expression in ovarian cancer: Role in cell proliferation and response to oxidative stress. *J. Biol. Chem.* **2005**, *280*, 39485–39492. [[CrossRef](#)] [[PubMed](#)]
- Pervaiz, S.; Clement, M.V. Tumor intracellular redox status and drug resistance—serendipity or a causal relationship? *Curr. Pharm. Des.* **2004**, *10*, 1969–1977. [[CrossRef](#)]
- Clerkin, J.S.; Naughton, R.; Quiney, C.; Cotter, T.G. Mechanisms of ROS modulated cell survival during carcinogenesis. *Cancer Lett.* **2008**, *266*, 30–36. [[CrossRef](#)]
- Trachootham, D.; Lu, W.; Ogasawara, M.A.; Nilisa, R.D.; Huang, P. Redox regulation of cell survival. *Antioxid. Redox Signal.* **2008**, *10*, 1343–1374. [[CrossRef](#)] [[PubMed](#)]
- Meier, B.; Radeke, H.H.; Selle, S.; Younes, M.; Sies, H.; Resch, K.; Habermehl, G.G. Human fibroblasts release reactive oxygen species in response to interleukin-1 or tumour necrosis factor-alpha. *Biochem. J.* **1989**, *263*, 539–545. [[CrossRef](#)]
- Ohba, M.; Shibamura, M.; Kuroki, T.; Nose, K. Production of hydrogen peroxide by transforming growth factor-beta 1 and its involvement in induction of egr-1 in mouse osteoblastic cells. *J. Cell Biol.* **1994**, *126*, 1079–1088. [[CrossRef](#)]
- Lo, Y.Y.; Cruz, T.F. Involvement of reactive oxygen species in cytokine and growth factor induction of c-fos expression in chondrocytes. *J. Biol. Chem.* **1995**, *270*, 11727–11730. [[CrossRef](#)]
- Sundaresan, M.; Yu, Z.X.; Ferrans, V.J.; Irani, K.; Finkel, T. Requirement for generation of H₂O₂ for platelet-derived growth factor signal transduction. *Science* **1995**, *270*, 296–299. [[CrossRef](#)]
- Roy, D.; Sarkar, S.; Felty, Q. Levels of IL-1 beta control stimulatory/inhibitory growth of cancer cells. *Front. Biosci.* **2006**, *11*, 889–898. [[CrossRef](#)]
- Irani, K.; Xia, Y.; Zweier, J.L.; Sollott, S.J.; Der, C.J.; Fearon, E.R.; Sundaresan, M.; Finkel, T.; GoldschmidtClermont, P.J. Mitogenic signaling mediated by oxidants in ras-transformed fibroblasts. *Science* **1997**, *275*, 1649–1652. [[CrossRef](#)]
- Mitsushita, J.; Lambeth, J.D.; Kamata, T. The superoxide-generating oxidase Nox1 is functionally required for Ras oncogene transformation. *Cancer Res.* **2004**, *64*, 3580–3585. [[CrossRef](#)]
- Weinberg, F.; Hamanaka, R.; Wheaton, W.W.; Weinberg, S.; Joseph, J.; Lopez, M.; Kalyanaraman, B.; Mutlu, G.M.; Budinger, G.R.; Chandel, N.S. Mitochondrial metabolism and ROS generation are essential for Kras-mediated tumorigenicity. *Proc. Natl. Acad. Sci. USA* **2010**, *107*, 8788–8793. [[CrossRef](#)] [[PubMed](#)]
- Ogrunc, M.; Di Micco, R.; Lontos, M.; Bombardelli, L.; Mione, M.; Fumagalli, M.; Gorgoulis, V.G.; d’Adda di Fagagna, F. Oncogene-induced reactive oxygen species fuel hyperproliferation and DNA damage response activation. *Cell Death Differ.* **2014**, *21*, 998–1012. [[CrossRef](#)] [[PubMed](#)]

24. Bae, Y.S.; Kang, S.W.; Seo, M.S.; Baines, I.C.; Tekle, E.; Chock, P.B.; Rhee, S.G. Epidermal growth factor (EGF)-induced generation of hydrogen peroxide—Role in EGF receptor-mediated tyrosine phosphorylation. *J. Biol. Chem.* **1997**, *272*, 217–221. [[CrossRef](#)]
25. Sirokmány, G.; Pató, A.; Zana, M.; Donkó, Á.; Bíró, A.; Nagy, P.; Geiszt, M. Epidermal growth factor-induced hydrogen peroxide production is mediated by dual oxidase 1. *Free Radic. Biol. Med.* **2016**, *97*, 204–211. [[CrossRef](#)] [[PubMed](#)]
26. Salmeen, A.; Andersen, J.N.; Myers, M.P.; Meng, T.C.; Hinks, J.A.; Tonks, N.K.; Barford, D. Redox regulation of protein tyrosine phosphatase 1B involves a sulphenyl-amide intermediate. *Nature* **2003**, *423*, 769–773. [[CrossRef](#)] [[PubMed](#)]
27. Koundouros, N.; Poulogiannis, G. Phosphoinositide 3-Kinase/Akt Signaling and Redox Metabolism in Cancer. *Front. Oncol.* **2018**, *8*, 160. [[CrossRef](#)] [[PubMed](#)]
28. Li, J.; Yen, C.; Liaw, D.; Podsypanina, K.; Bose, S.; Wang, S.I.; Puc, J.; Miliareisis, C.; Rodgers, L.; McCombie, R.; et al. PTEN, a Putative Protein Tyrosine Phosphatase Gene Mutated in Human Brain, Breast, and Prostate Cancer. *Science* **1997**, *275*, 1943. [[CrossRef](#)]
29. Wu, H.; Goel, V.; Haluska, F.G. PTEN signaling pathways in melanoma. *Oncogene* **2003**, *22*, 3113–3122. [[CrossRef](#)]
30. Verrastro, I.; Tveen-Jensen, K.; Woscholski, R.; Spickett, C.M.; Pitt, A.R. Reversible oxidation of phosphatase and tensin homolog (PTEN) alters its interactions with signaling and regulatory proteins. *Free Radic. Biol. Med.* **2016**, *90*, 24–34. [[CrossRef](#)]
31. Seth, D.; Rudolph, J. Redox Regulation of MAP Kinase Phosphatase 3. *Biochemistry* **2006**, *45*, 8476–8487. [[CrossRef](#)] [[PubMed](#)]
32. Son, Y.; Cheong, Y.-K.; Kim, N.-H.; Chung, H.-T.; Kang, D.; Pae, H.-O. Mitogen-Activated Protein Kinases and Reactive Oxygen Species: How Can ROS Activate MAPK Pathways? *J. Signal. Transduct.* **2011**, *2011*, 792639. [[CrossRef](#)]
33. Zhang, J.; Johnston, G.; Stebler, B.; Keller, E.T. Hydrogen Peroxide Activates NFκB and the Interleukin-6 Promoter Through NFκB-Inducing Kinase. *Antioxid. Redox Signal.* **2001**, *3*, 493–504. [[CrossRef](#)]
34. Morgan, M.J.; Liu, Z.-g. Crosstalk of reactive oxygen species and NF-κB signaling. *Cell Res.* **2011**, *21*, 103–115. [[CrossRef](#)] [[PubMed](#)]
35. Lingappan, K. NF-κB in Oxidative Stress. *Curr. Opin. Toxicol.* **2018**, *7*, 81–86. [[CrossRef](#)] [[PubMed](#)]
36. Xia, Y.; Shen, S.; Verma, I.M. NF-κB, an active player in human cancers. *Cancer Immunol. Res.* **2014**, *2*, 823–830. [[CrossRef](#)]
37. Li, F.; Zhang, J.; Arfuso, F.; Chinnathambi, A.; Zayed, M.E.; Alharbi, S.A.; Kumar, A.P.; Ahn, K.S.; Sethi, G. NF-kappaB in cancer therapy. *Arch. Toxicol.* **2015**, *89*, 711–731. [[CrossRef](#)]
38. Panieri, E.; Santoro, M.M. ROS homeostasis and metabolism: A dangerous liason in cancer cells. *Cell Death Dis.* **2016**, *7*, e2253. [[CrossRef](#)]
39. Ushio-Fukai, M.; Nakamura, Y. Reactive oxygen species and angiogenesis: NADPH oxidase as target for cancer therapy. *Cancer Lett.* **2008**, *266*, 37–52. [[CrossRef](#)]
40. Wu, W.S. The signaling mechanism of ROS in tumor progression. *Cancer Metastasis Rev.* **2006**, *25*, 695–705. [[CrossRef](#)]
41. Nishikawa, M. Reactive oxygen species in tumor metastasis. *Cancer Lett.* **2008**, *266*, 53–59. [[CrossRef](#)]
42. Xia, C.; Meng, Q.; Liu, L.-Z.; Rojanasakul, Y.; Wang, X.-R.; Jiang, B.-H. Reactive Oxygen Species Regulate Angiogenesis and Tumor Growth through Vascular Endothelial Growth Factor. *Cancer Res.* **2007**, *67*, 10823. [[CrossRef](#)] [[PubMed](#)]
43. Komatsu, D.; Kato, M.; Nakayama, J.; Miyagawa, S.; Kamata, T. NADPH oxidase 1 plays a critical mediating role in oncogenic Ras-induced vascular endothelial growth factor expression. *Oncogene* **2008**, *27*, 4724–4732. [[CrossRef](#)]
44. Chandel, N.S.; McClintock, D.S.; Feliciano, C.E.; Wood, T.M.; Melendez, J.A.; Rodriguez, A.M.; Schumacker, P.T. Reactive oxygen species generated at mitochondrial complex III stabilize hypoxia-inducible factor-1alpha during hypoxia: A mechanism of O2 sensing. *J. Biol. Chem.* **2000**, *275*, 25130–25138. [[CrossRef](#)]
45. Guzy, R.D.; Hoyos, B.; Robin, E.; Chen, H.; Liu, L.; Mansfield, K.D.; Simon, M.C.; Hammerling, U.; Schumacker, P.T. Mitochondrial complex III is required for hypoxia-induced ROS production and cellular oxygen sensing. *Cell Metab.* **2005**, *1*, 401–408. [[CrossRef](#)]
46. Chandel, N.S.; Maltepe, E.; Goldwasser, E.; Mathieu, C.E.; Simon, M.C.; Schumacker, P.T. Mitochondrial reactive oxygen species trigger hypoxia-induced transcription. *Proc. Natl. Acad. Sci. USA* **1998**, *95*, 11715–11720. [[CrossRef](#)] [[PubMed](#)]
47. Bell, E.L.; Klimova, T.A.; Eisenbart, J.; Schumacker, P.T.; Chandel, N.S. Mitochondrial reactive oxygen species trigger hypoxia-inducible factor-dependent extension of the replicative life span during hypoxia. *Mol. Cell Biol.* **2007**, *27*, 5737–5745. [[CrossRef](#)]
48. Semenza, G.L. Hypoxia-inducible factors: Coupling glucose metabolism and redox regulation with induction of the breast cancer stem cell phenotype. *EMBO J.* **2017**, *36*, 252–259. [[CrossRef](#)]
49. Al Tameemi, W.; Dale, T.P.; Al-Jumaily, R.M.K.; Forsyth, N.R. Hypoxia-Modified Cancer Cell Metabolism. *Front. Cell Dev. Biol.* **2019**, *7*, 4. [[CrossRef](#)] [[PubMed](#)]
50. Binker, M.G.; Binker-Cosen, A.A.; Richards, D.; Oliver, B.; Cosen-Binker, L.I. EGF promotes invasion by PANC-1 cells through Rac1/ROS-dependent secretion and activation of MMP-2. *Biochem. Biophys. Res. Commun.* **2009**, *379*, 445–450. [[CrossRef](#)]
51. Kar, S.; Subbaram, S.; Carrico, P.M.; Melendez, J.A. Redox-control of matrix metalloproteinase-1: A critical link between free radicals, matrix remodeling and degenerative disease. *Respir. Physiol. Neurobiol.* **2010**, *174*, 299–306. [[CrossRef](#)]
52. Meacham, C.E.; Morrison, S.J. Tumour heterogeneity and cancer cell plasticity. *Nature* **2013**, *501*, 328–337. [[CrossRef](#)]
53. Diehn, M.; Cho, R.W.; Lobo, N.A.; Kalisky, T.; Dorie, M.J.; Kulp, A.N.; Qian, D.; Lam, J.S.; Ailles, L.E.; Wong, M.; et al. Association of reactive oxygen species levels and radioresistance in cancer stem cells. *Nature* **2009**, *458*, 780–783. [[CrossRef](#)]
54. Ryoo, I.-g.; Lee, S.-h.; Kwak, M.-K. Redox Modulating NRF2: A Potential Mediator of Cancer Stem Cell Resistance. *Oxidative Med. Cell. Longev.* **2016**, *2016*, 2428153. [[CrossRef](#)]
55. Rojo de la Vega, M.; Chapman, E.; Zhang, D.D. NRF2 and the Hallmarks of Cancer. *Cancer Cell* **2018**, *34*, 21–43. [[CrossRef](#)]

56. Zimta, A.-A.; Cenariu, D.; Irimie, A.; Magdo, L.; Nabavi, S.M.; Atanasov, A.G.; Berindan-Neagoe, I. The Role of Nrf2 Activity in Cancer Development and Progression. *Cancers* **2019**, *11*, 1755. [[CrossRef](#)] [[PubMed](#)]
57. Reddy, N.M.; Kleeberger, S.R.; Yamamoto, M.; Kensler, T.W.; Scollick, C.; Biswal, S.; Reddy, S.P. Genetic dissection of the Nrf2-dependent redox signaling-regulated transcriptional programs of cell proliferation and cytoprotection. *Physiol. Genom.* **2007**, *32*, 74–81. [[CrossRef](#)]
58. Nioi, P.; Hayes, J.D. Contribution of NAD(P)H:quinone oxidoreductase 1 to protection against carcinogenesis, and regulation of its gene by the Nrf2 basic-region leucine zipper and the arylhydrocarbon receptor basic helix-loop-helix transcription factors. *Mutat. Res.* **2004**, *555*, 149–171. [[CrossRef](#)]
59. Hayes, J.D.; McMahon, M. NRF2 and KEAP1 mutations: Permanent activation of an adaptive response in cancer. *Trends Biochem. Sci.* **2009**, *34*, 176–188. [[CrossRef](#)]
60. Kerins, M.J.; Ooi, A. A catalogue of somatic NRF2 gain-of-function mutations in cancer. *Sci. Rep.* **2018**, *8*, 12846. [[CrossRef](#)]
61. DeNicola, G.M.; Karreth, F.A.; Humpton, T.J.; Gopinathan, A.; Wei, C.; Frese, K.; Mangal, D.; Yu, K.H.; Yeo, C.J.; Calhoun, E.S.; et al. Oncogene-induced Nrf2 transcription promotes ROS detoxification and tumorigenesis. *Nature* **2011**, *475*, 106–109. [[CrossRef](#)]
62. Hayes, J.D.; McMahon, M. The double-edged sword of Nrf2: Subversion of redox homeostasis during the evolution of cancer. *Mol. Cell* **2006**, *21*, 732–734. [[CrossRef](#)]
63. Wu, S.; Lu, H.; Bai, Y. Nrf2 in cancers: A double-edged sword. *Cancer Med.* **2019**, *8*, 2252–2267. [[CrossRef](#)] [[PubMed](#)]
64. Fiocchetti, M.; Fernandez, V.S.; Montalesi, E.; Marino, M. Neuroglobin: A Novel Player in the Oxidative Stress Response of Cancer Cells. *Oxid Med. Cell Longev* **2019**, *2019*, 6315034. [[CrossRef](#)]
65. Solar Fernandez, V.; Cipolletti, M.; Ascenzi, P.; Marino, M.; Fiocchetti, M. Neuroglobin As Key Mediator in the 17beta-Estradiol-Induced Antioxidant Cell Response to Oxidative Stress. *Antioxid Redox Signal.* **2020**, *32*, 217–227. [[CrossRef](#)]
66. Fiocchetti, M.; Solar Fernandez, V.; Segatto, M.; Leone, S.; Cercola, P.; Massari, A.; Cavaliere, F.; Marino, M. Extracellular Neuroglobin as a Stress-Induced Factor Activating Pre-Adaptation Mechanisms against Oxidative Stress and Chemotherapy-Induced Cell Death in Breast Cancer. *Cancers* **2020**, *12*, 2451. [[CrossRef](#)] [[PubMed](#)]
67. Coussens, L.M.; Werb, Z. Inflammation and cancer. *Nature* **2002**, *420*, 860–867. [[CrossRef](#)]
68. Valacchi, G.; Virgili, F.; Cervellati, C.; Pecorelli, A. OxInflammation: From Subclinical Condition to Pathological Biomarker. *Front. Physiol.* **2018**, *9*, 858. [[CrossRef](#)] [[PubMed](#)]
69. Nathan, C.; Cunningham-Bussell, A. Beyond oxidative stress: An immunologist's guide to reactive oxygen species. *Nat. Rev. Immunol.* **2013**, *13*, 349–361. [[CrossRef](#)] [[PubMed](#)]
70. Chen, X.; Song, M.; Zhang, B.; Zhang, Y. Reactive Oxygen Species Regulate T Cell Immune Response in the Tumor Microenvironment. *Oxid Med. Cell Longev* **2016**, *2016*, 1580967. [[CrossRef](#)]
71. Franchina, D.G.; Dostert, C.; Brenner, D. Reactive Oxygen Species: Involvement in T Cell Signaling and Metabolism. *Trends Immunol.* **2018**, *39*, 489–502. [[CrossRef](#)] [[PubMed](#)]
72. Kong, H.; Chandel, N.S. Regulation of redox balance in cancer and T cells. *J. Biol. Chem.* **2018**, *293*, 7499–7507. [[CrossRef](#)]
73. Kotsafti, A.; Scarpa, M.; Castagliuolo, I.; Scarpa, M. Reactive Oxygen Species and Antitumor Immunity-From Surveillance to Evasion. *Cancers* **2020**, *12*, 1748. [[CrossRef](#)]
74. Mullen, L.; Mengozzi, M.; Hanschmann, E.M.; Alberts, B.; Ghezzi, P. How the redox state regulates immunity. *Free Radic. Biol. Med.* **2020**, *157*, 3–14. [[CrossRef](#)] [[PubMed](#)]
75. Muri, J.; Kopf, M. Redox regulation of immunometabolism. *Nat. Rev. Immunol.* **2020**. [[CrossRef](#)] [[PubMed](#)]
76. Van Loenhout, J.; Peeters, M.; Bogaerts, A.; Smits, E.; Deben, C. Oxidative Stress-Inducing Anticancer Therapies: Taking a Closer Look at Their Immunomodulating Effects. *Antioxidants* **2020**, *9*, 1188. [[CrossRef](#)]
77. Reth, M. Hydrogen peroxide as second messenger in lymphocyte activation. *Nat. Immunol.* **2002**, *3*, 1129–1134. [[CrossRef](#)]
78. Sena, L.A.; Li, S.; Jairaman, A.; Prakriya, M.; Ezponda, T.; Hildeman, D.A.; Wang, C.R.; Schumacker, P.T.; Licht, J.D.; Perlman, H.; et al. Mitochondria are required for antigen-specific T cell activation through reactive oxygen species signaling. *Immunity* **2013**, *38*, 225–236. [[CrossRef](#)]
79. Hildeman, D.A.; Mitchell, T.; Teague, T.K.; Henson, P.; Day, B.J.; Kappler, J.; Marrack, P.C. Reactive oxygen species regulate activation-induced T cell apoptosis. *Immunity* **1999**, *10*, 735–744. [[CrossRef](#)]
80. Kono, K.; Salazar-Onfray, F.; Petersson, M.; Hansson, J.; Masucci, G.; Wasserman, K.; Nakazawa, T.; Anderson, P.; Kiessling, R. Hydrogen peroxide secreted by tumor-derived macrophages down-modulates signal-transducing zeta molecules and inhibits tumor-specific T cell-and natural killer cell-mediated cytotoxicity. *Eur. J. Immunol.* **1996**, *26*, 1308–1313. [[CrossRef](#)]
81. Nakamura, K.; Matsunaga, K. Susceptibility of natural killer (NK) cells to reactive oxygen species (ROS) and their restoration by the mimics of superoxide dismutase (SOD). *Cancer Biother. Radiopharm.* **1998**, *13*, 275–290. [[CrossRef](#)]
82. Malmberg, K.J.; Arulampalam, V.; Ichihara, F.; Petersson, M.; Seki, K.; Andersson, T.; Lenkei, R.; Masucci, G.; Pettersson, S.; Kiessling, R. Inhibition of activated/memory (CD45RO(+)) T cells by oxidative stress associated with block of NF-kappaB activation. *J. Immunol.* **2001**, *167*, 2595–2601. [[CrossRef](#)] [[PubMed](#)]
83. Mak, T.W.; Grusdat, M.; Duncan, G.S.; Dostert, C.; Nonnenmacher, Y.; Cox, M.; Binsfeld, C.; Hao, Z.; Brustle, A.; Itsumi, M.; et al. Glutathione Primes T Cell Metabolism for Inflammation. *Immunity* **2017**, *46*, 1089–1090. [[CrossRef](#)]
84. Kesarwani, P.; Al-Khami, A.A.; Scurti, G.; Thyagarajan, K.; Kaur, N.; Husain, S.; Fang, Q.; Naga, O.S.; Simms, P.; Beeson, G.; et al. Promoting thiol expression increases the durability of antitumor T-cell functions. *Cancer Res.* **2014**, *74*, 6036–6047. [[CrossRef](#)]

85. Scheffel, M.J.; Scurti, G.; Simms, P.; Garrett-Mayer, E.; Mehrotra, S.; Nishimura, M.I.; Voelkel-Johnson, C. Efficacy of Adoptive T-cell Therapy Is Improved by Treatment with the Antioxidant N-Acetyl Cysteine, Which Limits Activation-Induced T-cell Death. *Cancer Res.* **2016**, *76*, 6006–6016. [[CrossRef](#)] [[PubMed](#)]
86. Pilipow, K.; Scamardella, E.; Puccio, S.; Gautam, S.; De Paoli, F.; Mazza, E.M.; De Simone, G.; Polletti, S.; Buccilli, M.; Zanon, V.; et al. Antioxidant metabolism regulates CD8+ T memory stem cell formation and antitumor immunity. *JCI Insight* **2018**, *3*. [[CrossRef](#)]
87. Scheffel, M.J.; Scurti, G.; Wyatt, M.M.; Garrett-Mayer, E.; Paulos, C.M.; Nishimura, M.I.; Voelkel-Johnson, C. N-acetyl cysteine protects anti-melanoma cytotoxic T cells from exhaustion induced by rapid expansion via the downmodulation of Foxo1 in an Akt-dependent manner. *Cancer Immunol. Immunother.* **2018**, *67*, 691–702. [[CrossRef](#)]
88. Ligtenberg, M.A.; Mouggiakakos, D.; Mukhopadhyay, M.; Witt, K.; Lladser, A.; Chmielewski, M.; Riet, T.; Abken, H.; Kiessling, R. Coexpressed Catalase Protects Chimeric Antigen Receptor-Redirected T Cells as well as Bystander Cells from Oxidative Stress-Induced Loss of Antitumor Activity. *J. Immunol.* **2016**, *196*, 759–766. [[CrossRef](#)]
89. Yang, Y.; Neo, S.Y.; Chen, Z.; Cui, W.; Chen, Y.; Guo, M.; Wang, Y.; Xu, H.; Kurzay, A.; Alici, E.; et al. Thioredoxin activity confers resistance against oxidative stress in tumor-infiltrating NK cells. *J. Clin. Invest.* **2020**, *130*, 5508–5522. [[CrossRef](#)] [[PubMed](#)]
90. Mantegazza, A.R.; Savina, A.; Vermeulen, M.; Perez, L.; Geffner, J.; Hermine, O.; Rosenzweig, S.D.; Faure, F.; Amigorena, S. NADPH oxidase controls phagosomal pH and antigen cross-presentation in human dendritic cells. *Blood* **2008**, *112*, 4712–4722. [[CrossRef](#)]
91. Weiskopf, D.; Schwanninger, A.; Weinberger, B.; Almanzar, G.; Parson, W.; Buus, S.; Lindner, H.; Grubeck-Loebenstien, B. Oxidative stress can alter the antigenicity of immunodominant peptides. *J. Leukoc. Biol.* **2010**, *87*, 165–172. [[CrossRef](#)]
92. Trujillo, J.A.; Croft, N.P.; Dudek, N.L.; Channappanavar, R.; Theodossis, A.; Webb, A.I.; Dunstone, M.A.; Illing, P.T.; Butler, N.S.; Fett, C.; et al. The cellular redox environment alters antigen presentation. *J. Biol. Chem.* **2014**, *289*, 27979–27991. [[CrossRef](#)]
93. Malhotra, J.D.; Kaufman, R.J. Endoplasmic reticulum stress and oxidative stress: A vicious cycle or a double-edged sword? *Antioxid Redox Signal.* **2007**, *9*, 2277–2293. [[CrossRef](#)] [[PubMed](#)]
94. Kepp, O.; Menger, L.; Vacchelli, E.; Locher, C.; Adjemian, S.; Yamazaki, T.; Martins, I.; Sukkurwala, A.Q.; Michaud, M.; Senovilla, L.; et al. Crosstalk between ER stress and immunogenic cell death. *Cytokine Growth Factor Rev.* **2013**, *24*, 311–318. [[CrossRef](#)] [[PubMed](#)]
95. Cao, S.S.; Kaufman, R.J. Endoplasmic reticulum stress and oxidative stress in cell fate decision and human disease. *Antioxid Redox Signal.* **2014**, *21*, 396–413. [[CrossRef](#)] [[PubMed](#)]
96. Panaretakis, T.; Kepp, O.; Brockmeier, U.; Tesniere, A.; Bjorklund, A.C.; Chapman, D.C.; Durchschlag, M.; Joza, N.; Pierron, G.; van Endert, P.; et al. Mechanisms of pre-apoptotic calreticulin exposure in immunogenic cell death. *EMBO J.* **2009**, *28*, 578–590. [[CrossRef](#)]
97. Deng, H.; Zhou, Z.; Yang, W.; Lin, L.S.; Wang, S.; Niu, G.; Song, J.; Chen, X. Endoplasmic Reticulum Targeting to Amplify Immunogenic Cell Death for Cancer Immunotherapy. *Nano Lett.* **2020**, *20*, 1928–1933. [[CrossRef](#)]
98. Kazama, H.; Ricci, J.E.; Herndon, J.M.; Hoppe, G.; Green, D.R.; Ferguson, T.A. Induction of immunological tolerance by apoptotic cells requires caspase-dependent oxidation of high-mobility group box-1 protein. *Immunity* **2008**, *29*, 21–32. [[CrossRef](#)] [[PubMed](#)]
99. Deng, H.; Yang, W.; Zhou, Z.; Tian, R.; Lin, L.; Ma, Y.; Song, J.; Chen, X. Targeted scavenging of extracellular ROS relieves suppressive immunogenic cell death. *Nat. Commun.* **2020**, *11*, 4951. [[CrossRef](#)] [[PubMed](#)]
100. Kraaij, M.D.; Savage, N.D.; van der Kooij, S.W.; Koekkoek, K.; Wang, J.; van den Berg, J.M.; Ottenhoff, T.H.; Kuijpers, T.W.; Holmdahl, R.; van Kooten, C.; et al. Induction of regulatory T cells by macrophages is dependent on production of reactive oxygen species. *Proc. Natl. Acad. Sci. USA* **2010**, *107*, 17686–17691. [[CrossRef](#)]
101. Yan, Z.; Garg, S.K.; Banerjee, R. Regulatory T cells interfere with glutathione metabolism in dendritic cells and T cells. *J. Biol. Chem.* **2010**, *285*, 41525–41532. [[CrossRef](#)] [[PubMed](#)]
102. Efimova, O.; Szankasi, P.; Kelley, T.W. Ncf1 (p47phox) is essential for direct regulatory T cell mediated suppression of CD4+ effector T cells. *PLoS ONE* **2011**, *6*, e16013. [[CrossRef](#)]
103. Wen, Z.; Shimojima, Y.; Shirai, T.; Li, Y.; Ju, J.; Yang, Z.; Tian, L.; Goronzy, J.J.; Weyand, C.M. NADPH oxidase deficiency underlies dysfunction of aged CD8+ Tregs. *J. Clin. Invest.* **2016**, *126*, 1953–1967. [[CrossRef](#)] [[PubMed](#)]
104. Mouggiakakos, D.; Johansson, C.C.; Kiessling, R. Naturally occurring regulatory T cells show reduced sensitivity toward oxidative stress-induced cell death. *Blood* **2009**, *113*, 3542–3545. [[CrossRef](#)]
105. Mouggiakakos, D.; Johansson, C.C.; Jitschin, R.; Bottcher, M.; Kiessling, R. Increased thioredoxin-1 production in human naturally occurring regulatory T cells confers enhanced tolerance to oxidative stress. *Blood* **2011**, *117*, 857–861. [[CrossRef](#)]
106. Kurniawan, H.; Franchina, D.G.; Guerra, L.; Bonetti, L.; Baguet, L.S.; Grusdat, M.; Schlicker, L.; Hunewald, O.; Dostert, C.; Merz, M.P.; et al. Glutathione Restricts Serine Metabolism to Preserve Regulatory T Cell Function. *Cell Metab* **2020**, *31*, 920–936. [[CrossRef](#)]
107. Maj, T.; Wang, W.; Crespo, J.; Zhang, H.; Wang, W.; Wei, S.; Zhao, L.; Vatan, L.; Shao, I.; Szeliga, W.; et al. Oxidative stress controls regulatory T cell apoptosis and suppressor activity and PD-L1-blockade resistance in tumor. *Nat. Immunol.* **2017**, *18*, 1332–1341. [[CrossRef](#)] [[PubMed](#)]
108. Iida, N.; Dzutsev, A.; Stewart, C.A.; Smith, L.; Bouladoux, N.; Weingarten, R.A.; Molina, D.A.; Salcedo, R.; Back, T.; Cramer, S.; et al. Commensal bacteria control cancer response to therapy by modulating the tumor microenvironment. *Science* **2013**, *342*, 967–970. [[CrossRef](#)]

109. Schmielau, J.; Finn, O.J. Activated granulocytes and granulocyte-derived hydrogen peroxide are the underlying mechanism of suppression of t-cell function in advanced cancer patients. *Cancer Res.* **2001**, *61*, 4756–4760. [[PubMed](#)]
110. Aarts, C.E.M.; Hiemstra, I.H.; Beguin, E.P.; Hoogendijk, A.J.; Bouchmal, S.; van Houdt, M.; Tool, A.T.J.; Mul, E.; Jansen, M.H.; Janssen, H.; et al. Activated neutrophils exert myeloid-derived suppressor cell activity damaging T cells beyond repair. *Blood Adv.* **2019**, *3*, 3562–3574. [[CrossRef](#)]
111. Otsuji, M.; Kimura, Y.; Aoe, T.; Okamoto, Y.; Saito, T. Oxidative stress by tumor-derived macrophages suppresses the expression of CD3 zeta chain of T-cell receptor complex and antigen-specific T-cell responses. *Proc. Natl. Acad. Sci. USA* **1996**, *93*, 13119–13124. [[CrossRef](#)]
112. Nagaraj, S.; Gupta, K.; Pisarev, V.; Kinarsky, L.; Sherman, S.; Kang, L.; Herber, D.L.; Schneck, J.; Gabilovich, D.I. Altered recognition of antigen is a mechanism of CD8(+) T cell tolerance in cancer. *Nat. Med.* **2007**, *13*, 828–835. [[CrossRef](#)] [[PubMed](#)]
113. Liu, Y.; Wei, J.; Guo, G.; Zhou, J. Norepinephrine-induced myeloid-derived suppressor cells block T-cell responses via generation of reactive oxygen species. *Immunopharmacol. Immunotoxicol.* **2015**, *37*, 359–365. [[CrossRef](#)] [[PubMed](#)]
114. Corzo, C.A.; Cotter, M.J.; Cheng, P.Y.; Cheng, F.D.; Kusmartsev, S.; Sotomayor, E.; Padhya, T.; McCaffrey, T.V.; McCaffrey, J.C.; Gabilovich, D.I. Mechanism Regulating Reactive Oxygen Species in Tumor-Induced Myeloid-Derived Suppressor Cells. *J. Immunol.* **2009**, *182*, 5693–5701. [[CrossRef](#)]
115. Kusmartsev, S.; Gabilovich, D.I. Inhibition of myeloid cell differentiation in cancer: The role of reactive oxygen species. *J. Leukoc Biol.* **2003**, *74*, 186–196. [[CrossRef](#)] [[PubMed](#)]
116. Beury, D.W.; Carter, K.A.; Nelson, C.; Sinha, P.; Hanson, E.; Nyandjo, M.; Fitzgerald, P.J.; Majeed, A.; Wali, N.; Ostrand-Rosenberg, S. Myeloid-Derived Suppressor Cell Survival and Function Are Regulated by the Transcription Factor Nrf2. *J. Immunol.* **2016**, *196*, 3470–3478. [[CrossRef](#)] [[PubMed](#)]
117. Kusmartsev, S.; Nefedova, Y.; Yoder, D.; Gabilovich, D.I. Antigen-specific inhibition of CD8+ T cell response by immature myeloid cells in cancer is mediated by reactive oxygen species. *J. Immunol.* **2004**, *172*, 989–999. [[CrossRef](#)]
118. Lu, T.; Gabilovich, D.I. Molecular pathways: Tumor-infiltrating myeloid cells and reactive oxygen species in regulation of tumor microenvironment. *Clin. Cancer Res.* **2012**, *18*, 4877–4882. [[CrossRef](#)]
119. Ohl, K.; Tenbrock, K. Reactive Oxygen Species as Regulators of MDSC-Mediated Immune Suppression. *Front. Immunol.* **2018**, *9*, 2499. [[CrossRef](#)] [[PubMed](#)]
120. Ostrand-Rosenberg, S.; Beury, D.W.; Parker, K.H.; Horn, L.A. Survival of the fittest: How myeloid-derived suppressor cells survive in the inhospitable tumor microenvironment. *Cancer Immunol. Immunother.* **2020**, *69*, 215–221. [[CrossRef](#)]
121. Wang, J.; Yi, J. Cancer cell killing via ROS: To increase or decrease, that is the question. *Cancer Biol. Ther.* **2008**, *7*, 1875–1884. [[CrossRef](#)]
122. Galadari, S.; Rahman, A.; Pallichankandy, S.; Thayyullathil, F. Reactive oxygen species and cancer paradox: To promote or to suppress? *Free Radic. Biol. Med.* **2017**, *104*, 144–164. [[CrossRef](#)]
123. Raza, M.H.; Siraj, S.; Arshad, A.; Waheed, U.; Aldakheel, F.; Alduraywish, S.; Arshad, M. ROS-modulated therapeutic approaches in cancer treatment. *J. Cancer Res. Clin. Oncol.* **2017**, *143*, 1789–1809. [[CrossRef](#)] [[PubMed](#)]
124. Kim, S.J.; Kim, H.S.; Seo, Y.R. Understanding of ROS-Inducing Strategy in Anticancer Therapy. *Oxid Med. Cell Longev* **2019**, *2019*, 5381692. [[CrossRef](#)] [[PubMed](#)]
125. Perillo, B.; Di Donato, M.; Pezone, A.; Di Zazzo, E.; Giovannelli, P.; Galasso, G.; Castoria, G.; Migliaccio, A. ROS in cancer therapy: The bright side of the moon. *Exp. Mol. Med.* **2020**, *52*, 192–203. [[CrossRef](#)]
126. Khan, N.; Afaq, F.; Mukhtar, H. Cancer chemoprevention through dietary antioxidants: Progress and promise. *Antioxid Redox Signal.* **2008**, *10*, 475–510. [[CrossRef](#)] [[PubMed](#)]
127. Gao, P.; Zhang, H.; Dinavahi, R.; Li, F.; Xiang, Y.; Raman, V.; Bhujwalla, Z.M.; Felsner, D.W.; Cheng, L.; Pevsner, J.; et al. HIF-dependent antitumorigenic effect of antioxidants in vivo. *Cancer Cell* **2007**, *12*, 230–238. [[CrossRef](#)]
128. Nishikawa, M.; Hyoudou, K.; Kobayashi, Y.; Umeyama, Y.; Takakura, Y.; Hashida, M. Inhibition of metastatic tumor growth by targeted delivery of antioxidant enzymes. *J. Control. Release* **2005**, *109*, 101–107. [[CrossRef](#)] [[PubMed](#)]
129. Venkataraman, S.; Jiang, X.; Weydert, C.; Zhang, Y.; Zhang, H.J.; Goswami, P.C.; Ritchie, J.M.; Oberley, L.W.; Buettner, G.R. Manganese superoxide dismutase overexpression inhibits the growth of androgen-independent prostate cancer cells. *Oncogene* **2005**, *24*, 77–89. [[CrossRef](#)]
130. Liu, J.; Du, J.; Zhang, Y.; Sun, W.; Smith, B.J.; Oberley, L.W.; Cullen, J.J. Suppression of the malignant phenotype in pancreatic cancer by overexpression of phospholipid hydroperoxide glutathione peroxidase. *Hum. Gene Ther.* **2006**, *17*, 105–116. [[CrossRef](#)]
131. Nelson, S.K.; Bose, S.K.; Grunwald, G.K.; Myhill, P.; McCord, J.M. The induction of human superoxide dismutase and catalase in vivo: A fundamentally new approach to antioxidant therapy. *Free Radic. Biol. Med.* **2006**, *40*, 341–347. [[CrossRef](#)] [[PubMed](#)]
132. Teoh-Fitzgerald, M.L.; Fitzgerald, M.P.; Zhong, W.; Askeland, R.W.; Domann, F.E. Epigenetic reprogramming governs EcSOD expression during human mammary epithelial cell differentiation, tumorigenesis and metastasis. *Oncogene* **2014**, *33*, 358–368. [[CrossRef](#)]
133. The Effect of Vitamin E and Beta Carotene on the Incidence of Lung Cancer and Other Cancers in Male Smokers. *N. Engl. J. Med.* **1994**, *330*, 1029–1035. [[CrossRef](#)]
134. Omenn, G.S.; Goodman, G.E.; Thornquist, M.D.; Balmes, J.; Cullen, M.R.; Glass, A.; Keogh, J.P.; Meyskens, F.L.; Valanis, B.; Williams, J.H.; et al. Effects of a combination of beta carotene and vitamin A on lung cancer and cardiovascular disease. *N. Engl. J. Med.* **1996**, *334*, 1150–1155. [[CrossRef](#)] [[PubMed](#)]

135. D'Andrea, G.M. Use of antioxidants during chemotherapy and radiotherapy should be avoided. *CA Cancer J. Clin.* **2005**, *55*, 319–321. [[CrossRef](#)]
136. Seifried, H.E.; Anderson, D.E.; Fisher, E.I.; Milner, J.A. A review of the interaction among dietary antioxidants and reactive oxygen species. *J. Nutr. Biochem.* **2007**, *18*, 567–579. [[CrossRef](#)]
137. Klein, E.A.; Thompson, I.M., Jr.; Tangen, C.M.; Crowley, J.J.; Lucia, M.S.; Goodman, P.J.; Minasian, L.M.; Ford, L.G.; Parnes, H.L.; Gaziano, J.M.; et al. Vitamin E and the risk of prostate cancer: The Selenium and Vitamin E Cancer Prevention Trial (SELECT). *JAMA* **2011**, *306*, 1549–1556. [[CrossRef](#)]
138. Chandel, N.S.; Tuveson, D.A. The promise and perils of antioxidants for cancer patients. *N. Engl. J. Med.* **2014**, *371*, 177–178. [[CrossRef](#)]
139. Le Gal, K.; Ibrahim, M.X.; Wiel, C.; Sayin, V.I.; Akula, M.K.; Karlsson, C.; Dalin, M.G.; Akyurek, L.M.; Lindahl, P.; Nilsson, J.; et al. Antioxidants can increase melanoma metastasis in mice. *Sci. Transl. Med.* **2015**, *7*, 308re308. [[CrossRef](#)] [[PubMed](#)]
140. Peiris-Pages, M.; Martinez-Outschoorn, U.E.; Sotgia, F.; Lisanti, M.P. Metastasis and Oxidative Stress: Are Antioxidants a Metabolic Driver of Progression? *Cell Metab.* **2015**, *22*, 956–958. [[CrossRef](#)]
141. Piskounova, E.; Agathocleous, M.; Murphy, M.M.; Hu, Z.; Huddlestun, S.E.; Zhao, Z.; Leitch, A.M.; Johnson, T.M.; DeBerardinis, R.J.; Morrison, S.J. Oxidative stress inhibits distant metastasis by human melanoma cells. *Nature* **2015**, *527*, 186–191. [[CrossRef](#)]
142. Wiel, C.; Le Gal, K.; Ibrahim, M.X.; Jahangir, C.A.; Kashif, M.; Yao, H.; Ziegler, D.V.; Xu, X.; Ghosh, T.; Mondal, T.; et al. BACH1 Stabilization by Antioxidants Stimulates Lung Cancer Metastasis. *Cell* **2019**, *178*, 330–345. [[CrossRef](#)]
143. Firczuk, M.; Bajor, M.; Graczyk-Jarzynka, A.; Fidyk, K.; Goral, A.; Zagodzón, R. Harnessing altered oxidative metabolism in cancer by augmented prooxidant therapy. *Cancer Lett.* **2020**, *471*, 1–11. [[CrossRef](#)]
144. Berndtsson, M.; Hagg, M.; Panaretakis, T.; Havelka, A.M.; Shoshan, M.C.; Linder, S. Acute apoptosis by cisplatin requires induction of reactive oxygen species but is not associated with damage to nuclear DNA. *Int. J. Cancer* **2007**, *120*, 175–180. [[CrossRef](#)] [[PubMed](#)]
145. Hwang, P.M.; Bunz, F.; Yu, J.; Rago, C.; Chan, T.A.; Murphy, M.P.; Kelso, G.F.; Smith, R.A.; Kinzler, K.W.; Vogelstein, B. Ferredoxin reductase affects p53-dependent, 5-fluorouracil-induced apoptosis in colorectal cancer cells. *Nat. Med.* **2001**, *7*, 1111–1117. [[CrossRef](#)] [[PubMed](#)]
146. Muller, I.; Niethammer, D.; Bruchelt, G. Anthracycline-derived chemotherapeutics in apoptosis and free radical cytotoxicity (Review). *Int. J. Mol. Med.* **1998**, *1*, 491–494. [[CrossRef](#)]
147. De Boo, S.; Kopecka, J.; Brusa, D.; Gazzano, E.; Matera, L.; Ghigo, D.; Bosia, A.; Riganti, C. iNOS activity is necessary for the cytotoxic and immunogenic effects of doxorubicin in human colon cancer cells. *Mol. Cancer* **2009**, *8*, 108. [[CrossRef](#)]
148. Varbiro, G.; Veres, B.; Gallyas, F., Jr.; Sumegi, B. Direct effect of Taxol on free radical formation and mitochondrial permeability transition. *Free Radic. Biol. Med.* **2001**, *31*, 548–558. [[CrossRef](#)]
149. Ramanathan, B.; Jan, K.Y.; Chen, C.H.; Hour, T.C.; Yu, H.J.; Pu, Y.S. Resistance to paclitaxel is proportional to cellular total antioxidant capacity. *Cancer Res.* **2005**, *65*, 8455–8460. [[CrossRef](#)]
150. Chiu, W.H.; Luo, S.J.; Chen, C.L.; Cheng, J.H.; Hsieh, C.Y.; Wang, C.Y.; Huang, W.C.; Su, W.C.; Lin, C.F. Vinca alkaloids cause aberrant ROS-mediated JNK activation, Mcl-1 downregulation, DNA damage, mitochondrial dysfunction, and apoptosis in lung adenocarcinoma cells. *Biochem. Pharmacol.* **2012**, *83*, 1159–1171. [[CrossRef](#)]
151. Chou, W.C.; Jie, C.; Kenedy, A.A.; Jones, R.J.; Trush, M.A.; Dang, C.V. Role of NADPH oxidase in arsenic-induced reactive oxygen species formation and cytotoxicity in myeloid leukemia cells. *Proc. Natl. Acad. Sci. USA* **2004**, *101*, 4578–4583. [[CrossRef](#)]
152. Griffith, O.W.; Meister, A. Potent and specific inhibition of glutathione synthesis by buthionine sulfoximine (S-n-butyl homocysteine sulfoximine). *J. Biol. Chem.* **1979**, *254*, 7558–7560. [[CrossRef](#)]
153. Harris, I.S.; Treloar, A.E.; Inoue, S.; Sasaki, M.; Gorrini, C.; Lee, K.C.; Yung, K.Y.; Brenner, D.; Knobbe-Thomsen, C.B.; Cox, M.A.; et al. Glutathione and Thioredoxin Antioxidant Pathways Synergize to Drive Cancer Initiation and Progression (vol 27, pg 211, 2015). *Cancer Cell* **2015**, *27*, 314. [[CrossRef](#)]
154. Teppo, H.R.; Soini, Y.; Karihtala, P. Reactive Oxygen Species-Mediated Mechanisms of Action of Targeted Cancer Therapy. *Oxid Med. Cell Longev.* **2017**, *2017*, 1485283. [[CrossRef](#)] [[PubMed](#)]
155. Rodriguez-Hernandez, M.A.; de la Cruz-Ojeda, P.; Lopez-Grueso, M.J.; Navarro-Villaran, E.; Requejo-Aguilar, R.; Castejon-Vega, B.; Negrete, M.; Gallego, P.; Vega-Ochoa, A.; Victor, V.M.; et al. Integrated molecular signaling involving mitochondrial dysfunction and alteration of cell metabolism induced by tyrosine kinase inhibitors in cancer. *Redox. Biol.* **2020**, *36*, 101510. [[CrossRef](#)] [[PubMed](#)]
156. Trachootham, D.; Zhou, Y.; Zhang, H.; Demizu, Y.; Chen, Z.; Pelicano, H.; Chiao, P.J.; Achanta, G.; Arlinghaus, R.B.; Liu, J.S.; et al. Selective killing of oncogenically transformed cells through a ROS-mediated mechanism by beta-phenylethyl isothiocyanate. *Cancer Cell* **2006**, *10*, 241–252. [[CrossRef](#)]
157. Huang, S.X.; Yun, B.S.; Ma, M.; Basu, H.S.; Church, D.R.; Ingenhorst, G.; Huang, Y.; Yang, D.; Lohman, J.R.; Tang, G.L.; et al. Leinamycin E1 acting as an anticancer prodrug activated by reactive oxygen species. *Proc. Natl Acad Sci USA* **2015**, *112*, 8278–8283. [[CrossRef](#)]
158. Shaw, A.T.; Winslow, M.M.; Magendantz, M.; Ouyang, C.; Dowdle, J.; Subramanian, A.; Lewis, T.A.; Maglathin, R.L.; Tolliday, N.; Jacks, T. Selective killing of K-ras mutant cancer cells by small molecule inducers of oxidative stress. *Proc. Natl. Acad. Sci. USA* **2011**, *108*, 8773–8778. [[CrossRef](#)] [[PubMed](#)]

159. Ogura, A.; Oowada, S.; Kon, Y.; Hirayama, A.; Yasui, H.; Meike, S.; Kobayashi, S.; Kuwabara, M.; Inanami, O. Redox regulation in radiation-induced cytochrome c release from mitochondria of human lung carcinoma A549 cells. *Cancer Lett.* **2009**, *277*, 64–71. [[CrossRef](#)]
160. Maier, P.; Hartmann, L.; Wenz, F.; Herskind, C. Cellular Pathways in Response to Ionizing Radiation and Their Targetability for Tumor Radiosensitization. *Int. J. Mol. Sci.* **2016**, *17*, 102. [[CrossRef](#)]
161. Larkin, J.; Chiarion-Sileni, V.; Gonzalez, R.; Grob, J.J.; Rutkowski, P.; Lao, C.D.; Cowey, C.L.; Schadendorf, D.; Wagstaff, J.; Dummer, R.; et al. Five-Year Survival with Combined Nivolumab and Ipilimumab in Advanced Melanoma. *N. Engl. J. Med.* **2019**, *381*, 1535–1546. [[CrossRef](#)]
162. Brown, C.E.; Mackall, C.L. CAR T cell therapy: Inroads to response and resistance. *Nat. Rev. Immunol.* **2019**, *19*, 73–74. [[CrossRef](#)] [[PubMed](#)]
163. Habtetsion, T.; Ding, Z.C.; Pi, W.; Li, T.; Lu, C.; Chen, T.; Xi, C.; Spartz, H.; Liu, K.; Hao, Z.; et al. Alteration of Tumor Metabolism by CD4+ T Cells Leads to TNF-alpha-Dependent Intensification of Oxidative Stress and Tumor Cell Death. *Cell Metab.* **2018**, *28*, 228–242. [[CrossRef](#)]
164. Wang, W.; Green, M.; Choi, J.E.; Gijon, M.; Kennedy, P.D.; Johnson, J.K.; Liao, P.; Lang, X.; Kryczek, I.; Sell, A.; et al. CD8(+) T cells regulate tumour ferroptosis during cancer immunotherapy. *Nature* **2019**, *569*, 270–274. [[CrossRef](#)] [[PubMed](#)]
165. Wang, W.; Kryczek, I.; Dostal, L.; Lin, H.; Tan, L.; Zhao, L.; Lu, F.; Wei, S.; Maj, T.; Peng, D.; et al. Effector T Cells Abrogate Stroma-Mediated Chemoresistance in Ovarian Cancer. *Cell* **2016**, *165*, 1092–1105. [[CrossRef](#)] [[PubMed](#)]
166. Cramer, S.L.; Saha, A.; Liu, J.; Tadi, S.; Tiziani, S.; Yan, W.; Triplett, K.; Lamb, C.; Alters, S.E.; Rowlinson, S.; et al. Systemic depletion of L-cyst(e)ine with cyst(e)inase increases reactive oxygen species and suppresses tumor growth. *Nat. Med.* **2017**, *23*, 120–127. [[CrossRef](#)]
167. Tang, J.; Ramis-Cabrer, D.; Wang, X.; Barreiro, E. Immunotherapy with Monoclonal Antibodies in Lung Cancer of Mice: Oxidative Stress and Other Biological Events. *Cancers* **2019**, *11*, 1301. [[CrossRef](#)] [[PubMed](#)]
168. Chen, Q.; Espey, M.G.; Krishna, M.C.; Mitchell, J.B.; Corpe, C.P.; Buettner, G.R.; Shacter, E.; Levine, M. Pharmacologic ascorbic acid concentrations selectively kill cancer cells: Action as a pro-drug to deliver hydrogen peroxide to tissues. *Proc. Natl. Acad. Sci. USA* **2005**, *102*, 13604–13609. [[CrossRef](#)]
169. Chen, Q.; Espey, M.G.; Sun, A.Y.; Lee, J.H.; Krishna, M.C.; Shacter, E.; Choyke, P.L.; Pooput, C.; Kirk, K.L.; Buettner, G.R.; et al. Ascorbate in pharmacologic concentrations selectively generates ascorbate radical and hydrogen peroxide in extracellular fluid in vivo. *Proc. Natl. Acad. Sci. USA* **2007**, *104*, 8749–8754. [[CrossRef](#)] [[PubMed](#)]
170. Chen, Q.; Espey, M.G.; Sun, A.Y.; Pooput, C.; Kirk, K.L.; Krishna, M.C.; Khosh, D.B.; Drisko, J.; Levine, M. Pharmacologic doses of ascorbate act as a prooxidant and decrease growth of aggressive tumor xenografts in mice. *Proc. Natl. Acad. Sci. USA* **2008**, *105*, 11105–11109. [[CrossRef](#)]
171. Du, J.; Cullen, J.J.; Buettner, G.R. Ascorbic acid: Chemistry, biology and the treatment of cancer. *Biochim. Biophys. Acta* **2012**, *1826*, 443–457. [[CrossRef](#)] [[PubMed](#)]
172. Ma, Y.; Chapman, J.; Levine, M.; Polireddy, K.; Drisko, J.; Chen, Q. High-dose parenteral ascorbate enhanced chemosensitivity of ovarian cancer and reduced toxicity of chemotherapy. *Sci. Transl. Med.* **2014**, *6*, 222ra218. [[CrossRef](#)] [[PubMed](#)]
173. Yun, J.; Mullarky, E.; Lu, C.; Bosch, K.N.; Kavalier, A.; Rivera, K.; Roper, J.; Chio, I.I.; Giannopoulou, E.G.; Rago, C.; et al. Vitamin C selectively kills KRAS and BRAF mutant colorectal cancer cells by targeting GAPDH. *Science* **2015**, *350*, 1391–1396. [[CrossRef](#)]
174. Wei, X.; Xu, Y.; Xu, F.F.; Chaiswing, L.; Schnell, D.; Noel, T.; Wang, C.; Chen, J.; St Clair, D.K.; St Clair, W.H. RelB Expression Determines the Differential Effects of Ascorbic Acid in Normal and Cancer Cells. *Cancer Res.* **2017**, *77*, 1345–1356. [[CrossRef](#)] [[PubMed](#)]
175. Shenoy, N.; Creagan, E.; Witzig, T.; Levine, M. Ascorbic Acid in Cancer Treatment: Let the Phoenix Fly. *Cancer Cell* **2018**, *34*, 700–706. [[CrossRef](#)]
176. Vissers, M.C.M.; Das, A.B. Potential Mechanisms of Action for Vitamin C in Cancer: Reviewing the Evidence. *Front. Physiol.* **2018**, *9*, 809. [[CrossRef](#)]
177. Creagan, E.T.; Moertel, C.G.; O'Fallon, J.R.; Schutt, A.J.; O'Connell, M.J.; Rubin, J.; Frytak, S. Failure of high-dose vitamin C (ascorbic acid) therapy to benefit patients with advanced cancer. A controlled trial. *N. Engl. J. Med.* **1979**, *301*, 687–690. [[CrossRef](#)] [[PubMed](#)]
178. Moertel, C.G.; Fleming, T.R.; Creagan, E.T.; Rubin, J.; O'Connell, M.J.; Ames, M.M. High-dose vitamin C versus placebo in the treatment of patients with advanced cancer who have had no prior chemotherapy. A randomized double-blind comparison. *N. Engl. J. Med.* **1985**, *312*, 137–141. [[CrossRef](#)]
179. Padayatty, S.J.; Sun, H.; Wang, Y.; Riordan, H.D.; Hewitt, S.M.; Katz, A.; Wesley, R.A.; Levine, M. Vitamin C pharmacokinetics: Implications for oral and intravenous use. *Ann. Intern. Med.* **2004**, *140*, 533–537. [[CrossRef](#)]
180. Verrax, J.; Calderon, P.B. Pharmacologic concentrations of ascorbate are achieved by parenteral administration and exhibit antitumoral effects. *Free Radic. Biol. Med.* **2009**, *47*, 32–40. [[CrossRef](#)]
181. Nauman, G.; Gray, J.C.; Parkinson, R.; Levine, M.; Paller, C.J. Systematic Review of Intravenous Ascorbate in Cancer Clinical Trials. *Antioxidants* **2018**, *7*, 89. [[CrossRef](#)] [[PubMed](#)]
182. Schoenfeld, J.D.; Sibenthaler, Z.A.; Mapuskar, K.A.; Wagner, B.A.; Cramer-Morales, K.L.; Furqan, M.; Sandhu, S.; Carlisle, T.L.; Smith, M.C.; Abu Hejleh, T.; et al. O₂(-) and H₂O₂-Mediated Disruption of Fe Metabolism Causes the Differential Susceptibility of NSCLC and GBM Cancer Cells to Pharmacological Ascorbate. *Cancer Cell* **2017**, *32*, 268. [[CrossRef](#)] [[PubMed](#)]

183. Spitz, D.R.; Sim, J.E.; Ridnour, L.A.; Galoforo, S.S.; Lee, Y.J. Glucose deprivation-induced oxidative stress in human tumor cells. A fundamental defect in metabolism? *Ann. N Y Acad. Sci.* **2000**, *899*, 349–362. [[CrossRef](#)]
184. Aykin-Burns, N.; Ahmad, I.M.; Zhu, Y.; Oberley, L.W.; Spitz, D.R. Increased levels of superoxide and H₂O₂ mediate the differential susceptibility of cancer cells versus normal cells to glucose deprivation. *Biochem. J.* **2009**, *418*, 29–37. [[CrossRef](#)]
185. Caltagirone, A.; Weiss, G.; Pantopoulos, K. Modulation of cellular iron metabolism by hydrogen peroxide. Effects of H₂O₂ on the expression and function of iron-responsive element-containing mRNAs in B6 fibroblasts. *J. Biol. Chem.* **2001**, *276*, 19738–19745. [[CrossRef](#)]
186. Torti, S.V.; Torti, F.M. Iron and cancer: More ore to be mined. *Nat. Rev. Cancer* **2013**, *13*, 342–355. [[CrossRef](#)] [[PubMed](#)]
187. Galaris, D.; Barbouti, A.; Pantopoulos, K. Iron homeostasis and oxidative stress: An intimate relationship. *Biochim. Biophys. Acta Mol. Cell Res.* **2019**, *1866*, 118535. [[CrossRef](#)]
188. Shenoy, N.; Bhagat, T.; Nieves, E.; Stenson, M.; Lawson, J.; Choudhary, G.S.; Habermann, T.; Nowakowski, G.; Singh, R.; Wu, X.; et al. Upregulation of TET activity with ascorbic acid induces epigenetic modulation of lymphoma cells. *Blood Cancer J.* **2017**, *7*, e587. [[CrossRef](#)] [[PubMed](#)]
189. Shenoy, N.; Bhagat, T.D.; Cheville, J.; Lohse, C.; Bhattacharyya, S.; Tischer, A.; Machha, V.; Gordon-Mitchell, S.; Choudhary, G.; Wong, L.F.; et al. Ascorbic acid-induced TET activation mitigates adverse hydroxymethylcytosine loss in renal cell carcinoma. *J. Clin. Invest.* **2019**, *129*, 1612–1625. [[CrossRef](#)]
190. Cimmino, L.; Dolgalev, I.; Wang, Y.; Yoshimi, A.; Martin, G.H.; Wang, J.; Ng, V.; Xia, B.; Witkowski, M.T.; Mitchell-Flack, M.; et al. Restoration of TET2 Function Blocks Aberrant Self-Renewal and Leukemia Progression. *Cell* **2017**, *170*, 1079–1095. [[CrossRef](#)] [[PubMed](#)]
191. Luchtel, R.A.; Bhagat, T.; Pradhan, K.; Jacobs, W.R., Jr.; Levine, M.; Verma, A.; Shenoy, N. High-dose ascorbic acid synergizes with anti-PD1 in a lymphoma mouse model. *Proc. Natl. Acad. Sci. USA* **2020**, *117*, 1666–1677. [[CrossRef](#)]
192. Magri, A.; Germano, G.; Lorenzato, A.; Lamba, S.; Chila, R.; Montone, M.; Amodio, V.; Ceruti, T.; Sassi, F.; Arena, S.; et al. High-dose vitamin C enhances cancer immunotherapy. *Sci. Transl. Med.* **2020**, *12*, eaay8707. [[CrossRef](#)]
193. Brune, K.; Patrignani, P. New insights into the use of currently available non-steroidal anti-inflammatory drugs. *J. Pain Res.* **2015**, *8*, 105–118. [[CrossRef](#)] [[PubMed](#)]
194. Janne, P.A.; Mayer, R.J. Chemoprevention of colorectal cancer. *N. Engl. J. Med.* **2000**, *342*, 1960–1968. [[CrossRef](#)] [[PubMed](#)]
195. Keller, J.J.; Giardiello, F.M. Chemoprevention strategies using NSAIDs and COX-2 inhibitors. *Cancer Biol Ther* **2003**, *2*, S140–S149. [[CrossRef](#)]
196. Rao, C.V.; Reddy, B.S. NSAIDs and chemoprevention. *Curr. Cancer Drug Targets* **2004**, *4*, 29–42. [[CrossRef](#)] [[PubMed](#)]
197. Wang, D.; Dubois, R.N. Prostaglandins and cancer. *Gut* **2006**, *55*, 115–122. [[CrossRef](#)]
198. Finetti, F.; Travelli, C.; Ercoli, J.; Colombo, G.; Buoso, E.; Trabalzini, L. Prostaglandin E2 and Cancer: Insight into Tumor Progression and Immunity. *Biology* **2020**, *9*, 434. [[CrossRef](#)]
199. Tinsley, H.N.; Gary, B.D.; Keeton, A.B.; Lu, W.; Li, Y.; Piazza, G.A. Inhibition of PDE5 by sulindac sulfide selectively induces apoptosis and attenuates oncogenic Wnt/beta-catenin-mediated transcription in human breast tumor cells. *Cancer Prev. Res.* **2011**, *4*, 1275–1284. [[CrossRef](#)]
200. Li, N.; Xi, Y.; Tinsley, H.N.; Gурpinar, E.; Gary, B.D.; Zhu, B.; Li, Y.; Chen, X.; Keeton, A.B.; Abadi, A.H.; et al. Sulindac selectively inhibits colon tumor cell growth by activating the cGMP/PKG pathway to suppress Wnt/beta-catenin signaling. *Mol. Cancer Ther.* **2013**, *12*, 1848–1859. [[CrossRef](#)]
201. Li, N.; Chen, X.; Zhu, B.; Ramirez-Alcantara, V.; Canzoneri, J.C.; Lee, K.; Sigler, S.; Gary, B.; Li, Y.; Zhang, W.; et al. Suppression of beta-catenin/TCF transcriptional activity and colon tumor cell growth by dual inhibition of PDE5 and 10. *Oncotarget* **2015**, *6*, 27403–27415. [[CrossRef](#)] [[PubMed](#)]
202. Li, N.; Lee, K.; Xi, Y.; Zhu, B.; Gary, B.D.; Ramirez-Alcantara, V.; Gурpinar, E.; Canzoneri, J.C.; Fajardo, A.; Sigler, S.; et al. Phosphodiesterase 10A: A novel target for selective inhibition of colon tumor cell growth and beta-catenin-dependent TCF transcriptional activity. *Oncogene* **2015**, *34*, 1499–1509. [[CrossRef](#)] [[PubMed](#)]
203. Tsutsumi, S.; Gotoh, T.; Tomisato, W.; Mima, S.; Hoshino, T.; Hwang, H.J.; Takenaka, H.; Tsuchiya, T.; Mori, M.; Mizushima, T. Endoplasmic reticulum stress response is involved in nonsteroidal anti-inflammatory drug-induced apoptosis. *Cell Death Differ.* **2004**, *11*, 1009–1016. [[CrossRef](#)]
204. Adachi, M.; Sakamoto, H.; Kawamura, R.; Wang, W.; Imai, K.; Shinomura, Y. Nonsteroidal anti-inflammatory drugs and oxidative stress in cancer cells. *Histol. Histopathol.* **2007**, *22*, 437–442. [[CrossRef](#)] [[PubMed](#)]
205. Ou, Y.C.; Yang, C.R.; Cheng, C.L.; Raung, S.L.; Hung, Y.Y.; Chen, C.J. Indomethacin induces apoptosis in 786-O renal cell carcinoma cells by activating mitogen-activated protein kinases and AKT. *Eur. J. Pharmacol.* **2007**, *563*, 49–60. [[CrossRef](#)]
206. Du, H.; Li, W.; Wang, Y.; Chen, S.; Zhang, Y. Celecoxib induces cell apoptosis coupled with up-regulation of the expression of VEGF by a mechanism involving ER stress in human colorectal cancer cells. *Oncol. Rep.* **2011**, *26*, 495–502. [[CrossRef](#)] [[PubMed](#)]
207. Zhang, X.; Lee, S.H.; Min, K.W.; McEntee, M.F.; Jeong, J.B.; Li, Q.; Baek, S.J. The involvement of endoplasmic reticulum stress in the suppression of colorectal tumorigenesis by tolfenamic acid. *Cancer Prev. Res.* **2013**, *6*, 1337–1347. [[CrossRef](#)] [[PubMed](#)]
208. Cha, W.; Park, S.W.; Kwon, T.K.; Hah, J.H.; Sung, M.W. Endoplasmic reticulum stress response as a possible mechanism of cyclooxygenase-2-independent anticancer effect of celecoxib. *Anticancer Res.* **2014**, *34*, 1731–1735. [[PubMed](#)]
209. Ralph, S.J.; Pritchard, R.; Rodriguez-Enriquez, S.; Moreno-Sanchez, R.; Ralph, R.K. Hitting the Bull’s-Eye in Metastatic Cancers—NSAIDs Elevate ROS in Mitochondria, Inducing Malignant Cell Death. *Pharmaceuticals* **2015**, *8*, 62–106. [[CrossRef](#)]

210. Marchetti, M.; Resnick, L.; Gamliel, E.; Kesaraju, S.; Weissbach, H.; Binnering, D. Sulindac enhances the killing of cancer cells exposed to oxidative stress. *PLoS ONE* **2009**, *4*, e5804. [[CrossRef](#)]
211. Raza, H.; John, A.; Benedict, S. Acetylsalicylic acid-induced oxidative stress, cell cycle arrest, apoptosis and mitochondrial dysfunction in human hepatoma HepG2 cells. *Eur. J. Pharmacol.* **2011**, *668*, 15–24. [[CrossRef](#)] [[PubMed](#)]
212. Tse, A.K.; Cao, H.H.; Cheng, C.Y.; Kwan, H.Y.; Yu, H.; Fong, W.F.; Yu, Z.L. Indomethacin sensitizes TRAIL-resistant melanoma cells to TRAIL-induced apoptosis through ROS-mediated upregulation of death receptor 5 and downregulation of survivin. *J. Invest. Dermatol.* **2014**, *134*, 1397–1407. [[CrossRef](#)]
213. Pritchard, R.; Rodriguez-Enriquez, S.; Pacheco-Velazquez, S.C.; Bortnik, V.; Moreno-Sanchez, R.; Ralph, S. Celecoxib inhibits mitochondrial O₂ consumption, promoting ROS dependent death of murine and human metastatic cancer cells via the apoptotic signalling pathway. *Biochem. Pharmacol.* **2018**, *154*, 318–334. [[CrossRef](#)]
214. Ralph, S.J.; Nozuhur, S.; Moreno-Sánchez, R.; Rodríguez-Enriquez, S.; Pritchard, R. NSAID celecoxib: A potent mitochondrial pro-oxidant cytotoxic agent sensitizing metastatic cancers and cancer stem cells to chemotherapy. *J. Cancer Metastasis Treat.* **2018**, *4*, 49. [[CrossRef](#)]
215. Sun, Y.; Rigas, B. The thioredoxin system mediates redox-induced cell death in human colon cancer cells: Implications for the mechanism of action of anticancer agents. *Cancer Res.* **2008**, *68*, 8269–8277. [[CrossRef](#)]
216. Rousar, T.; Parik, P.; Kucera, O.; Bartos, M.; Cervinkova, Z. Glutathione reductase is inhibited by acetaminophen-glutathione conjugate in vitro. *Physiol. Res.* **2010**, *59*, 225–232. [[CrossRef](#)] [[PubMed](#)]
217. Raza, H.; John, A. Implications of altered glutathione metabolism in aspirin-induced oxidative stress and mitochondrial dysfunction in HepG2 cells. *PLoS ONE* **2012**, *7*, e36325. [[CrossRef](#)] [[PubMed](#)]
218. Hussain, M.; Javeed, A.; Ashraf, M.; Al-Zaubai, N.; Stewart, A.; Mukhtar, M.M. Non-steroidal anti-inflammatory drugs, tumour immunity and immunotherapy. *Pharmacol. Res.* **2012**, *66*, 7–18. [[CrossRef](#)]
219. Serafini, P.; Meckel, K.; Kelso, M.; Noonan, K.; Califano, J.; Koch, W.; Dolcetti, L.; Bronte, V.; Borrello, I. Phosphodiesterase-5 inhibition augments endogenous antitumor immunity by reducing myeloid-derived suppressor cell function. *J. Exp. Med.* **2006**, *203*, 2691–2702. [[CrossRef](#)]
220. Noonan, K.A.; Ghosh, N.; Rudraraju, L.; Bui, M.; Borrello, I. Targeting immune suppression with PDE5 inhibition in end-stage multiple myeloma. *Cancer Immunol. Res.* **2014**, *2*, 725–731. [[CrossRef](#)] [[PubMed](#)]
221. Spranger, S.; Bao, R.; Gajewski, T.F. Melanoma-intrinsic beta-catenin signalling prevents anti-tumour immunity. *Nature* **2015**, *523*, 231–235. [[CrossRef](#)]
222. Spranger, S.; Dai, D.; Horton, B.; Gajewski, T.F. Tumor-Residing Batf3 Dendritic Cells Are Required for Effector T Cell Trafficking and Adoptive T Cell Therapy. *Cancer Cell* **2017**, *31*, 711–723. [[CrossRef](#)]
223. Fletcher, R.; Tong, J.; Risnik, D.; Leibowitz, B.J.; Wang, Y.-J.; Concha-Benavente, F.; DeLiberty, J.M.; Stolz, D.B.; Pai, R.K.; Ferris, R.L.; et al. Non-steroidal anti-inflammatory drugs induce immunogenic cell death in suppressing colorectal tumorigenesis. *Oncogene* **2021**. [[CrossRef](#)] [[PubMed](#)]
224. Majchrzak, K.; Nelson, M.H.; Bowers, J.S.; Bailey, S.R.; Wyatt, M.M.; Wrangle, J.M.; Rubinstein, M.P.; Varela, J.C.; Li, Z.; Himes, R.A.; et al. beta-catenin and PI3Kdelta inhibition expands precursor Th17 cells with heightened stemness and antitumor activity. *JCI Insight* **2017**, *2*. [[CrossRef](#)] [[PubMed](#)]
225. Zelenay, S.; van der Veen, A.G.; Bottcher, J.P.; Snelgrove, K.J.; Rogers, N.; Acton, S.E.; Chakravarty, P.; Girotti, M.R.; Marais, R.; Quezada, S.A.; et al. Cyclooxygenase-Dependent Tumor Growth through Evasion of Immunity. *Cell* **2015**, *162*, 1257–1270. [[CrossRef](#)]
226. Liu, J.; Xia, X.; Huang, P. xCT: A Critical Molecule That Links Cancer Metabolism to Redox Signaling. *Mol. Ther.* **2020**, *28*, 2358–2366. [[CrossRef](#)]
227. Huang, Y.; Dai, Z.; Barbacioru, C.; Sadee, W. Cystine-glutamate transporter SLC7A11 in cancer chemosensitivity and chemoresistance. *Cancer Res.* **2005**, *65*, 7446–7454. [[CrossRef](#)]
228. Lo, M.; Wang, Y.Z.; Gout, P.W. The x(c)-cystine/glutamate antiporter: A potential target for therapy of cancer and other diseases. *J. Cell Physiol.* **2008**, *215*, 593–602. [[CrossRef](#)]
229. Daher, B.; Vucetic, M.; Pouyssegur, J. Cysteine Depletion, a Key Action to Challenge Cancer Cells to Ferroptotic Cell Death. *Front. Oncol.* **2020**, *10*, 723. [[CrossRef](#)]
230. Wang, W.; Zou, W. Amino Acids and Their Transporters in T Cell Immunity and Cancer Therapy. *Mol. Cell* **2020**, *80*, 384–395. [[CrossRef](#)] [[PubMed](#)]
231. Koppula, P.; Zhuang, L.; Gan, B. Cystine transporter SLC7A11/xCT in cancer: Ferroptosis, nutrient dependency, and cancer therapy. *Protein Cell* **2020**. [[CrossRef](#)]
232. Gout, P.W.; Buckley, A.R.; Simms, C.R.; Bruchovsky, N. Sulfasalazine, a potent suppressor of lymphoma growth by inhibition of the x(c)-cystine transporter: A new action for an old drug. *Leukemia* **2001**, *15*, 1633–1640. [[CrossRef](#)]
233. Nagane, M.; Kanai, E.; Shibata, Y.; Shimizu, T.; Yoshioka, C.; Maruo, T.; Yamashita, T. Sulfasalazine, an inhibitor of the cystine-glutamate antiporter, reduces DNA damage repair and enhances radiosensitivity in murine B16F10 melanoma. *PLoS ONE* **2018**, *13*, e0195151. [[CrossRef](#)] [[PubMed](#)]
234. Iida, Y.; Okamoto-Katsuyama, M.; Maruoka, S.; Mizumura, K.; Shimizu, T.; Shikano, S.; Hikichi, M.; Takahashi, M.; Tsuya, K.; Okamoto, S.; et al. Effective ferroptotic small-cell lung cancer cell death from SLC7A11 inhibition by sulforaphane. *Oncol. Lett.* **2021**, *21*, 71. [[CrossRef](#)] [[PubMed](#)]

235. Dixon, S.J.; Lemberg, K.M.; Lamprecht, M.R.; Skouta, R.; Zaitsev, E.M.; Gleason, C.E.; Patel, D.N.; Bauer, A.J.; Cantley, A.M.; Yang, W.S.; et al. Ferroptosis: An iron-dependent form of nonapoptotic cell death. *Cell* **2012**, *149*, 1060–1072. [[CrossRef](#)]
236. Liu, D.S.; Duong, C.P.; Haupt, S.; Montgomery, K.G.; House, C.M.; Azar, W.J.; Pearson, H.B.; Fisher, O.M.; Read, M.; Guerra, G.R.; et al. Inhibiting the system xC(-)/glutathione axis selectively targets cancers with mutant-p53 accumulation. *Nat. Commun.* **2017**, *8*, 14844. [[CrossRef](#)] [[PubMed](#)]
237. Sato, M.; Kusumi, R.; Hamashima, S.; Kobayashi, S.; Sasaki, S.; Komiyama, Y.; Izumikawa, T.; Conrad, M.; Bannai, S.; Sato, H. The ferroptosis inducer erastin irreversibly inhibits system xc- and synergizes with cisplatin to increase cisplatin's cytotoxicity in cancer cells. *Sci. Rep.* **2018**, *8*, 968. [[CrossRef](#)]
238. Cobler, L.; Zhang, H.; Suri, P.; Park, C.; Timmerman, L.A. xCT inhibition sensitizes tumors to gamma-radiation via glutathione reduction. *Oncotarget* **2018**, *9*, 32280–32297. [[CrossRef](#)] [[PubMed](#)]
239. Zhao, Y.; Li, Y.; Zhang, R.; Wang, F.; Wang, T.; Jiao, Y. The Role of Erastin in Ferroptosis and Its Prospects in Cancer Therapy. *Oncol. Targets Ther.* **2020**, *13*, 5429–5441. [[CrossRef](#)]
240. Badgley, M.A.; Kremer, D.M.; Maurer, H.C.; DelGiorno, K.E.; Lee, H.J.; Purohit, V.; Sagalovskiy, I.R.; Ma, A.; Kapilian, J.; Firl, C.E.M.; et al. Cysteine depletion induces pancreatic tumor ferroptosis in mice. *Science* **2020**, *368*, 85–89. [[CrossRef](#)]
241. Arensman, M.D.; Yang, X.S.; Leahy, D.M.; Toral-Barza, L.; Mileski, M.; Rosfjord, E.C.; Wang, F.; Deng, S.; Myers, J.S.; Abraham, R.T.; et al. Cystine-glutamate antiporter xCT deficiency suppresses tumor growth while preserving antitumor immunity. *Proc. Natl. Acad. Sci. USA* **2019**, *116*, 9533–9542. [[CrossRef](#)] [[PubMed](#)]
242. Lang, X.; Green, M.D.; Wang, W.; Yu, J.; Choi, J.E.; Jiang, L.; Liao, P.; Zhou, J.; Zhang, Q.; Dow, A.; et al. Radiotherapy and Immunotherapy Promote Tumoral Lipid Oxidation and Ferroptosis via Synergistic Repression of SLC7A11. *Cancer Discov.* **2019**, *9*, 1673–1685. [[CrossRef](#)] [[PubMed](#)]
243. Xu, X.; Saw, P.E.; Tao, W.; Li, Y.; Ji, X.; Bhasin, S.; Liu, Y.; Ayyash, D.; Rasmussen, J.; Huo, M.; et al. ROS-Responsive Polyprodrug Nanoparticles for Triggered Drug Delivery and Effective Cancer Therapy. *Adv. Mater.* **2017**, *29*, 1700141. [[CrossRef](#)] [[PubMed](#)]
244. Tao, W.; He, Z. ROS-responsive drug delivery systems for biomedical applications. *Asian J. Pharm. Sci.* **2018**, *13*, 101–112. [[CrossRef](#)]
245. Peiro Cadahia, J.; Previtali, V.; Troelsen, N.S.; Clausen, M.H. Prodrug strategies for targeted therapy triggered by reactive oxygen species. *Medchemcomm* **2019**, *10*, 1531–1549. [[CrossRef](#)]
246. Wang, Y.; Zhang, Y.; Ru, Z.; Song, W.; Chen, L.; Ma, H.; Sun, L. A ROS-responsive polymeric prodrug nanosystem with self-amplified drug release for PSMA (-) prostate cancer specific therapy. *J. Nanobiotechnol.* **2019**, *17*, 91. [[CrossRef](#)] [[PubMed](#)]
247. Yang, B.; Gao, J.; Pei, Q.; Xu, H.; Yu, H. Engineering Prodrug Nanomedicine for Cancer Immunotherapy. *Adv. Sci. (Weinh)* **2020**, *7*, 2002365. [[CrossRef](#)]
248. Gong, Y.; Chen, M.; Tan, Y.; Shen, J.; Jin, Q.; Deng, W.; Sun, J.; Wang, C.; Liu, Z.; Chen, Q. Injectable Reactive Oxygen Species-Responsive SN38 Prodrug Scaffold with Checkpoint Inhibitors for Combined Chemoimmunotherapy. *ACS Appl. Mater. Interfaces* **2020**, *12*, 50248–50259. [[CrossRef](#)]
249. Kuang, Y.; Balakrishnan, K.; Gandhi, V.; Peng, X. Hydrogen peroxide inducible DNA cross-linking agents: Targeted anticancer prodrugs. *J. Am. Chem. Soc.* **2011**, *133*, 19278–19281. [[CrossRef](#)]
250. Peng, X.; Gandhi, V. ROS-activated anticancer prodrugs: A new strategy for tumor-specific damage. *Ther. Deliv.* **2012**, *3*, 823–833. [[CrossRef](#)]
251. Chen, W.; Fan, H.; Balakrishnan, K.; Wang, Y.; Sun, H.; Fan, Y.; Gandhi, V.; Arnold, L.A.; Peng, X. Discovery and Optimization of Novel Hydrogen Peroxide Activated Aromatic Nitrogen Mustard Derivatives as Highly Potent Anticancer Agents. *J. Med. Chem.* **2018**, *61*, 9132–9145. [[CrossRef](#)]
252. Chen, W.; Balakrishnan, K.; Kuang, Y.; Han, Y.; Fu, M.; Gandhi, V.; Peng, X. Reactive oxygen species (ROS) inducible DNA cross-linking agents and their effect on cancer cells and normal lymphocytes. *J. Med. Chem.* **2014**, *57*, 4498–4510. [[CrossRef](#)] [[PubMed](#)]
253. Hagen, H.; Marzenell, P.; Jentzsch, E.; Wenz, F.; Veldwijk, M.R.; Mokhir, A. Aminoferrocene-based prodrugs activated by reactive oxygen species. *J. Med. Chem.* **2012**, *55*, 924–934. [[CrossRef](#)] [[PubMed](#)]
254. Schikora, M.; Reznikov, A.; Chaykovskaya, L.; Sachinska, O.; Polyakova, L.; Mokhir, A. Activity of aminoferrocene-based prodrugs against prostate cancer. *Bioorg. Med. Chem. Lett.* **2015**, *25*, 3447–3450. [[CrossRef](#)]
255. Daum, S.; Reshetnikov, M.S.V.; Sisa, M.; Dumych, T.; Lootsik, M.D.; Bilyy, R.; Bila, E.; Janko, C.; Alexiou, C.; Herrmann, M.; et al. Lysosome-Targeting Amplifiers of Reactive Oxygen Species as Anticancer Prodrugs. *Angew. Chem. Int. Ed. Engl.* **2017**, *56*, 15545–15549. [[CrossRef](#)] [[PubMed](#)]
256. Reshetnikov, V.; Daum, S.; Janko, C.; Karawacka, W.; Tietze, R.; Alexiou, C.; Paryzhak, S.; Dumych, T.; Bilyy, R.; Tripal, P.; et al. ROS-Responsive N-Alkylaminoferrocenes for Cancer-Cell-Specific Targeting of Mitochondria. *Angew. Chem. Int. Ed. Engl.* **2018**, *57*, 11943–11946. [[CrossRef](#)] [[PubMed](#)]
257. Yoo, H.J.; Liu, Y.; Wang, L.; Schubert, M.L.; Hoffmann, J.M.; Wang, S.; Neuber, B.; Huckelhoven-Krauss, A.; Gern, U.; Schmitt, A.; et al. Tumor-Specific Reactive Oxygen Species Accelerators Improve Chimeric Antigen Receptor T Cell Therapy in B Cell Malignancies. *Int. J. Mol. Sci.* **2019**, *20*, 2469. [[CrossRef](#)]

Review

Pro-Inflammatory Cytokines in the Formation of the Pre-Metastatic Niche

Ru Li, Annie Wen and Jun Lin * 

Department of Anesthesiology, Stony Brook University Health Sciences Center,
Stony Brook, NY 11794-8480, USA; ru.li@stonybrookmedicine.edu (R.L.); annie.wen@stonybrook.edu (A.W.)

* Correspondence: jun.lin@stonybrookmedicine.edu

Received: 30 November 2020; Accepted: 11 December 2020; Published: 13 December 2020



Simple Summary: The formation of the pre-metastatic niche, a favorable microenvironment in an organ distant from a primary tumor, is critical for tumor metastasis. We review the role of a key player, a class of proteins named pro-inflammatory cytokines secreted from both tumor cells and other cells in tissues, in helping to build the pre-metastatic niche. Various drugs have been developed to target pro-inflammatory cytokines, and their effects on tumor metastases are under investigation. Future clinical studies should focus on combining those drugs and applying them during cancer surgery, a critical moment for the establishment of the pre-metastatic niche.

Abstract: In the presence of a primary tumor, the pre-metastatic niche is established in secondary organs as a favorable microenvironment for subsequent tumor metastases. This process is orchestrated by bone marrow-derived cells, primary tumor-derived factors, and extracellular matrix. In this review, we summarize the role of pro-inflammatory cytokines including interleukin (IL)-6, IL-1 β , CC-chemokine ligand 2 (CCL2), granulocyte-colony stimulating factor (G-CSF), granulocyte-macrophage colony-stimulating factor (GM-CSF), stromal cell-derived factor (SDF)-1, macrophage migration inhibitory factor (MIF), and Chemokine (C-X-C motif) ligand 1 (CXCL1) in the formation of the pre-metastatic niche according to the most recent studies. Pro-inflammatory cytokines released from tumor cells or stromal cells act in both autocrine and paracrine manners to induce phenotype changes in tumor cells, recruit bone marrow-derived cells, and form an inflammatory milieu, all of which prime a secondary organ's microenvironment for metastatic cell colonization. Considering the active involvement of pro-inflammatory cytokines in niche formation, clinical strategies targeting them offer ways to inhibit the establishment of the pre-metastatic niche and therefore attenuate metastatic progression. We review clinical trials targeting different inflammatory cytokines in patients with metastatic cancers. Due to the pleiotropy and redundancy of pro-inflammatory cytokines, combined therapies should be designed in the future.

Keywords: pre-metastatic niche; pro-inflammatory cytokines; clinical trials

1. Introduction

Tumor metastasis is the main cause of therapeutic failure and mortality, with few effective treatment options. It has been suggested that the tumor microenvironment plays a prominent role in the formation of metastasis, collaborating with genetic and epigenetic networks in cancer cells [1,2]. A key step for the formation of tumor metastases is the extravasation of circulating tumor cells into distant organs and their adaption to new environments. Therefore, the reciprocal interactions between the disseminated cancer cells and the microenvironment in distant organs are imperative to successful metastasis. Primary tumor cells orchestrate the metastasis process through secreting a variety of molecules which promote the mobilization and recruitment of various types of cells to the

premetastatic sites and alter the expression of matrix proteins and the properties of the extracellular matrix (ECM) in secondary organs. All these events help create the so-called pre-metastatic niche (PMN), suitable for the engraftment of metastasizing tumor cells. The concept of PMN was first proposed by Dr. David Lyden in 2005 [3]. Since then, targeting the PMN to prevent metastasis has become a promising strategy for cancer treatment. However, much remains to be revealed about the factors that facilitate the establishment of the implantation site for tumor metastasis.

Priming of the organ-specific premetastatic sites is an important yet incompletely understood step during metastasis formation. Bone marrow-derived cells (BMDCs) and tumor-derived secreted factors are the two crucial components for pre-metastatic niche formation. The main type of BMDCs accumulated in the pre-metastatic niche is myeloid-derived suppressor cells (MDSCs). When infections and tissue injuries occur, the myeloid lineage is promptly expanded, and myeloid leukocytes in the bone marrow perform a protective role in host defense against such stresses and traumas. However, chronic inflammation associated with cancer induces the expression of pro-inflammatory cytokines that drive the differentiation of myeloid cells towards MDSCs. MDSCs are a heterogeneous population of immature myeloid cells including macrophages, granulocytes, neutrophils, and dendritic cells. They accumulate in the circulation of cancer patients and are recruited to peripheral lymphoid organs and tumor sites by growth factors released by cancer cells. Within the tumor microenvironment, MDSCs were shown to inhibit the proliferation and activity of killer T cells, promote angiogenesis, and improve tumor cells survival, thereby promoting tumor invasion and metastasis [4]. Besides the recruited MDSCs, the host stromal environment of the PMN also includes fibroblast, endothelial cells, and ECM.

Tumor-derived secreted factors play important roles in preparing distant organs for pre-metastatic niche formation. Tumor-derived secreted factors include cytokines, chemokines, growth factors, and extracellular vesicles (EV). Cytokines are a diverse family of small proteins secreted by cells, predominantly by helper T cells and macrophages for cell-to-cell communication. Cytokines could act on the cells releasing them (autocrine action), on nearby cells (paracrine action), or on distant cells (endocrine action) and are often produced in a cascade, as one cytokine stimulates its target cells to produce additional cytokines. The major subgroups of cytokines include interleukins, interferons, colony-stimulating factors, chemokines, and tumor necrosis factors. Cytokines exert their effects through binding to cytokine receptors on target cells, which activates a sequence of downstream proteins for the desired responses. It should be noted that the effects of different cytokines are sometimes redundant, with different cytokines eliciting similar responses [5,6]. Cytokines play a key role in tumor progression and metastasis by either directly regulating tumor growth, invasiveness, and metastasis or indirectly affecting stromal cells and immune cells [7]. Accumulating evidence suggests that pro-inflammatory cytokines are pivotal in the formation of the pre-metastatic niche. Tumor cell-derived pro-inflammatory cytokines and chemokines recruit a variety of regulatory and suppressive immune cells into distant sites to prime the local environment. The proliferative and invasive abilities of disseminated cancer cells are enhanced by proinflammatory cytokines from the surrounding microenvironment as paracrine signals. Thus, cancer cells can undergo epithelial-to-mesenchymal transition (EMT) to grow in distant tissues. In this review, we focus on the role of important pro-inflammatory cytokines in the establishment of the PMN and highlight the underlying mechanisms of PMN formation in various organs based on the most recent studies (Figure 1).

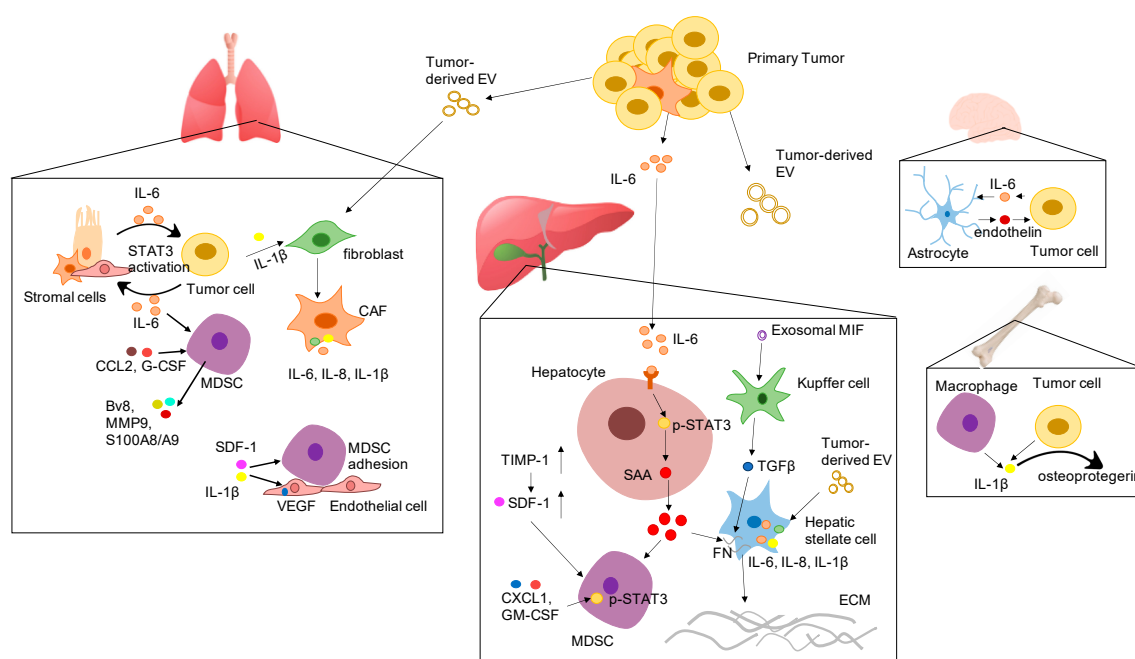


Figure 1. Proposed mechanisms by which various pro-inflammatory cytokines promote the formation of the pre-metastatic niche in different organs. Abbreviation: EV: extracellular vesicles; IL-6: interleukin 6; IL-1 β : interleukin-1 β ; SDF-1 α : stromal cell-derived factor 1; IL-8: interleukin 8; VEGF: vascular endothelial growth factor; G-CSF: granulocyte-colony stimulating factor; CCL2: CC-chemokine ligand 2; CXCL1: C-X-C motif ligand 1; MIF: macrophage migration inhibitory factor; TIMP-1: tissue inhibitor of metalloproteinases 1; GM-CSF: granulocyte-macrophage colony-stimulating factor; SAA: serum amyloid A; TGF- β : transforming growth factor beta; FN: fibronectin; ECM: extracellular matrix; STAT3: signal transducer and activator of transcription 3; CAF: cancer associated fibroblast; MDSC: myeloid-derived suppressor cells.

2. Interleukin 6

Interleukin 6 (IL-6) is recognized as a potent inflammatory cytokine that is widely expressed in a variety of immune cells and malignant tumors. IL-6 binds to its receptor to form a binary complex, which further dimerizes with its coreceptor glycoprotein 130 (GP130). Subsequently, GP130 activates Janus kinase (JAK), which then induces the phosphorylation of signal transducer and activator of transcription 3 (STAT3) [8]. The elevated IL-6 level and hyperactivation of the JAK/STAT3 pathway are often associated with poor patient outcomes [9–12]. JAK-mediated STAT3 tyrosine phosphorylation not only drives malignant cell proliferation, survival, and invasiveness, but also strongly compromises antitumor immunity in the tumor microenvironment [13–15]. In parallel, activated STAT3 can also promote IL-6 gene expression, resulting in a feed-forward autocrine loop. In the tumor microenvironment, the IL-6 signaling pathway affects a variety of stromal cells, including endothelial cells, fibroblasts, and cells of the immune system, which are active participants in angiogenesis and inflammatory and immune-suppressive responses [16].

During tumor progression, the induction of EMT is a key step for the transition from a quiescent to a metastatic tumor. In colorectal cancer cells, IL-6 activated STAT3 to suppress the MIR34A gene via a conserved STAT3-binding site in the first intron and further promoted EMT and invasion. Members of the miR-34 family are induced by tumor suppressor p53 and are known to suppress the early phases of metastasis through inhibiting EMT. They also directly target IL-6R and downregulate it. The IL6/STAT3/miR-34a feedback loop appears essential for EMT, invasion, and metastasis of colorectal, breast, and prostate cancer cells [17]. In addition to miR-34a, other microRNAs in EV profoundly affect the establishment of the PMN through various mechanisms including angiogenesis, EMT, metastatic colonization, as reviewed [18,19]. In breast cancer, adipocytes from the tumor microenvironment could

produce IL-6, which then activates STAT3 in cancer cells and induces the EMT phenotype by increasing the expression of PLOD2, which is important for matrix remodeling [20,21].

Liver metastases develop in nearly 25% of patients with colorectal cancer [22]. Ji et al. have shown in a colorectal cancer model that the primary tumor released integrin beta-like 1-rich extracellular vesicles to lungs and liver, which converted resident fibroblasts to cancer-associated fibroblast (CAF) in the lungs and activated hepatic stellate cells in the liver by stimulating TNFAIP3-mediated NF- κ B signaling pathway [23]. As one of the most abundant cell types in the tumor microenvironment, the activated CAFs modulate the inflammatory microenvironment by secreting pro-inflammatory cytokines including IL-6, IL-8, and IL-1 β and play a key role in depositing and the ECM. CAFs also produce high levels of transforming growth factor beta (TGF- β), α -SMA, and chemokine CXCL12, transforming fibroblasts into myofibroblasts. The interaction between CAFs and metastatic tumor cells has been studied extensively (as reviewed [24]). Pancreatic cancer also frequently spreads to the liver. Lee and colleagues investigated the role of IL-6 in forming the pre-metastatic niche in the liver in mouse models of pancreatic cancer [25]. The authors demonstrated that IL-6 derived from fibroblasts in a primary pancreatic tumor binds to its receptor on hepatocytes, the main cell type in the liver, and drives the expression and activation of STAT3. Subsequently, the activated hepatocytes secrete serum amyloid A1 (SAA1) and SAA2, which then attract myeloid cells into the liver. The accumulation of myeloid cells dampens immune surveillance by releasing cytokines that inhibit cancer-killing T cells. The activation of STAT3 also drives the deposition of extracellular matrix, which contributes to the initial anchoring and sustenance of metastatic cancer cells. All these events prepare the liver for the influx of cancer cells.

The lung is one of the most common sites of cancer metastasis, partially due to its efficiency at arresting circulating tumor cells because of the reduced capillary size. In experimental metastasis models, pre-metastatic events, including BMDC mobilization and the activation of inflammatory pathways, have been suggested to modify the lungs in order to facilitate the development of a pre-metastatic environment for circulating tumor cells [3,26,27]. Chang et al. showed that IL-6 derived from invasive breast cancer cells at advanced stages activated STAT3 through JAK in both the tumor itself and the surrounding stromal cells. It also regulated MDSC (CD11b+/Gr1+) expansion and macrophage (CD11b+/F480+) infiltration in distant organs like the lungs, leading to the establishment of an inflammatory microenvironment in pre-metastatic sites [28]. A recently published study investigated inter-lung metastasis of lung cancer. In lung tissue, GPRC5A (G-protein-coupled receptor, family C, member 5A) is predominately expressed and acts as a lung tumor suppressor gene [29]. The suppression of GPRC5A contributes to lung cancer development with chronic inflammation. The study showed that depletion of the upregulated IL-6 in GPRC5A knockout (Gprc5a-ko) mice almost completely eliminated lung metastasis. Dysregulated IL-6 signaling is intrinsically linked to the stem-like and immunosuppressive features of the metastatic tumor. IL-6 also induced recruitment of MDSCs and macrophage polarization, which inhibits host immunity. All these pieces of evidence indicated that IL-6 in Gprc5a-ko mouse lungs is essential for pre-metastatic niche formation [30]. IL-6/STAT3 signaling in tumor-containing lung tissue is activated via reciprocal interactions between metastatic tumor cells and stromal cells. Blockade of STAT3 signaling in lung cancer cells prevented lung metastasis in immune-competent syngeneic mice, but not in immune-deficient nude mice, which implies that STAT3-mediated immunosuppressive traits in tumor cells are functionally critical for lung metastasis in vivo [30]. Moreover, lymphatic endothelial cells of stromal lymphatic vessels in the pre-metastatic niche also contribute to metastasis. Primary tumor-secreted IL-6 activated STAT3 in lymphatic endothelial cells, which then induced the expression of hypoxia-inducible factor 1 (HIF-1), vascular endothelial growth factor (VEGF), and chemokine ligand 5 (CCL5). Tumor-conditioned lymphatic endothelial cells directed disseminated tumor cells into lungs and lymph nodes, promoted angiogenesis in distant organs, and allowed tumor extravasation and colonization [25].

Brain metastases of breast cancer, mostly in patients with HER2+ or triple-negative tumors, have exceeded the incident rate of 30% in metastatic breast cancer patients [31] and confer a poor

prognosis, with extremely short survival despite treatment [32]. Current systemic treatments include surgery and radiotherapy but have inadequate effects due to the enhanced resistance of metastatic tumor cells in the brain and limited access of drug to the brain because of the blood–brain barrier (BBB). It has been shown that the interaction between astrocyte and MDA-MB-231 cells induced the production of IL-6 and IL-8 by cancer cells. Cancer cell-derived IL-6 and IL-8 upregulated endothelin receptor expression on cancer cells and the production of endothelin from astrocytes. The endothelin axis then activated protein kinase B (AKT) and mitogen-activated protein kinase (MAPK) signaling pathways in MDA-MB-231 cells and protected the cancer cells from chemotherapeutic agents [33].

Through all these pre-clinical studies, we can conclude that IL-6 is a potent inflammatory cytokines and activator of STAT3, produced not only by tumor cells but also by cells in the PMN (Figure 1). It would suggest that tumor cells and stromal cells interdependently regulate IL-6 expression in cancers, which may account for the localized activation of the IL-6/STAT3 pathway. Although all these studies differed in murine models and cancer cells used, the therapeutic paradigm of targeting IL-6 pathway at the early stages of metastasis formation is promising. These discoveries should be investigated further, especially in aggressive tumors such as triple-negative breast cancer, pancreatic cancer, colorectal cancer, and lung cancer.

3. Interleukin-1 β

Interleukin-1 β (IL-1 β) is a pleiotropic cytokine that affects inflammatory responses, immune reactivity, and hemopoiesis in broad paracrine and endocrine manners. The potency of IL-1 β originates from its ability to induce the secretion of a network of proinflammatory molecules and the expression of adhesion molecules in diverse cells, thereby amplifying and sustaining its responses. As a mature secreted molecule, IL-1 β is one of the most potent pro-inflammatory cytokines abundant in primary tumor sites and in the tumor microenvironment in distant organs, which controls local proinflammatory cascades and thereby also affects the balance between antitumor cell immunity and destructive inflammation [34–36]. The local expression of IL-1 β in tumor sites has been correlated with increased invasiveness in experimental tumors and in cancer patients and is associated with a bad prognosis [34,37]. Neutralizing IL-1 β or blocking its receptor represents a direct targeted approach. Nowadays, several mediators blocking or neutralizing the IL-1 pathway such as antibodies and small-molecule inhibitors are in use or being tested for cancer treatment [38,39]. In this review, we will focus on the effect of IL-1 β on the establishment of pre-metastatic niches.

In breast cancer metastasis, Schmid and colleague found that IL-1 β was highly expressed in the microenvironment of murine lung, pancreatic, and breast tumors and was produced only by tumor-associated granulocytes and macrophage. The recruitment of myeloid cells induces inflammation in the premetastatic niche. IL-1 β works together with SDF-1 α to stimulate the adhesion of myeloid cells to the endothelium by activating integrin $\alpha 4\beta 1$ [40]. Furthermore, IL-1 β has been demonstrated to induce the expression and the release of IL-17 in $\gamma\delta$ T cells ($\gamma\delta$ T cells are a small subset of T cells that express heterodimeric T cell receptors composed of γ and δ chains) that led to the expansion and polarization of granulocyte-colony stimulating factor (G-CSF)-dependent neutrophils in mammary tumor-bearing mice. The accumulation of neutrophils and $\gamma\delta$ T cells in turn suppressed CD8⁺ T lymphocytes and allowed for pulmonary and lymph node metastasis formation [41]. A recent study showed that CXCR3-positive metastatic MDA-MB-231 cells (MDA-MB-231 cells expressing the chemokine receptor CXCR3) expressed high levels of IL-1 α/β via JNK signaling to evoke phenotypic changes in lung fibroblasts. Those fibroblasts in an inflammatory state produced the chemokines CXCL9 and CXCL10 through NF- κ B signaling, supporting the formation of the metastatic niche. CXCR3 is the only receptor known to bind and be activated by CXCL9 and CXCL10. Meanwhile, knockdown of IL-1 β was shown to limit the capability of cancer cells to colonize the lungs, demonstrating that IL-1 β is needed for lung metastasis formation and growth [42].

The poor prognosis of advance breast cancer patients with bone metastasis urges new therapeutic approaches. Knowledge of the molecular mechanism of breast cancer colonization of the bone

microenvironment is imperative for the development of future diagnostic and curative therapies. In breast cancer bone metastasis, it was suggested that IL-1 β contributed to the osteotropic nature of breast cancer cells. The analysis of tumor tissues from advanced-stage breast cancer patients demonstrated an increase in the likelihood of developing bone metastases in patients with IL-1 β -positive primary tumors compared to patients with IL-1 β -negative tumors. Based on that observation, Nutter and colleagues developed a bone-homing clone of the triple-negative breast cancer cells MDA-MB-231 and found that it had increased expression of IL-1 β and decreased expression of the cell adhesion molecule fibronectin and of the calcium-binding proteins S100A4 [43]. Besides the autocrine mechanism of breast-cancer derived IL-1 β in driving the cancer cell bone-seeking behavior, it was observed that MDA-MB-231 cells migrated to and colonized human bone tissue-conditioned medium that contained high levels of IL-1 β , which indicates that IL-1 β derived from the bone tissue microenvironment may also support the osteotropic breast cancer cell behavior [44]. Moreover, IL-1 β from macrophages or breast cancer cells themselves has been shown to induce the secretion of osteoprotegerin, a secreted member of the TNF receptor family involved in bone resorption, in breast cancer via the p38 and p42/22 MAPK signaling pathways. Inhibition of osteoprotegerin limits tumor invasion and metastasis, suggesting that osteoprotegerin and IL-1 β play a role in mediating breast cancer metastasis [45].

Another significant effect of IL-1 β promoting tumor metastasis is its ability to potentiate tumor angiogenesis. Carmi and colleague found that the cross-talk between IL-1 β and VEGF regulated the early angiogenic response, which procured a microenvironment suitable for angiogenesis and tumor development. VEGFR1⁺/IL-1R1⁺ immature myeloid cells produce IL-1 β along with other inflammatory chemokines and cytokines that enable endothelial cells to produce VEGF and other proangiogenic factors. In fact, IL-1 β appeared essential for the *in vivo* response of endothelial cells that impaired IL-1 β signaling and reduced the neo-angiogenic response in mice despite the presence of recombinant VEGF [46]. IL-1 β was also found to upregulate the production of VEGF and its receptor on vascular smooth muscle cells, which activates p38 MAPK and MAPK-activated protein kinase 2 via IL-1R1, promoting cell migration and angiogenesis [47]. One study also noted an increased expression of IL-1 β and E-selectin in premetastatic lungs in mice with melanoma, prior to the arrival of tumor cells. IL-1 β was produced by monocytic MDSCs in the premetastatic lungs, promoted E-selectin expression, and led to tumor cell adhesion to the vascular endothelium [48].

In contrast to most of the available data, metastasis-inhibiting effects have also been described for IL-1 β in breast cancer. Castano and colleague demonstrated that primary tumors elicited a response by innate immune cells that expressed IL-1 β , which infiltrated metastatic microenvironments. At the metastatic site, IL-1 β prevented metastatic cells from differentiating into highly proliferative E-cadherin-positive cells, which could form actively growing tumors. These authors also conducted a database analysis and revealed a beneficial effect of high primary tumor IL-1 β expression on overall survival and distant metastasis-free survival in patients with lymph node-positive breast cancer [49].

The role of inflammatory IL-1 β signaling in cancer is complex. Both pro-metastatic and anti-metastatic effects of IL-1 have been shown in mouse models, which are greatly dependent on the organ affected by cancer, cancer subtype, and the inflammatory background and stage of cancer. The source of IL-1 β is also critical to determine its effect. The chronic low levels of IL-1 β produced by the tumor itself may promote an immune-suppressive environment. On the other hand, exogenous administration of high levels of IL-1 β might elicit an anti-tumorigenic effect.

4. Other Cytokines

Besides IL-6 and IL-1 β , several other cytokine/chemokines are also studied in the PMN formation. CC-chemokine ligand 2 (CCL2), also known as monocyte chemoattractant protein-1 (MCP-1), is a member of the CC β cytokine family. Pollard and colleagues found that in the MMTV-PyMT mouse model of breast cancer, Gr1⁺ inflammatory monocytes expressing CCR2 (receptor for CCL2) were recruited to the premetastatic lung through CCL2 secreted by tumor and stromal cells and differentiated into tumor-associated macrophages (TAM) to promote the subsequent growth of metastatic cells.

Inhibition of CCL2 signaling or depletion of tumor cell-derived CCL2 diminished lung metastases in vivo [50]. However, monocytes are not the only population recruited to premetastatic lung by CCL2. Another study showed that tumor-entrained neutrophils also accumulated in the lungs via CCL2 and inhibited metastatic seeding in lungs by producing H₂O₂ [51]. Similar to IL-1 β , both pro-metastatic and anti-metastatic effects have been reported for CCL2. To understand if CCL2 can be a clinical target, it is necessary to define how the pro- and anti-metastatic effects are concomitantly regulated and which effect is dominant at each stage of metastasis.

Kowanetz and colleagues have indicated that tumor-secreted G-CSF expanded and mobilized Ly6G⁺Ly6C⁺ granulocytes from the bone marrow. G-CSF-mobilized Ly6G⁺Ly6C⁺ cells produced a series of pro-metastatic proteins such as Bv8, matrix-degrading enzyme MMP-9, inflammatory chemoattractants S100A8/A9 [52]. In addition to G-CSF, primary tumor-derived TNF- α and TGF β have also been implicated in the regulation of S100A8 and S100A9 expression in the pre-metastatic lungs, which were involved in the recruitment of MDSCs in distant organs [53]. Another colony-stimulating factor, tumor cell-secreted granulocyte-macrophage colony-stimulating factor (GM-CSF), has been shown to promote liver metastasis by inducing STAT3 phosphorylation in the liver MDSC. Activated STAT3 signaling promoted the expression of indoleamine 2,3-dioxygenase (IDO) and programmed death ligand 1 (PD-L1), both important mediators of T cell suppression. Inhibition of GM-CSF or GM-CSF-R markedly reduced IDO and PD-L1 expression in liver MDSCs, implicating tumor-derived GM-CSF in supporting the expression of immunoinhibitory molecules in MDSCs. Blockage of JAK2 and STAT3 also dramatically diminished IDO and PD-L1 expression in MDSCs, implying that STAT3 exerts transcriptional control over IDO and PD-L1 expression by binding to the *IDO1* and *PD-L1* promoters. All these results implicate GM-CSF and STAT3 as critical drivers of liver MDSC IDO/PD-L1 expression and potential mechanistic targets to enhance intrahepatic anti-tumor immunity [54].

One essential pathway governing tumor cell homing to the bone is the CXCL12–CXC chemokine receptor 4 (CXCR4) signaling axis. CXCL12 (stromal cell-derived factor 1, SDF-1) is a homeostatic chemokine predominantly produced by a diversity of stromal cells in the bone marrow including BM-MSCs, endothelial cells, CXCL12-abundant reticular (CAR) cells, and osteoblasts. Solid tumor cells overexpress the CXCL12 receptors CXCR4 and CXCR7 and migrate to CXCL12-expressing bone tissue via chemotaxis along a concentration gradient. In an experimental bone metastasis model of prostate cancer, prostate cancer cells target the hematopoietic stem cell (HSC) niche, use the CXCL12–CXCR4 axis to home to the niche, and compete with the HSC cells for niche support [55]. In colorectal cancer, a high systemic level of tissue inhibitor of metalloproteinases (TIMP)-1 led to increased hepatic SDF-1 level, which in turn promoted the recruitment of neutrophils to the liver. The activation of SDF-1 and the accumulation of neutrophils triggered the formation of a premetastatic niche and thus increased liver susceptibility towards metastasis. This promoted hepatic metastasis, independent of the origin or the intrinsic metastatic potential of tumor cells [56].

Macrophage migration inhibitory factor (MIF) is a well-known mediator of liver inflammation and fibrosis. For pancreatic cancer that metastasizes to the liver, exosomal MIF induced the release of TGF β by Kupffer cells in the liver, which further induced the deposit of fibronectin in the ECM by hepatic stellate cells. Fibronectin deposition subsequently summoned BMDCs and triggered PMN formation [57].

Chemokine (C–X–C motif) ligand 1 (CXCL1) is a member of the CXCL class of chemokines with neutrophil chemotactic and angiogenic properties. In an orthotopic mouse model of colorectal cancer, VEGF secreted by colorectal tumor cells stimulated the production of CXCL1 from TAM. The increase of CXCL1 in the liver recruited CXCR2-positive (CXCL1 receptor) MDSCs and facilitated the establishment of PMN in the liver [58].

5. Clinical Trials Targeting Pro-Inflammatory Cytokines in Metastatic Cancer

Pro-inflammatory cytokines are key mediators of innate and adaptive immunity at the crossroad of diverse pathways shaping pre-metastatic niches. Nowadays, several agents targeting IL-6, IL-6 receptor,

JAKs, or STAT3 have been used in the treatment of myeloma and tested in patients with solid tumors [8,59]. There are two FDA-approved antibodies directly targeting IL-6: siltuximab, a chimeric anti-IL-6 antibody [60], and tocilizumab, a humanized monoclonal antibody against the IL-6 receptor. Various global clinical trials, series, and pilot studies of off-label use of siltuximab and tocilizumab provide strong indications [61] that the anti-IL-6 therapy may be used for the treatment of blood cancers such as multiple myeloma [62] and leukemia [63] and of solid tumors such as prostate cancer [64], breast cancer [65], and ovarian cancer [66]. However, two phase II trials which employed siltuximab as second-line therapy for patients with metastatic prostate cancer showed an increase in plasma IL-6 after treatment and confirmed the poor prognosis associated with elevated IL-6 [60,67]. Two clinical trials, one (NCT04191421) evaluating siltuximab in metastatic pancreatic cancer patients and the other (NCT03135171) evaluating tocilizumab in metastatic HER2-positive breast cancer patients are in progress (Table 1).

Downstream in the IL-6 signaling pathway, JAK is another important drug target for cancer treatment. Among various JAK inhibitors, ruxolitinib is the most extensively investigated for cancer treatment. Approved by the FDA in 2011 for the treatment of myelofibrosis and post-polycythemia vera, ruxolitinib is a potent and selective oral JAK1 and JAK2 inhibitor. Studies on the safety and effectiveness of ruxolitinib in cancer patients with solid tumors such as breast cancer (NCT01594216), lung cancer (NCT02145637), colorectal cancer (NCT04303403), pancreatic cancer (NCT04303403), and head and neck cancer (NCT03153982) are ongoing. Additional early-phase trials of ruxolitinib have been focused on cancer metastasis, including patients with metastatic prostate cancer and metastatic breast cancer, as listed in Table 1. However, two phase III trials (NCT02119663 and NCT02117479) of ruxolitinib with capecitabine in metastatic pancreatic cancer patients were terminated due to no additional benefit over capecitabine alone [68]. The same also occurred with a phase II trial of ruxolitinib with capecitabine in patients with metastatic HER2-positive breast cancer (NCT02120417). Besides ruxolitinib, itacitinib, a JAK1 specific inhibitor, has also been employed in a phase I trial of metastatic soft tissue sarcomas.

The third potential target in the IL-6 signaling pathway is STAT3, with several compounds inhibiting the function or expression of STATs in clinical trials for various solid tumors [69]. BBI608, an oral cancer stemness inhibitor that blocks STAT3-mediated transcription of cancer stemness genes in the β -catenin pathway, has reached Phase II and III to treat metastatic colorectal cancer (Table 1). WP1066, a novel STAT3 inhibitor first published in 2010 [70], is in phase I for malignant glioma, metastatic melanoma in the brain, and pediatric brain tumors (Table 1).

Similarly, IL-1-blocking therapies have also been implicated in cancer-related inflammation [38,39]. Currently, clinically available anti-IL-1 strategies include anakinra (IL-1 receptor antagonist), canakinumab (a human anti-IL-1 β monoclonal antibody), CAN04 (an IL-1 receptor accessory protein binding protein), and isunakinra (a potent IL-1 receptor inhibitor). Accumulated evidence indicated that canakinumab is highly promising for the treatment of non-small-cell lung cancer, for which clinical trials are ongoing (NCT02090101, NCT01802970). Canakinumab is also being evaluated in metastatic pancreatic cancer, in a phase I clinical trial (Table 1). Another important anti-IL-1 drug for cancer treatment is anakinra, which is widely used to treat autoimmune and autoinflammatory diseases. It is also being tested as an adjunct therapy to reduce the inflammation associated with metastatic cancer, including colorectal cancer and breast cancer (Table 1).

In 2009, a phase II clinical trial has been conducted to test the effect of carlumab, a human mAb with high affinity and specificity for human CCL2, in patients with metastatic castration-resistant prostate cancer. In this trial, carlumab was unable to sustain a durable suppression of CCL2 and could not lead to meaningful clinical benefit responses (Table 1) [71]. Notably, the clinical application of CCL2 inhibitors for metastasis treatment requires a careful design.

Besides the extensively studied IL-6 and IL-1 β , there are several early-phase clinical trials exploring the efficacy of targeting CSF, SDF-1, and MIF in the treatment of various metastatic tumors, as summarized in Table 1. The trials with SDF-1 and MIF have been completed, but no results have been reported yet.

Table 1. Registered clinical trials targeting pro-inflammatory cytokines in patients with cancer metastases.

Tested Drug	NCT Number	Title	Status	Conditions	Phases	Enrollment	Start Date	Completion Date
IL-6 pathway								
IL-6								
Siltuximab, anti-IL-6 chimeric monoclonal antibody	NCT00433446	S0354, Anti-IL-6 Chimeric Monoclonal Antibody in Patients with Metastatic Prostate Cancer That Did Not Respond to Hormone Therapy	Completed	Metastatic Prostate Cancer	Phase 2	62	2007	2011
	NCT00385827	A Safety and Efficacy Study of Siltuximab (CNTO 328) in Male Subjects with Metastatic Hormone-Refractory Prostate Cancer (HRPC)	Terminated	Metastatic Prostate Cancer	Phase 2	106	2017	2021
	NCT04191421	Siltuximab and Spartalizumab in Patients with Metastatic Pancreatic Cancer	Recruiting	Metastatic Stage IV Pancreatic Cancer	Phase I Phase 2	42	2020	2022
Tocilizumab, humanized monoclonal antibody against IL-6 receptor	NCT03135171	Trastuzumab and Pertuzumab in Combination with Tocilizumab in Subjects with Metastatic HER2-Positive Breast Cancer Resistant to Trastuzumab	Recruiting	HER2+ Breast Cancer	Phase 1	20	2017	2021
	JAK							
Ruxolitinib, JAK1 and JAK2 inhibitor	NCT00638378	Study of Ruxolitinib (INCB018424) Administered Orally to Patients with Androgen-Independent Metastatic Prostate Cancer	Terminated	Prostate Cancer	Phase 2	22	2008	2009
	NCT01594216	Ruxolitinib in Estrogen Receptor-Positive Breast Cancer	Completed	Estrogen Receptor-Positive Invasive Metastatic Breast Cancer	Phase 2	29	2012	2016
	NCT02120417	A Study of Ruxolitinib in Combination with Capecitabine in Subjects with Advanced or Metastatic HER2-Negative Breast Cancer	Terminated	Breast Cancer	Phase 2	149	2014	2017
	NCT02041429	Ruxolitinib W/Preop Chemo for Triple-Negative Inflammatory Breast cancer	Active, not recruiting	Recurrent Breast Cancer Metastatic Breast Cancer	Phase I Phase 2	24	2014	2021
	NCT02066532	Ruxolitinib in Combination with Trastuzumab in Metastatic HER2-Positive Breast Cancer	Active, not recruiting	Metastatic Breast Cancer HER-2 Positive Breast Cancer	Phase I Phase 2	28	2014	2020

Table 1. Cont.

Tested Drug	NCT Number	Title	Status	Conditions	Phases	Enrollment	Start Date	Completion Date
	NCT03012230	Pembrolizumab and Ruxolitinib Phosphate in Treating Patients with Metastatic Stage IV Triple-Negative Breast Cancer	Recruiting	Metastatic Malignant Neoplasm in the Bone Stage IV Breast Cancer Triple-Negative Breast Carcinoma	Phase 1	18	2017	2021
	NCT02876302	Study of Ruxolitinib (INCB018424) With Preoperative Chemotherapy for Triple-Negative Inflammatory Breast Cancer	Recruiting	Inflammatory Breast Cancer	Phase 2	64	2017	2024
Itacitinib, JAK1 inhibitor	NCT03670069	Itacitinib in Treating Patients with Refractory Metastatic/Advanced Soft Tissue Sarcomas	Recruiting	Metastatic Leiomyosarcoma Metastatic Synovial Sarcoma	Phase 1	28	2019	2022
STAT								
	NCT03522649	A Phase III Clinical Study of Napabucasin (GP201) Plus FOLFIRI in Adult Patients with Metastatic Colorectal Cancer	Recruiting	Previously Treated Metastatic Colorectal Cancer	Phase 3	668	2018	2021
BBF608, STAT3 inhibitor	NCT03647839	Modulation of The Tumor Microenvironment Using Either Vascular Disrupting Agents or STAT3 Inhibition in Order to Synergize With PD1 Inhibition in Microsatellite-Stable, Refractory Colorectal Cancer Patients	Active, not recruiting	Colorectal Cancer Metastatic	Phase 2	90	2018	2022
WP1066, JAK2/STAT3 inhibitor	NCT01904123	STAT3 Inhibitor WP1066 in Treating Patients with Recurrent Malignant Glioma or Progressive Metastatic Melanoma in the Brain	Recruiting	Metastatic Malignant Neoplasm in the Brain Metastatic Melanoma	Phase 1	33	2018	2021
	NCT04334863	AflacSTI1901: Peds WP1066	Recruiting	Brain Tumor Medulloblastoma Brain Metastases	Phase 1	36	2020	2023
IL-1								
Canakinumab, human anti-IL-1 β monoclonal antibody	NCT03631199	Study of Efficacy and Safety of Pembrolizumab Plus Platinum-based Doublet Chemotherapy with or without Canakinumab in Previously Untreated Locally Advanced or Metastatic Non-Squamous and Squamous Non-Small Cell Lung Cancer (NSCLC) Subjects	Active, not recruiting	Non-Small Cell Lung Cancer	Phase 3	673	2018	2022

Table 1. Cont.

Tested Drug	NCT Number	Title	Status	Conditions	Phases	Enrollment	Start Date	Completion Date
Anakinra, human interleukin 1 receptor antagonist	NCT04581343	A Phase 1B Study of Canakinumab, Sparalizumab, Nab-Paclitaxel, and Gemcitabine in Metastatic PC Patients	Recruiting	Metastatic Pancreatic Ductal Adenocarcinoma	Phase 1	10	2020	2022
	NCT00072111	Anakinra in Treating Patients with Metastatic Cancer Expressing the Interleukin-1 Gene	Completed	Metastatic Cancer	Phase 1		2003	2015
	NCT02090101	Study Evaluating the Influence of LV5FU2 Bevacizumab Plus Anakinra Association on Metastatic Colorectal Cancer	Completed	Metastatic Colorectal Cancer	Phase 2	32	2014	2017
Anakinra, human interleukin 1 receptor antagonist	NCT01802970	Safety and Blood Immune Cell Study of Anakinra Plus Physician's Chemotherapy Choice in Metastatic Breast Cancer Patients	Completed	Metastatic Breast Cancer	Phase 1	10	2012	2017
	NCT01624766	Everolimus and Anakinra or Denosumab in Treating Participants with Relapsed or Refractory Advanced Cancers	Active, not recruiting	Advanced Malignant Neoplasm Metastatic Malignant Neoplasm Recurrent Malignant Neoplasm Refractory Malignant Neoplasm	Phase 1	57	2012	2020
CCL2								
Cartumab	NCT00992186	A Study of the Safety and Efficacy of Single-Agent Cartumab (an Anti-Chemokine Ligand 2 [CCL2]) in Participants with Metastatic Castrate-Resistant Prostate Cancer	Completed	Prostate cancer	Phase 2	46	2009	2011
	NCT03238027	A Phase 1 Study to Investigate SNDX-6352 Alone or in Combination With Durvalumab in Patients With Solid Tumors	Active, not recruiting	Solid Tumor Metastatic Tumor	Phase 1	45	2017	2021
CSF								
Olaptesed, binding to SDF-1	NCT03168139	Olaptesed (NOX-A12) Alone and in Combination with Pembrolizumab in Colorectal and Pancreatic Cancer Patients	Completed	Metastatic Colorectal Cancer Metastatic Pancreatic Cancer	Phase 1 Phase 2	20	2017	2020
	NCT01765790	Phase 1 Study of Anti-Macrophage Migration Inhibitory Factor (Anti-MIF) Antibody in Solid Tumors	Completed	Metastatic Adenocarcinoma of the Colon or Rectum	Phase 1	68	2012	2016
MIF								

6. Conclusions

Cancer metastasis poses significant challenges to the development of curative therapies due to insufficient knowledge of the mechanisms governing this process. Targeting the molecular interactions that build the PMN has the potential to prevent and eradicate metastases before they manifest. It would be most useful to block the signaling systems that promote the establishment of the PMN right after dissecting a primary tumor, i.e., in the critical post-operative window when no visible metastases are observed but PMN formation is probably ongoing. Compelling evidence implies the rise of pro-inflammatory cytokines and the suppression of the immune function during the peri-operative and post-operative periods [72,73], which all contribute to PMN formation. However, the combination of pro-inflammatory cytokines in the PMN is still under investigation and may vary in different types of cancer or even in individual patients. The advanced ‘omics’ technology could help design more precise and individualized therapeutic approaches in future clinical trials. Admittedly, some clinical trials targeting IL-6 or IL-1 have failed in preventing metastasis. Human solid tumors are more complex than mouse models, and the heterogeneity of cancer cells could be a factor affecting treatment efficacy. Thus, monotherapy to inhibit a single cytokine may not be sufficient to treat advanced tumors. Taking in consideration the pleiotropy and redundancy of pro-inflammatory cytokines, further in vitro and in vivo studies should be designed to determine the joint power of pro-inflammatory cytokines in PMN formation, as well as to analyze their combined targeting in cancer metastasis.

Author Contributions: Literature search, R.L. and A.W.; IL-6 writing, R.L.; IL-1 writing, A.W.; original draft preparation, R.L.; writing—review and editing, J.L.; supervision, J.L. All authors have read and agreed to the published version of the manuscript.

Funding: This research was funded by New York State Department of Health, grant number DOH01-C33915GG, and Stony Brook University (56562).

Conflicts of Interest: The authors declare no conflict of interest.

List of Abbreviations

ECM:	extracellular matrix
PMN:	pre-metastatic niche
BMDC:	bone marrow-derived cells
MDSC:	myeloid-derived suppressor cells
TAM:	tumor-associated macrophage
EV:	extracellular vesicles
EMT:	epithelial-to-mesenchymal transition
CAF:	cancer associated fibroblast
HSC:	hematopoietic stem cell
BBB:	blood–brain barrier
IL-6:	interleukin 6
IL-1 β :	interleukin-1 β
CXCL12/SDF-1 α :	stromal cell-derived factor 1
IL-8:	interleukin 8
VEGF:	vascular endothelial growth factor
G-CSF:	granulocyte-colony stimulating factor
MIF:	macrophage migration inhibitory factor
TIMP-1:	tissue inhibitor of metalloproteinases 1
GM-CSF:	granulocyte–macrophage colony-stimulating factor
SAA:	serum amyloid A
TGF- β :	transforming growth factor beta
HIF-1:	hypoxia-inducible factor 1
CCL2:	CC-chemokine ligand 2
CCL5:	chemokine ligand 5

CXCL1:	C–X–C motif ligand 1
JAK:	Janus kinase
STAT3:	signal transducer and activator of transcription 3
AKT:	protein kinase B
MAPK:	mitogen-activated protein kinase
IDO:	indoleamine 2,3-dioxygenase
PD-L1:	programmed death ligand 1

References

1. Vanharanta, S.; Massagué, J. Origins of metastatic traits. *Cancer Cell* **2013**, *24*, 410–421. [[CrossRef](#)] [[PubMed](#)]
2. Joyce, J.A.; Pollard, J.W. Microenvironmental regulation of metastasis. *Nat. Rev. Cancer* **2009**, *9*, 239–252. [[CrossRef](#)] [[PubMed](#)]
3. Kaplan, R.N.; Riba, R.D.; Zacharoulis, S.; Bramley, A.H.; Vincent, L.; Costa, C.; MacDonald, D.D.; Jin, D.K.; Shido, K.; Kerns, S.A.; et al. VEGFR1-positive haematopoietic bone marrow progenitors initiate the pre-metastatic niche. *Nature* **2005**, *438*, 820–827. [[CrossRef](#)]
4. Law, A.M.K.; Valdes-Mora, F.; Gallego-Ortega, D. Myeloid-Derived Suppressor Cells as a Therapeutic Target for Cancer. *Cells* **2020**, *9*, 561. [[CrossRef](#)] [[PubMed](#)]
5. Ozaki, K.; Leonard, W.J. Cytokine and cytokine receptor pleiotropy and redundancy. *J. Biol. Chem.* **2002**, *277*, 29355–29358. [[CrossRef](#)]
6. Altan-Bonnet, G.; Mukherjee, R. Cytokine-mediated communication: A quantitative appraisal of immune complexity. *Nat. Rev. Immunol.* **2019**, *19*, 205–217. [[CrossRef](#)]
7. Dranoff, G. Cytokines in cancer pathogenesis and cancer therapy. *Nat. Rev. Cancer* **2004**, *4*, 11–22. [[CrossRef](#)]
8. Johnson, D.E.; O’Keefe, R.A.; Grandis, J.R. Targeting the IL-6/JAK/STAT3 signalling axis in cancer. *Nat. Rev. Clin. Oncol.* **2018**, *15*, 234. [[CrossRef](#)]
9. Ludwig, H.; Nachbaur, D.M.; Fritz, E.; Krainer, M.; Huber, H. Interleukin-6 is a prognostic factor in multiple myeloma. *Blood* **1991**, *77*, 2794–2795. [[CrossRef](#)]
10. Macha, M.A.; Matta, A.; Kaur, J.; Chauhan, S.S.; Thakar, A.; Shukla, N.K.; Gupta, S.D.; Ralhan, R. Prognostic significance of nuclear pSTAT3 in oral cancer. *Head Neck* **2011**, *33*, 482–489. [[CrossRef](#)]
11. Chen, Y.; Wang, J.; Wang, X.; Liu, X.; Li, H.; Lv, Q.; Zhu, J.; Wei, B.; Tang, Y. STAT3, a Poor Survival Predictor, Is Associated with Lymph Node Metastasis from Breast Cancer. *J. Breast Cancer* **2013**, *16*, 40–49. [[CrossRef](#)] [[PubMed](#)]
12. Kusaba, T.; Nakayama, T.; Yamazumi, K.; Yakata, Y.; Yoshizaki, A.; Inoue, K.; Nagayasu, T.; Sekine, I. Activation of STAT3 is a marker of poor prognosis in human colorectal cancer. *Oncol. Rep.* **2006**, *15*, 1445–1451. [[CrossRef](#)] [[PubMed](#)]
13. Yu, H.; Kortylewski, M.; Pardoll, D. Crosstalk between cancer and immune cells: Role of STAT3 in the tumour microenvironment. *Nat. Rev. Immunol.* **2007**, *7*, 41. [[CrossRef](#)] [[PubMed](#)]
14. Yu, H.; Lee, H.; Herrmann, A.; Buettner, R.; Jove, R. Revisiting STAT3 signalling in cancer: New and unexpected biological functions. *Nat. Rev. Cancer* **2014**, *14*, 736. [[CrossRef](#)]
15. Kortylewski, M.; Kujawski, M.; Wang, T.; Wei, S.; Zhang, S.; Pilon-Thomas, S.; Niu, G.; Kay, H.; Mule, J.; Kerr, W.G.; et al. Inhibiting Stat3 signaling in the hematopoietic system elicits multicomponent antitumor immunity. *Nat. Med.* **2005**, *11*, 1314–1321. [[CrossRef](#)]
16. Jones, S.A.; Jenkins, B.J. Recent insights into targeting the IL-6 cytokine family in inflammatory diseases and cancer. *Nat. Rev. Immunol.* **2018**, *18*, 773–789. [[CrossRef](#)]
17. Rokavec, M.; Oner, M.G.; Li, H.; Jackstadt, R.; Jiang, L.; Lodygin, D.; Kaller, M.; Horst, D.; Ziegler, P.K.; Schwitalla, S.; et al. IL-6R/STAT3/miR-34a feedback loop promotes EMT-mediated colorectal cancer invasion and metastasis. *J. Clin. Investig.* **2014**, *124*, 1853–1867. [[CrossRef](#)]
18. Leone, P.; Buonavoglia, A.; Fasano, R.; Solimando, A.G.; De Re, V.; Cicco, S.; Vacca, A.; Racanelli, V. Insights into the Regulation of Tumor Angiogenesis by Micro-RNAs. *J. Clin. Med.* **2019**, *8*, 2030. [[CrossRef](#)]
19. Kim, J.; Yao, F.; Xiao, Z.; Sun, Y.; Ma, L. MicroRNAs and metastasis: Small RNAs play big roles. *Cancer Metastasis Rev.* **2018**, *37*, 5–15. [[CrossRef](#)]
20. Gyamfi, J.; Lee, Y.-H.; Eom, M.; Choi, J. Interleukin-6/STAT3 signalling regulates adipocyte induced epithelial-mesenchymal transition in breast cancer cells. *Sci. Rep.* **2018**, *8*, 8859. [[CrossRef](#)]

21. He, J.Y.; Wei, X.H.; Li, S.J.; Liu, Y.; Hu, H.L.; Li, Z.Z.; Kuang, X.H.; Wang, L.; Shi, X.; Yuan, S.T.; et al. Adipocyte-derived IL-6 and leptin promote breast Cancer metastasis via upregulation of Lysyl Hydroxylase-2 expression. *Cell Commun. Signal.* **2018**, *16*, 100. [[CrossRef](#)] [[PubMed](#)]
22. Abbruzzese, J.L.; Abbruzzese, M.C.; Lenzi, R.; Hess, K.R.; Raber, M.N. Analysis of a diagnostic strategy for patients with suspected tumors of unknown origin. *J. Clin. Oncol.* **1995**, *13*, 2094–2103. [[CrossRef](#)] [[PubMed](#)]
23. Ji, Q.; Zhou, L.; Sui, H.; Yang, L.; Wu, X.; Song, Q.; Jia, R.; Li, R.; Sun, J.; Wang, Z.; et al. Primary tumors release ITGBL1-rich extracellular vesicles to promote distal metastatic tumor growth through fibroblast-niche formation. *Nat. Commun.* **2020**, *11*, 1211. [[CrossRef](#)] [[PubMed](#)]
24. Erdogan, B.; Webb, D.J. Cancer-associated fibroblasts modulate growth factor signaling and extracellular matrix remodeling to regulate tumor metastasis. *Biochem. Soc. Trans.* **2017**, *45*, 229–236. [[CrossRef](#)]
25. Lee, E.; Fertig, E.J.; Jin, K.; Sukumar, S.; Pandey, N.B.; Popel, A.S. Breast cancer cells condition lymphatic endothelial cells within pre-metastatic niches to promote metastasis. *Nat. Commun.* **2014**, *5*, 4715. [[CrossRef](#)]
26. Huang, Y.; Song, N.; Ding, Y.; Yuan, S.; Li, X.; Cai, H.; Shi, H.; Luo, Y. Pulmonary vascular destabilization in the premetastatic phase facilitates lung metastasis. *Cancer Res.* **2009**, *69*, 7529–7537. [[CrossRef](#)]
27. Hiratsuka, S.; Ishibashi, S.; Tomita, T.; Watanabe, A.; Akashi-Takamura, S.; Murakami, M.; Kijima, H.; Miyake, K.; Aburatani, H.; Maru, Y. Primary tumours modulate innate immune signalling to create pre-metastatic vascular hyperpermeability foci. *Nat. Commun.* **2013**, *4*, 1853. [[CrossRef](#)]
28. Chang, Q.; Bournazou, E.; Sansone, P.; Berishaj, M.; Gao, S.P.; Daly, L.; Wels, J.; Theilen, T.; Granitto, S.; Zhang, X.; et al. The IL-6/JAK/Stat3 feed-forward loop drives tumorigenesis and metastasis. *Neoplasia* **2013**, *15*, 848–862. [[CrossRef](#)]
29. Tao, Q.; Fujimoto, J.; Men, T.; Ye, X.; Deng, J.; Lacroix, L.; Clifford, J.L.; Mao, L.; Van Pelt, C.S.; Lee, J.J.; et al. Identification of the retinoic acid-inducible Gprc5a as a new lung tumor suppressor gene. *J. Natl. Cancer Inst.* **2007**, *99*, 1668–1682. [[CrossRef](#)]
30. Jing, B.; Wang, T.; Sun, B.; Xu, J.; Xu, D.; Liao, Y.; Song, H.; Guo, W.; Li, K.; Hu, M.; et al. IL6/STAT3 Signaling Orchestrates Premetastatic Niche Formation and Immunosuppressive Traits in Lung. *Cancer Res.* **2020**, *80*, 784–797. [[CrossRef](#)]
31. Tabouret, E.; Chinot, O.; Metellus, P.; Tallet, A.; Viens, P.; Goncalves, A. Recent trends in epidemiology of brain metastases: An overview. *Anticancer Res.* **2012**, *32*, 4655–4662. [[PubMed](#)]
32. Witzel, I.; Laakmann, E.; Weide, R.; Neunhöffer, T.; Park-Simon, T.J.; Schmidt, M.; Fasching, P.A.; Hesse, T.; Polasik, A.; Mohrmann, S.; et al. Treatment and outcomes of patients in the Brain Metastases in Breast Cancer Network Registry. *Eur. J. Cancer* **2018**, *102*, 1–9. [[CrossRef](#)] [[PubMed](#)]
33. Kim, S.W.; Choi, H.J.; Lee, H.J.; He, J.; Wu, Q.; Langley, R.R.; Fidler, I.J.; Kim, S.J. Role of the endothelin axis in astrocyte- and endothelial cell-mediated chemoprotection of cancer cells. *Neuro Oncol.* **2014**, *16*, 1585–1598. [[CrossRef](#)] [[PubMed](#)]
34. Apte, R.N.; Voronov, E. Interleukin-1—a major pleiotropic cytokine in tumor-host interactions. *Semin. Cancer Biol.* **2002**, *12*, 277–290. [[CrossRef](#)]
35. Dinarello, C.A. Overview of the IL-1 family in innate inflammation and acquired immunity. *Immunol. Rev.* **2018**, *281*, 8–27. [[CrossRef](#)] [[PubMed](#)]
36. Bent, R.; Moll, L.; Grabbe, S.; Bros, M. Interleukin-1 Beta-A Friend or Foe in Malignancies? *Int. J. Mol. Sci.* **2018**, *19*, 2155. [[CrossRef](#)]
37. Krelin, Y.; Voronov, E.; Dotan, S.; Elkabets, M.; Reich, E.; Fogel, M.; Huszar, M.; Iwakura, Y.; Segal, S.; Dinarello, C.A.; et al. Interleukin-1beta-driven inflammation promotes the development and invasiveness of chemical carcinogen-induced tumors. *Cancer Res.* **2007**, *67*, 1062–1071. [[CrossRef](#)]
38. Dinarello, C.A.; Simon, A.; van der Meer, J.W. Treating inflammation by blocking interleukin-1 in a broad spectrum of diseases. *Nat. Rev. Drug Discov.* **2012**, *11*, 633–652. [[CrossRef](#)]
39. Molgora, M.; Supino, D.; Mantovani, A.; Garlanda, C. Tuning inflammation and immunity by the negative regulators IL-1R2 and IL-1R8. *Immunol. Rev.* **2018**, *281*, 233–247. [[CrossRef](#)]
40. Schmid, M.C.; Avraamides, C.J.; Foubert, P.; Shaked, Y.; Kang, S.W.; Kerbel, R.S.; Varner, J.A. Combined blockade of integrin- α 4 β 1 plus cytokines SDF-1 α or IL-1 β potently inhibits tumor inflammation and growth. *Cancer Res.* **2011**, *71*, 6965–6975. [[CrossRef](#)]
41. Coffelt, S.B.; Kersten, K.; Doornebal, C.W.; Weiden, J.; Vrijland, K.; Hau, C.S.; Versteegen, N.J.M.; Ciampricotti, M.; Hawinkels, L.; Jonkers, J.; et al. IL-17-producing gammadelta T cells and neutrophils conspire to promote breast cancer metastasis. *Nature* **2015**, *522*, 345–348. [[CrossRef](#)] [[PubMed](#)]

42. Pein, M.; Insua-Rodriguez, J.; Hongu, T.; Riedel, A.; Meier, J.; Wiedmann, L.; Decker, K.; Essers, M.A.G.; Sinn, H.P.; Spaich, S.; et al. Metastasis-initiating cells induce and exploit a fibroblast niche to fuel malignant colonization of the lungs. *Nat. Commun.* **2020**, *11*, 1494. [[CrossRef](#)] [[PubMed](#)]
43. Nutter, F.; Holen, I.; Brown, H.K.; Cross, S.S.; Evans, C.A.; Walker, M.; Coleman, R.E.; Westbrook, J.A.; Selby, P.J.; Brown, J.E.; et al. Different molecular profiles are associated with breast cancer cell homing compared with colonisation of bone: Evidence using a novel bone-seeking cell line. *Endocr. Relat. Cancer* **2014**, *21*, 327–341. [[CrossRef](#)] [[PubMed](#)]
44. Templeton, Z.S.; Lie, W.R.; Wang, W.; Rosenberg-Hasson, Y.; Alluri, R.V.; Tamareisis, J.S.; Bachmann, M.H.; Lee, K.; Maloney, W.J.; Contag, C.H.; et al. Breast Cancer Cell Colonization of the Human Bone Marrow Adipose Tissue Niche. *Neoplasia* **2015**, *17*, 849–861. [[CrossRef](#)]
45. Chung, S.T.; Geerts, D.; Roseman, K.; Renaud, A.; Connelly, L. Osteoprotegerin mediates tumor-promoting effects of Interleukin-1beta in breast cancer cells. *Mol. Cancer* **2017**, *16*, 27. [[CrossRef](#)]
46. Carmi, Y.; Dotan, S.; Rider, P.; Kaplanov, I.; White, M.R.; Baron, R.; Abutbul, S.; Huszar, M.; Dinarello, C.A.; Apte, R.N.; et al. The role of IL-1 β in the early tumor cell-induced angiogenic response. *J. Immunol.* **2013**, *190*, 3500–3509. [[CrossRef](#)]
47. Jung, Y.D.; Liu, W.; Reinmuth, N.; Ahmad, S.A.; Fan, F.; Gallick, G.E.; Ellis, L.M. Vascular endothelial growth factor is upregulated by interleukin-1 beta in human vascular smooth muscle cells via the P38 mitogen-activated protein kinase pathway. *Angiogenesis* **2001**, *4*, 155–162. [[CrossRef](#)]
48. Shi, H.; Zhang, J.; Han, X.; Li, H.; Xie, M.; Sun, Y.; Liu, W.; Ba, X.; Zeng, X. Recruited monocytic myeloid-derived suppressor cells promote the arrest of tumor cells in the premetastatic niche through an IL-1 β -mediated increase in E-selectin expression. *Int. J. Cancer* **2017**, *140*, 1370–1383. [[CrossRef](#)]
49. Castaño, Z.; San Juan, B.P.; Spiegel, A.; Pant, A.; DeCristo, M.J.; Laszewski, T.; Ubellacker, J.M.; Janssen, S.R.; Dongre, A.; Reinhardt, F.; et al. IL-1 β inflammatory response driven by primary breast cancer prevents metastasis-initiating cell colonization. *Nat. Cell Biol.* **2018**, *20*, 1084–1097. [[CrossRef](#)]
50. Qian, B.Z.; Li, J.; Zhang, H.; Kitamura, T.; Zhang, J.; Campion, L.R.; Kaiser, E.A.; Snyder, L.A.; Pollard, J.W. CCL2 recruits inflammatory monocytes to facilitate breast-tumour metastasis. *Nature* **2011**, *475*, 222–225. [[CrossRef](#)]
51. Granot, Z.; Henke, E.; Comen, E.A.; King, T.A.; Norton, L.; Benezra, R. Tumor entrained neutrophils inhibit seeding in the premetastatic lung. *Cancer Cell* **2011**, *20*, 300–314. [[CrossRef](#)] [[PubMed](#)]
52. Kowanetz, M.; Wu, X.; Lee, J.; Tan, M.; Hagenbeek, T.; Qu, X.; Yu, L.; Ross, J.; Korsisaari, N.; Cao, T.; et al. Granulocyte-colony stimulating factor promotes lung metastasis through mobilization of Ly6G+Ly6C+ granulocytes. *Proc. Natl. Acad. Sci. USA* **2010**, *107*, 21248–21255. [[CrossRef](#)] [[PubMed](#)]
53. Hiratsuka, S.; Watanabe, A.; Aburatani, H.; Maru, Y. Tumour-mediated upregulation of chemoattractants and recruitment of myeloid cells predetermines lung metastasis. *Nat. Cell Biol.* **2006**, *8*, 1369–1375. [[CrossRef](#)] [[PubMed](#)]
54. Thorn, M.; Guha, P.; Cunetta, M.; Espot, N.J.; Miller, G.; Junghans, R.P.; Katz, S.C. Tumor-associated GM-CSF overexpression induces immunoinhibitory molecules via STAT3 in myeloid-suppressor cells infiltrating liver metastases. *Cancer Gene Ther.* **2016**, *23*, 188–198. [[CrossRef](#)]
55. Shiozawa, Y.; Pedersen, E.A.; Havens, A.M.; Jung, Y.; Mishra, A.; Joseph, J.; Kim, J.K.; Patel, L.R.; Ying, C.; Ziegler, A.M.; et al. Human prostate cancer metastases target the hematopoietic stem cell niche to establish footholds in mouse bone marrow. *J. Clin. Investig.* **2001**, *121*, 1298–1312. [[CrossRef](#)]
56. Seubert, B.; Grünwald, B.; Kobuch, J.; Cui, H.; Schelter, F.; Schaten, S.; Siveke, J.T.; Lim, N.H.; Nagase, H.; Simonavicius, N.; et al. Tissue inhibitor of metalloproteinases (TIMP)-1 creates a premetastatic niche in the liver through SDF-1/CXCR4-dependent neutrophil recruitment in mice. *Hepatology* **2015**, *61*, 238–248. [[CrossRef](#)]
57. Costa-Silva, B.; Aiello, N.M.; Ocean, A.J.; Singh, S.; Zhang, H.; Thakur, B.K.; Becker, A.; Hoshino, A.; Mark, M.T.; Molina, H.; et al. Pancreatic cancer exosomes initiate pre-metastatic niche formation in the liver. *Nat. Cell Biol.* **2015**, *17*, 816–826. [[CrossRef](#)]
58. Wang, D.; Sun, H.; Wei, J.; Cen, B.; DuBois, R.N. CXCL1 Is Critical for Premetastatic Niche Formation and Metastasis in Colorectal Cancer. *Cancer Res.* **2017**, *77*, 3655–3665. [[CrossRef](#)]
59. Sansone, P.; Bromberg, J. Targeting the interleukin-6/Jak/stat pathway in human malignancies. *J. Clin. Oncol.* **2012**, *30*, 1005–1014. [[CrossRef](#)]

60. Dorff, T.B.; Goldman, B.; Pinski, J.K.; Mack, P.C.; Lara, P.N., Jr.; Van Veldhuizen, P.J., Jr.; Quinn, D.I.; Vogelzang, N.J.; Thompson, I.M., Jr.; Hussain, M.H. Clinical and correlative results of SWOG S0354: A phase II trial of CNTO328 (siltuximab), a monoclonal antibody against interleukin-6, in chemotherapy-pretreated patients with castration-resistant prostate cancer. *Clin. Cancer Res.* **2010**, *16*, 3028–3034. [[CrossRef](#)]
61. Kampan, N.C.; Xiang, S.D.; McNally, O.M.; Stephens, A.N.; Quinn, M.A.; Plebanski, M. Immunotherapeutic Interleukin-6 or Interleukin-6 Receptor Blockade in Cancer: Challenges and Opportunities. *Curr. Med. Chem.* **2018**, *25*, 4785–4806. [[CrossRef](#)] [[PubMed](#)]
62. Iftikhar, A.; Hassan, H.; Iftikhar, N.; Mushtaq, A.; Sohail, A.; Rosko, N.; Chakraborty, R.; Razzaq, F.; Sandeep, S.; Valent, J.N.; et al. Investigational Monoclonal Antibodies in the Treatment of Multiple Myeloma: A Systematic Review of Agents under Clinical Development. *Antibodies* **2019**, *8*, 34. [[CrossRef](#)]
63. Riegler, L.L.; Jones, G.P.; Lee, D.W. Current approaches in the grading and management of cytokine release syndrome after chimeric antigen receptor T-cell therapy. *Ther. Clin. Risk Manag.* **2019**, *15*, 323–335. [[CrossRef](#)] [[PubMed](#)]
64. Culig, Z.; Puh, M. Interleukin-6 and prostate cancer: Current developments and unsolved questions. *Mol. Cell. Endocrinol.* **2018**, *462*, 25–30. [[CrossRef](#)] [[PubMed](#)]
65. Masjedi, A.; Hashemi, V.; Hojjat-Farsangi, M.; Ghalamfarsa, G.; Azizi, G.; Yousefi, M.; Jadidi-Niaragh, F. The significant role of interleukin-6 and its signaling pathway in the immunopathogenesis and treatment of breast cancer. *Biomed. Pharmacother.* **2018**, *108*, 1415–1424. [[CrossRef](#)] [[PubMed](#)]
66. Angevin, E.; Taberero, J.; Elez, E.; Cohen, S.J.; Bahleda, R.; van Laethem, J.L.; Ottensmeier, C.; Lopez-Martin, J.A.; Clive, S.; Joly, F.; et al. A phase I/II, multiple-dose, dose-escalation study of siltuximab, an anti-interleukin-6 monoclonal antibody, in patients with advanced solid tumors. *Clin. Cancer Res.* **2014**, *20*, 2192–2204. [[CrossRef](#)] [[PubMed](#)]
67. Fizazi, K.; De Bono, J.S.; Flechon, A.; Heidenreich, A.; Voog, E.; Davis, N.B.; Qi, M.; Bandekar, R.; Vermeulen, J.T.; Cornfeld, M.; et al. Randomised phase II study of siltuximab (CNTO 328), an anti-IL-6 monoclonal antibody, in combination with mitoxantrone/prednisone versus mitoxantrone/prednisone alone in metastatic castration-resistant prostate cancer. *Eur. J. Cancer* **2012**, *48*, 85–93. [[CrossRef](#)]
68. Giaccone, G.; Sanborn, R.E.; Waqar, S.N.; Martinez-Marti, A.; Ponce, S.; Zhen, H.; Kennealey, G.; Erickson-Viitanen, S.; Schaefer, E. A Placebo-Controlled Phase II Study of Ruxolitinib in Combination With Pemetrexed and Cisplatin for First-Line Treatment of Patients With Advanced Nonsquamous Non-Small-Cell Lung Cancer and Systemic Inflammation. *Clin. Lung Cancer* **2018**, *19*, e567–e574. [[CrossRef](#)]
69. Zou, S.; Tong, Q.; Liu, B.; Huang, W.; Tian, Y.; Fu, X. Targeting STAT3 in Cancer Immunotherapy. *Mol. Cancer* **2020**, *19*, 145. [[CrossRef](#)]
70. Horiguchi, A.; Asano, T.; Kuroda, K.; Sato, A.; Asakuma, J.; Ito, K.; Hayakawa, M.; Sumitomo, M.; Asano, T. STAT3 inhibitor WP1066 as a novel therapeutic agent for renal cell carcinoma. *Br. J. Cancer* **2010**, *102*, 1592–1599. [[CrossRef](#)]
71. Pienta, K.J.; Machiels, J.P.; Schrijvers, D.; Alekseev, B.; Shkolnik, M.; Crabb, S.J.; Li, S.; Seetharam, S.; Puchalski, T.A.; Takimoto, C.; et al. Phase 2 study of carlumab (CNTO 888), a human monoclonal antibody against CC-chemokine ligand 2 (CCL2), in metastatic castration-resistant prostate cancer. *Investig. New Drugs* **2013**, *31*, 760–768. [[CrossRef](#)] [[PubMed](#)]
72. Li, R.; Huang, Y.; Lin, J. Distinct effects of general anesthetics on lung metastasis mediated by IL-6/JAK/STAT3 pathway in mouse models. *Nat. Commun.* **2020**, *11*, 642. [[CrossRef](#)] [[PubMed](#)]
73. Hiller, J.G.; Perry, N.J.; Poulgiannis, G.; Riedel, B.; Sloan, E.K. Perioperative events influence cancer recurrence risk after surgery. *Nat. Rev. Clin. Oncol.* **2018**, *15*, 205–218. [[CrossRef](#)] [[PubMed](#)]

Publisher’s Note: MDPI stays neutral with regard to jurisdictional claims in published maps and institutional affiliations.



© 2020 by the authors. Licensee MDPI, Basel, Switzerland. This article is an open access article distributed under the terms and conditions of the Creative Commons Attribution (CC BY) license (<http://creativecommons.org/licenses/by/4.0/>).

Article

Targeting of Evolutionarily Acquired Cancer Cell Phenotype by Exploiting pHi-Metabolic Vulnerabilities

Bryce Ordway ¹, Michal Tomaszewski ¹, Samantha Byrne ¹, Dominique Abrahams ¹, Pawel Swietach ², Robert J. Gillies ¹ and Mehdi Damaghi ^{1,3,*}

¹ Department of Cancer Physiology, Moffitt Cancer Center and Research Institute, Tampa, FL 33612, USA; bryce.ordway@moffitt.org (B.O.); michal.tomaszewski@moffitt.org (M.T.); samantha.byrne@moffitt.org (S.B.); dominique.abrahams@moffitt.org (D.A.); robert.gillies@moffitt.org (R.J.G.)

² Department of Physiology, Anatomy & Genetics, University of Oxford, Oxford OX1 3PT, UK; pawel.swietach@dpag.ox.ac.uk

³ Department of Oncologic Sciences, Morsani College of Medicine, University of South Florida, Tampa, FL 33612, USA

* Correspondence: Mehdi.damaghi@moffitt.org

Abstract: Evolutionary dynamics can be used to control cancers when a cure is not clinically considered to be achievable. Understanding Darwinian intratumoral interactions of microenvironmental selection forces can be used to steer tumor progression towards a less invasive trajectory. Here, we approach intratumoral heterogeneity and evolution as a dynamic interaction among subpopulations through the application of small, but selective biological forces such as intracellular pH (pHi) and/or extracellular pH (pHe) vulnerabilities. Increased glycolysis is a prominent phenotype of cancer cells under hypoxia or normoxia (Warburg effect). Glycolysis leads to an important aspect of cancer metabolism: reduced pHe and higher pHi. We recently showed that decreasing pHi and targeting pHi sensitive enzymes can reverse the Warburg effect (WE) phenotype and inhibit tumor progression. Herein, we used diclofenac (DIC) repurposed to control MCT activity, and Koningic acid (KA) that is a GAPDH partial inhibitor, and observed that we can control the subpopulation of cancer cells with WE phenotype within a tumor in favor of a less aggressive phenotype without a WE to control progression and metastasis. In a 3D spheroid co-cultures, we showed that our strategy can control the growth of more aggressive MDA-MB-231 cells, while sparing the less aggressive MCF7 cells. In an animal model, we show that our approach can reduce tumor growth and metastasis. We thus propose that evolutionary dynamics can be used to control tumor cells' clonal or sub-clonal populations in favor of slower growth and less damage to patients. We propose that this can result in cancer control for tumors where cure is not an option.

Keywords: evolutionary therapy; darwinian evolution; tumor microenvironment; cancer cells subpopulations; diclofenac; koningic acid; spheroid; 3D co-culture



Citation: Ordway, B.; Tomaszewski, M.; Byrne, S.; Abrahams, D.; Swietach, P.; Gillies, R.J.; Damaghi, M. Targeting of Evolutionarily Acquired Cancer Cell Phenotype by Exploiting pHi-Metabolic Vulnerabilities. *Cancers* **2021**, *13*, 64. <https://doi.org/10.3390/cancers13010064>

Received: 14 November 2020

Accepted: 23 December 2020

Published: 28 December 2020

Publisher's Note: MDPI stays neutral with regard to jurisdictional claims in published maps and institutional affiliations.



Copyright: © 2020 by the authors. Licensee MDPI, Basel, Switzerland. This article is an open access article distributed under the terms and conditions of the Creative Commons Attribution (CC BY) license (<https://creativecommons.org/licenses/by/4.0/>).

1. Introduction

The initiation and development of cancers is associated with major metabolic alterations in response to dynamically changing microenvironmental conditions such as hypoxia and acidosis [1]. These forces will select for the fittest phenotype in the context of the current microenvironment. Cancer cells that are more plastic and adaptable can acclimate to an increasing array of emergent microenvironmental selective forces. Combined, these factors define tumors as highly dynamic ecosystems in which many different cancer cell subpopulations compete for space and resources [2]. The microenvironment around the cells can alter the local fitness of cancer cell subpopulations in a tumor; leading to possible dramatically different evolutionary trajectories selecting for cells with different phenotypic and genotypic properties [3]. We have previously reported how acid-producing and acid-resistant phenotypes can engineer the tumor ecosystem in order to increase

their own fitness, allowing them to take over the population [3,4]. We have also showed the different strategies that cancer cells acquire to adapt to their microenvironment [3]. Here, we investigate the impact of switching off certain phenotypes that give cancer cells a competitive advantage. By switching these off, we can influence the distribution of sub-populations with the end game of turning the majority of the population into a less aggressive phenotype with decreased invasion and metastasis. The idea is to take away any evolutionarily acquired or selection driven advantages of the more aggressive clones in population to allow for non-aggressive cells to be able to compete [5].

Glycolysis is the prominent phenotype of cancer cells under hypoxia or normoxia (Warburg effect). Glycolysis produces acid, which must be removed from cells, resulting in an important aspect of cancer metabolism: i.e., reduced extracellular pH ($pH_e \sim 6.5\text{--}6.7$) and increased intracellular pH ($pH_i \geq 7.2$). For cells to compete they must adapt to these conditions and thus these adaptations can be used against them as a vulnerability [6]. Adaptive mechanisms include: increased expression and activity of acid extruders, such as monocarboxylate transporters (MCT) including: MCT1 and MCT4, $Na^+ - H^+$ exchanger 1 (NHE1) and V-ATPases, as well as membrane bound exofacial carbonic anhydrases such as CA9 or CA12 to maintain an optimal pH_i [6]. An optimal pH_i gives cancer cells some proliferative advantages [6]. Herewith, we use two drugs that we are repurposing to target pH_e and pH_i metabolic adaptations so that the more aggressive cancer cell sub-populations lose their selective advantage over the less aggressive phenotypes. The first drug is diclofenac, a clinically used non-steroidal anti-inflammatory drug (NSAID), that has been shown to have an inhibitory effect on MCTs [7,8]. Targeting MCTs is a promising approach that many groups are following to find treatment against the glycolytic phenotype of cancer cells such as MCT1/2 inhibitors [9]. However, these drugs have not yet been successful in treating cancer, as cells have shown the ability to switch isoforms from e.g., MCT1 to MCT4 [6,9]. Diclofenac is putatively a pan-MCT inhibitor [7].

The second drug is koningic acid (KA), a natural product produced by fungi, which inhibits the function of GAPDH [10,11].

In our previous work of systems analysis of cancer cells' metabolic vulnerabilities [6], we observed that GAPDH is highly pH_i sensitive and has a key role in promoting a WE phenotype. This pH sensitivity of GAPDH means that the effects of its inhibition on cell proliferation are enhanced at an acidic intracellular pH . This acidic pH_i vulnerability is the reasoning for coupling with diclofenac, which we demonstrated to be a potent inhibitor of MCT activity, causing decreased intracellular pH . Other groups also reported GAPDH as a selective WE phenotype target [10] that can be partially and irreversibly inhibited by KA.

Evolutionary-based therapies use Darwinian principles to delay the proliferation of aggressive populations regardless of their genotype states [3,5,12]. These therapies can be guided by the use of mathematical models of cell population dynamics based on competing mechanisms of cancer cell sub-population within the tumor [13,14]. Conventional maximum dose therapy (MDT) permits an unopposed proliferation of resistant and/or more plastic cells by removing sensitive and/or less plastic cancer cell populations, a phenomenon known as "competitive release" in ecology [5]. With "competitive release", clonal and sub-clonal population balance is not maintained amongst all different clones. Alternatively, evolution-based therapies use Darwinian principles to delay the proliferation of resistant populations [3,5], maintaining clonal and sub-clonal population balance. A form of evolutionary therapy is adaptive therapy (AT), where the competitive release of resistant clones is delayed by the application of intermittent or dose-varying therapeutic regimens, to maintain a balance between sensitive and resistant clones to successfully control tumor growth [5,15,16]. In our approach, we exploit metabolic adaptations to acidosis as a vulnerability for the more aggressive tumor cells in order to cancer growth. We selected our representative cell lines, less aggressive (MCF7) and more aggressive (MDA-MB-231), based on the previously described phenotypes [17–21].

2. Results

2.1. Diclofenac and Koningic Acid Reduce the Glycolytic Activity of Cancer Cells

H⁺-monocarboxylate transporters (MCTs) play a major role in transporting organic anions such as lactate across cell membranes. Since the transport cycle is coupled to H⁺ ions, the activity of MCTs also affects intracellular pH (pHi) within cells [22]. It has been shown that MCT inhibition decreases cancer cells' aggressive phenotypes [9,23,24] by reducing the lactate efflux, leading to acidification of pHi and buildup of intracellular [lactate] [6]. It has been shown that diclofenac can inhibit MCTs [7] and that koningic acid (KA) can inhibit GAPDH [10,25,26], which is very sensitive to pHi [6] (Figure 1A). As proof of principle, we measured the effect of diclofenac and KA on glucose consumption and lactate production of MCF7 and MDA-MB-231 breast cancer cell lines. In both cell lines, diclofenac and KA reduced the lactate production (Figure 1B) and glucose consumption (Figure 1C) significantly within 72 h of treatment. Notably the effect was larger in the more highly glycolytic MDA-mb-231 cells. We then measured the activity of both drugs in the 3D culture of MCF7 and MDA-MB-231 spheroids over time. We observed that both drugs showed effects as early as 24 h (Figure S1A,B). These results indicated that both drugs are effective in inhibiting glycolysis as proposed and can work both in 2D and 3D experiments. We also measured the glutamine and glutamate concentration in the media following treatments of both cell lines with both drugs under normoxia and hypoxia and found no differences among the groups (Figure S1C).

2.2. Diclofenac Inhibits MCT Activity

To test whether the effect of diclofenac treatment on glycolysis was due to inhibition of lactate export, we measured MCT activity before and after treatment with diclofenac using pHi as a reporter of transmembrane flux. To rule out if the effect on pHi change is because of NSAID activity of diclofenac, we also measured the MCT activity on the same cells treated with aspirin. Using a superfusion microscopy system and cells loaded with the pH reporter dye SNARF-1, we measured the time course of pHi during superfusate maneuvers that trigger net transmembrane flux of lactate (Figure 1D). When presented with extracellular lactate, cells acidified, and when extracellular lactate was withdrawn, cells alkalinized. The rate of these pHi changes are measures of MCT activity. In the presence of diclofenac, however, efflux of lactate was completely inhibited in both cell lines. Controls included another NSAID, aspirin, which was without effect. As these are acute effects, cell death was not expected to play a role (*vide infra*), and we further ruled it out, due to the inability of dead cells to retain the SNARF-1 dye. To confirm that diclofenac was acting on a specific transport process, *i.e.*, MCT, rather than causing a generalized tightening of membrane permeability, experiments were repeated with acetate in place of lactate. Compared to lactate, acetate can permeate the cell membrane in an MCT-independent manner by partitioning across the lipid matrix as acetic acid, and its efflux was unaffected by diclofenac (Figure 1E). This suggests that the action of diclofenac is targeted to MCT, the main route for lactate traffic in and out of cells. The results of this assay are not indicative of what is expected to be seen under physiological conditions. The large changes in pH observed in these experiments are not sustained for long periods of time, and are induced by superphysiological lactate levels. The purpose of these experiments was solely to determine the effects of Diclofenac on a cells ability to export lactate; not to demonstrate specific pHi values under drug treatment.

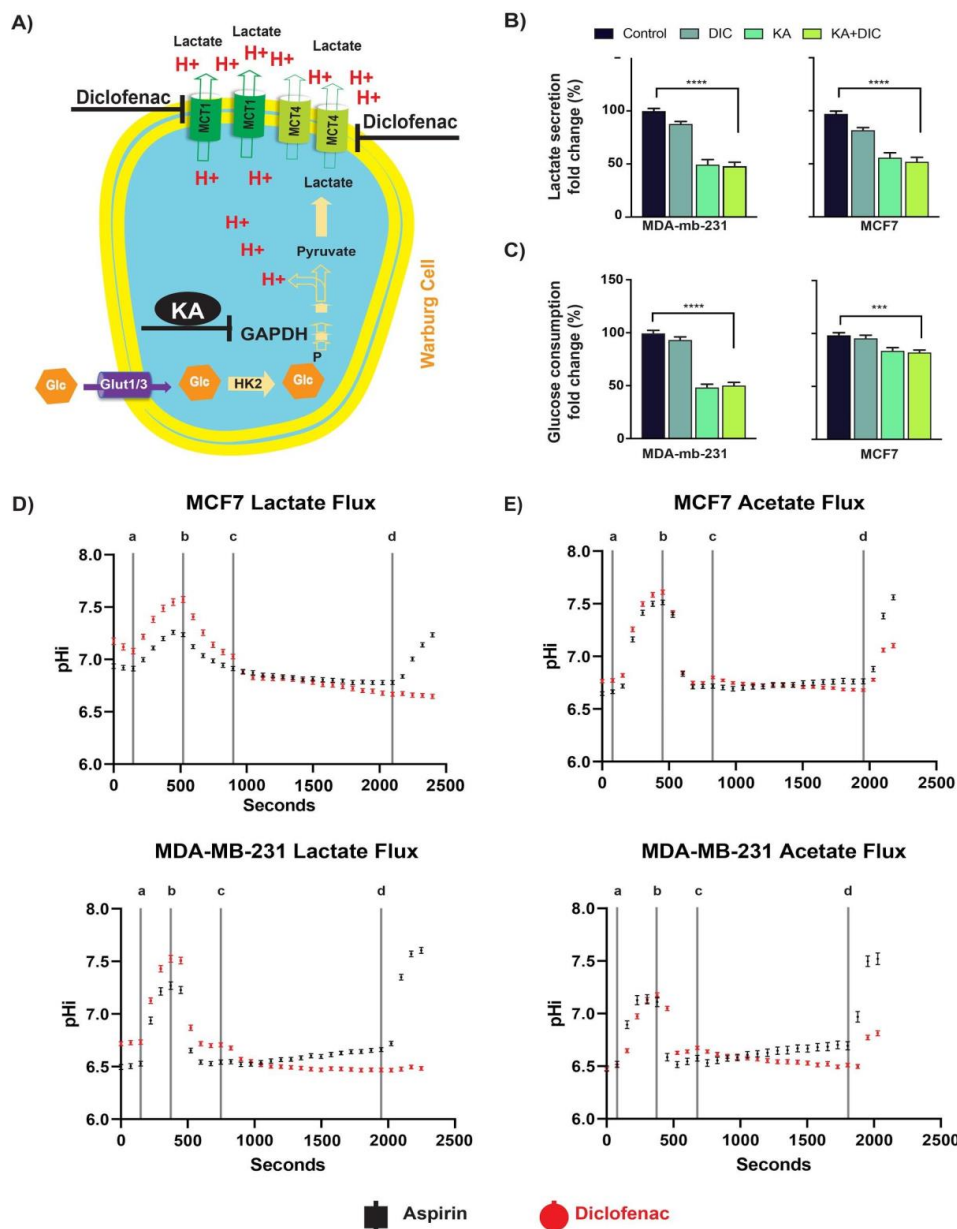


Figure 1. Diclofenac and koningic acid reduce the glycolytic activity of cancer cells. (A) Schematic showing effect of Diclofenac (1 μ M) to reduces the activity of MCT transporters leading to acidification of the intracellular pHi. Koningic acid (KA) reduces glycolytic activity by inhibiting GAPDH that has an alkaline pH optimum. (B) Lactate production was reduced in both MCF7 and MDA-MB-231 cells after treatment with diclofenac, KA, or both. (C) Glucose consumption was reduced in both MCF7 and MDA-MB-231 cells after treatment with diclofenac, KA, or both. (D) MCF7 and MDA-MB-231 cells were treated with diclofenac or Aspirin to measure the effect of drug on their lactate transport abilities. Line (a) represents the switch from a 30 mM lactate environment to a 0 mM Lactate environment. Line (b) represents the switch from a 0 mM lactate environment to a 30 mM lactate environment. Line (c) represents the switch from a 30 mM lactate environment – drug treatment to a 30 mM lactate environment + drug treatment. Line (d) represents the switch from a 30 mM lactate environment + drug treatment to a 0 mM lactate environment + drug treatment. (E) MCF7 and MDA-MB-231 cells were treated with diclofenac or Aspirin to measure the effect of drug on their pHi altering effects. Line (a) represents the switch from a 30 mM acetate environment to a 0 mM acetate environment. Line (b) represents the switch from a 0 mM acetate environment to a 30 mM acetate environment. Line (c) represents the switch from a 30 mM acetate environment – drug treatment to a 30 mM acetate environment + drug treatment. Line (d) represents the switch from a 30 mM acetate environment + drug treatment to a 0 mM acetate environment + drug treatment. *p*-values are represented as follows: *** *p* < 0.001, **** *p* < 0.0001.

2.3. Diclofenac and Koningic Acid Decrease the Viability of Cancer Cells

To test if the effects on glycolysis translate into the effective killing of cancer cells, we assessed the survival of cells using CCK8 viability assays and CelltiterGlo (see Methods) in both hypoxia and normoxia. We experimented with both normoxic and hypoxic conditions as they both commonly occur in the microenvironment of solid tumors such as breast cancer, and cell viability will be expected to be much more sensitivity to glycolysis inhibition under hypoxic conditions. In solid tumors, cells that are further than 160 micrometers from the vasculature they experience a hypoxic condition that makes the cells glycolysis dependent [27,28]. Many cancer cells overexpress or over-activate MCTs to deplete the lactate produced under the hypoxic conditions, although this response is not universal as shown in supplemental Figure S2. Under normoxia (Figure 2A) and hypoxia (Figure 2B) cell survival was measured after treatment with diclofenac, KA, or both in MCF7 and MDA-MB-231 cells. As shown in Figure 2A, diclofenac alone reduced the viability of MDA-mb-231, and MCF10/DCIS cells, which are highly glycolytic and tumorigenic, as well as MCF-7 cells which are tumorigenic and only moderately glycolytic. Notably there was no effect on viability of MCF10AT cells, which are neither tumorigenic nor glycolytic. More pronounced effects with a similar distribution were observed with KA and the combination of DIC + KA. Surprisingly, the effect of DIC on viability under hypoxia (Figure 2B) was less significant cf. normoxia (Figure 2A), whereas the effects of KA and the DIC + KA combination were no different. To test the activity of the drug on viability and H^+ export flux in the same experiment we performed a viability assay while monitoring the acidification of conditioned media. Inhibition of MCTs or GAPDH should reduce rate of media acidification. After treatment and before viability assays we measured the pHe of the media using the Five EasyTM/FiveGoTM pH meter (Mettler Toledo, Columbus, OH, USA see Methods). The acidification was reduced by both drugs and the pH of media was neutral, validating the effect of both diclofenac and KA on lowering glycolytic activity of cells (Figure S3).

To determine the effect of diclofenac and KA on the pHi of cancer cells, we measured the pHi of a panel of breast cancer cell lines (MDA-MB-231, MCF-DCIS, MCF7, 4T1, H605, and T47D), loaded with SNARF-1-AME (Figure 2C). For 16 h, cells were treated with diclofenac (100 μ M), KA (1 μ M), or aspirin (300 μ M), and then imaged in buffered RPMI media. All cell lines exhibited a significantly lower pHi with the treatment of diclofenac, and 4 of the 6 diclofenac treated cell lines had significantly lower pH than the aspirin group.

Considering the different microenvironment in solid tumors such as hypoxia and acidosis and their combination we wanted to test if inhibiting MCTs and GAPDH have an effect on the viability of cancer cells. These conditions are also very important to be targeted because they are specific for tumors and not experienced by normal cells. Therefore, we performed the survival assays on both MCF7 and MDA-MB-231 cells under four possible combinations of change in oxygen level and pH as following: (i) Normal pH-Normoxia, (ii) Low pH-Normoxia, (iii) Normal pH-Hypoxia, and (iv) Low pH-Hypoxia. Targeting MCTs and GAPDH under different microenvironments reduces the cancer cell's viability (Figure S4). The effect was greatest with the combination of both drugs and under the most unique condition of solid tumors -hypoxia, and acidic pH (Figure S4).

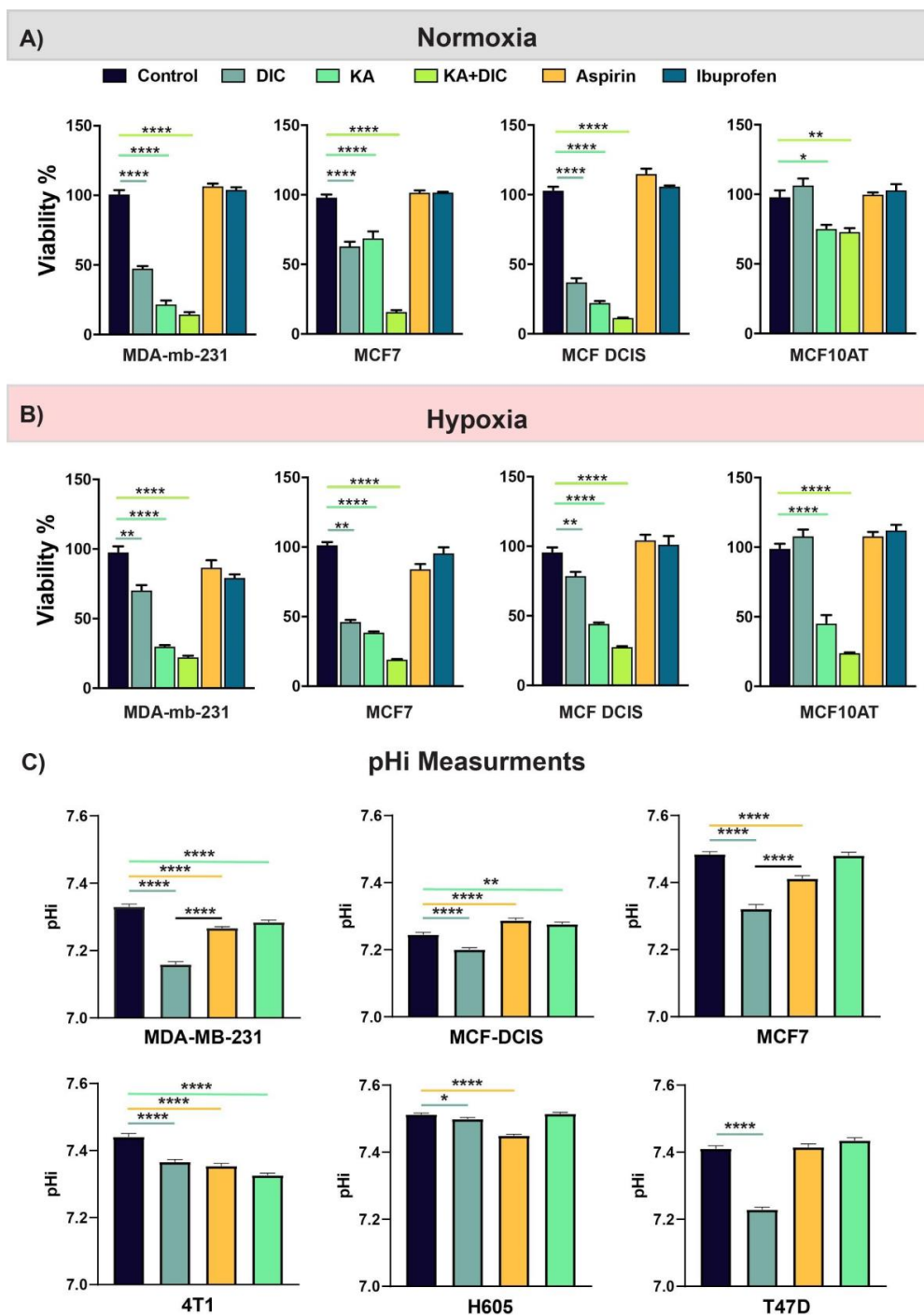


Figure 2. Diclofenac and koningic acid decrease the viability of cancer cells. (A,B) Viability of different breast cancer cell lines (MDA-MB-231, MCF7, MCF DCIS, MCF10AT) were measured in 2D using CCK8 kit under normoxia (A) and hypoxia (B) and different treatments. Diclofenac combination with GAPDH inhibition had the highest effect on cell viability. Interestingly other NSAID drugs such Aspirin or Ibuprofen didn't have any effect on cell viabilities. Error bars plotted as SD. (C) Intracellular pH measurement of MDA-MB-231, MCF-DCIS, MCF7, 4T1, H605, and T47D cancer cells using SNARF1, after 16 h treatment. Diclofenac decreased the pHi significantly in all cell lines. Error bars plotted as SEM. *p*-values are represented as follows: * *p* < 0.05, ** *p* < 0.01, *** *p* < 0.0001.

2.4. Diclofenac and Koningic Acid Reduce the Warburg Phenotype of Cancer Cells

The Warburg effect (WE) phenotype is defined by a high glycolytic rate even in the presence of oxygen (aerobic glycolysis) and is associated with the progression and

aggressiveness of cancers [29–32]. We recently showed that inhibiting proton pumps such as MCTs and pH-sensitive glycolytic enzymes such as GAPDH or GPI, reduces the WE phenotype of cancer cells [6]. Here we used the same strategy to reduce the WE phenotype by repurposing diclofenac from a NSAID to an MCT inhibitor and a natural product produced by fungi, koningic acid to target GAPDH. Above, we already showed that these compounds can reduce the glycolytic phenotype of cancer cells, and here we are using Seahorse measurements to confirm the inhibitor effect of these products on aerobic glycolysis. Seahorse can measure the glycolytic condition through simultaneous of proton efflux (ECAR) and mitochondrial respiration (OCR), which can be used to assess WE phenotype [6,33]. In the first experiment we interrogated at the real-time effect of diclofenac of KA on ECAR and OCR of MCF7 cancer cells (Figure 3A,B). KA and diclofenac monotonically increased the OCR compared to control and the combination of the two had the greatest effect (Figure 3A). KA and diclofenac both caused an initial drop of ECAR that lasted for 150 min that slowly returned to control levels. The recovery of ECAR to KA was more rapid compared to either conditions that contained diclofenac, which may be due to differences between GAPDH and MCT regulation (Figure 3B). This could imply that even if the cells over-activate or overexpress the GAPDH, because the pH_i is too low the phenotype can't be survived. We also measured the WE phenotype (ECAR/OCR) of these cells in three different time points: (i) right before drug injection, (ii) 5 h after injections, and (iii) 12 h after injections (black arrows in Figure 3A). These results showed that a combination of KA and diclofenac has the highest effect on decreasing the Warburg phenotype of cancer cells in mentioned time points (Figure 3C). To confirm this finding, we also performed a Seahorse experiment based on glycolytic rate assay that measured the maximum glycolytic capacity of cells by, first, shutting down mitochondrial respiration and then glycolysis (Methods). This assay also showed the highest inhibition of WE phenotype by the combination of KA and diclofenac in both MCF7 and MDA-MB-231 breast cancer cells (Figure 3D).

2.5. Reducing Warburg Phenotype Can Change Population Dynamics

Cancer evolution is a result of genetic diversification and clonal selection within the adaptive landscapes of tissue ecosystems. Therapeutic approaches can destroy some cancer clones, but it may also create a new space and different selective pressure resulting in expansion of resistant and most probably more aggressive clones aka “competitive release” in ecology and evolution. Evolutionary based therapeutic design can be used to control cancers when a cure is not possible. For that reason, understanding Darwinian intratumoral dynamics and their interactions with microenvironmental selection forces is critical to steer a tumor into a less invasive phenotype.

In 3D spheroid experiments we investigated the competitive release strategy to develop a new treatment design. Two distinct cell types were used to provide insight into the dynamic interactions among tumor cell subpopulations, a crucial element of intratumor heterogeneity. Mixed-culture competition experiments in spheroids can successfully track competitive outcomes amongst different cell types [34]. In 3D spheroid experiments differences in growth rates, carrying capacities and competition coefficients can be determined accurately [34]. For this experiment, we mono- and co-cultured MCF7-GFP and MDA-MB-231-RFP cells (1:1 ratio) and treated them with DMSO (control), diclofenac, KA, or combination of KA and diclofenac (Figure 4A–C). As a control experiment we grew spheroids in different microenvironmental conditions and with different ratios of MCF7 to MDA-MB-231 cells. In any microenvironmental condition and with any ratio of the two cancer cells, MDA-MB-231 cells always eventually dominated the MCF7 cells and took over the whole population (Figure S5). After treating the spheroids with diclofenac, KA, or the combination, we showed that these metabolically designed drugs can steer the population dynamics towards the less aggressive phenotype cells (MCF7-GFP) Figure 4A,B are controls showing effect of the agents on monocultures. Figure 4C shows that, in co-culture conditions, the green signal that belongs to MCF7-GFP was increased in

response to both drug and the combination, compared to the control group. These results show that it may be possible to control population dynamics in tumors based on their metabolic vulnerability.

2.6. Evolutionary Designed Therapy Controls Tumor Growth and Metastasis In Vivo

To translate our in vitro 2D and 3D results to in vivo we then performed animal experiments in female NSG mice. The experimental design was similar to the 3D spheroid experiment co-culture -MCF7 and MDA-MB-231 cells were mixed in 1:1 ratio and inoculated into the mice mammary fat pad. Mice were randomized into four groups of six mice per group and treated with diclofenac, KA, both, or none (DMSO). Primary tumor growth was unaffected by either monotherapy cf. controls, but there was a significant decrease caused by the combination of diclofenac and KA (Figure 5A).

At the end of the experiment we extracted the tumors and all the vital organs from each mouse and scored for metastasis. Notably, the diclofenac + KA combination group was metastasis-free, while all other groups had measurable metastases across multiple sites (Figure 5B). These results indicate that evolutionary therapeutic approaches based on metabolic targeting can be used to control tumor growth and even change aggressive phenotypes such as metastasis.

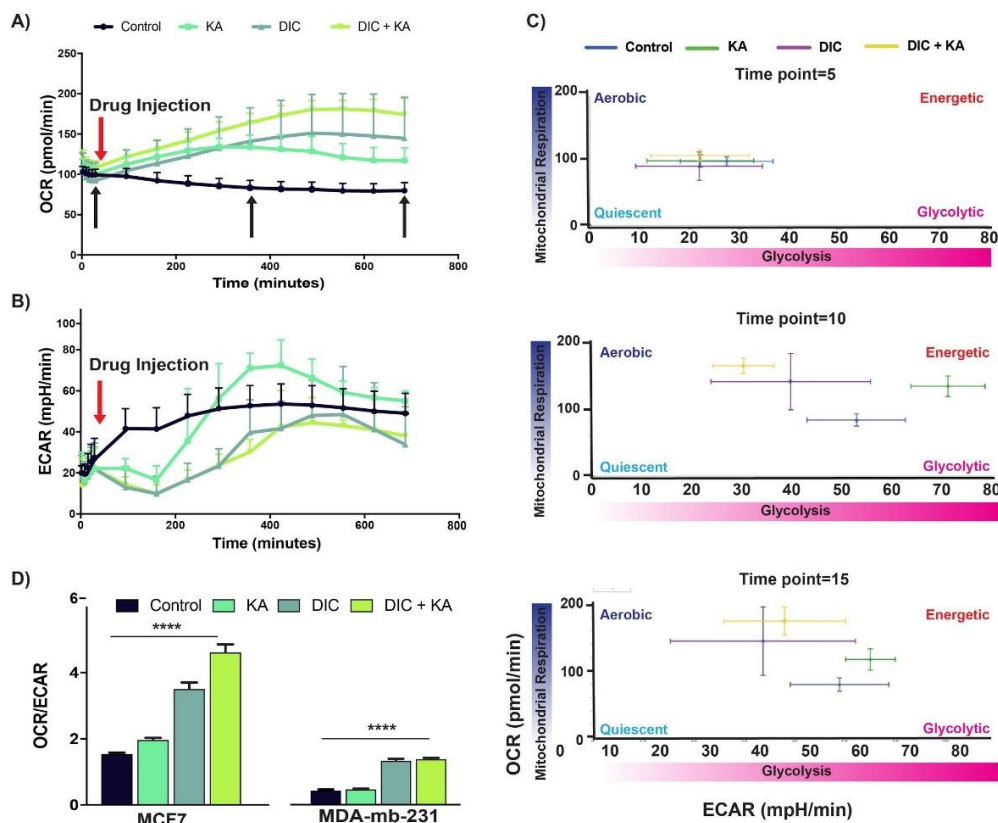


Figure 3. Diclofenac and koningic acid reduce the Warburg phenotype of cancer cells. (A) Oxygen Consumption Rate (OCR) and (B) Extracellular acidification rate (ECAR) of MCF7 cancer cells treated with, KA, diclofenac, and combination of both in real-time. (C) Energy map extracted from A and B under different treatments. A combination of KA and diclofenac had the highest effect on the reduction of WE phenotype in MCF7 breast cancer cells. (D) Glycolytic rate assay of both MCF7 and MDA-MB-231 cells confirmed the maximum reduction of WE phenotype with the combination of KA and diclofenac for 72 h. All the seahorse experiments were done in 6 replicates per condition and the data is normalized to the protein concentration of the cells per each well. The data is represented as the mean with the error bars as SD. p -values are represented as follows: **** $p < 0.0001$.

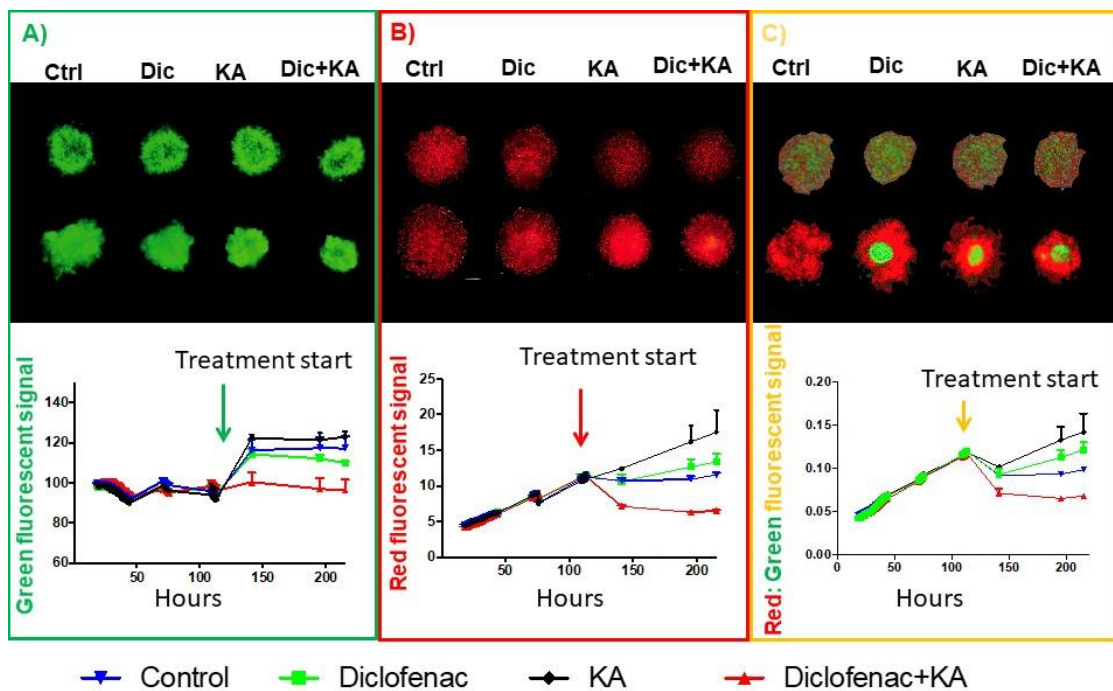


Figure 4. Spheroid 3D co-culture shows the role of evolutionary designed treatment in tumor cells population dynamics. (A) Images of the spheroids of MCF7 cells that were fluorescently tagged with GFP in monoculture. (B) Images of spheroids of MDA-MB-231 cells fluorescently tagged with RFP in monoculture. (C) Co-culture of MCF7-GFP and MDA-MB-231-RFP. The ratio in co-culture is 1:1 for experiment initiation. The top row are the pretreatment images and the bottom row for each condition is the last time point images. Underneath the images is a fluorescent signal analysis of the spheroid experiment under all four treatment conditions. Each experiment has 8 replicates. The data are represented as mean with the error bars as SD.

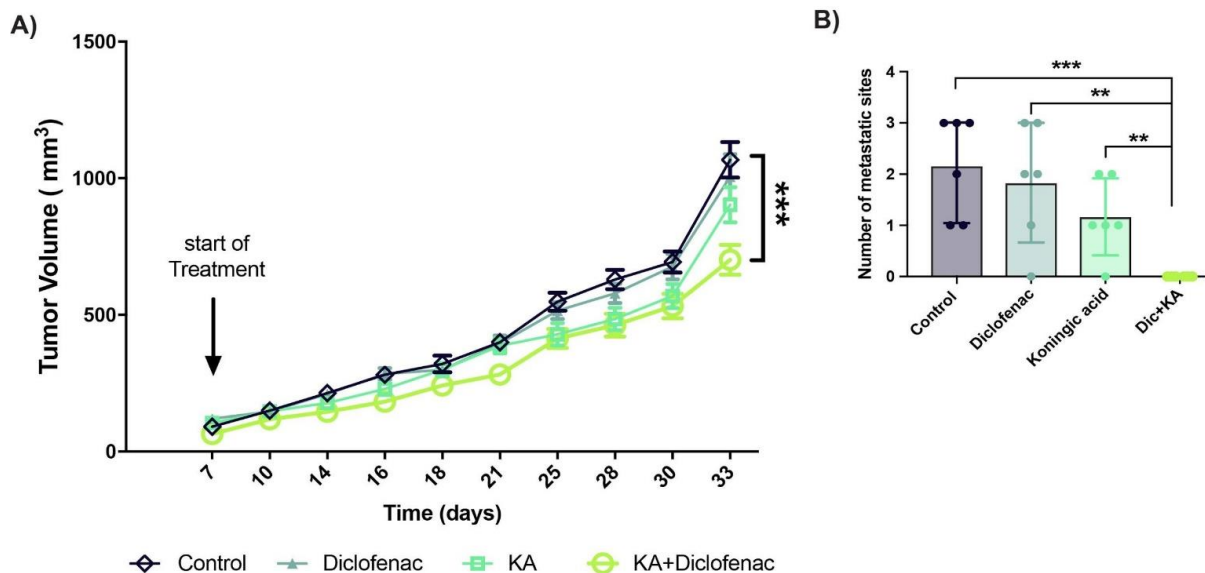


Figure 5. Animal experiments confirm the efficiency of evolutionary designed therapy. (A) Female NSG mice injected with a mixture of 5 million MCF7 and 5 million MDA-MB-231 breast cancer cells and randomized into four groups of 6 and treated with, DMSO, diclofenac, KA, and combination. Tumor size is measured every two or three days by calipers and also once a week with ultrasound. Data is presented as measurements by calipers and are mean with SD as their error bars. (B) The number of metastasis sites in vital organs such as liver, lungs, kidney, and spleen at the endpoint. The data is represented as mean with the error bars as the SD. *p*-values are represented as follows: ** *p* < 0.01, *** *p* < 0.001.

3. Discussion

Tumor evolution follows the Darwinian principles; meaning nature selects for phenotype not genotype [5]. When cancer initiates and develops, many clones and sub-clones emerge that are genetically heterogeneous with many of them presenting the same phenotype such as the Warburg effect (WE) phenotype [35]. The emergence of one phenotype from many clones with different genetic backgrounds implies the fitness of the selected phenotype to the selection forces. The WE phenotype is associated with progression and invasion of many cancers and is defined by a high glycolytic rate in the absence or presence of oxygen (aerobic glycolysis). Most cancer cells reprogram their metabolism in favor of aerobic glycolysis despite the presence of plentiful oxygen in their microenvironment, implying higher fitness of WE phenotype.

During the evolution of tumor cells and through adaptation to constantly variable microenvironment tumor cells adapt and acquire phenotypes helping them survive and grow. These acquired characteristics can be used as a new vulnerability against them. As mentioned previously, we recently showed that certain targets for inhibition of glycolysis have increased effects of inhibition at a lower intracellular pH [6]. To test this principle, we coupled Diclofenac, a compound we demonstrated to be a potent inhibitor of MCT's, with Koningic Acid, a known inhibitor of GAPDH. The MCT inhibition by Diclofenac provided the decrease in phi needed to enhance the effectiveness of KA. In this paper we showed that targeting the WE phenotype in more aggressive cancer cells can take their competitiveness from them so the less malignant cells can compete with them in a tumor niche. We used a simple model of co-culture of two cell lines with extremely opposing characteristics: MDA-MB-231 cells that are triple-negative fast proliferating, tumorigenic and metastatic in mouse xenograft models that are also highly glycolytic with WE phenotype and MCF7 cells that are ER/PR positive, slow-growing and tumorigenic in mouse xenografts with the help of estrogen pellets but not metastatic and very low glycolytic and not WE phenotype. The co-culture of these two cell lines was used as a simple population model of tumor heterogeneity to monitor the population dynamics of the tumor. In the future, these findings will be confirmed and expanded in a more complex, transgenic tumor model, to observe the effect of real intratumor heterogeneity in cell subpopulation. Using our metabolic targeted strategy, we showed that it is possible to control the population dynamic and heterogeneity. This population dynamic adjustment was able to successfully control tumor growth and metastasis in the mouse xenograft model. Therefore, we propose a novel strategy of cancer control for the tumor where a cure is not an option. We propose evolutionary principles of tumor growth that can be used to control tumor cells' clonal or sub-clonal population in favor of slower growth and less damage to patients.

4. Methods

4.1. Cell Culture

MCF-7 and MDA-MB-231 cells were acquired from American Type Culture Collection (ATCC, Manassas, VA, USA, 2007–2010) and were maintained in DMEM-F12 (Life Technologies, Carlsbad, CA, USA) supplemented with 10% fetal bovine serum (HyClone Laboratories, Logan, UT, USA). Cells were tested for mycoplasma contamination and authenticated using short tandem repeat DNA typing according to ATCC's guidelines. Cells were treated with diclofenac (1 μ M) and/or koningic acid (1 μ M) dissolved in the media of the cells.

4.2. Hypoxia Cell Culture

For hypoxia conditions we used a Biospherix X-Vivo Hypoxia Chamber. The conditions in each hypoxia chamber kept at 37 °C, 5% CO₂, with 0.1% O₂ and 94.9% N₂ or 1.0% O₂ and 95% N₂. The chamber was quality controlled and calibrated according to the manufacturer's specifications (Biospherix, Parish, NY, USA).

4.3. Transfection (GFP/RFP Plasmids)

To establish stable cell lines, the MCF-7 and MDA-MB-231 cells were infected with Plasmids expressing RFP or GFP using Fugene 6 (Promega, Madison, WI, USA) at early passage and were selected using 2 µg/mL puromycin (Sigma, St. Louis, MO, USA).

4.4. Mettler Toledo Five EasyTM/FiveGoTM pH Meter

The pH meter was first calibrated by using standard pre-made calibration buffer solutions for pH 4, 7, and 10. Then using the pH probe the pH of the control media used to grow the spheroids was measured. This pH was used as a baseline to compare the pH of the pHe media of the spheroids.

4.5. Viability Assays

4.5.1. CCK8

Cell viability was measured after treatment with drugs (diclofenac and koniginic acid or both) and DMSO as control using Cell Counting Kit-8 (CCK-8) under different microenvironmental conditions such as normoxia, hypoxia, normal pH, or low pH. CCK8 is a sensitive colorimetric-based viability assay based on Dojindo's highly water-soluble tetrazolium salt, with WST-8 as its active agent. CCK8 was used to measure viability as it is not pH sensitive and can be added to the cells directly in their niche, without fixation or change of media. For measuring viability, cells were seeded in a 96-well plate (with triplicate of the same samples), and viability was measured at the indicated intervals. The experiments were repeated at least two times.

4.5.2. CellTiter-Glo[®]

This 3D Cell Viability Assay is designed to determine the number of viable cells in 3D cell culture based on quantitation of the ATP through based on Luminescent Cell Viability Assay chemistry. The lytic capability of the reagents is much higher than the 2D assay and the assay is compatible with 96 well-plate formats of our spheroid experiments that make it ideal for high-throughput screening. In our assay 72 h after treatment of spheroid with inhibitors, the lysis buffer directly added to each well containing one sphere of MDA-MB-231 or MCF7 cells. The plates were incubated in RT for 10 min on a rocking shaker. Then the assay mixture containing luciferin and luciferase was added and the luminescent was measured after 5 min incubation in RT.

4.6. Glycolytic Rate Measurements (Seahorse)

Glycolytic rate of MCF7 and MDA-MB-231 cancer cells was measured using Seahorse XF96 extracellular flux analyzer and a glycolysis rate kit (Seahorse Biosciences, Billerica, MA, USA). All the seahorse experiment has been performed in the absence of CO₂/HCO₃³⁻. Oxygen consumption rate (OCR) and extracellular acidification rate (ECAR) of cancer cells were determined by seeding them on XF96 microplates in their growth medium until they reached over 90% confluence. In these studies, seeding started with 20,000 cells (80% of the well area). Measurements were determined 24 h later when the cells reached 90% confluence. One hour before the seahorse measurements culture media were removed and cells were washed 3 times with PBS followed by the addition of base medium (non-buffered DMEM supplemented with 25 mM glucose). Finally, data were normalized for total protein content of each well using the Bradford protein assay (ThermoFisher, Waltham, MA, USA). Seahorse measurements were performed with 4–6 technical replicates and these experiments were repeated at least 2 times. The WE phenotype ("Warburgness") can be expressed as the ratio of glycolysis (ECAR) to oxidative phosphorylation (expressed as the oxygen consumption rate, OCR) from the GST.

4.7. Metabolic Profiling

Cells were seeded in a regular 96-well plate for 2D culture and in U bottom 96 well plates for 3D spheroid culture in their growth medium containing 10% FBS under standard

culture condition. Once cells reach 90% confluence for 2D or carrying capacity for 3D (usually when the growth of spheres is steady and they don't get bigger), the growth media were removed and placed in a new 96 well plate with the same order as the original plate for metabolic profiling using YSI machine (YSI 2900 multi-analyte system (YSI, Yellow Springs, OH, USA)). We used at least 150 μ L of media in each well to make sure there was enough media for each assay in the machine. Sensors in YSI were changed weekly and calibrated before each experiment. Final data of the lactate, glucose, glutamine, and glutamate in conditioned media were normalized to the protein amount per well or the confluency of each well imaged right before metabolite measurements.

4.8. MCT Activity

Cells were plated on four chamber Lab-Tek chambered cover glass slides 1 day prior to experimenting, and cultured in RPMI media containing 10% FBS and 1% P/S. On day of experimentation, media was replaced with RPMI containing 10% FBS, 1% P/S, 25 mM HEPES, and 25 mM PIPES, to stabilize pH while outside of the 5% CO₂ incubator. Once the assay was ready to begin for a given group, 5-(and-6)-Carboxy SNARFTM-1, Acetoxymethyl Ester, Acetate was added 8 min prior to experimentation at a concentration of 10 μ g/mL. Prior to experimentation, the pH calibration curve of the 5-(and-6)-Carboxy SNARFTM-1, Acetoxymethyl Ester, Acetate dye was conducted using the nigericin method as described previously [36]. Once the 8 min incubation period was up, imaging began and superfusion with the 30 mM lactate solution (solutions listed in extended data file) and the SNARF-1 ratio was allowed to stabilize. The superfusion setup used in our experiments consists of a peristaltic to flow the media, a custom manufactured fluidic switch system which allows for the rapid changing of solutions, and a vacuum pump to aspirate media from the opposite side of the chamber. Once stabilized, cells were instantaneously switched to the 0 mM lactate solution and maintained in such until the velocity of the SNARF-1 ratio began to level off. Cells were then switched back to the 30 mM lactate condition and allowed to stabilize again. Once stabilized, the cells were switched to the same 30 mM lactate solution, this time either containing (X concentration of Diclofenac or Aspirin). Cells were maintained in the drug treatment solutions for 20 min in order for the drugs to take effect, and then switched to the 0 mM lactate solution containing the same concentration of drug they were treated with.

4.9. pHi Measurement

Cells were plated on four chamber Lab-Tek chambered cover glass slides 1 day prior to experimentation and cultured in RPMI media containing 10% FBS and 1% P/S. On day of experimentation, media was replaced with RPMI containing 10% FBS, 1% P/S, 25 mM HEPES, and 25 mM PIPES, to stabilize pH while outside of the 5% CO₂ incubator. Once the assay was ready to begin for a given group, 5-(and-6)-Carboxy SNARFTM-1, Acetoxymethyl Ester, Acetate was added 10 min prior to experimentation at a concentration of 10 μ g/mL. After the 10 min, cells were washed 2 times with drug containing media and fresh drug containing media was resupplied to the cells. Change in pHi caused by each drug was measured by converting the SNARF-1 ratio to pHi and comparing pre- and post- treatment pHi's.

4.10. Spheroid Mono- and Co-Culture

Perfecta3[®]96-Well Hanging Drop Plates or non-adhesive U shape bottom 96 well plates were used to grow the primary spheres containing 10,000 total cells. 10% Matrigel was used for the primary spheroid construction as follows. After cells were counted they were diluted as 200 cells per μ L of media. Then the cells mixture was cooled down in ice for 10 min and 10% Matrigel (melted in ice in the 4-degree Celsius walk-in fridge overnight) was added and directly seeded in the U plates. The plates were centrifuged for 1 min 500 RPM. For each experimental condition, the ratio between MCF-7-GFP and MDA-MB-231-RFP was 0, 50, or 100 percent as follows: 0/100, 50/50, 100/0. Each ratio

had 4–8 replicates for each experiment. An Incucyte microscope kept at 37 °C and 5% CO₂ was used to image the spheroid growth every 6 h over approximately 30 days. Images and fluorescent intensity were analyzed in Incucyte built-in software and image J. Relative fluorescent units (RFUs) were normalized by averaging red/green fluorescence when the corresponding cell type was absent then subtracting this value from other fluorescent values of that cell type. Drug treatments were directly added to the growth media of the spheroids and renewed every 3 days.

4.11. Animal Experiments

MCF7 and MDA-MB-231 breast cancer cell lines were grown in T-225 flask and harvested at 70–80% confluency. Both cells were authenticated by short tandem repeat analysis and tested for mycoplasma. 10 million cells in 200 µL cold PBS and 10% Matrigel was inoculated into cleared mammary fat pads of SCID mice (eight- to ten-week old females). Tumor measurements were done by calipers every other day and ultrasound once a week. Mice had free access to water and food for the whole duration of the experiment. For mixed cultures, a 1:1 mixture of 5 million MDA-MB-231 and 5 million MCF7 cells were injected. One week before cell injection, an estrogen pellet (0.72 mg slow-release, Innovative Research of America) was implanted to allow for the growth of ER-positive MCF7 tumors. The concentration of diclofenac given to each mouse was 40 mg/kg. As for the KA the concentration was 1 mg/kg. These concentrations remained the same when the mice were treated with both drugs. The control mice were injected with DMSO in PBS. The mice were treated by intraperitoneal injections once on Monday, Wednesday, and Friday weekly. At the end of the experiment tumors were extracted, then the size and weight of them were measured. Vital organs were also extracted and looked for metastasis.

Animal studies were performed by the guidelines of the IACUC of the H. Lee Moffitt Cancer Center (that was approved by the University of South Florida IACUC committee: IACUC 5331R).

5. Conclusions

We propose a novel strategy of cancer control for the tumor when a cure is not an option. We propose evolutionary principles of tumor growth can be used to control tumor cells' clonal or sub-clonal population in favor of slower growth and less damage to patients. We showed that slight metabolic adaptations acquired during the evolution of cancer cells such as increased pHi can be used as vulnerability against them.

Supplementary Materials: The following are available online at <https://www.mdpi.com/2072-6694/13/1/64/s1>, Figure S1: Glutamine and glutamate concentration in conditioned media of MCF7 and MDA-MB-231 cells treated with diclofenac, Koningic acid, and both compared to non-treated control in hypoxia (0.1% oxygen) and normoxia, Figure S2: ICC Analysis of MCT1 and MCT4 expression in breast cancer cell lines. Figure S3: Extracellular pH measurements of cells exposed to various treatment conditions. Treatment with KA, DIC, or combination of both results in an increase in extracellular pH. Figure S4: Survival assay of breast cancer cell lines in different microenvironmental conditions. Targeting MCTs and GAPDH under different microenvironments reduces the cancer cells' viability. The effect is the most with the combination of both drug and under the most unique condition of solid tumors, hypoxia, and acidic pH. Data is normalized to non-treated for each cell line in each condition and presented as mean with SD as error bars. Each experiment has 4 replicates, Figure S5: Mono- and co-culture of fluorescently tagged breast cancer cell line. In different microenvironmental conditions and with any initial ration of MCF7: MDA-MB-231, the more aggressive cells, MDA-MB-231 always win. The spheroids are grown in normoxia but considering the size of spheres that reaches to 1–2 mm we know that oxygen concentration can vary from normoxia at the surface of spheres to hypoxia in the center.

Author Contributions: B.O. and M.T. performed experiments. M.D. conceived the study, developed the methodology, and designed and performed experiments. M.D. and B.O. performed computational analysis. S.B. and D.A. performed animal work. M.D. wrote the paper with contributions from all

authors. P.S. supervised superfusion microscopy and its data analysis. M.D. and R.J.G. directed the study. All authors have read and agreed to the published version of the manuscript.

Funding: M.D. and R.J.G. were supported by grants from NCI (R01CA077571) and NIH/NCI PSOC (1U54CA193489).

Institutional Review Board Statement: N/A.

Informed Consent Statement: N/A.

Data Availability Statement: N/A.

Conflicts of Interest: The authors declare no competing interest.


References

- Gatenby, R.A.; Gillies, R.J. Why do cancers have high aerobic glycolysis? *Nat. Rev. Cancer* **2004**, *4*, 891–899. [[CrossRef](#)]
- Gatenby, R.A.; Brown, J. Mutations, evolution and the central role of a self-defined fitness function in the initiation and progression of cancer. *Biochim. Biophys. Acta (BBA) Rev. Cancer* **2017**, *1867*, 162–166. [[CrossRef](#)]
- Ibrahim-Hashim, A.; Robertson-Tessi, M.; Enriquez-Navas, P.M.; Damaghi, M.; Balagurunathan, Y.; Wojtkowiak, J.W.; Russell, S.; Yoonseok, K.; Lloyd, M.C.; Bui, M.M.; et al. Defining Cancer Subpopulations by Adaptive Strategies Rather Than Molecular Properties Provides Novel Insights into Intratumoral Evolution. *Cancer Res.* **2017**, *77*, 2242–2254. [[CrossRef](#)]
- Estrella, V.; Chen, T.; Lloyd, M.; Wojtkowiak, J.; Cornnell, H.H.; Ibrahim-Hashim, A.; Bailey, K.; Balagurunathan, Y.; Rothberg, J.M.; Sloane, B.F.; et al. Acidity Generated by the Tumor Microenvironment Drives Local Invasion. *Cancer Res.* **2013**, *73*, 1524–1535. [[CrossRef](#)]
- Enriquez-Navas, P.M.; Kam, Y.; Das, T.; Hassan, S.; Silva, A.; Foroutan, P.; Ruiz, E.; Martinez, G.; Minton, S.; Gillies, R.J.; et al. Exploiting evolutionary principles to prolong tumor control in preclinical models of breast cancer. *Sci. Transl. Med.* **2016**, *8*, 327ra24. [[CrossRef](#)]
- Persi, E.; Duran-Frigola, M.; Damaghi, M.; Roush, W.R.; Aloy, P.; Cleveland, J.L.; Gillies, R.J.; Ruppin, E. Systems analysis of intracellular pH vulnerabilities for cancer therapy. *Nat. Commun.* **2018**, *9*, 1–11. [[CrossRef](#)]
- Renner, K.; Bruss, C.; Schnell, A.; Koehl, G.; Becker, H.M.; Fante, M.; Menevse, A.-N.; Kauer, N.; Blazquez, R.; Hacker, L.; et al. Restricting Glycolysis Preserves T Cell Effector Functions and Augments Checkpoint Therapy. *Cell Rep.* **2019**, *29*, 135–150.e9. [[CrossRef](#)]
- Gan, T.J. Diclofenac: An update on its mechanism of action and safety profile. *Curr. Med. Res. Opin.* **2010**, *26*, 1715–1731. [[CrossRef](#)]
- Doherty, J.R.; Yang, C.; Scott, K.E.N.; Cameron, M.D.; Fallahi, M.; Li, W.; Hall, M.A.; Amelio, A.L.; Mishra, J.K.; Li, F.; et al. Blocking Lactate Export by Inhibiting the Myc Target MCT1 Disables Glycolysis and Glutathione Synthesis. *Cancer Res.* **2014**, *74*, 908–920. [[CrossRef](#)]
- Liberti, M.V.; Dai, Z.; Wardell, S.E.; Baccile, J.A.; Liu, X.; Gao, X.; Baldi, R.; Mehrmohamadi, M.; Johnson, M.O.; Madhukar, N.S.; et al. A Predictive Model for Selective Targeting of the Warburg Effect through GAPDH Inhibition with a Natural Product. *Cell Metab.* **2017**, *26*, 648–659.e8. [[CrossRef](#)]
- Liberti, M.V.; Allen, A.E.; Ramesh, V.; Dai, Z.; Singleton, K.R.; Guo, Z.; Liu, J.O.; Wood, K.C.; Locasale, J.W. Evolved resistance to partial GAPDH inhibition results in loss of the Warburg effect and in a different state of glycolysis. *J. Biol. Chem.* **2019**, *295*, 111–124. [[CrossRef](#)] [[PubMed](#)]
- Commander, R.; Wei, C.; Sharma, A.; Mouw, J.K.; Burton, L.J.; Summerbell, E.R.; Mahboubi, D.; Peterson, R.J.; Konen, J.; Zhou, W.; et al. Subpopulation targeting of pyruvate dehydrogenase and GLUT1 decouples metabolic heterogeneity during collective cancer cell invasion. *Nat. Commun.* **2020**, *11*, 1–17. [[CrossRef](#)] [[PubMed](#)]
- Picco, N.; Sahai, E.; Maini, P.K.; Anderson, A.R. Integrating Models to Quantify Environment-Mediated Drug Resistance. *Cancer Res.* **2017**, *77*, 5409–5418. [[CrossRef](#)] [[PubMed](#)]
- Nichol, D.; Jeavons, P.; Fletcher, A.G.; Bonomo, R.A.; Maini, P.K.; Paul, J.L.; Gatenby, R.A.; Anderson, A.R.; Scott, J.G. Steering Evolution with Sequential Therapy to Prevent the Emergence of Bacterial Antibiotic Resistance. *PLoS Comput. Biol.* **2015**, *11*, e1004493. [[CrossRef](#)] [[PubMed](#)]
- West, J.; You, L.; Zhang, J.; Gatenby, R.A.; Brown, J.S.; Newton, P.K.; Anderson, A.R.A. Towards Multidrug Adaptive Therapy. *Cancer Res.* **2020**, *80*, 1578–1589. [[CrossRef](#)]
- Zhang, J.; Cunningham, J.J.; Brown, J.S.; Gatenby, R.A. Integrating evolutionary dynamics into treatment of metastatic castrate-resistant prostate cancer. *Nat. Commun.* **2017**, *8*, 1–9. [[CrossRef](#)]
- Holliday, D.L.; Speirs, V. Choosing the right cell line for breast cancer research. *Breast Cancer Res.* **2011**, *13*, 1–7. [[CrossRef](#)]
- Neve, R.M.; Chin, K.; Fridlyand, J.; Yeh, J.; Baehner, F.L.; Fevr, T.; Clark, L.; Bayani, N.; Coppe, J.-P.; Tong, F.; et al. A collection of breast cancer cell lines for the study of functionally distinct cancer subtypes. *Cancer Cell* **2006**, *10*, 515–527. [[CrossRef](#)]
- Kao, J.; Salari, K.; Bocanegra, M.; Choi, Y.-L.; Girard, L.; Gandhi, J.; Kwei, K.A.; Hernandez-Boussard, T.; Wang, P.; Gazdar, A.F. Molecular profiling of breast cancer cell lines defines relevant tumor models and provides a resource for cancer gene discovery. *PLoS ONE* **2009**, *4*, e6146. [[CrossRef](#)]

20. Horwitz, K.B.; Costlow, M.; McGuire, W.L. MCF-7: A human breast cancer cell line with estrogen, androgen, progesterone, and glucocorticoid receptors. *Steroids* **1975**, *26*, 785–795. [[CrossRef](#)]
21. Levenson, A.S.; Jordan, V.C. MCF-7: The first hormone-responsive breast cancer cell line. *Cancer Res.* **1997**, *57*, 3071–3078. [[PubMed](#)]
22. Andersen, A.P.; Flinck, M.; Oernbo, E.K.; Pedersen, N.B.; Viuff, B.M.; Pedersen, S.F. Roles of acid-extruding ion transporters in regulation of breast cancer cell growth in a 3-dimensional microenvironment. *Mol. Cancer* **2016**, *15*, 45. [[CrossRef](#)] [[PubMed](#)]
23. Caruso, J.P.; Koch, B.J.; Benson, P.D.; Varughese, E.; Monterey, M.D.; Lee, A.E.; Dave, A.M.; Kioussis, S.; Sloan, A.E.; Mathupala, S.P. pH, Lactate, and Hypoxia: Reciprocity in Regulating High-Affinity Monocarboxylate Transporter Expression in Glioblastoma. *Neoplasia* **2017**, *19*, 121–134. [[CrossRef](#)]
24. Counillon, L.; Bouret, Y.; Marchiq, I.; Pouysségur, J. Na⁺/H⁺ antiporter (NHE1) and lactate/H⁺ symporters (MCTs) in pH homeostasis and cancer metabolism. *Biochim. Biophys. Acta (BBA) Mol. Cell Res.* **2016**, *1863*, 2465–2480. [[CrossRef](#)] [[PubMed](#)]
25. Liberti, M.V.; Locasale, J.W. The Warburg Effect: How Does it Benefit Cancer Cells? *Trends Biochem. Sci.* **2016**, *41*, 211–218. [[CrossRef](#)] [[PubMed](#)]
26. Endo, A.; Hasum, K.; Sakai, K.; Kanbe, T. Specific inhibition of glyceraldehyde-3-phosphate dehydrogenase by koniginic acid (Heptelidic acid). *J. Antibiot.* **1985**, *38*, 920–925. [[CrossRef](#)] [[PubMed](#)]
27. Damaghi, M.; Tafreshi, N.K.; Lloyd, M.C.; Sprung, R.; Estrella, V.; Wojtkowiak, J.W.; Morse, D.L.; Koomen, J.M.; Bui, M.M.; Gatenby, R.A.; et al. Chronic acidosis in the tumour microenvironment selects for overexpression of LAMP2 in the plasma membrane. *Nat. Commun.* **2015**, *6*, 8752. [[CrossRef](#)]
28. Damaghi, M.; Gillies, R. Phenotypic changes of acid-adapted cancer cells push them toward aggressiveness in their evolution in the tumor microenvironment. *Cell Cycle* **2017**, *16*, 1739–1743. [[CrossRef](#)]
29. Warburg, O. The chemical constitution of respiration ferment. *Science* **2006**, *68*, 437–443. [[CrossRef](#)]
30. Warburg, O. On respiratory impairment in cancer cells. *Science* **1956**, *124*, 269.
31. Warburg, O. On the Origin of Cancer Cells. *Science* **1956**, *123*, 309–314. [[CrossRef](#)] [[PubMed](#)]
32. Warburg, O.; Wind, F.; Negelein, E. The metabolism of tumors in the body. *J. Gen. Physiol.* **2004**, *8*, 519–530. [[CrossRef](#)] [[PubMed](#)]
33. De Luca, A.; Fiorillo, M.; Peiris-Pagès, M.; Ozsvari, B.; Smith, D.L.; Sanchez-Alvarez, R.; Martinez-Outschoorn, U.E.; Cappello, A.R.; Pezzi, V.; Lisanti, M.P.; et al. Mitochondrial biogenesis is required for the anchorage-independent survival and propagation of stem-like cancer cells. *Oncotarget* **2015**, *6*, 14777–14795. [[CrossRef](#)] [[PubMed](#)]
34. Freischel, A.R.; Damaghi, M.; Cunningham, J.J.; Ibrahim-Hashim, A.; Gillies, R.J.; Gatenby, R.A.; Brown, J.S. Frequency-dependent interactions determine outcome of competition between two breast cancer cell lines. *BioRxiv* **2020**. [[CrossRef](#)]
35. Gatenby, R.A.; Gillies, R.J. A microenvironmental model of carcinogenesis. *Nat. Rev. Cancer* **2008**, *8*, 56–61. [[CrossRef](#)]
36. Hulikova, A.; Aveyard, N.; Harris, A.L.; Vaughan-Jones, R.D.; Swietach, P. Intracellular Carbonic Anhydrase Activity Sensitizes Cancer Cell pH Signaling to Dynamic Changes in CO₂ Partial Pressure. *J. Biol. Chem.* **2014**, *289*, 25418–25430. [[CrossRef](#)]

Review

The Match between Molecular Subtypes, Histology and Microenvironment of Pancreatic Cancer and Its Relevance for Chemoresistance

Javier Martinez-Useros ^{*,†}, Mario Martin-Galan  and Jesus Garcia-Foncillas ^{*,†}

Translational Oncology Division, OncoHealth Institute, Health Research Institute-Fundacion Jimenez Diaz University Hospital, Av. Reyes Catolicos 2, 28040 Madrid, Spain; mariomgtics@gmail.com

* Correspondence: javier.museros@quironsalud.es (J.M.-U.); jesus.garciafoncillas@oncohealth.eu (J.G.-F.);

Tel.: +34-91-550-48-00 (J.M.-U. & J.G.-F.)

† These authors share equal senior authorship.

Simple Summary: Based on the four molecular subtypes of pancreatic cancer described by Bailey et al. 2016, in the present article we match the molecular, histology and microenvironment features of pancreatic cancer. This approach may help to understand the molecular basis of this kind of tumor, and how their microenvironment may affect treatment response. Moreover, we compile information about crucial factors that could serve as potential targets for drug design to achieve higher anti-tumor activity, and how histological evaluation of tumor microenvironment could provide first signs about treatment response.

Abstract: In the last decade, several studies based on whole transcriptomic and genomic analyses of pancreatic tumors and their stroma have come to light to supplement histopathological stratification of pancreatic cancers with a molecular point-of-view. Three main molecular studies: Collisson et al. 2011, Moffitt et al. 2015 and Bailey et al. 2016 have found specific gene signatures, which identify different molecular subtypes of pancreatic cancer and provide a comprehensive stratification for both a personalized treatment or to identify potential druggable targets. However, the routine clinical management of pancreatic cancer does not consider a broad molecular analysis of each patient, due probably to the lack of target therapies for this tumor. Therefore, the current treatment decision is taken based on patients' clinicopathological features and performance status. Histopathological evaluation of tumor samples could reveal many other attributes not only from tumor cells but also from their microenvironment specially about the presence of pancreatic stellate cells, regulatory T cells, tumor-associated macrophages, myeloid derived suppressor cells and extracellular matrix structure. In the present article, we revise the four molecular subtypes proposed by Bailey et al. and associate each subtype with other reported molecular subtypes. Moreover, we provide for each subtype a potential description of the tumor microenvironment that may influence treatment response according to the gene expression profile, the mutational landscape and their associated histology.

Keywords: molecular subtypes of pancreatic cancer; microenvironment; chemotherapy response; pancreatic stellate cells; regulatory T cells; tumor-associated macrophages; myeloid derived suppressor cells



Citation: Martinez-Useros, J.; Martin-Galan, M.; Garcia-Foncillas, J. The Match between Molecular Subtypes, Histology and Microenvironment of Pancreatic Cancer and Its Relevance for Chemoresistance. *Cancers* **2021**, *13*, 322. <https://doi.org/10.3390/cancers13020322>

Received: 30 November 2020

Accepted: 14 January 2021

Published: 17 January 2021

Publisher's Note: MDPI stays neutral with regard to jurisdictional claims in published maps and institutional affiliations.



Copyright: © 2021 by the authors. Licensee MDPI, Basel, Switzerland. This article is an open access article distributed under the terms and conditions of the Creative Commons Attribution (CC BY) license (<https://creativecommons.org/licenses/by/4.0/>).

1. Introduction

Pancreatic cancer (PC) incidence has increased in developed countries and its trend for 2030 is to be higher reaching the second cause of cancer-related deaths [1]. When tumors are <2 cm in size, the 5-year survival rate is around 50% while for tumors <1 cm could average as much as 100% [2]. Regrettably, pancreatic cancer symptoms are often misdiagnosed and commonly treated ambulatory that leads to a late diagnosis with metastatic disease in distant organs; then, their 5-year survival rate decreased to 3% [3,4]. PC could be

detected by elevated levels of CA19-9 serum marker [5]. However, CA19-9 is not PC specific and its levels are also high after biliary obstruction [6]. Recently, CA19-9 serum level in combination with IGF-1 and albumin have increased the sensitivity up to 93.6% and the specificity up to 95% to identify PC patients [7].

Risk factors of PC are cigarette smoking associated to 20–25% cases [8,9], chronic pancreatitis (4%) [10], diabetes (30%) [11], and some infectious agents like *Helicobacter pylori* (65%) presents an increased risk [12].

Surgical resection is considered the best treatment approach against PC. Histopathological characteristics of resected tumor like margins of resection (R), differentiation of tumor cells (G) or lymph-node status (N) could predict patient prognosis [13]. After resection, adjuvant treatment will depend on patient performance status but is usually based on gemcitabine [14], 5-fluorouracil and their combination with other cytotoxics [15]. The combination of gemcitabine with capecitabine exhibited better survival rates [16]. Other regimens based on FOLFIRINOX (folinic acid, 5-fluorouracil, irinotecan and oxaliplatin) or gemcitabine in combination with nano-albumin-bound paclitaxel (nab-paclitaxel) is administered to borderline resectable tumors as neoadjuvant treatment [17]. Another option for R1 patients, borderline resectable or locally advanced unresectable tumors is chemoradiotherapy [18,19]. However, PC exhibits chemoresistance due to a complex link between tumor cells and their microenvironment [20]. The tumor microenvironment TME is referred to the local environment where tumors developed [21]. The TME of PC is composed by tumor cells, extracellular matrix and stromal cells (pancreatic stellate cells (PSCs), regulatory T cells (Tregs), tumor-associated macrophages (TAMs), and myeloid derived suppressor cells (MDSCs). All these TME components foster high levels of hypoxia, which confer several metabolic advantages to tumor cells. Some studies have shown how PC microenvironment regulates proliferation, invasion and metastasis, chemoresistance and immune evasion [22,23].

Microenvironment of PC has immunosuppressive characteristics that lead to escape from the immune system, which enhances tumor progression. Cell populations from TME could induce the deposition of extracellular molecules such as matrix metalloproteinases, extracellular matrix molecules, growth factors and transforming growth factor β (TGF- β) to maintain the enabling microenvironment [24]. PSCs are able to produce a collagenous stroma and its role is crucial in both normal pancreas and tumor development. PSCs cooperate with cancer cells to build a perfect niche of tumor development with invasive abilities [25]. While in a normal physiological state, PSCs are quiescent and express nestin, vimentin, GFAP and desmin; activated PSCs become myofibroblast-like cells with overexpression of collagen type I and III, fibronectin and laminin, and present high proliferation and migration abilities [26]. Furthermore, activated PSCs allow pancreatic cancer-related fibrosis [27]. Interestingly, PSCs with an activated phenotype present expression of α -SMA [26], while CD10 positive PSCs have the ability to promote an invasive phenotype in PC [28]. There are subgroups of PSCs that interact with pancreatic β -cells called islet stellate cells. These islets are able to induce β -cell apoptosis, inhibit their proliferation, and diminish β -cell function [29,30]. Indeed, activated PSCs could impair pancreatic islet endocrine function. Since PSCs are glucose intolerant, this cell population is involved in development of type 2 diabetes, which directly promotes invasive phenotype because high levels of glucose are related to epithelial-to-mesenchymal transition [29,31]. PSCs promote also epithelial-to-mesenchymal transition of PC tumor cells [26].

Another TME cell population is Tregs that are a CD4+T cells subpopulation generated from naïve T cells with expression of FOXP3 and CD25. They are present in TME and they are able to suppress autoimmunity in physiological conditions, but also inhibit anti-tumor immune response. This fact could be explained because Tregs can impact tumor-associated CD11c+ dendritic cells to inhibit the activation of CD8+ T cells [32]. Recently, it has been described how Tregs induce differentiation of cancer-associated fibroblasts that promote tumor development [33]. Shevchenko et al. reported that gemcitabine at low doses reduce Tregs population in PC and provide a modest increase in survival [34]. Another study

described how neutrophil-lymphocyte ratio and a high proportion of Treg cells in pancreatic tumors are potential pathological biomarkers for poor outcome [35]. On the other hand, TAMs imply a subtype of immune cells that are commonly expressed in several solid tumors, and closely related to cancer-derived inflammation. Specially M2-polarized TAMs (CD163+ cells) are those cells with direct implication in cancer-derived inflammation; in addition, M2-polarized TAMs enable epithelial-to-mesenchymal transition through activation of TLR4/IL-10 signaling and inhibition of E-cadherin [36]. Additionally, TAMs promote angiogenesis, dedifferentiation and stem-cell phenotype in PC [37]. TAMs show several tumor-prone characteristics based on the release of some immunosuppressive and angiogenic cytokines [38]. In PC, TAMs present a high expression of BMP-4, BMP-7, TGF- β 1 and TGF- β 2 [39]. The infiltration of M2-polarized TAMs in PC stroma seems to be preferentially located in the body and tail of the pancreas, and similarly with other TME cell populations, M2-polarized TAM confers shorter overall survival to patients [40]. It has been reported how metformin could reduce desmoplasia of PC, reversion of epithelial-to-mesenchymal transition, and tumor-related inflammation via modulation of the AMPK/STAT3 that decreases levels of IL-1 β and hampers infiltration of M2-polarized TAMs [41]. Indeed, metformin in combination with simvastatin and digoxin is being evaluated in a phase IB trial to target crucial factors for PC development like PDX1 or BIRC5 (NCT03889795) [42]. In PC, M2-polarized TAM population rises significantly after gemcitabine administration, and it has been reported how aspirin could improve the effects of gemcitabine and decrease not only M2-polarized TAMs but also MDSCs populations [43]. MDSCs are a very heterogeneous immature myeloid cell population derived from the myeloid lineage that act as a multipotent progenitor cells. They are involved in development of obesity and several pathologies like autoimmune disease, chronic inflammation and tumorigenesis [44], and they are characterized by the expression of CD11b and Gr-1 surface markers [45]. Sangaletti et al. revealed how downregulation of SPARC decreased immunosuppression and reverted invasive phenotype triggered by the presence of MDSCs [46]. Immunosuppression by MDSCs is also driven by downregulation of JAK3, MHC class II and STAT5 that inhibit activation of T-cells or induce their apoptosis [44]. Another study revealed that the pro-inflammatory microenvironment that promotes MDSCs proliferation and recruitment is produced by a cytokine cascade, which includes the release of IL-1 β , IL-6, IL-13, IL-17, TNF- α , TGF- β and VEGF [47]. Similarly, other factors such as ARG-1, COX-2, Cybb, Cytochrome b-245, iNOS2 and PAUF are related to MDSCs activation [48]. MDSCs also impair chemo- and radiotherapy response. In fact, high levels of proinflammatory cytokines associated with MDSCs have been found in previously treated versus untreated patients or healthy samples [49]. Since radiotherapy induces the release of lactate by tumor cells that lead to activation of MDSCs, a proposed treatment strategy would imply target lactate to increase radiotherapy response [50]. Another mechanism described recently against MDSCs is by omega 3 administration due to its anti-inflammatory properties. Indeed, the combination of omega 3 with gemcitabine drastically stabilizes Tregs population and decreases MDSCs in advanced PC [51]. Other treatment approaches, like anti-CXCR2, have been described to counteract MDSCs [52], or an anti-ENO1 that limits the invasion of MDSCs and causes the subsequent disruption of TME interactions with tumor cells, which may improve survival or PC patients [53].

Other studies have proposed the administration of triterpenoid to hamper the activation of MDSCs and their immunosuppressive action in PC, which lead to an increased immune surveillance and immune response [54,55]. Therefore, diminish MDSCs population is a potential target for the treatment of PC and increase its chemoradiosensitivity.

Molecularly, PC is characterized by inactivating mutations in *TP53*, *RB*, *CDKN1A*, *CDKN2A*, or those associated to heritable PC such as *BRCA1* and *BRCA2* [56,57]. The effect of tumor suppressor genes could be blinded by overexpression of other oncogenes like *MYC*, *CCNE1* or *RAF* [58]. Broad genomic analysis has revealed different subtypes of PC. Bailey et al., identified four molecular subtypes of PC associated with specific histopathological characteristics: Squamous, progenitor, immunogenic and aberrantly

differentiated endocrine/exocrine (ADEX) [59]. The squamous molecular subtype is associated to squamous differentiation, TP63N activation, inflammation, hypoxia, metabolic reprogramming, dense extracellular matrix, TGF- β and WNT signaling pathway, increased proliferation, activation of MYC, autophagy and enhanced RNA processing. Progenitor and immunogenic subtypes share several characteristics like activation of FOXA2 and FOXA3 networks, xenobiotic metabolism, fatty acid oxidation and mucins metabolism. However, immunogenic subtype also involves the presence of several immune pathways like B cell, CD4 and CD8 T cell signaling, TLR signaling, and other factors associated with antigen presentation. ADEX is characterized by upregulation of NR5A2, RBPJL transcriptional regulation pathway, exocrine differentiation, development of pancreatic β -cell, epithelial cells differentiation and presents mutations in KRAS. Moffitt et al., proposed other molecular subtypes based on analyses of patient prognostic and gene expression profile of tumors (classical or basal-like tumors) and stroma (normal or activated stroma) compared with healthy samples [60]. Collisson et al., also proposed three molecular subtypes by a transcriptional profile analysis: Classical, which overlaps with Moffitt's classical subtype and exhibit high expression of molecules necessary for cell adhesion and epithelial morphology; quasi-mesenchymal subtype that shows high expression levels of genes associated to mesenchymal morphology; and exocrine-like subtype with overexpression of genes required for digestive enzymes release [61]. These diverse molecular subtypes exhibit several similarities with each other and highlight several opportunities for novel therapeutic strategies and targeted drug design.

TME of PC should be different according to different molecular subtypes and their response to chemotherapy should be different too. In the present article, we review the four molecular subtypes of pancreatic cancer proposed by Bailey et al., and we used them as backbone to supplement their features with other PC molecular subtypes proposed by Moffitt et al., and Collisson et al. Furthermore, we match each molecular subtype to a specific tumor histology and microenvironment, and how each complex network may influence treatment response.

2. Squamous Subtype

Squamous and adenosquamous tumors represent 1–4% of all PCs, are often generated in the head of the pancreas [62], and present the worst survival ratios even detected at early stages [63]. These tumors frequently carry TP53 mutations and present 3p loss compared to adenocarcinomas (Figure 1 and Table 1). Losses in 3p21.1–11.1 imply downregulation in several anti-oncogenic genes like ROBO1, ROBO2, WNT5A, FHIT. The squamous histology also presents upregulation of the WNT/ β -Catenin signaling pathway and downregulation of some chromatin modification factors [64]. These tumors are characterized by several cell layers with irregular borders, protruding intercellular junctions, high eosinophilic cytoplasm and keratin deposition, with denotes a rich and dense extracellular matrix (Figure 1 and Table 1) [65].

The squamous molecular subtype proposed by Bailey et al., presents MYC activation and overexpression of proteins TP63 and CD7 (TP40) as well as its target factors [59]. This molecular subtype was associated with presence of TP53 and KDM6A mutations [59,66].

Interestingly, overexpression of TP63 in combination with TP53 mutation is able to induce epithelial-to-mesenchymal transition to promote aggressive phenotype [67]. Squamous tumors also express integrins $\alpha 6\beta 1$, $\alpha 6\beta 4$ and EGF. Concerning epigenetic modifications, this subtype exhibits an hypermethylator phenotype that downregulates protein expression of PDX1, MNX1, GATA6 or HNF1B (Figure 1 and Table 1). However, it presents upregulation of LOX, which is associated with metastasis development [68]. Squamous molecular subtype exhibit an hypoxic, inflamed and autophagic microenvironment that correlates with squamous histology [59]. Moreover, Moffitt et al. found a squamous subtype characterized by overexpression associated with several components of the extracellular matrix like laminins and keratins [60]. This matrix composition allows an oncogenic microenvironment that fosters proliferation of PC tumor cells. This dense

extracellular matrix generates a physical barrier for drug delivery that leads to a chemoresistant phenotype [69]. This rich extracellular matrix contributes to generation of hypoxic conditions and expression of hypoxia-inducible factor 1 (HIF1) [70], and overexpression of MUC1, VEGF and PDGF that enhance the endothelial tube formation, proliferation and migration ability [71]. The squamous molecular subtype also presents activation of TGF- β signaling pathway [59], and overexpression of EGFR and S100A2 [72]. These findings support the presence and important role of PSCs in the development of squamous tumor microenvironment since cytokines TGF- β , PDGF, Angiotensin II could bind to the PSCs receptors and activate downstream signaling pathways such as ERK, c-Jun, P38, MAPK or JAK-STAT to promote the activation and proliferation of PSCs. Moreover, activated PSCs can produce and secrete to stroma a variety of growth factors through paracrine mechanism, to activate EGFR, PI3K-AKT, and mTOR signaling pathways, and then promote proliferation and inhibition of apoptosis of PC cells [73,74]. One study has reported that squamous PC cells are able to recruit neutrophils that convert PSCs into tumor-associated fibroblasts (TAFs) that overexpress inflammatory cytokines like IL1A and CXCL1 [75]. TAFs also contribute to generate a rich tumor prone extracellular matrix by secretion of fibroblast activating protein (FAP) that participate in angiogenesis and affect the activity of IFN- γ and TNF- α [76].

On the other hand, the squamous molecular subtype proposed by Bailey et al. linked with “basal-like” and “activated” stroma signatures proposed by Moffitt et al. (Figure 1 and Table 1). The “basal-like” and “activated” stroma signatures also exhibited the worst survivals compared to “classical” and “normal” stroma subgroups, which goes in accordance with both squamous molecular subtype of Bailey et al., and the squamous histology of PC [60]. “Basal-like” subtype presents *KRAS*^{G12D} mutation, while “activated” stroma subtype expresses SPARC, WNT family members WNT2 and WNT5A, gelatinase B (MMP9), stromelysin 3 (MMP11), and FAP that contribute to tumor development [60]. Furthermore, “activated” stroma subgroup is characterized by other factors like the chemokine ligands CCL13 and CCL18, and integrin ITGAM, which are associated with the presence of macrophages [60]. This fact suggests the important role of macrophages in the tumor microenvironment to promote angiogenesis and chemoresistance [77]. In this sense, it has been described how TAMs enable chemoresistance to gemcitabine and nab-paclitaxel by expression of insulin growth factor (IGF) that activates IGF-1 receptors [78]. It has been reported that PSCs also promote gemcitabine resistance mediated by secretion of deoxycytidine that modulate nucleoside transporters [79]. Moreover, PSCs reduce the sensitivity of PC cells to radiotherapy by regulation of epithelial-to-mesenchymal transition and increasing cancer stem cell markers [80]. Furthermore, these authors provide a rationale for the use of an anti-TGF- β neutralizing antibody to inhibit epithelial-to-mesenchymal transition and cancer stem cells to sensitize cells to radiation and reduce tumors [80]. Other cell population like tumor associated fibroblasts can secrete proinflammatory factors like IL-6, which activates STAT3, and secrete CXCL12 that inhibit T-cells infiltration in tumors [81]. In addition, CXCL12 in combination with anti-PD-L1 immunotherapy has shown a synergic anti-tumor effect and is considered a potential target for those PCs with high FAP expression [82].

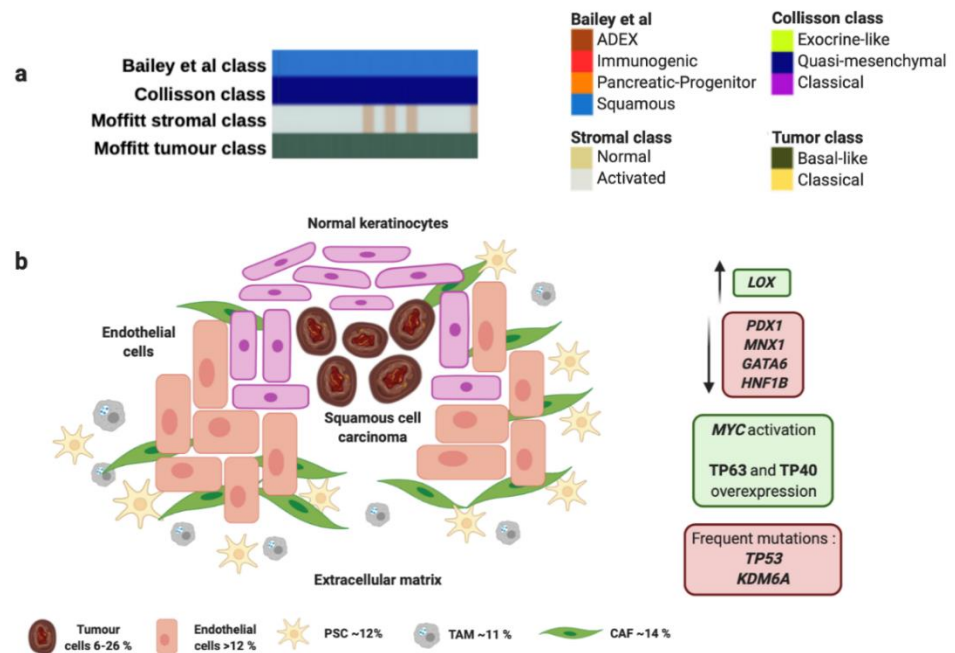


Figure 1. Squamous molecular profile and microenvironment. (a) Squamous subtype is associated with specific histological characteristics such as squamous and adenosquamous carcinomas. (b) Squamous subtype proposed by Bailey et al., matches perfectly with “quasi-mesenchymal” tumor subtype proposed by Collisson et al., and “basal-like” tumors and “activated” stroma subtypes proposed by Moffitt et al. Green boxes contain upregulated significant factors and activated pathways associated to squamous molecular subtype. Red boxes contain downregulated significant factors (up) and most common mutations found in squamous molecular subtype (down). Percentage of each subcellular population has been obtained from Peng et al., [86]. Abbreviations: TAM: Tumor-associated macrophage; CAF: Cancer-associated fibroblast; PSC: Pancreatic stellate cell.

Table 1. Molecular features of each pancreatic cancer subtype according to their main subcellular population.

Bailey et al. Molecular Subtype	Cellular Subpopulations	Molecular Profile of Cellular Subpopulation	Expression of Cytokines, Chemokines and Receptors	Clinical Significance
Squamous	Tumor cells	<i>TP53</i> and <i>KDM6A</i> mutations [59,66]; <i>KRAS-G12D</i> - mutation [60]; overexpression of <i>LOX</i> [68]; upregulation of <i>TP63</i> , <i>TP40</i> and <i>IDO1</i> [59]; activation of <i>WNT/β-Catenin</i> pathway [64], <i>MYC</i> activation [59]; overexpression of <i>HIF1</i> [70], <i>MUC1</i> and <i>PDGF</i> [71], <i>ROBO1</i> , <i>ROBO2</i> , <i>WNT5A</i> , <i>FHIT</i> [64]; downregulation of <i>PDX1</i> , <i>MNX1</i> , <i>GATA6</i> and <i>HNF1B</i> [59]; Activation of <i>ERK</i> , <i>c-Jun</i> , <i>P38</i> , <i>MAPK</i> , <i>JAK-STAT</i> , <i>PI3K-AKT</i> , <i>mTOR</i> and cancer stem cell markers [73,74]; overexpression of <i>RGS5</i> , <i>ACTA2</i> , <i>PDGFRB</i> , <i>SOD3</i> , <i>NOTCH3</i> , <i>COL18A1</i> , <i>COL4A1</i> , <i>NDUFA4L2</i> , <i>COL4A2</i> , <i>SEPT4</i> , <i>COL14A1</i> and <i>SPARC</i> [86]	Laminins and keratins [60]; PD-L1 y PD-L2 [59]; CEACAM6, <i>MUC1</i> , <i>EPCAM</i> , <i>CEACAM5</i> , <i>MMP7</i> , <i>CEACAM1</i> , <i>IL18</i> , <i>VEGFA</i> , <i>IL32</i> [86]	Immunotherapy resistance and aggressive phenotype [83,84]
	Stellate cell	Integrins $\alpha6\beta1$, $\alpha6\beta4$ and <i>EGF</i> [59]; <i>TGF-β</i> [59]; Angiotensin II and deoxycytidine [79]	Gemcitabine and radiotherapy resistance [79,80]	
	Endothelial cells	Overexpression of <i>COL15A1</i> , <i>RAMP2</i> , <i>CDH5</i> , <i>SPARCL1</i> , <i>NOTCH4</i> , <i>SMAD9</i> and <i>JAM2</i> [86]	<i>VEGF</i> [71]	Angiogenesis [87]
	Macrophages	Overexpression of <i>AIF1</i> , <i>APOC1</i> , <i>APOE</i> , <i>C1QB</i> , <i>C1QA</i> , <i>C1QC</i> , <i>NCF2</i> and <i>CCL2</i> [86]	<i>IGF</i> , <i>CCL13</i> , <i>CCL18</i> and integrin <i>ITGAM</i> [60,78]; <i>HLA-DRA</i> , <i>HLA-DPA1</i> , <i>HLA-DPB1</i> , <i>CD14</i> , <i>CD53</i> , <i>CD68</i> , <i>CD74</i> , <i>FTH1</i> , <i>FTL</i> , <i>TGFBI</i> , <i>IL8</i> and <i>IL13RA1</i> [86]	Enable chemoresistance to gemcitabine and nab-paclitaxel [78]
	Fibroblasts	<i>SFRP2</i> , <i>LUM</i> , <i>COL1A1</i> , <i>COL1A2</i> , <i>DCN</i> , <i>COL3A1</i> , <i>MMP11</i> , <i>COL6A3</i> , <i>COL10A1</i> , <i>COL5A2</i> , <i>SPARC</i> , <i>COL6A2</i> , <i>COL5A1</i> , <i>COL6A1</i> , <i>COL8A1</i> , <i>COL12A1</i> , <i>MMP14</i> , <i>FGF7</i> , <i>FAP</i> [86]	<i>EGFR</i> and <i>S100A2</i> [72]; <i>IL1A</i> and <i>CXCL1</i> [75]; <i>IFN-γ</i> , <i>TNF-α</i> , <i>IL-6</i> , <i>CXCL12</i> and <i>FAP</i> [76,81,82]	Inhibit T-cells infiltration activity [85]

Table 1. Cont.

Bailey et al. Molecular Subtype	Cellular Subpopulations	Molecular Profile of Cellular Subpopulation	Expression of Cytokines, Chemokines and Receptors	Clinical Significance
Progenitor	Tumor cells	<i>KRAS-G12V</i> - mutation [60]; <i>TGFB2</i> mutation [59]; overexpression of MUC5AC and MUC1 [59]; upregulation of HES1, HNF1A, HNF1B, HNF4A, HNF4G, FOXA2, FOXA3, LAMA1, MNX1 and EP300 [59]; overexpression of PDX1 [88], GATA6 [60] and CDX2 [89,90]; downregulation of IDO1 [59], LOX and S100A [59]	High mucin production [60]; low levels of EGFR, CTLA4, PD-L1 and PD-L2 [59]	Chemoresistance, immune evasion and upregulation of cell survival pathways [91,92]; poor response to platinum-based therapy [60]
	Ductal cells type 2	Overexpression of SOX9 [86]	CEACAM1, CEACAM5, CEACAM6, EPCAM, IL18, IL32, KRT19, MMP7, MUC1, MUC5AC, VEGFA [86,93]	Poor clinical prognosis [86]
Immunogenic	Tumor cells	<i>KRAS-G12V</i> - mutation [60]; Overexpression of CDX2 [89,90] and GATA6 [60]		<i>KRAS-G12V</i> - highlights the presence of Tregs infiltration [94]; GATA6 expression inhibits cell dissemination [91] and confers poor response to platinum based therapy [60]
	B cells	Upregulation of LIMD2, IRF8, BANK1 and RAC2 [86]	CD19, CD20, CD37, CD52, CD53, CD74, CD79A, CD79B, CXCR4, IL16 and VPREB3 [86]	High B cells infiltration [86]
	T cells	Upregulation of FOXP3 [59]; Upregulation of RAC2 [86]	CD4, CD8, CD25, CTLA4 and PD1 [59]; CCL5, CD2, CD3E, CD3D, CD3G, CD7, CD45, CD52, CD69, CXCR4, IL2RG, IL7R, IL32, KLRB1, LTB [86]	Promote tumor immunosuppression [95]; CD8 cells secrete perforin and granzymes with cytolytic effect [96]
	Macrophages	Upregulation of AIF1, APOC1, APOE, C1QB, C1QA, C1QC, FTH1, NCF2 [86]	IL10 and TGF- β [97]; CSF1R, TLR4, TLR7, TLR8, PD-L2 [59]; CD14, CD53, CD68, CD74, CCL2, HLA-DRA, HLA-DPA1, HLA-DPB1, IL8, IL13RA1, TGFBI, and VEGFR [86]	Chemoresistance [78]
ADEX	Tumor cells	Presence of mutations in: <i>FAT1</i> , <i>FAT3</i> , and <i>FAT4</i> (57%), <i>BRCA2</i> (42%), <i>SMAD4</i> (26%), <i>JAK1</i> (17%), <i>RB1</i> (13%), <i>TP53</i> (13%), <i>CTNNB1</i> (11%), <i>APC</i> (9%), <i>ARID1A</i> (9%), <i>GNAS</i> (9%), <i>MLL3</i> (9%), <i>PTEN</i> (9%), <i>RNF43</i> (4%) and <i>MEN1</i> (4%); however, <i>KRAS</i> mutations are scarce [98,99]; upregulation of <i>AMY2B</i> , <i>CEL</i> , <i>INS</i> , <i>PRSS1</i> , <i>PRSS3</i> [59]; and <i>RBPJL</i> , <i>NR5A2</i> , <i>MIST1</i> [100,101]		Better clinical outcome [60]
	Acinar cells	Expression of BCL-10 [65]	IL32, PRSS1, REG1A, REG1B, REG3A, REG3G, [86]; ELA3A and CFTR [61]	Exhibit high exocrine features [65]
	Stellate cell	Overexpression of ACTA2, DES and VIM [60,102]; COL18A1, COL4A1, COL4A2, COL14A1, NDUFA4L2, NOTCH3, RGS5, SEPT4, SOD3 and SPARC [86]	VEGF [103] and PDGFRB [86]	Impairs drug delivery, stimulates epithelial-to-mesenchymal transition, increases genetic instability and chemoresistance [104]; increased apoptosis of pancreatic β -cells [105]
	Endocrine cells	Overexpression of <i>INS</i> , <i>NEUROD1</i> , <i>NKX2-2</i> , <i>MAFA</i> [59], and <i>ABCC8</i> [86]	CHGA, CHGB, IAPP, PCSK1N and TTR [86]	Endocrine/exocrine differentiation and association with initiation of diabetes [59]

Unfortunately, Bailey et al., support that squamous molecular subtype exhibits the highest expression of PD-L1, PD-L2 and IDO1 [59], thus, they sustain that these tumors are not good candidates for immunotherapy administration [83,84].

However, the combination of IDO1 inhibitor and anti-PD-1/PD-L1 treatment could achieve promising results and become a potential strategy to induce intratumoral T-cell infiltration [85]. In the light of the foregoing, the microenvironment of the squamous molecular subtype presents a complex interaction between different cell populations and extracellular components to confer chemoresistance of PC.

3. Progenitor and Immunogenic Subtypes

The progenitor molecular subtype proposed by Bailey et al. presents activation on transcriptional networks that exhibit high expression of the proteins HES1, HNF1A, HNF1B, HNF4A, HNF4G, FOXA2, FOXA3, LAMA1, MNX1 and EP300 (Figure 2 and Table 1) [59]. These transcription factors are considered crucial for determination and development of the pancreatic endoderm. While the squamous subtype presented downregulation of PDX1, which is also critical for pancreatic development, the progenitor subtype overexpresses PDX1 (Figure 2 and Table 1) [88]. Moreover, progenitor molecular subtype expresses multiple genes necessary for the metabolism of mucins, fatty acids, steroid hormones, and also involves drug metabolism. Indeed, progenitor molecular subtype overexpresses MUC5AC and MUC1 (Figure 2 and Table 1) [59]. Interestingly, both progenitor and immunogenic molecular subtypes share the same histology derived from premalignant lesions like mucinous non-cystic adenocarcinomas and intraductal papillary mucinous neoplasms (IPMN), characterized by a high mucin production (Figure 2 and Table 1) [106], different epithelial-to-mesenchymal transition markers [107], and immunohistochemical staining of CDX2 [89,90].

The immunogenic molecular subtype also presents many other similarities in the gene expression profile with the progenitor subtype; however, immunogenic subtype exhibit a significantly higher immune infiltrate [59]. Gene expression analysis identified upregulation in those genes associated with nine different populations of immune cells [108], being the most significant those involved with B and T cells infiltration (CD4, CD8, CD25, FOXP3) (Figure 2 and Table 1). Furthermore, immunogenic subtype presents activation of CTLA4 and PD1, which suggests that this molecular subtype could be feasible treated with immunecheckpoints inhibitors [59]. In contrast, the pancreatic progenitor subtype presents the lowest levels of CTLA4, PD-L1, PD-L2, and IDO1 [59]. The immunogenic subtype also has enrichment in genes for Toll-like receptors that play a key role in the innate immune system. These genes include TLR4, TLR7, TLR8, PD-L2 and CSF1R (Figure 2 and Table 1) [59]. These receptors usually are expressed on sentinel cells such as macrophages and dendritic cells, which reveal the strong link between the immunogenic molecular subtype with the presence of immune cell population in the TME (Figure 2 and Table 1). In this sense, TAMs present in PC, especially those M2-type macrophages can promote neovasculature formation to feed tumor cells and induce chemoresistance, proliferation, invasion and metastasis of PC tumor cells [77]. TAMs could be recruited to neoplastic foci by cytokines and vascular endothelial growth factors (VEGF). Once there, TAMs promote proliferation of PC cells through the release of growth factors like Il10 or TGF- β [97]. In addition, the presence of TAMs in the TME is associated with chemoresistance [78].

On the other hand, the immunogenic molecular subtype of PC present inflammation, caused by abundant Tregs infiltration and high expression of cytotoxic T lymphocyte-associated protein 4 (CTLA-4). These factors promote tumor immunosuppression through the inhibition of the killing ability of effector cells [95]. The presence of CD8+ T cells in immunogenic subtype can decrease the capability of anti-tumor immune cells due to the ability of CD8+T cells to express FAS-ligand and secrete perforin and granzymes with cytolytic effect [96]. Despite the immunosuppressive skills of immunogenic subtype, patients with this kind of tumor present the best outcome out of the four molecular subtypes [59].

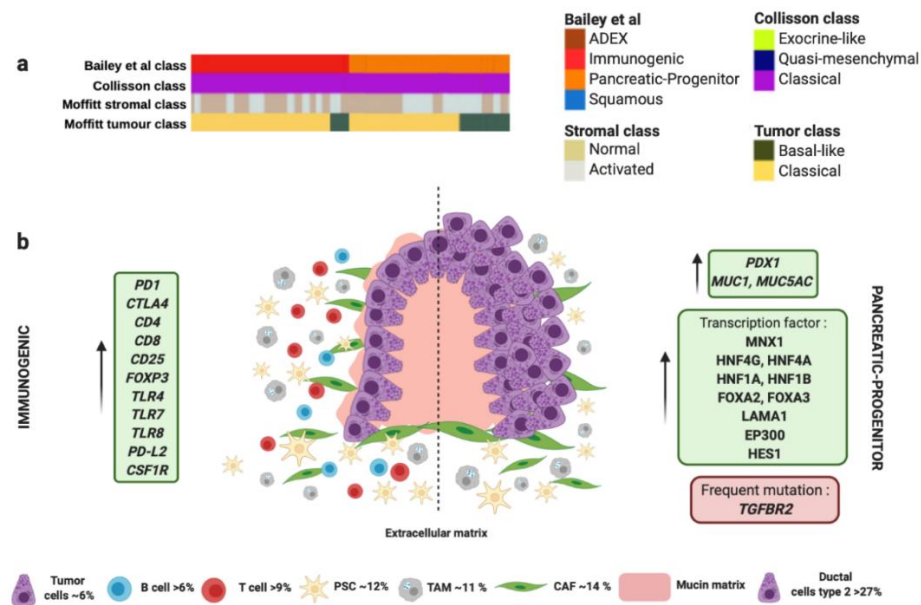


Figure 2. Immunogenic and progenitor molecular profiles and their microenvironment. (a) Both subtypes proposed by Bailey et al., match perfectly with “classical” tumor subtype proposed by Collisson et al., and “classical” tumor subtype proposed by Moffitt et al. (b) Both subtypes share the same histology derived from premalignant lesions like mucinous non-cystic adenocarcinomas and intraductal papillary mucinous neoplasms (IPMN) characterized by high mucin production. Dotted line separates schematic representation of two subtypes. Green boxes contain upregulated significant factors associated to each subtype. Red box contains the most characteristic gene mutation in progenitor molecular subtype. Pink color represents mucin production. Percentage of each subcellular population has been obtained from Peng et al., [86]. Abbreviations: TAM: tumor-associated macrophage; CAF: cancer-associated fibroblast; PSC: pancreatic stellate cell.4. Microenvironment of ADEX Subtype.

Interestingly, both progenitor and immunogenic subtypes correlate with “classical” tumor subtype proposed by Moffitt et al., which also share the expression of extracellular mucin in more than 10% (Figure 2 and Table 1) [60]. Similarly to immunogenic molecular subtype, “classical” tumors present better outcome compared to those “basal-like” tumors [60]. Remarkably, progenitor and immunogenic molecular subtypes by Bailey et al. and “classical” tumor subtype by Moffitt et al., correlate with the same gene expression signature of “classical” tumor subtype proposed by Collisson et al. (Figure 2 and Table 1) [109]. This fact supports the presence of the G12V variant of *KRAS* mutation that is associated with the “classical” subtype [60]. “Classical” molecular subtype also presents enrichment in genes associated with *GATA6* overexpression responsible for promoting epithelial cell differentiation [60]. However, other authors propose the loss of *GATA6* expression in tumors confers a shorter survival and they have a poor response to adjuvant treatment based on 5-fluorouracil (5-FU)/leucovorin [91]. In this sense, “classical” molecular subtype tumors also exhibit poor response to platinum based therapy [60]. Therefore, the adjuvant treatment used for the management of immunogenic/progenitor/classical molecular subtype tumors would be more aggressive to overcome the chemoresistance. For this, immunotherapy has arisen as one of the most effective anti-tumor treatments. PC overexpress important factors for targeted therapies, such as MUC-1, CEA, PSC, VEGF, MSLN and mutation *KRAS* [110]. However, the most important targets for immunotherapy currently are PD-1, PD-L1 and CTLA-4. In animal models, anti-PD-1 or anti-PD-L1 treatment boosted infiltration of CD8+ T cells in the tumor and enhanced efficacy of immunotherapy.

Regrettably, immunotherapy against PC has presented no benefit in clinical trials so far [111,112]. Currently, the failure of anti-PD-1/anti-PD-L1 based therapy is mainly

attributed to the lack of T-cell infiltration in the TME of PC. Therefore, the immunogenic molecular subtype that presents elevated genes for B- and T-cell infiltration is a potential responder for immunotherapy. Other type of immunotherapy based on CAR-T cells has obtained promising results. Some clinical trials have focused on modified CAR-T cells able to target MUC1 or Mesothelin (MSLN) [113]. Although MUC1 is overexpressed in approximately 85% of PC, those tumors present overexpression of IDO1, COX1/2, and Gal-9 that conferred resistance to these anti-MUC1 CAR-T cells [114]. However, the use of inhibitors of IDO1, COX1/2, and Gal-9 overcame this resistance in combination with anti-MUC1 CAR-T cells [114]. In this concern, a phase I/II trial has been designed with resectable PC patients' T cells modified to allow identification and kill of MUC1 positive tumor cells (NCT02587689). CAR-T cells could be engineered to target other antigens such as Mesothelin, and they have achieved encouraging results in solid malignancies [115], which has established the bases for a subsequent clinical trial with anti-MSLN CAR-T cells (NCT04203459). Although CAR-T cell therapy has achieved favorable results, it is crucial to evaluate the potential side effects on T-cell exhaustion.

The ADEX molecular subtype by Bailey et al., is defined by the orchestrated expression of factors necessary for the exocrine and endocrine pancreatic cell-fate determination. ADEX presents upregulation in transcription factors involved in healing and regeneration after pancreatitis events such as RBPJL, NR5A2, MIST1 and their associated downstream cascade factors (Figure 3 and Table 1) [100,101]. This molecular subtype exhibits an expression profile associated with extremely rare acinar histopathology (Figure 3 and Table 1) [59,63]. Macroscopically, this histology shows large tumors, frequently presented in encapsulated form and well circumscribed. It also presents cystic evolution, necrosis, and upper digestive hemorrhage [116]. In clinical practice, diagnosis of acinar carcinomas is performed by immunohistochemical evaluation of pancreatic enzymes like trypsin and chymotrypsin that are produced in the rough endoplasmic reticulum of acinar cells. It also presents high specificity for BCL-10 immunostaining [65]. Furthermore, somatic mutational index of acinar subtype is higher than adenocarcinoma being the most frequent mutations in the following genes: *FAT1*, *FAT3*, and *FAT4* (57%), *BRCA2* (42%), *SMAD4* (26%), *JAK1* (17%), *RB1* (13%), *TP53* (13%), *CTNBN1* (11%), *APC* (9%), *ARID1A* (9%), *GNAS* (9%), *MLL3* (9%), *PTEN* (9%), *RNF43* (4%) and *MEN1* (4%); however, *KRAS* mutations are not often observed in acinar subtype (Figure 3 and Table 1) [98,99]. In this sense, Bailey et al. found in ADEX molecular subtype high expression levels of *INS*, *NEUROD1*, *NKX2-2* and *MAFA*, which are associated with endocrine differentiation and sudden occurrence of diabetes type MODY (Figure 3 and Table 1).

Importantly, most PC-derived cell lines present enrichment in genes found in ADEX molecular subtype like *AMY2B*, *CEL*, *INS*, *PRSS1* and *PRSS3* [59].

ADEX molecular subtype proposed by Bailey et al., matches perfectly with “exocrine-like” subtype proposed by Collisson et al., which shows relatively high expression of tumor cell-derived digestive enzymes like ELA3A and CFTR, which controls Cl⁻ and Na⁺ ions, and water flux (Figure 3 and Table 1) [61]. In addition, ADEX molecular subtype correlates with “normal stroma” subtype proposed by Moffitt et al., which exhibit longer survival rates (Figure 3 and Table 1) [60]. “Normal stroma” is also distinguished by high expression levels of PSCs markers: Smooth muscle actin (*ACTA2*), Desmin (*DES*) and Vimentin (*VIM*) [60,102]. This fact highlights the importance of the PSCs population in the ADEX microenvironment. PSCs role go in accordance with ADEX origin, since they present expression markers of stem and progenitor cells needed to maintain differentiation and regeneration of pancreas [117]. Indeed, PSCs are necessary to trigger desmoplastic reaction by the synthesise of large amounts of extracellular matrix proteins, such as collagens, and amplify endostatin production of cancer cells that contributes to an hypoxic milieu [103,118]. Moreover, PSCs produce VEGF to increase endothelial cell growth in the peritumoral stroma [103]. All the above supports the role of PSCs in induction of fibrosis [119], that impairs drug delivery, stimulates epithelial-to-mesenchymal transition, and increases genetic instability leading to a more chemoresistant tumor [104]. Furthermore, PSCs play a

crucial role in islet cell dysfunction since PSCs decrease insulin expression and an increased apoptosis of pancreatic β -cells that connects to initiation of diabetes [105]. One study supported that PC cells cultured with extracellular matrix proteins produced by PSCs were able to develop resistance to 5-FU, cisplatin and doxorubicin [120]. As above mentioned, the presence of PSCs in ADEX molecular subtype could imply resistance to gemcitabine [79] and a reduced sensitivity to radiotherapy [80].

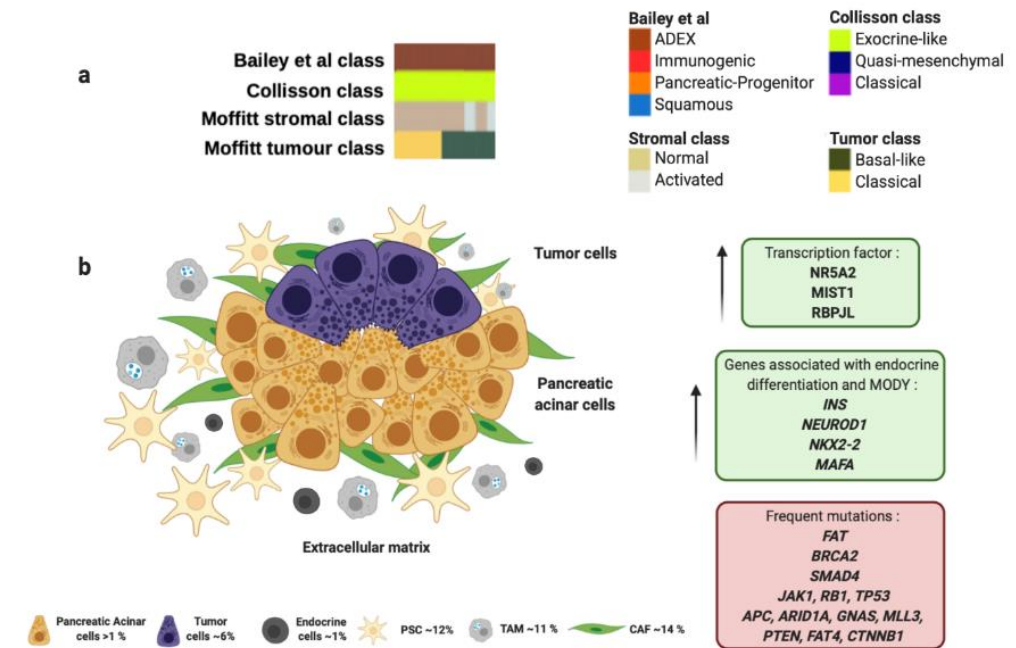


Figure 3. ADEX molecular profile and microenvironment. (a) ADEX subtype proposed by Bailey et al., matches perfectly with “exocrine-like” subtype proposed by Collisson et al., and most of “normal stroma” subtype cases analyzed by Moffitt et al. (b) ADEX molecular subtype is associated with the rare acinar histology. Green boxes contain upregulated transcription factors and other genes involved in ADEX molecular subtype. Red box contains genes commonly mutated in ADEX. Percentage of each subcellular population has been obtained from Peng et al., [86]. Abbreviations: TAM: tumor-associated macrophage; CAF: cancer-associated fibroblast; PSC: pancreatic stellate cell; MODY: maturity onset diabetes of the young.

4. Conclusions and Future Perspectives

The match between molecular features at genomic, epigenomic and expression levels combined with the biological behavior of PC is bringing new therapeutic strategies for the clinical management of these patients. In addition, the study of the TME could explain chemoresistance of PC previously attributed only to tumor cells. The TME and especially the role of its immune cell population in tumor initiation, development and immune evasion is changing the paradigm of PC diagnosis and treatment approach with the identification of new molecular subtypes (Table 2).

Table 2. On-going clinical trials that include different subtypes of pancreatic cancer.

Clinical Trial	Study Type	Treatment	Patients	Aim
NCT03977233	Phase II	Neoadjuvant FOLFIRINOX (oxaliplatin, leucovorin, irinotecan, 5-FU) First-line systemic chemotherapy with either FOLFIRINOX or cisplatin plus gemcitabine based regimens	Untreated patients with resectable, borderline resectable and unresectable locally advanced pancreatic ductal adenocarcinoma	Assess the impact of tumor and stromal molecular subtypes on the efficacy of neoadjuvant FOLFIRINOX
NCT02869802	Observational Prospective		Tumor samples, baseline and serial blood and urine samples from metastatic pancreatic ductal adenocarcinoma	Patients will undergo fresh tumor biopsy at study enrollment for comprehensive molecular characterization

Table 2. Cont.

Clinical Trial	Study Type	Treatment	Patients	Aim
NCT04246710	Observational Prospective	Not specified	Resectable, borderline resectable, locally advanced, metastatic and recurrent pancreatic cancer	Molecular characterization and identification of markers for therapeutic stratification by endoscopic ultrasound tissue core biopsies
NCT04683315	Phase II	Patients with “classical” subtype will receive FOLFIRINOX; and patients with “basal” subtype will receive gemcitabine/nab-paclitaxel.	Patients with “classical” or “basal” subtype pancreatic cancer	Molecular subtyping of pretreated endoscopic ultrasound fine needle aspiration samples to determine pancreatic cancer subtype
NCT03820921	Observational Prospective	PD-1 inhibitor (pembrolizumab)	Unresectable or metastatic, microsatellite instability-high (MSI-H) or mismatch repair-deficient (dMMR) pancreatic cancer that have progressed following prior treatment and have no satisfactory alternative treatment options.	Assess of tumor PD-L1/dMMR expression in patients with pancreatic cancer using endoscopic ultrasound fine needle aspiration biopsy samples, and the prospective correlation of MMR status and PD-L1 expression with overall survival and progression-free survival of PDAC patients.
NCT04436679	Observational Retrospective	None	Excreto-pancreatic adenocarcinoma of the pancreas, ductal adenocarcinoma or “classical” adenocarcinoma	Analyze the microscopic characteristics of the stroma, tumor budding and mucin expression using a comparative approach of long-survivor/short-survival patients.
NCT03840460	Observational Prospective	Not specified	Early and advanced pancreatic adenocarcinoma, precursor lesions or pancreatic neuroendocrine tumors.	Study the molecular profile of pancreatic lesions and their microenvironment at various stages to predict treatment response, treatment toxicity and prognostic. Additionally, investigate the particular micro-organisms colonizing individual patients and association with patient’s outcome

Although treatment strategies based on immuncheckpoint inhibitors have shown disappointing results, new studies are ongoing with novel drug design to improve patient response, and to avoid tumor immune evasion. In this concern, a randomized clinical trial (NCT02030860) aimed to evaluate paricalcitol that target vitamin D metabolism in the TME in combination with gemcitabine plus nab-paclitaxel in the neoadjuvant scenario for resectable PC patients. Another phase I/II clinical trial is designed to evaluate the safety and tolerability of the microenvironment modifier drug, L-DOS47, in combination with doxorubicin. The L-DOS47 is reported to neutralize the acid extracellular matrix that protects the tumor (NCT04203641) [121]. Recently, other treatments like GVAX or CRS-207 have appeared with promising results against PC [122]. GVAX is a vaccine based on granulocyte-macrophage colony-stimulating factor that inhibits Tregs and induces T cells; while CRS-207 is a vaccine based on live-attenuated *Listeria monocytogenes*-expressing mesothelin that has been described to induce innate and adaptive immune response against tumor cells and has achieved longer survivals of PC patients (NCT03161379; NCT02451982) [122]. Other drugs are based on nucleic acid, this is the case of olaptesed pegol a L-RNA Spiegelmer that exhibits a high affinity against CXCL12, a factor previously described responsible for TAMs recruitment (NCT03168139) [123]. These new treatment approaches highlight the importance of targeting not only tumor cells but also TME. Although translational research and drug design are working synergistically to improve outcome of PC patients, clinical research must not ignore that patients might be stratified not only based on performance

status of patients and/or the molecular characteristics of tumors, but also according to their TME features to obtain better treatment responses and longer survivals.

Author Contributions: Conceptualization, J.M.-U. and J.G.-F. writing—original draft preparation, J.M.-U. figures and tables, M.M.-G.; writing—review and editing, M.M.-G. and J.M.-U. visualization, M.M.-G. supervision, J.G.-F. funding acquisition, J.G.-F. All authors have read and agreed to the published version of the manuscript.

Funding: This research received no external funding.

Acknowledgments: We especially thank oncologist Aberto Orta-Ruiz (MD, PhD) from the Medical Oncology Department (Fundacion Jimenez Diaz University Hospital) for his appreciated revision, suggestions and criticism for the present review article. All figures have been designed with BioRender.com.

Conflicts of Interest: The authors declare no conflict of interest.

References

- Rahib, L.; Smith, B.D.; Aizenberg, R.; Rosenzweig, A.B.; Fleshman, J.M.; Matrisian, L.M. Projecting Cancer Incidence and Deaths to 2030: The Unexpected Burden of Thyroid, Liver, and Pancreas Cancers in the United States. *Cancer Res.* **2014**, *74*, 2913–2921. [[CrossRef](#)] [[PubMed](#)]
- Tamm, E.P.; Bhosale, P.R.; Vikram, R.; de Almeida Marcal, L.P.; Balachandran, A. Imaging of Pancreatic Ductal Adenocarcinoma: State of the Art. *World J. Radiol.* **2013**, *5*, 98–105. [[CrossRef](#)] [[PubMed](#)]
- Kelsen, D.P.; Portenoy, R.; Thaler, H.; Tao, Y.; Brennan, M. Pain as a Predictor of Outcome in Patients with Operable Pancreatic Carcinoma. *Surgery* **1997**, *122*, 53–59. [[CrossRef](#)]
- Siegel, R.L.; Miller, K.D.; Jemal, A. Cancer Statistics, 2019. *CA Cancer J. Clin.* **2019**, *69*, 7–34. [[CrossRef](#)] [[PubMed](#)]
- Duffy, M.J.; Sturgeon, C.; Lamerz, R.; Haglund, C.; Holubec, V.L.; Klapdor, R.; Nicolini, A.; Topolcan, O.; Heinemann, V. Tumor Markers in Pancreatic Cancer: A European Group on Tumor Markers (EGTM) Status Report. *Ann. Oncol.* **2010**, *21*, 441–447. [[CrossRef](#)] [[PubMed](#)]
- Kim, J.-E.; Lee, K.T.; Lee, J.K.; Paik, S.W.; Rhee, J.C.; Choi, K.W. Clinical Usefulness of Carbohydrate Antigen 19-9 as a Screening Test for Pancreatic Cancer in an Asymptomatic Population. *J. Gastroenterol. Hepatol.* **2004**, *19*, 182–186. [[CrossRef](#)]
- Ferri, M.J.; Saez, M.; Figueras, J.; Fort, E.; Sabat, M.; López-Ben, S.; de Llorens, R.; Aleixandre, R.N.; Peracaula, R. Improved Pancreatic Adenocarcinoma Diagnosis in Jaundiced and Non-Jaundiced Pancreatic Adenocarcinoma Patients through the Combination of Routine Clinical Markers Associated to Pancreatic Adenocarcinoma Pathophysiology. *PLoS ONE* **2016**, *11*, e0147214. [[CrossRef](#)]
- Blackford, A.; Parmigiani, G.; Kensler, T.W.; Wolfgang, C.; Jones, S.; Zhang, X.; Parsons, D.W.; Lin, J.C.-H.; Leary, R.J.; Eshleman, J.R.; et al. Genetic Mutations Associated with Cigarette Smoking in Pancreatic Cancer. *Cancer Res.* **2009**, *69*, 3681–3688. [[CrossRef](#)]
- Bosetti, C.; Lucenteforte, E.; Silverman, D.T.; Petersen, G.; Bracci, P.M.; Ji, B.T.; Negri, E.; Li, D.; Risch, H.A.; Olson, S.H.; et al. Cigarette Smoking and Pancreatic Cancer: An Analysis from the International Pancreatic Cancer Case-Control Consortium (Panc4). *Ann. Oncol.* **2012**, *23*, 1880–1888. [[CrossRef](#)]
- Lowenfels, A.B.; Maisonneuve, P.; DiMagno, E.P.; Elitsur, Y.; Gates, L.K.; Perrault, J.; Whitcomb, D.C. Hereditary Pancreatitis and the Risk of Pancreatic Cancer. International Hereditary Pancreatitis Study Group. *J. Natl. Cancer Inst.* **1997**, *89*, 442–446. [[CrossRef](#)]
- Chari, S.T.; Leibson, C.L.; Rabe, K.G.; Timmons, L.J.; Ransom, J.; de Andrade, M.; Petersen, G.M. Pancreatic Cancer-Associated Diabetes Mellitus: Prevalence and Temporal Association with Diagnosis of Cancer. *Gastroenterology* **2008**, *134*, 95–101. [[CrossRef](#)] [[PubMed](#)]
- Chen, X.-Z.; Wang, R.; Chen, H.-N.; Hu, J.-K. Cytotoxin-Associated Gene A-Negative Strains of Helicobacter Pylori as a Potential Risk Factor of Pancreatic Cancer: A Meta-Analysis Based on Nested Case-Control Studies. *Pancreas* **2015**, *44*, 1340–1344. [[CrossRef](#)] [[PubMed](#)]
- Neoptolemos, J.P.; Urrutia, R.; Abbruzzese, J.L.; Büchler, M.W. *Pancreatic Cancer*; Springer: Berlin/Heidelberg, Germany, 2018; ISBN 9781493971930.
- Oettle, H.; Post, S.; Neuhaus, P.; Gellert, K.; Langrehr, J.; Ridwelski, K.; Schramm, H.; Fahlke, J.; Zuelke, C.; Burkart, C.; et al. Adjuvant Chemotherapy with Gemcitabine vs. Observation in Patients Undergoing Curative-Intent Resection of Pancreatic Cancer: A Randomized Controlled Trial. *J. Am. Med. Assoc.* **2007**, *297*, 267–277. [[CrossRef](#)] [[PubMed](#)]
- Neoptolemos, J.P.; Stocken, D.D.; Bassi, C.; Ghaneh, P.; Cunningham, D.; Goldstein, D.; Padbury, R.; Moore, M.J.; Gallinger, S.; Mariette, C.; et al. Adjuvant Chemotherapy with Fluorouracil plus Folinic Acid vs. Gemcitabine Following Pancreatic Cancer Resection: A Randomized Controlled Trial. *JAMA J. Am. Med. Assoc.* **2010**, *304*, 1073–1081. [[CrossRef](#)] [[PubMed](#)]
- Neoptolemos, J.P.; Palmer, D.; Ghaneh, P.; Valle, J.W.; Cunningham, D.; Wadsley, J.; Meyer, T.; Anthony, A.; Glimelius, B.; Falk, S.; et al. ESPAC-4: A Multicenter, International, Open-Label Randomized Controlled Phase III Trial of Adjuvant Combination

- Chemotherapy of Gemcitabine (GEM) and Capecitabine (CAP) versus Monotherapy Gemcitabine in Patients with Resected Pancreatic Ductal Adenocarcin. *J. Clin. Oncol.* **2016**, *34*. [[CrossRef](#)]
17. Vera, R.; Dotor, E.; Feliu, J.; González, E.; Laquente, B.; Macarulla, T.; Martínez, E.; Maurel, J.; Salgado, M.; Manzano, J.L. SEOM Clinical Guideline for the Treatment of Pancreatic Cancer. *Clin. Transl. Oncol.* **2016**, *18*, 1172–1178. [[CrossRef](#)]
 18. Mukherjee, S.; Hurt, C.N.; Bridgewater, J.; Falk, S.; Cummins, S.; Wasan, H.; Crosby, T.; Jephcott, C.; Roy, R.; Radhakrishna, G.; et al. Gemcitabine-Based or Capecitabine-Based Chemoradiotherapy for Locally Advanced Pancreatic Cancer (SCALOP): A Multicentre, Randomised, Phase 2 Trial. *Lancet Oncol.* **2013**, *14*, 317–326. [[CrossRef](#)]
 19. Hammel, P.; Huguet, F.; Van Laethem, J.-L.; Goldstein, D.; Glimelius, B.; Artru, P.; Borbath, I.; Bouche, O.; Shannon, J.; André, T.; et al. Comparison of Chemoradiotherapy (CRT) and Chemotherapy (CT) in Patients with a Locally Advanced Pancreatic Cancer (LAPC) Controlled after 4 Months of Gemcitabine with or without Erlotinib: Final Results of the International Phase III LAP 07 Study. *J. Clin. Oncol.* **2013**, *31*. [[CrossRef](#)]
 20. Zeng, S.; Pöttler, M.; Lan, B.; Grützmann, R.; Pilarsky, C.; Yang, H. Chemoresistance in Pancreatic Cancer. *Int. J. Mol. Sci.* **2019**, *20*, 4504. [[CrossRef](#)]
 21. Ioannides, C.G.; Whiteside, T.L. T Cell Recognition of Human Tumors: Implications for Molecular Immunotherapy of Cancer. *Clin. Immunol. Immunopathol.* **1993**, *66*, 91–106. [[CrossRef](#)]
 22. Apte, M.V.; Xu, Z.; Pothula, S.; Goldstein, D.; Pirola, R.C.; Wilson, J.S. Pancreatic Cancer: The Microenvironment Needs Attention Too! *Pancreatology* **2015**, *15*, S32–S38. [[CrossRef](#)] [[PubMed](#)]
 23. Chang, J.H.; Jiang, Y.; Pillarisetty, V.G. Role of Immune Cells in Pancreatic Cancer from Bench to Clinical Application: An Updated Review. *Medicine* **2016**, *95*, e5541. [[CrossRef](#)] [[PubMed](#)]
 24. Roberts, N.J.; Norris, A.L.; Petersen, G.M.; Bondy, M.L.; Brand, R.; Gallinger, S.; Kurtz, R.C.; Olson, S.H.; Rustgi, A.K.; Schwartz, A.G.; et al. Whole Genome Sequencing Defines the Genetic Heterogeneity of Familial Pancreatic Cancer. *Cancer Discov.* **2016**, *6*, 166–175. [[CrossRef](#)] [[PubMed](#)]
 25. Pothula, S.P.; Pirola, R.C.; Wilson, J.S.; Apte, M.V. Pancreatic Stellate Cells: Aiding and Abetting Pancreatic Cancer Progression. *Pancreatology* **2020**, *20*, 409–418. [[CrossRef](#)] [[PubMed](#)]
 26. Xue, R.; Jia, K.; Wang, J.; Yang, L.; Wang, Y.; Gao, L.; Hao, J. A Rising Star in Pancreatic Diseases: Pancreatic Stellate Cells. *Front. Physiol.* **2018**, *9*, 754. [[CrossRef](#)]
 27. Che, M.; Kweon, S.-M.; Teo, J.-L.; Yuan, Y.-C.; Melstrom, L.G.; Waldron, R.T.; Lugea, A.; Urrutia, R.A.; Pandol, S.J.; Lai, K.K.Y. Targeting the CBP/ β -Catenin Interaction to Suppress Activation of Cancer-Promoting Pancreatic Stellate Cells. *Cancers* **2020**, *12*, 1476. [[CrossRef](#)]
 28. Ikenaga, N.; Ohuchida, K.; Mizumoto, K.; Cui, L.; Kayashima, T.; Morimatsu, K.; Moriyama, T.; Nakata, K.; Fujita, H.; Tanaka, M. CD10+ Pancreatic Stellate Cells Enhance the Progression of Pancreatic Cancer. *Gastroenterology* **2010**, *139*, 1041–1051. [[CrossRef](#)]
 29. Zha, M.; Xu, W.; Zhai, Q.; Li, F.; Chen, B.; Sun, Z. High Glucose Aggravates the Detrimental Effects of Pancreatic Stellate Cells on Beta-Cell Function. *Int. J. Endocrinol.* **2014**, *2014*, 165612. [[CrossRef](#)]
 30. Li, F.-F.; Chen, B.-J.; Li, W.; Li, L.; Zha, M.; Zhou, S.; Bachem, M.G.; Sun, Z.-L. Islet Stellate Cells Isolated from Fibrotic Islet of Goto-Kakizaki Rats Affect Biological Behavior of Beta-Cell. *J. Diabetes Res.* **2016**, *2016*, 6924593. [[CrossRef](#)]
 31. Lee, E.; Ryu, G.R.; Ko, S.-H.; Ahn, Y.-B.; Song, K.-H. A Role of Pancreatic Stellate Cells in Islet Fibrosis and β -Cell Dysfunction in Type 2 Diabetes Mellitus. *Biochem. Biophys. Res. Commun.* **2017**, *485*, 328–334. [[CrossRef](#)]
 32. Jang, J.-E.; Hajdu, C.H.; Liot, C.; Miller, G.; Dustin, M.L.; Bar-Sagi, D. Crosstalk between Regulatory T Cells and Tumor-Associated Dendritic Cells Negates Anti-Tumor Immunity in Pancreatic Cancer. *Cell Rep.* **2017**, *20*, 558–571. [[CrossRef](#)] [[PubMed](#)]
 33. Aykut, B.; Chen, R.; Miller, G. Regulatory T Cells Keep Pancreatic Cancer at Bay. *Cancer Discov.* **2020**, *10*, 345–347. [[CrossRef](#)] [[PubMed](#)]
 34. Shevchenko, I.; Karakhanova, S.; Soltek, S.; Link, J.; Bayry, J.; Werner, J.; Umansky, V.; Bazhin, A.V. Low-Dose Gemcitabine Depletes Regulatory T Cells and Improves Survival in the Orthotopic Panc02 Model of Pancreatic Cancer. *Int. J. Cancer* **2013**, *133*, 98–107. [[CrossRef](#)] [[PubMed](#)]
 35. Cheng, H.; Luo, G.; Lu, Y.; Jin, K.; Guo, M.; Xu, J.; Long, J.; Liu, L.; Yu, X.; Liu, C. The Combination of Systemic Inflammation-Based Marker NLR and Circulating Regulatory T Cells Predicts the Prognosis of Resectable Pancreatic Cancer Patients. *Pancreatology* **2016**, *16*, 1080–1084. [[CrossRef](#)]
 36. Liu, C.-Y.; Xu, J.-Y.; Shi, X.-Y.; Huang, W.; Ruan, T.-Y.; Xie, P.; Ding, J.-L. M2-Polarized Tumor-Associated Macrophages Promoted Epithelial-Mesenchymal Transition in Pancreatic Cancer Cells, Partially through TLR4/IL-10 Signaling Pathway. *Lab. Invest.* **2013**, *93*, 844–854. [[CrossRef](#)]
 37. Meng, F.; Li, C.; Li, W.; Gao, Z.; Guo, K.; Song, S. Interaction between Pancreatic Cancer Cells and Tumor-Associated Macrophages Promotes the Invasion of Pancreatic Cancer Cells and the Differentiation and Migration of Macrophages. *IUBMB Life* **2014**, *66*, 835–846. [[CrossRef](#)]
 38. Malmberg, K.-J. Effective Immunotherapy against Cancer: A Question of Overcoming Immune Suppression and Immune Escape? *Cancer Immunol. Immunother.* **2004**, *53*, 879–892. [[CrossRef](#)]
 39. Shen, Z.; Seppänen, H.; Kauttu, T.; Vainionpää, S.; Ye, Y.; Wang, S.; Mustonen, H.; Puolakkainen, P. Vasohibin-1 Expression Is Regulated by Transforming Growth Factor- β /Bone Morphogenic Protein Signaling Pathway Between Tumor-Associated Macrophages and Pancreatic Cancer Cells. *J. Interferon. Cytokine Res.* **2013**, *33*, 428–433. [[CrossRef](#)]

40. Hu, H.; Hang, J.-J.; Han, T.; Zhuo, M.; Jiao, F.; Wang, L.-W. The M2 Phenotype of Tumor-Associated Macrophages in the Stroma Confers a Poor Prognosis in Pancreatic Cancer. *Tumour Biol.* **2016**, *37*, 8657–8664. [[CrossRef](#)]
41. Incio, J.; Suboj, P.; Chin, S.M.; Vardam-Kaur, T.; Liu, H.; Hato, T.; Babykutty, S.; Chen, I.; Deshpande, V.; Jain, R.K.; et al. Metformin Reduces Desmoplasia in Pancreatic Cancer by Reprogramming Stellate Cells and Tumor-Associated Macrophages. *PLoS ONE* **2015**, *10*, e0141392. [[CrossRef](#)]
42. Liu, S.-H.; Yu, J.; Creeden, J.F.; Sutton, J.M.; Markowiak, S.; Sanchez, R.; Nemunaitis, J.; Kalinoski, A.; Zhang, J.-T.; Damoiseaux, R.; et al. Repurposing Metformin, Simvastatin and Digoxin as a Combination for Targeted Therapy for Pancreatic Ductal Adenocarcinoma. *Cancer Lett.* **2020**, *491*, 97–107. [[CrossRef](#)] [[PubMed](#)]
43. Liu, Q.; Li, Y.; Niu, Z.; Zong, Y.; Wang, M.; Yao, L.; Lu, Z.; Liao, Q.; Zhao, Y. Atorvastatin (Lipitor) Attenuates the Effects of Aspirin on Pancreatic Cancerogenesis and the Chemotherapeutic Efficacy of Gemcitabine on Pancreatic Cancer by Promoting M2 Polarized Tumor Associated Macrophages. *J. Exp. Clin. Cancer Res.* **2016**, *35*, 33. [[CrossRef](#)] [[PubMed](#)]
44. Gabrilovich, D.I.; Nagaraj, S. Myeloid-Derived Suppressor Cells as Regulators of the Immune System. *Nat. Rev. Immunol.* **2009**, *9*, 162–174. [[CrossRef](#)] [[PubMed](#)]
45. Talmadge, J.E.; Gabrilovich, D.I. History of Myeloid-Derived Suppressor Cells. *Nat. Rev. Cancer* **2013**, *13*, 739–752. [[CrossRef](#)] [[PubMed](#)]
46. Sangaletti, S.; Talarico, G.; Chiodoni, C.; Cappetti, B.; Botti, L.; Portararo, P.; Gulino, A.; Consonni, F.M.; Sica, A.; Randon, G.; et al. SPARC Is a New Myeloid-Derived Suppressor Cell Marker Licensing Suppressive Activities. *Front. Immunol.* **2019**, *10*. [[CrossRef](#)] [[PubMed](#)]
47. Karakhanova, S.; Link, J.; Heinrich, M.; Shevchenko, I.; Yang, Y.; Hassenpflug, M.; Bunge, H.; von Ahn, K.; Brecht, R.; Mathes, A.; et al. Characterization of Myeloid Leukocytes and Soluble Mediators in Pancreatic Cancer: Importance of Myeloid-Derived Suppressor Cells. *Oncoimmunology* **2015**, *4*, e998519. [[CrossRef](#)] [[PubMed](#)]
48. Song, J.; Lee, J.; Kim, J.; Jo, S.; Kim, Y.J.; Baek, J.E.; Kwon, E.-S.; Lee, K.-P.; Yang, S.; Kwon, K.-S.; et al. Pancreatic Adenocarcinoma Up-Regulated Factor (PAUF) Enhances the Accumulation and Functional Activity of Myeloid-Derived Suppressor Cells (MDSCs) in Pancreatic Cancer. *Oncotarget* **2016**, *7*, 51840–51853. [[CrossRef](#)]
49. Markowitz, J.; Brooks, T.R.; Duggan, M.C.; Paul, B.K.; Pan, X.; Wei, L.; Abrams, Z.; Luedke, E.; Lesinski, G.B.; Mundy-Bosse, B.; et al. Patients with Pancreatic Adenocarcinoma Exhibit Elevated Levels of Myeloid-Derived Suppressor Cells upon Progression of Disease. *Cancer Immunol. Immunother.* **2015**, *64*, 149–159. [[CrossRef](#)]
50. Yang, X.; Lu, Y.; Hang, J.; Zhang, J.; Zhang, T.; Huo, Y.; Liu, J.; Lai, S.; Luo, D.; Wang, L.; et al. Lactate-Modulated Immunosuppression of Myeloid-Derived Suppressor Cells Contributes to the Radioresistance of Pancreatic Cancer. *Cancer Immunol. Res.* **2020**, *8*, 1440–1451. [[CrossRef](#)]
51. Isherwood, J.; Arshad, A.; Chung, W.Y.; Runau, F.; Cooke, J.; Pollard, C.; Howells, L.; Fishwick, J.; Thompson, J.; Metcalfe, M.; et al. Myeloid Derived Suppressor Cells Are Reduced and T Regulatory Cells Stabilised in Patients with Advanced Pancreatic Cancer Treated with Gemcitabine and Intravenous Omega 3. *Ann. Transl. Med.* **2020**, *8*, 172. [[CrossRef](#)]
52. Ijichi, H.; Chytil, A.; Gorska, A.E.; Aakre, M.E.; Bierie, B.; Tada, M.; Mohri, D.; Miyabayashi, K.; Asaoka, Y.; Maeda, S.; et al. Inhibiting Cxcr2 Disrupts Tumor-Stromal Interactions and Improves Survival in a Mouse Model of Pancreatic Ductal Adenocarcinoma. *J. Clin. Invest.* **2011**, *121*, 4106–4117. [[CrossRef](#)] [[PubMed](#)]
53. Cappello, P.; Tonoli, E.; Curto, R.; Giordano, D.; Giovarelli, M.; Novelli, F. Anti- α -Enolase Antibody Limits the Invasion of Myeloid-Derived Suppressor Cells and Attenuates Their Restraining Effector T Cell Response. *Oncoimmunology* **2016**, *5*, e1112940. [[CrossRef](#)] [[PubMed](#)]
54. Nagaraj, S.; Youn, J.-I.; Weber, H.; Iclozan, C.; Lu, L.; Cotter, M.J.; Meyer, C.; Becerra, C.R.; Fishman, M.; Antonia, S.; et al. Anti-Inflammatory Triterpenoid Blocks Immune Suppressive Function of MDSCs and Improves Immune Response in Cancer. *Clin. Cancer Res.* **2010**, *16*, 1812–1823. [[CrossRef](#)] [[PubMed](#)]
55. Ling, X.; Konopleva, M.; Zeng, Z.; Ruvolo, V.; Stephens, L.C.; Schober, W.; McQueen, T.; Dietrich, M.; Madden, T.L.; Andreeff, M. The Novel Triterpenoid C-28 Methyl Ester of 2-Cyano-3, 12-Dioxoolen-1, 9-Dien-28-Oic Acid Inhibits Metastatic Murine Breast Tumor Growth through Inactivation of STAT3 Signaling. *Cancer Res.* **2007**, *67*, 4210–4218. [[CrossRef](#)] [[PubMed](#)]
56. Martinez-Useros, J.; Garcia-Foncillas, J. Can Molecular Biomarkers Change the Paradigm of Pancreatic Cancer Prognosis? *Biomed. Res. Int.* **2016**, *2016*, 4873089. [[CrossRef](#)] [[PubMed](#)]
57. Martinez-Useros, J.; Garcia-Foncillas, J. The Role of BRCA2 Mutation Status as Diagnostic, Predictive, and Prognosis Biomarker for Pancreatic Cancer. *Biomed. Res. Int.* **2016**, *2016*, 1869304. [[CrossRef](#)]
58. Sabharwal, S.S.; Schumacker, P.T. Mitochondrial ROS in Cancer: Initiators, Amplifiers or an Achilles' Heel? *Nat. Rev. Cancer* **2014**, *14*, 709–721. [[CrossRef](#)] [[PubMed](#)]
59. Bailey, P.; Chang, D.K.; Nones, K.; Johns, A.L.; Patch, A.-M.; Gingras, M.-C.; Miller, D.K.; Christ, A.N.; Bruxner, T.J.C.; Quinn, M.C.; et al. Genomic Analyses Identify Molecular Subtypes of Pancreatic Cancer. *Nature* **2016**, *531*, 47–52. [[CrossRef](#)]
60. Moffitt, R.A.; Marayati, R.; Flate, E.L.; Volmar, K.E.; Loeza, S.G.H.; Hoadley, K.A.; Rashid, N.U.; Williams, L.A.; Eaton, S.C.; Chung, A.H.; et al. Virtual Microdissection Identifies Distinct Tumor- and Stroma-Specific Subtypes of Pancreatic Ductal Adenocarcinoma. *Nat. Genet.* **2015**, *47*, 1168–1178. [[CrossRef](#)]
61. Collisson, E.A.; Sadanandam, A.; Olson, P.; Gibb, W.J.; Truitt, M.; Gu, S.; Cooc, J.; Weinkle, J.; Kim, G.E.; Jakkula, L.; et al. Subtypes of Pancreatic Ductal Adenocarcinoma and Their Differing Responses to Therapy. *Nat. Med.* **2011**, *17*, 500–503. [[CrossRef](#)]



62. Feng, Y.-F.; Chen, J.-Y.; Chen, H.-Y.; Wang, T.-G.; Shi, D.; Lu, Y.-F.; Pan, Y.; Shao, C.-W.; Yu, R.-S. 110 Patients with Adenosquamous Carcinomas of the Pancreas (PASC): Imaging Differentiation of Small (≤ 3 Cm) versus Large (>3 Cm) Tumors. *Abdom. Radiol. (N. Y.)* **2019**, *44*, 2466–2473. [[CrossRef](#)] [[PubMed](#)]
63. Niger, M.; Prisciandaro, M.; Antista, M.; Monica, M.A.T.; Cattaneo, L.; Prinzi, N.; Manglaviti, S.; Nichetti, F.; Brambilla, M.; Torchio, M.; et al. One Size Does Not Fit All for Pancreatic Cancers: A Review on Rare Histologies and Therapeutic Approaches. *World J. Gastrointest. Oncol.* **2020**, *12*, 833–849. [[CrossRef](#)] [[PubMed](#)]
64. Fang, Y.; Su, Z.; Xie, J.; Xue, R.; Ma, Q.; Li, Y.; Zhao, Y.; Song, Z.; Lu, X.; Li, H.; et al. Genomic Signatures of Pancreatic Adenosquamous Carcinoma (PASC). *J. Pathol.* **2017**, *243*, 155–159. [[CrossRef](#)] [[PubMed](#)]
65. Bosman, F.T.; Carneiro, F.; Hruban, R.H.; Theise, N.D. *WHO Classification of Tumours of the Digestive System—NLM Catalog—NCBI*; IARC Press: Lyon, France, 2010.
66. Cancer Genome Atlas Research Network. By The Cancer Genome Atlas Research Network. Integrated Genomic Characterization of Pancreatic Ductal Adenocarcinoma. *Cancer Cell* **2017**, *32*, 185–203. [[CrossRef](#)] [[PubMed](#)]
67. Engelmann, D.; Pützer, B.M. Emerging from the Shade of P53 Mutants: N-Terminally Truncated Variants of the P53 Family in EMT Signaling and Cancer Progression. *Sci. Signal* **2014**, *7*, re9. [[CrossRef](#)] [[PubMed](#)]
68. Miller, B.W.; Morton, J.P.; Pinese, M.; Saturno, G.; Jamieson, N.B.; McGhee, E.; Timpson, P.; Leach, J.; McGarry, L.; Shanks, E.; et al. Targeting the LOX/Hypoxia Axis Reverses Many of the Features That Make Pancreatic Cancer Deadly: Inhibition of LOX Abrogates Metastasis and Enhances Drug Efficacy. *EMBO Mol. Med.* **2015**, *7*, 1063–1076. [[CrossRef](#)]
69. Hosein, A.N.; Brekken, R.A.; Maitra, A. Pancreatic Cancer Stroma: An Update on Therapeutic Targeting Strategies. *Nat. Rev. Gastroenterol. Hepatol.* **2020**, *17*, 487–505. [[CrossRef](#)]
70. Bristow, R.G.; Hill, R.P. Hypoxia and Metabolism. Hypoxia, DNA Repair and Genetic Instability. *Nat. Rev. Cancer* **2008**, *8*, 180–192. [[CrossRef](#)]
71. Kitamoto, S.; Yokoyama, S.; Higashi, M.; Yamada, N.; Takao, S.; Yonezawa, S. MUC1 Enhances Hypoxia-Driven Angiogenesis through the Regulation of Multiple Proangiogenic Factors. *Oncogene* **2013**, *32*, 4614–4621. [[CrossRef](#)]
72. Biankin, A.V.; Kench, J.G.; Colvin, E.K.; Segara, D.; Scarlett, C.J.; Nguyen, N.Q.; Chang, D.K.; Morey, A.L.; Lee, C.-S.; Pinese, M.; et al. Expression of S100A2 Calcium-Binding Protein Predicts Response to Pancreatectomy for Pancreatic Cancer. *Gastroenterology* **2009**, *137*, 558–568. [[CrossRef](#)]
73. Mews, P.; Phillips, P.; Fahmy, R.; Korsten, M.; Pirola, R.; Wilson, J.; Apte, M. Pancreatic Stellate Cells Respond to Inflammatory Cytokines: Potential Role in Chronic Pancreatitis. *Gut* **2002**, *50*, 535–541. [[CrossRef](#)] [[PubMed](#)]
74. Masamune, A.; Satoh, M.; Kikuta, K.; Suzuki, N.; Shimosegawa, T. Activation of JAK-STAT Pathway Is Required for Platelet-Derived Growth Factor-Induced Proliferation of Pancreatic Stellate Cells. *World J. Gastroenterol.* **2005**, *11*, 3385–3391. [[CrossRef](#)] [[PubMed](#)]
75. Somerville, T.D.; Biffi, G.; Daßler-Plenker, J.; Hur, S.K.; He, X.-Y.; Vance, K.E.; Miyabayashi, K.; Xu, Y.; Maia-Silva, D.; Klingbeil, O.; et al. Squamous Trans-Differentiation of Pancreatic Cancer Cells Promotes Stromal Inflammation. *Elife* **2020**, *9*, e53381. [[CrossRef](#)] [[PubMed](#)]
76. Öhlund, D.; Handy-Santana, A.; Biffi, G.; Elyada, E.; Almeida, A.S.; Ponz-Sarvisé, M.; Corbo, V.; Oni, T.E.; Hearn, S.A.; Lee, E.J.; et al. Distinct Populations of Inflammatory Fibroblasts and Myofibroblasts in Pancreatic Cancer. *J. Exp. Med.* **2017**, *214*, 579–596. [[CrossRef](#)]
77. Lankadasari, M.B.; Mukhopadhyay, P.; Mohammed, S.; Harikumar, K.B. TAMing Pancreatic Cancer: Combat with a Double Edged Sword. *Mol. Cancer* **2019**, *18*, 48. [[CrossRef](#)]
78. Ireland, L.; Santos, A.; Ahmed, M.S.; Rainer, C.; Nielsen, S.R.; Quaranta, V.; Weyer-Czernilofsky, U.; Engle, D.D.; Perez-Mancera, P.A.; Coupland, S.E.; et al. Chemoresistance in Pancreatic Cancer Is Driven by Stroma-Derived Insulin-Like Growth Factors. *Cancer Res.* **2016**, *76*, 6851–6863. [[CrossRef](#)]
79. Dalin, S.; Sullivan, M.R.; Lau, A.N.; Grauman-Boss, B.; Mueller, H.S.; Kreidl, E.; Fenoglio, S.; Luengo, A.; Lees, J.A.; Vander Heiden, M.G.; et al. Deoxycytidine Release from Pancreatic Stellate Cells Promotes Gemcitabine Resistance. *Cancer Res.* **2019**, *79*, 5723–5733. [[CrossRef](#)]
80. Al-Assar, O.; Demiciorglu, F.; Lunardi, S.; Gaspar-Carvalho, M.M.; McKenna, W.G.; Muschel, R.M.; Brunner, T.B. Contextual Regulation of Pancreatic Cancer Stem Cell Phenotype and Radioresistance by Pancreatic Stellate Cells. *Radiother. Oncol.* **2014**, *111*, 243–251. [[CrossRef](#)]
81. Panni, R.Z.; Sanford, D.E.; Belt, B.A.; Mitchem, J.B.; Worley, L.A.; Goetz, B.D.; Mukherjee, P.; Wang-Gillam, A.; Link, D.C.; Denardo, D.G.; et al. Tumor-Induced STAT3 Activation in Monocytic Myeloid-Derived Suppressor Cells Enhances Stemness and Mesenchymal Properties in Human Pancreatic Cancer. *Cancer Immunol. Immunother.* **2014**, *63*, 513–528. [[CrossRef](#)]
82. Feig, C.; Jones, J.O.; Kraman, M.; Wells, R.J.B.; Deonarine, A.; Chan, D.S.; Connell, C.M.; Roberts, E.W.; Zhao, Q.; Caballero, O.L.; et al. Targeting CXCL12 from FAP-Expressing Carcinoma-Associated Fibroblasts Synergizes with Anti-PD-L1 Immunotherapy in Pancreatic Cancer. *Proc. Natl. Acad. Sci. USA* **2013**, *110*, 20212–20217. [[CrossRef](#)]
83. Jenkins, R.W.; Barbie, D.A.; Flaherty, K.T. Mechanisms of Resistance to Immune Checkpoint Inhibitors. *Br. J. Cancer* **2018**, *118*, 9–16. [[CrossRef](#)]
84. Holmgaard, R.B.; Zamarin, D.; Munn, D.H.; Wolchok, J.D.; Allison, J.P. Indoleamine 2,3-Dioxygenase Is a Critical Resistance Mechanism in Antitumor T Cell Immunotherapy Targeting CTLA-4. *J. Exp. Med.* **2013**, *210*, 1389–1402. [[CrossRef](#)] [[PubMed](#)]

85. Blair, A.B.; Kleponis, J.; Thomas, D.L.; Muth, S.T.; Murphy, A.G.; Kim, V.; Zheng, L. IDO1 Inhibition Potentiates Vaccine-Induced Immunity against Pancreatic Adenocarcinoma. *J. Clin. Investig.* **2019**, *129*, 1742–1755. [[CrossRef](#)] [[PubMed](#)]
86. Peng, J.; Sun, B.-F.; Chen, C.-Y.; Zhou, J.-Y.; Chen, Y.-S.; Chen, H.; Liu, L.; Huang, D.; Jiang, J.; Cui, G.-S.; et al. Single-Cell RNA-Seq Highlights Intra-Tumoral Heterogeneity and Malignant Progression in Pancreatic Ductal Adenocarcinoma. *Cell Res.* **2019**, *29*, 725–738. [[CrossRef](#)] [[PubMed](#)]
87. Shi, S.; Xu, J.; Zhang, B.; Ji, S.; Xu, W.; Liu, J.; Jin, K.; Liang, D.; Liang, C.; Liu, L.; et al. VEGF Promotes Glycolysis in Pancreatic Cancer via HIF1 α Up-Regulation. *Curr. Mol. Med.* **2016**, *16*, 394–403. [[CrossRef](#)]
88. Hale, M.A.; Kagami, H.; Shi, L.; Holland, A.M.; Elsässer, H.-P.; Hammer, R.E.; MacDonald, R.J. The Homeodomain Protein PDX1 Is Required at Mid-Pancreatic Development for the Formation of the Exocrine Pancreas. *Dev. Biol.* **2005**, *286*, 225–237. [[CrossRef](#)]
89. Patra, K.C.; Bardeesy, N.; Mizukami, Y. Diversity of Precursor Lesions For Pancreatic Cancer: The Genetics and Biology of Intraductal Papillary Mucinous Neoplasm. *Clin. Transl. Gastroenterol.* **2017**, *8*, e86. [[CrossRef](#)]
90. Baker, M.L.; Seeley, E.S.; Pai, R.; Suriawinata, A.A.; Mino-Kenudson, M.; Zamboni, G.; Klöppel, G.; Longnecker, D.S. Invasive Mucinous Cystic Neoplasms of the Pancreas. *Exp. Mol. Pathol.* **2012**, *93*, 345–349. [[CrossRef](#)]
91. Martinelli, P.; Carrillo-de Santa Pau, E.; Cox, T.; Sainz, B.; Dusetti, N.; Greenhalf, W.; Rinaldi, L.; Costello, E.; Ghaneh, P.; Malats, N.; et al. GATA6 Regulates EMT and Tumour Dissemination, and Is a Marker of Response to Adjuvant Chemotherapy in Pancreatic Cancer. *Gut* **2017**, *66*, 1665–1676. [[CrossRef](#)]
92. Suh, H.; Pillai, K.; Morris, D.L. Mucins in Pancreatic Cancer: Biological Role, Implications in Carcinogenesis and Applications in Diagnosis and Therapy. *Am. J. Cancer Res.* **2017**, *7*, 1372–1383.
93. Pompella, L.; Tirino, G.; Pappalardo, A.; Caterino, M.; Ventriglia, A.; Nacca, V.; Orditura, M.; Ciardiello, F.; De Vita, F. Pancreatic Cancer Molecular Classifications: From Bulk Genomics to Single Cell Analysis. *Int. J. Mol. Sci.* **2020**, *21*, 2814. [[CrossRef](#)] [[PubMed](#)]
94. Cheng, H.; Luo, G.; Jin, K.; Fan, Z.; Huang, Q.; Gong, Y.; Xu, J.; Yu, X.; Liu, C. Kras Mutation Correlating with Circulating Regulatory T Cells Predicts the Prognosis of Advanced Pancreatic Cancer Patients. *Cancer Med.* **2020**, *9*, 2153–2159. [[CrossRef](#)] [[PubMed](#)]
95. Bauer, C.A.; Kim, E.Y.; Marangoni, F.; Carrizosa, E.; Claudio, N.M.; Mempel, T.R. Dynamic Treg Interactions with Intratumoral APCs Promote Local CTL Dysfunction. *J. Clin. Invest.* **2014**, *124*, 2425–2440. [[CrossRef](#)] [[PubMed](#)]
96. Trivedi, P.M.; Fynch, S.; Kennedy, L.M.; Chee, J.; Krishnamurthy, B.; O'Reilly, L.A.; Strasser, A.; Kay, T.W.H.; Thomas, H.E. Soluble FAS Ligand Is Not Required for Pancreatic Islet Inflammation or Beta-Cell Destruction in Non-Obese Diabetic Mice. *Cell Death Discov.* **2019**, *5*, 136. [[CrossRef](#)] [[PubMed](#)]
97. Sideras, K.; Braat, H.; Kwekkeboom, J.; van Eijck, C.H.; Peppelenbosch, M.P.; Sleijfer, S.; Bruno, M. Role of the Immune System in Pancreatic Cancer Progression and Immune Modulating Treatment Strategies. *Cancer Treat. Rev.* **2014**, *40*, 513–522. [[CrossRef](#)] [[PubMed](#)]
98. Jiao, Y.; Yonescu, R.; Offerhaus, G.J.A.; Klimstra, D.S.; Maitra, A.; Eshleman, J.R.; Herman, J.G.; Poh, W.; Pelosof, L.; Wolfgang, C.L.; et al. Whole-Exome Sequencing of Pancreatic Neoplasms with Acinar Differentiation. *J. Pathol.* **2014**, *232*, 428–435. [[CrossRef](#)]
99. Furukawa, T.; Sakamoto, H.; Takeuchi, S.; Ameri, M.; Kuboki, Y.; Yamamoto, T.; Hatori, T.; Yamamoto, M.; Sugiyama, M.; Ohike, N.; et al. Whole Exome Sequencing Reveals Recurrent Mutations in BRCA2 and FAT Genes in Acinar Cell Carcinomas of the Pancreas. *Sci. Rep.* **2015**, *5*, 8829. [[CrossRef](#)]
100. Von Figura, G.; Morris, J.P.; Wright, C.V.E.; Hebrok, M. Nr5a2 Maintains Acinar Cell Differentiation and Constrains Oncogenic Kras-Mediated Pancreatic Neoplastic Initiation. *Gut* **2014**, *63*, 656–664. [[CrossRef](#)]
101. Hale, M.A.; Swift, G.H.; Hoang, C.Q.; Deering, T.G.; Masui, T.; Lee, Y.-K.; Xue, J.; MacDonald, R.J. The Nuclear Hormone Receptor Family Member NR5A2 Controls Aspects of Multipotent Progenitor Cell Formation and Acinar Differentiation during Pancreatic Organogenesis. *Development* **2014**, *141*, 3123–3133. [[CrossRef](#)]
102. Mathison, A.; Liebl, A.; Bharucha, J.; Mukhopadhyay, D.; Lomberk, G.; Shah, V.; Urrutia, R. Pancreatic Stellate Cell Models for Transcriptional Studies of Desmoplasia-Associated Genes. *Pancreatology* **2010**, *10*, 505–516. [[CrossRef](#)]
103. Erkan, M.; Reiser-Erkan, C.; Michalski, C.W.; Deucker, S.; Sauliunaite, D.; Streit, S.; Esposito, I.; Friess, H.; Kleeff, J. Cancer-Stellate Cell Interactions Perpetuate the Hypoxia-Fibrosis Cycle in Pancreatic Ductal Adenocarcinoma. *Neoplasia* **2009**, *11*, 497–508. [[CrossRef](#)] [[PubMed](#)]
104. Wang, Z.; Li, Y.; Ahmad, A.; Banerjee, S.; Azmi, A.S.; Kong, D.; Sarkar, F.H. Pancreatic Cancer: Understanding and Overcoming Chemoresistance. *Nat. Rev. Gastroenterol. Hepatol.* **2011**, *8*, 27–33. [[CrossRef](#)] [[PubMed](#)]
105. Mekapogu, A.R.; Pothula, S.P.; Pirola, R.C.; Wilson, J.S.; Apte, M.V. Multifunctional Role of Pancreatic Stellate Cells in Pancreatic Cancer. *Ann. Pancreat. Cancer* **2019**, *2*. [[CrossRef](#)]
106. Franses, J.W.; Basar, O.; Kadayifci, A.; Yuksel, O.; Choz, M.; Kulkarni, A.S.; Tai, E.; Vo, K.D.; Arora, K.S.; Desai, N.; et al. Improved Detection of Circulating Epithelial Cells in Patients with Intraductal Papillary Mucinous Neoplasms. *Oncologist* **2018**, *23*, 1260. [[CrossRef](#)]
107. Lahat, G.; Lubezky, N.; Loewenstein, S.; Nizri, E.; Gan, S.; Pasmanik-Chor, M.; Hayman, L.; Barazowsky, E.; Ben-Haim, M.; Klausner, J.M. Epithelial-to-Mesenchymal Transition (EMT) in Intraductal Papillary Mucinous Neoplasm (IPMN) Is Associated with High Tumor Grade and Adverse Outcomes. *Ann. Surg. Oncol.* **2014**, *21*, S750–S757. [[CrossRef](#)]
108. Rooney, M.S.; Shukla, S.A.; Wu, C.J.; Getz, G.; Hacohen, N. Molecular and Genetic Properties of Tumors Associated with Local Immune Cytolytic Activity. *Cell* **2015**, *160*, 48–61. [[CrossRef](#)]

109. Yachida, S.; Jones, S.; Bozic, I.; Antal, T.; Leary, R.; Fu, B.; Kamiyama, M.; Hruban, R.H.; Eshleman, J.R.; Nowak, M.A.; et al. Distant Metastasis Occurs Late during the Genetic Evolution of Pancreatic Cancer. *Nature* **2010**, *467*, 1114–1117. [[CrossRef](#)]
110. A Phase I/II Study of a MUC1 Peptide Pulsed Autologous Dendritic Cell Vaccine as Adjuvant Therapy in Patients with Resected Pancreatic and Biliary Tumors—PubMed. Available online: <https://pubmed.ncbi.nlm.nih.gov/19129927/> (accessed on 11 November 2020).
111. Hu, G.; He, N.; Cai, C.; Cai, F.; Fan, P.; Zheng, Z.; Jin, X. HDAC3 Modulates Cancer Immunity via Increasing PD-L1 Expression in Pancreatic Cancer. *Pancreatology* **2019**, *19*, 383–389. [[CrossRef](#)]
112. Park, H.; Bang, J.-H.; Nam, A.-R.; Eun Park, J.; Hua Jin, M.; Bang, Y.-J.; Oh, D.-Y. Prognostic Implications of Soluble Programmed Death-Ligand 1 and Its Dynamics during Chemotherapy in Unresectable Pancreatic Cancer. *Sci. Rep.* **2019**, *9*, 11131. [[CrossRef](#)]
113. Saka, D.; Gökalp, M.; Piyade, B.; Cevik, N.C.; Arik Sever, E.; Unutmaz, D.; Ceyhan, G.O.; Demir, I.E.; Asimgil, H. Mechanisms of T-Cell Exhaustion in Pancreatic Cancer. *Cancers* **2020**, *12*, 2274. [[CrossRef](#)]
114. Yazdanifar, M.; Zhou, R.; Grover, P.; Williams, C.; Bose, M.; Moore, L.J.; Wu, S.-T.; Maher, J.; Dreau, D.; Mukherjee, A.P. Overcoming Immunological Resistance Enhances the Efficacy of A Novel Anti-TMUC1-CAR T Cell Treatment against Pancreatic Ductal Adenocarcinoma. *Cells* **2019**, *8*, 1070. [[CrossRef](#)] [[PubMed](#)]
115. Beatty, G.L.; Haas, A.R.; Maus, M.V.; Torigian, D.A.; Soulen, M.C.; Plesa, G.; Chew, A.; Zhao, Y.; Levine, B.L.; Albelda, S.M.; et al. Mesothelin-Specific Chimeric Antigen Receptor MRNA-Engineered T Cells Induce Anti-Tumor Activity in Solid Malignancies. *Cancer Immunol. Res.* **2014**, *2*, 112–120. [[CrossRef](#)] [[PubMed](#)]
116. Diaz Sanchez, A.; Ponferrada Diaz, Á.; Senosiain Labiano, M.; Huerta Madrigal, A. Hemorragia digestiva alta como presentación de un carcinoma acinar pancreático. *Gastroenterol. Hepatol.* **2006**, *29*, 380. [[CrossRef](#)]
117. Kordes, C.; Sawitzka, I.; Götze, S.; Häussinger, D. Stellate Cells from Rat Pancreas Are Stem Cells and Can Contribute to Liver Regeneration. *PLoS ONE* **2012**, *7*, e51878. [[CrossRef](#)] [[PubMed](#)]
118. Tang, D.; Wang, D.; Yuan, Z.; Xue, X.; Zhang, Y.; An, Y.; Chen, J.; Tu, M.; Lu, Z.; Wei, J.; et al. Persistent Activation of Pancreatic Stellate Cells Creates a Microenvironment Favorable for the Malignant Behavior of Pancreatic Ductal Adenocarcinoma. *Int. J. Cancer* **2013**, *132*, 993–1003. [[CrossRef](#)]
119. Masamune, A.; Kikuta, K.; Watanabe, T.; Satoh, K.; Hirota, M.; Shimosegawa, T. Hypoxia Stimulates Pancreatic Stellate Cells to Induce Fibrosis and Angiogenesis in Pancreatic Cancer. *Am. J. Physiol. Gastrointest. Liver Physiol.* **2008**, *295*, G709–G717. [[CrossRef](#)]
120. Miyamoto, H.; Murakami, T.; Tsuchida, K.; Sugino, H.; Miyake, H.; Tashiro, S. Tumor-Stroma Interaction of Human Pancreatic Cancer: Acquired Resistance to Anticancer Drugs and Proliferation Regulation Is Dependent on Extracellular Matrix Proteins. *Pancreas* **2004**, *28*, 38–44. [[CrossRef](#)]
121. Tian, B.; Wong, W.Y.; Uger, M.D.; Wisniewski, P.; Chao, H. Development and Characterization of a Camelid Single Domain Antibody-Urease Conjugate That Targets Vascular Endothelial Growth Factor Receptor 2. *Front. Immunol.* **2017**, *8*, 956. [[CrossRef](#)]
122. Le, D.T.; Wang-Gillam, A.; Picozzi, V.; Greten, T.F.; Crocenzi, T.; Springett, G.; Morse, M.; Zeh, H.; Cohen, D.; Fine, R.L.; et al. Safety and Survival With GVAX Pancreas Prime and *Listeria Monocytogenes*-Expressing Mesothelin (CRS-207) Boost Vaccines for Metastatic Pancreatic Cancer. *J. Clin. Oncol.* **2015**, *33*, 1325–1333. [[CrossRef](#)]
123. Roccaro, A.M.; Sacco, A.; Purschke, W.G.; Moschetta, M.; Buchner, K.; Maasch, C.; Zboralski, D.; Zöllner, S.; Vonhoff, S.; Mishima, Y.; et al. SDF-1 Inhibition Targets the Bone Marrow Niche for Cancer Therapy. *Cell Rep.* **2014**, *9*, 118–128. [[CrossRef](#)]

Review

Cancer Cells Resistance Shaping by Tumor Infiltrating Myeloid Cells

Marcin Domagala ^{1,2,3}, Chloé Laplagne ^{1,2,3}, Edouard Leveque ^{1,2,3}, Camille Laurent ^{1,2,3,4},
Jean-Jacques Fournié ^{1,2,3}, Eric Espinosa ^{1,2,3}  and Mary Poupot ^{1,2,3,*} 

- ¹ Centre de Recherches en Cancérologie de Toulouse, Inserm UMR1037, 31037 Toulouse, France; marcin.domagala@inserm.fr (M.D.); chloe.laplagne@inserm.fr (C.L.); edouard.leveque@inserm.fr (E.L.); Laurent.Camille@iuct-oncopole.fr (C.L.); jean-jacques.fournie@inserm.fr (J.-J.F.); eric.espinosa@inserm.fr (E.E.)
- ² Université Toulouse III Paul-Sabatier, 31400 Toulouse, France
- ³ ERL 5294 CNRS, 31037 Toulouse, France
- ⁴ IUCT-O, 31000 Toulouse, France
- * Correspondence: mary.poupot@inserm.fr; Tel.: +33-582741662

Simple Summary: The tumor is a complex system that is composed of tumor cells, themselves surrounded by many other different cell types. Among these cells, myeloid cells have to eliminate cancer cells to reduce tumor size, but they are also able, depending on the tumor stage, to favor tumor development. Therefore, different cellular interactions and soluble factors that are produced by all these cells can participate to maintain tumor cell survival and favor their proliferation, migration, and resistance to cytotoxic immune cells and therapies. This review aims to detail the physiological function of myeloid cells, their pathological function, and how they shape tumor cells to be resistant to apoptotic, to immune effector cells, and to therapies.

Abstract: Interactions between malignant cells and neighboring stromal and immune cells profoundly shape cancer progression. New forms of therapies targeting these cells have revolutionized the treatment of cancer. However, in order to specifically address each population, it was essential to identify and understand their individual roles in interaction between malignant cells, and the formation of the tumor microenvironment (TME). In this review, we focus on the myeloid cell compartment, a prominent, and heterogeneous group populating TME, which can initially exert an anti-tumoral effect, but with time actively participate in disease progression. Macrophages, dendritic cells, neutrophils, myeloid-derived suppressor cells, mast cells, eosinophils, and basophils act alone or in concert to shape tumor cells resistance through cellular interaction and/or release of soluble factors favoring survival, proliferation, and migration of tumor cells, but also immune-escape and therapy resistance.

Keywords: microenvironment; resistance; myeloid cells; cancer development



Citation: Domagala, M.; Laplagne, C.; Leveque, E.; Laurent, C.; Fournié, J.-J.; Espinosa, E.; Poupot, M. Cancer Cells Resistance Shaping by Tumor Infiltrating Myeloid Cells. *Cancers* **2021**, *13*, 165. <https://doi.org/10.3390/cancers13020165>

Received: 30 November 2020

Accepted: 30 December 2020

Published: 6 January 2021

Publisher's Note: MDPI stays neutral with regard to jurisdictional claims in published maps and institutional affiliations.



Copyright: © 2021 by the authors. Licensee MDPI, Basel, Switzerland. This article is an open access article distributed under the terms and conditions of the Creative Commons Attribution (CC BY) license (<https://creativecommons.org/licenses/by/4.0/>).

1. Introduction

Nowadays, tumor microenvironment (TME) is recognized as an essential element of tumor development and progression. It not only remains in constant contact with the tumor, but it also mediates complex dialog between malignant cells and surrounding tissues. The cellular components of this dynamic network are represented by normal and tumoral tissue-resident cells with a large proportion of recruited immune cells alongside: fibroblasts, neuroendocrine, adipose, endothelial, and mesenchymal cells [1]. All of the cellular and molecular actors of the TME are involved in carcinogenesis through the promotion of tumor: growth, dormancy, invasion, and metastasis. The infiltrating immune cells can be represented by lymphoid cells, such as: CD8, CD4, and $\gamma\delta$ T lymphocytes, B cells, and natural killer (NK) cells, and myeloid cells, such as: monocytes/macrophages, dendritic

cells (DC), neutrophils, myeloid-derived suppressor cells (MDSC), basophils/eosinophils, and mast cells. In the initial states of oncogenesis, all of these cell populations can help in the elimination of mutated cells. However, after the tumor dormancy and editing phase, the loss of oncoantigens and MHC lead to the immune escape, allowing for further tumor development [2]. TME, including immune cells, is then modified to actively support and promote cancerogenesis and shape the character of emerging tumors [3]. This review aims at summarizing the role of the tumor infiltrating immune cells and, particularly, myeloid cells shaping cancer cells resistance to apoptosis, immune response, and therapy. Following the text, the readers can refer to the figures that resume the role of the different tumor-associated myeloid cells in cancer cells survival, proliferation, and migration (Figure 1), and in cancer cells immune-escape and therapy resistance (Figure 2).

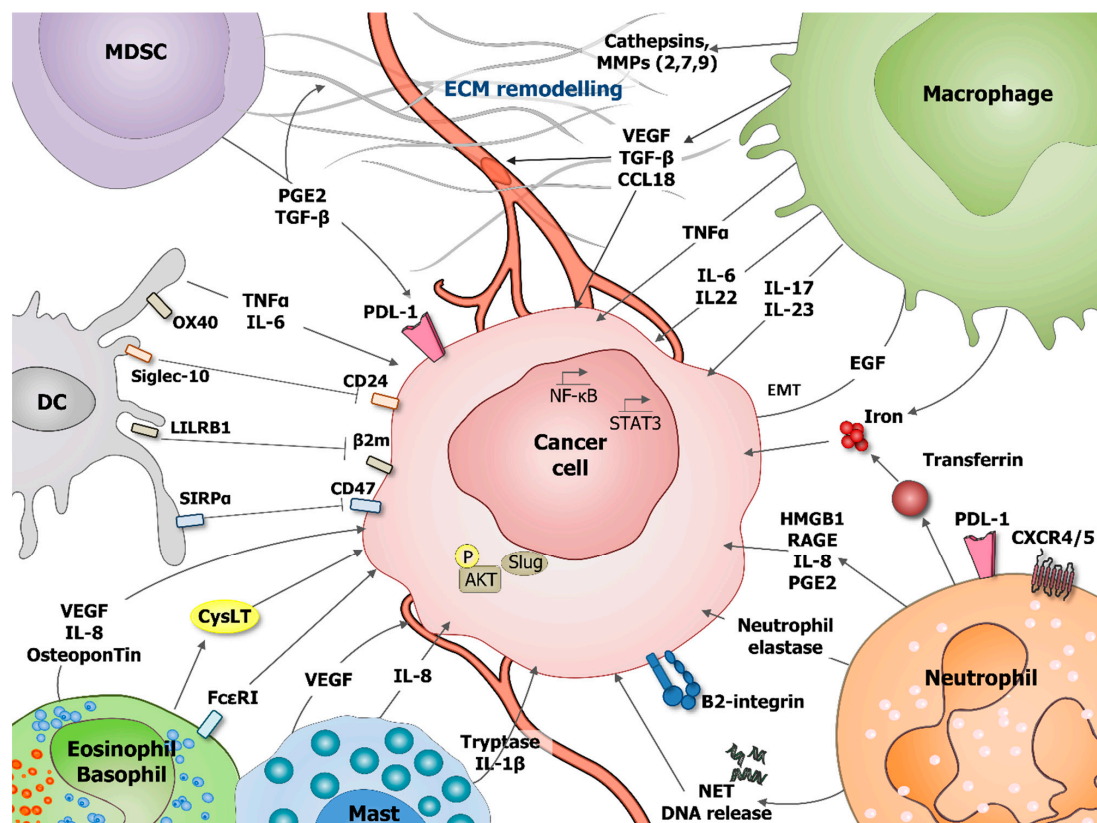


Figure 1. Role of tumor-associated myeloid cells in cancer cells survival, proliferation and migration. During tumorigenesis various myeloid cells populations, including: dendritic cells (DC), myeloid-derived suppressor cells (MDSC), macrophages, neutrophils, eosinophils, basophils, and mast cells can support cancer cells survival, proliferation, and migration. These processes can be stimulated by direct effect on tumoral cells or indirectly by influencing tumor microenvironment (TME), including extracellular matrix (ECM) remodeling and angiogenesis stimulation. Direct effects are mediated through production of interleukin IL-6, IL-8, IL-17, IL-22, IL-23, prostaglandin E2 (PGE2), transforming growth factor beta (TGF- β), vascular endothelial growth factor A (VEGF-A), osteopontin, and tumor necrosis factor α (TNF- α). Neutrophils secrete the iron-transporting protein transferrin which is a major mitogen for tumor cells and release of neutrophil extracellular traps (NET), including their deoxyribonucleic acid (DNA). Neutrophils produce neutrophil elastase favoring tumor cell proliferation and regulate the HMGB1/RAGE/IL-8 axis favoring the crosstalk between glioma cells and the TME. Mast cells release tryptase and IL-1 beta (IL-1 β) mediating malignant pleural effusion. Basophils express Fc ϵ Receptor I, promoting their tissue infiltration and producing cysteinyl leukotrienes (CysLT), allowing for proangiogenic activity of activated basophils. DC express OX40, Siglec-10, leukocyte immunoglobulin-like receptor B1 (LILRB1), and SIRP α , which, respectively, recognize OX40 ligand (OX40L), CD24, MHC class I-associated β 2M subunits, and CD47 at the surface of tumor cells blocking phagocytosis. Macrophages are an important source of various metalloproteinases (MMPs, MMP2, 7, 9) and cathepsins that provide conduits for tumor cells in the extracellular matrix (ECM). VEGF that is produced by myeloid cells is a major stimulator of angiogenesis.

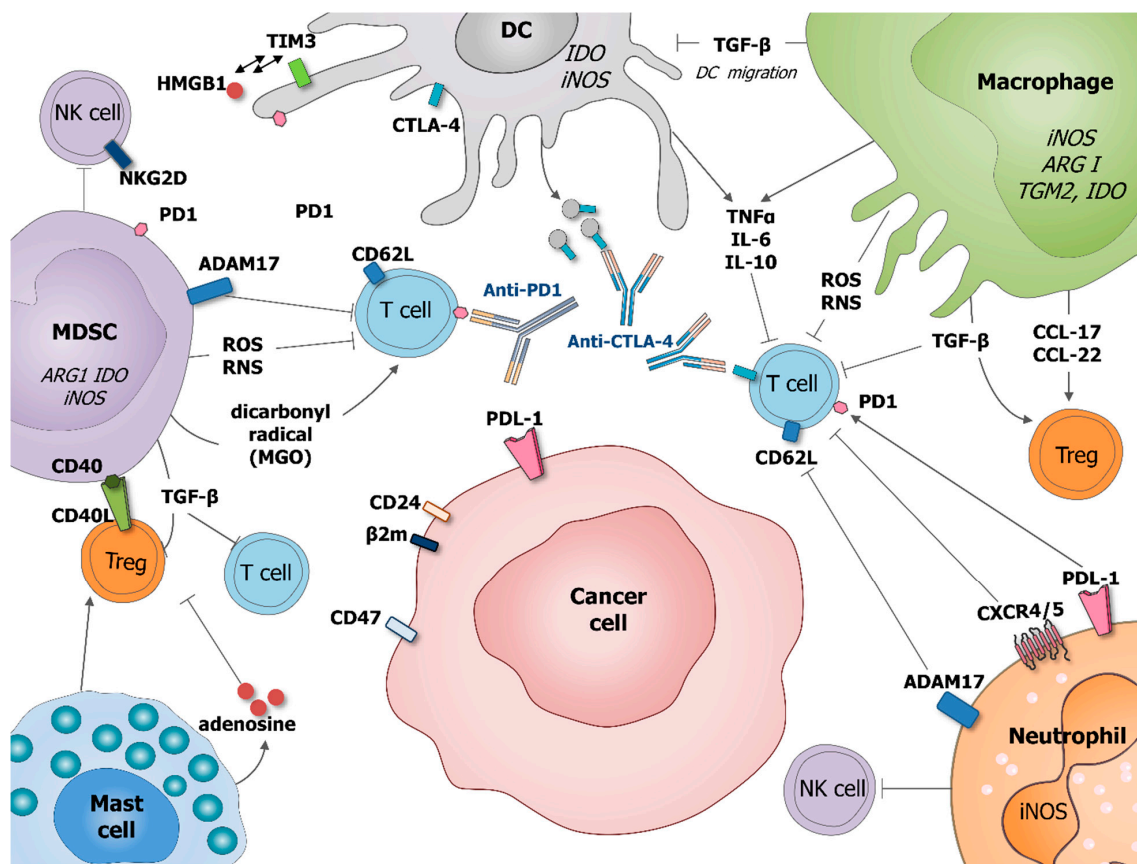


Figure 2. Role of tumor-associated myeloid cells in cancer cells immune-escape and therapy resistance. Macrophages and MDSC produce transforming growth factor beta (TGF- β) which inhibits DC migration at the tumor site, promote regulatory T cells (Treg) and block T cell activation. Macrophages potentiate Treg activation by production of chemokines CCL-17 and CCL-22. DC express immune checkpoint receptors, such as cytotoxic T-lymphocyte-associated protein 4 (CTLA-4), which can be released on the surface of microvesicles that could block costimulatory molecules, such as CD80/86. DC express also programmed cell death protein 1 (PD-1) and T cell immunoglobulin and mucin domain-containing protein 3 (Tim-3) interacting with HMGB1. MDSC suppress T cell functions by producing ROS and RNS inducing the nitration of TCR and MHC-I, as well as producing dicarbonyl radical methylglyoxal in the TME inhibiting CD8 T cells. MDSC express CD40 interacting with its ligand CD40L present on the surface of Treg. Mast cells can stimulate Treg numbers and secrete adenosine, which inhibits T cell proliferation. Neutrophil, as MDSC, expresses a disintegrin and metalloproteinase 17 (ADAM17) that cleaves the ectodomain of L-selectin (CD62L) on T cells. Neutrophil and cancer cells might express PD1 ligand (PDL-1) which inhibits activation of T cells expressing PD1. Neutrophils express CXCR4/5 leading to the immunosuppression of T-cell proliferation. MDSC and neutrophils, are also able to suppress NK cell cytotoxicity. By diminishing the response of various immune cells, tumor-associated myeloid cells can also negatively influence outcome of anti-cancer therapies, especially various immunotherapies.

2. Macrophages

Macrophages in cancer represent a major part of the immune cells within the TME and they are more frequently associated with a bad prognosis. Understanding the origin and physiological roles of macrophages provides improved insight into their role in cancer.

2.1. Origin and Physiological Roles of Macrophages

It was recently shown that most resident macrophages (MPs) in normal tissues are not only derived from bone marrow (BM) progenitors, as previously thought, but also from yolk sac or foetal liver and they are maintained by self-renewal [4,5]. However, during adult life, the rate of resident MPs can also be maintained by the infiltration of blood-derived MPs, except for microglia in the brain [6]. Therefore, monocytes from blood

and bone marrow are able to infiltrate tissues and differentiate into specific tissue MPs, but whether they can be considered to be tissue-resident MPs is still a debate. In the blood, two types of monocytes can be distinguished by the expression of the Ly6C marker in mice, Ly6C⁺ monocytes being originate from bone-marrow, and Ly6C⁻ from circulating Ly6C⁺ monocytes [7]. If Ly6C⁺ monocytes respond to damage by infiltrating and differentiating in MPs in the tissues, Ly6C⁻ monocytes remain in the vessels to detect and remove damaged endothelial cells [8]. Therefore, the ratio of these two monocytes populations in the blood can change, depending on different stimuli, including external stimuli. In human blood, three main monocytes populations have been identified, a classical one, CD14⁺⁺CD16⁻, a non-classical one, CD14^{int}CD16⁺, and an intermediate one, CD14⁺CD16⁺ [9]. These two latter populations are differentiated from a uniform population CD14⁺⁺CD16⁻ egressing from the bone marrow [10].

Resident macrophages display key roles in growth, tissue development, homeostasis, and remodelling, and they have site-specific phenotypes and functions [11]. It was proposed that the specialization of the resident MPs takes place inside the target tissue, due to close contacts with tissue-specific cells as well as to soluble factors in the tissue environment [12]. Microglia, in the brain and spinal cord, contribute to synaptic maturation during brain development and the clearance of immature or defective neuronal synapses [13]. In the lung, alveolar MPs mediate approximately 30% of the surfactant lipid metabolism. Langerhans cells with cutaneous MPs in the skin are specialized in the formation of the extracellular matrix and in skin layer differentiation. Cardiac-resident MPs are required during heart development and they take part in the regulation of the cardiac rhythm [14]. Kupffer cells in the liver are involved in the modulation of metabolism in hepatocytes, preventing the pathogenic accumulation of lipids [15]. Tissue-resident MPs that are located in the red-pulp region of the spleen have important functions in iron processing connected with the clearance of damaged red blood cells and the erythropoiesis [16]. Besides, MPs from the white-pulp region phagocytose lymphocytes avoiding B cell accumulation and auto antibody production [17].

Apart from physiological functions, monocytes/MPs also display pathological functions in infection/inflammation contexts, tissue repair, and cancer.

2.2. Pathological Functions of Macrophages

MPs are very plastic cells that are able to respond to molecular or cellular signals from the tissue environment. The molecular signals can be endocrine or paracrine signals that originate from phagocytosed cells or microorganisms and from the extracellular matrix/proteins. MPs can also directly interact with other tissue-resident cells, such as immune cells recruited during injury. Indeed, monocytes and MPs are recruited from the bone marrow to the tissue injury site via the chemoattractant CCL2 that is secreted by resident MPs, endothelial cells, myocytes, and fibroblasts [18]. The CCL2 receptor, CCR2, is highly expressed by Ly6C⁺ mouse monocytes [19]. In humans, classical monocytes (CD14⁺CD16⁻) display a high expression of CCR2 and they are involved in responses to bacterial infection and inflammation, in inflammasome signalling, and in low density lipoprotein uptake. In contrast, non-classical monocytes (CD14^{int}CD16⁺) display a high expression of genes that are involved in cytoskeletal dynamics, tissue invasion during inflammation and genes suggesting terminal differentiation and cellular maturity [20].

Therefore, monocytes-derived and tissue-resident MPs colocalize to take part in healing and then to the resolution, thanks to the production of cytotoxic and pro-inflammatory mediators, the clearance of invading microorganisms, or removal of apoptotic and damaged cells [21]. On the arrival at the injury site, blood-derived MPs can adopt a pro-inflammatory/M1/classical or anti-inflammatory/M2/alternative phenotype, depending on the cytokines that are present in the microenvironment [22,23]. Regarding the plasticity of MPs, although the framework of M1/M2 polarization is a very useful system for in vitro studies, it is unclear how similar clear-cut phenotypes can be appended during in vivo injury and repair [24]. This M1/M2 paradigm is well pictured by the high expression of

M2 markers by tissue-resident MPs when compared to the mature phenotype of monocyte-derived MPs [25,26]. Early on after damage or injury, infiltrated Ly6C⁺ monocytes scavenge apoptotic debris or pathogens or infected cells thanks to the expression of pattern recognition receptors (PRR), Toll like receptors (TLR), scavenger receptors, and Fc receptors that, respectively, recognize microbial antigens, danger signals, or immunoglobulins. These events lead to the activation of transcription factors such as interferon (IFN) regulatory factors and nuclear factor kappa B (NFκB), inducing an M1 polarization and initiation of the inflammatory response [27]. These blood-derived M1 MPs then release pro-inflammatory cytokines (e.g., IL-1β, IL-6, IL-12, IL-23, and TNF-α) and type-1 cell-attracting chemokines (e.g., CXCL9 and CXCL10), favouring the recruitment of more macrophages and leucocytes to help with injury resolution [28]. Once the acute injury has been resolved, MPs are in charge of suppressing inflammation and initiating wound repair. After clearing debris, MPs produce growth factors and mediators, which abrogate the pro-inflammatory function of T cells and other immune cells [29]. This is accompanied by a progressive repolarization of the blood-derived MPs towards a phenotype and functions that are increasingly similar to those of homeostatic tissue-resident MPs [30].

Specific plasma membrane receptors induce pro- and anti-inflammatory pathways in MPs. If IFNγ mediates the classical/M1 activation with upregulation of MHCII antigens, induction of nitric oxide synthase (i-NOS) and the production of pro-inflammatory molecules, interleukin-4 and -13 (IL-4 and IL-13) induce the alternative/M2 phenotype that is characterized by the upregulation of CD206, transglutaminase 2, arginase, and the production of IL-10 and chemokines, such as CCL17, CCL22 and CCL24 [28,31]. Like other immune cells, specific functions of MPs are, therefore, coupled to specific phenotypes, even when considering their plasticity, MPs can display intermediate phenotypes in certain inflammatory diseases and cancer [32,33].

2.3. Macrophages in Cancer

MPs in cancer are called tumor associated macrophages (TAM) and they represent the major immune component of the TME. According to oxygen ratio and tumor progression, TAM display either a M1 or M2 phenotype. They play a major role in tumor growth, metastatic dissemination, and therapy failure, promoting angiogenesis and secreting different factors that are involved in extracellular matrix (ECM) remodelling that facilitate tumor cell motility and intravasation. High TAM infiltration is generally correlated with poor outcomes in several types of cancer.

2.3.1. Origin and Functions of TAM

Until recently, TAM were considered to exclusively originate from blood-derived MPs undergoing differentiation upon tissue infiltration in response to chemokine and growth factors that are produced by stromal and tumor cells in the TME. Colony-stimulating factor 1 (CSF-1), vascular endothelial growth factor A (VEGF-A), and different CCL (2, 18, 20) were found to act as chemotactic molecules in various cancer [34–36]. However, evidence shows that tissue-resident MPs can coexist in tumors with blood-derived MPs and their phenotype can rapidly evolve, depending on the stage of the tumor and the characteristics of the molecular and cellular actors in the TME.

In early stage tumor development, IFN-α polarizes resident MPs towards an M1 phenotype and activates the infiltration of blood derived-M1 MPs. These MPs directly phagocytize tumor cells expressing low levels of the “don’t eat me” signal CD47, release pro-inflammatory factors that activate Th1 and Th17 immune responses and can also produce TNF-related apoptosis-inducing ligand (TRAIL) that result in TRAIL-induced cancer cell apoptosis [37,38]. In contrast, in more advanced tumors, TAM are polarized to an M2 related phenotype. This polarization occurs, thanks to anti-inflammatory mediators that are produced by the tumor cell itself and by stromal and immune cells in the TME, but also by MPs themselves. CSF-1, CCL2, 3, 14, and IL-4 are common tumor-derived factors driving the recruitment, proliferation, and M2-polarization of MPs [39–41]. Other factors

are more specific to the type of cancer, such as prostate cancer-derived cathelicidin-related antimicrobial peptide [42] or hypoxic cancer cell-derived cytokines Oncostatin M and Eotaxin [43]. IL-4 can also be secreted in the TME by Th2-polarized CD4 cells as well as IL-10 or IL-13, which lead to STAT-6 activation [44–46]. Besides, migration-stimulating factor (MSF), IL-4, and CXCL12 can be secreted by MPs to promote self-polarization [47–49]. Finally, hypoxia-inducible factors (HIF-1 α and 2 α), high-mobility group box 1 protein (HMGB1), extracellular ATP, or tumor-derived ECM components are also potential factors that promote M2 polarization [50–52].

2.3.2. How Can TAM Shape Cancer Cell Resistance?

M2-like MPs in TME are highly involved in cancer cell resistance by promoting cancer initiation, angiogenesis, the establishment of a premalignant niche, metastasis, and immune suppression.

It has been shown that an inflammatory microenvironment promotes genetic instability, leading to the proliferation of epithelial cells, but also the infiltration of immune cells, such as macrophages. On site, TAM can secrete IL-23 and IL-17, which promote cancer cell proliferation. IL-23 signaling in tumor cells is important for the intra-tumoral production of downstream cytokines, which are either direct (IL-6, IL-22) or indirect (IL-17A) STAT3 activators [53]. IL-6 that is produced by TAM also promotes tumor cells proliferation and invasive potential via STAT3 signaling [54]. TAMs also represent a strong source of iron, which is essential in tumor cell division, growth, and survival, and motility through the remodeling of the extracellular matrix [55].

TNF- α , which is a key player in NF κ B upregulation, is produced in the TME by, amongst others, TAM and it induces migration and invasion potential of cancer cells [56]. Cancer cells motility is also favored by various metalloproteinases (MMPs) and cathepsins that are produced by TAM activated by TGF- β in the TME [57,58]. Some chemokines, such as CCL18 produced by TAM, also promote the migration of cancer cells and metastasis through the clusterization of integrins [59]. A mouse study showed that mouse MPs-derived insulin growth factor 1 (IGF-1) induces the migration of epithelial ovarian cell lines [60]. Finally, it has been shown that MPs-derived microRNA (miR-223) also regulate tumor invasion [61].

TAM also take part in the promotion of the formation of blood vessels within the tumor providing nutrition for tumor growth [62]. Several pro-angiogenic factors, such as TGF- β , VEGF, PDGF, and angiogenic chemokines, are produced by TAM in the TME. CCL18 produced by TAM promote, synergically with VEGF, the endothelial cell migration and angiogenesis [63]. Other chemokines, such as CXCL1, 8, 12, 13, and CCL2, 5 produced by TAM, help with the angiogenesis switch in tumor tissues [28]. Finally, TAM can be found in hypoxic parts of the tumor and it can express HIF-1 α , which regulates the transcription of VEGF largely associated with angiogenesis [58].

The epithelial-mesenchymal transition (EMT) is a fundamental process for tumor progression and metastasis, during which TAM plays an active role through interactions with tumor cells and the production of facilitating factors of EMT. Through the production of EGF, TAM can induce the EMT of cancer cells by activating the EGFR/ERK1/2 signaling pathway [64].

TAM are also able to protect tumor cells from immune attacks, inhibiting T cell proliferation, function, and recruitment through the release of immunosuppressive cytokines. They are able to neutralize the recruitment and functions of cytotoxic CD8 T-cells and natural killer cells through the secretion of IL-10 and TGF- β in the TME [65,66]. TAM-derived TGF- β also decreases antigen presentation, which reduces DC migration and increases apoptosis [67]. On the contrary, the production of CCL17 and CCL22 by TAM promotes the infiltration of Th2 and Treg populations in tumors [68]. TAM-derived prostaglandin E2 (PGE2), IL-10, and indoleamine 2,3-dioxygenase (IDO) play important roles in the suppression of cytolytic T lymphocytes and in the induction of Treg function [69,70]. IL-10, alone or in concert with IL-6, causes the upregulation of macrophage B7-H4 expression, which is

responsible for the suppression of tumor-associated antigen-specific T cell immunity [71]. Moreover, IL-10 and PGE2 can induce the expression of immune-checkpoint ligands (PD-L1) in myeloid cells, which can inhibit cytolytic T lymphocytes responses [72,73]. Finally, IL-10 acts in an autocrine circuit in TAM in order to restrain their expression of IL-12 and also inhibits the release of IFN- γ [48].

The resistance of tumor cells to cytotoxic T cells can also be induced by reactive oxygen species (ROS) and reactive nitrogen species (RNS) that are produced by TAM through iNOS and arginase I, two enzymes that are very active in TAM [74].

TAM can also be responsible for tumor resistance to treatments. TAM-derived exosomes have been shown to be involved in mediating the resistance of gastric cancer cells to cisplatin [75]. Endocrine resistance in breast cancer cells can be increased by TAM-derived CCL2 through the activation of the PI3K/Akt/mTOR signaling pathway [40]. Autophagy in hepatocellular carcinomas cells can be induced by TAM, leading to oxaliplatin resistance [76]. It was recently shown that depletion of TAM by an anti-CSF-1R enhanced the anti-tumor effect of docetaxel in a murine epithelial ovarian cancer [74]. In Chronic Lymphocytic Leukemia (CLL), the nurse like cells (NLC), which are the specific protumoral TAM of the CLL reside in lymph nodes, spleen and bone marrow where they protect CLL B cells against apoptosis but also against chemotherapies such as ibrutinib [77,78]. This protection has been shown to depend on cell contact and soluble factors that are produced by TAM and, in an autocrine manner, by CLL B cells themselves [79–82].

Anticancer immunotherapies may also be reduced by TAM when their suppression of TME correlates with an increase of DC-vaccination therapy in a malignant mesothelioma mouse model [83] or an increase of anti-PD1 treatment favoring CD8 T cells recruitment to the tumor site [84,85]. Finally, high levels of TAM in the TME were also shown to increase the resistance of tumor cells to Vascular-targeted photodynamic: paldeliporfin (VTP) therapy in a prostate mouse model [86].

3. Dendritic Cells

Dendritic cells (DC) are derived from bone marrow progenitors and they can infiltrate the TME. They represent a small fraction in the TME, but they can play a key role in the sensing of infiltrated T cells or have an immunosuppressive role, leading to the tumor resistance.

3.1. Origin and Roles of Dendritic Cells

DC represent the regulators of innate and adaptive immune responses. These cells are able to present antigens to T lymphocytes. Several subsets of DC can be distinguished, depending on the tissue, e.g., classical/conventional DC (cDC) and plasmacytoid DC (pDC). Amongst cDC, the cDC1 present exogenous cell-associated antigens to CD8+ T cells, regulating their cytotoxic responses to intracellular pathogens [87] and cancer cells. In addition, cDC1 regulate innate immune responses through the production of IL-12 to activate the expression of IFN- γ by NK cells [88]. The cDC2, which present soluble antigens to CD4 T cells, are involved in the regulation of responses to extracellular pathogens, parasites, and allergens [89]. As for pDC, they rapidly respond to pathogens thanks to their expression of TLR7 and TLR9, which recognize single-stranded RNA and CpG dinucleotides, respectively. Through the production of type I and II interferons, these cells regulate the expansion of NK cells and CD8 T cells, but they also induce the maturation of cDC1 [90]. cDC and pDC derive from the common DC progenitor by a differentiation that is strictly restricted to this hematopoietic lineage. The common DC progenitor derive from the differentiation of hematopoietic stem cells (HSC) in bone marrow, the same progenitor as for monocytes and neutrophils [91]. After specification in the bone marrow, cDC progenitors are able to proliferate in lymphoid organs and peripheral tissues [92]. The development of all subsets of DC is dependent on the cytokine FMS-like tyrosine kinase 3 ligand (FLT3L) [93] and the differentiation into DC subtypes is controlled by different transcription factors. cDC1 differentiation is controlled by IFN-regulatory factor 8 (IRF8),

DNA-binding protein inhibitor ID2, basic leucine zipper transcriptional factor ATF-like 3, and nuclear factor IL-3-regulated protein. cDC2 development depends on RELB, PU.1, recombining the binding protein suppressor of hairless and IRF4 [87]. The transcription factor E2-2 regulates pDC development [94]. Immature DC migrate out of the bone marrow to colonize peripheral tissues, where they encounter antigens, such as danger-associated molecular patterns (DAMPs), which are recognized by pattern recognition receptors (PRR) that are expressed by each subset of DC. Concerning the phenotype of these DC, cDC1 are characterized by CD141, cDC2 by CD1c, and pDC by CD123.

3.2. Dendritic Cells in Cancer

In cancer, DC predominantly play an anti-tumorigenic role through the cross-presenting of exogenous antigens via MHC class I and class II to CD8 T cells and CD4 T cells, respectively, and through the secretion of immune-stimulatory cytokines. In a tumor context, cDC1 are both lymph node residents and migratory populations. These cells sample antigens in blood and lymph fluid to deliver them to lymph nodes. In the tumor, these cells are an important source of CXCL9 and CXCL10, which allow for the infiltration of both naïve and pre-activated T cells [95]. They can also produce high levels of IL-12 and type I IFN, which promote DC-mediated cross-priming of anti-tumor T cell responses, but also help to maintain CTL effector functions within the TME [96]. In contrast, cDC2 induce CD4 T cell responses and activate TH17 cells, but they do not deliver antigens to lymph nodes [97]. DC can also derive from circulating monocytes in the context of cancer or inflammation. These moDC, for monocyte-derived DC, can have the same presenting role as the resident cDC1 [98] and produce high levels of IL-15 in order to support anti-tumor T helper cell type I responses [99] or express TRAIL to mediate tumor cell apoptosis [100].

Alongside these anti-tumorigenic capacities, DC can, under certain circumstances, act as pro-tumoral cells in the TME. Despite the capacity of pDC to produce pro-inflammatory type I IFN, their presence can be associated with a poor prognosis in breast cancer, melanoma, and ovarian cancer [101,102]. Indeed, the poor activation of pDC in the TME and their active instruction by tumor cells lead to an immunosuppressive function through the production of IDO, IL-10, or OX40 [103]. The strong interaction of pDC and multiple myeloma (MM) cells induce the secretion of IL-3, which stimulates both pDC survival and MM cell survival and proliferation [104]. moDC in the TME can also be efficient producers of iNOS, TNF- α , IL-6, and IL-10 and hamper T cell proliferation [97,98].

Additionally, DC express the SIRP α receptor and the leukocyte immunoglobulin-like receptor B1 (LILRB1), which, respectively, recognize CD47 and MHC class I-associated β 2M subunits at the surface of tumor cells, blocking phagocytosis [105,106]. CD24 expressed by tumor cells can also inhibit phagocytosis by DC after engagement of Siglec-10 [107].

Immune checkpoints, such as CTLA-4 and PD-1, have been shown to negatively regulate the activity of DC. DC can express CTLA-4 and secrete it within microvesicles that could interact with costimulatory molecules, e.g., CD80/CD86 on bystander DC leading to the loss of expression of these molecules and, thus, to the non-activation of CD8 T cells [108]. DC can also express PD-1, limiting the production of the pro-inflammatory cytokines IL-12 and TNF- α during ex-vivo restimulation [109]. The ligation of PD-1⁺ DC to PD-1L expressed by ovarian tumor cells induced the suppression of antigen presentation, costimulatory molecule expression, and pro-inflammatory cytokine secretion [110]. TIM3 also expressed by DC negatively regulates IFN- α production by pDC [111] and CXCL9 production by cDC1 limiting the recruitment of cytotoxic T cells into the tumor [112]. Moreover, the interaction of HMGB1 and TIM3 on DC interferes with nucleic acid recruitment to endosomal compartments impairing the innate immune sensing of nucleic acids released by dying tumor cells [113].

In addition, the tumor can also interfere with the anti-tumorigenic functions of DC. Tumor-derived IL-6 and CSF-1 affect DC differentiation, promoting lineage commitment toward suppressive monocytes [114] and VEGF inhibits DC maturation by suppressing

NF κ B signaling in hematopoietic progenitors [115] as well as the tumor-derived TGF- β can inhibit antigen uptake [116].

4. Neutrophils

Neutrophils play an important role in the innate immune response against pathogens through phagocytosis, the release of anti-microbial peptides/proteases, and release of neutrophil extracellular traps (NETs). However, they are also able to modulate cancer growth and metastatic progression.

4.1. Origin and Physiological Roles of Neutrophils

Neutrophils represent 60% of all leukocytes in the bone marrow and their homeostasis is maintained thanks to an equilibrium between granulopoiesis, storage in bone marrow and release, and migration toward peripheral tissues. These cells have a relatively short life, but they are essential for pathogen elimination and represent an important link between innate and adaptive immunity.

In the bone marrow, the common myeloid progenitors are differentiated into common granulocyte monocyte progenitors (GMP), which can either lead to the monocyte lineage, depending on the C/EBP- α , or to the neutrophil and eosinophil lineage, thanks to the C/EBP- ϵ [117,118]. The acetylation of C/EBP- ϵ and the lack of expression of GATA-1 then lead to the ultimate differentiation into neutrophils [118]. Granulopoiesis is the formation of granules within neutrophil development; these granules are essential for the neutrophil functions. This process begins at the GMP stage, which progresses through a series of progenitors, including myeloblasts, promyelocytes, and myelocytes, which are able to proliferate, before becoming metamyelocytes that no longer proliferate, leading finally to mature neutrophils [119]. However, neutrophils are also plastic-like macrophages and they appear to be disease- or tissue-specific, and distinct neutrophils subsets can therefore be distinguished through their appearance, their density, or their surface receptor expression profiles. Neutrophils can be polarized *in vitro* into pro-inflammatory N1 by LPS and IFN- or anti-inflammatory N2 by IL-4 [120]. However, the question of plasticity with the N1/N2 switch remains unclear, knowing that neutrophils have a much shorter life-span than macrophages.

Neutrophils contribute to tissue injury by amplifying the inflammatory response, by the release of toxic effectors and the phagocytosis of pathogens. First, neutrophils have to be recruited in peripheral organs thanks to chemokines (G-CSF, CXCL1, CCL2, CXCL10) that are produced by conventional DC that encounter pathogens [121]. In addition, endothelial cells that are activated through PRR that detect pathogens upregulate P-, L-, and E-selectins that maximize neutrophils recruitment through their capture by endothelial cells, their rolling, and transmigration [122]. Neutrophils express cellular adhesion molecules (ICAM-1, ICAM-2, VCAM-1), which are essential to pass through endothelial junctions [123]. At the site infection, neutrophils are able to internalize microorganisms through Fc γ receptors, C-type lectins, or complement receptors. Following engulfment, primary and secondary granules fuse to the phagosome and release their antimicrobial contents and reactive oxygen species (ROS) to kill the microbe. Neutrophil cytoplasmic granules containing various cytotoxic factors also play an important role in killing pathogens [124]. Under flow conditions in the blood, neutrophils develop an additional mechanism for engaging and capturing circulating pathogens. Upon sensing bacteria in the blood, neutrophils release their DNA in a netlike configuration to create and release traps, called NETs. NETs are covered with elastase, histones, and other toxic molecules that kill pathogens [125]. However, if the release of anti-microbial molecules and NETs are essential for killing pathogens, then this can cause some toxic effects in the surrounding cells leading to tissue injury and thereafter contribute to the development of many non-infectious diseases, such as lung injury or rheumatoid arthritis [126]. Thus, neutrophils functions are tightly regulated.

Subsequently, neutrophils can be involved in the tissue repair following tissue injury; first, as professional phagocytes to remove tissue debris at the site of injury. Secondly, neutrophils can release growth factors and pro-angiogenic factors that contribute to regeneration and revascularization [127]; and, thirdly, neutrophils become apoptotic and they are cleared by macrophages, which also leads to the release of the tissue-repairing cytokines TGF- β and IL-10 [128].

Therefore, neutrophils have some beneficial effects on the resolution of infection, but they can also have detrimental activities and the unbalance between these effects can favor disease development [129].

4.2. Neutrophils in Cancer

In cancer, the dysregulation of granulopoiesis leads to different subsets with specific roles in tumor progression.

Two neutrophil subsets, high-density neutrophils (HDNs) considered as mature, and low-density neutrophils (LDNs), a mixture of mature and immature neutrophils, were identified in various tumor models by differential density centrifugation. The increase of these LDNs in the peripheral blood was associated with tumor growth and metastasis [130]. In addition, the two categories, N1 and N2, were clearly described in cancer through their respective anti- and pro-tumorigenic functions with the concept of plasticity as for TAM, which has not yet been shown in infectious processes. The neutrophils that are found in the TME are referred to as TAN (tumor associated neutrophils). The CXCR2 axis controls the mobilization of neutrophils from blood towards the tumor [131]. When compared to neutrophils in infectious disease, where they have a short life span, TAN display a high longevity and N1/N2 TAN can be converted into each other [132]. TME enriched in TGF- β or G-CSF induces the polarization towards the N2 phenotype, whereas IFN- γ , IFN- β , or LPS lead to N1 polarization [133,134].

The anti-tumor activities of neutrophils have been shown in different contexts and notably in a colon cancer mouse model, in which the depletion of neutrophils was associated with an increase of proliferation, growth, and invasiveness of tumor cells [135]. The mechanisms of anti-tumor functions of neutrophils are varied. Through the generation of ROS, such as H₂O₂, neutrophils were shown to be able to kill tumor cells in vitro and in tumor mouse models [136]. The production of ROS by neutrophils can also suppress the pro-tumorigenic role of the IL-17-secreting $\gamma\delta$ T cells in tumors, which inhibits their proliferation [137]. By inhibiting STAT5, neutrophils are able to induce the apoptosis of prostate cancer cells [138], and their secretion of granzyme B in the TME in colon cancer mouse models leads to the killing of tumor cells [139]. Moreover, neutrophils are able to kill cancer cell in a contact-dependent manner through the interaction of cathepsin G at their surface with the receptor for advanced glycation end products (RAGE) [140]. Thanks to the production of pro-inflammatory factors, such as CCL2, IL-8, CCL3, and IL-6, and their crosstalk with activated T cells, TANs, in early-stage human lung cancer, are actively involved in the stimulation of T cells responses limiting tumor progression [141]. In addition, IFN- γ produced by recruited monocytes in lung tumors activates the encoding of the TMEM173 gene for the protein STING (stimulator of interferon genes) within neutrophils, which stimulates the neutrophil-mediated killing of disseminated cancer cells [142]. Finally, it was shown that infiltration by neutrophils enhances the prognostic significance of colorectal cancer infiltration by CD8 T cells, improving survival in human colorectal cancer [143].

On the contrary, neutrophils display pro-tumorigenic functions that enhance tumor cell proliferation, invasion, angiogenesis, metastasis, and immune suppression. Tumor cell proliferation can be promoted by interaction with neutrophils in hypoxic conditions and mediated by the production of neutrophil elastase [136], as in the case of the acute promyelocytic leukemia progression [144]. The enhancement of non-small cell lung cancer cells proliferation is also favored by elastase that is produced following their interaction with neutrophils as well as the production of immunosuppressive PGE₂ [145]. NET over-

production was also involved in promoting tumor cells proliferation, but also migration and invasion, favoring the crosstalk between glioma cells and the TME by regulating the HMGB1/RAGE/IL-8 axis [146] or by activating pancreatic tumor growth through the DNA releases from NET [147].

The role of neutrophils in the metastatic process was shown by the association between neutrophil and circulating tumor cells within the bloodstream in breast cancer patients and mouse models [148]. By a proteomic approach, the iron-transporting protein transferrin was identified as the major mitogen for tumor cells that are secreted by neutrophils and the depletion of neutrophils suppressed transferrin production and lung metastasis [149]. Neutrophils have also been suggested to promote cancer cell adherence and, thereby, mediate metastasis in a murine model of liver metastasis [150]. Finally, human neutrophils were shown to induce tumor cell migration and interact with melanoma cells via $\beta 2$ integrin [151].

Neutrophils also play an important immunosuppressive role in impairing T cells proliferation and the activation in the TME in ovarian cancer for instance [152]. A high mature neutrophils/T cell ratio in multiple myeloma patients was correlated with a weak progression-free survival that was associated with an immunosuppressive profile of the infiltrated neutrophils [153]. In advanced stages of primary melanomas, TAN were shown as expressing PD-L1, CXCR4, CCR5, Adam17, and Nos2, leading to the immunosuppression of T-cell proliferation [154]. The expression of PD-L1 by TAN was correlated with the induction of PD-1 on CD8 T cells and their in vivo depletion delayed tumor growth with a significant increase of the frequency of proliferating IFN- γ -producing CD8 T cells [155]. Besides, the expression of PD-L1 by neutrophils can be promoted by IL-6 that is produced by human ovarian tumor cells under the effect of long non-coding RNA [156]. Finally, neutrophils are also able to suppress NK cell cytotoxicity, which results in defective antitumor responses and promotes metastasis in mice [157].

This balance between pro- and anti-tumor effects shows the plasticity of neutrophils, depending on different factors and cell contacts in the TME.

5. MDSC

MDSC form a heterogeneous group that consists of activated immature myeloid cells at different stages of hematopoiesis, which are able to exert strong anti-inflammatory response. In contrast to previously discussed cell types, MDSC presence in healthy individual is limited, as they are a product of chronic inflammation. In the context of cancer however, they are stated as one of the main actors in immune-escape and maintenance of immunosuppressive TME and their presence is repeatedly connected with failure in response to ICI therapies [158].

5.1. Origins and Roles of MDSCs

By nature, these cells are the result of a disrupted hematopoiesis and they are usually discussed in the context of cancer. However, they are gaining increasing recognition in physiological inflammation and aging, injury, trauma, and systemic infections, such as sepsis. MDSC generation is aimed at restraining hyper-inflammation and protecting the host from autoimmunity [159]. A good example of this phenomenon can be observed in severe COVID-19 cases, where there is a substantial increase in the percentage of MDSC in peripheral blood of patient up to 90% of all PBMC (normally MDSC constitute around 1% of all PBMC in healthy donor), which again decreases upon the end of infection [160]. MDSC consist of two main groups of cells: polymorphonuclear (PMN-MDSC) initially called granulocytic (G-MDSC) and monocytic (M-MDSC) [161]. Further research enabled the distinction of the third group, which is represented by even less specialized cells, termed as early-stage MDSC (eMDSC) [162]. Normally, immature myeloid cells reside in the BM and they leave this site when they reach a certain maturation stage. Nonetheless, in the presence of stress signals, they are recruited from the BM in their immature state [163]. High levels of cytokines, such as: GM-CSF, G-CSF,

and M-CSF, in conjunction with IL-6, IL-1 β , VEGF, and FGF- β produced by stromal or tumoral cells, are responsible for a disturbance of hematopoiesis and expansion of MDSCs. GM-CSF and M-CSF are crucial in the case of M-MDSC, whilst G-CSF is a key cytokine for PMN-MDSC. The phenotypical characterization of MDSC and their distinction from mature myeloid cells can be a serious problem and often requires the comparison of multiple surface markers and the performance of functional assays [164]. In mice, MDSC can be characterized as Gr-1⁺CD11b⁺ cells and, further, M-MDSC were described as CD11b⁺Ly6C^{high}Ly6G⁻ cells, while PMN-MDSC as CD11b⁺Ly6C^{low}Ly6G⁺ expressing cells [165,166]. In humans, a great number of surface phenotypes have been described with high variations between individuals. The mouse equivalent of PMN-MDSC was defined as CD11b⁺CD14⁻CD15⁺ or CD11b⁺CD14⁻CD66b⁺CD33^{DIM}, whereas M-MDSC are CD11b⁺CD14⁺CD15⁻HLADR^{-/low}CD33^{+/high} [165,167,168]. eMDSC were defined as Lin⁻(CD3, CD14, CD15, CD19, CD56)HLADR⁻CD33⁺ [164]. Additionally, the use of more recent markers allowed to further distinguish MDSC from their mature counterparts. For example M-MDSC are S100a9^{high}, whilst mature monocytes are S100a9^{low} [169,170]. In the human PMN population, the LOX1 marker turned out to be expressed on PMN-MDSC in contrast to mature neutrophils [171,172]. Additional to the phenotypic features detailed above, mouse studies showed that CD84 expressed on PMN-MDSC helps to distinguish them from neutrophils [173]. It is worth mentioning that the PMN-MDSC population is partially enriched in a mononuclear cell fraction during centrifugation in the Ficoll gradient, due to the decreased granularity of those cells [164]. In humans, MDSC can therefore be distinguished from neutrophils and monocytes based on their phenotypic markers, density gradient, but also by their unique functionality. Physiologically myeloid activation subsides quickly after the cessation of stimuli; that said, MDSCs, as a product of chronic inflammation, show continuous activation with an impaired ability to produce pro-inflammatory factors. MDSC are also characterized by very limited phagocytic properties. Instead, they excel in the field of immune suppression [171]. The repression of the immune response by MDSC takes place through a wide range of different mechanisms. In humans, PMN-MDSC are mostly known to inhibit T cells via the production of ROS [174]. M-MDSC mediate T cell suppression through the inducible nitric oxide synthase (iNOS) generation of NO, release of suppressive cytokines, such as IL-10, and prostaglandin PGE2 [175–177]. For instance, iNOS play an essential role in MDSC-mediated T cell suppression inhibiting antigen specific T cell proliferation in mice with proteoglycan-induced autoimmune arthritis [178]. PMN-MDSC also expressed immune checkpoint receptors, such as PD1, which can be upregulated in multiple sclerosis and leads to T cell inhibition [179].

5.2. MDSCs in Cancer

Initial remarks on the presence of MDSC were made at the beginning of the 20th century upon the characterization of tumorigenesis. With time, it has been shown that the numerous myeloid cell populations detected in different cancers were able to negatively impact T cell proliferation and activation. Moreover, it has been observed that these cells lack some of the markers of immune cell populations, such as T cell, NK cell, or macrophages, and, therefore, were initially named Null cells or Natural suppressor cells (NS) [163]. Only recently the term Myeloid Derived-Suppressor Cells was introduced to more appropriately represent the nature and functionality of these cells [163,180]. In humans, single cells RNA experiments of pancreatic lesions revealed an increased infiltration of MDSC, depending on the severity of the disease [181]. Indeed, MDSC can constitute up to 51% of non-epithelial cells in Pancreatic Ductal Adenocarcinoma (PDAC) when compared to 5% in non-invasive Intraductal Papillary Mucinous Neoplasms (IPMNs) correlated with a loss of cytotoxic T cells in early lesions and a gain of immunosuppressive myeloid populations in progressing diseases. A multicenter analysis showed that PMN-MDSC are a leading population of MDSC in solid tumors and their expansion is especially intensified in the context of tumorigenesis when compared to other inflammatory states [172]. Interestingly, mouse research showed that, in TAM rich tumors, M-CSF/M-CSFR signaling indirectly

blocks the recruitment of PMN-MDSC to the tumor site. This phenomenon was observed after anti CSF-1R therapy, which causes increased infiltration of the tumor by PMN-MDSC (and it is stated as one of the reasons for failure of CSF-1R targeted monotherapy) [182].

The MDSC differentiation program is associated with abnormal STAT3 signaling and the inhibition of the IRF 8 branch, leading to sustained cell proliferation and the inhibition of their terminal differentiation. STAT3 activation also leads to the expression of S100A9, which plays an essential role in MDSC biology. It is important in the stabilization of the STAT3/C/EBP β complex, which is crucial for the blocking of terminal differentiation and maintenance of the immune-suppressive function of MDSC [183,184]. For example, S100A9 KO mice exhibit a very potent antitumor response that is reversed upon the transfer of S100A9 positive MDSCs [185]. Furthermore, it has been shown that the administration of S100A9 protein alone to KO mice can restore the MDSC phenotype [184].

MDSCs are able to suppress both the innate and adaptive immune systems through various mechanisms. MDSC suppress T cell functions by producing ROS and RNS inducing the nitration of TCR and MHC-I, which hinders peptide recognition and disrupts T cell IL-2 signaling [174,186]. MDSC can be involved in the depletion of amino acids that are essential for T cell functions and proliferation. MDSC expression of the arginase 1 leads to the depletion of L-arginine, an important nutrient for T cell and NK cell proliferation [187]. By sequestering cysteine, MDSC limit the availability of this amino acid in the microenvironment, thereby hindering T cells activation and functions [188]. Tryptophan, which is also essential for T cell survival and functions, can also be depleted by MDSC through the expression of IDO that is involved in the catabolism and degradation of tryptophan [189]. Furthermore, CD8 T cells can be inhibited or paralyzed, as stated by the authors, by MDSC in the TME through expression of dicarbonyl radical methylglyoxal [190]. The intratumoral migration of T cells can also be impaired by MDSC through the peroxynitration, which alters CCL2 levels or through their plasma membrane expression of ADAM17 (a disintegrin and metalloproteinase 17) that cleaves the ectodomain of L-selectin (CD62L) on T cells [191,192]. MDSC have also been shown to impair NK cell functions. They can block the IFN- γ production by NK cells by affecting Stat5 activity and reducing NKG2D expression by NK cells through cell–cell interactions, leading to the suppression of NK cell cytotoxicity in tumor-bearing mice [193,194]. The production of PGE2 by MDSC was shown to enhance the stemness of uterine cervical cancer and the promotion of PD-L1 expression in epithelial ovarian cancer [195,196].

Moreover, MDSC can drive immune tolerance to tumors by increasing the number of Treg in the tumor. This is related to the interaction of the immune stimulatory receptor CD40 on MDSC with the CD40L that is expressed on Treg, and indirectly to the secretion of IL-10, TGF- β by IFN- γ stimulated MDSC [197,198].

Finally, MDSC confers resistance to immune checkpoint inhibitors, as MDSC depletion was shown to enhance the efficacy of anti-PD1 and anti-CTLA4 treatment with a complete tumor regression and a decrease of metastasis in an aggressive breast tumor mouse model [199]. Moreover, through the expression of Arg-1, MDSC confers resistance to bortezomib in human myeloma cell lines [200], which can be reversed while using Arg-1 inhibitors that were shown to decrease the L-arginase activity in correlation with a reduction of tumor growth in multiple mouse models of cancer [187].

Therefore, MDSC also play an important role in the resistance of tumor cells against the immune system to certain therapies.

6. Mast Cells

Mast cells (MCs) are innate immune cells that are located in virtually all tissues and they are particularly numerous in barrier tissues, such as skin and mucosa. They are characterized by the co-expression of CD117 (KIT) and Fc ϵ RI. They constitute a versatile population of sentinel cells that are endowed with multiple immune defenses and regulation capabilities, such as: defense against parasites and micro-organisms, defense against

venoms, initiation of the inflammatory vascular phase, interactions with CD4 and CD8 T cells, and positive or negative modulation of the immune response.

6.1. Origin and Physiological Roles of Mast Cells

MC precursors are produced in the bone marrow through the stem cell factor (SCF)-driven differentiation of hematopoietic stem cells [201,202]. These precursors circulate in the blood and are home to tissues thanks to the expression of $\alpha 4\beta 7$ integrins and positive chemotaxis for SCF [203]. MCs differentiate globally into two subsets, depending on the type of tissue they colonize and its microenvironment. Homing to the mucosa drives the differentiation of mucosal mast cells (MMCs in mice) or MCT (in humans, for tryptase expressing MC). Homing to connective tissue or serosa (such as skin or peritonea) drives the differentiation of CTMCs (connective tissue MCs in mice) or MCTC (in human, for tryptase and chymase expressing MCs). CTMC maturation is driven by SCF, NGF, and IL-9 provided by neighboring cells, such as epithelial cells or immune cells.

It was recently reported in a murine model that, like macrophages, mast cells have dual developmental origins, which arise from primitive and adult hematopoiesis [204]. Largely of yolk sac origin in early life, they are progressively replaced by mast cells that are derived from adult HSCs.

Like granulocytes, MCs store several bioactive molecules in their granules (such as histamine, tryptase, chymase, chemokine, TNF) that can be swiftly released upon activation by degranulation [205]. Bioactive components within the granules are embedded in a matrix of proteoglycan that allows for their storage and regulation of their biological activity [206]. Upon degranulation, the matrix is exteriorized and it acts as a bio-diffusor that take part in regulating half-life and bio-activity of the mediators [207]. MC also produce neosynthesized mediators such as eicosanoids (PGD₂, PGE₂, Cysteinyl leukotrienes), chemokines (CXCL8, CCL2, CCL3, CCL4) and cytokines (IL-5, IL-6, TNF, IL-13, IL-10, IL-1 β). Finally, MCs can play the role of antigen presenting cells [208–210].

MCs are abundant in barrier tissues that are exposed to the external environment. They play the role of surveillance outposts that sense their environment. Indeed, MCs respond to both innate and adaptive immunity stimuli and to changes in tissue homeostasis [211,212]. MC express several PRRs, which allows them to sense pathogens or danger signals [213]. Moreover, MC biological responses are deeply impacted by the alarmins IL-33 and TSLP [214]. They strongly express the IL-33 receptor ST2, allowing for them to sense stressed or dying cells in their neighborhood. IL-33 swiftly potentializes several MC functions, such as degranulation or cytokine production [215,216]. MCs indirectly recognize antigens via Abs/Fc receptors. MCs express Fc receptors for IgE and IgG, depending on the subset. The expression of the high affinity receptor for IgE is a hallmark of mast cells, enabling interactions with IgE-targeted antigens and their involvement in immediate hypersensitivity reactions. MCs also express activatory and inhibitory (in rodents) receptors for IgG [217]. For instance, IgG-opsonized pathogens are recognized by human MCs via Fc γ RIIA and they induce a polarized degranulation, called ADDS (antibody-dependent degranulatory synapse). Finally, connective tissue MCs express a receptor for cationic secretagogues, MRGPRX2 in humans (the ortholog of Mrgprb2 in rodent) [218]. This receptor recognizes a vast array of cationic compounds, such as neuropeptides (Substance P, Vaso-intestinal peptide), antimicrobial peptides (cathelicidin, human α -defensin2), or bacterial quorum sensing molecules [219], and triggers MC degranulation and cytokine production [207,220,221].

The production of such a large array of receptors and mediators endows MCs with the unique ability to detect tissue damages and interact with vascular, immune, and nervous systems. MCs can exhibit direct microbicidal activity [222]; nevertheless, it seems that the principal role of MCs against pathogens is to trigger an alarm and organize the inflammatory response. This task is enabled by their strategic location in tissues: near blood vessels, nerve endings, and lymphocyte-rich areas [222].

MCs are responsible for the main vascular changes that accompany the inflammatory response, thanks to the production of potent vasoactive compounds, such as histamine, TNF, and tryptase. They take part in the recruitment of immune effector cells in inflamed tissues by producing several chemokines. Several studies have reported the close proximity between MC and nerve fiber in skin and intestine [223–225]. It appears increasingly clearly that MCs and sensory neurons form a functional unit in the skin and the gut, and that nerve cell-MC crosstalk is an important functional module in the response to tissue aggressions [210,226,227]. Moreover, MCs are found near T cell rich areas in tissues and they can interact with several T cell subsets, such as CD4 Th cells [209], CD8 T cells [228], and $\gamma\delta$ T cells. Upon IFN- γ stimulation, MCs express MHC class II and costimulatory molecules and were shown to influence Th cell cytokine production in vitro [229,230]. Likewise, cognate and non-cognate crosstalk between MC and CD4 T cells were shown to mold both MC and T cell responses [230–233].

Finally, MCs also contribute to tissue repair, matrix remodeling, fibrosis [234], and wound healing [235]. MC proteases, such as tryptase and chymase, can inactivate inflammatory factors and avoid excessive tissue damage [236], and participate directly or indirectly in tissue remodeling [237].

In conclusion, MCs are versatile immune cells that take part in numerous processes of the immune response and are involved in several pathophysiological mechanisms [238,239]. A partial understanding of their complex role is especially apparent in the context of cancer.

6.2. Mast Cells in Cancer

Because of their natural presence in all tissues, MCs are immune components of the TME and are de facto present there from the first stage of carcinogenesis. Nevertheless, their role in the cancer pathophysiology remains elusive.

Numerous studies (reviewed extensively in [240]) have reported that MCs can adopt different roles toward cancer cells, depending on the type of tumor, stage of the disease, and their localization in TME. All of those conditions dictate whether MCs will display pro- or anti-tumoral properties or will simply remain bystanders. A good example of contribution of MCs to tumor development dependent on the stage of the disease was described in prostate cancer, where MCs play a pro-tumorigenic function at an early stage, but became dispensable at a later stage [241] or in NSCLC where peritumoral MC density is of favorable prognostic in stage I, but not in stage II [242]. Recently, it was highlighted that not only the density, but also micro-localization, of MCs can modify their involvement in cancer development. Differences in the pro or anti-tumorigenic role of MCs according to their localization have been reported at least in Melanoma [243], lung [244], and prostate cancer [245,246]. In lung cancer, the infiltration of MCs inside tumor islets was associated with a better outcome independent of tumor stage [244]. In prostate cancer, intratumoral MC density was associated with a good prognosis [246], whilst high peritumoral MC density was described to promote tumor growth [245].

One of the clearest functions of MCs in TME is their participation in angiogenesis through VEGF secretion. MC density was positively correlated with angiogenesis in Melanoma [247,248], colorectal, lung [249], and pancreas cancer [250]. Interestingly, a recent study showed that VEGF production by MCs can be directly triggered by cancer cells-derived extracellular vesicles [251].

MCs have also been described to take part in epithelial to mesenchymal transition (EMT). In thyroid cancer, Visciano and colleagues showed that MCs promote EMT via CXCL8 production, leading to AKT phosphorylation and Slug expression by thyroid cancer cells [252]. The involvement of MCs in EMT was also suggested in a pre-clinical model of lung metastasis. Mice lacking MCs (Mcpt5-Cre) showed a reduced melanoma colonization in the lung. This observation is associated with a higher expression of E-cadherin and reduced expression of Twist in MC deficient mice when compared to control mice, indicating a change in epithelial/mesenchymal orientation [253]. MCs also mediate

malignant pleural effusion via tryptase and IL-1 β release after recruitment via tumor derived CCL2 and activation by osteopontin [254].

Other studies have suggested a possible role of MCs inside the TME through their ability to interact with other immune cells and to favor or suppress immune responses. In a subcutaneous cancer model, Huang and colleagues showed that SCF-activated MCs can intensify immunosuppression by increasing Treg frequency and secreting adenosine that acts directly on both T cells, by reducing their proliferation, and on NK cells, by decreasing IFN- production [255].

Interestingly, MC/T cells cooperation inside the TME was described as an important factor in predicting responses to neoadjuvant chemotherapy in inflammatory breast cancer [256]. The characterization of the tumor microenvironment revealed that having a lower pretreatment MC density was significantly associated with achieving a complete pathological response to neoadjuvant chemotherapy. Moreover, spatial analysis revealed a close proximity between CD8 T cells and MCs when a complete pathological response was not achieved, highlighting MC as an interesting therapeutic target that could improve current therapeutic strategies. Targeting MCs to improve therapeutic strategies was also suggested in a pre-clinical model of melanoma, where Kaesler and colleagues identified MCs accumulating in and around melanomas after anti-CTLA-4 treatment and showed that effective melanoma immune control was dependent on LPS-activated MCs that secreted CXCL10, which promoted the recruitment of effector T cells. They highlighted a new way to target MCs and to involve them in the tumor immune defense [257].

These observations suggested different mechanisms by which MCs can impact the TME and influence tumor development. Nevertheless, many other mediators commonly produced by MCs play a role in tumor development, such as: PGE2 [258], IL-13 [259], histamine [260], and TNF [261]. Whether MCs produce these mediators inside the TME remains to be elucidated.

7. Eosinophils and Basophils

Just as mast cells, eosinophils and basophils are specialized effector cells playing key roles in the defense against parasites and hypersensitivity type I reactions. These cells share typical receptors and cytokines, but display specific effector functions. Basophils can be found in the bloodstream of healthy individuals and they are rapidly recruited within tissues in the presence of inflammation. Eosinophils circulate and they are resident in the hematopoietic and lymphoid organs, being ready to migrate to the site of allergic reactions. In addition, these cells can also play some pro-tumor roles.

7.1. Origin and Functions

Basophils stem from the differentiation of GMP in the bone marrow and then circulate [262]. Eosinophils also differentiate in the bone marrow from IL-5 receptor alpha progenitors and then migrate into the bloodstream [263], and the presence of intracellular acidophilic granules discriminates them from basophils and neutrophils. IL-3 is the most important growth and activating cytokine for human and murine basophils that are produced by the inflamed tissue, but also in an autocrine manner [264]. Basophils, such as mast cells, express the Fc ϵ Receptor I, which has a high affinity for the immunoglobulin E (IgE). IgE is produced during type I hypersensitivity reactions that are observed in various allergic diseases (e.g., asthma, sinusitis, rhinitis, food allergies, chronic urticarial, and atopic dermatitis), but also in the defense against parasites (protozoa and helminths) [265]. Upon activation through the Fc ϵ RI, basophils release their granules content, being composed of inflammatory mediators into the environment. These mediators comprise histamine, protease, cytokines, and chemokines, which will activate other inflammatory cells, but also vessels and smooth muscle [266]. Amongst these cytokines, IL4 and IL-13 are potent mediators of the type 2 immune response. Additionally, basophils produce IL-6 and TNF- α [267].

On the contrary, eosinophils weakly express FcεRI, but express other cell surface molecules that are involved in their activation, such as FcγRIIA (receptor for IgG), FcαRI (receptor for IgA), complement receptors, cytokine receptors, especially receptors for IL-3, IL-5, and GM-CSF, chemokine receptors (CCR1 and CCR3), but also some adhesion molecules and TLR7/8 [268]. Through their expression of the ST2 receptor, eosinophil differentiation can be stimulated by IL-33 during inflammatory responses in an IL-5-dependent manner [269]. Several receptors that are present at the surface of eosinophils, upon stimulation, mediate piecemeal degranulation. However, the molecules released depends on the stimulus, as eosinophils are able to secrete cytokines mediating opposite effects. For instance, IFN-γ stimulation induces the secretion of IL-1, whereas stimulation with eotaxin (CCL11) leads to the secretion of IL-4, despite the fact that these two interleukins are stored in the same granules [270,271]. As for neutrophils, when exposed to bacteria, eosinophils are able to release mitochondrial DNA in order to form an extracellular trap containing granule proteins, eosinophil cationic protein, and eosinophil major basic protein 1 that bind and kill bacteria, for instance in inflammatory skin diseases [272]. Moreover, eosinophils also express several inhibitory receptors, such as FcγRIIB, ILT5/LIR3, CD33, Siglec-8/10, p140, and IRp60/CD300a (reviewed in [273]). Eosinophils are thus complex cells that can be either stimulated or inhibited in their proliferation, survival, or functions through these inhibitory receptors.

7.2. Basophils and Eosinophils in Cancer

The presence of basophils and eosinophils was detected in several types of tumors. Taking under consideration plasticity and a range of factors, these cells can express it is impossible to unambiguously define their role in cancer. Depending on the circumstances, they can show anti-tumoral effects or favor angiogenesis, cancer cell invasiveness, and maintenance of an immunosuppressive environment.

In a mouse model of breast cancer, a low level of circulating basophils has been correlated with an increased number of pulmonary metastases [274]. In addition, a study of over 400 women that were diagnosed with colorectal cancer revealed that eosinophil infiltration of the tumor, particularly in the stromal tissue, was associated with a decreased mortality rate [275]. Eosinophils were also found to be potentiators of anti-CTLA4 therapy in breast cancer patients, being correlated with their level of accumulation within the tumor [276]. A direct anti-tumor effect of eosinophils in a melanoma mouse model was shown to be dependent on the presence of IL-33 in the TME [277]. High relative circulating basophils and activated infiltrated basophils were positively associated with improved outcome in melanoma or ovarian cancer patients and, according to several data, basopenia was associated with a poor prognosis in colorectal cancer [278–280].

However, these two types of cells could also favor tumor development. Basophils are preferentially circulating, but some lung-resident basophils exhibit a specific phenotype that is involved in the development of alveolar macrophages and their polarization towards a pro-tumor M2 state. Therefore, basophils may be involved in regulating the activity of TAM in the TME [281]. Moreover, recruitment of basophils in tumor-draining lymph nodes of pancreatic ductal adenocarcinoma patients has been shown to be activated by T-cell-derived IL-3 to produce IL-4, inducing a tumor-promoting Th2 inflammation [282]. Eosinophils are also able to exert an IL-4 mediated immunomodulatory function, which induces the switch from a Th1 immune response to a Th2 one. In the same way, it has been postulated that basophils recruited within the skin, in an inflammation-driven model of epithelial carcinogenesis, could promote tumor development via their FcεRI signaling [283].

Alongside their role in the immunomodulation, basophils and eosinophils are able to act on angiogenesis. Infiltrating basophils in human nasal polyps contain VEGF-A localized in secretory granules, which can be released by their IgE-mediated activation. Moreover, these cells also express on their membrane VEGFR-2 and the co-receptors NRP1 and NRP2 involved in the infiltration of basophils at the site of chronic inflammation, such as tumor site [284]. Other angiogenic factors, such as angiopoietins or HGF, can be

released by basophils upon activation [285,286]. Some lipids mediators, such as cysteinyl leukotrienes (CysLT), produced by activated basophils [287], also display proangiogenic activities and can activate the expression of the CysLT2 receptor in tumor blood endothelial cells [288]. Eosinophils present in hypoxic tumor microenvironments could also play pro-tumorigenic roles by promoting tumoral angiogenesis via the release of VEGF-A, IL-8, and osteopontin [289–291].

Finally, by sequestering circulating tumor cells, NET was clearly shown to promote cancer metastasis in murine models and in humans [292]. The extracellular trap that is produced by activated basophils and eosinophils could also have some impact on tumor growth and metastasis, but this remains to be investigated.

Basophils and eosinophils display a plastic phenotype with numerous factors that can be involved in pro-tumor processes and certainly in the resistance of tumor cells to immune cells or to chemotherapies as yet to be investigated.

8. Conclusions

In cancer, myeloid cells form a diverse group and are able to adapt their phenotype to the TME, depending on cell interaction, oncogenic drivers, altered metabolism, hypoxia, and various secreted factors. Therefore, these plastic cells are able to both initiate or suppress anti-tumor immune response. Whether macrophages or DC or neutrophils or MDSC or mast cells or eosinophils and basophils, all of these cells have an important role in shaping tumor cells to be resistant against apoptosis, immune cells attacks, or therapeutic agents, and, therefore, to grow and migrate for metastasis formation. Therefore, targeting these cells in the TME is a good opportunity to find new specific targeting therapies or to enhance current therapies by therapies combination.

Author Contributions: M.D., C.L. (Chloé Laplagne), E.L., C.L. (Camille Laurent), J.-J.F., E.E. and M.P. participated to the writing of this review. All authors have read and agreed to the published version of the manuscript.

Funding: This research was funded by Inserm, CNRS and University Toulouse III.

Conflicts of Interest: No conflicts of Interest.

References

1. Wang, M.; Zhao, J.; Zhang, L.; Wei, F.; Lian, Y.; Wu, Y.; Gong, Z.; Zhang, S.; Zhou, J.; Cao, K.; et al. Role of Tumor Microenvironment in Tumorigenesis. *J. Cancer* **2017**, *8*, 761–773. [[CrossRef](#)] [[PubMed](#)]
2. Schreiber, R.D.; Old, L.J.; Smyth, M.J. Cancer Immunoediting: Integrating Immunity's Roles in Cancer Suppression and Promotion. *Science* **2011**, *331*, 1565–1570. [[CrossRef](#)] [[PubMed](#)]
3. Hanahan, D.; Coussens, L.M. Accessories to the Crime: Functions of Cells Recruited to the Tumor Microenvironment. *Cancer Cell* **2012**, *21*, 309–322. [[CrossRef](#)]
4. Wynn, T.A.; Chawla, A.; Pollard, J.W. Macrophage Biology in Development, Homeostasis and Disease. *Nature* **2013**, *496*, 445–455. [[CrossRef](#)] [[PubMed](#)]
5. Ginhoux, F.; Schultze, J.L.; Murray, P.J.; Ochando, J.; Biswas, S.K. New Insights into the Multidimensional Concept of Macrophage Ontogeny, Activation and Function. *Nat. Immunol.* **2016**, *17*, 34–40. [[CrossRef](#)]
6. Ajami, B.; Bennett, J.L.; Kriegler, C.; Tetzlaff, W.; Rossi, F.M.V. Local Self-Renewal Can Sustain CNS Microglia Maintenance and Function throughout Adult Life. *Nat. Neurosci.* **2007**, *10*, 1538–1543. [[CrossRef](#)]
7. Hettinger, J.; Richards, D.M.; Hansson, J.; Barra, M.M.; Joschko, A.-C.; Krijgsveld, J.; Feuerer, M. Origin of Monocytes and Macrophages in a Committed Progenitor. *Nat. Immunol.* **2013**, *14*, 821–830. [[CrossRef](#)]
8. Geissmann, F.; Jung, S.; Littman, D.R. Blood Monocytes Consist of Two Principal Subsets with Distinct Migratory Properties. *Immunity* **2003**, *19*, 71–82. [[CrossRef](#)]
9. Passlick, B.; Flieger, D.; Ziegler-Heitbrock, H.W. Identification and Characterization of a Novel Monocyte Subpopulation in Human Peripheral Blood. *Blood* **1989**, *74*, 2527–2534. [[CrossRef](#)]
10. Patel, A.A.; Zhang, Y.; Fullerton, J.N.; Boelen, L.; Rongvaux, A.; Maini, A.A.; Bigley, V.; Flavell, R.A.; Gilroy, D.W.; Asquith, B.; et al. The Fate and Lifespan of Human Monocyte Subsets in Steady State and Systemic Inflammation. *J. Exp. Med.* **2017**, *214*, 1913–1923. [[CrossRef](#)]
11. Theret, M.; Mounier, R.; Rossi, F. The Origins and Non-Canonical Functions of Macrophages in Development and Regeneration. *Development* **2019**, *146*, 1–14. [[CrossRef](#)] [[PubMed](#)]

12. Gautier, E.L.; Yvan-Charvet, L. Understanding Macrophage Diversity at the Ontogenic and Transcriptomic Levels. *Immunol. Rev.* **2014**, *262*, 85–95. [[CrossRef](#)] [[PubMed](#)]
13. Amit, I.; Winter, D.R.; Jung, S. The Role of the Local Environment and Epigenetics in Shaping Macrophage Identity and Their Effect on Tissue Homeostasis. *Nat. Immunol.* **2016**, *17*, 18–25. [[CrossRef](#)] [[PubMed](#)]
14. Hulsmans, M.; Clauss, S.; Xiao, L.; Aguirre, A.D.; King, K.R.; Hanley, A.; Huckler, W.J.; Wülfers, E.M.; Seemann, G.; Courties, G.; et al. Macrophages Facilitate Electrical Conduction in the Heart. *Cell* **2017**, *169*, 510–522.e20. [[CrossRef](#)]
15. Odegaard, J.I.; Ricardo-Gonzalez, R.R.; Red Eagle, A.; Vats, D.; Morel, C.R.; Goforth, M.H.; Subramanian, V.; Mukundan, L.; Ferrante, A.W.; Chawla, A. Alternative M2 Activation of Kupffer Cells by PPARdelta Ameliorates Obesity-Induced Insulin Resistance. *Cell Metab.* **2008**, *7*, 496–507. [[CrossRef](#)]
16. Kohyama, M.; Ise, W.; Edelson, B.T.; Wilker, P.R.; Hildner, K.; Mejia, C.; Frazier, W.A.; Murphy, T.L.; Murphy, K.M. Role for Spi-C in the Development of Red Pulp Macrophages and Splenic Iron Homeostasis. *Nature* **2009**, *457*, 318–321. [[CrossRef](#)] [[PubMed](#)]
17. de Back, D.Z.; Kostova, E.B.; van Kraaij, M.; van den Berg, T.K.; van Bruggen, R. Of Macrophages and Red Blood Cells: A Complex Love Story. *Front. Physiol.* **2014**, *5*, 9. [[CrossRef](#)] [[PubMed](#)]
18. Yoshimura, T.; Galligan, C.; Takahashi, M.; Chen, K.; Liu, M.; Tessarollo, L.; Wang, J.M. Non-Myeloid Cells Are Major Contributors to Innate Immune Responses via Production of Monocyte Chemoattractant Protein-1/CCL2. *Front. Immunol.* **2014**, *4*, 482. [[CrossRef](#)] [[PubMed](#)]
19. Boring, L.; Gosling, J.; Chensue, S.W.; Kunkel, S.L.; Farese, R.V.; Broxmeyer, H.E.; Charo, I.F. Impaired Monocyte Migration and Reduced Type 1 (Th1) Cytokine Responses in C-C Chemokine Receptor 2 Knockout Mice. *J. Clin. Investig.* **1997**, *100*, 2552–2561. [[CrossRef](#)]
20. Anbazhagan, K.; Duroux-Richard, I.; Jorgensen, C.; Apparailly, F. Transcriptomic Network Support Distinct Roles of Classical and Non-Classical Monocytes in Human. *Int. Rev. Immunol.* **2014**, *33*, 470–489. [[CrossRef](#)]
21. Laskin, D.L.; Sunil, V.R.; Gardner, C.R.; Laskin, J.D. Macrophages and Tissue Injury: Agents of Defense or Destruction? *Annu. Rev. Pharmacol. Toxicol.* **2011**, *51*, 267–288. [[CrossRef](#)] [[PubMed](#)]
22. Mills, C.D.; Kincaid, K.; Alt, J.M.; Heilman, M.J.; Hill, A.M. M-1/M-2 Macrophages and the Th1/Th2 Paradigm. *J. Immunol.* **2000**, *164*, 6166–6173. [[CrossRef](#)] [[PubMed](#)]
23. Martinez, F.O.; Sica, A.; Mantovani, A.; Locati, M. Macrophage Activation and Polarization. *Front. Biosci.* **2008**, *13*, 453–461. [[CrossRef](#)] [[PubMed](#)]
24. Xue, J.; Schmidt, S.V.; Sander, J.; Draffehn, A.; Krebs, W.; Quester, I.; De Nardo, D.; Gohel, T.D.; Emde, M.; Schmidleithner, L.; et al. Transcriptome-Based Network Analysis Reveals a Spectrum Model of Human Macrophage Activation. *Immunity* **2014**, *40*, 274–288. [[CrossRef](#)] [[PubMed](#)]
25. Lavin, Y.; Winter, D.; Blecher-Gonen, R.; David, E.; Keren-Shaul, H.; Merad, M.; Jung, S.; Amit, I. Tissue-Resident Macrophage Enhancer Landscapes Are Shaped by the Local Microenvironment. *Cell* **2014**, *159*, 1312–1326. [[CrossRef](#)]
26. Mould, K.J.; Jackson, N.D.; Henson, P.M.; Seibold, M.; Janssen, W.J. Single Cell RNA Sequencing Identifies Unique Inflammatory Airspace Macrophage Subsets. *JCI Insight* **2019**, *4*, 1–17. [[CrossRef](#)]
27. Kawai, T.; Akira, S. The Role of Pattern-Recognition Receptors in Innate Immunity: Update on Toll-like Receptors. *Nat. Immunol.* **2010**, *11*, 373–384. [[CrossRef](#)]
28. Mantovani, A.; Sica, A.; Sozzani, S.; Allavena, P.; Vecchi, A.; Locati, M. The Chemokine System in Diverse Forms of Macrophage Activation and Polarization. *Trends Immunol.* **2004**, *25*, 677–686. [[CrossRef](#)]
29. Vannella, K.M.; Wynn, T.A. Mechanisms of Organ Injury and Repair by Macrophages. *Annu. Rev. Physiol.* **2017**, *79*, 593–617. [[CrossRef](#)]
30. Olingy, C.E.; San Emeterio, C.L.; Ogle, M.E.; Krieger, J.R.; Bruce, A.C.; Pfau, D.D.; Jordan, B.T.; Peirce, S.M.; Botchwey, E.A. Non-Classical Monocytes Are Biased Progenitors of Wound Healing Macrophages during Soft Tissue Injury. *Sci. Rep.* **2017**, *7*, 447. [[CrossRef](#)]
31. Martinez, F.O.; Helming, L.; Milde, R.; Varin, A.; Melgert, B.N.; Draijer, C.; Thomas, B.; Fabbri, M.; Crawshaw, A.; Ho, L.P.; et al. Genetic Programs Expressed in Resting and IL-4 Alternatively Activated Mouse and Human Macrophages: Similarities and Differences. *Blood* **2013**, *121*, e57–e69. [[CrossRef](#)] [[PubMed](#)]
32. Vogel, D.Y.S.; Vereyken, E.J.F.; Glim, J.E.; Heijnen, P.D.A.M.; Moeton, M.; van der Valk, P.; Amor, S.; Teunissen, C.E.; van Horssen, J.; Dijkstra, C.D. Macrophages in Inflammatory Multiple Sclerosis Lesions Have an Intermediate Activation Status. *J. Neuroinflamm.* **2013**, *10*, 35. [[CrossRef](#)] [[PubMed](#)]
33. Pettersen, J.S.; Fuentes-Duculan, J.; Suárez-Fariñas, M.; Pierson, K.C.; Pitts-Kiefer, A.; Fan, L.; Belkin, D.A.; Wang, C.Q.F.; Bhuvanendran, S.; Johnson-Huang, L.M.; et al. Tumor-Associated Macrophages in the Cutaneous SCC Microenvironment Are Heterogeneously Activated. *J. Invest. Dermatol.* **2011**, *131*, 1322–1330. [[CrossRef](#)] [[PubMed](#)]
34. Franklin, R.A.; Liao, W.; Sarkar, A.; Kim, M.V.; Bivona, M.R.; Liu, K.; Pamer, E.G.; Li, M.O. The Cellular and Molecular Origin of Tumor-Associated Macrophages. *Science* **2014**, *344*, 921–925. [[CrossRef](#)] [[PubMed](#)]
35. Linde, N.; Lederle, W.; Depner, S.; van Rooijen, N.; Gutschalk, C.M.; Mueller, M.M. Vascular Endothelial Growth Factor-Induced Skin Carcinogenesis Depends on Recruitment and Alternative Activation of Macrophages. *J. Pathol.* **2012**, *227*, 17–28. [[CrossRef](#)] [[PubMed](#)]

36. Nandi, B.; Shapiro, M.; Samur, M.K.; Pai, C.; Frank, N.Y.; Yoon, C.; Prabhala, R.H.; Munshi, N.C.; Gold, J.S. Stromal CCR6 Drives Tumor Growth in a Murine Transplantable Colon Cancer through Recruitment of Tumor-Promoting Macrophages. *Oncoimmunology* **2016**, *5*, e1189052. [[CrossRef](#)]
37. Zhao, H.; Wang, J.; Kong, X.; Li, E.; Liu, Y.; Du, X.; Kang, Z.; Tang, Y.; Kuang, Y.; Yang, Z.; et al. CD47 Promotes Tumor Invasion and Metastasis in Non-Small Cell Lung Cancer. *Sci. Rep.* **2016**, *6*, 29719. [[CrossRef](#)]
38. Griffith, T.S.; Wiley, S.R.; Kubin, M.Z.; Sedger, L.M.; Maliszewski, C.R.; Fanger, N.A. Monocyte-Mediated Tumoricidal Activity via the Tumor Necrosis Factor-Related Cytokine, TRAIL. *J. Exp. Med.* **1999**, *189*, 1343–1354. [[CrossRef](#)]
39. De, I.; Steffen, M.D.; Clark, P.A.; Patros, C.J.; Sokn, E.; Bishop, S.M.; Litscher, S.; Maklakova, V.I.; Kuo, J.S.; Rodriguez, F.J.; et al. CSF1 Overexpression Promotes High-Grade Glioma Formation without Impacting the Polarization Status of Glioma-Associated Microglia and Macrophages. *Cancer Res.* **2016**, *76*, 2552–2560. [[CrossRef](#)]
40. Li, D.; Ji, H.; Niu, X.; Yin, L.; Wang, Y.; Gu, Y.; Wang, J.; Zhou, X.; Zhang, H.; Zhang, Q. Tumor-Associated Macrophages Secrete CC-Chemokine Ligand 2 and Induce Tamoxifen Resistance by Activating PI3K/Akt/MTOR in Breast Cancer. *Cancer Sci.* **2020**, *111*, 47–58. [[CrossRef](#)]
41. Zhao, P.; Gao, D.; Wang, Q.; Song, B.; Shao, Q.; Sun, J.; Ji, C.; Li, X.; Li, P.; Qu, X. Response Gene to Complement 32 (RGC-32) Expression on M2-Polarized and Tumor-Associated Macrophages Is M-CSF-Dependent and Enhanced by Tumor-Derived IL-4. *Cell Mol. Immunol.* **2015**, *12*, 692–699. [[CrossRef](#)] [[PubMed](#)]
42. Cha, H.-R.; Lee, J.H.; Hensel, J.A.; Sawant, A.B.; Davis, B.H.; Lee, C.M.; Deshane, J.S.; Ponnazhagan, S. Prostate Cancer-Derived Cathelicidin-Related Antimicrobial Peptide Facilitates Macrophage Differentiation and Polarization of Immature Myeloid Progenitors to Protumorigenic Macrophages. *Prostate* **2016**, *76*, 624–636. [[CrossRef](#)] [[PubMed](#)]
43. Tripathi, C.; Tewari, B.N.; Kanchan, R.K.; Baghel, K.S.; Nautiyal, N.; Shrivastava, R.; Kaur, H.; Bhatt, M.L.B.; Bhadauria, S. Macrophages Are Recruited to Hypoxic Tumor Areas and Acquire a Pro-Angiogenic M2-Polarized Phenotype via Hypoxic Cancer Cell Derived Cytokines Oncostatin M and Eotaxin. *Oncotarget* **2014**, *5*, 5350–5368. [[CrossRef](#)] [[PubMed](#)]
44. Gocheva, V.; Wang, H.-W.; Gadea, B.B.; Shree, T.; Hunter, K.E.; Garfall, A.L.; Berman, T.; Joyce, J.A. IL-4 Induces Cathepsin Protease Activity in Tumor-Associated Macrophages to Promote Cancer Growth and Invasion. *Genes Dev.* **2010**, *24*, 241–255. [[CrossRef](#)] [[PubMed](#)]
45. DeNardo, D.G.; Barreto, J.B.; Andreu, P.; Vasquez, L.; Tawfik, D.; Kolhatkar, N.; Coussens, L.M. CD4(+) T Cells Regulate Pulmonary Metastasis of Mammary Carcinomas by Enhancing Protumor Properties of Macrophages. *Cancer Cell* **2009**, *16*, 91–102. [[CrossRef](#)]
46. Pedroza-Gonzalez, A.; Xu, K.; Wu, T.-C.; Aspod, C.; Tindle, S.; Marches, F.; Gallegos, M.; Burton, E.C.; Savino, D.; Hori, T.; et al. Thymic Stromal Lymphopoietin Fosters Human Breast Tumor Growth by Promoting Type 2 Inflammation. *J. Exp. Med.* **2011**, *208*, 479–490. [[CrossRef](#)]
47. Solinas, G.; Schiarea, S.; Liguori, M.; Fabbri, M.; Pesce, S.; Zammataro, L.; Pasqualini, F.; Nebuloni, M.; Chiabrando, C.; Mantovani, A.; et al. Tumor-Conditioned Macrophages Secrete Migration-Stimulating Factor: A New Marker for M2-Polarization, Influencing Tumor Cell Motility. *J. Immunol.* **2010**, *185*, 642–652. [[CrossRef](#)]
48. Sica, A.; Saccani, A.; Bottazzi, B.; Polentarutti, N.; Vecchi, A.; van Damme, J.; Mantovani, A. Autocrine Production of IL-10 Mediates Defective IL-12 Production and NF-Kappa B Activation in Tumor-Associated Macrophages. *J. Immunol.* **2000**, *164*, 762–767. [[CrossRef](#)]
49. Sánchez-Martín, L.; Estechea, A.; Samaniego, R.; Sánchez-Ramón, S.; Vega, M.Á.; Sánchez-Mateos, P. The Chemokine CXCL12 Regulates Monocyte-Macrophage Differentiation and RUNX3 Expression. *Blood* **2011**, *117*, 88–97. [[CrossRef](#)]
50. Doedens, A.L.; Stockmann, C.; Rubinstein, M.P.; Liao, D.; Zhang, N.; DeNardo, D.G.; Coussens, L.M.; Karin, M.; Goldrath, A.W.; Johnson, R.S. Macrophage Expression of Hypoxia-Inducible Factor-1 Alpha Suppresses T-Cell Function and Promotes Tumor Progression. *Cancer Res.* **2010**, *70*, 7465–7475. [[CrossRef](#)]
51. Kim, S.; Takahashi, H.; Lin, W.-W.; Descargues, P.; Grivennikov, S.; Kim, Y.; Luo, J.-L.; Karin, M. Carcinoma-Produced Factors Activate Myeloid Cells through TLR2 to Stimulate Metastasis. *Nature* **2009**, *457*, 102–106. [[CrossRef](#)]
52. Deligne, C.; Murdamoothoo, D.; Gammage, A.N.; Gschwandtner, M.; Erne, W.; Loustau, T.; Marzeda, A.M.; Carapito, R.; Paul, N.; Velazquez-Quesada, I.; et al. Matrix-Targeting Immunotherapy Controls Tumor Growth and Spread by Switching Macrophage Phenotype. *Cancer Immunol. Res.* **2020**, *8*, 368–382. [[CrossRef](#)]
53. Grivennikov, S.I.; Wang, K.; Mucida, D.; Stewart, C.A.; Schnabl, B.; Jauch, D.; Taniguchi, K.; Yu, G.-Y.; Osterreicher, C.H.; Hung, K.E.; et al. Adenoma-Linked Barrier Defects and Microbial Products Drive IL-23/IL-17-Mediated Tumour Growth. *Nature* **2012**, *491*, 254–258. [[CrossRef](#)]
54. Kong, L.; Zhou, Y.; Bu, H.; Lv, T.; Shi, Y.; Yang, J. Deletion of Interleukin-6 in Monocytes/Macrophages Suppresses the Initiation of Hepatocellular Carcinoma in Mice. *J. Exp. Clin. Cancer Res.* **2016**, *35*, 131. [[CrossRef](#)]
55. Jung, M.; Mertens, C.; Tomat, E.; Brüne, B. Iron as a Central Player and Promising Target in Cancer Progression. *Int. J. Mol. Sci.* **2019**, *20*, 273. [[CrossRef](#)] [[PubMed](#)]
56. Hong, L.; Wang, S.; Li, W.; Wu, D.; Chen, W. Tumor-Associated Macrophages Promote the Metastasis of Ovarian Carcinoma Cells by Enhancing CXCL16/CXCR6 Expression. *Pathol. Res. Pract.* **2018**, *214*, 1345–1351. [[CrossRef](#)] [[PubMed](#)]
57. Wang, R.; Zhang, J.; Chen, S.; Lu, M.; Luo, X.; Yao, S.; Liu, S.; Qin, Y.; Chen, H. Tumor-Associated Macrophages Provide a Suitable Microenvironment for Non-Small Lung Cancer Invasion and Progression. *Lung Cancer* **2011**, *74*, 188–196. [[CrossRef](#)] [[PubMed](#)]

58. Wen, Z.; Liu, H.; Li, M.; Li, B.; Gao, W.; Shao, Q.; Fan, B.; Zhao, F.; Wang, Q.; Xie, Q.; et al. Increased Metabolites of 5-Lipoxygenase from Hypoxic Ovarian Cancer Cells Promote Tumor-Associated Macrophage Infiltration. *Oncogene* **2015**, *34*, 1241–1252. [[CrossRef](#)]
59. Chen, J.; Yao, Y.; Gong, C.; Yu, F.; Su, S.; Chen, J.; Liu, B.; Deng, H.; Wang, F.; Lin, L.; et al. CCL18 from Tumor-Associated Macrophages Promotes Breast Cancer Metastasis via PITPNM3. *Cancer Cell* **2011**, *19*, 541–555. [[CrossRef](#)]
60. Liu, L.; Wang, X.; Li, X.; Wu, X.; Tang, M.; Wang, X. Upregulation of IGF1 by Tumor-Associated Macrophages Promotes the Proliferation and Migration of Epithelial Ovarian Cancer Cells. *Oncol. Rep.* **2018**, *39*, 818–826. [[CrossRef](#)]
61. Yang, M.; Chen, J.; Su, F.; Yu, B.; Su, F.; Lin, L.; Liu, Y.; Huang, J.-D.; Song, E. Microvesicles Secreted by Macrophages Shuttle Invasion-Potentiating MicroRNAs into Breast Cancer Cells. *Mol. Cancer* **2011**, *10*, 117. [[CrossRef](#)] [[PubMed](#)]
62. Qian, B.; Pollard, J.W. Macrophage Diversity Enhances Tumor Progression and Metastasis. *Cell* **2010**, *141*, 39. [[CrossRef](#)] [[PubMed](#)]
63. Lin, L.; Chen, Y.-S.; Yao, Y.-D.; Chen, J.-Q.; Chen, J.-N.; Huang, S.-Y.; Zeng, Y.-J.; Yao, H.-R.; Zeng, S.-H.; Fu, Y.-S.; et al. CCL18 from Tumor-Associated Macrophages Promotes Angiogenesis in Breast Cancer. *Oncotarget* **2015**, *6*, 34758–34773. [[CrossRef](#)] [[PubMed](#)]
64. Gao, L.; Zhang, W.; Zhong, W.-Q.; Liu, Z.-J.; Li, H.-M.; Yu, Z.-L.; Zhao, Y.-F. Tumor Associated Macrophages Induce Epithelial to Mesenchymal Transition via the EGFR/ERK1/2 Pathway in Head and Neck Squamous Cell Carcinoma. *Oncol. Rep.* **2018**, *40*, 2558. [[CrossRef](#)] [[PubMed](#)]
65. Takenaka, M.C.; Gabriely, G.; Rothhammer, V.; Mascanfroni, I.D.; Wheeler, M.A.; Chao, C.-C.; Gutiérrez-Vázquez, C.; Kenison, J.; Tjon, E.C.; Barroso, A.; et al. Control of Tumor-Associated Macrophages and T Cells in Glioblastoma via AHR and CD39. *Nat. Neurosci.* **2019**, *22*, 729–740. [[CrossRef](#)] [[PubMed](#)]
66. Kato, Y.; Tabata, K.; Kimura, T.; Yachie-Kinoshita, A.; Ozawa, Y.; Yamada, K.; Ito, J.; Tachino, S.; Hori, Y.; Matsuki, M.; et al. Lenvatinib plus Anti-PD-1 Antibody Combination Treatment Activates CD8+ T Cells through Reduction of Tumor-Associated Macrophage and Activation of the Interferon Pathway. *PLoS ONE* **2019**, *14*, e0212513. [[CrossRef](#)] [[PubMed](#)]
67. Ito, M.; Minamiya, Y.; Kawai, H.; Saito, S.; Saito, H.; Nakagawa, T.; Imai, K.; Hirokawa, M.; Ogawa, J. Tumor-Derived TGFβ1 Induces Dendritic Cell Apoptosis in the Sentinel Lymph Node. *J. Immunol.* **2006**, *176*, 5637–5643. [[CrossRef](#)]
68. Solinas, G.; Germano, G.; Mantovani, A.; Allavena, P. Tumor-Associated Macrophages (TAM) as Major Players of the Cancer-Related Inflammation. *J. Leukoc. Biol.* **2009**, *86*, 1065–1073. [[CrossRef](#)]
69. Lievens, L.A.; Cornelissen, R.; Bezemer, K.; Kaijen-Lambers, M.E.H.; Hegmans, J.P.J.; Aerts, J.G.J.V. Pleural Effusion of Patients with Malignant Mesothelioma Induces Macrophage-Mediated T Cell Suppression. *J. Thorac. Oncol.* **2016**, *11*, 1755–1764. [[CrossRef](#)]
70. Campesato, L.F.; Budhu, S.; Tchaicha, J.; Weng, C.-H.; Gigoux, M.; Cohen, I.J.; Redmond, D.; Mangarin, L.; Pourpe, S.; Liu, C.; et al. Blockade of the AHR Restricts a Treg-Macrophage Suppressive Axis Induced by L-Kynurenine. *Nat. Commun.* **2020**, *11*, 4011. [[CrossRef](#)]
71. Chen, C.; Qu, Q.-X.; Shen, Y.; Mu, C.-Y.; Zhu, Y.-B.; Zhang, X.-G.; Huang, J.-A. Induced Expression of B7-H4 on the Surface of Lung Cancer Cell by the Tumor-Associated Macrophages: A Potential Mechanism of Immune Escape. *Cancer Lett.* **2012**, *317*, 99–105. [[CrossRef](#)] [[PubMed](#)]
72. Kuang, D.-M.; Zhao, Q.; Peng, C.; Xu, J.; Zhang, J.-P.; Wu, C.; Zheng, L. Activated Monocytes in Peritumoral Stroma of Hepatocellular Carcinoma Foster Immune Privilege and Disease Progression through PD-L1. *J. Exp. Med.* **2009**, *206*, 1327–1337. [[CrossRef](#)] [[PubMed](#)]
73. Prima, V.; Kaliberova, L.N.; Kaliberov, S.; Curiel, D.T.; Kusmartsev, S. COX2/MPGES1/PGE2 Pathway Regulates PD-L1 Expression in Tumor-Associated Macrophages and Myeloid-Derived Suppressor Cells. *Proc. Natl. Acad. Sci. USA* **2017**, *114*, 1117–1122. [[CrossRef](#)] [[PubMed](#)]
74. Lu, T.; Ramakrishnan, R.; Altiok, S.; Youn, J.-I.; Cheng, P.; Celis, E.; Pisarev, V.; Sherman, S.; Sporn, M.B.; Gabilovich, D. Tumor-Infiltrating Myeloid Cells Induce Tumor Cell Resistance to Cytotoxic T Cells in Mice. *J. Clin. Investig.* **2011**, *121*, 4015–4029. [[CrossRef](#)]
75. Zheng, P.; Chen, L.; Yuan, X.; Luo, Q.; Liu, Y.; Xie, G.; Ma, Y.; Shen, L. Exosomal Transfer of Tumor-Associated Macrophage-Derived miR-21 Confers Cisplatin Resistance in Gastric Cancer Cells. *J. Exp. Clin. Cancer Res.* **2017**, *36*, 53. [[CrossRef](#)]
76. Fu, X.-T.; Song, K.; Zhou, J.; Shi, Y.-H.; Liu, W.-R.; Shi, G.-M.; Gao, Q.; Wang, X.-Y.; Ding, Z.-B.; Fan, J. Tumor-Associated Macrophages Modulate Resistance to Oxaliplatin via Inducing Autophagy in Hepatocellular Carcinoma. *Cancer Cell Int.* **2019**, *19*, 71. [[CrossRef](#)]
77. Burger, J.A.; Tsukada, N.; Burger, M.; Zvaifler, N.J.; Dell'Aquila, M.; Kipps, T.J. Blood-Derived Nurse-like Cells Protect Chronic Lymphocytic Leukemia B Cells from Spontaneous Apoptosis through Stromal Cell-Derived Factor-1. *Blood* **2000**, *96*, 2655–2663. [[CrossRef](#)]
78. Boissard, F.; Fournié, J.-J.; Quillet-Mary, A.; Ysebaert, L.; Poupot, M. Nurse-like Cells Mediate Ibrutinib Resistance in Chronic Lymphocytic Leukemia Patients. *Blood Cancer J.* **2015**, *5*, e355. [[CrossRef](#)]
79. Boissard, F.; Laurent, C.; Ramsay, A.G.; Quillet-Mary, A.; Fournié, J.-J.; Poupot, M.; Ysebaert, L. Nurse-like Cells Impact on Disease Progression in Chronic Lymphocytic Leukemia. *Blood Cancer J.* **2016**, *6*, e381. [[CrossRef](#)]
80. Boissard, F.; Tosolini, M.; Ligat, L.; Quillet-Mary, A.; Lopez, F.; Fournié, J.-J.; Ysebaert, L.; Poupot, M. Nurse-like Cells Promote CLL Survival through LFA-3/CD2 Interactions. *Oncotarget* **2017**, *8*, 52225–52236. [[CrossRef](#)]
81. Caligaris-Cappio, F. Role of the Microenvironment in Chronic Lymphocytic Leukaemia. *Br. J. Haematol.* **2003**, *123*, 380–388. [[CrossRef](#)] [[PubMed](#)]

82. Nishio, M.; Endo, T.; Tsukada, N.; Ohata, J.; Kitada, S.; Reed, J.C.; Zvaifler, N.J.; Kipps, T.J. Nurse-like Cells Express BAFF and APRIL, Which Can Promote Survival of Chronic Lymphocytic Leukemia Cells via a Paracrine Pathway Distinct from That of SDF-1 α . *Blood* **2005**, *106*, 1012–1020. [[CrossRef](#)] [[PubMed](#)]
83. Dammeijer, F.; Lievense, L.A.; Kaijen-Lambers, M.E.; van Nimwegen, M.; Bezemer, K.; Hegmans, J.P.; van Hall, T.; Hendriks, R.W.; Aerts, J.G. Depletion of Tumor-Associated Macrophages with a CSF-1R Kinase Inhibitor Enhances Antitumor Immunity and Survival Induced by DC Immunotherapy. *Cancer Immunol. Res.* **2017**, *5*, 535–546. [[CrossRef](#)] [[PubMed](#)]
84. Peranzoni, E.; Lemoine, J.; Vimeux, L.; Feuillet, V.; Barrin, S.; Kantari-Mimoun, C.; Bercovici, N.; Guérin, M.; Biton, J.; Ouakrim, H.; et al. Macrophages Impede CD8 T Cells from Reaching Tumor Cells and Limit the Efficacy of Anti-PD-1 Treatment. *Proc. Natl. Acad. Sci. USA* **2018**, *115*, E4041–E4050. [[CrossRef](#)] [[PubMed](#)]
85. Panni, R.Z.; Herndon, J.M.; Zuo, C.; Hegde, S.; Hogg, G.D.; Knolhoff, B.L.; Breden, M.A.; Li, X.; Krisnawan, V.E.; Khan, S.Q.; et al. Agonism of CD11b Reprograms Innate Immunity to Sensitize Pancreatic Cancer to Immunotherapies. *Sci. Transl. Med.* **2019**, *11*. [[CrossRef](#)] [[PubMed](#)]
86. Lebdaï, S.; Gigoux, M.; Alvim, R.; Somma, A.; Nagar, K.; Azzouzi, A.R.; Cussenot, O.; Merghoub, T.; Wolchok, J.D.; Scherz, A.; et al. Potentiating Vascular-Targeted Photodynamic Therapy through CSF-1R Modulation of Myeloid Cells in a Preclinical Model of Prostate Cancer. *Oncoimmunology* **2019**, *8*, e1581528. [[CrossRef](#)]
87. Guilliams, M.; Ginhoux, F.; Jakubzick, C.; Naik, S.H.; Onai, N.; Schraml, B.U.; Segura, E.; Tussiwand, R.; Yona, S. Dendritic Cells, Monocytes and Macrophages: A Unified Nomenclature Based on Ontogeny. *Nat. Rev. Immunol.* **2014**, *14*, 571–578. [[CrossRef](#)]
88. Askenase, M.H.; Han, S.-J.; Byrd, A.L.; da Fonseca, D.M.; Bouladoux, N.; Wilhelm, C.; Konkel, J.E.; Hand, T.W.; Lacerda-Queiroz, N.; Su, X.; et al. Bone-Marrow-Resident NK Cells Prime Monocytes for Regulatory Function during Infection. *Immunity* **2015**, *42*, 1130–1142. [[CrossRef](#)]
89. Vu Manh, T.-P.; Bertho, N.; Hosmalin, A.; Schwartz-Cornil, I.; Dalod, M. Investigating Evolutionary Conservation of Dendritic Cell Subset Identity and Functions. *Front. Immunol.* **2015**, *6*, 260. [[CrossRef](#)]
90. Brewitz, A.; Eickhoff, S.; Dähling, S.; Quast, T.; Bedoui, S.; Kroczeck, R.A.; Kurts, C.; Garbi, N.; Barchet, W.; Iannaccone, M.; et al. CD8⁺ T Cells Orchestrate PDC-XCR1⁺ Dendritic Cell Spatial and Functional Cooperativity to Optimize Priming. *Immunity* **2017**, *46*, 205–219. [[CrossRef](#)]
91. Anderson, D.A.; Dutertre, C.-A.; Ginhoux, F.; Murphy, K.M. Genetic Models of Human and Mouse Dendritic Cell Development and Function. *Nat. Rev. Immunol.* **2020**. [[CrossRef](#)] [[PubMed](#)]
92. Liu, K.; Vitoria, G.D.; Schwickert, T.A.; Guermonprez, P.; Meredith, M.M.; Yao, K.; Chu, F.-F.; Randolph, G.J.; Rudensky, A.Y.; Nussenzweig, M. In Vivo Analysis of Dendritic Cell Development and Homeostasis. *Science* **2009**, *324*, 392–397. [[CrossRef](#)] [[PubMed](#)]
93. McKenna, H.J.; Stocking, K.L.; Miller, R.E.; Brasel, K.; De Smedt, T.; Maraskovsky, E.; Maliszewski, C.R.; Lynch, D.H.; Smith, J.; Pulendran, B.; et al. Mice Lacking Flt3 Ligand Have Deficient Hematopoiesis Affecting Hematopoietic Progenitor Cells, Dendritic Cells, and Natural Killer Cells. *Blood* **2000**, *95*, 3489–3497. [[CrossRef](#)] [[PubMed](#)]
94. Ghosh, H.S.; Cisse, B.; Bunin, A.; Lewis, K.L.; Reizis, B. Continuous Expression of the Transcription Factor E2-2 Maintains the Cell Fate of Mature Plasmacytoid Dendritic Cells. *Immunity* **2010**, *33*, 905–916. [[CrossRef](#)] [[PubMed](#)]
95. Spranger, S.; Dai, D.; Horton, B.; Gajewski, T.F. Tumor-Residing Batf3 Dendritic Cells Are Required for Effector T Cell Trafficking and Adoptive T Cell Therapy. *Cancer Cell* **2017**, *31*, 711–723.e4. [[CrossRef](#)]
96. Garris, C.S.; Arlauckas, S.P.; Kohler, R.H.; Trefny, M.P.; Garren, S.; Piot, C.; Engblom, C.; Pfirschke, C.; Siwicki, M.; Gungabeesoon, J.; et al. Successful Anti-PD-1 Cancer Immunotherapy Requires T Cell-Dendritic Cell Crosstalk Involving the Cytokines IFN- γ and IL-12. *Immunity* **2018**, *49*, 1148–1161.e7. [[CrossRef](#)]
97. Laoui, D.; Keirse, J.; Morias, Y.; Van Overmeire, E.; Geeraerts, X.; Elkrim, Y.; Kiss, M.; Bolli, E.; Lahmar, Q.; Sichen, D.; et al. The Tumour Microenvironment Harbours Ontogenically Distinct Dendritic Cell Populations with Opposing Effects on Tumour Immunity. *Nat. Commun.* **2016**, *7*, 13720. [[CrossRef](#)]
98. Veglia, F.; Gabrilovich, D.I. Dendritic Cells in Cancer: The Role Revisited. *Curr. Opin. Immunol.* **2017**, *45*, 43–51. [[CrossRef](#)]
99. Santini, S.M.; Di Pucchio, T.; Lapenta, C.; Parlato, S.; Logozzi, M.; Belardelli, F. The Natural Alliance between Type I Interferon and Dendritic Cells and Its Role in Linking Innate and Adaptive Immunity. *J. Interferon Cytokine Res.* **2002**, *22*, 1071–1080. [[CrossRef](#)]
100. Vanderheyde, N.; Aksoy, E.; Amraoui, Z.; Vandenabeele, P.; Goldman, M.; Willems, F. Tumoricidal Activity of Monocyte-Derived Dendritic Cells: Evidence for a Caspase-8-Dependent, Fas-Associated Death Domain-Independent Mechanism. *J. Immunol.* **2001**, *167*, 3565–3569. [[CrossRef](#)]
101. Sisirak, V.; Faget, J.; Vey, N.; Blay, J.-Y.; Ménétrier-Caux, C.; Caux, C.; Bendriss-Vermare, N. Plasmacytoid Dendritic Cells Deficient in IFN α Production Promote the Amplification of FOXP3⁺ Regulatory T Cells and Are Associated with Poor Prognosis in Breast Cancer Patients. *Oncoimmunology* **2013**, *2*, e22338. [[CrossRef](#)]
102. Pinto, A.; Rega, A.; Crother, T.R.; Sorrentino, R. Plasmacytoid Dendritic Cells and Their Therapeutic Activity in Cancer. *Oncoimmunology* **2012**, *1*, 726–734. [[CrossRef](#)] [[PubMed](#)]
103. Aspod, C.; Leccia, M.-T.; Charles, J.; Plumas, J. Melanoma Hijacks Plasmacytoid Dendritic Cells to Promote Its Own Progression. *Oncoimmunology* **2014**, *3*, e27402. [[CrossRef](#)] [[PubMed](#)]
104. Ray, A.; Das, D.S.; Song, Y.; Macri, V.; Richardson, P.; Brooks, C.L.; Chauhan, D.; Anderson, K.C. A Novel Agent SL-401 Induces Anti-Myeloma Activity by Targeting Plasmacytoid Dendritic Cells, Osteoclastogenesis and Cancer Stem-like Cells. *Leukemia* **2017**, *31*, 2652–2660. [[CrossRef](#)] [[PubMed](#)]

105. Blazar, B.R.; Lindberg, F.P.; Ingulli, E.; Panoskaltsis-Mortari, A.; Oldenborg, P.A.; Iizuka, K.; Yokoyama, W.M.; Taylor, P.A. CD47 (Integrin-Associated Protein) Engagement of Dendritic Cell and Macrophage Counterreceptors Is Required to Prevent the Clearance of Donor Lymphohematopoietic Cells. *J. Exp. Med.* **2001**, *194*, 541–549. [[CrossRef](#)]
106. Barkal, A.A.; Weiskopf, K.; Kao, K.S.; Gordon, S.R.; Rosental, B.; Yiu, Y.Y.; George, B.M.; Markovic, M.; Ring, N.G.; Tsai, J.M.; et al. Engagement of MHC Class I by the Inhibitory Receptor LILRB1 Suppresses Macrophages and Is a Target of Cancer Immunotherapy. *Nat. Immunol.* **2018**, *19*, 76–84. [[CrossRef](#)]
107. Chen, G.-Y.; Tang, J.; Zheng, P.; Liu, Y. CD24 and Siglec-10 Selectively Repress Tissue Damage-Induced Immune Responses. *Science* **2009**, *323*, 1722–1725. [[CrossRef](#)]
108. Halpert, M.M.; Konduri, V.; Liang, D.; Chen, Y.; Wing, J.B.; Paust, S.; Levitt, J.M.; Decker, W.K. Dendritic Cell-Secreted Cytotoxic T-Lymphocyte-Associated Protein-4 Regulates the T-Cell Response by Downmodulating Bystander Surface B7. *Stem. Cells Dev.* **2016**, *25*, 774–787. [[CrossRef](#)]
109. Yao, S.; Wang, S.; Zhu, Y.; Luo, L.; Zhu, G.; Flies, S.; Xu, H.; Ruff, W.; Broadwater, M.; Choi, I.-H.; et al. PD-1 on Dendritic Cells Impedes Innate Immunity against Bacterial Infection. *Blood* **2009**, *113*, 5811–5818. [[CrossRef](#)]
110. Karyampudi, L.; Lamichhane, P.; Krempski, J.; Kalli, K.R.; Behrens, M.D.; Vargas, D.M.; Hartmann, L.C.; Janco, J.M.T.; Dong, H.; Hedin, K.E.; et al. PD-1 Blunts the Function of Ovarian Tumor-Infiltrating Dendritic Cells by Inactivating NF-KB. *Cancer Res.* **2016**, *76*, 239–250. [[CrossRef](#)]
111. Schwartz, J.A.; Clayton, K.L.; Mujib, S.; Zhang, H.; Rahman, A.K.M.N.-U.; Liu, J.; Yue, F.Y.; Benko, E.; Kovacs, C.; Ostrowski, M.A. Tim-3 Is a Marker of Plasmacytoid Dendritic Cell Dysfunction during HIV Infection and Is Associated with the Recruitment of IRF7 and P85 into Lysosomes and with the Submembrane Displacement of TLR9. *J. Immunol.* **2017**, *198*, 3181–3194. [[CrossRef](#)]
112. de Mingo Pulido, Á.; Gardner, A.; Hiebler, S.; Soliman, H.; Rugo, H.S.; Krummel, M.F.; Coussens, L.M.; Ruffell, B. TIM-3 Regulates CD103+ Dendritic Cell Function and Response to Chemotherapy in Breast Cancer. *Cancer Cell* **2018**, *33*, 60–74.e6. [[CrossRef](#)]
113. Chiba, S.; Baghdadi, M.; Akiba, H.; Yoshiyama, H.; Kinoshita, I.; Dosaka-Akita, H.; Fujioka, Y.; Ohba, Y.; Gorman, J.V.; Colgan, J.D.; et al. Tumor-Infiltrating DCs Suppress Nucleic Acid-Mediated Innate Immune Responses through Interactions between the Receptor TIM-3 and the Alarmin HMGB1. *Nat. Immunol.* **2012**, *13*, 832–842. [[CrossRef](#)]
114. Menetrier-Caux, C.; Montmain, G.; Dieu, M.C.; Bain, C.; Favrot, M.C.; Caux, C.; Blay, J.Y. Inhibition of the Differentiation of Dendritic Cells from CD34(+) Progenitors by Tumor Cells: Role of Interleukin-6 and Macrophage Colony-Stimulating Factor. *Blood* **1998**, *92*, 4778–4791. [[CrossRef](#)]
115. Oyama, T.; Ran, S.; Ishida, T.; Nadaf, S.; Kerr, L.; Carbone, D.P.; Gabrilovich, D.I. Vascular Endothelial Growth Factor Affects Dendritic Cell Maturation through the Inhibition of Nuclear Factor-Kappa B Activation in Hemopoietic Progenitor Cells. *J. Immunol.* **1998**, *160*, 1224–1232.
116. Tauriello, D.V.F.; Palomo-Ponce, S.; Stork, D.; Berenguer-Llergo, A.; Badia-Ramentol, J.; Iglesias, M.; Sevillano, M.; Ibiza, S.; Cañellas, A.; Hernando-Mombona, X.; et al. TGFβ Drives Immune Evasion in Genetically Reconstituted Colon Cancer Metastasis. *Nature* **2018**, *554*, 538–543. [[CrossRef](#)]
117. Paul, F.; Arkin, Y.; Giladi, A.; Jaitin, D.A.; Kenigsberg, E.; Keren-Shaul, H.; Winter, D.; Lara-Astiaso, D.; Gury, M.; Weiner, A.; et al. Transcriptional Heterogeneity and Lineage Commitment in Myeloid Progenitors. *Cell* **2015**, *163*, 1663–1677. [[CrossRef](#)]
118. Bartels, M.; Govers, A.M.; Fleskens, V.; Lourenço, A.R.; Pals, C.E.; Vervoort, S.J.; van Gent, R.; Brenkman, A.B.; Bierings, M.B.; Ackerman, S.J.; et al. Acetylation of C/EBPε Is a Prerequisite for Terminal Neutrophil Differentiation. *Blood* **2015**, *125*, 1782–1792. [[CrossRef](#)]
119. Cowland, J.B.; Borregaard, N. Granulopoiesis and Granules of Human Neutrophils. *Immunol. Rev.* **2016**, *273*, 11–28. [[CrossRef](#)]
120. Ma, Y.; Yabluchanskiy, A.; Iyer, R.P.; Cannon, P.L.; Flynn, E.R.; Jung, M.; Henry, J.; Cates, C.A.; Deleon-Pennell, K.Y.; Lindsey, M.L. Temporal Neutrophil Polarization Following Myocardial Infarction. *Cardiovasc. Res.* **2016**, *110*, 51–61. [[CrossRef](#)]
121. Jiao, J.; Dragomir, A.-C.; Kocabayoglu, P.; Rahman, A.H.; Chow, A.; Hashimoto, D.; Leboeuf, M.; Kraus, T.; Moran, T.; Carrasco-Avino, G.; et al. Central Role of Conventional Dendritic Cells in Regulation of Bone Marrow Release and Survival of Neutrophils. *J. Immunol.* **2014**, *192*, 3374–3382. [[CrossRef](#)]
122. Phillipson, M.; Kubes, P. The Neutrophil in Vascular Inflammation. *Nat. Med.* **2011**, *17*, 1381–1390. [[CrossRef](#)]
123. Petri, B.; Phillipson, M.; Kubes, P. The Physiology of Leukocyte Recruitment: An in Vivo Perspective. *J. Immunol.* **2008**, *180*, 6439–6446. [[CrossRef](#)]
124. Sheshachalam, A.; Srivastava, N.; Mitchell, T.; Lacy, P.; Eitzen, G. Granule Protein Processing and Regulated Secretion in Neutrophils. *Front. Immunol.* **2014**, *5*, 448. [[CrossRef](#)]
125. Kolaczowska, E.; Jenne, C.N.; Surewaard, B.G.J.; Thanabalasuriar, A.; Lee, W.-Y.; Sanz, M.-J.; Mowen, K.; Opdenakker, G.; Kubes, P. Molecular Mechanisms of NET Formation and Degradation Revealed by Intravital Imaging in the Liver Vasculature. *Nat. Com.* **2015**, *6*, 6673. [[CrossRef](#)]
126. Jorch, S.K.; Kubes, P. An Emerging Role for Neutrophil Extracellular Traps in Noninfectious Disease. *Nat. Med.* **2017**, *23*, 279–287. [[CrossRef](#)]
127. Dalli, J.; Montero-Melendez, T.; Norling, L.V.; Yin, X.; Hinds, C.; Haskard, D.; Mayr, M.; Perretti, M. Heterogeneity in Neutrophil Microparticles Reveals Distinct Proteome and Functional Properties. *Mol. Cell Prot.* **2013**, *12*, 2205–2219. [[CrossRef](#)]
128. Frangogiannis, N.G. Regulation of the Inflammatory Response in Cardiac Repair. *Circul. Res.* **2012**, *110*, 159–173. [[CrossRef](#)]
129. Wang, J. Neutrophils in Tissue Injury and Repair. *Cell Tissue Res.* **2018**, *371*, 531–539. [[CrossRef](#)]

130. Sagiv, J.Y.; Michaeli, J.; Assi, S.; Mishalian, I.; Kisos, H.; Levy, L.; Damti, P.; Lumbroso, D.; Polyansky, L.; Sionov, R.V.; et al. Phenotypic Diversity and Plasticity in Circulating Neutrophil Subpopulations in Cancer. *Cell Rep.* **2015**, *10*, 562–573. [[CrossRef](#)]
131. Fridlender, Z.G.; Albelda, S.M. Tumor-Associated Neutrophils: Friend or Foe? *Carcinogenesis* **2012**, *33*, 949–955. [[CrossRef](#)]
132. Andzinski, L.; Wu, C.-F.; Lienenklaus, S.; Kröger, A.; Weiss, S.; Jablonska, J. Delayed Apoptosis of Tumor Associated Neutrophils in the Absence of Endogenous IFN- β . *Int. J. Cancer* **2015**, *136*, 572–583. [[CrossRef](#)]
133. Andzinski, L.; Kasnitz, N.; Stahnke, S.; Wu, C.-F.; Gereke, M.; von Köckritz-Blickwede, M.; Schilling, B.; Brandau, S.; Weiss, S.; Jablonska, J. Type I IFNs Induce Anti-Tumor Polarization of Tumor Associated Neutrophils in Mice and Human. *Int. J. Cancer* **2016**, *138*, 1982–1993. [[CrossRef](#)]
134. Ohms, M.; Möller, S.; Laskay, T. An Attempt to Polarize Human Neutrophils Toward N1 and N2 Phenotypes In Vitro. *Front. Immunol.* **2020**, *11*, 532. [[CrossRef](#)]
135. Triner, D.; Devenport, S.N.; Ramakrishnan, S.K.; Ma, X.; Frieler, R.A.; Greenson, J.K.; Inohara, N.; Nunez, G.; Colacino, J.A.; Mortensen, R.M.; et al. Neutrophils Restrict Tumor-Associated Microbiota to Reduce Growth and Invasion of Colon Tumors in Mice. *Gastroenterology* **2019**, *156*, 1467–1482. [[CrossRef](#)]
136. Mahiddine, K.; Blaisdell, A.; Ma, S.; Créquer-Grandhomme, A.; Lowell, C.A.; Erlebacher, A. Relief of Tumor Hypoxia Unleashes the Tumoricidal Potential of Neutrophils. *J. Clin. Investig.* **2020**, *130*, 389–403. [[CrossRef](#)]
137. Mensurado, S.; Rei, M.; Lança, T.; Ioannou, M.; Gonçalves-Sousa, N.; Kubo, H.; Malissen, M.; Papayannopoulos, V.; Serre, K.; Silva-Santos, B. Tumor-Associated Neutrophils Suppress pro-Tumoral IL-17+ $\Gamma\delta$ T Cells through Induction of Oxidative Stress. *PLoS Biol.* **2018**, *16*, e2004990. [[CrossRef](#)]
138. Costanzo-Garvey, D.L.; Keeley, T.; Case, A.J.; Watson, G.F.; Alsamrae, M.; Yu, Y.; Su, K.; Heim, C.E.; Kielian, T.; Morrissey, C.; et al. Neutrophils Are Mediators of Metastatic Prostate Cancer Progression in Bone. *Cancer Immunol. Immunother.* **2020**, *69*, 1113–1130. [[CrossRef](#)]
139. Martin, A.; Seignez, C.; Racoeur, C.; Isambert, N.; Mabrouk, N.; Scagliarini, A.; Reveneau, S.; Arnould, L.; Bettaieb, A.; Jeannin, J.-F.; et al. Tumor-Derived Granzyme B-Expressing Neutrophils Acquire Antitumor Potential after Lipid A Treatment. *Oncotarget* **2018**, *9*, 28364–28378. [[CrossRef](#)]
140. Sionov, R.V.; Fainsod-Levi, T.; Zelter, T.; Polyansky, L.; Pham, C.T.; Granot, Z. Neutrophil Cathepsin G and Tumor Cell RAGE Facilitate Neutrophil Anti-Tumor Cytotoxicity. *Oncoimmunology* **2019**, *8*, e1624129. [[CrossRef](#)]
141. Eruslanov, E.B.; Bhojnagarwala, P.S.; Quatromoni, J.G.; Stephen, T.L.; Ranganathan, A.; Deshpande, C.; Akimova, T.; Vachani, A.; Litzky, L.; Hancock, W.W.; et al. Tumor-Associated Neutrophils Stimulate T Cell Responses in Early-Stage Human Lung Cancer. *J. Clin. Investig.* **2014**, *124*, 5466–5480. [[CrossRef](#)]
142. Hagerling, C.; Gonzalez, H.; Salari, K.; Wang, C.-Y.; Lin, C.; Robles, I.; van Gogh, M.; Dejmeck, A.; Jirstrom, K.; Werb, Z. Immune Effector Monocyte-Neutrophil Cooperation Induced by the Primary Tumor Prevents Metastatic Progression of Breast Cancer. *Proc. Natl. Acad. Sci. USA* **2019**, *116*, 21704–21714. [[CrossRef](#)]
143. Governa, V.; Trella, E.; Mele, V.; Tornillo, L.; Amicarella, F.; Cremonesi, E.; Muraro, M.G.; Xu, H.; Droeser, R.; Däster, S.R.; et al. The Interplay Between Neutrophils and CD8+ T Cells Improves Survival in Human Colorectal Cancer. *Clin. Cancer Res.* **2017**, *23*, 3847–3858. [[CrossRef](#)]
144. Yu, L.; Zhong, L.; Xiong, L.; Dan, W.; Li, J.; Ye, J.; Wan, P.; Luo, X.; Chu, X.; Liu, C.; et al. Neutrophil Elastase-Mediated Proteolysis of the Tumor Suppressor P200 CUX1 Promotes Cell Proliferation and Inhibits Cell Differentiation in APL. *Life Sci.* **2020**, *242*, 117229. [[CrossRef](#)]
145. Hattar, K.; Franz, K.; Ludwig, M.; Sibelius, U.; Wilhelm, J.; Lohmeyer, J.; Savai, R.; Subtil, F.S.B.; Dahlem, G.; Eul, B.; et al. Interactions between Neutrophils and Non-Small Cell Lung Cancer Cells: Enhancement of Tumor Proliferation and Inflammatory Mediator Synthesis. *Cancer Immunol. Immunother.* **2014**, *63*, 1297–1306. [[CrossRef](#)]
146. Zha, C.; Meng, X.; Li, L.; Mi, S.; Qian, D.; Li, Z.; Wu, P.; Hu, S.; Zhao, S.; Cai, J.; et al. Neutrophil Extracellular Traps Mediate the Crosstalk between Glioma Progression and the Tumor Microenvironment via the HMGB1/RAGE/IL-8 Axis. *Cancer Biol. Med.* **2020**, *17*, 154–168. [[CrossRef](#)]
147. Miller-Ocuin, J.L.; Liang, X.; Boone, B.A.; Doerfler, W.R.; Singhi, A.D.; Tang, D.; Kang, R.; Lotze, M.T.; Zeh, H.J. DNA Released from Neutrophil Extracellular Traps (NETs) Activates Pancreatic Stellate Cells and Enhances Pancreatic Tumor Growth. *Oncoimmunology* **2019**, *8*, e1605822. [[CrossRef](#)]
148. Szczerba, B.M.; Castro-Giner, F.; Vetter, M.; Krol, I.; Gkountela, S.; Landin, J.; Scheidmann, M.C.; Donato, C.; Scherrer, R.; Singer, J.; et al. Neutrophils Escort Circulating Tumour Cells to Enable Cell Cycle Progression. *Nature* **2019**, *566*, 553–557. [[CrossRef](#)]
149. Liang, W.; Li, Q.; Ferrara, N. Metastatic Growth Instructed by Neutrophil-Derived Transferrin. *Proc. Natl. Acad. Sci. USA* **2018**, *115*, 11060–11065. [[CrossRef](#)]
150. Spicer, J.D.; McDonald, B.; Cools-Lartigue, J.J.; Chow, S.C.; Giannias, B.; Kubes, P.; Ferri, L.E. Neutrophils Promote Liver Metastasis via Mac-1-Mediated Interactions with Circulating Tumor Cells. *Cancer Res.* **2012**, *72*, 3919–3927. [[CrossRef](#)]
151. Huh, S.J.; Liang, S.; Sharma, A.; Dong, C.; Robertson, G.P. Transiently Entrapped Circulating Tumor Cells Interact with Neutrophils to Facilitate Lung Metastasis Development. *Cancer Res.* **2010**, *70*, 6071–6082. [[CrossRef](#)] [[PubMed](#)]
152. Singel, K.L.; Emmons, T.R.; Khan, A.N.H.; Mayor, P.C.; Shen, S.; Wong, J.T.; Morrell, K.; Eng, K.H.; Mark, J.; Bankert, R.B.; et al. Mature Neutrophils Suppress T Cell Immunity in Ovarian Cancer Microenvironment. *JCI Insight* **2019**, *4*. [[CrossRef](#)] [[PubMed](#)]

153. Perez, C.; Botta, C.; Zabaleta, A.; Puig, N.; Cedena, M.-T.; Goicoechea, I.; Alameda, D.; San José-Eneriz, E.; Merino, J.; Rodríguez-Otero, P.; et al. Immunogenomic Identification and Characterization of Granulocytic Myeloid-Derived Suppressor Cells in Multiple Myeloma. *Blood* **2020**, *136*, 199–209. [[CrossRef](#)] [[PubMed](#)]
154. Forsthuber, A.; Lipp, K.; Andersen, L.; Ebersberger, S.; Graña-Castro, O.; Ellmeier, W.; Petzelbauer, P.; Lichtenberger, B.M.; Loewe, R. CXCL5 as Regulator of Neutrophil Function in Cutaneous Melanoma. *J. Investig. Dermatol.* **2019**, *139*, 186–194. [[CrossRef](#)]
155. Khou, S.; Popa, A.; Luci, C.; Bihl, F.; Meghraoui-Kheddar, A.; Bourdely, P.; Salavagione, E.; Cosson, E.; Rubod, A.; Cazareth, J.; et al. Tumor-Associated Neutrophils Dampen Adaptive Immunity and Promote Cutaneous Squamous Cell Carcinoma Development. *Cancers* **2020**, *12*, 1860. [[CrossRef](#)]
156. Shang, A.; Wang, W.; Gu, C.; Chen, C.; Zeng, B.; Yang, Y.; Ji, P.; Sun, J.; Wu, J.; Lu, W.; et al. Long Non-Coding RNA HOTTIP Enhances IL-6 Expression to Potentiate Immune Escape of Ovarian Cancer Cells by Upregulating the Expression of PD-L1 in Neutrophils. *J. Exp. Clin. Cancer Res.* **2019**, *38*, 411. [[CrossRef](#)]
157. Sceneay, J.; Chow, M.T.; Chen, A.; Halse, H.M.; Wong, C.S.F.; Andrews, D.M.; Sloan, E.K.; Parker, B.S.; Bowtell, D.D.; Smyth, M.J.; et al. Primary Tumor Hypoxia Recruits CD11b+/Ly6Cmed/Ly6G+ Immune Suppressor Cells and Compromises NK Cell Cytotoxicity in the Premetastatic Niche. *Cancer Res.* **2012**, *72*, 3906–3911. [[CrossRef](#)]
158. Weber, R.; Fleming, V.; Hu, X.; Nagibin, V.; Groth, C.; Altevogt, P.; Utikal, J.; Umansky, V. Myeloid-Derived Suppressor Cells Hinder the Anti-Cancer Activity of Immune Checkpoint Inhibitors. *Front. Immunol.* **2018**, *9*, 1310. [[CrossRef](#)]
159. Khaled, Y.S.; Ammori, B.J.; Elkord, E. Myeloid-Derived Suppressor Cells in Cancer: Recent Progress and Prospects. *Immunol. Cell Biol.* **2013**, *91*, 493–502. [[CrossRef](#)]
160. Agrati, C.; Sacchi, A.; Bordoni, V.; Cimini, E.; Notari, S.; Grassi, G.; Casetti, R.; Tartaglia, E.; Lalle, E.; D’Abramo, A.; et al. Expansion of Myeloid-Derived Suppressor Cells in Patients with Severe Coronavirus Disease (COVID-19). *Cell Death Differ.* **2020**, *27*, 3196–3207. [[CrossRef](#)]
161. Gabrilovich, D.I.; Ostrand-Rosenberg, S.; Bronte, V. Coordinated Regulation of Myeloid Cells by Tumours. *Nat. Rev. Immunol.* **2012**, *12*, 253–268. [[CrossRef](#)] [[PubMed](#)]
162. Dumitru, C.A.; Moses, K.; Trellakis, S.; Lang, S.; Brandau, S. Neutrophils and Granulocytic Myeloid-Derived Suppressor Cells: Immunophenotyping, Cell Biology and Clinical Relevance in Human Oncology. *Cancer Immunol. Immunother.* **2012**, *61*, 1155–1167. [[CrossRef](#)]
163. Talmadge, J.E.; Gabrilovich, D.I. History of Myeloid-Derived Suppressor Cells. *Nat. Rev. Cancer* **2013**, *13*, 739–752. [[CrossRef](#)]
164. Bronte, V.; Brandau, S.; Chen, S.-H.; Colombo, M.P.; Frey, A.B.; Greten, T.F.; Mandruzzato, S.; Murray, P.J.; Ochoa, A.; Ostrand-Rosenberg, S.; et al. Recommendations for Myeloid-Derived Suppressor Cell Nomenclature and Characterization Standards. *Nat. Commun.* **2016**, *7*, 12150. [[CrossRef](#)]
165. Poschke, I.; Kiessling, R. On the Armament and Appearances of Human Myeloid-Derived Suppressor Cells. *Clin. Immunol.* **2012**, *144*, 250–268. [[CrossRef](#)]
166. Youn, J.-I.; Gabrilovich, D.I. The Biology of Myeloid-Derived Suppressor Cells: The Blessing and the Curse of Morphological and Functional Heterogeneity. *Eur. J. Immunol.* **2010**, *40*, 2969–2975. [[CrossRef](#)]
167. Meirou, Y.; Kanterman, J.; Baniyash, M. Paving the Road to Tumor Development and Spreading: Myeloid-Derived Suppressor Cells Are Ruling the Fate. *Front. Immunol.* **2015**, *6*, 523. [[CrossRef](#)]
168. Lahat, N.; Rahat, M.A.; Ballan, M.; Weiss-Cerem, L.; Engelmayer, M.; Bitterman, H. Hypoxia Reduces CD80 Expression on Monocytes but Enhances Their LPS-Stimulated TNF-Alpha Secretion. *J. Leukoc. Biol.* **2003**, *74*, 197–205. [[CrossRef](#)]
169. Huang, M.; Wu, R.; Chen, L.; Peng, Q.; Li, S.; Zhang, Y.; Zhou, L.; Duan, L. S100A9 Regulates MDSCs-Mediated Immune Suppression via the RAGE and TLR4 Signaling Pathways in Colorectal Carcinoma. *Front. Immunol.* **2019**, *10*, 2243. [[CrossRef](#)]
170. Zhao, F.; Hoehst, B.; Duffy, A.; Gamrekelashvili, J.; Fioravanti, S.; Manns, M.P.; Greten, T.F.; Korangy, F. S100A9 a New Marker for Monocytic Human Myeloid-Derived Suppressor Cells. *Immunology* **2012**, *136*, 176–183. [[CrossRef](#)]
171. Condamine, T.; Dominguez, G.A.; Youn, J.-I.; Kossenkov, A.V.; Mony, S.; Alicea-Torres, K.; Tcyganov, E.; Hashimoto, A.; Nefedova, Y.; Lin, C.; et al. Lectin-Type Oxidized LDL Receptor-1 Distinguishes Population of Human Polymorphonuclear Myeloid-Derived Suppressor Cells in Cancer Patients. *Sci. Immunol.* **2016**, *1*. [[CrossRef](#)] [[PubMed](#)]
172. Cassetta, L.; Bruderek, K.; Skrzeczynska-Moncznik, J.; Osiecka, O.; Hu, X.; Rundgren, I.M.; Lin, A.; Santegoets, K.; Horzum, U.; Godinho-Santos, A.; et al. Differential Expansion of Circulating Human MDSC Subsets in Patients with Cancer, Infection and Inflammation. *J. Immunother. Cancer* **2020**, *8*, 1–13. [[CrossRef](#)] [[PubMed](#)]
173. Alshetaiwi, H.; Pervolarakis, N.; McIntyre, L.L.; Ma, D.; Nguyen, Q.; Rath, J.A.; Nee, K.; Hernandez, G.; Evans, K.; Torosian, L.; et al. Defining the Emergence of Myeloid-Derived Suppressor Cells in Breast Cancer Using Single-Cell Transcriptomics. *Sci. Immunol.* **2020**, *5*, 2–28. [[CrossRef](#)] [[PubMed](#)]
174. Nagaraj, S.; Gupta, K.; Pisarev, V.; Kinarsky, L.; Sherman, S.; Kang, L.; Herber, D.L.; Schneck, J.; Gabrilovich, D.I. Altered Recognition of Antigen Is a Mechanism of CD8+ T Cell Tolerance in Cancer. *Nat. Med.* **2007**, *13*, 828–835. [[CrossRef](#)]
175. Raber, P.L.; Thevenot, P.; Sierra, R.; Wyczechowska, D.; Halle, D.; Ramirez, M.E.; Ochoa, A.C.; Fletcher, M.; Velasco, C.; Wilk, A.; et al. Subpopulations of Myeloid-Derived Suppressor Cells Impair T Cell Responses through Independent Nitric Oxide-Related Pathways. *Int. J. Cancer* **2014**, *134*, 2853–2864. [[CrossRef](#)]
176. Zhou, L.; Miao, K.; Yin, B.; Li, H.; Fan, J.; Zhu, Y.; Ba, H.; Zhang, Z.; Chen, F.; Wang, J.; et al. Cardioprotective Role of Myeloid-Derived Suppressor Cells in Heart Failure. *Circulation* **2018**, *138*, 181–197. [[CrossRef](#)]

177. Crook, K.R.; Jin, M.; Weeks, M.F.; Rampersad, R.R.; Baldi, R.M.; Glekas, A.S.; Shen, Y.; Esserman, D.A.; Little, P.; Schwartz, T.A.; et al. Myeloid-Derived Suppressor Cells Regulate T Cell and B Cell Responses during Autoimmune Disease. *J. Leukoc. Biol.* **2015**, *97*, 573–582. [[CrossRef](#)]
178. Kurkó, J.; Vida, A.; Ocskó, T.; Tryniszewska, B.; Rauch, T.A.; Glant, T.T.; Szekanecz, Z.; Mikecz, K. Suppression of Proteoglycan-Induced Autoimmune Arthritis by Myeloid-Derived Suppressor Cells Generated in Vitro from Murine Bone Marrow. *PLoS ONE* **2014**, *9*, e111815. [[CrossRef](#)]
179. Ioannou, M.; Alissafi, T.; Lazaridis, I.; Deraos, G.; Matsoukas, J.; Gravanis, A.; Mastorodemos, V.; Plaitakis, A.; Sharpe, A.; Boumpas, D.; et al. Crucial Role of Granulocytic Myeloid-Derived Suppressor Cells in the Regulation of Central Nervous System Autoimmune Disease. *J. Immunol.* **2012**, *188*, 1136–1146. [[CrossRef](#)]
180. Bergenfelz, C.; Leandersson, K. The Generation and Identity of Human Myeloid-Derived Suppressor Cells. *Front. Oncol.* **2020**, *10*, 109. [[CrossRef](#)]
181. Bernard, V.; Semaan, A.; Huang, J.; San Lucas, F.A.; Mulu, F.C.; Stephens, B.M.; Guerrero, P.A.; Huang, Y.; Zhao, J.; Kamyabi, N.; et al. Single-Cell Transcriptomics of Pancreatic Cancer Precursors Demonstrates Epithelial and Microenvironmental Heterogeneity as an Early Event in Neoplastic Progression. *Clin. Cancer Res.* **2019**, *25*, 2194–2205. [[CrossRef](#)] [[PubMed](#)]
182. Kumar, V.; Donthireddy, L.; Marvel, D.; Condamine, T.; Wang, F.; Lavilla-Alonso, S.; Hashimoto, A.; Vonteddu, P.; Behera, R.; Goins, M.A.; et al. Cancer-Associated Fibroblasts Neutralize the Anti-Tumor Effect of CSF1 Receptor Blockade by Inducing PMN-MDSC Infiltration of Tumors. *Cancer Cell* **2017**, *32*, 654–668.e5. [[CrossRef](#)] [[PubMed](#)]
183. Gao, Y.; Sun, W.; Shang, W.; Li, Y.; Zhang, D.; Wang, T.; Zhang, X.; Zhang, S.; Zhang, Y.; Yang, R. Lnc-C/EBP β Negatively Regulates the Suppressive Function of Myeloid-Derived Suppressor Cells. *Cancer Immunol. Res.* **2018**, *6*, 1352–1363. [[CrossRef](#)] [[PubMed](#)]
184. Alkhateeb, T.; Kumbhare, A.; Bah, I.; Youssef, D.; Yao, Z.Q.; McCall, C.E.; El Gazzar, M. S100A9 Maintains Myeloid-Derived Suppressor Cells in Chronic Sepsis by Inducing MiR-21 and MiR-181b. *Mol. Immunol.* **2019**, *112*, 72–81. [[CrossRef](#)] [[PubMed](#)]
185. Cheng, P.; Corzo, C.A.; Luetteke, N.; Yu, B.; Nagaraj, S.; Bui, M.M.; Ortiz, M.; Nacken, W.; Sorg, C.; Vogl, T.; et al. Inhibition of Dendritic Cell Differentiation and Accumulation of Myeloid-Derived Suppressor Cells in Cancer Is Regulated by S100A9 Protein. *J. Exp. Med.* **2008**, *205*, 2235–2249. [[CrossRef](#)]
186. Mazzoni, C.J.; Gomes, C.A.; Souza, N.A.; de Queiroz, R.G.; Justiniano, S.C.B.; Ward, R.D.; Kyriacou, C.P.; Peixoto, A.A. Molecular Evolution of the Period Gene in Sandflies. *J. Mol. Evol.* **2002**, *55*, 553–562. [[CrossRef](#)]
187. Steggerda, S.M.; Bennett, M.K.; Chen, J.; Emberley, E.; Huang, T.; Janes, J.R.; Li, W.; MacKinnon, A.L.; Makkouk, A.; Marguier, G.; et al. Inhibition of Arginase by CB-1158 Blocks Myeloid Cell-Mediated Immune Suppression in the Tumor Microenvironment. *J. Immunother. Cancer* **2017**, *5*, 101. [[CrossRef](#)]
188. Srivastava, M.K.; Sinha, P.; Clements, V.K.; Rodriguez, P.; Ostrand-Rosenberg, S. Myeloid-Derived Suppressor Cells Inhibit T-Cell Activation by Depleting Cystine and Cysteine. *Cancer Res.* **2010**, *70*, 68–77. [[CrossRef](#)]
189. Yu, J.; Du, W.; Yan, F.; Wang, Y.; Li, H.; Cao, S.; Yu, W.; Shen, C.; Liu, J.; Ren, X. Myeloid-Derived Suppressor Cells Suppress Antitumor Immune Responses through IDO Expression and Correlate with Lymph Node Metastasis in Patients with Breast Cancer. *J. Immunol.* **2013**, *190*, 3783–3797. [[CrossRef](#)]
190. Baumann, T.; Dunkel, A.; Schmid, C.; Schmitt, S.; Hiltensperger, M.; Lohr, K.; Laketa, V.; Donakonda, S.; Ahting, U.; Lorenz-Depiereux, B.; et al. Regulatory Myeloid Cells Paralyze T Cells through Cell-Cell Transfer of the Metabolite Methylglyoxal. *Nat. Immunol.* **2020**, *21*, 555–566. [[CrossRef](#)]
191. Molon, B.; Ugel, S.; Del Pozzo, F.; Soldani, C.; Zilio, S.; Avella, D.; De Palma, A.; Mauri, P.; Monegal, A.; Rescigno, M.; et al. Chemokine Nitration Prevents Intratumoral Infiltration of Antigen-Specific T Cells. *J. Exp. Med.* **2011**, *208*, 1949–1962. [[CrossRef](#)] [[PubMed](#)]
192. Hanson, E.M.; Clements, V.K.; Sinha, P.; Ilkovitch, D.; Ostrand-Rosenberg, S. Myeloid-Derived Suppressor Cells down-Regulate L-Selectin Expression on CD4+ and CD8+ T Cells. *J. Immunol.* **2009**, *183*, 937–944. [[CrossRef](#)] [[PubMed](#)]
193. Liu, C.; Yu, S.; Kappes, J.; Wang, J.; Grizzle, W.E.; Zinn, K.R.; Zhang, H.-G. Expansion of Spleen Myeloid Suppressor Cells Represses NK Cell Cytotoxicity in Tumor-Bearing Host. *Blood* **2007**, *109*, 4336–4342. [[CrossRef](#)] [[PubMed](#)]
194. Elkabets, M.; Ribeiro, V.S.G.; Dinarello, C.A.; Ostrand-Rosenberg, S.; Di Santo, J.P.; Apte, R.N.; Vosshenrich, C.A.J. IL-1 β Regulates a Novel Myeloid-Derived Suppressor Cell Subset That Impairs NK Cell Development and Function. *Eur. J. Immunol.* **2010**, *40*, 3347–3357. [[CrossRef](#)] [[PubMed](#)]
195. Kuroda, H.; Mabuchi, S.; Yokoi, E.; Komura, N.; Kozasa, K.; Matsumoto, Y.; Kawano, M.; Takahashi, R.; Sasano, T.; Shimura, K.; et al. Prostaglandin E2 Produced by Myeloid-Derived Suppressive Cells Induces Cancer Stem Cells in Uterine Cervical Cancer. *Oncotarget* **2018**, *9*, 36317–36330. [[CrossRef](#)] [[PubMed](#)]
196. Komura, N.; Mabuchi, S.; Shimura, K.; Yokoi, E.; Kozasa, K.; Kuroda, H.; Takahashi, R.; Sasano, T.; Kawano, M.; Matsumoto, Y.; et al. The Role of Myeloid-Derived Suppressor Cells in Increasing Cancer Stem-like Cells and Promoting PD-L1 Expression in Epithelial Ovarian Cancer. *Cancer Immunol. Immunother.* **2020**, *69*, 2477–2499. [[CrossRef](#)]
197. Pan, P.-Y.; Ma, G.; Weber, K.J.; Ozao-Choy, J.; Wang, G.; Yin, B.; Divino, C.M.; Chen, S.-H. Immune Stimulatory Receptor CD40 Is Required for T-Cell Suppression and T Regulatory Cell Activation Mediated by Myeloid-Derived Suppressor Cells in Cancer. *Cancer Res.* **2010**, *70*, 99–108. [[CrossRef](#)]

198. Huang, B.; Pan, P.-Y.; Li, Q.; Sato, A.I.; Levy, D.E.; Bromberg, J.; Divino, C.M.; Chen, S.-H. Gr-1+CD115+ Immature Myeloid Suppressor Cells Mediate the Development of Tumor-Induced T Regulatory Cells and T-Cell Anergy in Tumor-Bearing Host. *Cancer Res.* **2006**, *66*, 1123–1131. [CrossRef]
199. Kim, K.; Skora, A.D.; Li, Z.; Liu, Q.; Tam, A.J.; Blosser, R.L.; Diaz, L.A.; Papadopoulos, N.; Kinzler, K.W.; Vogelstein, B.; et al. Eradication of Metastatic Mouse Cancers Resistant to Immune Checkpoint Blockade by Suppression of Myeloid-Derived Cells. *Proc. Natl. Acad. Sci. USA* **2014**, *111*, 11774–11779. [CrossRef]
200. Romano, A.; Parrinello, N.L.; La Cava, P.; Tibullo, D.; Giallongo, C.; Camiolo, G.; Puglisi, F.; Parisi, M.; Piroso, M.C.; Martino, E.; et al. PMN-MDSC and Arginase Are Increased in Myeloma and May Contribute to Resistance to Therapy. *Expert Rev. Mol. Diagn.* **2018**, *18*, 675–683. [CrossRef]
201. Maaninka, K.; Lappalainen, J.; Kovanen, P.T. Human Mast Cells Arise from a Common Circulating Progenitor. *J. Allergy Clin. Immunol.* **2013**, *132*, 463–469.e3. [CrossRef] [PubMed]
202. Schmetzer, O.; Valentin, P.; Church, M.K.; Maurer, M.; Siebenhaar, F. Murine and Human Mast Cell Progenitors. *Eur. J. Pharmacol.* **2016**, *778*, 2–10. [CrossRef]
203. Gurish, M.F.; Boyce, J.A. Mast Cell Growth, Differentiation, and Death. *Clin. Rev. Allergy Immunol.* **2002**, *22*, 107–118. [CrossRef]
204. Gentek, R.; Ghigo, C.; Hoeffel, G.; Bulle, M.J.; Msallam, R.; Gautier, G.; Launay, P.; Chen, J.; Ginhoux, F.; Bajénoff, M. Hemogenic Endothelial Fate Mapping Reveals Dual Developmental Origin of Mast Cells. *Immunity* **2018**, *48*, 1160–1171.e5. [CrossRef] [PubMed]
205. Lundquist, A.; Pejler, G. Biological Implications of Preformed Mast Cell Mediators. *Cell Mol. Life Sci.* **2011**, *68*, 965–975. [CrossRef] [PubMed]
206. Wernersson, S.; Pejler, G. Mast Cell Secretory Granules: Armed for Battle. *Nat. Rev. Immunol.* **2014**, *14*, 478–494. [CrossRef]
207. Espinosa, E.; Valitutti, S. New Roles and Controls of Mast Cells. *Curr. Opin. Immunol.* **2018**, *50*, 39–47. [CrossRef]
208. Komi, D.E.A.; Rambasek, T.; Wöhr, S. Mastocytosis: From a Molecular Point of View. *Clin. Rev. Allergy Immunol.* **2018**, *54*, 397–411. [CrossRef]
209. Gaudenzio, N.; Laurent, C.; Valitutti, S.; Espinosa, E. Human Mast Cells Drive Memory CD4+ T Cells toward an Inflammatory IL-22+ Phenotype. *J. Allergy Clin. Immunol.* **2013**, *131*, 1400–1407.e11. [CrossRef]
210. Galli, S.J.; Nakae, S.; Tsai, M. Mast Cells in the Development of Adaptive Immune Responses. *Nat. Immunol.* **2005**, *6*, 135–142. [CrossRef]
211. Gilfillan, A.M.; Tkaczyk, C. Integrated Signalling Pathways for Mast-Cell Activation. *Nat. Rev. Immunol.* **2006**, *6*, 218–230. [CrossRef] [PubMed]
212. Recent Advances in Mast Cell Activation and Regulation–PubMed. Available online: <https://pubmed.ncbi.nlm.nih.gov/32226609/> (accessed on 20 November 2020).
213. Agier, J.; Pastwińska, J.; Brzezińska-Błaszczyk, E. An Overview of Mast Cell Pattern Recognition Receptors. *Inflamm. Res.* **2018**, *67*, 737–746. [CrossRef] [PubMed]
214. Saluja, R.; Zoltowska, A.; Ketelaar, M.E.; Nilsson, G. IL-33 and Thymic Stromal Lymphopoietin in Mast Cell Functions. *Eur. J. Pharmacol.* **2016**, *778*, 68–76. [CrossRef] [PubMed]
215. Joulia, R.; Mailhol, C.; Valitutti, S.; Didier, A.; Espinosa, E. Direct Monitoring of Basophil Degranulation by Using Avidin-Based Probes. *J. Allergy Clin. Immunol.* **2017**, *140*, 1159–1162.e6. [CrossRef] [PubMed]
216. Rönnberg, E.; Ghaib, A.; Ceriol, C.; Enoksson, M.; Arock, M.; Säfholm, J.; Ekoff, M.; Nilsson, G. Divergent Effects of Acute and Prolonged Interleukin 33 Exposure on Mast Cell IgE-Mediated Functions. *Front. Immunol.* **2019**, *10*, 1361. [CrossRef]
217. Jönsson, F.; Daëron, M. Mast Cells and Company. *Front. Immunol.* **2012**, *3*, 16. [CrossRef] [PubMed]
218. McNeil, B.D.; Pundir, P.; Meeker, S.; Han, L.; Udem, B.J.; Kulka, M.; Dong, X. Identification of a Mast-Cell-Specific Receptor Crucial for Pseudo-Allergic Drug Reactions. *Nature* **2015**, *519*, 237–241. [CrossRef]
219. Pundir, P.; Liu, R.; Vasavda, C.; Serhan, N.; Limjunyawong, N.; Yee, R.; Zhan, Y.; Dong, X.; Wu, X.; Zhang, Y.; et al. A Connective Tissue Mast-Cell-Specific Receptor Detects Bacterial Quorum-Sensing Molecules and Mediates Antibacterial Immunity. *Cell Host Microbe* **2019**, *26*, 114–122.e8. [CrossRef]
220. Corbière, A.; Loste, A.; Gaudenzio, N. MRGPRX2 Sensing of Cationic Compounds—A Bridge between Nociception and Skin Diseases? *Exp. Dermatol.* **2020**. [CrossRef]
221. Lu, L.; Kulka, M.; Unsworth, L.D. Peptide-Mediated Mast Cell Activation: Ligand Similarities for Receptor Recognition and Protease-Induced Regulation. *J. Leukoc. Biol.* **2017**, *102*, 237–251. [CrossRef]
222. Abraham, S.N.; St John, A.L. Mast Cell-Orchestrated Immunity to Pathogens. *Nat. Rev. Immunol.* **2010**, *10*, 440–452. [CrossRef]
223. Arizono, N.; Matsuda, S.; Hattori, T.; Kojima, Y.; Maeda, T.; Galli, S.J. Anatomical Variation in Mast Cell Nerve Associations in the Rat Small Intestine, Heart, Lung, and Skin. Similarities of Distances between Neural Processes and Mast Cells, Eosinophils, or Plasma Cells in the Jejunal Lamina Propria. *Lab. Investig.* **1990**, *62*, 626–634. [PubMed]
224. Barbara, G.; Stanghellini, V.; De Giorgio, R.; Cremon, C.; Cottrell, G.S.; Santini, D.; Pasquinelli, G.; Morselli-Labate, A.M.; Grady, E.F.; Bunnett, N.W.; et al. Activated Mast Cells in Proximity to Colonic Nerves Correlate with Abdominal Pain in Irritable Bowel Syndrome. *Gastroenterology* **2004**, *126*, 693–702. [CrossRef] [PubMed]
225. Serhan, N.; Basso, L.; Sibillano, R.; Petitfils, C.; Meixiong, J.; Bonnart, C.; Reber, L.L.; Marichal, T.; Starkl, P.; Cenac, N.; et al. House Dust Mites Activate Nociceptor-Mast Cell Clusters to Drive Type 2 Skin Inflammation. *Nat. Immunol.* **2019**, *20*, 1435–1443. [CrossRef]

226. Suzuki, J.; Isobe, M.; Izawa, A.; Takahashi, W.; Yamazaki, S.; Okubo, Y.; Amano, J.; Sekiguchi, M. Differential Th1 and Th2 Cell Regulation of Murine Cardiac Allograft Acceptance by Blocking Cell Adhesion of ICAM-1/LFA-1 and VCAM-1/VLA-4. *Transpl. Immunol.* **1999**, *7*, 65–72. [[CrossRef](#)]
227. Siiskonen, H.; Harvima, I. Mast Cells and Sensory Nerves Contribute to Neurogenic Inflammation and Pruritus in Chronic Skin Inflammation. *Front. Cell Neurosci.* **2019**, *13*, 422. [[CrossRef](#)] [[PubMed](#)]
228. Stelekati, E.; Bahri, R.; D’Orlando, O.; Orinska, Z.; Mittrücker, H.-W.; Langenhaun, R.; Glatzel, M.; Bollinger, A.; Paus, R.; Bulfone-Paus, S. Mast Cell-Mediated Antigen Presentation Regulates CD8+ T Cell Effector Functions. *Immunity* **2009**, *31*, 665–676. [[CrossRef](#)] [[PubMed](#)]
229. Lotfi-Emran, S.; Ward, B.R.; Le, Q.T.; Pozez, A.L.; Manjili, M.H.; Woodfolk, J.A.; Schwartz, L.B. Human Mast Cells Present Antigen to Autologous CD4+ T Cells. *J. Allergy Clin. Immunol.* **2018**, *141*, 311–321.e10. [[CrossRef](#)]
230. Gaudenzio, N.; Espagnol, N.; Mars, L.T.; Liblau, R.; Valitutti, S.; Espinosa, E. Cell-Cell Cooperation at the T Helper Cell/Mast Cell Immunological Synapse. *Blood* **2009**, *114*, 4979–4988. [[CrossRef](#)]
231. Nakae, S.; Suto, H.; Iikura, M.; Kakurai, M.; Sedgwick, J.D.; Tsai, M.; Galli, S.J. Mast Cells Enhance T Cell Activation: Importance of Mast Cell Costimulatory Molecules and Secreted TNF. *J. Immunol.* **2006**, *176*, 2238–2248. [[CrossRef](#)]
232. Shefler, I.; Salamon, P.; Levi-Schaffer, F.; Mor, A.; Hershko, A.Y.; Mekori, Y.A. MicroRNA-4443 Regulates Mast Cell Activation by T Cell-Derived Microvesicles. *J. Allergy Clin. Immunol.* **2018**, *141*, 2132–2141.e4. [[CrossRef](#)] [[PubMed](#)]
233. Shefler, I.; Salamon, P.; Reshef, T.; Mor, A.; Mekori, Y.A. T Cell-Induced Mast Cell Activation: A Role for Microparticles Released from Activated T Cells. *J. Immunol.* **2010**, *185*, 4206–4212. [[CrossRef](#)] [[PubMed](#)]
234. Bradding, P.; Pejler, G. The Controversial Role of Mast Cells in Fibrosis. *Immunol. Rev.* **2018**, *282*, 198–231. [[CrossRef](#)] [[PubMed](#)]
235. Ud-Din, S.; Wilgus, T.A.; Bayat, A. Mast Cells in Skin Scarring: A Review of Animal and Human Research. *Front. Immunol.* **2020**, *11*, 552205. [[CrossRef](#)]
236. Pejler, G.; Rönnerberg, E.; Waern, I.; Wernersson, S. Mast Cell Proteases: Multifaceted Regulators of Inflammatory Disease. *Blood* **2010**, *115*, 4981–4990. [[CrossRef](#)]
237. Vanganswinkel, T.; Lemmens, S.; Geurts, N.; Quanten, K.; Dooley, D.; Pejler, G.; Hendrix, S. Mouse Mast Cell Protease 4 Suppresses Scar Formation after Traumatic Spinal Cord Injury. *Sci. Rep.* **2019**, *9*, 3715. [[CrossRef](#)]
238. Galli, S.J.; Gaudenzio, N.; Tsai, M. Mast Cells in Inflammation and Disease: Recent Progress and Ongoing Concerns. *Annu. Rev. Immunol.* **2020**, *38*, 49–77. [[CrossRef](#)]
239. Varricchi, G.; Rossi, F.W.; Galdiero, M.R.; Granata, F.; Criscuolo, G.; Spadaro, G.; de Paulis, A.; Marone, G. Physiological Roles of Mast Cells: Collegium Internationale Allergologicum Update 2019. *Int. Arch. Allergy Immunol.* **2019**, *179*, 247–261. [[CrossRef](#)]
240. Varricchi, G.; Galdiero, M.R.; Loffredo, S.; Marone, G.; Iannone, R.; Marone, G.; Granata, F. Are Mast Cells MASTers in Cancer? *Front. Immunol.* **2017**, *8*, 1–13. [[CrossRef](#)]
241. Pittoni, P.; Tripodo, C.; Piconese, S.; Mauri, G.; Parenza, M.; Rigoni, A.; Sangaletti, S.; Colombo, M.P. Mast Cell Targeting Hampers Prostate Adenocarcinoma Development but Promotes the Occurrence of Highly Malignant Neuroendocrine Cancers. *Cancer Res.* **2011**, *71*, 5987–5997. [[CrossRef](#)]
242. Carlini, M.J.; Dalurzo, M.C.L.; Lastiri, J.M.; Smith, D.E.; Vasallo, B.C.; Puricelli, L.I.; Lauría de Cidre, L.S. Mast Cell Phenotypes and Microvessels in Non-Small Cell Lung Cancer and Its Prognostic Significance. *Hum. Pathol.* **2010**, *41*, 697–705. [[CrossRef](#)] [[PubMed](#)]
243. Siiskonen, H.; Poukka, M.; Bykachev, A.; Tynnelä-Korhonen, K.; Sironen, R.; Pasonen-Seppänen, S.; Harvima, I.T. Low Numbers of Tryptase+ and Chymase+ Mast Cells Associated with Reduced Survival and Advanced Tumor Stage in Melanoma. *Melanoma Res.* **2015**, *25*, 479–485. [[CrossRef](#)] [[PubMed](#)]
244. Welsh, T.J.; Green, R.H.; Richardson, D.; Waller, D.A.; O’Byrne, K.J.; Bradding, P. Macrophage and Mast-Cell Invasion of Tumor Cell Islets Confers a Marked Survival Advantage in Non-Small-Cell Lung Cancer. *J. Clin. Oncol.* **2005**, *23*, 8959–8967. [[CrossRef](#)] [[PubMed](#)]
245. Johansson, A.; Rudolfsson, S.; Hammarsten, P.; Halin, S.; Pietras, K.; Jones, J.; Stattin, P.; Egevad, L.; Granfors, T.; Wikström, P.; et al. Mast Cells Are Novel Independent Prognostic Markers in Prostate Cancer and Represent a Target for Therapy. *Am. J. Pathol.* **2010**, *177*, 1031–1041. [[CrossRef](#)]
246. Fleischmann, A.; Schlomm, T.; Köllermann, J.; Sekulic, N.; Huland, H.; Mirlacher, M.; Sauter, G.; Simon, R.; Erbersdobler, A. Immunological Microenvironment in Prostate Cancer: High Mast Cell Densities Are Associated with Favorable Tumor Characteristics and Good Prognosis. *Prostate* **2009**, *69*, 976–981. [[CrossRef](#)]
247. Ribatti, D.; Vacca, A.; Ria, R.; Marzullo, A.; Nico, B.; Filotico, R.; Roncali, L.; Dammacco, F. Neovascularisation, Expression of Fibroblast Growth Factor-2, and Mast Cells with Tryptase Activity Increase Simultaneously with Pathological Progression in Human Malignant Melanoma. *Eur. J. Cancer* **2003**, *39*, 666–674. [[CrossRef](#)]
248. Takebayashi, S.; Jimi, S.; Kawamoto, N. Cutaneous Malignant Melanoma: Correlation between Neovascularization and Peritumor Accumulation of Mast Cells Overexpressing Vascular Endothelial Growth Factor. *Hum. Pathol.* **2000**, *31*, 955–960. [[CrossRef](#)]
249. Imada, A.; Shijubo, N.; Kojima, H.; Abe, S. Mast Cells Correlate Angiogenesis and Poor Outcome in Stage I Lung Adenocarcinoma. *Eur. Respir. J.* **2000**, *15*, 1087–1093. [[CrossRef](#)]
250. Esposito, I.; Menicagli, M.; Funel, N.; Bergmann, F.; Boggi, U.; Mosca, F.; Bevilacqua, G.; Campani, D. Inflammatory Cells Contribute to the Generation of an Angiogenic Phenotype in Pancreatic Ductal Adenocarcinoma. *J. Clin. Pathol.* **2004**, *57*, 630–636. [[CrossRef](#)]

251. Gorzalczyk, Y.; Merimsky, O.; Sagi-Eisenberg, R. Mast Cells Are Directly Activated by Cancer Cell-Derived Extracellular Vesicles by a CD73- and Adenosine-Dependent Mechanism. *Transl. Oncol.* **2019**, *12*, 1549–1556. [[CrossRef](#)]
252. Visciano, C.; Liotti, F.; Prevede, N.; Cali', G.; Franco, R.; Collina, F.; De Paulis, A.; Marone, G.; Santoro, M.; Melillo, R.M. Mast Cells Induce Epithelial-to-Mesenchymal Transition and Stem Cell Features in Human Thyroid Cancer Cells through an IL-8-Akt-Slug Pathway. *Oncogene* **2015**, *34*, 5175–5186. [[CrossRef](#)] [[PubMed](#)]
253. Öhrvik, H.; Grujic, M.; Waern, I.; Gustafson, A.M.; Ernst, N.; Roers, A.; Hartmann, K.; Pejler, G. Mast Cells Promote Melanoma Colonization of Lungs. *Oncotarget* **2016**, *7*, 68990–69001. [[CrossRef](#)] [[PubMed](#)]
254. Giannou, A.D.; Marazioti, A.; Spella, M.; Kanellakis, N.I.; Apostolopoulou, H.; Psallidas, I.; Prijovich, Z.M.; Vreka, M.; Zazara, D.E.; Lilis, I.; et al. Mast Cells Mediate Malignant Pleural Effusion Formation. *J. Clin. Investig.* **2015**, *125*, 2317–2334. [[CrossRef](#)] [[PubMed](#)]
255. Huang, B.; Lei, Z.; Zhang, G.M.; Li, D.; Song, C.; Li, B.; Liu, Y.; Yuan, Y.; Unkeless, J.; Xiong, H.; et al. SCF-Mediated Mast Cell Infiltration and Activation Exacerbate the Inflammation and Immunosuppression in Tumor Microenvironment. *Blood* **2008**, *112*, 1269–1279. [[CrossRef](#)]
256. Reddy, S.M.; Reuben, A.; Barua, S.; Jiang, H.; Zhang, S.; Wang, L.; Gopalakrishnan, V.; Hudgens, C.W.; Tetzlaff, M.T.; Reuben, J.M.; et al. Poor Response to Neoadjuvant Chemotherapy Correlates with Mast Cell Infiltration in Inflammatory Breast Cancer. *Cancer Immunol. Res.* **2019**, *7*, 1025–1035. [[CrossRef](#)]
257. Kaesler, S.; Wölbing, F.; Kempf, W.E.; Skabytska, Y.; Köberle, M.; Volz, T.; Sinnberg, T.; Amaral, T.; Möckel, S.; Yazdi, A.; et al. Targeting Tumor-Resident Mast Cells for Effective Anti-Melanoma Immune Responses. *JCI Insight* **2019**, *4*. [[CrossRef](#)]
258. Zelenay, S.; Van Der Veen, A.G.; Böttcher, J.P.; Snelgrove, K.J.; Rogers, N.; Acton, S.E.; Chakravarty, P.; Girotti, M.R.; Marais, R.; Quezada, S.A.; et al. Cyclooxygenase-Dependent Tumor Growth through Evasion of Immunity. *Cell* **2015**, *162*, 1257–1270. [[CrossRef](#)]
259. Terabe, M.; Park, J.M.; Berzofsky, J.A. Role of IL-13 in Regulation of Anti-Tumor Immunity and Tumor Growth. *Cancer Immunol. Immunother.* **2004**, *53*, 79–85. [[CrossRef](#)]
260. Kennedy, L.; Hodges, K.; Meng, F.; Alpini, G.; Francis, H. Histamine and Histamine Receptor Regulation of Gastrointestinal Cancers. *Transl. Gastrointest. Cancer* **2012**, *1*, 215–227.
261. Balkwill, F. Tumour Necrosis Factor and Cancer. *Nat. Rev. Cancer* **2009**, *9*, 361–371. [[CrossRef](#)]
262. Arinobu, Y.; Iwasaki, H.; Gurish, M.F.; Mizuno, S.; Shigematsu, H.; Ozawa, H.; Tenen, D.G.; Austen, K.F.; Akashi, K. Developmental Checkpoints of the Basophil/Mast Cell Lineages in Adult Murine Hematopoiesis. *Proc. Natl. Acad. Sci. USA* **2005**, *102*, 18105–18110. [[CrossRef](#)] [[PubMed](#)]
263. Kopf, M.; Brombacher, F.; Hodgkin, P.D.; Ramsay, A.J.; Milbourne, E.A.; Dai, W.J.; Ovington, K.S.; Behm, C.A.; Köhler, G.; Young, I.G.; et al. IL-5-Deficient Mice Have a Developmental Defect in CD5+ B-1 Cells and Lack Eosinophilia but Have Normal Antibody and Cytotoxic T Cell Responses. *Immunity* **1996**, *4*, 15–24. [[CrossRef](#)]
264. Schroeder, J.T.; Chichester, K.L.; Bieneman, A.P. Human Basophils Secrete IL-3: Evidence of Autocrine Priming for Phenotypic and Functional Responses in Allergic Disease. *J. Immunol.* **2009**, *182*, 2432–2438. [[CrossRef](#)] [[PubMed](#)]
265. Gould, H.J.; Sutton, B.J.; Beavil, A.J.; Beavil, R.L.; McCloskey, N.; Coker, H.A.; Fear, D.; Smurthwaite, L. The Biology of IGE and the Basis of Allergic Disease. *Annu. Rev. Immunol.* **2003**, *21*, 579–628. [[CrossRef](#)] [[PubMed](#)]
266. Knol, E.F.; Gibbs, B.F. Basophil Stimulation and Signaling Pathways. *Methods Mol. Biol.* **2014**, *1192*, 193–203. [[CrossRef](#)] [[PubMed](#)]
267. Yuk, C.M.; Park, H.J.; Kwon, B.-I.; Lah, S.J.; Chang, J.; Kim, J.-Y.; Lee, K.-M.; Park, S.-H.; Hong, S.; Lee, S.-H. Basophil-Derived IL-6 Regulates TH17 Cell Differentiation and CD4 T Cell Immunity. *Sci. Rep.* **2017**, *7*, 41744. [[CrossRef](#)] [[PubMed](#)]
268. Johansson, M.W. Eosinophil Activation Status in Separate Compartments and Association with Asthma. *Front. Med.* **2017**, *4*, 75. [[CrossRef](#)]
269. Johnston, L.K.; Hsu, C.-L.; Krier-Burris, R.A.; Chhiba, K.D.; Chien, K.B.; McKenzie, A.; Berdnikovs, S.; Bryce, P.J. IL-33 Precedes IL-5 in Regulating Eosinophil Commitment and Is Required for Eosinophil Homeostasis. *J. Immunol.* **2016**, *197*, 3445–3453. [[CrossRef](#)]
270. Zimmermann, N.; Hogan, S.P.; Mishra, A.; Brandt, E.B.; Bodette, T.R.; Pope, S.M.; Finkelman, F.D.; Rothenberg, M.E. Murine Eotaxin-2: A Constitutive Eosinophil Chemokine Induced by Allergen Challenge and IL-4 Overexpression. *J. Immunol.* **2000**, *165*, 5839–5846. [[CrossRef](#)]
271. Bandeira-Melo, C.; Sugiyama, K.; Woods, L.J.; Weller, P.F. Cutting Edge: Eotaxin Elicits Rapid Vesicular Transport-Mediated Release of Preformed IL-4 from Human Eosinophils. *J. Immunol.* **2001**, *166*, 4813–4817. [[CrossRef](#)]
272. Simon, D.; Hoesli, S.; Roth, N.; Staedler, S.; Yousefi, S.; Simon, H.-U. Eosinophil Extracellular DNA Traps in Skin Diseases. *J. Allergy Clin. Immunol.* **2011**, *127*, 194–199. [[CrossRef](#)] [[PubMed](#)]
273. Munitz, A.; Levi-Schaffer, F. Inhibitory Receptors on Eosinophils: A Direct Hit to a Possible Achilles Heel? *J. Allergy Clin. Immunol.* **2007**, *119*, 1382–1387. [[CrossRef](#)] [[PubMed](#)]
274. Wang, C.; Chen, Y.-G.; Gao, J.-L.; Lyu, G.-Y.; Su, J.; Zhang, Q.I.; Ji, X.; Yan, J.-Z.; Qiu, Q.-L.; Zhang, Y.-L.; et al. Low Local Blood Perfusion, High White Blood Cell and High Platelet Count Are Associated with Primary Tumor Growth and Lung Metastasis in a 4T1 Mouse Breast Cancer Metastasis Model. *Oncol. Lett.* **2015**, *10*, 754–760. [[CrossRef](#)] [[PubMed](#)]
275. Prizment, A.E.; Vierkant, R.A.; Smyrk, T.C.; Tillmans, L.S.; Lee, J.J.; Sriramarao, P.; Nelson, H.H.; Lynch, C.F.; Thibodeau, S.N.; Church, T.R.; et al. Tumor Eosinophil Infiltration and Improved Survival of Colorectal Cancer Patients: Iowa Women's Health Study. *Mod. Pathol.* **2016**, *29*, 516–527. [[CrossRef](#)]

276. Zheng, X.; Zhang, N.; Qian, L.; Wang, X.; Fan, P.; Kuai, J.; Lin, S.; Liu, C.; Jiang, W.; Qin, S.; et al. CTLA4 Blockade Promotes Vessel Normalization in Breast Tumors via the Accumulation of Eosinophils. *Int. J. Cancer* **2020**, *146*, 1730–1740. [[CrossRef](#)]
277. Lucarini, V.; Ziccheddu, G.; Macchia, I.; La Sorsa, V.; Peschiaroli, F.; Buccione, C.; Sistigu, A.; Sanchez, M.; Andreone, S.; D’Urso, M.T.; et al. IL-33 Restricts Tumor Growth and Inhibits Pulmonary Metastasis in Melanoma-Bearing Mice through Eosinophils. *Oncoimmunology* **2017**, *6*, e1317420. [[CrossRef](#)]
278. Rosner, S.; Kwong, E.; Shoushtari, A.N.; Friedman, C.F.; Betof, A.S.; Brady, M.S.; Coit, D.G.; Callahan, M.K.; Wolchok, J.D.; Chapman, P.B.; et al. Peripheral Blood Clinical Laboratory Variables Associated with Outcomes Following Combination Nivolumab and Ipilimumab Immunotherapy in Melanoma. *Cancer Med.* **2018**, *7*, 690–697. [[CrossRef](#)]
279. Bax, H.J.; Chauhan, J.; Stavrika, C.; Khiabany, A.; Nakamura, M.; Pellizzari, G.; Ilieva, K.M.; Lombardi, S.; Gould, H.J.; Corrigan, C.J.; et al. Basophils from Cancer Patients Respond to Immune Stimuli and Predict Clinical Outcome. *Cells* **2020**, *9*, 1631. [[CrossRef](#)]
280. Wei, Y.; Zhang, X.; Wang, G.; Zhou, Y.; Luo, M.; Wang, S.; Hong, C. The Impacts of Pretreatment Circulating Eosinophils and Basophils on Prognosis of Stage I–III Colorectal Cancer. *Asia Pac. J. Clin. Oncol.* **2018**, *14*, e243–e251. [[CrossRef](#)]
281. Cohen, M.; Giladi, A.; Gorki, A.-D.; Solodkin, D.G.; Zada, M.; Hladik, A.; Miklosi, A.; Salame, T.-M.; Halpern, K.B.; David, E.; et al. Lung Single-Cell Signaling Interaction Map Reveals Basophil Role in Macrophage Imprinting. *Cell* **2018**, *175*, 1031–1044.e18. [[CrossRef](#)]
282. De Monte, L.; Wörmann, S.; Brunetto, E.; Heltai, S.; Magliacane, G.; Reni, M.; Paganoni, A.M.; Recalde, H.; Mondino, A.; Falconi, M.; et al. Basophil Recruitment into Tumor-Draining Lymph Nodes Correlates with Th2 Inflammation and Reduced Survival in Pancreatic Cancer Patients. *Cancer Res.* **2016**, *76*, 1792–1803. [[CrossRef](#)] [[PubMed](#)]
283. Crawford, G.; Hayes, M.D.; Seoane, R.C.; Ward, S.; Dalessandri, T.; Lai, C.; Healy, E.; Kipling, D.; Proby, C.; Moyes, C.; et al. Epithelial Damage and Tissue $\gamma\delta$ T Cells Promote a Unique Tumor-Protective IgE Response. *Nat. Immunol.* **2018**, *19*, 859–870. [[CrossRef](#)] [[PubMed](#)]
284. de Paulis, A.; Prevete, N.; Fiorentino, I.; Rossi, F.W.; Staibano, S.; Montuori, N.; Ragno, P.; Longobardi, A.; Liccardo, B.; Genovese, A.; et al. Expression and Functions of the Vascular Endothelial Growth Factors and Their Receptors in Human Basophils. *J. Immunol.* **2006**, *177*, 7322–7331. [[CrossRef](#)] [[PubMed](#)]
285. Prevete, N.; Staiano, R.I.; Granata, F.; Detoraki, A.; Necchi, V.; Ricci, V.; Triggiani, M.; De Paulis, A.; Marone, G.; Genovese, A. Expression and Function of Angiopoietins and Their Tie Receptors in Human Basophils and Mast Cells. *J. Biol. Regul. Homeost. Agents* **2013**, *27*, 827–839.
286. Cerny-Reiterer, S.; Ghanim, V.; Hoermann, G.; Aichberger, K.J.; Herrmann, H.; Muellauer, L.; Repa, A.; Sillaber, C.; Walls, A.F.; Mayerhofer, M.; et al. Identification of Basophils as a Major Source of Hepatocyte Growth Factor in Chronic Myeloid Leukemia: A Novel Mechanism of BCR-ABL1-Independent Disease Progression. *Neoplasia* **2012**, *14*, 572–584. [[CrossRef](#)]
287. MacGlashan, D.W.; Peters, S.P.; Warner, J.; Lichtenstein, L.M. Characteristics of Human Basophil Sulfidopeptide Leukotriene Release: Releasability Defined as the Ability of the Basophil to Respond to Dimeric Cross-Links. *J. Immunol.* **1986**, *136*, 2231–2239.
288. Duah, E.; Teegala, L.R.; Kondeti, V.; Adapala, R.K.; Keshamouni, V.G.; Kanaoka, Y.; Austen, K.F.; Thodeti, C.K.; Paruchuri, S. Cysteinyl Leukotriene 2 Receptor Promotes Endothelial Permeability, Tumor Angiogenesis, and Metastasis. *Proc. Natl. Acad. Sci. USA* **2019**, *116*, 199–204. [[CrossRef](#)]
289. Horiuchi, T.; Weller, P.F. Expression of Vascular Endothelial Growth Factor by Human Eosinophils: Upregulation by Granulocyte Macrophage Colony-Stimulating Factor and Interleukin-5. *Am. J. Respir. Cell Mol. Biol.* **1997**, *17*, 70–77. [[CrossRef](#)]
290. Ben Efraim, A.H.N.; Eliashar, R.; Levi-Schaffer, F. Hypoxia Modulates Human Eosinophil Function. *Clin. Mol. Allergy* **2010**, *8*, 10. [[CrossRef](#)]
291. Puxeddu, I.; Berkman, N.; Ribatti, D.; Bader, R.; Haitchi, H.M.; Davies, D.E.; Howarth, P.H.; Levi-Schaffer, F. Osteopontin Is Expressed and Functional in Human Eosinophils. *Allergy* **2010**, *65*, 168–174. [[CrossRef](#)]
292. Cools-Lartigue, J.; Spicer, J.; McDonald, B.; Gowing, S.; Chow, S.; Giannias, B.; Bourdeau, F.; Kubes, P.; Ferri, L. Neutrophil Extracellular Traps Sequester Circulating Tumor Cells and Promote Metastasis. *J. Clin. Investig.* **2013**, *123*, 3446–3458. [[CrossRef](#)] [[PubMed](#)]

Review

Plasmin and Plasminogen System in the Tumor Microenvironment: Implications for Cancer Diagnosis, Prognosis, and Therapy

Alamelu G. Bharadwaj ¹, Ryan W. Holloway ¹, Victoria A. Miller ¹  and David M. Waisman ^{1,2,*}¹ Department of Pathology, Dalhousie University, Halifax, NS B3H 4R2, Canada;

Alamelu.Bharadwaj@dal.ca (A.G.B.); Ryan.Holloway@dal.ca (R.W.H.); Victoria.Miller@dal.ca (V.A.M.)

² Department of Biochemistry & Molecular Biology, Dalhousie University, Halifax, NS B3H 4R2, Canada

* Correspondence: david.waisman@dal.ca

Simple Summary: In this review, we present a detailed discussion of how the plasminogen-activation system is utilized by tumor cells in their unrelenting attack on the tissues surrounding them. Plasmin is an enzyme which is responsible for digesting several proteins that hold the tissues surrounding solid tumors together. In this process tumor cells utilize the activity of plasmin to digest tissue barriers in order to leave the tumour site and spread to other parts of the body. We specifically focus on the role of plasminogen receptor—p11 which is an important regulatory protein that facilitates the conversion of plasminogen to plasmin and by this means promotes the attack by the tumour cells on their surrounding tissues.



Citation: Bharadwaj, A.G.; Holloway, R.W.; Miller, V.A.; Waisman, D.M. Plasmin and Plasminogen System in the Tumor Microenvironment: Implications for Cancer Diagnosis, Prognosis, and Therapy. *Cancers* **2021**, *13*, 1838. <https://doi.org/10.3390/cancers13081838>

Academic Editors: Hilary Collier and Patricia Alexandra Saraiva Madureira

Received: 1 January 2021

Accepted: 24 March 2021

Published: 12 April 2021

Publisher's Note: MDPI stays neutral with regard to jurisdictional claims in published maps and institutional affiliations.



Copyright: © 2021 by the authors. Licensee MDPI, Basel, Switzerland. This article is an open access article distributed under the terms and conditions of the Creative Commons Attribution (CC BY) license (<https://creativecommons.org/licenses/by/4.0/>).

Abstract: The tumor microenvironment (TME) is now being widely accepted as the key contributor to a range of processes involved in cancer progression from tumor growth to metastasis and chemoresistance. The extracellular matrix (ECM) and the proteases that mediate the remodeling of the ECM form an integral part of the TME. Plasmin is a broad-spectrum, highly potent, serine protease whose activation from its precursor plasminogen is tightly regulated by the activators (uPA, uPAR, and tPA), the inhibitors (PAI-1, PAI-2), and plasminogen receptors. Collectively, this system is called the plasminogen activation system. The expression of the components of the plasminogen activation system by malignant cells and the surrounding stromal cells modulates the TME resulting in sustained cancer progression signals. In this review, we provide a detailed discussion of the roles of plasminogen activation system in tumor growth, invasion, metastasis, and chemoresistance with specific emphasis on their role in the TME. We particularly review the recent highlights of the plasminogen receptor S100A10 (p11), which is a pivotal component of the plasminogen activation system.

Keywords: plasmin; plasminogen; S100A10; macrophages; tumor microenvironment; uPA; uPAR; PAI-1; PAI-2; metastasis; tumor growth

1. Introduction

A tumor is a heterogenous multicellular organ comprised of not only cancer cells but also supporting stromal cells. The environment surrounding the tumor mass is known as the tumor microenvironment (TME). TME is composed of stromal cells that are of diverse types, including fibroblasts, adipocytes, infiltrating lymphocytes and macrophages, lymphatic and vascular network, and most importantly the extracellular matrix (ECM). Moreover, the TME is also composed of secreted proteins, RNAs, exosomes, and microvesicles. The TME is now viewed as one of the hallmarks of cancer because it plays an instrumental role in tumor growth, progression, and metastasis; mediates immune escape; and promotes local therapeutic resistance. The ECM is composed of a diverse array of proteins that are constantly synthesized and remodeled and provide biochemical and biophysical functionality to the TME, which further modulate tumor cell behavior (reviewed

in [1,2]). The dynamic remodeling of the ECM and TME is mediated by proteases, such as matrix metalloproteases (MMPs) (reviewed in [3]) cathepsins, and plasmin [4]. Fibrinogen and fibrin are important components of the ECM. Enhanced plasminogen activation is not only associated with increased invasive and metastatic potential of tumor cells but also contributes to tumor growth by activating growth factors and cytokines. In this review, we will discuss the individual components of the plasmin activation system (PAS) and their contribution toward modulating the TME.

2. Proteases in the Tumor Microenvironment

The TME is composed of the ECM and surrounding stromal cells, such as fibroblasts and adipocytes; and infiltrating immune cells, such as macrophages, lymphocytes; pericytes; and endothelial cells [5,6]. The ECM is composed of a network of proteins, such as collagen, elastins, laminin, fibronectin, and proteoglycans, each interacting with one other to form tissue support and architecture [7]. A specialized component of the ECM, the basement membrane (BM), forms the acellular layer that serves as a platform for epithelial and endothelial cells and surrounds fat cells, muscle cells and peripheral nerves. The BM also plays important roles in compartmentalization within tissues and maintenance of epithelial integrity and is a regulator of cell differentiation, proliferation, migration, and survival. The BM contains a variety of proteins including type IV collagen, entactin, laminin, and sulfated proteoglycans. The ECM not only provides biochemical signals for tumor growth, invasion, and metastasis, but it equally contributes to biomechanical properties, such as stiffness, which also influence cellular behavior and phenotype [8,9]. Tumor growth and metastasis not only depend on autocrine signals from tumor cells, but they largely depend on many converging paracrine signals elicited by the host microenvironment and ECM.

Fibrinogen is a soluble protein produced by hepatocytes and secreted into plasma, where it functions in hemostasis. Thrombin released at the site of vascular injury converts fibrinogen to the insoluble molecule fibrin that forms the major constituent of the blood clot. In 1878, Billroth had reported that tumor cells surround themselves with a fibrin thrombus. Based on this observation, he proposed that fibrin promotes tumor growth and invasion [10]. More recent studies have supported and extended this concept, showing that many hemostatic factors, including fibrinogen, fibrin, and components of the fibrinolytic system, are involved in cancer growth and metastasis [11–13]. Fibrinogen but not fibrin is abundant throughout the connective tissue in breast cancer but not in nonmalignant tissues [14]. In contrast, in many other forms of cancer, both fibrin and fibrinogen are present in the tumor stroma [14–17]. Meta-analysis of studies showed that elevated plasma fibrinogen levels show poor clinical outcome in solid tumors and hematological cancers, though the results for hematological cancers were contradictory [18,19]. It appears that fibrin promotes cell migration by providing a matrix for tumor cell migration and by interacting with adhesive molecules of the cancer cells. Fibrinogen can serve as a scaffold that binds tumor cells and platelets as they leave the tumor site. As an extracellular protein matrix, fibrinogen not only promotes the migration of tumor cells but also protects tumor cells from the innate immune surveillance system [20]. However, it also presents a barrier that must be breached before extravasation into the blood can occur. Therefore, proteolysis of fibrin must be carefully regulated as excessive fibrinolysis will prevent its utilization for the migration of the cancer cells and insufficient fibrinolysis will not allow the cancer cells to pass through the fibrin barrier [21–23].

Enhanced protease expression and proteolytic activity are hallmarks of cancer progression [24,25]. These proteases participate in the invasion and metastasis of tumor cells by promoting the degradation of the ECM. However, it has been recently suggested that their role is much more complicated, and they participate in multiple stages of cancer progression. Extensive studies have demonstrated that proteolytic activity is elicited not only by tumor cells but also by stromal cells; this concerted proteolytic activity is responsible for ECM degradation and remodeling in a TME [26]. There are five classes of proteases

that are categorized based on their mechanism of activity and active site residue, namely aspartic, cysteine, metallo, serine, and threonine proteases [26–30]. The activity of these proteases is tightly regulated by the presence of protease inhibitors which are classified based on the proteases they inhibit. Cystatins inhibit cysteine proteases; serpins (serine protease inhibitors) inhibit serine proteases; and tissue inhibitors inhibit metalloproteases. The threonine proteases are inhibited by bortezomib [31,32]. Further regulation of proteolytic activity is mediated by gene expression and epigenetic regulation, localization and compartmentalization, trafficking, post-translational modification, and zymogen activation [33]. Although this review focuses on the plasminogen/plasmin system it is important to point out that the other classes of proteases also play an important role in the disease process. For example, overexpression of the cysteine protease, cathepsin B has a well-established link to tumor growth, invasion, angiogenesis and metastasis [34,35]. The threonine protease activity of the proteasome plays a key role in protein degradation and its deregulation has been linked to malignant progression [36]. The caspases, are a family of cysteine-dependent aspartate-specific proteases that have an important function in the maintenance of cellular and organismal homeostasis by functioning as mediators of the inflammatory response and apoptosis [37]. The topic of the role of the different classes of proteases in cancer has been reviewed in [38] and will not be the focus of detailed discussion in this review.

3. Overview of the Plasmin–Plasminogen Activation System

The first publication by Virchow on the decomposition of fibrin in the blood of dissected human bodies appeared in 1846. The term fibrinolysis was introduced in 1893 by Dastre who published observations on the dissolution of clotted dog's blood [39]. Fibrinolysis is the process of degradation of fibrin, which is the major component of a thrombus [40,41]. The process involves interactions between multiple components of the fibrinolytic system, which play a major role in the dissolution of clots during wound healing and restoration of circulation. The fibrinolytic system is involved not only in homeostasis but also in the progression of several pathological conditions, such as cardiovascular diseases; angiogenesis; and tumor invasion and metastasis [42]. In fact, extracellular matrix (ECM) degradation is one of the most crucial steps involved in local invasion and distant metastasis [1]. The critical mediator of fibrinolysis is plasmin—a potent serine protease. Plasmin also plays a key role in ECM degradation directly and indirectly by activating many of the proteases that function in matrix degradation. Plasmin is generated from its precursor zymogen, plasminogen, by the cleavage of the Arg561–Val562 peptide bond by tissue plasminogen activator (tPA) and urokinase-type plasminogen activator (uPA) [43]. A number of key papers from MacFarlane in 1946 and Astrup in identified the presence of plasminogen activators and regulators [44,45].

Plasminogen is synthesized and secreted by the liver [46]. In processes, such as wound healing and tissue remodeling that occurs in the TME, uPA is the predominant form of plasminogen activator, whereas tPA is the primary activator in the circulation [47]. While tPA is found in the ECM of most tissues, uPA is localized to cell surfaces by its receptor uPAR. The activities of both tPA and uPA are regulated by plasminogen activator inhibitor (PAI)-1 [48] and PAI-2 [49], whereas the activity of plasmin itself is inhibited by α 2-antiplasmin [50,51] and α 2-macroglobulin [52] (Figure 1). Overall, a complicated interplay between the plasminogen activators and inhibitors determines the extent of tissue remodeling, fibrinolysis, and tumor invasion and metastasis [53,54]. In the TME, this is further complicated by the fact that the expression of the activators and inhibitors are not restricted to tumor cells alone, but the stromal cells are also involved in the expression and secretion of activators and inhibitors.

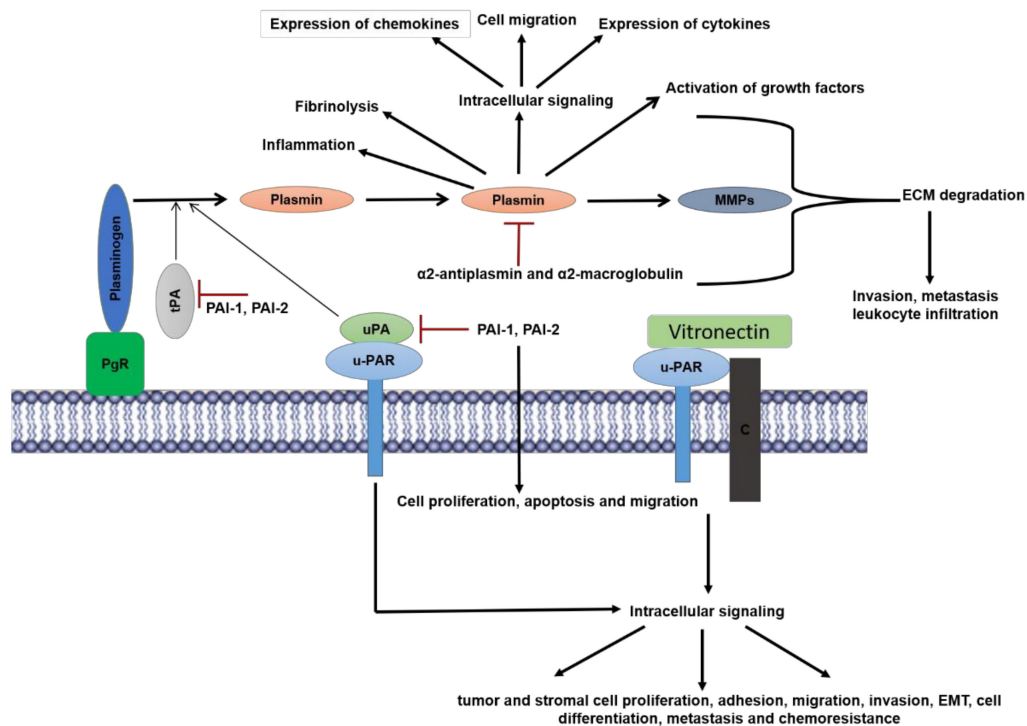


Figure 1. Overview of components and functions of plasminogen-activation system: Plasminogen is activated to the serine protease plasmin by a multicomponent system comprised of plasminogen receptors (PgR), urokinase-type-plasminogen activator (uPA), and tissue-plasminogen activator (tPA). uPA is bound to its receptor urokinase-plasminogen activator receptor (uPAR) whereas in most cases tPA is bound by the PgR. The activity of tPA and uPA are inhibited by the plasminogen-activator-inhibitor 1, 2 (PAI-1, PAI-2), of which PAI-1 is a more potent inhibitor. PAI-1 also promotes cellular proliferation, apoptosis, and migration. Plasmin activity is directly regulated by inhibitors α 2 anti-plasmin and α 2-macroglobulin. Plasmin mediates its physiological effects by virtue of its protease dependent and independent activities. Plasmin proteolytically activates other proteases such as matrix metalloproteinases (MMPs) that along with plasmin is involved in the degradation of extracellular matrix proteins (ECM) which promotes inflammation including leukocyte infiltration in tumors, cancer cell invasion and metastasis. Plasmin promotes tumor growth by proteolytically activating nascent growth factors in the ECM. Intracellular signaling by plasmin via several receptors (described above) mediates a plethora of effects that include expression of cytokines and chemokines, cell migration and inflammation. uPA and uPAR function both in plasminogen-dependent (protease activity) and plasminogen-independent mechanisms that promote multiple cellular responses. uPAR functions independently of uPA by binding to vitronectin and co-receptors (C) such as integrins, to promote intracellular signaling, which result in tumor and stromal cell proliferation, adhesion, migration, invasion, epithelial-mesenchymal-transition (EMT), cell differentiation, metastasis and chemoresistance in cancer cells.

Plasmin generation proceeds at a slow rate but is accelerated by a group of cell surface proteins that bind plasminogen, called plasminogen receptors [55–57]. Plasminogen receptors localize the bound plasminogen near the vicinity of the tumor cell, allowing easy access by uPAR-bound uPA. Plasminogen receptors are also present on the cells of the TME, including endothelial cells, activated myofibroblasts, and macrophages. Thus, there is substantial interaction between the tumor and host cells for plasminogen binding, plasmin generation, and signaling crosstalk between the two components. These interactions play a vital role in cancer progression by modulating cell proliferation, angiogenesis, invasion, and metastasis.

4. Structure and Function of Plasminogen and Plasmin

Plasminogen is a 92–94 kilodalton protein that circulates as a zymogen in the blood. The variation in molecular weight is due to glycosylation differences, discussed further below. Plasminogen, like many hemostatic proteins, is produced in the liver and is found

at a concentration of approximately 2 μM in the plasma [58]. It is a multidomain protein, comprised of an amino (N)-terminal peptide domain, five kringle domains, and the serine protease domain [59]. The classical catalytic triad is located within the serine protease domain: Histidine 603, Aspartate 646, and Serine 741. This domain has a homology with the active site of other serine proteases, such as trypsin and elastase [60]. The kringle domains of plasminogen are so-called due to their physical resemblance to kringle pastries [61]. The 3-dimensional structure of the kringle domains revealed that multiple intra-molecular disulfide bonds contribute to the structural rigidity of these domains [62]. The kringle domains contain sites that bind lysine residues. The lysine-binding sites (LBS) of plasminogen kringles bind lysine residues both within the plasminogen molecule and those contributed by fibrin blood clots and cell-surface plasminogen receptors [60]. The crystal structure of plasminogen has been solved and revealed much about the architecture of the molecule [63,64]. The LBS of all kringle (Kr) domains, except Kr are engaged in intramolecular interactions, while only Kr1-LBS is readily available for extra molecular binding. Plasminogen circulates in a “closed conformation,” with Lys50, Arg68, and Arg70 from the N-terminal peptide domain interacting with the LBS of Kr4 and Kr5, respectively, and Lys708 interacting with the LBS of Kr2. In contrast, the LBS of Kr1 and Kr4 have an LBS that binds with higher affinity to the C-terminal lysines of fibrin structures. These interactions between the N-terminal domain and intramolecular residues are critical for maintaining plasminogen in a tight closed conformation. The proteolytic cleavage at Lys77 by plasmin results in the removal of the N-terminal region, which results in the formation of a truncated form of plasminogen called Lys-plasminogen [65–67]. This form of plasminogen is in a more open conformation. Law [64] had proposed that a plasminogen receptor likely interacted with both Kr1 and Kr5. The interaction with Kr1 was responsible for the tethering of the molecule to the plasminogen receptor, whereas the subsequent interaction with Kr5 unleashed the series of conformational changes responsible for the exposure of the activation loop to cleavage by plasminogen activators.

Both, the rate, and location of plasmin formation, are tightly controlled. To ensure hemostasis, plasmin generation is typically restricted to the sites of thrombosis and angiogenesis and the sites of ECM remodeling. Unrestrained plasmin generation is a factor in the depletion of pro-coagulant proteins in disseminated intravascular coagulation [68]. Plasmin generation on the surface of tumor cells leads to cell invasion and metastasis [69]. Local surfaces play a part in plasmin generation; both the fibrin surface and cell surface carry out a similar regulatory role [70]. Plasminogen receptors found on the cell surface, some of which also bind tPA, colocalize with other receptors that specifically bind plasminogen activators [71–74]. The plasminogen receptors also provide lysine residues for binding plasminogen and in certain cases, a site for binding tPA. As has been shown for p11, the binding of tPA and plasminogen/plasmin to this receptor protects tPA from inactivation by PAI-1 and plasmin from inactivation by alpha-2 anti-plasmin [75]. Similarly, on the fibrin clot surface, C-terminal lysine residues are interspersed within the fibrin network. Restricting plasmin activation to either a cell surface or the clot surface allows for proteolytic targeting as well as some protection from circulating inhibitors. In addition to its cleavage to form plasmin, plasminogen can also be proteolysed into several bioactive molecules called angiostatins [76]. The angiostatins are a group of proteolytic products derived from plasminogen, which retain some of the kringle domains but lack the proteolytic domain. Structures include Kr1-Kr3, Kr1-Kr4, and Kr1-Kr5 [77]. Our laboratory demonstrated that the autoproteolytic cleavage of the Lys468–Gly469 bond and reduction of the plasmin Cys462–Cys541 disulfide of plasmin resulted in the formation of an angiostatin, A61 (Lys78–Lys468) [78]. The angiostatins are crucial inhibitors of vascular endothelial cell proliferation, tube formation, and migration; they can also promote vascular endothelial cell apoptosis [79].

Plasmin has proteolytic activity against a broad range of substrates, such as syndecans [80], laminins, fibronectin [81], vascular cell adhesion protein 1 [82], and vitronectin [83]. The broad range of substrates results in an extensive range of processes,

both physiologic and pathologic, in which plasmin participates. These processes include fibrinolysis, signaling pathways, cell migration, wound healing, inflammation, and oncogenesis [84]. Plasmin releases growth factors such as fibroblast growth factor-2 (FGF-2), hepatocyte growth factor (HGF), and vascular endothelial growth factor (VEGF) that are sequestered by the ECM [85–88]. Additionally, plasmin activates MMPs, such as MMP 1, 2, 3, 9, and 14, and indirectly affects tumor cell invasion [89]. Plasmin also promotes intracellular signaling through various pathways to promote cell migration of peripheral blood monocytes through Protease-activated-receptor 1 (PAR-1) [90,91]. Stimulation of monocytes by plasmin results in enhanced expression of inflammatory cytokines (tumor necrosis factor-alpha (TNF α), interleukin (IL)-6, IL-1 α/β , CD40) and chemokines (monocyte chemoattractant protein (MCP)-1/CCL2), tissue factors, and lipid mediators via activation of AP-1 and nuclear factor-kappa (NF- κ B) transcription factors [90]. Plasmin has been shown to activate multiple signaling pathways, such as Janus Kinase/Signal Transducer and Activator of Transcription (JAK/STAT), p38 mitogen-activated protein kinase (MAPK), extracellular signal-regulated protein kinase (ERK)1/2 [92]. With HT29-M6 intestinal epithelial cells, Diaz et al. showed that plasmin plays a dual role in promoting cell scattering as a result of its ECM degrading proteolytic activity and in intracellular signaling by the induction of ERK1/2 activation [93]. Some cells, such as Chinese Hamster Ovary and BA3 cells, utilize both the proteolytic activity and the signaling function of plasmin to induce cell migration. Specifically, Tarui et al. showed that plasmin bound to α v β 3 integrin and promoted cell migration in these cells, whereas treatment with plasmin inhibitor aprotinin abrogated signaling and migration [94]. In summary, plasmin activates several cell types, such as monocytes, macrophages, fibroblasts, endothelial cells, epithelial cells, and platelets, that form a part of the TME and promotes their migration.

5. Plasminogen Activators

There are two physiologic activators of plasminogen—uPA and tPA—which are used clinically as thrombolytic therapeutics [40]. Both tPA and uPA are multidomain proteases. The active forms of each of these enzymes are inhibited by PAI-1 and PAI-2. The tPA is a 70 kDa protein of 527 amino acids [95]. It consists of 2 kringle domains, a finger domain, epidermal growth factor (EGF)-like domain, and serine protease domain [96]. The tPA interacts with fibrin via its finger domain as well as kringle-2. Like most of the kringle domains of plasminogen, kringle-2 is a lysine binding site; however, kringle-1 has a serine residue at the site of a usual tryptophan residue within the hydrophobic cleft that alters its ability to bind to lysine residues [97,98]. The tPA is synthesized and secreted by endothelial cells as well as many brain cells, including neurons, astrocytes, microglia, and oligodendrocytes [96,98]. The plasma protein concentration of tPA is in the range of 5–10 μ g/L. The protein is synthesized as a proenzyme single chain, cross-linked polypeptide, glycosylated at threonine Thr61 (O-linked), asparagine Asn117, Asn184, and Asn448 (N-linked). The proenzyme has a low serine protease activity. This single-chain form is fully activated by cleavage of the arginine Arg275-isoleucine Ile276 bond by plasmin, kallikrein, or coagulation factor Xa. This 2-chain form is held together by a single disulfide bond between Cys264 and Cys395 [96]. The interaction of tPA with endothelial cells and vascular smooth muscle cells can lead to increased activation of plasminogen. Previous studies have proposed that a C-terminal lysine or arginine residue on annexin A2 (also known as p36), generated by an unknown protease as the binding site for plasminogen [99,100]. Subsequent studies have thrown doubt on the existence of proteolyzed annexin A2 as the binding site; it is more likely to be the binding partner of annexin A2, p11, which possesses a C-terminal lysine residue [100,101]. Like tPA, uPA is found in the plasma at approximately the same concentration of 5–10 μ g/L, but it is produced by cells in the lungs, kidneys as well as keratinocytes and endothelial cells. The uPA is synthesized as a 55 kDa single-chain protein consisting of 411 amino acids [102]. This multidomain protein has an EGF-like domain, one kringle domain, and a serine protease domain. Additionally, like tPA, it is glycosylated: Thr18 (O-linked) and Asn302 (N-linked). Additionally, it has 2 phos-

phorylation sites: serine Ser138 and Ser303. The secreted protein is a zymogen and requires cleavage of its Lys158–Ile159 bond to demonstrate its full activity. The two-chain form is held together by a single disulfide bond between Cys148 and Cys279. The Lys–Ile bond is cut by plasmin, kallikrein, coagulation factor XIIa, or cathepsin B [103,104]. This results in the high molecular weight form of active uPA. Additionally, there is a low molecular weight form, primarily found in the urine and is generated by plasmin or auto-proteolysis at the Lys135–Lys136 bond. The single-chain pro-uPA is 250-fold less potent in the activation of plasminogen than the two-chain uPA. Different proteases have been reported to function in mediating the cleavage of pro-uPA. Plasmin most effectively converts the pro-uPA into active uPA [105]. Among the other proteases that can activate pro-uPA includes cathepsin B and L, nerve growth factor-g, trypsin, kallikrein, thermolysin, and mast cell tryptase [103,104,106–109]. uPA is primarily responsible for cell surface-associated plasminogen activation. This is accomplished by the binding of the single-chain proenzyme to the glycosylphosphatidylinositol (GPI)-anchored uPAR, where the proenzyme is activated by plasmin, cathepsin B, or kallikrein [54]. The activation of cell-bound plasminogen by receptor-bound uPA is characterized by a 40-fold reduction in the K_m for plasminogen activation [74]. The co-localization of uPAR with plasminogen receptors localizes the resultant plasmin activity to the cell surface. The cell membrane-bound plasmin activity created by cell-bound plasminogen is protected by inactivation from plasma-borne inhibitors, but its activity can be indirectly reduced by the PAI-1 and PAI-2 through the inhibition of tPA and uPA [110,111]. In parallel, plasmin bound to the surface of cells cleaves pro-uPA bound to uPAR at a rate 50-fold that of plasmin in solution [41]. This directed activation on the cell surface gives those cells an invasive phenotype. Invasive cells make use of the broad substrate specificity of the resulting plasmin to degrade the various proteins of the ECM, including fibronectin, laminin, vitronectin, and proteoglycans. As discussed, plasmin can also activate pro-MMPs, resulting in the degradation of collagen [54].

The coordination of the uPA system consisting of plasmin and uPA along with the inhibitors alpha2-antiplasmin, PAI-1 and PAI-2 together with the receptor uPAR, plays an important role in the regulation of cancer progression and metastasis [54,58]. The first evidence of a possible causative role of plasminogen activator in malignancy was shown by the sharp increase in fibrinolytic activity in virally transformed fibroblasts [112]. This plasminogen activator was later identified to be uPA [113]. Increased concentration of uPA in the plasma is correlative of poor prognosis in breast, bladder, gastric, and prostate cancers; head and neck and colorectal cancers; and melanoma [114].

As discussed, uPAR is a GPI-anchored membrane receptor for uPA, that regulates protease activity on the cell surface. Later studies have shown that it binds to vitronectin from the ECM with the aid of co-receptors, such as integrins, caveolin, and G-protein-coupled receptors, and promotes intracellular signaling and gene expression [115,116]. Interestingly, binding of uPA to uPAR also activates intracellular signaling that is mediated by the N-terminal region of uPA and is independent of the active site domain, suggesting a plasmin-independent mechanism [117]. The cell signaling cascade initiated by uPAR promotes cancer cell invasion, migration, epithelial to mesenchymal transition, cell differentiation, proliferation, and metastasis. The expression of uPA and uPAR gene is elevated in many cancers compared to non-cancerous tissues. The uPAR binds to uPA and at the same time binds to vitronectin, which is relevant for the downstream signaling by uPAR. The uPAR promoter is activated by several transcription factors, such as activator protein 1, NF- κ B, and hypoxia-inducible factor 1 α , which are upregulated by the RAS-ERK-MAPK pathway and TME factors such as hypoxia (reviewed in [118]). The uPAR is also cleaved at its GPI-anchor by a specific phospholipase and is found as a soluble form (suPAR) in the plasma and urine [119]. The suPAR can activate the G-protein coupled chemotactic receptor FPRL1/LXA4R. The expression of uPAR is upregulated by various inflammatory cytokines, such as TNF- α , interferon-gamma (IFN- γ), IL-1, and IL-2 [120]. More recently, it has been demonstrated that uPAR is upregulated during senescence and uPAR specific-chimeric antigen receptor T-cell therapy enhances the survival of mice with lung adenocarcinoma [121].

Expression of uPA and uPAR has been observed in various hematopoietic cells, and both these proteins play an important role in the regulation of innate and adaptive immune response through the modulation of cell adhesion and migration of neutrophils, monocytes, macrophages, and myeloid-derived-suppressor cells and activation of T-cells [114]. Thus, the uPA–uPAR axis potentiates tissue remodeling not only in the cancer cells but also in the immune cells by allowing their invasion, migration, and adhesion in the stroma where they modulate tumor growth and metastasis. The uPA–uPAR axis also regulates apoptosis. When uPA and uPAR were downregulated simultaneously, a dramatic decrease in the invasiveness of breast cancer cells was observed along with the activation of the apoptotic cascade [122]. Furthermore, antibody-targeted inhibition of u-PAR reduced metastasis and induced apoptosis in ovarian cancer cells In Vitro and In Vivo [123].

6. Plasminogen Activation Inhibitors

PAI-1 is a 379-amino acid serine protease inhibitor that inhibits the activity of tPA and uPA [124–126] which is associated with inflammation and tumorigenesis. Interestingly although PAI-1 functions as an inhibitor of uPA and tPA, it serves a pro-tumorigenic role in various cancers such as lung and breast [127–129]. This is clearly because PAI-1 is a multifunctional protein not only regulating plasmin generation but also modulating cell proliferation, migration, and apoptosis (reviewed in [130]). Moreover, PAI-1 plays both an autocrine and paracrine role in tumorigenesis and is produced by both tumor cells and cells of the TME such as adipocytes, macrophages, fibroblasts, smooth muscle cells, and endothelial cells. Much of our knowledge of the pro-tumorigenic and metastatic role of PAI-1 was deciphered from PAI-1-deficient mouse models and transgenic tumor models. Interestingly, the tumor growth and metastasis phenotype in syngeneic models and genetically engineered mouse tumor models provided contradictory results. The implantation of PAI-1 deficient syngeneic tumor cells in PAI-1 knockout (KO) mice demonstrated that both host and tumor cells PAI-1 contributed positively to tumor growth, angiogenesis, and metastasis in a dose-dependent manner [128,131]. However, loss of PAI-1 in the transgenic breast [132] and ocular [133] tumor models did not show any significant effect on tumor development and progression possibly due to the compensation by other members of the PAI family and other protease inhibitors [134]. The function of PAI-1 in tumor angiogenesis, migration/invasion, and apoptosis is mediated by distinct structural domains. For instance, the pro-angiogenic function is due to the vitronectin binding domain and uPA-binding domain (anti-protease). This is primarily by two mechanisms one is plasmin dependent and the other is plasmin independent. First, the inhibition of uPA by PAI-1 binding prevents the activation of plasminogen to plasmin, which further prevents cleavage of Fas-L on the cell surface and consequently, Fas-mediated apoptosis of endothelial cells is inhibited [129]. Second, PAI-1 binding to vitronectin allows the release of endothelial cells from vitronectin and migration for promoting angiogenesis [135]. Finally, the ability of PAI-1 to bind to its receptor low density lipoprotein receptor-related protein 1 (LRP1) promotes intracellular signaling and tumor cell and endothelial cell migration [136]. A recent study has highlighted the mechanistic role of the pro-tumorigenic function of PAI-1 in the TME. This study demonstrated that PAI-1 mediates a pro-tumorigenic effect by recruiting and polarizing macrophages to M2 phenotype in the TME. Interestingly, this dual role is promoted by two different structural domains of PAI-1. The LRP1 domain mediates the monocyte migration and recruitment, and the uPA interacting domain causes the M2 polarization via activation of the IL-6/STAT3 pathway which in turn is induced by the p38-MAPK and NF- κ B signaling pathways. Although it is unclear how PAI-1 activates these signaling pathway, the authors speculate that reduced plasmin in the presence of PAI-1 potentially prevents receptor protein degradation and enhances downstream signaling [137].

PAI-2, although originally identified as a less potent inhibitor of uPA, is a 47 kDa protein. It has been now shown to having a predominantly intracellular function and has been discovered to be a modulator of proteotoxic stress [138] unrelated to plasminogen activation/uPA inhibition. The loss of PAI-2 gene in mice is not accompanied by any major

phenotypic changes associated with fibrinolysis or hemostasis unlike the PAI-1 deficient mice [139,140]. However, bioinformatics analysis and expression data from macrophages have revealed that PAI-2 is modulated with genes associated with cell migration and movement. There are some reports suggesting a role for monocyte-derived PAI-2 in promoting uPA mediated fibrinolysis or clot resolution [141].

7. Plasminogen Receptors

Plasminogen binds to cells with low affinity ($K_d = 0.3\text{--}2\ \mu\text{M}$) and high capacity ($10^4\text{--}10^7$ binding sites per cell) [73,142]. The plasminogen-binding sites on cells are mediated by both proteins and non-proteins such as glycosaminoglycans and gangliosides.

Plasminogen receptors serve as anchoring sites for plasminogen on the cell surface. The binding of plasminogen to these receptors increases the rate of local plasmin generation. Plasminogen receptors are found on the surface of most cell types (except for red blood cells) at a high density, dependent on cell type: 1 to 200×10^5 /endothelial cell, 5×10^5 /lymphocyte, and 35,000/platelet [57,68].

The current dogma states that although both internal lysines and the carboxyl-terminal lysine of plasminogen receptors bind to plasminogen, it is the plasminogen receptors with carboxyl-terminal lysine residues that preferentially induce a conformational change in plasminogen that greatly facilitates its activation by the plasminogen activators. This dogma is based on the report that treatment of U937 cells with carboxypeptidase B (CpB) reduced plasminogen binding by about 60% whereas plasminogen activation was reduced by about 95% [72]. Since CpB proteolytically removes lysine and arginine residues from the carboxyl-terminal of proteins, it was concluded that only a subset of plasminogen receptors, that have a carboxyl-terminal lysine residue, participate in plasminogen activation. The analysis of the effect of CpB on plasminogen activation by THP-1 monocytes, THP-1 macrophages, and human umbilical vein endothelial cells revealed that carboxyl-terminal lysines played only a minor role in plasminogen activation [143]. Similarly, CpB treatment of activated platelets reduced plasminogen activation by only about 20% [144]. These studies have suggested that plasminogen receptors with internal lysine residues also participate in plasminogen activation by plasminogen receptors.

An understanding of the mechanism of interaction of an internal or C-terminal lysine with the LBS of plasminogen comes from structural studies. The interaction of lysine with the LBS is mediated by hydrophobic interaction as well as by charged residues. Lysine is a basic aliphatic amino acid with a side chain consisting of a 4-carbon chain hydrophobic region and a positively charged amine group. The amino group of lysine interacts with negatively charged aspartic acid residues within the binding pocket of the LBS, whereas the hydrophobic chain interacts with the hydrophobic cleft of the LBS [60]. Compared to an internal lysine residue, the carboxyl-terminal lysine possesses a negatively charged carboxyl group which interacts with the cationic center of the LBS of plasminogen.

Localizing plasmin activity at the cell surface grants the cell various abilities. The broad spectrum of plasmin activity means that in addition to direct extracellular proteolysis, plasmin can also activate other proteinases, thereby increasing the overall proteolytic activity of the cell. Plasmin is also able to process latent growth factors and cytokines in the ECM that induces signaling events to modulate cellular functions such as cell migration.

Plasminogen receptors are often found co-localized with receptors for plasminogen activators or bind tPA itself [145,146]. The co-localization of plasminogen and its activators aids in restricting the activity of the resulting plasmin to the cell surface.

Many proteins have been identified as potential plasminogen receptors. Most of these proteins have C-terminal lysines. Those that have a C-terminal lysine include α -enolase [142], histone H2B [147,148], S100A4 [149], the annexin A2 heterotetramer (annexin A2 in complex with p11 also known as AIIIt) [101], plasminogen (Plg)-RKT [150], TIP49a [151], and cytokeratin 8 [152]. Examples of plasminogen receptors that do not have the classic C-terminal lysine residue include high mobility group box-1 protein (HMGB-1) [56] (also known as amphoterin) and integrins, primarily those of the $\beta 2$ inte-

grin family [57] and glucose-regulated protein 78 [153]. It has been shown that a significant amount of the plasmin generating activity of malignant cancer cells is due to a novel, unidentified class of plasminogen receptors. These plasminogen receptors are generated by the action of plasmin on unknown cell surface proteins, resulting in the generation of a new carboxyl-terminal lysine and hence a new plasminogen-binding site. For example, the majority of the plasmin-generating capacity of several malignant breast cancer cell lines is due to these unidentified, cryptic plasminogen receptors [154].

Many of the plasminogen receptors are associated with cancer and are found on the surface of most tumors [155]. Examples of plasminogen receptors that are upregulated in cancer include p11 (reviewed in [156]), S100A4 [157,158], α -enolase [159], and cytokeratin K8 [152]. Interestingly, the majority of plasminogen receptors function in tumor-stromal cross-talk during cancer progression. The expression of plasminogen receptors, such as p11 and Plg-RKT, in macrophages, promote pro-tumorigenic phenotype in animal models. Importantly, these receptors have been shown to play a predominant role in macrophage recruitment to tumor sites and during inflammation and will be discussed in detail in the later sections. In this review, we will focus on the plasminogen receptor p11 that has contributed greatly to our understanding of plasminogen receptors in the TME and tumor progression.

8. AIIIt Structure, Function, and Regulation

The annexin A2-S100A10 heterotetramer, is also known as AIIIt [78,101,160]. AIIIt is composed of two subunits of annexin A2 (also called p36) and a dimer of p11. The AIIIt heterotetramer acts as a platform for promoting interactions with other cellular proteins. It regulates multiple ion channels, such as Cl^- , K^+ , Na^+ , Ca^{2+} , cystic fibrosis transmembrane conductance regulator, transient receptor potential vanilloid type 5 and 6, NaV1.8, Acid-Sensing Ion Channel-1, and TASK1 using distinct mechanisms, which has been reviewed in detail elsewhere and will not be discussed in this review [161].

AIIIt is also a significant contributor to plasmin generation of many cell types. AIIIt binds both tPA and plasminogen on the cell surface and converts plasminogen to plasmin. The p11 subunit (Mr 11 kDa) of AIIIt is one of 20 different members of the S100 family made of calcium-binding, dimeric EF hand-type proteins. p11 is present in several tissues, such as the brain, heart, gastrointestinal tract, kidney, liver, lung, spleen, testes, epidermis, aorta, and thymus. It is highly expressed in many cell types, such as endothelial, cardiomyocytes, monocytes, T lymphocytes, and neurons [162]. The p11 subunit of the AIIIt heterotetramer is one of the most highly regulated plasminogen receptors. These regulators include physiological signals such as EGF [163,164] and $\text{IFN-}\gamma$ [165,166]. p11 is also regulated by oncogenes, such as KRAS [167], which is present in about 30% of all human cancers and promyelocytic leukemia-retinoic acid receptor alpha (PML/RAR α) oncoprotein [168], the oncogene responsible for acute promyelocytic leukemia (Figure 2). Our laboratory has shown that p11 is regulated by oncogenic RAS by the Ral-GDS pathway and depletion of p11 in RAS transformed cells results in a substantial reduction in plasmin generation and plasminogen dependent invasion [167] (Figure 2). The expression of p11 is also regulated by glucocorticoids, cytokines, growth factors, and neurotransmitters [162,169]. The expression of p11 is aberrantly regulated in many pathological conditions, such as cancer, depressive mood disorder, and neurodegeneration [170].

The large subunit of AIIIt, p36, is a 36-kDa protein belonging to a group of calcium-dependent, phospholipid-binding proteins known as the annexin family [162,171,172]. The formation of the AIIIt heterotetramer occurs intracellularly when the p11 homodimer becomes attached to two copies of a p36 subunit. Within the heterotetramer, p36 has two key functions: (1) to facilitate the localization of p11 to the cell surface, [173] and (2) to prevent the rapid degradation of newly translated p11 since the binding of p36 and p11 blocks p11 from ubiquitylation and degradation [174–176].

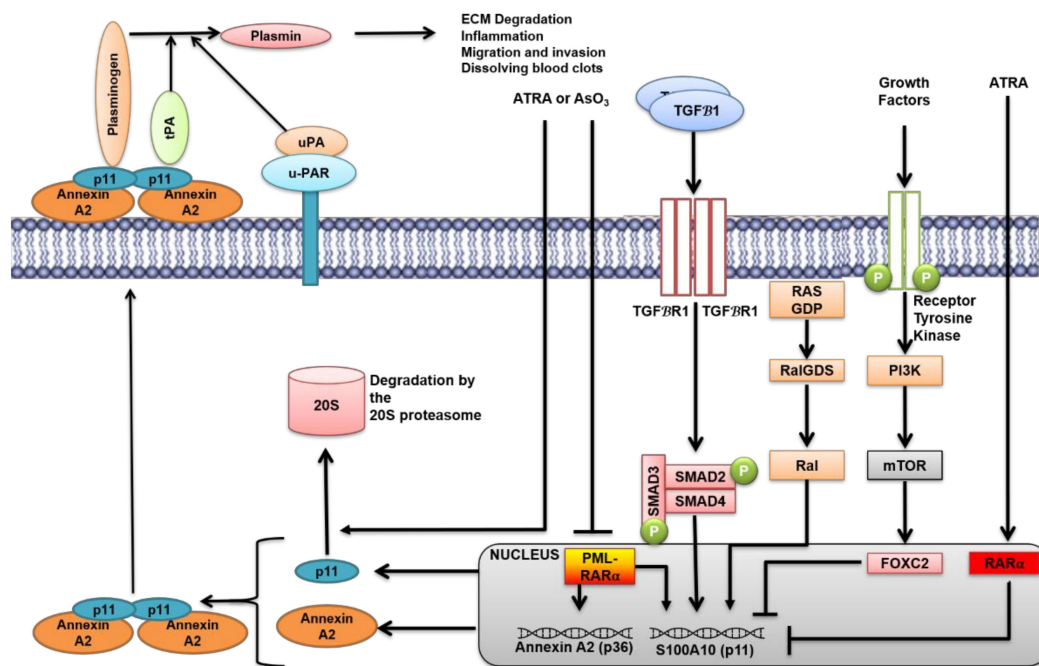


Figure 2. Regulation of S100A10 (p11): P11 is transactivated by (1) the promyelocytic leukemia-retinoic acid receptor alpha (PML-RAR α) fusion oncoprotein, (2) TGF β 1-dependent activation of the SMAD pathway, and (3) oncogenic RAS-mediated activation of the Ral-GDS/Ral pathway. Conversely, transcriptional repression of P11 is mediated by (1) ATRA- and arsenic trioxide (AsO $_3$)-induced degradation of the PML-RAR α fusion oncoprotein, (2) growth factor-induction of the PI3K/mTOR pathway and consequent FOXC2-dependent transcriptional repression of p11, and (3) ATRA-activation of RAR α . Newly transcribed p11 and p36 (Annexin A2) proteins rapidly form the AIIt heterotetramer complex within the cytoplasm prior to being transported to the cell surface. Although the p11–p36 interaction protects p11 from degradation by the 26S proteasome, ATRA and AsO $_3$ both induced the ubiquitin-independent degradation of p11 by the 20S proteasome. Once at the cell surface, AIIt acts as a dual receptor for plasminogen and tissue plasminogen activator (tPA) and co-localizes with and urokinase-type-plasminogen activator/uPAR complex. By localizing plasminogen and its activators, AIIt catalyzes the cleavage of plasminogen to produce plasmin, a serine protease involved in ECM degradation, inflammation, cellular migration and invasion, and blood clot dissolution.

It was initially proposed that in the absence of p36, the p11 protein was rapidly ubiquitinated on lysines in the carboxyl-terminal region of p11, consequently directing it to the proteasome for degradation [174]. In the study by He et al., overexpression of a series of carboxyl-terminal mutants of p11 and ubiquitin in HEK293 cells showed that ubiquitylation was likely to involve Lys92 or Lys94 of the p11 carboxyl-terminal sequence ⁸⁹VHMKQKGKK⁹⁷. In these experiments, cellular proteins were immunoprecipitated using ubiquitin antibodies and immunoblotted for p11 to determine whether p11 was ubiquitinated. However, it is possible that the proteins immunoprecipitated by the ubiquitin antibodies were ubiquitylated proteins that had bound to p11. Additionally, ubiquitin conjugation of p11 was not confirmed using mass spectrometry. In contrast to the model of ubiquitylation of p11 on carboxy-terminal lysines presented by He et al., Wagner et al. [177] identified Lys47, Lys54, and Lys57 as the potential ubiquitylated lysines in p11 by mass spectrometry analysis of endogenous proteins isolated from murine tissues. However, the study did not address the proportion of p11 of the total population that was ubiquitylated and why ubiquitylated p11 was detected in only two of the five tissues examined. Furthermore, the proposed ubiquitylation sites of p11 were not confirmed by site-directed mutagenesis. Consistent with the findings by Wagner et al., Holloway et al. [178] applied mass spectrometric analysis of overexpressed p11 and identified Lys57 as the primary target of ubiquitylation. This observation was confirmed by site-directed mutagenesis and it was shown that mutagenesis of Lys57 prevented p11 ubiquitylation. Importantly, ubiquitylation of p11 was only observed after overexpression of both p11 and ubiquitin.

As the overexpression of proteins can produce cellular anomalies that may induce anomalous ubiquitylation [179], it is unclear if ubiquitylation of p11 occurs under physiological conditions. The formation of ubiquitin chains on the lysine residues of proteins is considered a signal for proteasomal degradation. To form a ubiquitin chain, ubiquitin moieties can be conjugated through one of their lysine residues (K6, K11, K27, K29, K33, K48, and K63) although K29 and K48 are thought to be particularly important. He et al. co-expressed p11 with mutant ubiquitin in which Lys29 or Lys48 of ubiquitin were mutated to arginine (ub-K29R and ub-K48R) in HEK293 cells. They observed that the overexpression of p11 and the ubiquitin mutants increased p11 protein levels, presumably by blocking proteasomal degradation. However, the effect of the mutant ubiquitins was not compared to wild-type ubiquitin to determine if wild-type ubiquitin also modulated p11 expression. Using both the wild-type and a mutant ubiquitin with all lysines mutated to arginine (ub-K0) to prevent any chain formation and any possible proteasomal targeting, Holloway et al. found p11 expression increased in HEK293 cells transfected with both p11 and ubiquitin-wild type (WT) compared to p11 alone. Surprisingly, p11 expression was more dramatically increased when overexpressed with ub-K0, therefore suggesting that ubiquitin chain formation and ubiquitin-dependent proteasomal degradation were not responsible for p11 degradation. Higher molecular weight forms of p11 were detected only when p11 was overexpressed with ubiquitin, and interestingly, multiple molecular weight species of p11 were observed in cells transfected with ub-K0, suggesting the existence of multiple ubiquitin sites in p11 when both proteins were overexpressed. Holloway concluded that the reported ubiquitin-dependent proteasomal degradation of p11 was likely due to an artifact of protein overexpression.

Holloway et al. identified the mechanism of regulation of p11 levels [178]. Using all-trans-retinoic acid (ATRA)-treated acute promyelocytic leukemia (APL) cells, they reported that inhibition of the proteasome with lactacystin prevented the ATRA-induced loss of p11, but the ubiquitylation inhibitor PYR-41 had no effect, suggesting that p11 levels were regulated by a ubiquitin-independent proteasomal mechanism. Furthermore, when proteasomal degradation was inhibited, higher molecular weight ubiquitin-p11 complexes were not detected, although the accumulation of other ubiquitylated proteins was observed. Moreover, incubation of purified p11, p36, and AII α proteins with the 20S proteasome resulted in the degradation of these proteins *In Vitro*. Since the 20S proteasome degrades proteins in a ubiquitin-independent manner [180], the authors further concluded that p11 was regulated by a ubiquitin-independent mechanism (Figure 2). In contrast, when p11 and ubiquitin were overexpressed in HEK293T cells, ubiquitylated p11 species were observed. Mass spectrometry analysis of these ubiquitylated p11 species identified lysines 27, 37, and 57 of p11 as sites of ubiquitylation, whereas lysine 57 was the primary site of ubiquitylation, as reported earlier by Wagner et al. [177].

APL is characterized by expression of the PML/RAR α , which blocks granulocyte differentiation and has been shown to increase p11 and p36 expression. Treatment of NB4 cells with ATRA, which binds to and activates the destruction of PML/RAR α also causes a rapid loss in the expression of p11 and p36 protein. Our laboratory performed an extensive analysis of the mechanism of ATRA-dependent loss of p11 and p36 expression using wild-type NB4 cells, a mutant NB4 cell line resistant to ATRA-induced differentiation (NB4-MR), PR9 cells in which the PML/RAR α oncoprotein can be induced by Zn²⁺ treatment, and PML/RAR α -negative cells (HL-60, U937, and MCF-7) [178]. We observed that ATRA treatment resulted in the loss of p11 total protein levels in parental and ATRA-induced differentiation-resistant NB4 cells, demonstrating that ATRA-mediated promyelocyte differentiation did not affect p11 or p36 expression. ATRA treatment also diminished p11 and p36 levels in PR9 cells in which PML/RAR α was induced and unexpectedly in MCF-7 breast cancer cells, indicating that ATRA affected p11 expression in MCF-7 cells independently of the PML/RAR α fusion protein. This suggested that the receptor of ATRA, RAR α is involved in regulating p11 transcription. *In silico* analysis also revealed several potential binding sites for RAR α were present in the ± 10 kb re-

gion from the p11 transcriptional start-site. In addition to this finding, previous studies have reported that ATRA treatment of BEAS-2B lung epithelial cells [181] and dendritic cells [182] also resulted in the downregulation of p11 expression. Lokman et al. found that ATRA treatment resulted in downregulation of p11 and p36 mRNA and cell surface protein levels with a concomitant reduction in plasmin activity, and invasion, in the serous ovarian cancer cell line (OAW28) [183]. Interestingly, a proteomic analysis of tamoxifen-resistant MCF-7-derived cell line with elevated expression of RAR α (Lewis lung carcinoma cells [LLC] 2) showed that p11 and several other members of the S100 proteins were reduced compared to parental MCF-7 cells [184]. Considering the presence of potential RAR α binding sites in the p11 promoter and that ATRA can modulate p11 expression in the absence of PML/RAR α , the use of ATRA may have a therapeutic value in the depletion of p11 and plasmin activity in cancers other than APL. Consistently, the potential of ATRA as a promising new therapy for serous ovarian cancer has been explored by the Ricciardelli group, particularly its effect on regulation of p11 and p36. Their findings suggest that ATRA predominantly downregulated p11 mRNA and protein expression in serous ovarian cancer cells, which resulted in decreased plasminogen activation and invasion in these cells [183].

Carnitine palmitoyltransferase 1A has been shown to mediate the succinylation of p11 [185] and that the succinylated form of p11 was upregulated in gastric cancer. The authors showed that p11 was succinylated at lysine residue 47 (K47), which stabilized the protein against proteosomal degradation. Moreover, overexpression of a succinylation mimetic mutant K47E p11 increased the invasion and migration of gastric cancer cells. Interestingly, inhibition of ubiquitination enhanced succinylation of p11. Further studies would be of interest to determine if succinylation modulates the interaction of p11 with p36, plasminogen, or tPA, thus affecting the plasminogen activation functionality.

Another potential unexplored mode of post-translation modification and regulation of p11 could be via arginylation. Protein arginylation is a post-translation protein modification that is mediated by arginyl-tRNA-protein transferase (ATE1) via the transfer of arginine from t-RNA to N-terminal region of aspartic acid, glutamic acid, or cysteines in proteins [186]. Studies using global arginylation profiling in ATE1 KO mouse models have identified p11 as one of the targets, which was arginylated. The site of arginylation was identified as Ser3 [187]. The physiological significance of arginylation of p11 is yet to be identified, but it would be of interest to determine if arginylation of p11 affects the interaction with its binding partner p36 or other proteins or its localization to the cell surface, stability, and plasminogen receptor function on the cell surface.

Epithelial-mesenchymal-transition (EMT) is a well-regulated process defined by the gradual loss of epithelial characteristics of the cell and the gain of mesenchymal properties. EMT is crucial not only for embryogenesis and tissue repair but also during cancer progression and dissemination [188,189]. During EMT, the cancer cell acquires enhanced migratory and invasive properties, which include increased expression and production of ECM degrading enzymes such as MMPs [190]. This ultimately leads to cancer metastasis and colonization in distant secondary organs, such as the lungs, bone, brain, and liver, depending on the cancer type. It has been well documented that activation of the transforming growth factor-beta 1 (TGF β 1) signaling pathway orchestrates downstream signaling events and transcriptional programming for the EMT process [191]. Although it has been established that EMT is coupled with increased activity of proteolytic enzymes as the MMPs [192–194], the role of the plasminogen activation system has been poorly understood. We have recently shown that p11 is regulated through canonical Smad4-dependent TGF β 1 signaling and repressed by FOXC2-mediated PI3K-mTOR signaling in cells undergoing EMT. Specifically, the components of the plasminogen activation system, namely p11, PAI-1, and uPAR, were differentially regulated during EMT. Interestingly, p11 was the only known plasminogen receptor that was regulated in the A549, a lung cell model, in response to TGF β 1 signaling [195]. This result is further supported by proteomic data by other groups that showed that p11 was one of the few proteins upregulated in mesenchymal

prostate cancer cells and A549 cells after TGF β 1 treatment [196,197]. Our studies showed that although total cellular p11 expression was increased in response to TGF β treatment, plasmin generation or invasiveness was not enhanced (Figure 2). This was primarily due to increased PAI-1 expression and reduced cell surface expression of p11 [195]. Other studies have observed that both uPAR signaling and PAI-1 expression are required for activation of EMT in breast cancer [198] and fibroblasts [199], respectively. These studies have suggested that p11 is one of the crucial plasminogen receptors for EMT and that cell surface expression of p11 drives the plasminogen activation during EMT. Although paradoxical that PAI-1, a major plasminogen activation inhibitor, is upregulated during EMT, it is potentially necessary to maintain the delicate balance between plasminogen activation and inhibition during the invasive escape of cancer cells.

9. Role of p11 in Plasmin Generation

The AIIIt heterotetramer is a co-receptor for both plasminogen and tPA. The p36 subunit serves to anchor the complex to the cell surface while the p11 subunit serves as a plasminogen receptor. Plasminogen was initially shown to bind to the carboxy-terminal lysine of the p11 subunit [162,172]. p11 has a high affinity for tPA (Kd of 0.68 μ M) and plasminogen (Kd of 0.11 μ M). As with other plasminogen receptors, plasminogen binding to p11 induces an open conformation of plasminogen that promotes its activation [100,162]. Since the cleavage of the carboxyl-terminal lysines of p11 by carboxy peptidase B or their removal by site-directed mutagenesis results in a loss in plasminogen binding and activation, it has been assumed that the carboxy-terminal lysine of p11 is the key regulators of plasminogen binding and activation. However, our laboratory recently showed that the substitution of the carboxyl-terminal lysines with isoleucine (p11K95,96I) or arginine (p11K95,96R) did not result in a loss in p11-dependent plasminogen activation [100]. Furthermore, we reported that ϵ -aminocaproic acid, a lysine analog that blocks the lysine-binding kringle domains of plasminogen, blocked acceleration of plasminogen activation by the p11K95,96I mutant. Hence, these findings suggested that p11 uses internal lysine residues to bind plasminogen and tPA and that loss of the last two carboxyl-terminal residues of p11 may result in destabilizing p11 such that the internal lysine residue is not available for plasminogen activation.

In the same study, we also investigated the structural interactions between p11, tPA, and plasminogen. We observed that in contrast to the reported critical function of the finger domain of tPA in fibrin-stimulated plasmin generation, the kringle-2 domain of tPA played a key role in p11-dependent plasmin generation. We then showed that the kringle-2 domain of tPA was critical for plasminogen activation by other plasminogen receptors including, enolase-1, S100A4, histone H2B, cytokeratin 8, and high mobility group box-1 protein. Next, we used a series of plasminogen kringle mutants to identify the domain of plasminogen key for p11-dependent plasminogen activation. The kringle-1 domain of plasminogen, previously shown to be indispensable for fibrin-binding was shown to also be critical for p11-dependent plasmin generation.

The depletion of p11 via shRNA has been shown to dramatically reduce plasmin generation in a variety of cell types. For example, the depletion of p11 in HT1080 fibrosarcoma cells reduced plasmin generation by up to 95%, and ECM hydrolysis was reduced by 70% compared to HT1080 control cells [200]. AIIIt purified from bovine lung was initially reported to dramatically stimulate plasmin generation; yet, purified annexin proteins, including p36, were shown to have a marginal effect on plasmin generation [160]. Later, Kassam et al. [75] found that plasmin generation by the AIIIt heterotetramer stimulated activation of glu-plasminogen by 341-fold, whereas the p36 monomer stimulated activation by 6-fold. They also investigated the role of p11 in plasmin generation by comparing human recombinant proteins. They found that tPA-dependent plasmin generation was stimulated 77-fold by AIIIt that was formed by the combination of recombinant p11 and p36, 46-fold by p11, and only 2-fold by p36. They also observed that the combination of p11 with the first 15 amino acids of the p36-amino-terminus, which contained the p11-binding

sites, was like AIIIt formed with the full-length p36. Hajjar's group has reported that Cys-8 in the amino-terminal domain of p36 forms the binding site for tPA and binds tPA with a K_d of 48 nM [201]. They also reported that the Cys-8 residue of p36 is a key target for homocysteinylation and that this residue forms a disulfide bond with homocysteine. Importantly, the homocysteinylation of this site, reported by this group, was shown to block plasmin generation by p36 In Vitro and to account for the hemostatic imbalance displayed by patients with hyperhomocysteinemia. However, we reported that the AIIIt composed of p36 (Cys-8-Ser)/p11 wild-type (WT) (AIIIt Cys8Ser) exhibited greater acceleration of tPA-dependent plasminogen activation than the wild-type AIIIt. This rules out the postulated role of the Cys-8 residue of p36 in plasminogen activation. Hence, our data firmly support the concept that the p11 subunit and not p36 is the critical regulator of plasmin generation by the AIIIt heterotetramer. As part of AIIIt, the p11 subunit has a key function in the binding of plasminogen and facilitating its activation by binding and co-localizing plasminogen activators, yet p11 is also capable of binding newly generated plasmin to protect it from inactivation by α_2 -anti-plasmin [75].

Kwon et al. [78] also found that plasmin binding to p11 could promote plasmin-autoproteolysis. The specific plasminogen fragments produced from plasmin autoproteolysis are called angiostatins. These are a group of angiogenesis inhibitors. Kwon demonstrated that cells convert plasminogen to a form of angiostatin called A61 (Lys78–Lys468) in a three-step process. Initially, uPA cleaves the Arg561–Val562 of plasminogen which results in the formation of plasmin. Next, plasmin autoproteolysis results in the cleavage of the Lys77–Lys78 and Lys468–Gly469 bond. However, the presence of a Cys462–Cys541 disulfide prevents release of A61 (Lys78–Lys468) from the plasmin molecule. Last, AIIIt catalyzes the reduction of the Cys462–Cys541 disulfide of plasmin, which allows the release of A61 from plasmin. Mutagenesis of p36 Cys334Ser and either p11 Cys61Ser or p11 Cys82Ser was observed to inactivate the plasmin reductase activity of the isolated subunits, which suggested that specific cysteine residues of both p36 and p11 participated in the plasmin reductase activity of AIIIt.

10. Involvement of p11 in Biological Processes and Cancer

As described above, since AIIIt heterotetramer serves as a scaffold protein for protein–protein interactions with several other proteins, p11 plays a crucial role in several other biological processes via the virtue of this interaction. These processes include Na^+ absorption, pain processing, neuroprotective role in amyotrophic lateral sclerosis and traumatic model of motor neuron degeneration, and finally depression. The role of p11 in these processes has been discussed extensively elsewhere and will not be the focus of this review [161].

Plasmin generation by the p11 subunit of AIIIt is involved in multiple biological processes including monocyte and macrophage recruitment in inflammatory responses [202,203], fibrinolysis by endothelial cells [204], and cancer cell metastasis [167,200,205]. The presence of p11 at the cell surface of endothelial cells plays a vital role in plasmin generation that participates in vascular fibrinolysis. The shRNA-depletion of p11 from telomerase immortalized microvascular endothelial cells resulted in the dramatic decrease of plasminogen binding and plasmin generation by 50% and 60%, respectively, without affecting the presence of p36 at the cell surface [204]. Interestingly, the depletion of p36 reduced plasminogen binding and plasmin generation to a similar extent in these cells. As p36 has been shown to play a vital role in the stabilization and localization of p11, the findings indicate p11 is essential for the plasmin generation in endothelial cells, whereas p36 plays a role in the stabilization of p11. Surette et al. [204] also found that endothelial cell p11 was required for plasmin-dependent fibrinolysis In Vivo. In p11-KO mice, fibrin deposition was increased compared to p11-WT mice, and this was found to be independent of coagulation since there was no difference in prothrombin time and activated partial thromboplastin time between p11-WT and p11-KO mice. Using a tail-clip experiment to characterize the length of time for bleeding to stop, the time to stop bleeding for p11-KO mice was 4-fold less

than the p11-WT group, thus indicating that the loss of p11 reduced plasmin-dependent fibrinolytic activity.

Cell surface plasmin generation via p11 plays a major role in the migration of macrophages to the site of inflammation [203] and tumor sites [202]. The plasmin generated at the cell surface of macrophages facilitates their migration through tissues by direct hydrolysis of the protein that forms the ECM and by activating MMPs [206] that will further degrade the ECM upon activation. Other studies have shown that p11 plays a crucial role in sepsis in animal models by negatively regulating macrophage Toll-Like-Receptor (TLR) signaling [207].

The aberrant expression of p11 has been found to promote the invasiveness of tumor cells and metastasis by numerous studies. In mouse xenograft models, transplantation of p11-depleted HT1080 fibrosarcoma cells showed a 3-fold reduction in the number of metastatic foci in the lungs compared to mice injected with HT1080 cells with WT levels of p11 [200]. In contrast, the overexpression of p11 in the HT1080 fibrosarcoma cells resulted in a 16-fold increase in the number of metastatic foci in the lungs [200]. Depletion of p11 in colorectal cell line CCL-222 reduced plasminogen binding by 45% and plasmin generation by 65%, and these cells were unable to migrate through a Matrigel barrier in a plasmin-dependent manner [205]. Recently, Bydoun et al. demonstrated that loss of p11 in a pancreatic cancer cell line (Panc1) resulted in decreased plasminogen activation and plasminogen-dependent invasion with no alteration in tumor cell proliferation *In Vitro*. Interestingly, the injection of the p11 depleted pancreatic tumor cells in immunocompromised non-obese diabetic (NOD)/severe combined immunodeficiency (SCID) mice resulted in reduced tumor growth compared to control cells, suggesting the involvement and interaction with TME in tumor growth [208]. Many studies in other cancer models have also associated p11 in tumorigenesis through plasminogen-independent mechanisms. For example, loss of p11 in ovarian cancer cells resulted in reduced tumor growth in NOD/SCID mice *In Vivo* with concurrent reduction of cell proliferation, colony formation, migration, and invasion *In Vitro*. Moreover, p11-depleted cells show decreased resistance to carboplatin *In Vitro* [209]. Li Y et al., recently demonstrated the importance of p11 in gastric cancer tumorigenesis. Overexpression of p11 in gastric cancer cells resulted in increased tumor burden in subcutaneous tumors in BALB/c-nude mice. Rapamycin treatment of the subcutaneous tumors from p11 overexpressing cells resulted in a significant reduction in tumor weight and size suggesting that p11 promotes tumor growth in gastric cancer cells via mTOR signaling pathway. Consistently, these authors also observed a positive correlation between p11 expression and mTOR signaling in Gene Set Enrichment Analysis from The Cancer Genome Atlas database. More specifically, these studies have indicated that p11 stimulates aerobic glycolysis in gastric cancer cells via activation of Src/ANXA2/AKT/mTOR signaling pathway, ultimately leading to enhanced cell proliferation and resistance to apoptosis. This is the first investigation directly implicating p11 in aerobic glycolysis [210]. Two recent studies have highlighted the importance of p11 in modulating gene expression of pluripotency factors in breast cancer stem cells (CSC). Studies by Yanagi et al. have shown that p11 was dramatically upregulated in CD44+ metastasized CSC in mouse patient-derived xenotransplant (PDX) mammary tumors compared to CD44– metastasized and CD44+ and CD44– primary CSC. Moreover, overexpression of p11 in human breast cancer cell line MDA MB 231 resulted in increased organoid-forming, invasive, and metastatic capacity, whereas loss of p11 resulted in a reduced number of organoids. Interestingly, these studies also established that p11 upregulated stem cell-related genes, such as OCT4, SOX2, and NANOG, in the organoids, suggesting a novel function of p11 in promoting metastasis of CSC [211]. Lu et al., observed that chemotherapy (paclitaxel or carboplatin)-induced p11 is mediated by HIF-1, which further promotes epigenetic modulation and transcriptional activation and expression of pluripotency factors, such as NANOG, SOX2 and KLF4, in breast cancer cell lines. Moreover, loss of p11 resulted in increased sensitivity to paclitaxel in orthotopic mammary tumors [212]. Both these studies emphasize the pivotal role of p11 in facilitating the enrichment of CSC in

breast cancer. Although these authors did not investigate the plasminogen activation function of p11 in these cell models, it is highly likely that p11 plays both plasminogen-dependent and -independent function in tumor cell proliferation, migration, and invasion. Identification of the lysine residue involved in plasminogen binding and generation of p11 mutant mice incapable to activating plasminogen will further our understanding of plasminogen-dependent and -independent functions of p11 in cancer progression.

11. Plasmin Functions in the Tumor Microenvironment—Regulation of Macrophage Function

In the past two decades, the major focus on the plasminogen activation system has been on the various components specifically the activators, inhibitors, and receptors. However, the effects of the proteolytic plasmin on cancer progression have been poorly understood. Plasmin can cleave a broad range of ECM substrates, growth factors, and cytokines. The plasmin-mediated function in TME can be classified into two categories—proteolytic processing of substrates and proteins and plasmin signaling at the cell surface.

Plasmin has been indirectly implicated in the development and progression of tumors by activating various growth factors, such as TGF β , FGF-2, and HGF. TGF β and uPA are coordinately and tightly regulated in cancer progression. TGF β upregulates uPA expression, which further enhances plasmin generation and activates TGF β which contributes to the tumor progression via its effects on EMT, invasion, and metastasis (reviewed in [213,214]).

As discussed, several components of the plasminogen-plasmin system including activators, inhibitors, and receptors, are expressed on stromal cells and concurrently support tumor growth and progression. For instance, uPA is expressed on myofibroblasts and uPAR; plasminogen receptors, such as Plg-RKT and p11, are expressed on the macrophages; and PAI-1 on macrophages, endothelial cells, and fibroblasts. Studies using transgenic and ectopic mouse tumor models have played a tremendous role in our understanding of the stromal and cancer cell contribution of the plasminogen-plasmin system components toward cancer progression.

The role of the proinflammatory function of plasmin during tissue injury and atherosclerosis is well known. Studies have demonstrated that binding of plasmin to monocytes induces expression of proinflammatory cytokines, such TNF- α and IL-6, via the activation of NF- κ B and JAK/STAT pathway [215]. AII is required not only for plasmin binding on monocytes but also for plasmin-mediated downstream signaling. This function of plasmin is independent of the catalytic/proteolytic function of plasmin [216].

The generation of plasmin from plasminogen by tPA has been shown to regulate the balance of soluble and cell-bound levels of the chemokine CCL21 in the immune system, particularly in the dendritic and T-cells. This chemokine has a crucial role in the migration and homing of T-lymphocytes and antigen-presenting dendritic cells [217]. In another study, plasmin stimulated chemotaxis of monocyte-derived dendritic cells via the activation of Akt2 and p38 mitogen-activated signaling pathway [218]. These studies suggest that plasmin is a potent chemoattractant for immune cells acting via its proteolytic and signaling function. Although studies for the role of plasmin signaling have not been performed in the context of tumor growth, progression, and TME, it is well established that tumor-infiltrating immune cells play an important role by either interfering or promoting tumor progression [219].

In the context of cancer, studies have shown the dual requirement of the proteolytic and signaling properties of plasmin for promoting a motogenic phenotype. For example, in HT29-M6 intestinal cell lines, treatment with phorbol 12-myristate 13-acetate (PMA) resulted in a cascade of events, which involved initial upregulation of uPA, proteolysis of uPAR, activation of plasminogen to plasmin degradation of ECM, and scattering of cells. Activation of ERK1/2 was required for the cell scattering event that was mediated by plasmin intracellular signaling [93].

The plasminogen-activation system plays a pivotal role in macrophage biology, specifically macrophage migration and phagocytosis. In one of the first studies, Ploplis et al. used plasminogen-deficient mice and demonstrated that upon inflammatory stimulus

with thioglycolate, monocyte and lymphocyte recruitment to the peritoneal cavity was dramatically retarded [220]. More recently, Silva et al. demonstrated that the decrease in macrophage recruitment could be partly attributed to a decrease in plasmin-mediated fibrinolysis in these mice. In this study, they showed that reduced peritoneal infiltration of macrophages in plasminogen-depleted mice was restored by fibrinogen deficiency [221]. Further evidence for the signaling role of plasmin in mediating monocyte migration was obtained from studies by Carmo et al. These studies have shown that plasmin facilitates monocyte migration via PAR-1, MEK/ERK, and CCL2/CCR2-mediated signaling [90]. Das et al. showed a remarkable decrease in macrophage-mediated phagocytosis of apoptotic thymocytes in spleen and reduced uptake by peritoneal macrophages in plasminogen knockout mice. Overall, the spleen and liver from these plasminogen-deficient mice displayed downregulation of genes involved in phagocytosis [222].

Aligned with the role of plasminogen in macrophage recruitment (summarized in Figure 3), depletion of several plasminogen receptors results in a phenotype resembling that in plasminogen-deficient mice. The role of plasminogen receptors on monocyte migration was mostly studied using an inflammation model. Receptors, such as enolase-1, histone H2B, Plg-RKT, and p11, played predominant roles in thioglycolate elicited monocyte migration both In Vivo and In Vitro. Enolase-1 was shown to play a crucial role in lipopolysaccharide (LPS)-driven monocyte migration and matrix degradation In Vitro and LPS-dependent recruitment of alveolar monocytes In Vivo. LPS upregulated enolase-1 in human blood monocytes and U937 cells, which in turn resulted in plasminogen-dependent enhancement in monocyte recruitment [223]. Das et al., showed that although multiple plasminogen receptors, such as enolase-1, AIIIt, and histone H2B, are expressed in the macrophage cell lines RAW 264 and JA774.1 cells, histone H2B contributed to 50% of the plasminogen activation function in these cells [147]. The newest member of the plasminogen receptor family, Plg-RKT, is the only transmembrane plasminogen receptor. This receptor is expressed in blood monocytes and monocytoid cells. Inhibition of Plg-RKT by blocking antibodies resulted in a dramatic reduction in plasmin generation, monocyte migration, and invasion through a Matrigel-coated chamber. Moreover, in the thioglycolate dependent peritonitis model, treatment with Plg-RKT antibody also resulted in the reduction of macrophage recruitment in the peritoneal cavity [224,225]. Our laboratory has shown the role of p11 in plasmin-dependent macrophage infiltration in both inflammation and tumor models. The availability of p11-KO mouse models has enabled an elegant demonstration of the important contribution of p11 toward macrophage recruitment. O'Connell et al. [203] examined how the loss of p11 affected the migration of macrophages using the thioglycollate-induced peritonitis as a model of inflammation. In p11-KO mice, the number of macrophages that migrated into the peritoneal cavity upon thioglycolate treatment was reduced by 53% compared to the macrophages of p11-WT mice. Furthermore, the p11-KO macrophages displayed limited invasive capability using the Matrigel plug assay In Vivo.

Phipps et al. [202] discovered that the expression of p11 in macrophages plays an essential role in facilitating macrophage migration to tumors. Using a xenograft mouse model in which LLC cells were transplanted into p11-WT and p11-KO mice, tumor growth was arrested after seven days in p11-KO mice. In contrast, tumor growth continued in the p11-WT mice, where tumors were 10-fold larger than those in p11-KO mice. In p11-WT mice, the immunohistochemical analysis determined that macrophages were present throughout the tumor. In contrast, macrophages were present at the periphery of tumors in p11-KO mice, indicating that macrophages lacking p11 were incapable of infiltrating into tumors. To determine the impact that p11-expression in macrophages has in affecting tumor growth in the p11-KO mice, p11-WT macrophages were injected peritoneally into p11-KO mice before transplantation of LLC cells. Tumors in the p11-KO mice transplanted with p11-WT macrophages presented tumors comparable to the tumors observed in p11-WT mice, hence indicating that p11-dependent plasmin generation in macrophages plays a critical role in facilitating tumorigenesis.

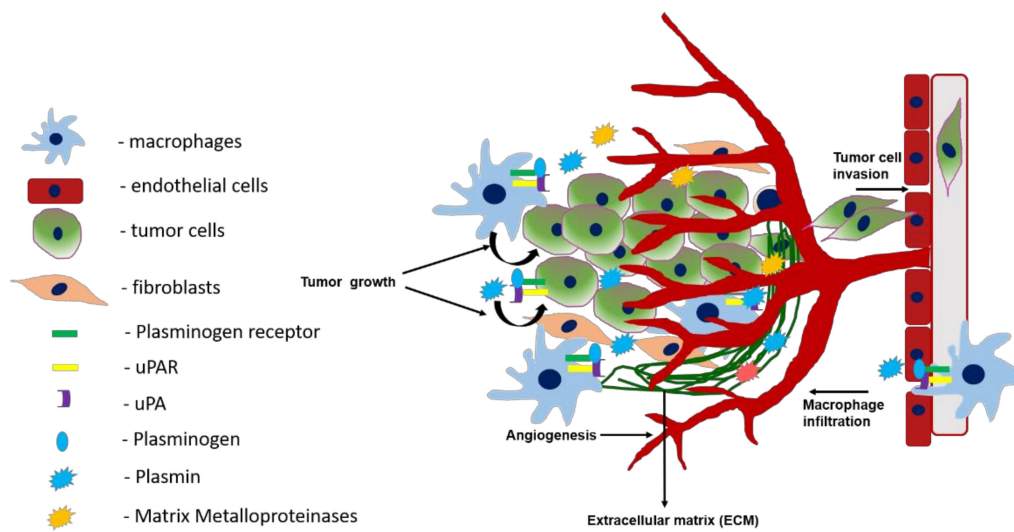


Figure 3. Role of the plasminogen activation system in tumor growth, angiogenesis, macrophage infiltration, and invasion. Activation of plasminogen bound to plasminogen receptors at the cell surface of macrophages and tumor cells is mediated by uPA bound to uPAR. This results in the production of plasmin which activates matrix metalloproteinases and together these proteases play a key role in the infiltration of macrophages to tumor sites. At the tumor site, macrophages promote tumor growth, angiogenesis, and metastasis. Plasmin produced by the tumor cells mediates tumor cell migration and invasion both by protease dependent and independent mechanisms.

Currently, research on the role of p11 in tumorigenesis has been predominately conducted in ectopic tumor models. Transgenic mouse models of cancer are histologically and genetically accurate models of human cancer. Recently, we utilized the mouse mammary tumor virus-polyoma middle tumor (MMTV-PyMT) transgenic model to interrogate the role of p11 in breast cancer in WT and p11-KO mice [226]. The MMTV-PyMT transgenic model-specific expression of the oncogene PyMT under the MMTV promoter, results in widespread tumor growth in the mammary glands and spontaneous metastasis to the lymph nodes and lungs. This mouse model is very similar to human breast cancer in that the tumors display histological and molecular characteristics mirroring the progression of human breast cancer. With this model system, we have shown that p11 is exclusively expressed in the stromal compartment, and the loss of p11 dramatically reduces tumor onset, growth, and progression. Spontaneous and experimental pulmonary metastasis were also substantially reduced in the absence of p11. Surprisingly, tumors and tumor cell lines isolated from these animals do not demonstrate a decrease in plasminogen activation with the loss of p11. We hypothesize that plasmin generation by stromal cells, such as macrophages, is critical for tumor growth and progression of breast cancer in this model system. Many dysregulated pathways and processes observed in breast cancer progression mimic those observed during normal mammary gland development and tissue remodeling. During puberty, and under the control of hormones and other factors, the ductal epithelium of the rudimentary mammary gland invades into the mammary fat pad in a process referred to as branching morphogenesis. ECM-degrading enzymes, including MMPs and their inhibitors, tissue inhibitors of metalloproteinases are involved in this process [227]. Plasminogen-deficient mice show a delay in early ductal development and many are unable to lactate because of a lack of secretory epithelium [228]. Since p11 is involved in cancer cell invasion we investigated the possibility that p11 might also be involved in branching morphogenesis. We observed a reduction in length of the ductal branches in the p11-KO mammary glands at the early time points of 6 and 8 weeks and was comparable to the WT at 10 and 12 weeks. This suggests that p11 regulates the invasion of both normal and cancer cells.

Hence, there is ample evidence linking the plasminogen activation system components to macrophage invasion and migration (Figure 3). Several studies have demonstrated that

plasminogen plays an important role in macrophage-driven phagocytic function in the context of liver injury and wound healing. Using plasminogen and uPA KO mice, Kawao et al. showed that in a liver injury model, plasminogen was important for macrophage-specific phagocytosis of cellular debris [229]. On the contrary, Rosenwald et al. showed that plasminogen does not induce macrophage-specific phagocytosis but rather affects the prey cells [230]. Finally, Das et al. showed using plasminogen-deficient mice that many genes involved in phagocytosis are downregulated in these mice and that plasminogen is a key regulator of macrophage-specific phagocytosis [222]. Although there is no direct evidence of the role of plasminogen and phagocytosis in the context of tumor and TME, this might be mainly relevant in chemotherapy and radiation therapy. In this scenario, potentially damage associated molecular patterns induced by dying tumor cells can activate endothelial cells and promote migration of myeloid cells, such as macrophages, which in turn results in the clearance of apoptotic tumor cells by phagocytosis. Future studies should be aimed at identifying the plasminogen receptors responsible for the phagocytosis process.

Initially, the role of the uPA, uPAR, plasminogen, PAI-1, and plasminogen receptors in cancer growth was studied using transplantable and ectopic tumor models in NOD/SCID and syngeneic mice and antibody-targeting and anti-sense gene knock-down technology. These studies primarily utilized LLC cells, melanoma, squamous lung carcinoma, and prostate cancer models [105,231–237]. Overall, these studies showed that inhibition of uPA and uPAR resulted in decreased metastasis. More recently, due to the availability of gene knockout transgenic mouse models, the role of plasminogen, uPA, uPAR, PAI-1, and plasminogen receptors in tumor growth and metastasis have been extensively studied. The MMTV-PyMT transgenic model has been extensively used to study the function and expression of the various components of the plasminogen activation system (reviewed in [238]). More importantly, this model is relevant to understanding the expression and contribution of the plasminogen activation components by both TME and tumor cells in cancer growth and progression. In situ hybridization and immunohistochemistry have revealed that the expression of uPA, uPAR, and PAI-1 is predominantly increased in the stromal compartment, by cells that include fibroblasts, macrophages, and endothelial cells. Interestingly, this mirrors the expression and localization pattern in human breast cancer, where the highest uPA [239] and uPAR [240] expression is found in stromal cells including the macrophages in the periphery of breast cancer cells, whereas PAI-1 expression is found predominantly in the myofibroblasts [241]. Studies with plasminogen-deficient mice that express the MMTV-PyMT oncogene presented contrasting results among different groups. The first studies performed in the late '90s by the Bugge group showed that loss of plasminogen decreased spontaneous pulmonary metastasis with no effect on tumor onset and growth [53]. In contrast, studies reported by the Lundt group more than a decade later showed that loss of plasminogen did not decrease spontaneous metastasis to the lung. The latter group attributed this confounding result to the extensive backcrossing of their mice before initiating these studies [242]. In the MMTV-PyMT model, there is no significant difference in tumor growth and vascularization between WT and uPA, uPAR, and PAI-1 deficient animals [238]. The uPA deficiency shows the most significant decrease in metastasis, and PAI-1 depletion has a slight metastasis promoting effect (although not statistically significant); uPAR loss does not affect metastasis (reviewed in [238]). Interestingly, the effect of uPA on cancer progression depends on the organ and cancer types. In the case of melanoma, uPA deficiency in mice results in decreased invasion and progression, whereas inhibition of uPA does not affect the progression of pancreatic cancer in the RIP-Tag2 transgenic mouse model [243,244]. Among the PgRs, genetic depletion of S100A4 resulted in a dramatic decrease in pulmonary metastatic burden without any alteration in tumor onset and growth kinetics. This was accompanied by significant suppression of T-cell infiltration in the tumors depleted of S100A4. S100A4 secretion in the TME resulted in the influx of T-cells which release cytokines resulting in enhanced metastasis [245]. Our studies with the MMTV-PyMT transgenic model in which the p11 gene was knocked

out was the only instance of a plasminogen activation system component (p11) playing a dynamic role in tumor onset, growth, progression, and metastasis.

12. Plasminogen Activation Components and Role in Chemoresistance

There are two main molecular targets in breast cancer based on the expression of estrogen receptor alpha (ER α) and epidermal growth factor receptor 2 (HER2). Tamoxifen is the main component for the treatment of ER α positive breast cancer, which accounts for about 70% of all breast cancers. Tamoxifen acts by competing with estrogen for its binding with ER α resulting in the inhibition of estrogen effect on cancer cell proliferation (reviewed in [246,247]). Although tamoxifen therapy has significantly resulted in reduction in mortality rate in ER-positive breast cancer patients, a significant proportion of patients present with recurrence due to intrinsic or acquired resistance to tamoxifen. Components of the plasminogen activation system have been involved in predicting tamoxifen resistance in hormone responsive breast cancer. A high tumor expression of uPA, uPAR, and PAI-1 was associated with poor response to tamoxifen in patients with recurrent breast cancer [248,249].

Chemotherapy is the primary mode of treatment for metastatic and aggressive breast cancer especially triple-negative breast cancer. Triple-negative breast cancer is characterized by loss of ER, progesterone receptor and HER2 and is highly aggressive and metastatic. Chemotherapeutic agents, such as paclitaxel and carboplatin, are commonly used to treat aggressive breast cancer. Although these drugs reduce overall primary tumor burden, many patients develop recurrent and metastatic disease which are subsequently resistant to these drugs. Hence, chemoresistance remains a major barrier to successful treatment of aggressive and metastatic breast cancer. Several mechanisms contribute toward chemoresistance that is well studied specifically for breast cancer. These include but are not restricted to increased drug metabolism and excretion of the drugs, mechanisms for resisting apoptosis and enhancing cell survival pathways, EMT, activation of cancer stem cells, efficient DNA damage response and repair, and finally, alterations in the TME to promote drug resistance (reviewed in [250,251]).

p11 has been linked to resistance to several chemotherapeutic agents. Proteomic analysis of acquired tamoxifen resistance in MCF-7 breast cancer cells has identified p11 as one of the top five upregulated proteins in tamoxifen-resistant cells [252]. Similarly, proteomic analysis showed that p11 was significantly increased in relapsing patients associated with tamoxifen resistance [184]. Overexpression of p11 has also been linked to reduced sensitivity of colorectal cancer cells [253] to oxaliplatin and depletion of p11 in leukemic cells increases sensitivity to vincristine [254]. Finally, p11 was part of an 11-member signature panel associated with multi-drug resistance in ovarian cancer [255]. The functional significance of p11 in promoting chemotherapy resistance has not yet been elucidated, but these studies allude to its potential as a prognostic marker.

13. The Role of the Plasmin and Plasminogen System as Biomarkers in Cancers

Cancer biomarkers are most often used as aid in diagnosis but can also be useful to determine tumor aggressiveness. Biomarkers also play a key role in identifying new personalized targets depending on the aggressiveness of the disease and toxicity to the therapeutic agents. In order for personalized therapies to be effective we require validated novel biomarkers for predicting aggressive vs. non-aggressive cancer, response to therapy and therapeutic resistance, and for predicting therapeutic side-effects and toxicity [256]. The best-established cancer biomarkers are uPA/uPAR and PAI-I [42,257]. As discussed, many components of the fibrinolytic system play an important pathologic role in tumor growth and metastases. Ultimately, plasmin plays two distinct roles in the transformation process. First, plasmin participates in the proteolytic activation of several growth factors such as TGF β , FGF2, ILGF-1, and hepatocyte growth factor. Second, plasmin participates in tumor growth and metastasis via degradation of components of the extracellular matrix which form a barrier to metastasis. Plasmin also participates in the activation of several proteases, such as the MMPs, that also proteolyze extracellular matrix components.

The uPA/uPAR complex also plays a role in signal transduction and cellular adhesion. Substantially increased levels of uPA were observed in various cancers of the breast, stomach, colon and rectum, esophagus, pancreas, glioma, lung, kidney, prostate, uterine cervix, ovary, liver and bone as evaluated by tissue extraction, immunohistochemical and in situ hybridization methods [257]. Subsequently, the increased expression of uPA, uPAR, and/or PAI-1 has been demonstrated to be associated with poorer overall prognosis in multiple cancer types, including cancer of breast [258], bone [259], colon and rectum [260–262], pancreas [263], glioma [264], kidney [265,266], prostate [267,268], lung [269], cervix [270], ovary [271], esophagus [272], liver [273] and stomach [274].

Of the various cancers, the best-established case for the utilization of uPA/PAI-1 as biomarkers is for breast cancer. The use of uPA/PAI-1 as prognostic biomarkers in lymph node-negative breast cancer has been confirmed by randomized prospective clinical trials involving pooled analysis of data from retrospective and prospective studies [275]. In this regard they are used for the identification of lymph node-negative patients who have HER-2-negative tumors and who can be safely spared the toxicity and costs of adjuvant chemotherapy.

The association of uPA and PAI-1 with tumor aggressiveness and patient response has been supported by an extensive array of studies spanning over 30 years. However, the use of uPA/uPAR and PAI-1 as biomarkers in clinical practice has been very limited. A major reason for this has been the fact that while inhibition of uPA, uPAR or PAI-1 by inhibitory monoclonal antibodies, by gene manipulations such as the transfection of PAI-1 into experimental tumors, and by synthetic small molecules designed to target uPA, uPAR or PAI-1 have shown in many cases dramatic inhibition of tumor growth and metastasis in experimental animals, these approaches have had minimal impact on human tumors and metastases. In the absence of clinical trials showing significant effects on human cancers, there has been a reluctance to use these components as biomarkers.

The studies on the expression of plasminogen receptors as cancer biomarkers have been performed on a few known plasminogen receptors such as p11, Enolase 1, and cytokeratin 8 [155,156,159]. Many of the plasminogen receptors are multifunctional proteins with both intracellular and extracellular expression and functionality in cancer progression. Hence, it is imperative to specifically delineate the intracellular and membranous (or secreted) expression patterns of the receptors when describing the diagnostic, and prognostic value of the receptors in human cancers. Nevertheless, overexpression of several of the plasminogen receptors has been correlated with poor overall survival and prognosis.

Clinical analysis has demonstrated that p11 gene and protein expression are up-regulated in several cancers, such as blood, brain, colorectal, gallbladder, kidney, lung, lymphatic, ovary, pancreas, prostate, skin, stomach, and thyroid, and it has been extensively documented in recent reviews [156,276,277]. Our laboratory has recently established the potential of p11 as a diagnostic and prognostic biomarker in pancreatic and breast cancer. In silico analysis of pancreatic tumors and cell lines demonstrated upregulation of p11 mRNA expression. p11 mRNA expression and methylation status were predictive of overall survival and recurrence-free survival (RFS) in pancreatic ductal adenocarcinoma patients. Furthermore, protein expression of p11 significantly increased in during progression from normal to pancreatic ductal adenocarcinoma as demonstrated in tissue microarray analysis in human patients [208].

Expression of p11 in breast cancer has been analyzed in multiple studies with inconsistent observations. In one of the early studies, Carlsson et al. performed an analysis in ductal carcinoma in situ and invasive and metastatic breast tumors using serial analysis of gene expression. They found that p11 gene expression was downregulated in breast cancer irrespective of pathological grade [278]. In contrast, Yu et al. demonstrated that p11 was one of the 170 genes that were activated at the intravasation step during metastasis [279] in breast cancer patients. Studies by Zhang et al., using Kaplan—Meier plotter database showed that elevated p11 mRNA expression was predictive of worse overall survival (OS) in basal-type breast cancer, and there was no significant association of p11 expression in

other subtypes based on clinicopathological grades [280]. Since p11 protein expression is subjected to multiple post-translational modifications and interactions with several binding partners, gene expression analysis alone will not suffice to understand the clinical significance of p11 expression. To date, only two studies have examined the expression of p11 protein in clinical samples from breast cancer patients. The first analysis by Arai et al. demonstrated membranous overexpression of p11 in high-grade tumor status correlating with high mitotic counts, severe nuclear pleomorphism, high Ki67 positivity index and low ER status [281]. They did not observe any correlation of p11 protein expression with stromal invasion. Our laboratory has utilized both gene expression profiling and immunohistochemical staining for p11 in breast cancer patient tissues. We observed that p11 mRNA expression was significantly associated with poor patient prognosis and significantly elevated in high-grade, triple-negative tumors, and tumors with high proliferative index. Most impressively, we observed that the high mRNA levels of p11 were significantly associated with poor patient OS and a hazard ratio of 3.34. Although membranous expression of p11 protein as evaluated by immunohistochemistry was significantly elevated in tumor cells compared to normal mammary epithelium, there was no correlation between high p11 expression and clinical and pathological tumor grade or with molecular subtype in human breast cancer samples. The discrepancy between p11 mRNA and protein expression in human tissues can be partially attributed to the contribution of p11 by stromal cells in the TME, which has not been examined in the immunohistochemistry analysis. Future studies should be focused on employing a larger cohort of tissues for a detailed evaluation of stromal and tumor cell expression of p11 in breast cancer [226].

Similarly, mRNA and protein for cytokeratin 8 is overexpressed in several cancers such as breast, colon, gastric, head and neck, liver, lung, skin and uterus (reviewed in [155]). Enolase 1 has also been evaluated for its use as a biomarker in several cancers, where it is shown to be upregulated such as bone, breast, head and neck, liver, lung and pancreas where it suggests to have a prognostic significance (reviewed in [155]). Since many of the plasminogen receptors play a key role in the macrophage function in animal models as described previously it will be interesting to determine if macrophages in human tumors from patients show elevated expression of plasminogen receptors, which can further be used as a prognostic indicator of cancer progression and therapeutic interventions.

14. Concluding Remarks

Overall, the interpretation of the role of the plasminogen activation system in tumor progression has been more complicated than expected due to the multifunctionality of the components and their plasmin-independent role in tumor progression. For instance, plasmin apart from its enzymatic function also promotes cell signaling which potentially contributes toward tumor growth and metastasis. uPAR is a pleiotropic protein that regulates cell adhesion, migration, proliferation, via intracellular signaling and independent of its plasmin activating function.

In summary, from these studies, we can infer that plasmin-mediated proteolysis contributes to the degradation of ECM, which can directly or indirectly affect tumor stroma formation, angiogenesis, and dissemination. Plasmin generation by stromal cells, such as macrophages is critical for tumor growth and progression in many forms of cancer including breast cancer. In this regard, the plasminogen receptors play a key role in regulating plasmin generation. Our work has highlighted the importance of the plasminogen receptor, p11, in the interaction of cancer cells with the stroma.

Author Contributions: Writing—original draft preparation, A.G.B., R.W.H., V.A.M., D.M.W.; writing—review and editing, A.G.B., R.W.H., V.A.M., D.M.W.; supervision, D.M.W.; project administration, D.M.W.; funding acquisition, D.M.W. All authors have read and agreed to the published version of the manuscript.

Funding: A.G.B. is supported by a trainee award from the Beatrice Hunter Cancer Research Institute with funds provided by the Harvey Graham Cancer Research Fund as part of The Terry Fox Strategic

Health Research Training Program in Cancer Research at Canadian Institute of Health Research (CIHR). D.M.W. and this research is supported by a grant from the CIHR.

Conflicts of Interest: The authors declare no conflict of interest.

References

- Lu, P.; Takai, K.; Weaver, V.M.; Werb, Z. Extracellular matrix degradation and remodeling in development and disease. *Cold Spring Harb. Perspect. Biol.* **2011**, *3*, a005058. [CrossRef] [PubMed]
- Hynes, R.O. Extracellular matrix: Not just pretty fibrils. *Science* **2009**, *326*, 1216–1219. [CrossRef] [PubMed]
- Walker, C.; Mojares, E.; Del Río Hernández, A. Role of Extracellular Matrix in Development and Cancer Progression. *Int. J. Mol. Sci.* **2018**, *19*, 3028. [CrossRef] [PubMed]
- Deryugina, E.I.; Quigley, J.P. Cell surface remodeling by plasmin: A new function for an old enzyme. *J. Biomed. Biotechnol.* **2012**, *2012*, 564259. [CrossRef]
- Hanahan, D.; Coussens, L.M. Accessories to the crime: Functions of cells recruited to the tumor microenvironment. *Cancer Cell* **2012**, *21*, 309–322. [CrossRef]
- Place, A.E.; Jin Huh, S.; Polyak, K. The microenvironment in breast cancer progression: Biology and implications for treatment. *Breast Cancer Res.* **2011**, *13*, 227. [CrossRef]
- Mouw, J.K.; Ou, G.; Weaver, V.M. Extracellular matrix assembly: A multiscale deconstruction. *Nat. Rev. Mol. Cell Biol.* **2014**, *15*, 771–785. [CrossRef]
- Kai, F.; Laklai, H.; Weaver, V.M. Force Matters: Biomechanical Regulation of Cell Invasion and Migration in Disease. *Trends Cell Biol.* **2016**, *26*, 486–497. [CrossRef]
- Deville, S.S.; Cordes, N. The Extracellular, Cellular, and Nuclear Stiffness, a Trinity in the Cancer Resistome-A Review. *Front. Oncol.* **2019**, *9*, 1376. [CrossRef]
- Billroth, T. Lectures on surgical pathology and therapeutics. In *A Handbook for Students and Practitioners*; The New Sydenham Society: London, UK, 1877; Available online: <https://catalog.hathitrust.org/Record/002090469> (accessed on 1 March 2021).
- Iwasaki, T. Histological and experimental observations on the destruction of tumour cells in the blood vessels. *J. Pathol. Bacteriol.* **1915**, *20*, 85–105. [CrossRef]
- DeWys, W.D.; Kwaan, H.C.; Bathina, S. Effect of defibrination on tumor growth and response to chemotherapy. *Cancer Res.* **1976**, *36*, 3584–3587.
- Danø, K.; Andreasen, P.A.; Grøndahl-Hansen, J.; Kristensen, P.; Nielsen, L.S.; Skriver, L. Plasminogen activators, tissue degradation, and cancer. *Adv. Cancer Res.* **1985**, *44*, 139–266.
- Costantini, V.; Zacharski, L.R.; Memoli, V.A.; Kisiel, W.; Kudryk, B.J.; Rousseau, S.M. Fibrinogen deposition without thrombin generation in primary human breast cancer tissue. *Cancer Res.* **1991**, *51*, 349–353.
- Costantini, V.; Zacharski, L.R.; Memoli, V.A.; Kisiel, W.; Kudryk, B.J.; Rousseau, S.M.; Stump, D.C. Fibrinogen deposition and macrophage-associated fibrin formation in malignant and nonmalignant lymphoid tissue. *J. Lab. Clin. Med.* **1992**, *119*, 124–131.
- Ornstein, D.L.; Zacharski, L.R.; Memoli, V.A.; Kisiel, W.; Kudryk, B.J.; Hunt, J.; Rousseau, S.M.; Stump, D.C. Coexisting macrophage-associated fibrin formation and tumor cell urokinase in squamous cell and adenocarcinoma of the lung tissues. *Cancer* **1991**, *68*, 1061–1067. [CrossRef]
- Dvorak, H.F.; Senger, D.R.; Dvorak, A.M. Fibrin as a component of the tumor stroma: Origins and biological significance. *Cancer Metastasis Rev.* **1983**, *2*, 41–73. [CrossRef]
- Dai, K.; Zhang, Q.; Li, Y.; Wu, L.; Zhang, S.; Yu, K. Plasma fibrinogen levels correlate with prognosis and treatment outcome in patients with non-M3 acute myeloid leukemia. *Leuk. Lymphoma* **2019**, *60*, 1503–1511. [CrossRef]
- Wada, H.; Mori, Y.; Okabayashi, K.; Gabazza, E.C.; Kushiya, F.; Watanabe, M.; Nishikawa, M.; Shiku, H.; Nobori, T. High plasma fibrinogen level is associated with poor clinical outcome in DIC patients. *Am. J. Hematol.* **2003**, *72*, 1–7. [CrossRef]
- Zheng, S.; Shen, J.; Jiao, Y.; Liu, Y.; Zhang, C.; Wei, M.; Hao, S.; Zeng, X. Platelets and fibrinogen facilitate each other in protecting tumor cells from natural killer cytotoxicity. *Cancer Sci.* **2009**, *100*, 859–865. [CrossRef]
- Simpson-Haidaris, P.J.; Rybarczyk, B. Tumors and fibrinogen. The role of fibrinogen as an extracellular matrix protein. *Ann. N. Y. Acad. Sci.* **2001**, *936*, 406–425. [CrossRef]
- Reijerkerk, A.; Voest, E.E.; Gebbink, M.F. No grip, no growth: The conceptual basis of excessive proteolysis in the treatment of cancer. *Eur. J. Cancer* **2000**, *36*, 1695–1705. [CrossRef]
- Al-Mehdi, A.B.; Tozawa, K.; Fisher, A.B.; Shientag, L.; Lee, A.; Muschel, R.J. Intravascular origin of metastasis from the proliferation of endothelium-attached tumor cells: A new model for metastasis. *Nat. Med.* **2000**, *6*, 100–102. [CrossRef]
- Sevenich, L.; Joyce, J.A. Pericellular proteolysis in cancer. *Genes Dev.* **2014**, *28*, 2331–2347. [CrossRef]
- Mason, S.D.; Joyce, J.A. Proteolytic Networks in Cancer. *Trends Cell Biol.* **2011**, *21*. Available online: <https://www.ncbi.nlm.nih.gov/pmc/articles/PMC3840715/> (accessed on 5 June 2020). [CrossRef]
- Koblinski, J.E.; AhrAm, M.; Sloane, B.F. Unraveling the role of proteases in cancer. *Clin. Chim. Acta* **2000**, *291*, 113–135. [CrossRef]
- Ward, O.P. Proteases. *Compr. Biotechnol.* **2011**, *604–615*, 571–582.
- Twining, S.S. Regulation of Proteolytic Activity in Tissues. *Crit. Rev. Biochem. Mol. Biol.* **1994**, *29*, 315–383. [CrossRef]
- Noël, A.; Gilles, C.; Bajou, K.; Devy, L.; Kebers, F.; Lewalle, J.M.; Maquoui, E.; Munaut, C.; Remacle, A.; Foidart, J.M. Emerging roles for proteinases in cancer. *Invasion Metastasis* **1997**, *17*, 221–239.

30. Garcia-Carreón, F.L.; Toro, M.A.N.D. Classification of proteases without tears. *Biochem. Educ.* **1997**, *25*, 161–167. [CrossRef]
31. Otlewski, J.; Jelen, F.; Zakrzewska, M.; Oleksy, A. The many faces of protease–protein inhibitor interaction. *EMBO J.* **2005**, *24*, 1303–1310. [CrossRef]
32. Rawlings, N.D.; Tolle, D.P.; Barrett, A.J. Evolutionary families of peptidase inhibitors. *Biochem. J.* **2004**, *378*, 705–716. [CrossRef] [PubMed]
33. López-Otín, C.; Bond, J.S. Proteases: Multifunctional Enzymes in Life and Disease. *J. Biol. Chem.* **2008**, *283*, 30433–30437. [CrossRef] [PubMed]
34. Poreba, M.; Groborz, K.; Vizovisek, M.; Maruggi, M.; Turk, D.; Turk, B.; Powis, G.; Drag, M.; Salvesen, G.S. Fluorescent probes towards selective cathepsin B detection and visualization in cancer cells and patient samples. *Chem. Sci.* **2019**, *10*, 8461–8477. [CrossRef] [PubMed]
35. Mai, J.; Waisman, D.M.; Sloane, B.F. Cell surface complex of cathepsin B/annexin II tetramer in malignant progression. *Biochim. Biophys. Acta* **2000**, *1477*, 215–230. [CrossRef]
36. Buac, D.; Shen, M.; Schmitt, S.; Kona, F.R.; Deshmukh, R.; Zhang, Z.; Neslund-Dudas, C.; Mitra, B.; Dou, Q.P. From bortezomib to other inhibitors of the proteasome and beyond. *Curr. Pharm. Des.* **2013**, *19*, 4025–4038. [CrossRef]
37. Werner, A.B.; Tait, S.W.; de Vries, E.; Eldering, E.; Borst, J. Requirement for aspartate-cleaved bid in apoptosis signaling by DNA-damaging anti-cancer regimens. *J. Biol. Chem.* **2004**, *279*, 28771–28780. [CrossRef]
38. Eatemadi, A.; Aiyelabegan, H.T.; Negahdari, B.; Mazlomi, M.A.; Daraee, H.; Daraee, N.; Eatemadi, R.; Sadroddiny, E. Role of protease and protease inhibitors in cancer pathogenesis and treatment. *Biomed. Pharmacother.* **2017**, *86*, 221–231. [CrossRef]
39. Dastre: Fibrinolyse Dans le Sang—Google Scholar. Available online: https://scholar.google.com/scholar_lookup?title=Fibrinolyse%20dans%20le%20sang&author=A.%20Dastre&journal=Arch%20Physiol%20Norm%20Pathol&volume=5&pages=661-663&publication_year=1893 (accessed on 3 March 2021).
40. Longstaff, C.; Kolev, K. Basic mechanisms and regulation of fibrinolysis. *J. Thromb. Haemost.* **2015**, *13*, S98–S105. [CrossRef]
41. Yang, Z.; Mochalkin, I.; Doolittle, R.F. A model of fibrin formation based on crystal structures of fibrinogen and fibrin fragments complexed with synthetic peptides. *PNAS* **2000**, *97*, 14156–14161. [CrossRef]
42. Kwaan, H.C.; Lindholm, P.F. Fibrin and Fibrinolysis in Cancer. *Semin. Thromb. Hemost.* **2019**, *45*, 413–422. [CrossRef]
43. Saksela, O. Plasminogen activation and regulation of pericellular proteolysis. *Biochim. Biophys. Acta* **1985**, *823*, 35–65. [CrossRef]
44. Macfarlane, R.G.; Pilling, J. Observations on fibrinolysis plasminogen, plasmin, and antiplasmin content of human blood. *Lancet* **1946**, *248*, 562–565. [CrossRef]
45. Astrup, T.; Permin, P.M. Fibrinolysis in the Animal Organism. *Nature* **1947**, *159*, 681–682. [CrossRef]
46. Raum, D.; Marcus, D.; Alper, C.A.; Levey, R.; Taylor, P.D.; Starzl, T.E. Synthesis of human plasminogen by the liver. *Science* **1980**, *208*, 1036–1037. [CrossRef]
47. Romer, J.; Bugge, T.H.; Pyke, C.; Lund, L.R.; Flick, M.J.; Degen, J.L.; Danø, K. Impaired wound healing in mice with a disrupted plasminogen gene. *Nat. Med.* **1996**, *2*, 287–292. [CrossRef]
48. Declerck, P.J.; Gils, A. Three decades of research on plasminogen activator inhibitor-1: A multifaceted serpin. *Semin. Thromb. Hemost.* **2013**, *39*, 356–364.
49. Dear, A.E.; Medcalf, R.L. The cellular and molecular biology of plasminogen activator inhibitor type-2. *Fibrinolysis* **1995**, *9*, 321–330. [CrossRef]
50. Aoki, N. Discovery of alpha2-plasmin inhibitor and its congenital deficiency. *J. Thromb. Haemost.* **2005**, *3*, 623–631. [CrossRef]
51. Gallimore, M.J. More on: Discovery of alpha2-plasmin inhibitor and its congenital deficiency. *J. Thromb. Haemost.* **2006**, *4*, 284–285. [CrossRef]
52. De Boer, J.P.; Creasey, A.A.; Chang, A.; Abbink, J.J.; Roem, D.; Eerenberg, A.J. Alpha-2-macroglobulin functions as an inhibitor of fibrinolytic, clotting, and neutrophilic proteinases in sepsis: Studies using a baboon model. *Infect. Immun.* **1993**, *61*, 5035–5043. [CrossRef]
53. Bugge, T.H.; Lund, L.R.; Kombrinck, K.K.; Nielsen, B.S.; Holmbäck, K.; Drew, A.F.; Flick, M.J.; Witte, D.P.; Danø, K.; Degen, J.L. Reduced metastasis of Polyoma virus middle T antigen-induced mammary cancer in plasminogen-deficient mice. *Oncogene* **1998**, *16*, 3097–3104. [CrossRef]
54. Stoppelli, M.P. The Plasminogen Activation System in Cell Invasion. Madame Curie Bioscience Database. Landes Bioscience. 2013. Available online: <https://www.ncbi.nlm.nih.gov/books/NBK6146/> (accessed on 6 August 2020).
55. Miles, L.A.; Parmer, R.J. Plasminogen Receptors: The First Quarter Century. *Semin. Thromb. Hemost.* **2013**, *39*, 329–337.
56. Miles, L.A.; Ny, L.; Wilczynska, M.; Shen, Y.; Ny, T.; Parmer, R.J. Plasminogen Receptors and Fibrinolysis. *Int. J. Mol. Sci.* **2021**, *22*, 1712. [CrossRef]
57. Godier, A.; Hunt, B.J. Plasminogen receptors and their role in the pathogenesis of inflammatory, autoimmune and malignant disease. *J. Thromb. Haemost.* **2013**, *11*, 26–34. [CrossRef]
58. Ranson, M.; Andronicos, N.M. Plasminogen binding and cancer: Promises and pitfalls. *Front. Biosci.* **2003**, *8*, s294–s304. [CrossRef]
59. Forsgren, M.; Råden, B.; Israelsson, M.; Larsson, K.; Hedén, L.O. Molecular cloning and characterization of a full-length cDNA clone for human plasminogen. *FEBS Lett.* **1987**, *213*, 254–260. [CrossRef]
60. Castellino, F.J.; McCance, S.G. The kringle domains of human plasminogen. *Ciba Found. Symp.* **1997**, *212*, 46–60.

61. Robbins, K.C.; Bernabe, P.; Arzadon, L.; Summaria, L. The primary structure of human plasminogen. I. The NH₂-terminal sequences of human plasminogen and the S-carboxymethyl heavy (A) and light (B) chain derivatives of plasmin. *J. Biol. Chem.* **1972**, *247*, 6757–6762. [[CrossRef](#)]
62. Ponting, C.P.; Marshall, J.M.; Cederholm-Williams, S.A. Plasminogen: A structural review. *Blood Coagul. Fibrinolysis* **1992**, *3*, 605–614. [[CrossRef](#)]
63. Xue, Y.; Bodin, C.; Olsson, K. Crystal structure of the native plasminogen reveals an activation-resistant compact conformation. *J. Thromb. Haemost.* **2012**, *10*, 1385–1396. [[CrossRef](#)]
64. Law, R.H.; Caradoc-Davies, T.T.; Cowieson, N.; Horvath, A.J.; Quek, A.J.; Encarnacao, J.A.; Steer, D.; Cowan, A.; Zhang, Q.; Lu, B.G.; et al. The X-ray crystal structure of full-length human plasminogen. *Cell Rep.* **2012**, *1*, 185–190. [[CrossRef](#)] [[PubMed](#)]
65. Wallén, P.; Wiman, B. Characterization of human plasminogen: I. On the relationship between different molecular forms of plasminogen demonstrated in plasma and found in purified preparations. *Biochim. Biophys. Acta (BBA) Protein Struct.* **1970**, *221*, 20–30. [[CrossRef](#)]
66. Markus, G.; Priore, R.L.; Wissler, F.C. The binding of tranexamic acid to native (Glu) and modified (Lys) human plasminogen and its effect on conformation. *J. Biol. Chem.* **1979**, *254*, 1211–1216. [[CrossRef](#)]
67. Hoylaerts, M.; Rijken, D.C.; Lijnen, H.R.; Collen, D. Kinetics of the activation of plasminogen by human tissue plasminogen activator. Role of fibrin. *J. Biol. Chem.* **1982**, *257*, 2912–2919. [[CrossRef](#)]
68. The cell biology of the plasminogen system. Faseb, J. 1995. Available online: <https://faseb.onlinelibrary.wiley.com/doi/abs/10.1096/fasebj.9.10.7615163> (accessed on 6 August 2020).
69. Poddar, N.K.; Maurya, S.K.; Saxena, V. Role of Serine Proteases and Inhibitors in Cancer. In *Proteases in Physiology and Pathology*; Chakraborti, S., Dhalla, N.S., Eds.; Springer: Singapore, 2017; pp. 257–287. [[CrossRef](#)]
70. Fleury, V.; Anglés-Cano, E. Characterization of the binding of plasminogen to fibrin surfaces: The role of carboxy-terminal lysines. *Biochemistry* **1991**, *30*, 7630–7638. [[CrossRef](#)]
71. Miles, L.A.; Plow, E.F. Binding and activation of plasminogen on the platelet surface. *J. Biol. Chem.* **1985**, *260*, 4303–4311. [[CrossRef](#)]
72. Félez, J.; Miles, L.A.; Fábregas, P.; Jardí, M.; Plow, E.F.; Lijnen, R.H. Characterization of cellular binding sites and interactive regions within reactants required for enhancement of plasminogen activation by tPA on the surface of leukocytic cells. *Thromb. Haemost.* **1996**, *76*, 577–584. [[CrossRef](#)]
73. Plow, E.F.; Freaney, D.E.; Plescia, J.; Miles, L.A. The plasminogen system and cell surfaces: Evidence for plasminogen and urokinase receptors on the same cell type. *J. Cell Biol.* **1986**, *103*, 2411–2420. [[CrossRef](#)]
74. Ellis, V.; Behrendt, N.; Danø, K. Plasminogen activation by receptor-bound urokinase. A kinetic study with both cell-associated and isolated receptor. *J. Biol. Chem.* **1991**, *266*, 12752–12758. [[CrossRef](#)]
75. Kassam, G.; Le, B.-H.; Choi, K.-S.; Kang, H.-M.; Fitzpatrick, S.L.; Louie, P.; Waisman, D.M. The p11 subunit of the annexin II tetramer plays a key role in the stimulation of t-PA-dependent plasminogen activation. *Biochemistry* **1998**, *37*, 16958–16966. [[CrossRef](#)]
76. O'Reilly, M.S.; Holmgren, L.; Shing, Y.; Chen, C.; Rosenthal, R.A.; Moses, M.; Lane, W.S.; Cao, Y.; Sage, E.; Folkman, J. Angiostatin: A novel angiogenesis inhibitor that mediates the suppression of metastases by a Lewis lung carcinoma. *Cell* **1994**, *79*, 315–328. [[CrossRef](#)]
77. Geiger, J.H.; Cnudde, S.E. What the structure of angiostatin may tell us about its mechanism of action. *J. Thromb. Haemost.* **2004**, *2*, 23–34. [[CrossRef](#)]
78. Kwon, M.; Caplan, J.F.; Filipenko, N.R.; Choi, K.-S.; Fitzpatrick, S.L.; Zhang, L.; Waisman, D.M. Identification of annexin II heterotetramer as a plasmin reductase. *J. Biol. Chem.* **2002**, *277*, 10903–10911. [[CrossRef](#)]
79. Cao, Y.; Xue, L. Angiostatin. *Semin. Thromb. Hemost.* **2004**, *30*, 83–93.
80. Schmidt, A.; Echtermeyer, F.; Alozie, A.; Brands, K.; Buddecke, E. Plasmin- and thrombin-accelerated shedding of syndecan-4 ectodomain generates cleavage sites at Lys(114)-Arg(115) and Lys(129)-Val(130) bonds. *J. Biol. Chem.* **2005**, *280*, 34441–34446. [[CrossRef](#)]
81. Liotta, L.A.; Goldfarb, R.H.; Brundage, R.; Siegal, G.P.; Terranova, V.; Garbisa, S. Effect of plasminogen activator (urokinase), plasmin, and thrombin on glycoprotein and collagenous components of basement membrane. *Cancer Res.* **1981**, *41*, 4629–4636.
82. Tjwa, M.; Moura, R.; Moons, L.; Plaisance, S.; De Mol, M.; Jansen, S.; Dewerchin, M.; Verfaillie, C.; Carmeliet, P. Fibrinolysis-independent role of plasmin and its activators in the haematopoietic recovery after myeloablation. *J. Cell Mol. Med.* **2009**, *13*, 4587–4595. [[CrossRef](#)]
83. Gechtman, Z.; Sharma, R.; Kreizman, T.; Fridkin, M.; Shaltiel, S. Synthetic peptides derived from the sequence around the plasmin cleavage site In Vitronectin: Use in mapping the PAI-1 binding site. *FEBS Lett.* **1993**, *315*, 293–297. [[CrossRef](#)]
84. Andreassen, P.A.; Egelund, R.; Petersen, H.H. The plasminogen activation system in tumor growth, invasion, and metastasis. *CMLS Cell Mol. Life Sci.* **2000**, *57*, 25–40. [[CrossRef](#)]
85. Pedrozo, H.A.; Schwartz, Z.; Robinson, M.; Gomez, R.; Dean, D.D.; Bonewald, L.F.; Boyan, B.D. Potential Mechanisms for the Plasmin-Mediated Release and Activation of Latent Transforming Growth Factor- β 1 from the Extracellular Matrix of Growth Plate Chondrocytes. *Endocrinology* **1999**, *140*, 5806–5816. [[CrossRef](#)]
86. Matsuoka, H.; Sisson, T.H.; Nishiuma, T.; Simon, R.H. Plasminogen-mediated activation and release of hepatocyte growth factor from extracellular matrix. *Am. J. Respir. Cell Mol. Biol.* **2006**, *35*, 705–713. [[CrossRef](#)]

87. George, S.J.; Johnson, J.L.; Smith, M.A.; Jackson, C.L. Plasmin-mediated fibroblast growth factor-2 mobilisation supports smooth muscle cell proliferation in human saphenous vein. *J. Vasc. Res.* **2001**, *38*, 492–501. [[CrossRef](#)]
88. McColl, B.K.; Baldwin, M.; Roufai, S.; Freeman, C.; Alitalo, K.; A Stacker, S.; Achen, M.G. Plasmin activates VEGF-C and VEGF-D. *Int. Congr. Ser.* **2004**, *1262*, 79–82. [[CrossRef](#)]
89. Murphy, G.; Stanton, H.; Cowell, S.; Butler, G.; Knäuper, V.; Atkinson, S.; Gavrilovic, J. Mechanisms for pro matrix metalloproteinase activation. *APMIS* **1999**, *107*, 38–44. [[CrossRef](#)]
90. Carmo, A.A.F.; Costa, B.R.C.; Vago, J.P.; De Oliveira, L.C.; Tavares, L.P.; Nogueira, C.R.C.; Ribeiro, A.L.C.; Garcia, C.C.; Barbosa, A.S.; Brasil, B.S.A.F.; et al. Plasmin Induces In Vivo Monocyte Recruitment through Protease-Activated Receptor-1-, MEK/ERK-, and CCR2-Mediated Signaling. *J. Immunol.* **2014**, *193*, 3654–3663. [[CrossRef](#)]
91. Majumdar, M.; Tarui, T.; Shi, B.; Akakura, N.; Ruf, W.; Takada, Y. Plasmin-induced migration requires signaling through protease-activated receptor 1 and integrin alpha(9)beta(1). *J. Biol. Chem.* **2004**, *279*, 37528–37534. [[CrossRef](#)]
92. Burysek, L.; Syrovets, T.; Simmet, T. The serine protease plasmin triggers expression of MCP-1 and CD40 in human primary monocytes via activation of p38 MAPK and janus kinase (JAK)/STAT signaling pathways. *J. Biol. Chem.* **2002**, *277*, 33509–33517. [[CrossRef](#)]
93. Díaz, V.M.; Hurtado, M.; Kort, E.J.; Resnati, M.; Blasi, F.; Thomson, T.; Paciucci, R. Requirement of the enzymatic and signaling activities of plasmin for phorbol-ester-induced scattering of colon cancer cells. *Exp. Cell Res.* **2006**, *312*, 2203–2213. [[CrossRef](#)]
94. Tarui, T.; Majumdar, M.; Miles, L.; Ruf, W.; Takada, Y. Plasmin-induced Migration of Endothelial Cells. *J. Biol. Chem.* **2002**, *277*, 33564–33570. [[CrossRef](#)]
95. Pennica, D.; Holmes, W.E.; Kohr, W.J.; Harkins, R.N.; Vehar, G.A.; Ward, C.A.; Bennett, W.F.; Yelverton, E.; Seeburg, P.H.; Heyneker, H.L.; et al. Cloning and expression of human tissue-type plasminogen activator cDNA in *E. coli*. *Nature* **1983**, *301*, 214–221. [[CrossRef](#)]
96. Schaller, J.; Gerber, S.S. The plasmin–antiplasmin system: Structural and functional aspects. *Cell Mol. Life Sci.* **2011**, *68*, 785–801. [[CrossRef](#)] [[PubMed](#)]
97. De Vos, A.M.; Ultsch, M.H.; Kelley, R.F.; Padmanabhan, K.; Tulinsky, A.; Westbrook, M.L. Crystal structure of the kringle 2 domain of tissue plasminogen activator at 2.4-Å resolution. *Biochemistry* **1992**, *31*, 270–279. [[CrossRef](#)] [[PubMed](#)]
98. Hébert, M.; Lesept, F.; Vivien, D.; Macrez, R. The story of an exceptional serine protease, tissue-type plasminogen activator (tPA). *Rev. Neurol. Paris* **2016**, *172*, 186–197. [[CrossRef](#)] [[PubMed](#)]
99. Hajjar, K.A.; Jacovina, A.T.; Chacko, J.A. An endothelial cell receptor for plasminogen/tissue plasminogen activator. I. Identity with annexin II. *J. Biol. Chem.* **1994**, *269*, 21191–21197. [[CrossRef](#)]
100. Miller, V.A.; Madureira, P.A.; Kamaludin, A.A.; Komar, J.; Sharma, V.; Sahni, G.; Thelwell, C.; Longstaff, C.; Waisman, D.M. Mechanism of plasmin generation by S100A10. *Thromb. Haemost.* **2017**, *117*, 1058–1071. [[CrossRef](#)]
101. Kwon, M.; MacLeod, T.J.; Zhang, Y.; Waisman, D.M. S100A10, annexin A2, and annexin a2 heterotetramer as candidate plasminogen receptors. *Front. Biosci.* **2005**, *10*, 300–325. [[CrossRef](#)]
102. Kasai, S.; Arimura, H.; Nishida, M.; Suyama, T. Primary structure of single-chain pro-urokinase. *J. Biol. Chem.* **1985**, *260*, 12382–12389. [[CrossRef](#)]
103. Kobayashi, H.; Kanayama, N.; Schmitt, M.; Goretzki, L.; Chucholowski, N.; Calvete, J.; Kramer, M.; Günzler, W.A.; Jänicke, F.; Terao, T.; et al. Cathepsin B efficiently activates the soluble and the tumor cell receptor-bound form of the proenzyme urokinase-type plasminogen activator (Pro-uPA). *J. Biol. Chem.* **1991**, *266*, 5147–5152. [[CrossRef](#)]
104. Ichinose, A.; Fujikawa, K.; Suyama, T. The activation of pro-urokinase by plasma kallikrein and its inactivation by thrombin. *J. Biol. Chem.* **1986**, *261*, 3486–3489. [[CrossRef](#)]
105. Schmitt, M.; Goretzki, L.; Jänicke, F.; Calvete, J.; Eulitz, M.; Kobayashi, H.; Chucholowski, N.; Graeff, H. Biological and clinical relevance of the urokinase-type plasminogen activator (uPA) in breast cancer. *Biomed. Biochim. Acta* **1991**, *50*, 731–741.
106. Petersen, L.C.; Lund, L.R.; Nielsen, L.S.; Danø, K.; Skriver, L. One-chain urokinase-type plasminogen activator from human sarcoma cells is a proenzyme with little or no intrinsic activity. *J. Biol. Chem.* **1988**, *263*, 11189–11195. [[CrossRef](#)]
107. Stack, M.S.; Johnson, D.A. Human mast cell tryptase activates single-chain urinary-type plasminogen activator (pro-urokinase). *J. Biol. Chem.* **1994**, *269*, 9416–9419. [[CrossRef](#)]
108. Goretzki, L.; Schmitt, M.; Mann, K.; Calvete, J.; Chucholowski, N.; Kramer, M. Effective activation of the proenzyme form of the urokinase-type plasminogen activator (pro-uPA) by the cysteine protease cathepsin L. *FEBS Lett.* **1992**, *297*, 112–118. [[CrossRef](#)]
109. Wolf, B.B.; Vasudevan, J.; Henkin, J.; Gonias, S.L. Nerve growth factor-gamma activates soluble and receptor-bound single chain urokinase-type plasminogen activator. *J. Biol. Chem.* **1993**, *268*, 16327–16331. [[CrossRef](#)]
110. Cubellis, M.V.; Wun, T.C.; Blasi, F. Receptor-mediated internalization and degradation of urokinase is caused by its specific inhibitor PAI-1. *EMBO J.* **1990**, *9*, 1079–1085. [[CrossRef](#)]
111. Hall, S.W.; Humphries, J.E.; Gonias, S.L. Inhibition of cell surface receptor-bound plasmin by alpha 2-antiplasmin and alpha 2-macroglobulin. *J. Biol. Chem.* **1991**, *266*, 12329–12336. [[CrossRef](#)]
112. Ossowski, L.; Quigley, J.P.; Kellerman, G.M.; Reich, E. Fibrinolysis associated with oncogenic transformation. Requirement of plasminogen for correlated changes in cellular morphology, colony formation in agar, and cell migration. *J. Exp. Med.* **1973**, *138*, 1056–1064. [[CrossRef](#)]
113. Åstedt, B.; Holmberg, L. Immunological identity of urokinase and ovarian carcinoma plasminogen activator released in tissue culture. *Nature* **1976**, *261*, 595–597. [[CrossRef](#)]

114. Mahmood, N.; Mihalciou, C.; Rabbani, S.A. Multifaceted Role of the Urokinase-Type Plasminogen Activator (uPA) and Its Receptor (uPAR): Diagnostic, Prognostic, and Therapeutic Applications. *Front. Oncol.* **2018**, *8*, 24. [CrossRef]
115. Wei, Y.; Waltz, D.A.; Rao, N.; Drummond, R.J.; Rosenberg, S.; Chapman, H.A. Identification of the urokinase receptor as an adhesion receptor for vitronectin. *J. Biol. Chem.* **1994**, *269*, 32380–32388. [CrossRef]
116. Blasi, F.; Carmeliet, P. uPAR: A versatile signalling orchestrator. *Nat. Rev. Mol. Cell Biol.* **2002**, *3*, 932–943. [CrossRef]
117. Nguyen, D.H.; Hussaini, I.M.; Gonias, S.L. Binding of urokinase-type plasminogen activator to its receptor in MCF-7 cells activates extracellular signal-regulated kinase 1 and 2 which is required for increased cellular motility. *J. Biol. Chem.* **1998**, *273*, 8502–8507. [CrossRef]
118. Smith, H.W.; Marshall, C.J. Regulation of cell signalling by uPAR. *Nat. Rev. Mol. Cell Biol.* **2010**, *11*, 23–36. [CrossRef]
119. Montuori, N.; Visconte, V.; Rossi, G.; Ragno, P. Soluble and cleaved forms of the urokinase-receptor: Degradation products or active molecules? *Thromb. Haemost.* **2005**, *93*, 192–198. [CrossRef]
120. Mondino, A.; Blasi, F. uPA and uPAR in fibrinolysis, immunity and pathology. *Trends Immunol.* **2004**, *25*, 450–455. [CrossRef]
121. Amor, C.; Feucht, J.; Leibold, J.; Ho, Y.-J.; Zhu, C.; Alonso-Curbelo, D.; Mansilla-Soto, J.; Boyer, J.A.; Li, X.; Giavridis, T.; et al. Senolytic CAR T cells reverse senescence-associated pathologies. *Nature* **2020**, *583*, 127–132. [CrossRef]
122. Subramanian, R.; Gondi, C.S.; Lakka, S.S.; Jutla, A.; Rao, J.S. siRNA-mediated Simultaneous downregulation of uPA and its receptor inhibits angiogenesis and invasiveness triggering apoptosis in breast cancer cells. *Int. J. Oncol.* **2006**, *28*, 831–839. [CrossRef]
123. Kenny, H.A.; Leonhardt, P.; Ladanyi, A.; Yamada, S.D.; Montag, A.; Im, H.K.; Jagadeeswaran, S.; Shaw, D.E.; Mazar, A.P.; Lengyel, E. Targeting the Urokinase Plasminogen Activator Receptor Inhibits Ovarian Cancer Metastasis. *Clin. Cancer Res.* **2011**, *17*, 459–471. [CrossRef]
124. Dosne, A.M.; Dupuy, E.; Bodevin, E. Production of a fibrinolytic inhibitor by cultured endothelial cells derived from human umbilical vein. *Thromb. Res.* **1978**, *12*, 377–387. [CrossRef]
125. Loskutoff, D.J.; van Mourik, J.A.; Erickson, L.A.; Lawrence, D. Detection of an unusually stable fibrinolytic inhibitor produced by bovine endothelial cells. *Proc. Natl. Acad. Sci. USA* **1983**, *80*, 2956–2960. [CrossRef]
126. Ginsburg, D.; Zeheb, R.; Yang, A.Y.; Rafferty, U.M.; A Andreasen, P.; Nielsen, L.; Dano, K.; Lebo, R.V.; Gelehrter, T.D. cDNA cloning of human plasminogen activator-inhibitor from endothelial cells. *J. Clin. Investig.* **1986**, *78*, 1673–1680. [CrossRef] [PubMed]
127. Bajou, K.; Noel, A.; Gerard, R.D.; Masson, V.; Brunner, N.; Holsthansen, C.; Skobe, M.; E Fusenig, N.; Carmeliet, P.; Collen, D.; et al. Absence of host plasminogen activator inhibitor 1 prevents cancer invasion and vascularization. *Nat. Med.* **1998**, *4*, 923–928. [CrossRef]
128. Bajou, K.; Maillard, C.; Jost, M.; Lijnen, R.H.; Gils, A.; Declerck, P.; Carmeliet, P.; Foidart, J.-M.; Noël, A. Host-derived plasminogen activator inhibitor-1 (PAI-1) concentration is critical for In Vivo tumoral angiogenesis and growth. *Oncogene* **2004**, *23*, 6986–6990. [CrossRef] [PubMed]
129. Bajou, K.; Peng, H.; Laug, W.E.; Maillard, C.; Noel, A.; Foidart, J.M. Plasminogen Activator Inhibitor-1 Protects Endothelial Cells from FasL-Mediated Apoptosis. *Cancer Cell.* **2008**, *14*, 324–334. [CrossRef] [PubMed]
130. Balsara, R.D.; Ploplis, V.A. Plasminogen Activator Inhibitor-1: The Double Edged Sword in Apoptosis. *Thromb. Haemost.* **2008**, *100*, 1029–1036. [CrossRef] [PubMed]
131. Gutierrez, L.S.; Schulman, A.; Brito-Robinson, T.; Noria, F.; Ploplis, V.A.; Castellino, F.J. Tumor development is retarded in mice lacking the gene for urokinase-type plasminogen activator or its inhibitor, plasminogen activator inhibitor-1. *Cancer Res.* **2000**, *60*, 5839–5847. [PubMed]
132. Almholt, K.; Nielsen, B.S.; Frandsen, T.L.; Brünner, N.; Danø, K.; Johnsen, M. Metastasis of transgenic breast cancer in plasminogen activator inhibitor-1 gene-deficient mice. *Oncogene* **2003**, *22*, 4389–4397. [CrossRef]
133. Maillard, C.; Bouquet, C.; Petitjean, M.; Mestdagt, M.; Frau, E.; Jost, M.; Masset, A.; Opolon, P.; Beermann, F.; Abitbol, M.; et al. Reduction of brain metastases in plasminogen activator inhibitor-1-deficient mice with transgenic ocular tumors. *Carcinogenesis* **2008**, *29*, 2236–2242. [CrossRef]
134. Kubala, M.H.; DeClerck, Y.A. The Plasminogen Activator Inhibitor-1 Paradox in Cancer: A Mechanistic Understanding. *Cancer Metastasis Rev.* **2019**, *38*, 483–492. [CrossRef]
135. Isogai, C.; E Laug, W.; Shimada, H.; Declerck, P.J.; Stins, M.F.; Durden, D.L.; Erdreich-Epstein, A.; Declerck, Y. Plasminogen Activator Inhibitor-1 Promotes Angiogenesis by Stimulating Endothelial Cell Migration toward Fibronectin. *Cancer Res.* **2001**, *61*, 5587–5594.
136. Czekay, R.-P.; Wilkins-Port, C.E.; Higgins, S.P.; Freytag, J.; Overstreet, J.M.; Klein, R.M.; Higgins, C.E.; Samarakoon, R.; Higgins, P.J. PAI-1: An Integrator of Cell Signaling and Migration. *Int. J. Cell Biol.* **2011**, *2011*. Available online: <https://www.ncbi.nlm.nih.gov/pmc/articles/PMC3151495/> (accessed on 21 December 2020). [CrossRef]
137. Kubala, M.H.; Punj, V.; Placencio-Hickok, V.R.; Fang, H.; Fernandez, G.E.; Sposto, R.; DeClerck, Y.A. Plasminogen Activator Inhibitor-1 Promotes the Recruitment and Polarization of Macrophages in Cancer. *Cell Rep.* **2018**, *25*, 2177–2191.e7. [CrossRef]
138. Lee, J.A.; Yerbury, J.J.; Farrawell, N.; Shearer, R.F.; Constantinescu, P.; Hatters, D.M.; Schroder, W.A.; Suhrbier, A.; Wilson, M.R.; Saunders, D.N.; et al. SerpinB2 (PAI-2) Modulates Proteostasis via Binding Misfolded Proteins and Promotion of Cytoprotective Inclusion Formation. *PLoS ONE* **2015**, *10*, e0130136. [CrossRef]

139. Farrehi, P.M.; Ozaki, C.K.; Carmeliet, P.; Fay, W.P. Regulation of arterial thrombolysis by plasminogen activator inhibitor-1 in mice. *Circulation* **1998**, *97*, 1002–1008. [[CrossRef](#)]
140. Dougherty, K.M.; Pearson, J.M.; Yang, A.Y.; Westrick, R.J.; Baker, M.S.; Ginsburg, D. The plasminogen activator inhibitor-2 gene is not required for normal murine development or survival. *Proc. Natl. Acad. Sci. USA* **1999**, *96*, 686–691. [[CrossRef](#)]
141. Ritchie, H.; Robbie, L.A.; Kinghorn, S.; Exley, R.; Booth, N.A. Monocyte plasminogen activator inhibitor 2 (PAI-2) inhibits u-PA-mediated fibrin clot lysis and is cross-linked to fibrin. *Thromb. Haemost.* **1999**, *81*, 96–103.
142. Miles, L.A.; Dahlberg, C.M.; Plescia, J.; Felez, J.; Kato, K.; Plow, E.F. Role of cell-surface lysines in plasminogen binding to cells: Identification of alpha-enolase as a candidate plasminogen receptor. *Biochemistry* **1991**, *30*, 1682–1691. [[CrossRef](#)]
143. Romagnuolo, R.; Marcovina, S.M.; Boffa, M.B.; Koschinsky, M.L. Inhibition of plasminogen activation by apo(a): Role of carboxyl-terminal lysines and identification of inhibitory domains in apo(a). *J. Lipid Res.* **2014**, *55*, 625–634. [[CrossRef](#)]
144. Lenich, C.; Liu, J.-N.; Gurewich, V. Thrombin Stimulation of Platelets Induces Plasminogen Activation Mediated by Endogenous Urokinase-Type Plasminogen Activator. *Blood* **1997**, *90*, 3579–3586. [[CrossRef](#)]
145. Felez, J.; Chanquia, C.J.; Fabregas, P.; Plow, E.F.; Miles, L.A. Competition between plasminogen and tissue plasminogen activator for cellular binding sites. *Blood* **1993**, *82*, 2433–2441. [[CrossRef](#)]
146. Andronicos, N.M.; Ranson, M. The topology of plasminogen binding and activation on the surface of human breast cancer cells. *Br. J. Cancer* **2001**, *85*, 909–916. [[CrossRef](#)]
147. Das, R.; Burke, T.; Plow, E.F. Histone H2B as a functionally important plasminogen receptor on macrophages. *Blood* **2007**, *110*, 3763–3772. [[CrossRef](#)] [[PubMed](#)]
148. Herren, T.; Burke, T.A.; Das, R.; Plow, E.F. Identification of histone H2B as a regulated plasminogen receptor. *Biochemistry* **2006**, *45*, 9463–9474. [[CrossRef](#)] [[PubMed](#)]
149. Semov, A.; Moreno, M.J.; Onichtchenko, A.; Abulrob, A.; Ball, M.; Ekiel, I.; Pietrzynski, G.; Stanimirovic, D.; Alakhov, V. Metastasis-associated protein S100A4 induces angiogenesis through interaction with Annexin II and accelerated plasmin formation. *J. Biol. Chem.* **2005**, *280*, 20833–20841. [[CrossRef](#)] [[PubMed](#)]
150. Miles, L.A. *Identification of the Novel Plasminogen Receptor, Plg-RKT*; IntechOpen: London, UK, 2012.
151. Hawley, S.B.; Tamura, T.; Miles, L.A. Purification, Cloning, and Characterization of a Profibrinolytic Plasminogen-binding Protein, TIP49a. *J. Biol. Chem.* **2001**, *276*, 179–186. [[CrossRef](#)] [[PubMed](#)]
152. Gonias, S.L.; Hembrough, T.A.; Sankovic, M. Cytokeratin 8 functions as a major plasminogen receptor in select epithelial and carcinoma cells. *Front. Biosci.* **2001**, *6*, D1403–D1411. [[CrossRef](#)] [[PubMed](#)]
153. Gonzalez-Gronow, M.; Gomez, C.F.; de Ridder, G.G.; Ray, R.; Pizzo, S.V. Binding of tissue-type plasminogen activator to the glucose-regulated protein 78 (GRP78) modulates plasminogen activation and promotes human neuroblastoma cell proliferation In Vitro. *J. Biol. Chem.* **2014**, *289*, 25166–25176. [[CrossRef](#)] [[PubMed](#)]
154. Stillfried, G.E.; Saunders, D.N.; Ranson, M. Plasminogen binding and activation at the breast cancer cell surface: The integral role of urokinase activity. *Breast Cancer Res.* **2007**, *9*, R14. [[CrossRef](#)]
155. Ceruti, P.; Principe, M.; Capello, M.; Cappello, P.; Novelli, F. Three are better than one: Plasminogen receptors as cancer theranostic targets. *Exp. Hematol. Oncol.* **2013**, *2*, 12. [[CrossRef](#)]
156. Tanty, N.A.; Karyadi, A.S.; Rasman, S.Z.; Salim, M.R.G.; Devina, A.; Sumarpo, A. The prognostic value of S100A10 expression in cancer. *Oncol. Lett.* **2019**, *17*, 1417–1424. [[CrossRef](#)]
157. Bettum, I.J.; Vasiliaskaite, K.; Nygaard, V.; Clancy, T.; Pettersen, S.J.; Tenstad, E.; Mælandsmo, G.M.; Prasmickaite, L. Metastasis-associated protein S100A4 induces a network of inflammatory cytokines that activate stromal cells to acquire pro-tumorigenic properties. *Cancer Lett.* **2014**, *344*, 28–39. [[CrossRef](#)]
158. Klingelhöfer, J.; Grum-Schwensen, B.; Beck, M.K.; Knudsen, R.S.P.; Grigorian, M.; Lukanidin, E.; Ambartsumian, N. Anti-S100A4 Antibody Suppresses Metastasis Formation by Blocking Stroma Cell Invasion. *Neoplasia* **2012**, *14*, 1260–1268. [[CrossRef](#)]
159. Capello, M.; Ferri-Borgogno, S.; Cappello, P.; Novelli, F. α -Enolase: A promising therapeutic and diagnostic tumor target. *FEBS J.* **2011**, *278*, 1064–1074. [[CrossRef](#)]
160. Choi, K.-S.; Fitzpatrick, S.L.; Filipenko, N.R.; Fogg, D.K.; Kassam, G.; Magliocco, A.M.; Waisman, D.M. Regulation of plasmin-dependent fibrin clot lysis by annexin II heterotetramer. *J. Biol. Chem.* **2001**, *276*, 25212–25221. [[CrossRef](#)]
161. Seo, J.-S.; Svenningsson, P. Modulation of Ion Channels and Receptors by p11 (S100A10). *Trends Pharmacol. Sci.* **2020**, *41*, 487–497. [[CrossRef](#)]
162. Madureira, P.A.; O’Connell, P.A.; Surette, A.P.; Miller, V.A.; Waisman, D.M. The biochemistry and regulation of S100A10: A multifunctional plasminogen receptor involved in oncogenesis. *J. Biomed Biotechnol.* **2012**, *2012*, 353687. [[CrossRef](#)]
163. Munz, B.; Gerke, V.; Gillitzer, R.; Werner, S. Differential expression of the calpactin I subunits annexin II and p11 in cultured keratinocytes and during wound repair. *J. Invest. Dermatol.* **1997**, *108*, 307–312. [[CrossRef](#)]
164. Huang, X.-L.; Pawliczak, R.; Cowan, M.J.; Gladwin, M.T.; Madara, P.; Logun, C.; Shelhamer, J.H. Epidermal growth factor induces p11 gene and protein expression and down-regulates calcium ionophore-induced arachidonic acid release in human epithelial cells. *J. Biol. Chem.* **2002**, *277*, 38431–38440. [[CrossRef](#)]
165. Huang, X.; Pawliczak, R.; Yao, X.; Cowan, M.J.; Gladwin, M.T.; Walter, M.J. Interferon-gamma induces p11 gene and protein expression in human epithelial cells through interferon-gamma-activated sequences in the p11 promoter. *J. Biol. Chem.* **2003**, *278*, 9298–9308. [[CrossRef](#)]

166. Fang, Y.-T.; Lin, C.-F.; Wang, C.-Y.; Anderson, R.; Lin, Y.-S. Interferon- γ stimulates p11-dependent surface expression of annexin A2 in lung epithelial cells to enhance phagocytosis. *J. Cell Physiol.* **2012**, *227*, 2775–2787. [CrossRef]
167. Madureira, P.A.; Bharadwaj, A.G.; Bydoun, M.; Garant, K.; O'Connell, P.; Lee, P.; Waisman, D.M. Cell surface protease activation during RAS transformation: Critical role of the plasminogen receptor, S100A10. *Oncotarget* **2016**, *7*, 47720–47737. [CrossRef] [PubMed]
168. O'Connell, P.A.; Madureira, P.A.; Berman, J.N.; Liwski, R.S.; Waisman, D.M. Regulation of S100A10 by the PML-RAR- α oncoprotein. *Blood* **2011**, *117*, 4095–4105. [CrossRef] [PubMed]
169. Svenningsson, P.; Greengard, P. p11 (S100A10)—an inducible adaptor protein that modulates neuronal functions. *Curr. Opin. Pharmacol.* **2007**, *7*, 27–32. [CrossRef] [PubMed]
170. Warner-Schmidt, J.L.; Chen, E.Y.; Zhang, X.; Marshall, J.J.; Morozov, A.; Svenningsson, P.; Greengard, P. A role for p11 in the antidepressant action of brain-derived neurotrophic factor. *Biol. Psychiatry* **2010**, *68*, 528–535. [CrossRef] [PubMed]
171. Waisman, D.M. Annexin II tetramer: Structure and function. *Mol. Cell Biochem.* **1995**, *149–150*, 301–322. [CrossRef] [PubMed]
172. Bharadwaj, A.; Bydoun, M.; Holloway, R.; Waisman, D. Annexin A2 heterotetramer: Structure and function. *Int. J. Mol. Sci.* **2013**, *14*, 6259–6305. [CrossRef] [PubMed]
173. Thiel, C.; Osborn, M.; Gerke, V. The tight association of the tyrosine kinase substrate annexin II with the submembranous cytoskeleton depends on intact p11- and Ca(2+)-binding sites. *J. Cell Sci.* **1992**, *103*, 733–742.
174. He, K.-L.; Deora, A.B.; Xiong, H.; Ling, Q.; Weksler, B.B.; Niesvizky, R.; Hajjar, K.A. Endothelial cell annexin A2 regulates polyubiquitination and degradation of its binding partner S100A10/p11. *J. Biol. Chem.* **2008**, *283*, 19192–19200. [CrossRef]
175. He, K.-L.; Sui, G.; Xiong, H.; Broekman, M.J.; Huang, B.; Marcus, A.J.; Hajjar, K.A. Feedback regulation of endothelial cell surface plasmin generation by PKC-dependent phosphorylation of annexin A2. *J. Biol. Chem.* **2011**, *286*, 15428–15439. [CrossRef]
176. Puisieux, A.; Ji, J.; Ozturk, M. Annexin II up-regulates cellular levels of p11 protein by a post-translational mechanisms. *Biochem. J.* **1996**, *313*, 51–55. [CrossRef]
177. Wagner, S.A.; Beli, P.; Weinert, B.T.; Schölz, C.; Kelstrup, C.D.; Young, C.; Nielsen, M.L.; Olsen, J.V.; Brakebusch, C.; Choudhary, C. Proteomic analyses reveal divergent ubiquitylation site patterns in murine tissues. *Mol. Cell Proteom.* **2012**, *11*, 1578–1585. [CrossRef]
178. Holloway, R.W.; Thomas, M.L.; Cohen, A.M.; Bharadwaj, A.G.; Rahman, M.; Marcato, P.; Marignani, P.A.; Waisman, D.M. Regulation of cell surface protease receptor S100A10 by retinoic acid therapy in acute promyelocytic leukemia (APL) \star . *Cell Death Dis.* **2018**, *9*, 920. [CrossRef]
179. Moriya, H. Quantitative nature of overexpression experiments. *Mol. Biol. Cell.* **2015**, *26*, 3932–3939. [CrossRef]
180. Coux, O.; Tanaka, K.; Goldberg, A.L. Structure and functions of the 20S and 26S proteasomes. *Annu. Rev. Biochem.* **1996**, *65*, 801–847. [CrossRef]
181. Gladwin, M.T.; Yao, X.L.; Cowan, M.; Huang, X.L.; Schneider, R.; Grant, L.R.; Logun, C.; Shelhamer, J.H. Retinoic acid reduces p11 protein levels in bronchial epithelial cells by a posttranslational mechanism. *Am. J. Physiol. Lung Cell Mol. Physiol.* **2000**, *279*, L1103–L1109. [CrossRef]
182. Jie, Z.; Liang, Y.; Yi, P.; Tang, H.; Soong, L.; Cong, Y.; Zhang, K.; Sun, J. Retinoic Acid Regulates Immune Responses by Promoting IL-22 and Modulating S100 Proteins in Viral Hepatitis. *J. Immunol.* **2017**, *198*, 3448–3460. [CrossRef]
183. Lokman, N.A.; Ho, R.; Gunasegaran, K.; Bonner, W.M.; Oehler, M.K.; Ricciardelli, C. Anti-tumour effects of all-trans retinoid acid on serous ovarian cancer. *J. Exp. Clin. Cancer Res.* **2019**, *38*, 10. [CrossRef]
184. Johansson, H.J.; Sanchez, B.C.; Forshed, J.; Stål, O.; Fohlin, H.; Lewensohn, R.; Hall, P.; Bergh, J.; Lehtiö, J.; Linderholm, B.K. Proteomics profiling identify CAPS as a potential predictive marker of tamoxifen resistance in estrogen receptor positive breast cancer. *Clin. Proteom.* **2015**, *12*, 1–10. Available online: <https://www.ncbi.nlm.nih.gov/pmc/articles/PMC4389343/> (accessed on 25 December 2020). [CrossRef]
185. Wang, C.; Zhang, C.; Li, X.; Shen, J.; Xu, Y.; Shi, H.; Mu, X.; Pan, J.; Zhao, T.; Li, M.; et al. CPT1A-mediated succinylation of S100A10 increases human gastric cancer invasion. *J. Cell Mol. Med.* **2019**, *23*, 293–305. [CrossRef]
186. Balzi, E.; Choder, M.; Chen, W.N.; Varshavsky, A.; Goffeau, A. Cloning and functional analysis of the arginyl-tRNA-protein transferase gene ATE1 of *Saccharomyces cerevisiae*. *J. Biol. Chem.* **1990**, *265*, 7464–7471. [CrossRef]
187. Wong, C.C.L.; Xu, T.; Rai, R.; Bailey, A.O.; Yates, J.R.; Wolf, Y.I. Global Analysis of Posttranslational Protein Arginylation. *PLoS Biol.* **2007**, *5*, e258. [CrossRef] [PubMed]
188. Dongre, A.; Weinberg, R.A. New insights into the mechanisms of epithelial–mesenchymal transition and implications for cancer. *Nat. Rev. Mol. Cell Biol.* **2019**, *20*, 69–84. [CrossRef] [PubMed]
189. Thiery, J.P.; Acloque, H.; Huang, R.Y.J.; Nieto, M.A. Epithelial-mesenchymal transitions in development and disease. *Cell* **2009**, *139*, 871–890. [CrossRef] [PubMed]
190. Kalluri, R.; Weinberg, R.A. The basics of epithelial-mesenchymal transition. *J. Clin. Investig.* **2009**, *119*, 1420–1428. [CrossRef]
191. Wendt, M.K.; Allington, T.M.; Schiemann, W.P. Mechanisms of Epithelial-Mesenchymal Transition by TGF- β . *Future Oncol.* **2009**, *5*, 1145–1168. [CrossRef]
192. Gilles, C.; Newgreen, D.F.; Sato, H.; Thompson, E.W. Matrix Metalloproteases and Epithelial-to-Mesenchymal Transition: Implications for Carcinoma Metastasis. In *Madame Curie Bioscience Database*; Landes Bioscience: Austin, TX, USA, 2013. Available online: <https://www.ncbi.nlm.nih.gov/books/NBK6387/> (accessed on 2 March 2021).

193. Radisky, E.S.; Radisky, D.C. Matrix Metalloproteinase-Induced Epithelial-Mesenchymal Transition in Breast Cancer. *J. Mammary Gland Biol. Neoplasia* **2010**, *15*, 201–212. [CrossRef]
194. Scheau, C.; Badarau, I.A.; Costache, R.; Caruntu, C.; Mihai, G.L.; Didilescu, A.C.; Constantin, C.; Neagu, M. The Role of Matrix Metalloproteinases in the Epithelial-Mesenchymal Transition of Hepatocellular Carcinoma. *Anal. Cell. Pathol. Hindawi* **2019**, *2019*, e9423907. [CrossRef]
195. Bydoun, M.; Sterea, A.; Weaver, I.C.G.; Bharadwaj, A.G.; Waisman, D.M. A novel mechanism of plasminogen activation in epithelial and mesenchymal cells. *Sci. Rep.* **2018**, *8*, 14091. [CrossRef]
196. Zhang, S.; Wang, X.; Osunkoya, A.O.; Iqbal, S.; Wang, Y.A.; Chen, Z.; Müller, S.; Jossen, S.; Coleman, I.M.; Nelson, P.S.; et al. EPLIN Downregulation Promotes Epithelial-Mesenchymal Transition in Prostate Cancer Cells and Correlates With Clinical Lymph Node Metastasis. *Oncogene* **2011**, *30*, 4941–4952. [CrossRef]
197. Keshamouni, V.G.; Michailidis, G.; Grasso, C.S.; Anthwal, S.; Strahler, J.R.; Walker, A.; Arenberg, D.A.; Reddy, R.C.; Akulapalli, S.; Thannickal, V.J.; et al. Differential protein expression profiling by iTRAQ-2DLC-MS/MS of lung cancer cells undergoing epithelial-mesenchymal transition reveals a migratory/invasive phenotype. *J. Proteome Res.* **2006**, *5*, 1143–1154. [CrossRef]
198. Jo, M.; Lester, R.D.; Montel, V.; Eastman, B.; Takimoto, S.; Gonias, S.L. Reversibility of Epithelial-Mesenchymal Transition (EMT) Induced in Breast Cancer Cells by Activation of Urokinase Receptor-dependent Cell Signaling. *J. Biol. Chem.* **2009**, *284*, 22825–22833. [CrossRef]
199. Omori, K.; Hattori, N.; Senoo, T.; Takayama, Y.; Masuda, T.; Nakashima, T.; Iwamoto, H.; Fujitaka, K.; Hamada, H.; Kohno, N. Inhibition of Plasminogen Activator Inhibitor-1 Attenuates Transforming Growth Factor- β -Dependent Epithelial Mesenchymal Transition and Differentiation of Fibroblasts to Myofibroblasts. *PLoS ONE* **2016**, *11*, e0148969. [CrossRef]
200. Choi, K.; Fogg, D.K.; Yoon, C.; Waisman, D.M. P11 regulates extracellular plasmin production and invasiveness of HT1080 fibrosarcoma cells. *FASEB J.* **2003**, *17*, 235–246. [CrossRef]
201. Hajjar, K.A.; Mauri, L.; Jacovina, A.T.; Zhong, F.; Mirza, U.A.; Padovan, J.C.; Chait, B.T. Tissue plasminogen activator binding to the annexin II tail domain. Direct modulation by homocysteine. *J. Biol. Chem.* **1998**, *273*, 9987–9993. [CrossRef]
202. Phipps, K.D.; Surette, A.P.; O'Connell, P.A.; Waisman, D.M. Plasminogen receptor S100A10 is essential for the migration of tumor-promoting macrophages into tumor sites. *Cancer Res.* **2011**, *71*, 6676–6683. [CrossRef]
203. O'Connell, P.A.; Surette, A.P.; Liwski, R.S.; Svenningsson, P.; Waisman, D.M. S100A10 regulates plasminogen-dependent macrophage invasion. *Blood* **2010**, *116*, 1136–1146. [CrossRef]
204. Surette, A.P.; Madureira, P.A.; Phipps, K.D.; Miller, V.A.; Svenningsson, P.; Waisman, D.M. Regulation of fibrinolysis by S100A10 In Vivo. *Blood* **2011**, *118*, 3172–3181. [CrossRef]
205. Zhang, L.; Fogg, D.K.; Waisman, D.M. RNA interference-mediated silencing of the S100A10 gene attenuates plasmin generation and invasiveness of Colo 222 colorectal cancer cells. *J. Biol. Chem.* **2004**, *279*, 2053–2062. [CrossRef]
206. Lijnen, H.R. Plasmin and matrix metalloproteinases in vascular remodeling. *Thromb. Haemost.* **2001**, *86*, 324–333. [CrossRef]
207. Lou, Y.; Han, M.; Liu, H.; Niu, Y.; Liang, Y.; Guo, J.; Zhang, W.; Wang, H. Essential roles of S100A10 in Toll-like receptor signaling and immunity to infection. *Cell. Mol. Immunol.* **2020**, *17*, 1053–1062. [CrossRef]
208. Bydoun, M.; Sterea, A.; Liptay, H.; Uzans, A.; Huang, W.; Rodrigues, G.J.; Weaver, I.C.; Gu, H.; Waisman, D.M. S100A10, a novel biomarker in pancreatic ductal adenocarcinoma. *Mol. Oncol.* **2018**, *12*, 1895–1916. [CrossRef] [PubMed]
209. Wang, L.; Yan, W.; Li, X.; Liu, Z.; Tian, T.; Chen, T.; Zou, L.; Cui, Z. S100A10 silencing suppresses proliferation, migration and invasion of ovarian cancer cells and enhances sensitivity to carboplatin. *J. Ovarian Res.* **2019**, *12*, 113. [CrossRef] [PubMed]
210. Li, Y.; Li, X.-Y.; Li, L.-X.; Zhou, R.-C.; Sikong, Y.; Gu, X. S100A10 Accelerates Aerobic Glycolysis and Malignant Growth by Activating mTOR-Signaling Pathway in Gastric Cancer. *Front. Cell Dev. Biol.* **2020**. Available online: <https://www.frontiersin.org/articles/10.3389/fcell.2020.559486/full> (accessed on 22 December 2020). [CrossRef] [PubMed]
211. Yanagi, H.; Watanabe, T.; Nishimura, T.; Hayashi, T.; Kono, S.; Tsuchida, H.; Hirata, M.; Kijima, Y.; Takao, S.; Okada, S.; et al. Upregulation of S100A10 in metastasized breast cancer stem cells. *Cancer Sci.* **2020**, *111*, 4359–4370. [CrossRef]
212. Lu, H.; Xie, Y.; Tran, L.; Lan, J.; Yang, Y.; Murugan, N.L.; Wang, R.; Wang, Y.J.; Semenza, G.L. Chemotherapy-induced S100A10 recruits KDM6A to facilitate OCT4-mediated breast cancer stemness. *J. Clin. Investig.* **2020**, *130*, 4607–4623. [CrossRef]
213. Santibanez, J.F.; Krstic, J. Transforming Growth Factor-Beta and Urokinase Type Plasminogen Interplay in Cancer. *Curr. Protein Pept. Sci.* **2018**, *19*, 1155–1163. [CrossRef]
214. Santibanez, J.F. *Transforming Growth Factor-Beta and Urokinase-Type Plasminogen Activator: Dangerous Partners in Tumorigenesis—Implications in Skin Cancer*; ISRN Dermatology; Hindawi: London, UK, 2013; Volume 2013, p. e597927. Available online: <https://www.hindawi.com/journals/isrn/2013/597927/> (accessed on 22 December 2020).
215. Qun, L.; Yves, L.; Tatiana, S.; Thomas, S. Plasmin Triggers Cytokine Induction in Human Monocyte-Derived Macrophages. *Arterioscler. Thromb. Vasc. Biol.* **2007**, *27*, 1383–1389.
216. Laumonier, Y.; Syrovets, T.; Burysek, L.; Simmet, T. Identification of the annexin A2 heterotetramer as a receptor for the plasmin-induced signaling in human peripheral monocytes. *Blood* **2006**, *107*, 3342–3349. [CrossRef]
217. Lorenz, N.; Loef, E.J.; Kelch, I.D.; Verdon, D.J.; Black, M.M.; Middleditch, M.J.; Greenwood, D.R.; Graham, E.S.; Brooks, A.E.; Dunbar, P.R.; et al. Plasmin and regulators of plasmin activity control the migratory capacity and adhesion of human T cells and dendritic cells by regulating cleavage of the chemokine CCL21. *Immunol. Cell Biol.* **2016**, *94*, 955–963. [CrossRef]







218. Li, X.; Syrovets, T.; Genze, F.; Pitterle, K.; Oberhuber, A.; Orend, K.-H.; Simmet, T. Plasmin triggers chemotaxis of monocyte-derived dendritic cells through an Akt2-dependent pathway and promotes a T-helper type-1 response. *Arterioscler. Thromb. Vasc. Biol.* **2010**, *30*, 582–590. [[CrossRef](#)]
219. Whiteside, T.L. The role of immune cells in the tumor microenvironment. *Cancer Treat. Res.* **2006**, *130*, 103–124.
220. Ploplis, V.A.; French, E.L.; Carmeliet, P.; Collen, D.; Plow, E.F. Plasminogen deficiency differentially affects recruitment of inflammatory cell populations in mice. *Blood* **1998**, *91*, 2005–2009. [[CrossRef](#)]
221. Silva, L.M.; Lum, A.G.; Tran, C.; Shaw, M.W.; Gao, Z.; Flick, M.J.; Moutsopoulos, N.M.; Bugge, T.H.; Mullins, E.S. Plasmin-mediated fibrinolysis enables macrophage migration in a murine model of inflammation. *Blood* **2019**, *134*, 291–303. [[CrossRef](#)]
222. Das, R.; Ganapathy, S.; Settle, M.; Plow, E.F. Plasminogen promotes macrophage phagocytosis in mice. *Blood* **2014**, *124*, 679–688. [[CrossRef](#)]
223. Wygrecka, M.; Marsh, L.M.; Morty, R.E.; Henneke, I.; Guenther, A.; Lohmeyer, J.; Markart, P.; Preissner, K.T. Enolase-1 promotes plasminogen-mediated recruitment of monocytes to the acutely inflamed lung. *Blood* **2009**, *113*, 5588–5598. [[CrossRef](#)]
224. Miles, L.A.; Lighvani, S.; Baik, N.; Parmer, C.M.; Khaldoyanidi, S.; Mueller, B.M.; Parmer, R.J. New insights into the role of Plg-RKT in macrophage recruitment. *Int. Rev. Cell Mol. Biol.* **2014**, *309*, 259–302.
225. Andronicos, N.M.; Chen, E.I.; Baik, N.; Bai, H.; Parmer, C.M.; Kiosses, W.B.; Kamps, M.P.; Yates, J.R.; Parmer, R.J.; Miles, L.A. Proteomics-based discovery of a novel, structurally unique, and developmentally regulated plasminogen receptor, Plg-RKT; a major regulator of cell surface plasminogen activation. *Blood* **2010**, *115*, 1319–1330. [[CrossRef](#)]
226. Bharadwaj, A.G.; Dahn, M.L.; Liu, R.-Z.; Colp, P.; Thomas, L.N.; Holloway, R.W. S100A10 Has a Critical Regulatory Function in Mammary Tumor Growth and Metastasis: Insights Using MMTV-PyMT Oncomice and Clinical Patient Sample Analysis. *Cancers* **2020**, *7*, 12.
227. Fata, J.E.; Werb, Z.; Bissell, M.J. Regulation of mammary gland branching morphogenesis by the extracellular matrix and its remodeling enzymes. *Breast Cancer Res.* **2004**, *6*, 1–11. [[CrossRef](#)]
228. Green, K.A.; Nielsen, B.S.; Castellino, F.J.; Rømer, J.; Lund, L.R. Lack of plasminogen leads to milk stasis and premature mammary gland involution during lactation. *Dev. Biol.* **2006**, *299*, 164–175. [[CrossRef](#)]
229. Kawao, N.; Nagai, N.; Tamura, Y.; Horiuchi, Y.; Okumoto, K.; Okada, K.; Suzuki, Y.; Umemura, K.; Yano, M.; Ueshima, S.; et al. Urokinase-type plasminogen activator and plasminogen mediate activation of macrophage phagocytosis during liver repair In Vivo. *Thromb. Haemost.* **2012**, *107*, 749–759. [[CrossRef](#)]
230. Rosenwald, M.; Koppe, U.; Keppeler, H.; Sauer, G.; Hennel, R.; Ernst, A.; Blume, K.E.; Peter, C.; Herrmann, M.; Belka, C.; et al. Serum-Derived Plasminogen Is Activated by Apoptotic Cells and Promotes Their Phagocytic Clearance. *J. Immunol.* **2012**, *189*, 5722–5728. [[CrossRef](#)]
231. Kobayashi, H.; Gotoh, J.; Fujie, M.; Shinohara, H.; Moniwa, N.; Terao, T. Inhibition of metastasis of Lewis lung carcinoma by a synthetic peptide within growth factor-like domain of urokinase in the experimental and spontaneous metastasis model. *Int. J. Cancer* **1994**, *57*, 727–733. [[CrossRef](#)]
232. Min, H.Y.; Doyle, L.V.; Vitt, C.R.; Zandonella, C.L.; Stratton-Thomas, J.R.; A Shuman, M.; Rosenberg, S. Urokinase receptor antagonists inhibit angiogenesis and primary tumor growth in syngeneic mice. *Cancer Res.* **1996**, *56*, 2428–2433.
233. Mueller, B.M.; Yu, Y.B.; Laug, W.E. Overexpression of plasminogen activator inhibitor 2 in human melanoma cells inhibits spontaneous metastasis in scid/scid mice. *Proc. Natl. Acad. Sci. USA* **1995**, *92*, 205–209. [[CrossRef](#)]
234. Ossowski, L.; Reich, E. Antibodies to plasminogen activator inhibit human tumor metastasis. *Cell* **1983**, *35*, 611–619. [[CrossRef](#)]
235. Kook, Y.H.; Adamski, J.; Zelent, A.; Ossowski, L. The effect of antisense inhibition of urokinase receptor in human squamous cell carcinoma on malignancy. *EMBO J.* **1994**, *13*, 3983–3991. [[CrossRef](#)]
236. Yu, H.; Schultz, R.M. Relationship between Secreted Urokinase Plasminogen Activator Activity and Metastatic Potential in Murine B16 Cells Transfected with Human Urokinase Sense and Antisense Genes. *Cancer Res.* **1990**, *50*, 7623–7633.
237. Crowley, C.W.; Cohen, R.L.; Lucas, B.K.; Liu, G.; Shuman, M.A.; Levinson, A.D. Prevention of metastasis by inhibition of the urokinase receptor. *Proc. Natl. Acad. Sci. USA* **1993**, *90*, 5021–5025. [[CrossRef](#)]
238. Almholt, K.; Green, K.A.; Juncker-Jensen, A.; Nielsen, B.S.; Lund, L.R.; Rømer, J. Extracellular proteolysis in transgenic mouse models of breast cancer. *J. Mammary Gland Biol. Neoplasia* **2007**, *12*, 83–97. [[CrossRef](#)]
239. Nielsen, B.S.; Sehested, M.; Duun, S.; Rank, F.; Timshel, S.; Rygaard, J.; Johnsen, M.; Danø, K. Urokinase plasminogen activator is localized in stromal cells in ductal breast cancer. *Lab. Invest.* **2001**, *81*, 1485–1501. [[CrossRef](#)] [[PubMed](#)]
240. Pyke, C.; Graem, N.; Ralfkiaer, E.; Rønne, E.; Høyer-Hansen, G.; Brünner, N.; Danø, K. Receptor for Urokinase Is Present in Tumor-associated Macrophages in Ductal Breast Carcinoma. *Cancer Res.* **1993**, *53*, 1911–1915. [[PubMed](#)]
241. Offersen, B.V.; Nielsen, B.S.; Høyer-Hansen, G.; Rank, F.; Hamilton-Dutoit, S.; Overgaard, J.; Andreasen, P.A. The myofibroblast is the predominant plasminogen activator inhibitor-1-expressing cell type in human breast carcinomas. *Am. J. Pathol.* **2003**, *163*, 1887–1899. [[CrossRef](#)]
242. Almholt, K.; Juncker-Jensen, A.; Lærum, O.D.; Johnsen, M.; Rømer, J.; Lund, L.R. Spontaneous metastasis in congenic mice with transgenic breast cancer is unaffected by plasminogen gene ablation. *Clin. Exp. Metastasis* **2013**, *30*, 277–288. [[CrossRef](#)]
243. Shapiro, R.L.; Duquette, J.G.; Roses, D.F.; Nunes, I.; Harris, M.N.; Kamino, H. Induction of primary cutaneous melanocytic neoplasms in urokinase-type plasminogen activator (uPA)-deficient and wild-type mice: Cellular blue nevi invade but do not progress to malignant melanoma in uPA-deficient animals. *Cancer Res.* **1996**, *56*, 3597–3604.

244. Bergers, G.; A Brekken, R.; McMahon, G.; Vu, T.H.; Itoh, T.; Tamaki, K.; Tanzawa, K.; E Thorpe, P.; Itohara, S.; Werb, Z.; et al. Matrix metalloproteinase-9 triggers the angiogenic switch during carcinogenesis. *Nat. Cell Biol.* **2000**, *2*, 737–744. [CrossRef]
245. Grum-Schwensen, B.; Klingelhöfer, J.; Grigorian, M.; Almholt, K.; Nielsen, B.S.; Lukanidin, E. Lung Metastasis Fails in MMTV-PyMT Oncomice Lacking S100A4 Due to a T-Cell Deficiency in Primary Tumors. *Cancer Res.* **2010**, *26*, 936–947. Available online: <https://cancerres.aacrjournals.org/content/early/2010/01/26/0008-5472.CAN-09-3220> (accessed on 25 December 2020). [CrossRef]
246. Waks, A.G.; Winer, E.P. Breast Cancer Treatment: A Review. *JAMA* **2019**, *321*, 288–300. [CrossRef]
247. Chang, M. Tamoxifen Resistance in Breast Cancer. *Biomol. Ther.* **2012**, *20*, 256–267. [CrossRef]
248. Foekens, J.A.; Look, M.P.; Peters, H.A.; van Putten, W.L.; Portengen, H.; Klijn, J.G. Urokinase-type plasminogen activator and its inhibitor PAI-1: Predictors of poor response to tamoxifen therapy in recurrent breast cancer. *J. Natl. Cancer Instig.* **1995**, *87*, 751–756. [CrossRef]
249. Gelder, M.E.M.; Look, M.P.; Peters, H.A.; Schmitt, M.; Brünner, N.; Harbeck, N. Urokinase-Type Plasminogen Activator System in Breast Cancer: Association with Tamoxifen Therapy in Recurrent Disease. *Cancer Res.* **2004**, *64*, 4563–4568. [CrossRef]
250. Bukowski, K.; Kciuk, M.; Kontek, R. Mechanisms of Multidrug Resistance in Cancer Chemotherapy. *Int. J. Mol. Sci.* **2020**, *21*, 3233. [CrossRef]
251. Ji, X.; Lu, Y.; Tian, H.; Meng, X.; Wei, M.; Cho, W.C. Chemoresistance mechanisms of breast cancer and their countermeasures. *Biomed. Pharmacother.* **2019**, *114*, 108800. [CrossRef]
252. Zhou, C.; Zhong, Q.; Rhodes, L.V.; Townley, I.; Bratton, M.R.; Zhang, Q.; Martin, E.C.; Elliott, S.; Collins-Burow, B.M.; E Burow, M.; et al. Proteomic analysis of acquired tamoxifen resistance in MCF-7 cells reveals expression signatures associated with enhanced migration. *Breast Cancer Res.* **2012**, *14*, R45. [CrossRef]
253. Suzuki, S.; Tanigawara, Y. Forced expression of S100A10 reduces sensitivity to oxaliplatin in colorectal cancer cells. *Proteome Sci.* **2014**, *12*, 26. [CrossRef]
254. Gopalakrishnapillai, A.; Kolb, E.A.; Dhanan, P.; Mason, R.W.; Napper, A.; Barwe, S.P. Disruption of Annexin II /p11 Interaction Suppresses Leukemia Cell Binding, Homing and Engraftment, and Sensitizes the Leukemia Cells to Chemotherapy. *PLoS ONE* **2015**, *10*, e0140564. [CrossRef]
255. Gillet, J.-P.; Calcagno, A.M.; Varma, S.; Davidson, B.; Elstrand, M.B.; Ganapathi, R.; Kamat, A.A.; Sood, A.K.; Ambudkar, S.V.; Seiden, M.V.; et al. Multidrug Resistance-Linked Gene Signature Predicts Overall Survival of Patients with Primary Ovarian Serous Carcinoma. *Clin. Cancer Res.* **2012**, *18*, 3197–3206. [CrossRef]
256. Duffy, M.J.; Crown, J. A Personalized Approach to Cancer Treatment: How Biomarkers Can Help. *Clin. Chem.* **2008**, *54*, 1770–1779. [CrossRef]
257. McMahon, B.J.; Kwaan, H.C. Components of the Plasminogen-Plasmin System as Biologic Markers for Cancer. In *Advances in Cancer Biomarkers: From Biochemistry to Clinic for a Critical Revision Advances in Experimental Medicine and Biology*; Scatena, R., Ed.; Springer: Dordrecht, The Netherlands, 2015; pp. 145–156. [CrossRef]
258. Duffy, M.J.; Duggan, C.; Mulcahy, H.E.; McDermott, E.W.; O’Higgins, N.J. Urokinase plasminogen activator: A prognostic marker in breast cancer including patients with axillary node-negative disease. *Clin. Chem.* **1998**, *44*, 1177–1183. [CrossRef]
259. Kirchheimer, J.C.; Pflüger, H.; Ritschl, P.; Hienert, G.; Binder, B.R. Plasminogen activator activity in bone metastases of prostatic carcinomas as compared to primary tumors. *Invasion Metastasis* **1985**, *5*, 344–355.
260. Stephens, R.W.; Nielsen, H.J.; Christensen, I.J.; Thorlacius-Ussing, O.; Sørensen, S.; Danø, K.; Brunner, N. Plasma urokinase receptor levels in patients with colorectal cancer: Relationship to prognosis. *J. Natl. Cancer Instig.* **1999**, *91*, 869–874. [CrossRef] [PubMed]
261. Skelly, M.M.; Troy, A.; Duffy, M.J.; E Mulcahy, H.; Duggan, C.; Connell, T.G.; O’Donoghue, D.P.; Sheahan, K. Urokinase-type plasminogen activator in colorectal cancer: Relationship with clinicopathological features and patient outcome. *Clin. Cancer Res.* **1997**, *3*, 1837–1840. [PubMed]
262. Ganesh, S.; Sier, C.F.; Heerding, M.M.; Griffioen, G.; Lamers, C.B.; Verspaget, H.W. Urokinase receptor and colorectal cancer survival. *Lancet* **1994**, *344*, 401–402. [CrossRef]
263. Takeuchi, Y.; Nakao, A.; Harada, A.; Nonami, T.; Fukatsu, T.; Takagi, H. Expression of plasminogen activators and their inhibitors in human pancreatic carcinoma: Immunohistochemical study. *Am. J. Gastroenterol.* **1993**, *88*, 1928–1933. [PubMed]
264. Landau, B.J.; Kwaan, H.C.; Verrusio, E.N.; Brem, S.S. Elevated levels of urokinase-type plasminogen activator and plasminogen activator inhibitor type-1 in malignant human brain tumors. *Cancer Res.* **1994**, *54*, 1105–1108. [CrossRef]
265. Hofmann, R.; Lehmer, A.; Buresch, M.; Hartung, R.; Ulm, K. Clinical relevance of urokinase plasminogen activator, its receptor, and its inhibitor in patients with renal cell carcinoma. *Cancer* **1996**, *78*, 487–492. [CrossRef]
266. Swiercz, R.; Wolfe, J.D.; Zaher, A.; Jankun, J. Expression of the plasminogen activation system in kidney cancer correlates with its aggressive phenotype. *Clin. Cancer Res.* **1998**, *4*, 869–877.
267. Miyake, H.; Hara, I.; Yamanaka, K.; Gohji, K.; Arakawa, S.; Kamidono, S. Elevation of serum levels of urokinase-type plasminogen activator and its receptor is associated with disease progression and prognosis in patients with prostate cancer. *Prostate* **1999**, *39*, 123–129. [CrossRef]
268. Hienert, G.; Kirchheimer, J.C.; Pflüger, H.; Binder, B.R. Urokinase-type plasminogen activator as a marker for the formation of distant metastases in prostatic carcinomas. *J. Urol.* **1988**, *140*, 1466–1469. [CrossRef]

269. Pavey, S.J.; Hawson, G.A.; Marsh, N.A. Impact of the fibrinolytic enzyme system on prognosis and survival associated with non-small cell lung carcinoma. *Blood Coagul. Fibrinolysis* **2001**, *12*, 51–58. [CrossRef]
270. Kobayashi, H.; Fujishiro, S.; Terao, T. Impact of urokinase-type plasminogen activator and its inhibitor type 1 on prognosis in cervical cancer of the uterus. *Cancer Res.* **1994**, *54*, 6539–6548.
271. Kuhn, W.; Schmalfeldt, B.; Reuning, U.; Pache, L.; Berger, U.; Ulm, K.; Harbeck, N.; Späthe, K.; Dettmar, P.; Höfler, H.; et al. Prognostic significance of urokinase (uPA) and its inhibitor PAI-1 for survival in advanced ovarian carcinoma stage FIGO IIIc. *Br. J. Cancer* **1999**, *79*, 1746–1751. [CrossRef]
272. Torzewski, M.; Sarbia, M.; Verreet, P.; Dutkowski, P.; Heep, H.; Willers, R.; Gabbert, H. Prognostic significance of urokinase-type plasminogen activator expression in squamous cell carcinomas of the esophagus. *Clin. Cancer Res.* **1997**, *3*, 2263–2268.
273. De Petro, G.; Taviani, D.; Copeta, A.; Portolani, N.; Giulini, S.M.; Barlati, S. Expression of urokinase-type plasminogen activator (u-PA), u-PA receptor, and tissue-type PA messenger RNAs in human hepatocellular carcinoma. *Cancer Res.* **1998**, *58*, 2234–2239.
274. Nekarda, H.; Schmitt, M.; Ulm, K.; Wenninger, A.; Vogelsang, H.; Becker, K.; Roder, J.D.; Fink, U.; Siewert, J.R. Prognostic impact of urokinase-type plasminogen activator and its inhibitor PAI-1 in completely resected gastric cancer. *Cancer Res.* **1994**, *54*, 2900–2907.
275. Duffy, M.J.; McGowan, P.M.; Harbeck, N.; Thomssen, C.; Schmitt, M. uPA and PAI-1 as biomarkers in breast cancer: Validated for clinical use in level-of-evidence-1 studies. *Breast Cancer Res.* **2014**, *16*, 428. [CrossRef]
276. Noye, T.; Lokman, N.; Oehler, M.; Ricciardelli, C. S100A10 in Cancer Progression and Chemotherapy Resistance: A Novel Therapeutic Target Against Ovarian Cancer. 2018. Available online: <https://www.preprints.org/manuscript/201810.0318/v1> (accessed on 25 December 2020).
277. Noye, T.M.; Lokman, N.A.; Oehler, M.K.; Ricciardelli, C. S100A10 and Cancer Hallmarks: Structure, Functions, and its Emerging Role in Ovarian Cancer. *Int. J. Mol. Sci.* **2018**, *1*, 4122. Available online: <https://www.ncbi.nlm.nih.gov/pmc/articles/PMC6321037/> (accessed on 18 February 2021). [CrossRef]
278. Carlsson, H.; Petersson, S.; Enerbäck, C. Cluster analysis of S100 gene expression and genes correlating to psoriasin (S100A7) expression at different stages of breast cancer development. *Int. J. Oncol.* **2005**, *27*, 1473–1481.
279. Yu, M.; Bardia, A.; Wittner, B.S.; Stott, S.L.; Smas, M.E.; Ting, D.T.; Isakoff, S.J.; Ciciliano, J.C.; Wells, M.N.; Shah, A.M.; et al. Circulating breast tumor cells exhibit dynamic changes in epithelial and mesenchymal composition. *Science* **2013**, *339*, 580–584. [CrossRef]
280. Zhang, S.; Wang, Z.; Liu, W.; Lei, R.; Shan, J.; Li, L.; Wang, X. Distinct prognostic values of S100 mRNA expression in breast cancer. *Sci. Rep.* **2017**, *7*, 39786. [CrossRef]
281. Arai, K.; Iwasaki, T.; Sonoda, A.; Endo, A. Membranous overexpression of S100A10 is associated with a high-grade cellular status of breast carcinoma. *Med. Mol. Morphol.* **2020**, *53*, 104–114. [CrossRef]

Article

S100A10 Has a Critical Regulatory Function in Mammary Tumor Growth and Metastasis: Insights Using MMTV-PyMT Oncomice and Clinical Patient Sample Analysis

Alamelu G. Bharadwaj ¹, Margaret L. Dahn ¹ , Rong-Zong Liu ² , Patricia Colp ¹, Lynn N. Thomas ³, Ryan W. Holloway ³, Paola A. Marignani ³ , Catherine K. L. Too ³, Penelope J. Barnes ¹ , Roseline Godbout ² , Paola Marcato ^{1,4}  and David M. Waisman ^{1,3,*}

¹ Department of Pathology, Dalhousie University, Halifax, NS B3H 4R2, Canada; Alamelu.Bharadwaj@dal.ca (A.G.B.); meg.thomas@dal.ca (M.L.D.); p.colp@dal.ca (P.C.); penny.barnesmd@nshealth.ca (P.J.B.); paola.marcato@dal.ca (P.M.)

² Department of Oncology, University of Alberta, Edmonton, AB T6G 2Z1, Canada; rongzong@ualberta.ca (R.-Z.L.); rgodbout@ualberta.ca (R.G.)

³ Department of Biochemistry & Molecular Biology, Dalhousie University, Halifax, NS B3H 4R2, Canada; Lynn.Thomas@Dal.Ca (L.N.T.); Ryan.W.Holloway@Dal.Ca (R.W.H.); paola.marignani@dal.ca (P.A.M.); catherine.too@dal.ca (C.K.L.T.)

⁴ Department of Microbiology and Immunology, Dalhousie University, NS B3H 4R2, Canada

* Correspondence: David.Waisman@dal.ca

Received: 30 September 2020; Accepted: 4 December 2020; Published: 7 December 2020



Simple Summary: The key challenges that face patients during breast cancer therapy is the metastatic spread and aggressiveness of the disease. Thus, the goal of current breast cancer research is to discover new therapeutic and diagnostic targets that limit the aggressive spread of the cancer. In this study, we investigated the role of protein S100A10 (p11) in breast tumor growth, progression, and metastasis using mouse cancer models and patient tumor sample analysis. We have demonstrated in our previous studies that p11 is critical for the function of a proteolytic enzyme–plasmin, which aids in the digestion of the tissues surrounding the tumor and allows the escape of the cancer cells from the breast tissue to organs such as the lungs and bone. Here, we present evidence that genetic deletion of p11 results in smaller and less aggressive mammary tumors in mice. We also observed that the cancer spread to the lungs is dramatically reduced in the absence of p11 gene in mice. Subsequent analysis of breast cancer patient tissues showed a correlation between higher p11 expression and both poor survival and aggressive cancer.

Abstract: S100A10 (p11) is a plasminogen receptor that regulates cellular plasmin generation by cancer cells. In the current study, we used the MMTV-PyMT mouse breast cancer model, patient tumor microarray, and immunohistochemical (IHC) analysis to investigate the role of p11 in oncogenesis. The genetic deletion of p11 resulted in significantly decreased tumor onset, growth rate, and spontaneous pulmonary metastatic burden in the PyMT/p11-KO (knock-out) mice. This phenotype was accompanied by substantial reduction in Ki67 positivity, macrophage infiltration, decreased vascular density in the primary tumors, and decrease in invasive carcinoma and pulmonary metastasis. Surprisingly, IHC analysis of wild-type MMTV-PyMT mice failed to detect p11 expression in the tumors or metastatic tumor cells and loss of p11 did not decrease plasmin generation in the PyMT tumors and cells. Furthermore, tumor cells expressing p11 displayed dramatically reduced lung metastasis when injected into p11-depleted mice, further strengthening the stromal role of p11 in tumor growth and metastasis. Transcriptome analysis of the PyMT tumors from p11-KO mice showed marked reduction in genes such as *Areg*, *Muc1*, and *S100a8* involved in breast cancer development, progression, and inflammation. The PyMT/p11-KO tumors displayed a remarkable increase in inflammatory cytokines

such as interleukin (*Il*)-6, *Il*-10, and interferon (*Ifn*)- γ . Gene expression profiling and IHC of primary breast cancer samples showed that p11 mRNA and protein levels were significantly higher in tumor tissues compared to normal mammary tissue. P11 mRNA expression was significantly associated with poor patient prognosis and significantly elevated in high grade, triple negative (TN) tumors, and tumors with high proliferative index. This is the first study examining the crucial role of p11 in breast tumor development and metastasis, thus emphasizing its potential as a diagnostic and prognostic biomarker in breast cancer.

Keywords: breast cancer; S100A10 (p11); tumor growth; tumor progression; macrophages; metastasis; carcinoma; mammary gland; triple negative

1. Introduction

Breast cancer is the leading cause of cancer death among women worldwide. The vast number of cancer-associated deaths are due to metastases rather than primary disease alone. Currently, strategies to treat and eliminate metastasis are limited and challenged by resistance to therapies. Thus, discovering the underlying molecular mechanisms that promote breast cancer metastasis and therapy resistance is critical for identifying novel treatment strategies.

Extracellular proteases promote degradation of the extracellular matrix and form a key component of the cascade of events contributing to cancer cell invasion and metastasis. [1–3]. Increasing evidence has shown elevated expression of proteases plasmin and matrix metalloproteases (MMPs) in breast cancer progression and has been extensively studied with mouse tumor models [4]. Plasminogen (Plg), synthesized by the liver is activated to plasmin (Pm) by tissue plasminogen activator (tPA) and urokinase plasminogen (uPA) activator, (reviewed in [5,6]). This process, normally slow, is accelerated by plasminogen receptors (PgR) on the cell surface. Our laboratory identified S100A10 (p11) as a plasminogen receptor that forms a complex with both plasminogen and plasminogen activator [7–10].

P11 is a multifunctional protein and a member of the S100 proteins. Several extracellular and intracellular functions have been identified for p11; the plasminogen receptor function is the most well studied so far [5]. P11, present on the extracellular surface, is complexed with its binding partner annexin A2 (p36). We have reported that p11 regulates plasminogen activation on the cell surface of many cancer cells including fibrosarcoma, colorectal, lung, and pancreatic cells [8,11–16]. We have also reported that p11 regulates the plasmin production of stromal cells, including macrophages and endothelial cells [17–19], and that p11-dependent plasmin generation is necessary for macrophage infiltration to the site of inflammation in subcutaneous tumor growth.

Several studies have shown correlations between p11 gene expression and poor prognosis and overall survival in lung [20–22], colorectal, ovarian, kidney, and gastric cancers, anaplastic thyroid carcinoma, melanoma and acute lymphoblastic leukemia (reviewed in [12]), and pancreatic ductal adenocarcinoma [16]. P11 is upregulated in basal-type breast cancer [23] and during the process of intravasation and epithelial mesenchymal transition [24].

Although we have shown that p11 is important for ectopic tumor growth in both NOD/SCID (Non-obese diabetic/severe combined immunodeficiency) and syngeneic mouse models for various cancer cell lines such as colorectal, fibrosarcoma, and pancreatic cancer, these studies have limitations. Firstly, they do not reproduce the complex multistep landscape of human oncogenesis. Secondly, the growth, invasion, and metastasis of cancer also depends on its interaction with the tumor microenvironment making it difficult to distinguish the individual contribution of tumor and stromal cells to cancer progression. To circumvent these experimental challenges, and to advance our understanding of the role of p11 in oncogenesis, we have established the MMTV-PyMT (mouse mammary tumor virus-polyoma middle tumor-antigen) transgenic breast cancer model in

wild-type and p11 knockout mice and have used this double transgenic model to investigate the role of p11 in breast cancer malignancy.

In the MMTV-PyMT transgenic mouse model, mammary gland specific expression of the oncogene PyMT under the MMTV promoter, results in widespread tumor growth in all ten mammary glands and spontaneous metastasis to the lymph nodes and lungs. This occurs with a mean latency of 92 days, with high penetrance and almost a 100% incidence of metastasis. This mouse model is very similar to human breast cancer in that the tumors display histological and molecular characteristics mirroring the progression of human breast cancer [25–27] and have a reactive stroma. This model has been widely used to establish the role of proteolytic activity in cancer cell malignancy. Proteases that affect metastasis in this model system include Plg [28,29], uPA [30], MMP-9 and MMP-3 [4,31,32], cathepsin B [33,34], and ADAMTS1 (short for disintegrin and metalloproteinase with thrombospondin motifs) [35]. Another important feature of the MMTV-PyMT model is that the increased metastatic potential is largely dependent on the presence of macrophages in the primary tumor [36,37]. Thus, the MMTV-PyMT model is a pertinent model to investigate the functional role of p11.

In the current study, we conducted a systematic, functional, and correlative analysis of the role of p11 in breast cancer oncogenesis using the MMTV-PyMT transgenic mouse model. We have also performed gene expression profiling and protein expression analysis of human breast cancer tissues. The studies described herein indicate that p11 plays a complex and multifunctional role in breast tumor growth, progression, and metastasis.

2. Results

2.1. Loss of p11 Results in Delayed Appearance of Multifocal Dysplastic Lesions

The fourth inguinal mammary gland from PyMT/p11-WT (wild-type) and PyMT/p11-KO (knock-out) mice was isolated at 8, 10, and 12 weeks of age, fixed and stained with carmine alum [37]. As early as 6 weeks of age, we observed the appearance of early hyperplastic lesion at a single focus or in some cases, multiple foci beneath the nipple in the older zone of the ductal tree in the PyMT/p11-WT. At 8 weeks, we observed the formation of multiple small nodules in the distal newer ducts, which then spread extensively to the entire length of mammary gland by 12 weeks of age. In contrast, PyMT/p11-KO mice showed complete absence of hyperplastic tumor foci at 6 weeks, which appeared first at 8 weeks of age, and were restricted to only a fraction of the older ductal structures even at 12 weeks. The most dramatic difference was the complete absence of multiple tumor foci throughout the mammary gland of the PyMT/p11-KO mice at 12 weeks (Figure 1). Hematoxylin and Eosin (H&E) staining of a representative tissue section (5 μ m) (Figure S1) showed increased hyperplastic lesions in the PyMT/p11-WT as age progressed from 6 weeks to 12 weeks, whereas none were observed in the PyMT/p11-KO tumors.

2.2. p11 Plays a Role in Mammary Tumor Growth and Progression

We employed a cohort of 27 PyMT/p11-WT and 28 PyMT/p11-KO mice and monitored the time of appearance and size of palpable tumors. A fraction of the mice was sacrificed at 20 weeks and the total tumor burden was determined. The remaining mice were monitored further until a combined tumor volume of 4000 mm³ was attained, the humane endpoint of the experiments.

The first palpable tumor appeared at 9 weeks in the PyMT/p11-WT mice compared to 11 weeks in the PyMT/p11-KO mice (Figure 2A). At 10 weeks, 77% of PyMT/p11-WT and 42% of PyMT/p11-KO mice developed palpable tumors. All the PyMT/p11-WT mice developed palpable tumors by 105 days of age (15 weeks), whereas only 89% of PyMT/p11-KO mice developed tumors at 20 weeks (Figure 2B). Overall, the mean tumor latency was increased by two weeks in the PyMT/p11-KO mice (Figure 2C). The tumor volume was dramatically decreased in the PyMT/p11-KO mice with a 4- and 6-fold decrease at 15 and 20 weeks, respectively (Figure 2D).

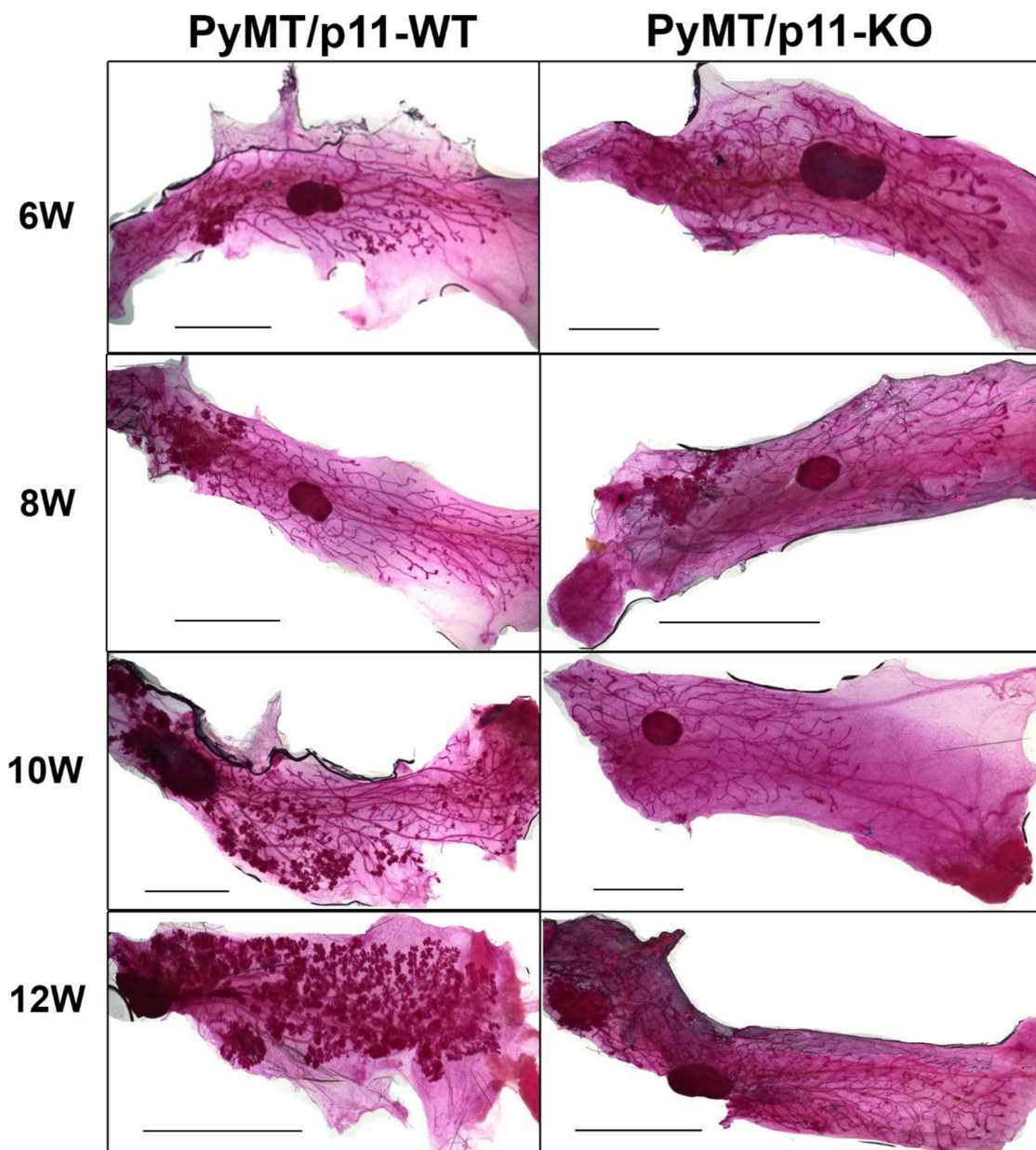


Figure 1. Loss of p11 affects formation of hyperplastic lesions in PyMT driven tumors. Whole mammary glands from PyMT/p11-WT (n = 3) and PyMT/p11-KO mice at 6 (6 W), 8 (8 W), 10 (10 W), 12 (12 W) weeks) were excised, fixed, and stained with carmine alum as per standard protocols (See Materials and Methods). Representative images from the 4th abdominal mammary gland from each group and time point are shown. Scale bar 2 mm.

Histopathological progression to late carcinoma stage was delayed in PyMT/p11-KO mice (Figure 2E). By 10 weeks of age, 83% of the PyMT/p11-WT mice and only 25% of the PyMT/p11-KO progressed to the early carcinoma stage. By 20 weeks, 82% of the PyMT/p11-WT mice and 6.25% of the PyMT/p11-KO had progressed to the late carcinoma stage. Interestingly, at this endpoint, 37.5% of PyMT/p11-KO mice showed normal mammary gland histopathology.

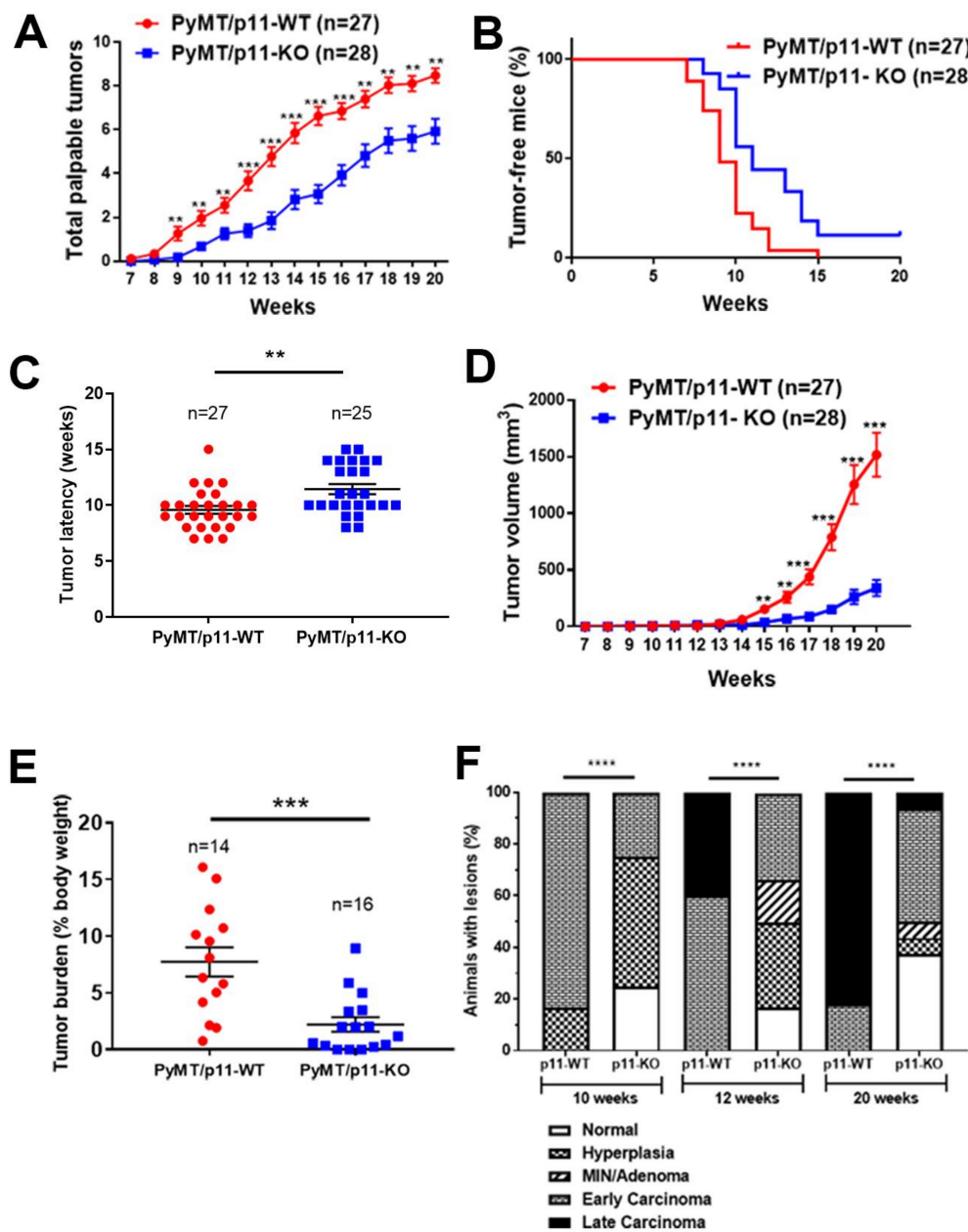


Figure 2. Tumor initiation, growth, burden, and progression are decreased and delayed in PyMT/p11-KO mice. (A) Appearance of palpable tumors was monitored weekly. (B) Percent tumor-free mice was calculated using Kaplan–Meier analysis (hazard ratio (HR)—2.24, $p = 0.0004$). (C) Tumor latency was plotted for each mouse based on the first appearance of palpable tumor. (D) Tumor volume was measured weekly using calipers. Total volume was plotted to represent tumor growth rate. (E) Total tumor weight at endpoint (20 weeks) was determined as a percentage of body weight. Data are a compilation of three independent experiments, except (D), which shows data from one independent experiment. Significance was determined by non-parametric t -test (Mann Whitney U test—unpaired, non-parametric test for means). (F) Mammary glands and tumors from PyMT/p11-WT and PyMT/p11-KO mice were harvested at 20 weeks, formalin-fixed, embedded, and sectioned at 5 μm thickness. The H&E and smooth muscle α -actin-stained sections were classified into histopathological stages by a pathologist in a blinded manner. (n = 6 to 12 mice in each group). Statistical analysis was performed by χ^2 -test ($p < 0.0001$). The asterix on each plot represents p -values as follows. ** $p < 0.01$, *** $p < 0.001$, **** $p < 0.0001$.

2.3. Loss of p11 Reduces Tumor Cell Proliferation, Vascular Density, and Macrophage Infiltration

The proliferative index of PyMT/p11-WT and PyMT/p11-KO tumors at endpoint (20 weeks) were measured using Ki67 positive immunoreactivity [38]. We observed a 2.9-fold reduction in mean Ki67 positive-cells in tumors from PyMT/p11-KO mice, suggesting that p11 functions in modulation of tumor cell proliferation (Figure 3A). Although there was a trend for increased apoptosis in the PyMT/p11-KO tumors, this was not of statistical significance (Figure S4A). We observed a 6-fold reduction in endothelial cell staining (CD31-positive) in the PyMT/p11-KO tumors compared to PyMT/p11-WT tumors (Figure 3B). In both groups of PyMT mice, the macrophages (F4/80-positive) were restricted to the peripheral area of the tumors. However, there was a significant (11.5-fold) decrease in the macrophage density in the tumors from PyMT/p11-KO mice compared to the PyMT/p11-WT mice (Figure 3C). We also observed a qualitative increase in CD3+ (total T cells) staining in the tumors, but this difference was not statistically significant (Figure S4B).

2.4. Loss of p11 Reduced Spontaneous and Experimental Metastasis

We harvested the lungs from 20-week old mice and performed histochemical analysis. We observed a significant 18-fold decrease in metastatic burden and a 14-fold decrease in number of metastatic foci (Figure 4A) in the PyMT/p11-KO mice. Furthermore, the presence of metastatic foci was observed only in 3 of 17 (17.6%) in the PyMT/p11-KO mice compared to 10 of 19 (53%) in the PyMT/p11-WT mice, suggesting an important role for p11 in spontaneous metastasis. Next, we injected the PyMT transformed cell line, Py8119 with WT p11 levels intravenously (lateral tail vein) in p11-WT and p11-KO mice. We observed a dramatic decrease in the metastatic burden (6-fold) and number of metastatic foci (2.5-fold) in the p11-KO mice (Figure 4B). These results suggest that stromal p11 is important for the extravasation process and establishment of metastases by these breast cancer cells.

2.5. p11 Expression Is Restricted to the Stromal Compartment in Mammary and Pulmonary Metastatic Tumors

To further investigate the expression and localization of p11 in the PyMT tumor and stromal compartment, we performed immunohistochemical analysis of tumors from both PyMT/p11-WT and PyMT/p11-KO cohorts. Interestingly, we observed that the majority of the p11 staining was localized to the stromal compartment in the PyMT/p11-WT mice. Only a fraction (33%) of tumors examined presented with diffuse p11 staining in the tumor cells (Figure 5A).

To further evaluate if p11 expression was induced in the metastatic tumor cells, we immunostained lung sections from PyMT/p11-WT mice and observed that the lung tissue but not the metastatic foci showed immunoreactivity for p11. (Figure 5B). This suggested that the tumor cells in the PyMT tumors do not express detectable levels of p11, whereas it is highly expressed in the stromal cells surrounding the tumors. Furthermore, there did not appear to be an induction of p11 in the cancer cells that left the tumor and metastasized to the lungs.

We also examined the lung tumors obtained after tail vein injection of Py8119 cells in p11-WT and p11-KO mice. Surprisingly, we observed that the metastatic foci obtained from the lungs of both genotypes showed strong membranous expression of p11. This was more evident in the p11-KO mice, where expression was restricted to the small tumor nodules and was completely absent in the surrounding lung tissues (Figure 5C). We further evaluated p11 expression in both the whole tumor homogenates and Py8119 cells by immunoblotting (Figure 5D,F). As anticipated, whole tumor homogenates from these groups also showed p11 expression in the PyMT/p11-WT tumors consistent with some expression in the stroma. Unlike the PyMT cancer cells, we observed that Py8119 tumor cells showed robust p11 expression (Figure 5F).

2.6. Loss of p11 Does Not Affect Plasminogen Activation (or Plasmin Generation) in PyMT Tumors

We previously observed that plasminogen activation is substantially reduced in p11-depleted cancer cells such as colorectal [14], fibrosarcoma [13], pancreatic [16], and lung [15]. We measured

plasmin generation in tumor homogenates and cell lines isolated from PyMT tumors and did not observe any difference (Figure 5E and Figure S5B). However, PyMT tumors from p11-WT and p11-KO mice showed a marked increase in plasminogen activation compared to normal mammary glands (Figure S5C). These data suggest that p11 does not play a significant role in tumor cell plasmin generation in the PyMT mammary tumors.

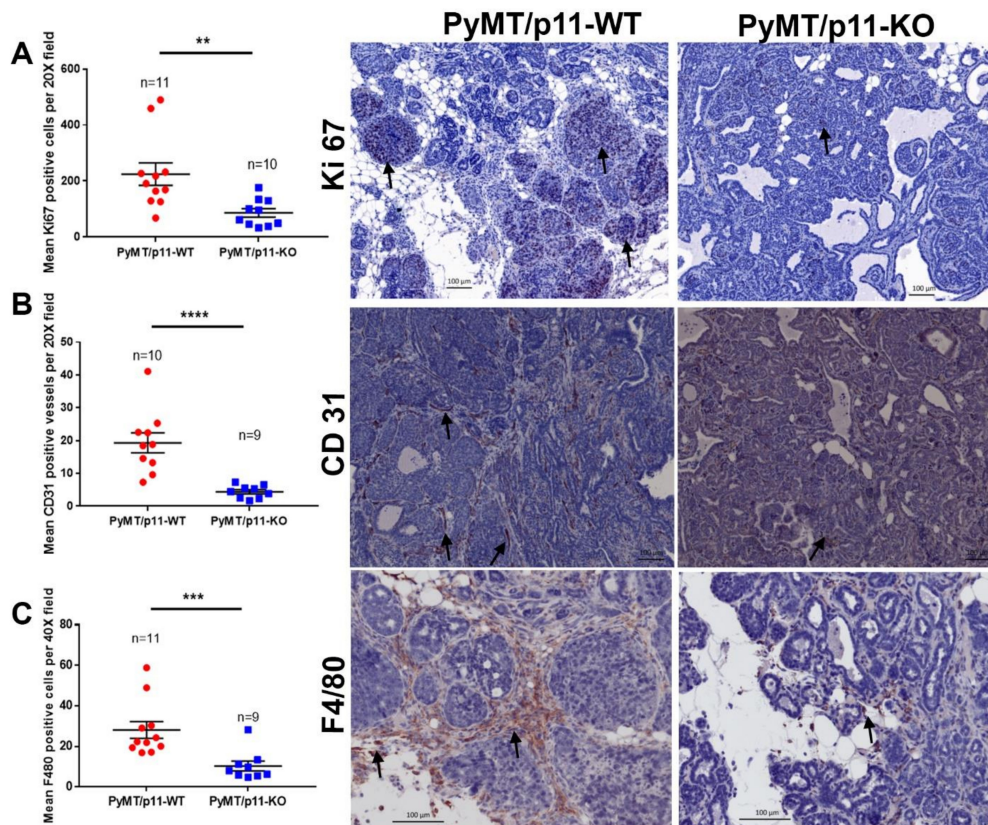


Figure 3. PyMT/p11-KO mice tumors show reduced proliferation, vascular density and macrophage infiltration. Formalin-fixed, paraffin-embedded, and sectioned tissues from PyMT/p11-WT ($n = 11$) and PyMT/p11-KO ($n = 10$) (end-point, 20 weeks) mice were immunostained for (A) Ki67 (proliferation marker), (B) CD31 (endothelial marker), and (C) F4/80 (mouse macrophage marker). (A) Immunostaining using anti-rabbit Ki67 antibody (Abcam, Cambridge, MA, USA). Stained sections were imaged using Zeiss Axio Imager Z1 W/color and monochrome camera (Carl Zeiss Canada, Toronto, ON, Canada) at 10 \times magnification. Left panel: The number of Ki67-positive cells was manually counted using Zen (2012) software in 7–10 random fields per tissue section/mouse. Significance was determined using Mann Whitney U test (unpaired, non-parametric test for means), $p = 0.0021$. Right panel: The representative image was captured at 20 \times magnification. Scale bar–100 μm . (B) Immunostaining using anti-rabbit CD31 antibody (Abcam, Cambridge, MA, USA). Stained sections were imaged using Aperio Scanning system (Leica Biosystems, Concord, Ontario) at 40 \times magnification. Left panel: The number of CD31-positive cells were manually counted using Imagescope software (Leica Biosystems, Concord, Ontario) in 7–10 random fields per tissue section/mouse. Mann Whitney U test (unpaired, non-parametric test for means) shows p value < 0.0001 . Right panel: Representative image at 20 \times magnification. Scale bar–100 μm . (C) Immunostaining using anti-rat F4/80 antibody (BM8, ThermoFisher Scientific, Waltham, MA, USA). Stained sections were imaged as in (A), but at 40 \times magnification. Left panel: The number of F4/80-positive cells were manually counted as in (A). Mann Whitney U test (unpaired, non-parametric test for means) showed $p < 0.0001$. Right panel: Representative image at 20 \times magnification. Scale bar–100 μm . The asterisk on each plot represents p -values as follows. ** $p < 0.01$, *** $p < 0.001$, **** $p < 0.0001$.

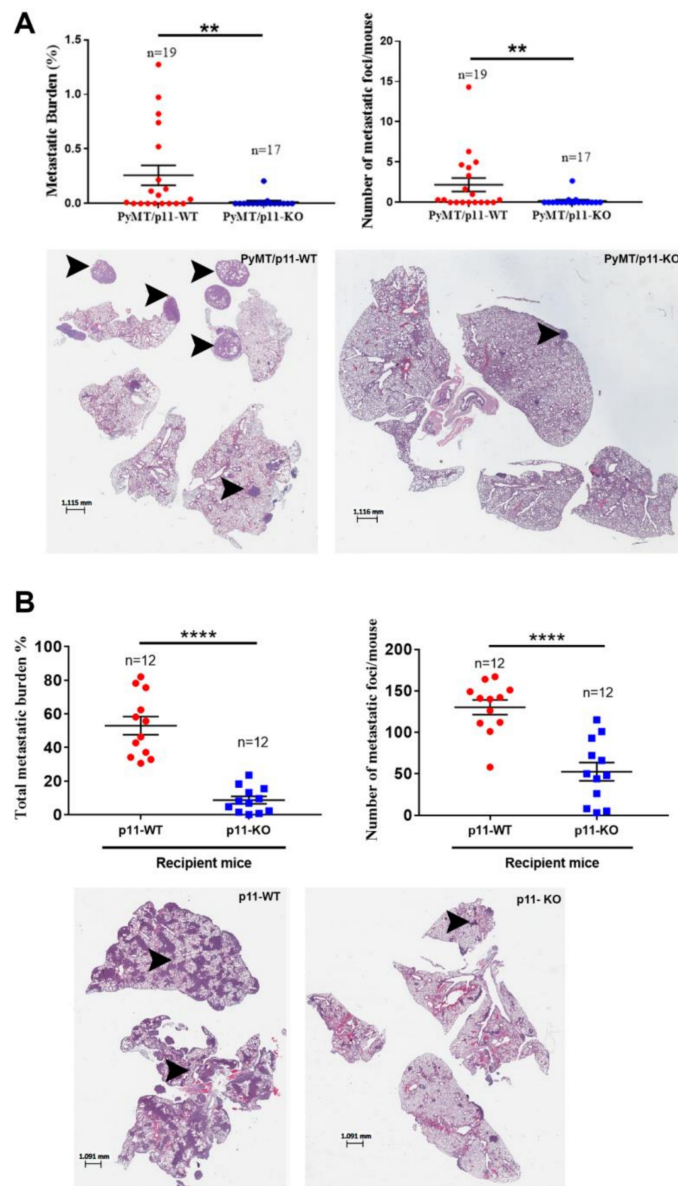


Figure 4. Metastasis is diminished in PyMT/p11-KO mice. **(A)** We evaluated pulmonary metastasis at the 20-week end point in (spontaneous model) PyMT/p11-WT and PyMT/p11-KO mice by microscopic examination of formalin-fixed, H&E-stained lung sections (5 μ m). Three lung sections each 100 μ m apart were used for staining. Quantification was performed using Aperio image analysis software (Imagescope). Mean values for three sections were used to calculate the metastatic burden and foci values. **(A)** We evaluated the metastatic burden by measuring the total metastatic area and total lung area, followed by normalization (A—upper left panel). Mann Whitney U test showed statistical significance with *p* value of 0.0062. The number of metastatic foci per mouse lung section was determined by manual counting of images (A—upper right panel). Mann Whitney U test showed *p* value of 0.0069. Lower panels: Representative lung images from WT and KO mice. **(B)** Experimental metastasis assay. We injected 2.5×10^5 Py8119 (p11-WT levels) cells into p11-WT and p11-KO mice (*n* = 12 mice per group). The lungs were harvested after 14 days, formalin-fixed, and sectioned at 5 μ m as described above. Mann Whitney non-parametric *t*-test (for means) for statistical significance was performed. Metastasis was pooled and combined from two independent experiments (*n* = 6 each). *p* < 0.0001. Lower panels: representative lung images from WT and KO mice. The asterisk on each plot represents *p*-values as follows. ** *p* < 0.01, **** *p* < 0.0001.

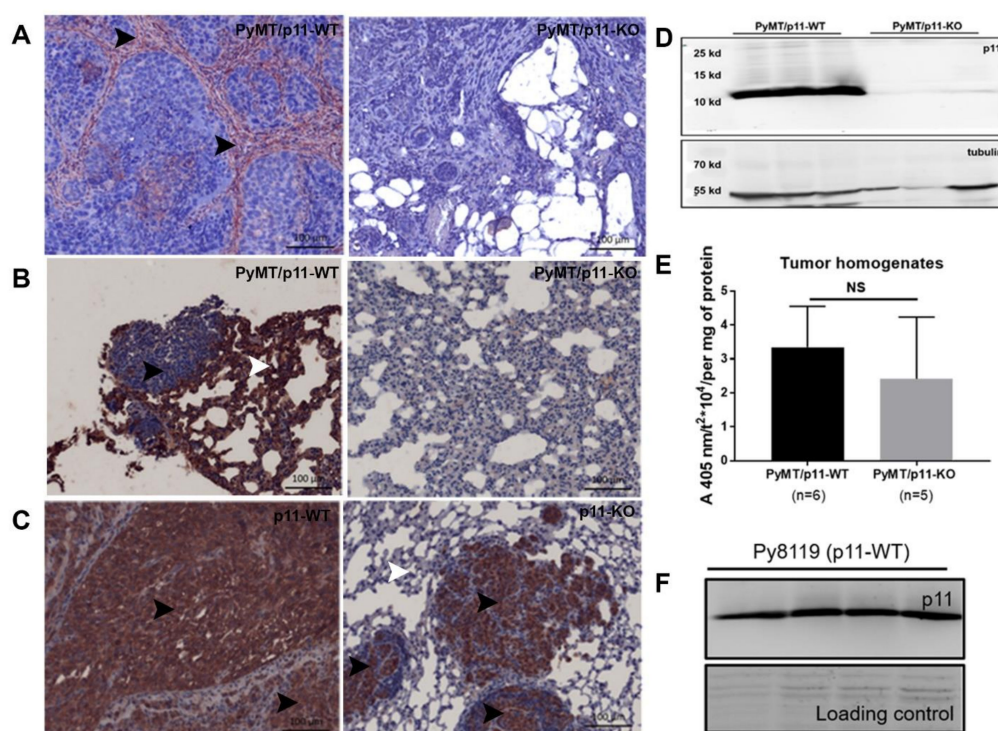


Figure 5. Expression of p11 in mammary and pulmonary metastatic tumors is restricted to the stromal compartment in the PyMT/p11-WT tumors. IHC staining was performed using anti-rabbit p11 antibody (Proteintech, Rosemont, IL, USA), on 5 μ m sections from 20-week end-point PyMT/p11-WT ($n = 10$) and PyMT/p11-KO tumors ($n = 3$), and lungs from spontaneous and experimental metastasis assay. (A) Representative images of p11 immunostained sections of PyMT mammary tumors. As anticipated, the tumors from PyMT/p11-KO mice showed no staining, validating the specificity of the antibody. (B) PyMT spontaneous lung metastasis from PyMT/p11-WT and PyMT/p11-KO mice, and (C) experimental metastasis of Py8119 cells injected in p11-WT ($n = 4$) and p11-KO ($n = 4$) mice are shown. Scale bar is 100 μ m. (D) Western blot of p11 expression in total cell tumor homogenates from PyMT/p11-WT ($n = 3$) and PyMT/p11-KO mice ($n = 3$). (E) Fresh and frozen tumors from both PyMT/p11-WT ($n = 6$ mice) and PyMT/p11-KO ($n = 5$ mice) were homogenized and equal protein (30–60 μ g) was used for plasmin generation assay as described in Materials and Methods and Supplemental Section. Mann Whitney U (unpaired, non-parametric test for means) t -test show $p = 0.3290$. NS, not significant (F) Western blot for p11 expression in total cell lysates in Py8119 cells obtained from ATCC (American Type Culture Collection) ($n = 4$) using goat anti-mouse antibody (R&D systems, Minneapolis, MN, USA).

2.7. P11 Regulates Expression of Genes and Cytokines Affecting Tumor Progression

To examine how p11 might regulate tumor growth and metastasis genes, we performed microarray gene expression profiling on mammary tumors from PyMT/p11-WT and PyMT/p11-KO mice ($n = 3$ per group). We observed that 891 transcripts were elevated and 269 were reduced by more than 1.5-fold ($p < 0.05$) in the PyMT/p11-KO tumors (Figure 6A). As anticipated, S100A10 expression was decreased by 3.08-fold in the PyMT/p11-KO tumors, supporting the validity of the gene expression data set. Of the 891 transcripts, 331 were annotated genes: 144 genes were downregulated and approximately 187 genes were upregulated in the PyMT/p11-KO mice (Supplemental file 1). We chose to validate seven downregulated genes (*Aldh1a2*, *Areg*, *Ctse*, *Muc1*, *S100a8*, *Thbs1*, and *Tnc*) and two upregulated genes (*Cdh19* and *Cpm*) using reverse transcriptase quantitative PCR (RT-qPCR) ($n = 11$ mice per group). We confirmed that amphiregulin (*Areg*), mucin 1 (*Muc1*), and *S100a8*, were downregulated, whereas cadherin 19 (*Cdh19*) was upregulated by qPCR (Figure 6B). In contrast to the microarray data,

Aldh1A2 and *Tnc* were shown to be upregulated by qPCR (Figure 6B and Figure S6A), which potentially represents false hits from microarray.

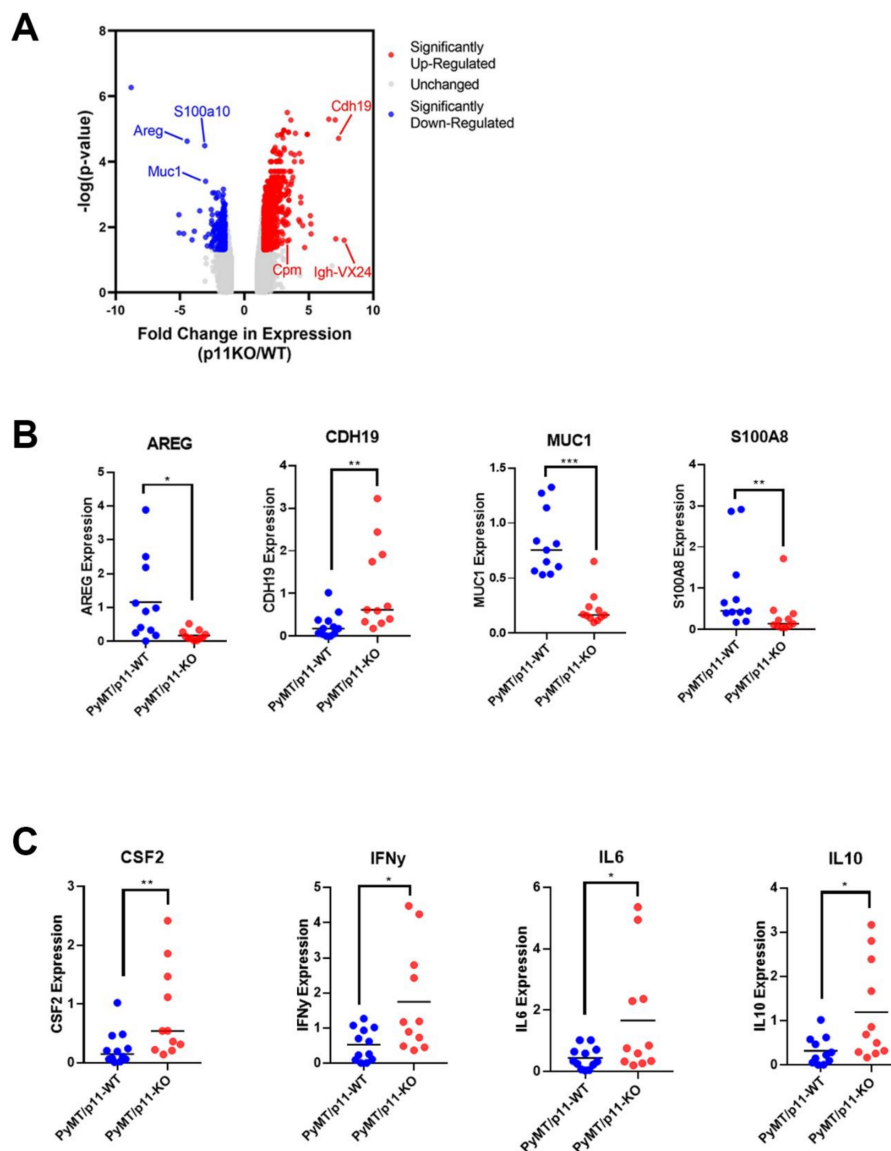


Figure 6. Tumor transcriptome of PyMT/p11-KO mice suggest the downregulation of tumor promoting genes. Gene expression profiling of PyMT/p11-WT and PyMT/p11-KO tumors were performed (n = 3 mice per group). (A) Volcano plot with (significant) p value of < 0.05 upregulated and downregulated genes in the PyMT/p11 KO mice (n = 3 mice in each group). The top 6 genes are highlighted. Genes which were up- or down-regulated more than 2-fold ($\log_2 = 0.678$) at a significance level of $p < 0.05$ were considered differentially expressed. (B) Validation of the top 9 differentially expressed genes using quantitative RT-PCR (10–11 mice per group). Significance was determined by unpaired t -test. Only the genes significantly altered are shown. (C) Loss of p11 in PyMT tumors results in differential cytokine expression profile. We performed quantitative RT-PCR on tumors isolated from PyMT/p11-WT and PyMT/p11KO mice (10–11 mice per group), using a CFX96 or CFX384 Touch Real-Time PCR Detection system (BioRad, Mississauga, ON, Canada). Relative mRNA expression was log-2 transformed prior to plotting and statistical analysis. Significance was determined by unpaired, t -test. Only those cytokines significantly altered are shown. The asterisk on each plot represents p -values as follows. * $p < 0.05$, ** $p < 0.01$, *** $p < 0.001$.

Quantitative PCR showed no significant change in the expression of cytokines associated with macrophage recruitment including *Csf1*, *Ccl5*, *Ccr5*, and *Ccl2* (Figure S6B). Comparison of expression of inflammatory cytokines between the two groups showed significant increases in *Ifn-γ* (3.36-fold), *Il-10* (3.7-fold), *Il-6* (3.7-fold), but no significant changes in *Il-12α*, *Il-4*, and *Tnf-α* (Figure 6C, Supporting Figure 4B). Interestingly, we observed a 3-fold increase in *Csf2* expression in the PyMT/p11-KO tumors (Figure 6C).

2.8. p11 Is Associated with Poor Clinical Outcomes

We employed a well-defined breast cancer patient cohort (n = 176) and stratified the patient population into S100A10 high and low mRNA levels. Kaplan–Meier survival analysis showed that high levels of S100A10 were significantly associated with both shorter overall survival (HR = 3.34, $p < 0.0001$) and recurrence-free cancer (HR = 2.27, $p < 0.001$) (Figure 7A,B). We further found that S100A10 levels were significantly increased in high histologic grade tumors compared with normal mammary tissues ($p < 0.01$) and low grade tumors ($p < 0.05$) (Figure 7C) Among the molecular subtypes, S100A10 mRNA levels were significantly higher in triple negative (TN) and human epidermal growth factor receptor 2 (HER2)-enriched breast tumors compared to normal breast tissues. TN tumors showed significantly higher S100A10 levels than luminal estrogen receptor (ER+) tumors (Figure 7D). In addition, tumors with high Ki67 immunoreactivity (percentage of positive cells >15%) showed significantly higher S100A10 levels than tumors with low Ki67 immunoreactivity ($\leq 15\%$) (Figure 7E).

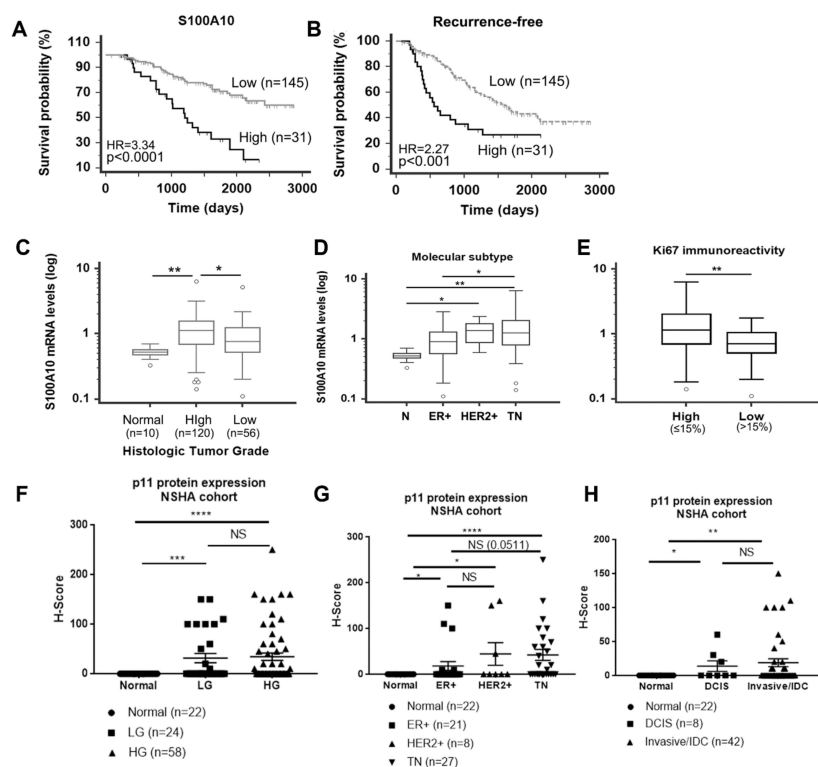


Figure 7. Expression of S100A10 (p11) expression in breast cancer patients. Treatment-naïve primary breast cancer samples (n = 176) were obtained through the Canadian Breast Cancer Foundation (CBCF) Tumor Bank and used for gene expression analysis. *S100A10* high and low mRNA levels were based on the signal intensity from our gene expression microarray profile using the Receiver Operating Characteristic (ROC) curve analysis. Correlation of *S100A10* mRNA with (A) overall survival probability. High mRNA levels of *S100A10* are significantly associated with poor patient overall survival (HR of 3.34). (B) Recurrence free survival, with HR 2.27. (C) For histological tumor grade, p11 is significantly upregulated in high grade (HG) tumors compared to normal breast and low-grade (LG) tumor tissues.

(D) For molecular subtype, p11 is significantly up-regulated in HER2+ and triple negative breast cancers compared to normal breast tissues. (E) In breast cancer patients, p11 mRNA levels are significantly higher in tumors with high Ki67 immunoreactivity. *S100A10* (p11) protein is overexpressed in breast tumors compared to normal mammary tissues. (F–H) IHC staining of p11 in normal breast tissues and in low grade (LG), high grade (HG), ductal carcinoma in situ (DCIS), IDC (Invasive Ductal Carcinoma)/Invasive, ER+, HER2+ and TN tumors was performed using anti-p11 antibody (Proteintech, Rosemont, IL, USA). These human tissues were obtained from Queen Elizabeth II Health Sciences Centre, Nova Scotia Health Authority (NSHA) (see Materials and Methods). The stained sections were scored (semi-quantitative) based on percent positive tumor cells and intensity of staining by a pathologist (blinded). H score was determined based on the formula described and the samples/tissues were separated and plotted based on (F) clinical/histological grade, (G) pathological grade, and (H) molecular subtype. Statistical analysis was performed by Mann Whitney U test (unpaired, non-parametric test for means *t*-test). The Asterisk on each plot represents *p*-values as follows. * *p* < 0.05, ** *p* < 0.01, *** *p* < 0.001, **** *p* < 0.0001.

Immunostaining of the NSHA patient cohort followed by semiquantitative scoring of the staining showed no p11 immunostaining (100% negative, H-score = 0) of epithelial cells that formed the normal mammary ducts but expression in the stromal areas surrounding the normal duct was observed (Figure S7A). Based on H-score, we found 25% of low grade, 29.3% of high grade, 37.5% of DCIS, 33% of IDC, 23.8% of ER+, 37.5% HER2+, and 52% of TN tissues/samples were positive for p11 expression. We observed a significant increase in H-score values between normal and low-grade, and normal and high-grade, but the difference between low grade and high grade was not significant (Figure 7F). Similarly, DCIS and IDC samples showed significantly higher H-score values compared to normal tissues. But there was no difference in p11 expression between DCIS and IDC samples, suggesting that p11 expression does not correlate with invasive progression (Figure 7G and Figure S7). We observed the most dramatic increase in p11 staining between normal tissue and TN tumors (*p* < 0.0001), consistent with the highest mean H-score value for the TN tumors. We also noted significant increase between normal and ER+, and normal and HER2+ tumors, but there was no significant increase between ER+ and HER2+ tumors. Interestingly, statistical comparison of ER+ and TN tumors showed increase in TN with respect to ER+ although the *p* value (0.0511) was only approaching significance (Figure 7H and Figure S7).

3. Discussion

The loss of components of the plasmin-plasminogen system decreased pulmonary metastasis but had no effect on tumor onset or growth in the PyMT model (reviewed in [4]). Interestingly, in this study, we observed a dramatic delay in tumor onset, growth, and progression to malignancy in the PyMT/p11KO mice. These results suggest a complex role for p11 in breast cancer oncogenesis beyond the regulation of plasmin generation.

We observed a dramatic decrease in metastatic burden (18-fold) and metastatic foci (14-fold) in PyMT/p11-KO mice. The histopathological progression to late carcinoma stage was delayed in PyMT/p11-KO mice (Figure 2E), potentially attributing the decrease in metastases to the delayed development of malignancy. However, pulmonary metastases in the PyMT model is an early event and independent of tumor size [39,40]. Interestingly, metastases formed by injection of the PyMT transformed cell line, Py8119, into the p11-KO mice were dramatically reduced, suggesting that the p11-deficient stroma is a less favorable environment for the establishment of metastases.

These results are consistent with our previous work showing a dramatic reduction in the growth of Lewis lung carcinomas and T241 fibrosarcomas in p11-deficient mice compared with WT mice [19] and that the tumor growth deficit corresponded with a decrease in macrophage and endothelial cell density. Consistent with delayed tumor onset and growth, we observed a dramatic decrease in Ki67 positivity in tumors from PyMT/p11-KO mice, suggesting a role for p11 in tumor cell proliferation. Although, apoptosis as shown by TUNEL staining was marginally decreased with loss of p11 in PyMT

tumors, this was not statistically significant and warrants further testing in a larger sample size. Nevertheless, this corroborates our finding with Ki67 staining/quantification. Tumor-associated macrophages (TAMs) significantly contribute to tumor progression, angiogenic switch, and metastasis [41,42], with loss of peritumoral TAMs resulting in delayed tumor progression [43]. Therefore, it is likely that a portion of the requirement of p11 for PyMT-driven tumor growth and metastasis is due to the function of p11 in macrophage recruitment.

We have previously reported that p11 is responsible for much of the plasmin generation in various cancer cell lines [5,15,16,44]. However, in the present study, we were unable to detect any differences in plasmin generation between cancer cells or tumor homogenates isolated from the PyMT/p11-KO and PyMT/p11-WT mice. Macrophages and endothelial cells utilize p11 for their physiological functions. We have shown that the loss of p11 slows migration of the macrophage to the tumor site. It was therefore surprising that we did not detect differences in the tumor homogenates isolated from PyMT/WT and PyMT/p11-KO mice. Although the PyMT/p11-KO mice tumor homogenates appeared to generate less plasmin, the difference did not meet statistical significance. The reason for this discrepancy is unclear at present but may be addressed by larger sample sizes. However, we observed that PyMT tumors from p11-WT and p11-KO mice showed a marked increase in plasmin generation compared to normal mammary glands (Figure S5D), suggesting compensation by other plasminogen receptors in this model. It is likely that distant peripheral macrophages utilize plasminogen receptors such as p11 to migrate and invade the tumors [19,45,46]. Furthermore, we detected weak p11 expression in some of the tumor cells and no expression in metastatic nodules of PyMT/p11-WT tumors. The similarity of F4/80 and p11 staining pattern in the PyMT-tumor stroma suggests that macrophages are the most prominent p11-staining cells in the stroma (Figure S8). However, detailed colocalization studies will be necessary to verify this prediction. In contrast, lung tumors obtained after tail vein injection of Py8119 cells in p11-WT and p11-KO mice showed robust p11 expression. Overall, the exclusive expression of p11 in the stroma *in vivo* parallels the stromal localization of other components of the plasminogen activation system including uPA, uPAR, tPA, and PAI-1 in mouse (PyMT) and human models [4]. The lack of p11 expression in the PyMT-expressing tumor cells and restriction of the majority of p11 expression to the stromal compartment were striking observations in the current study. The middle T (MT) region of PyMT is an effective oncogene and activates the PI3 kinase (PI3K) signaling pathway [47,48]. Recently we have shown that active PI3K signaling decreased p11 expression in several tumor cells via the FOXC2 transcription factor [15]. In addition, *in vitro* observations indicate a distinct rewiring of signaling in 2-D cell cultures resulting in increased p11 expression potentially due to de-repression of tumor-stroma signaling events observed *in vivo* [49,50]. Furthermore, the retention of p11 expression in the Py8119 tumor cells in the lung metastatic nodules, suggests the absence of inhibitory signals in the lung microenvironment.

Whole mount analysis of mammary glands indicated a decrease in multifocal dysplastic lesions as early as 6–8 weeks in the PyMT/p11-KO mice (Figure 1). By 10–12 weeks, these lesions had become quite dramatic, whereas dysplastic lesions in the mammary glands of the PyMT/p11-KO mice were sparse. An interesting observation was the reduction in length of the ductal branches in the PyMT/p11-KO mammary glands at the early time points of 6 and 8 weeks, and was comparable to the WT at 10 and 12 weeks (Figure S2). However, by 10 and 12 weeks, the ductal branching was indistinguishable, suggesting that the developmental deficit was no longer present (Figure S2). The mechanism by which the developmental deficit had been overcome at 10 weeks is unclear and will require a detailed study of the role of p11 in mammary development. However, it is unclear if this novel function of p11 in mammary development could account for the dramatic reduction in tumor growth observed in the PyMT/p11-KO mice. Other groups have shown that infiltration of macrophages is required for early mammary gland development [51]. It is likely that defective macrophage migration observed with p11-KO mice causes early defects in ductal branching in the mammary gland. This suggests that p11 may play a potential role during early stages of mammary gland development. More recently, another plasminogen receptor, Plg-Rkt, was shown to be critical for lactogenesis and mammary

lobuloalveolar development [52]. We were initially concerned that the delayed development might affect the expression of the PyMT oncogene in the epithelial cells and thereby contribute to the delay in oncogenesis observed in the p11-KO mice. However, we did not observe a decrease in PyMT expression in spontaneous tumors from p11-KO mice as evidenced from both qPCR and IHC expression analysis at several early and late time points (data not shown). This suggests that delay in development does not affect oncogene expression in p11-KO mice and therefore the effects of p11 on tumor development are direct. These data and the evidence from human patient tumor analysis strengthens our hypothesis that p11 plays a development-independent role in tumor growth and progression. Our future studies are focused on investigating the role of p11 in mammary gland development.

Quantitative PCR validation of microarray gene data confirmed the significant downregulation of *Areg*, *Muc1*, and *S100a8* genes in PyMT/p11-KO tumors. *Areg* (amphiregulin), a player in breast cancer proliferation, is abundant in the pubertal mammary gland and loss of *Areg* in mice results in stunted ductal morphogenesis. Our observation of decreased early mammary ductal morphogenesis might be due to the loss of *Areg* expression [53]. Loss of transmembrane glycoprotein *Muc1* results in significant delay in tumor progression and metastasis [54], consistent with delayed progression to malignancy displayed by PyMT/p11-KO tumors. *S100a8* is elevated in ER- and HER2+ subtypes of breast cancer and contributes towards cancer cell survival and metastasis [55], thereby contributing to delayed progression of PyMT/p11-KO tumors. It is unclear whether p11 plays a direct or indirect role in regulating these genes in vivo, or whether the alteration of these genes are markers of tumor growth and progression.

We also compared the levels of inflammatory modulators in PyMT/p11WT and PyMT/p11-KO tumors that might impact macrophage infiltration. The *Csf1*- gene, implicated in the proliferation, differentiation, and recruitment of macrophages in breast cancer [37], was unchanged. We saw a significant increase in *Csf2* expression in PyMT/p11-KO tumors but *Csf2* has not been shown to correlate with macrophage infiltration in breast tumors. We also observed a significant increase in cytokines such as *Ifn- γ* , *Il-6*, and *Il-10*. *Il-6* positively correlates with breast cancer progression and development of metastasis [56]. Studies on the role of *Il-10* in breast cancer showed contradicting results [56]. *Ifn- γ* plays an important role in antitumor immunity and tumor suppressive phenotype via the JAK/STAT pathway. It is possible that the tumor suppressive phenotype observed in the PyMT/p11-KO mice is ascribed to the increase in tumor suppressive cytokines such as *Il-10* and *Ifn- γ* .

Previous gene expression studies showed that p11 correlated to poor overall survival in basal-like breast cancer (reviewed in [57]). In elucidating the prognostic role of p11 in human breast cancer, we found that p11 mRNA (microarray) was overexpressed in human breast tumors, correlated positively with overall survival and recurrence-free survival, and was increased in high grade tumors compared to low grade tumors and normal tissue. P11 was highly expressed in TN breast cancer, ER+, and HER2+, suggesting a role in breast cancer progression. Interestingly, expression of p11 protein (IHC) was significantly elevated in tumor cells compared to normal mammary epithelium, but we did not observe any correlation between high p11 expression and clinical and pathological tumor grade or with molecular subtype in human breast cancer samples. The lack of consistency between our gene expression profiling and IHC data could be due to two reasons. First, microarray analysis was performed in tumors containing stroma and hence the increased p11 expression includes contribution from the tumor microenvironment (Figure 7A–E). Second, we conducted p11 immunostaining only in a small cohort of patient samples with a small sample size for ER+ and HER2+ tumors (Figure 7F–H and Figure S7), where the H-scores were ascribed based on the staining intensity in the tumor cells. Future studies will be aimed at increasing the sample size for IHC or by using a tissue microarray analysis and evaluating the expression pattern in the stroma. Overall, p11 expression was completely restricted to the stromal cells in the PyMT mouse model, whereas expression was seen in human tumor cells. This difference can potentially be attributed to the nature of oncogene and mutations between the murine and human breast tumors.

4. Materials and Methods

4.1. Mice

All animal experiments were performed according to protocol approved by the University Committee on Laboratory Animals, Dalhousie University, Canada. The C57Bl6 MMTV-PyMT mice were obtained from Dr. Mak (UHN, Toronto, Canada). The p11 WT and p11 KO mice were obtained from P. Svenningsson (Karolinska Institutet, Solna, Sweden). We employed a sequential breeding strategy to generate PyMT/p11-KO homozygous mice. We crossed the male PyMT/p11-WT mice with the female p11 KO mice to obtain heterozygotes for p11. The resultant F1 (PyMT/p11+/-) males were bred with the female (p11+/-) mice. This crossbreeding produced F2 females PyMT/p11-WT, (PyMT/p11+/-) and PyMT/p11-KO. Virgin female C57BL/6 mice heterozygous for the MMTV-PyMT transgene and homozygous KO (PyMT/p11-KO) or homozygous WT (PyMT/p11-WT) for the p11 gene were used in our studies. Genotyping of mice was performed by PCR of genomic DNA derived from ear clippings using published primers for PyMT and p11 (Table S1).

4.2. Cell Culture and Reagents

Py8119 cells were obtained from American Type Culture Collection (ATCC) and maintained in F12 Kaign's medium (Hyclone, Logan, UT, USA) with 5% Fetal Clone II serum (ThermoFisher Scientific, Waltham, MA, USA), 1% penicillin and streptomycin. Py8119 cells were tested for pathogen (Charles River Laboratory, Wilmington, MA, USA) before injecting into the mice. All cells were tested for mycoplasma (Lonza Mycoalert kit, Morristown, NJ, USA) and only mycoplasma-free cells were used.

4.3. Whole Mount Analysis

The harvested tissues were stretched and placed onto a cassette matrix and fixed overnight in Carnoy's fixative. The tissues were sequentially hydrated with 70%, 50%, 25% ethanol, followed by a final water wash. They were stained with carmine alum solution for four hours, followed by sequential dehydration in 70%, 95%, and 100% ethanol, and defatting of the tissues was carried out in two xylene washes for 30 min and overnight. The dehydrated and defatted tissues were then mounted on slides using Cytoseal (Richard-Allan Scientific, Thermo Scientific, Waltham, MA, USA) mounting medium. The slides were digitally imaged using a stereomicroscope under similar lighting and contrast conditions (Zeiss microscope).

4.4. Tumor Measurements

For the spontaneous PyMT tumor model, all the mammary glands were palpated once a week for 20–25 weeks to monitor tumor latency and progression. For evaluating the kinetics of tumor growth, the tumors were measured using Vernier calipers, and tumor volume was determined using the standard calculation for a hemi-ellipsoid; $0.5ab^2$, where a is the smaller and b is the larger diameter. Tumor burden was calculated at the endpoint (20 weeks) by determining the total tumor weight/body weight. We determined the percentage of tumor-free mice using Kaplan–Meier analysis (Graph pad prism, La Jolla, CA, USA) in the two PyMT mice groups. Animals were considered tumor-free until a palpable mass (>4.0 mm) persisted for longer than four days. All tumor growth and kinetics data were obtained from three independent experiments. Only virgin female mice were used for all the experiments.

4.5. Spontaneous and Experimental Metastasis Quantification

For evaluation and assessment of lung metastasis, lungs were harvested at 20 weeks, fixed in 10% buffered formalin for 48 h, and embedded in paraffin. The lungs were cut at 5 μ m thickness and 3–6 sections from each lung at 100 μ m apart were stained with H&E. The stained slides were scanned using Aperio microscope (Leica Biosystems, Concord, ON, Canada) and the number of metastatic

foci were counted using Imagescope (Leica Biosystems, Concord, ON, Canada). The total metastatic burden was determined using Imagescope by tracing the metastatic area as a ratio of the total lung area. For experimental metastasis assay, Py8119 cells were injected via the tail vein at a density of 2.5×10^5 cells. The lungs were harvested 14 days after injection and analyzed for metastatic burden and foci calculation as described for spontaneous metastasis quantification.

4.6. Tissue Processing and Immunohistochemistry

Tumors, mammary glands, and lungs were harvested and fixed in neutral 10% buffered formalin for 48 h and stored in 70% ethanol before embedding in paraffin. The embedded tissues were cut into 5 μ m thick sections, stained with H&E for pathological analysis, and adjacent sections were used for IHC. The tissue sections were deparaffinized with sequential washes in xylene, 100%, 95%, and 70% ethanol followed by water wash. The details of the antibody dilution, method of chromogen, and stain development are provided in the Table S2.

Antigen retrieval was performed by heat treatment using a pressure cooker in either Tris-EDTA (pH 9.0) or citrate buffer (pH 6.0). The slides were rinsed in Tris-buffered-saline (TBS) or Phosphate Buffered Saline (PBS), depending on the antibody and blocked with Rodent Block M (Biocare, Pacheco, CA, USA). The primary antibodies CD31, Ki67, smooth muscle α -actin (α -SMA), p11, F4/80, were incubated overnight at room temperature followed by secondary antibody and chromogen steps. For anti-rat, the slides were washed with TBS after primary incubation, followed by 15 min incubation with rat probe, subsequently the slides were washed and incubated with Rat on mouse HRP polymer for 15 min (Biocare, Pacheco, CA, USA), followed by three washes with TBS and stained with DAB (Biocare, Pacheco, CA, USA) and counter stained with hematoxylin. For anti-rabbit secondary antibodies, the slides were incubated with goat anti-rabbit secondary (Envision, DAKO, Beijing, China) for 30 min, followed by washes with TBS and counterstained with hematoxylin. For anti-mouse antibody, we used mouse-on-mouse HRP polymer kit (Biocare, Pacheco, CA, USA) and anti-goat antibodies we used rabbit-anti goat HRP polymer (DAKO), followed by staining with DAB and counterstaining with hematoxylin. All stained sections were washed in water and mounted with aqueous mounting medium (Vectamount, MJS Biolynx Inc., Brockville, ON, Canada). The immunostained sections were imaged using Zeiss Axio Imager Z1 W/color and monochrome camera (p11, Ki67, CD31, F4/80, α -SMA, H&E, CD3, and TUNEL staining) using 40X (for manual counting—F4/80, Ki67, CD3) and 20X for representation. To count the number of CD31 positive vessels, we scanned the slides using Aperio Scanning system, following which CD31-positive vessels were counted from 7–10 snapshots of random fields. To quantify the number of Ki67 positive, F4/80, CD3-positive, TUNEL positive, we captured images using Zeiss Axio Imager Z1 microscope, and manually counted the positive cells using the Zen software in 7–10 fields. The average of 7–10 fields for Ki67, CD31, and F4/80, was used for each mouse in the quantification bar graph. For human p11 staining, we followed the same procedure as for mouse tissues, but blocking was performed with Background Terminator (Biocare, Pacheco, CA, USA) for 10 min before incubating with primary antibody.

4.7. Gene Expression Profiling (Mouse Tumors)

Sample preparation, amplification, and hybridization to the Affymetrix Mouse gene 2.0 ST array, and data collection were performed by The Centre for Applied Genomics at the Hospital for Sick Children (Toronto, ON, Canada). The Transcriptome Analysis Console software (Thermo Fisher Scientific, Waltham, MA, USA) was used to normalize data and calculate fold changes in expression (GSE151579). Genes up- or downregulated by more than 2-fold ($\log_2 = 0.678$) at a significance level of $p < 0.05$ were considered differentially expressed.

4.8. Gene Expression Profiling (Human Tumors)

The gene expression microarray dataset was generated from a human breast cancer cohort consisting of 176 treatment-naïve primary tumor samples as previously described [58] (GSE22820).

Patient material and clinical information were collected under Research Ethics Board Protocol ETH-02-86-17. Patients received standardized guideline-based chemo and hormone therapies: i.e., hormone therapy for all patients with ER-positive tumors, trastuzumab for those with HER2-overexpression tumors, anthracycline chemotherapy for high risk node-negative disease, and anthracycline plus taxane chemotherapy for node-positive disease. The median follow-up time for surviving patients was 4.5 years.

4.9. Quantitative Polymerase Chain Reaction (Mouse Tumors)

Tumors from PyMT/p11-WT and PyMT/p11-KO mice at 20 weeks of age were excised, snap frozen in liquid nitrogen, and stored at -80°C . Total RNA was extracted using Trizol (Invitrogen, Thermofisher Scientific, Waltham, MA, USA) and the PureLink RNA kit (Invitrogen, Thermofisher Scientific, Waltham, MA, USA) with DNase treatment. Equal amounts of RNA ($0.5\ \mu\text{g}$) were reverse transcribed using iScript (BioRad, Mississauga, ON, Canada); qPCR reactions were performed with SsoAdvanced Universal SYBR Supermix (BioRad, Mississauga, ON, Canada) and gene-specific mouse primers (Table S2) on a CFX96 or CFX384 Touch Real-Time PCR Detection system (BioRad, Mississauga, ON, Canada). Standard curves for each primer set were generated, and primer efficiencies were incorporated into the CFX Manager software (BioRad, Mississauga, ON, Canada). mRNA expression of all samples was calculated using the $\Delta\Delta\text{Ct}$ method, with gene of interest made relative to two reference genes (rlp10 and PyMT) and an indicated control sample. Relative mRNA expression was \log_{-2} transformed prior to plotting and statistical analysis.

4.10. Human Patient Breast Tissue Collection, p11 Immunohistochemistry, and H-Score Assignment

Anatomical pathology electronic files (Cerner Millennium) for the Queen Elizabeth II Health Sciences Centre, Nova Scotia Health Authority (NSHA) were retrospectively searched for a cohort of invasive and in situ breast carcinomas beginning 1 January 2011. One formalin-fixed paraffin-embedded (FFPE) tumor block and one FFPE block of normal breast tissue were selected from each patient of an identified cohort of 119 patients. For this study, FFPE breast tissues were used with approval from the Nova Scotia Health Authority Research Ethics Board, and Materials Transfer and Collaboration Agreement between the NSHA and Dalhousie University. P11 immunostaining on patient tissue sections was performed as described earlier [16], using anti-rabbit polyclonal antibody to human p11 (Proteintech, Rosemont, IL, USA).

The stained sections were evaluated and assigned a semiquantitative score by a pathologist (PJB) in a blinded fashion based on percentage of positive cells and intensity of staining. The percentage of cells were identified as negative, weak, moderate, and strong for membrane staining in tumor cells. An H-score of less than 10% was considered negative. The H-score was determined using the formula ($\% \text{ negative} \times 0 + \% \text{ weak} \times 1 + \% \text{ moderate} \times 2 + \% \text{ strong} \times 3$). The semiquantitative H-score values ranged at 5–250. Nottingham grade 1 and 2 tumors were combined as ‘low grade’ and Nottingham grade 3 tumors were labeled ‘high grade’. A scatter plot was generated based on tumor grade (high and low grade, including samples from the molecular subtype category), tumor type (ductal carcinoma in situ (DCIS), variants of invasive ductal carcinoma and invasive lobular carcinoma, also including samples from the molecular subtype categories), and molecular subtype (estrogen receptor positive (ER+), Her2+, triple negative (TN)).

4.11. Isolation of Mouse PyMT Tumor Cell Lines

PyMT tumors from 20-week mice were excised and rinsed in (PBS), minced in RPMI with 5% FBS with penicillin and streptomycin containing 1 mg/mL of collagenase (Sigma, Oakville, Ontario, Canada). The tumor preparation was then incubated at 37°C for 1–2 h, followed by straining through a 70-micron mesh strainer. The cells were washed with Dulbecco’s Modified Eagle’s Medium (DMEM) with 10% FBS, passaged once and used in plasmin generation assays as described below. In some cases,

isolated cells were directly plated in 96-well plate without passaging and plasmin generation assay was performed as described.

4.12. Plasmin Generation Assay

Plasmin generation assay was determined in PyMT tumor homogenates. We employed fresh and frozen 20-week old PyMT tumors from PyMT/p11-WT and PyMT/p11-KO mice to prepare tumor homogenates. Briefly the tumors were homogenized in electric homogenizer (Pro Scientific, Oxford, CT, USA) in Dulbecco's phosphate-buffered saline (DPBS) with 1% Triton. We used 30–60 µg of protein for the assay. Plasmin generation assay was conducted as described in [19,44].

4.13. Immunoblotting

Immunoblotting was performed as described in [59] and anti-mouse p11 antibody (R&D systems, Minneapolis, MN, USA) and β-tubulin (Sigma, Mississauga, ON, Canada) was used for immune staining (details in Table S2).

4.14. Statistical Analysis

Three independent experiments with varying mice numbers in each were performed. For evaluation of total palpable tumors (tumor onset), tumor-free mice (survival), tumor growth (volume) and metastasis, we pooled the data/measurements from the three independent experiments. For determination of end-point tumor and metastatic burden and foci, we used data from one independent experiment (20-week endpoint). For time course measurements (whole mounts, tumor progression), we employed 3–12 mice at each endpoint. All statistical analyses were performed using Graph pad prism 5 software (La Jolla, CA, USA). Unless indicated in the figure legends, statistical significance was determined using the Mann Whitney non-parametric test for significantly different variances. * $p < 0.05$, ** $p < 0.01$, *** $p < 0.001$, **** $p < 0.0001$. Proportions were compared by χ^2 test. A significance threshold of $p < 0.05$ was used.

For human patient samples, all statistical analyses for gene expression profiling were performed using MedCalc Version 14.12.0 (MedCalc Software). Gene expression microarray signal intensity values were log-transformed to better fit the normal distribution assumption. One-way ANOVA was employed to test the statistical significance for the difference in S100A10 mRNA levels among molecular subtypes, tumor histologic grades, or Ki67 immunoreactivity classifications. Prognostic significance was analyzed using log rank test on Kaplan–Meier survival probabilities.

5. Conclusions

Our current study is the first comprehensive study using a transgenic mouse model to examine the role of p11 in breast cancer. The novel finding of this study is that p11 potentially plays a role in mammary gland development and future studies are aimed at delineating the mechanistic role of p11 in ductal branching morphogenesis and mammary gland development. Overall, our studies demonstrated that p11 plays a causal, complex, and definitive role in breast tumor development, progression, and metastasis, possibly via p11-dependent macrophage migration and tumor infiltration and regulation of tumor associated cytokines and genes involved in tumor progression. Surprisingly, our results suggest that stromal and not cancer cell p11 is crucial for mediating these effects specifically in the PyMT model. Since the majority of p11 was expressed by the stromal cells in the tumor periphery, our study also highlights the importance of tumor–stroma interactions and signaling for breast tumor progression. Further studies are required to conclusively demonstrate that p11 can be employed as a biomarker with diagnostic and prognostic value in breast cancer.

Supplementary Materials: The following are available online at <http://www.mdpi.com/2072-6694/12/12/3673/s1>, Figure S1: Loss of p11 affects multi-focal dysplastic lesions. Figure S2: Loss of p11 affects early stage mammary gland development. Figure S3: Loss of p11 delays progression to late carcinoma–H&E and α-smooth muscle actin IHC. Figure S4: Loss of p11 does not impact cell-death/apoptosis and T-cell infiltration. Figure S5: Loss of p11 does not decrease plasmin generation in PyMT tumors and cell lines. Figure S6: Gene expression profiling of

PyMT/p11-WT and PyMT/p11-KO tumors. Figure S7: IHC staining of p11 in human tissue sections. Figure S8: IHC staining of p11 and F4/80 in the PyMT/p11-WT tumors. Table S1: Sequences of primers employed in the q-PCR validation of microarray hits, q-PCR expression of cytokine in PyMT tumors and genotyping for PyMT and p11. Table S2: Antibodies used for immunoblotting and IHC. S1 File. Microarray hits for PyMT mouse tumor gene expression profiling. This file in an excel spread sheet listing all the hits obtained from gene expression profiling of PyMT tumors.

Author Contributions: Conceptualization: A.G.B., M.L.D., D.M.W.; Data Curation: A.G.B., M.L.D., R.-Z.L., D.M.W.; Formal Analysis: A.G.B., M.L.D., R.-Z.L., D.M.W.; Funding Acquisition: D.M.W.; Investigation: A.G.B., M.L.D., R.-Z.L., P.C., R.W.H., L.N.T., D.M.W.; Methodology: A.G.B., M.L.D., R.-Z.L., P.C., R.W.H., L.N.T., D.M.W.; Project Administration: D.M.W.; Resources: A.G.B., M.L.D., R.-Z.L., P.C., L.N.T., R.G., P.J.B., C.K.L.T., P.M., D.M.W.; Software: Supervision: P.A.M., R.G., P.J.B., C.K.L.T., P.M., D.M.W.; Validation: A.G.B., M.L.D., R.W.H., D.M.W.; Visualization: A.G.B., M.L.D., R.-Z.L., D.M.W.; Writing–Original Drafts: A.G.B., D.M.W.; Writing–Reviewing and Editing: A.G.B., M.L.D., R.-Z.L., P.C., L.N.T., P.A.M., C.K.L.T., P.J.B., R.G., P.M., and D.M.W. All authors have read and agreed to the published version of the manuscript.

Funding: A.G.B is supported by a trainee award from the Beatrice Hunter Cancer Research Institute with funds provided by the Harvey Graham Cancer Research Fund as part of The Terry Fox Strategic Health Research Training Program in Cancer Research at CIHR. M.L.D. is supported by CGS-D award from the CIHR, a Nova Scotia Health Research Foundation studentship, a Nova Scotia Research and Innovation Graduate scholarship, a Beatrice Hunter Cancer Research Institute Cancer Research Training Program studentship, and a Killam Laureate scholarship. P.A.M. is supported by funding from Dalhousie Medical Research Foundation (DMRF) and Breast Cancer Society of Canada (BCSC). R.G. is supported by a grant from Canadian Cancer Research Institute (grant No. 705455). C.K.L.T. is supported Canadian Breast Cancer Foundation/Atlantic, Canadian Cancer Society and Breast Cancer Society of Canada, QEII Foundation, Beatrice Hunter Cancer Research Institute, P.J.B. is supported by Breast Cancer Society of Canada, QEII Foundation, Beatrice Hunter Cancer Research Institute. P.M. is supported by CIHR, PJT 162313. D.M.W. and this research is supported by a grant from the CIHR.

Acknowledgments: The authors would like to thank Allison Glover, Eva Rogerson, Erica Meehan, Allison Letcher for their technical support. We would also like to thank Victoria Miller for their thoughtful comments and discussions.

Conflicts of Interest: The authors declare that they have no conflicts of interest with the contents of this article.

Ethics Declarations: All animal experiments were performed according to protocol approved by University Committee on Laboratory Animals, Dalhousie University, Halifax, NS, Canada.

Ethics Approval and Consent to Participate: Patient material and clinical information were collected under Research Ethics Board Protocol ETH-02-86-17.

References

1. Lambert, A.W.; Pattabiraman, D.R.; Weinberg, R.A. Emerging Biological Principles of Metastasis. *Cell* **2017**, *168*, 670–691. [[CrossRef](#)] [[PubMed](#)]
2. Behrendt, N.; Høyer-Hansen, G.; Johnsen, M.; Lund, L.R.; Ploug, M.; Rømer, J.; Danø, K. Plasminogen activation and cancer. *Thromb. Haemost.* **2005**, *93*, 676–681. [[CrossRef](#)]
3. Sevenich, L.; Joyce, J.A. Pericellular proteolysis in cancer. *Genes Dev.* **2014**, *28*, 2331–2347. [[CrossRef](#)] [[PubMed](#)]
4. Almholt, K.; Green, K.A.; Juncker-Jensen, A.; Nielsen, B.S.; Lund, L.R.; Rømer, J. Extracellular proteolysis in transgenic mouse models of breast cancer. *J. Mammary Gland Biol. Neoplasia* **2007**, *12*, 83–97. [[CrossRef](#)]
5. Madureira, P.A.; O’Connell, P.A.; Surette, A.P.; Miller, V.A.; Waisman, D.M. The biochemistry and regulation of S100A10: A multifunctional plasminogen receptor involved in oncogenesis. *J. Biomed. Biotechnol.* **2012**, *2012*, 353687. [[CrossRef](#)] [[PubMed](#)]
6. Kwon, M.; MacLeod, T.J.; Zhang, Y.; Waisman, D.M. S100A10, annexin A2, and annexin a2 heterotetramer as candidate plasminogen receptors. *Front. Biosci. J. Virtual Libr.* **2005**, *10*, 300–325. [[CrossRef](#)] [[PubMed](#)]
7. Kassam, G.; Le, B.-H.; Choi, K.-S.; Kang, H.-M.; Fitzpatrick, S.L.; Louie, P.; Waisman, D.M. The p11 Subunit of the Annexin II Tetramer Plays a Key Role in the Stimulation of t-PA-Dependent Plasminogen Activation. *Biochemistry* **1998**, *37*, 16958–16966. [[CrossRef](#)] [[PubMed](#)]
8. Kassam, G.; Choi, K.S.; Ghuman, J.; Kang, H.M.; Fitzpatrick, S.L.; Zackson, T.; Toba, M.; Shinomiya, A.; Waisman, D.M. The role of annexin II tetramer in the activation of plasminogen. *J. Biol. Chem.* **1998**, *273*, 4790–4799. [[CrossRef](#)]

9. Miller, V.A.; Madureira, P.A.; Kamaludin, A.A.; Komar, J.; Sharma, V.; Sahni, G.; Thelwell, C.; Longstaff, C.; Waisman, D.M. Mechanism of plasmin generation by S100A10. *Thromb. Haemost.* **2017**, *117*, 1058–1071. [[CrossRef](#)]
10. MacLeod, T.J.; Kwon, M.; Filipenko, N.R.; Waisman, D.M. Phospholipid-associated annexin A2-S100A10 heterotetramer and its subunits: Characterization of the interaction with tissue plasminogen activator, plasminogen, and plasmin. *J. Biol. Chem.* **2003**, *278*, 25577–25584. [[CrossRef](#)]
11. Bharadwaj, A.; Bydoun, M.; Holloway, R.; Waisman, D. Annexin A2 heterotetramer: Structure and function. *Int. J. Mol. Sci.* **2013**, *14*, 6259–6305. [[CrossRef](#)]
12. Noye, T.M.; Lokman, N.A.; Oehler, M.K.; Ricciardelli, C. S100A10 and Cancer Hallmarks: Structure, Functions, and its Emerging Role in Ovarian Cancer. *Int. J. Mol. Sci.* **2018**, *19*, 4122. [[CrossRef](#)] [[PubMed](#)]
13. Choi, K.-S.; Fogg, D.K.; Yoon, C.-S.; Waisman, D.M. p11 regulates extracellular plasmin production and invasiveness of HT1080 fibrosarcoma cells. *FASEB J. Off. Publ. Fed. Am. Soc. Exp. Biol.* **2003**, *17*, 235–246. [[CrossRef](#)] [[PubMed](#)]
14. Zhang, L.; Fogg, D.K.; Waisman, D.M. RNA interference-mediated silencing of the S100A10 gene attenuates plasmin generation and invasiveness of Colo 222 colorectal cancer cells. *J. Biol. Chem.* **2004**, *279*, 2053–2062. [[CrossRef](#)] [[PubMed](#)]
15. Bydoun, M.; Sterea, A.; Weaver, I.C.G.; Bharadwaj, A.D.; Waisman, D.M. A novel mechanism of plasminogen activation in epithelial and mesenchymal cells. *Sci. Rep.* **2018**, *8*, 14091. [[CrossRef](#)] [[PubMed](#)]
16. Bydoun, M.; Sterea, A.; Liptay, H.; Uzans, A.; Huang, W.; Rodrigues, G.J.; Weaver, I.C.; Gu, H.; Waisman, D.M. S100A10, a novel biomarker in pancreatic ductal adenocarcinoma. *Mol. Oncol.* **2018**, *12*, 1895–1916. [[CrossRef](#)]
17. O’Connell, P.A.; Surette, A.P.; Liwski, R.S.; Svenningsson, P.; Waisman, D.M. S100A10 regulates plasminogen-dependent macrophage invasion. *Blood* **2010**, *116*, 1136–1146. [[CrossRef](#)]
18. Surette, A.P.; Madureira, P.A.; Phipps, K.D.; Miller, V.A.; Svenningsson, P.; Waisman, D.M. Regulation of fibrinolysis by S100A10 in vivo. *Blood* **2011**, *118*, 3172–3181. [[CrossRef](#)]
19. Phipps, K.D.; Surette, A.P.; O’Connell, P.A.; Waisman, D.M. Plasminogen receptor S100A10 is essential for the migration of tumor-promoting macrophages into tumor sites. *Cancer Res.* **2011**, *71*, 6676–6683. [[CrossRef](#)]
20. Sato, K.; Saiki, Y.; Arai, K.; Ishizawa, K.; Fukushige, S.; Aoki, K.; Abe, J.; Takahashi, S.; Sato, I.; Sakurada, A.; et al. S100A10 upregulation associates with poor prognosis in lung squamous cell carcinoma. *Biochem. Biophys. Res. Commun.* **2018**, *505*, 466–470. [[CrossRef](#)]
21. Katono, K.; Sato, Y.; Jiang, S.-X.; Kobayashi, M.; Saito, K.; Nagashio, R.; Ryuge, S.; Satoh, Y.; Saegusa, M.; Masuda, N. Clinicopathological Significance of S100A10 Expression in Lung Adenocarcinomas. *Asian Pac. J. Cancer Prev.* **2016**, *17*, 289–294. [[CrossRef](#)] [[PubMed](#)]
22. Gocheva, V.; Naba, A.; Bhutkar, A.; Guardia, T.; Miller, K.M.; Caroline, K.-K.; Dayton, T.L.; Sanchez-Rivera, F.J.; Kim-Kiselak, C.; Jailkhani, N.; et al. Quantitative proteomics identify Tenascin-C as a promoter of lung cancer progression and contributor to a signature prognostic of patient survival. *Proc. Natl. Acad. Sci. USA* **2017**, *114*, E5625–E5634. [[CrossRef](#)] [[PubMed](#)]
23. McKiernan, E.; McDermott, E.W.; Evoy, D.; Crown, J.; Duffy, M.J. The role of S100 genes in breast cancer progression. *Tumour Biol. J. Int. Soc. Oncodevelopmental. Biol. Med.* **2011**, *32*, 441–450. [[CrossRef](#)]
24. Yu, M.; Bardia, A.; Wittner, B.S.; Stott, S.L.; Smas, M.E.; Ting, D.T.; Isakoff, S.J.; Ciciliano, J.C.; Wells, M.N.; Shah, A.M.; et al. Circulating breast tumor cells exhibit dynamic changes in epithelial and mesenchymal composition. *Science* **2013**, *339*, 580–584. [[CrossRef](#)] [[PubMed](#)]
25. Lin, E.Y.; Jones, J.G.; Li, P.; Zhu, L.; Whitney, K.D.; Muller, W.J.; Pollard, J.W. Progression to Malignancy in the Polyoma Middle T Oncoprotein Mouse Breast Cancer Model Provides a Reliable Model for Human Diseases. *Am. J. Pathol.* **2003**, *163*, 2113–2126. [[CrossRef](#)]
26. Maglione, J.E.; Moghanaki, D.; Young, L.J.; Manner, C.K.; Ellies, L.G.; O’Joseph, S.; Nicholson, B.; Cardiff, R.D.; MacLeod, C.L. Transgenic Polyoma middle-T mice model premalignant mammary disease. *Cancer Res.* **2001**, *61*, 8298–8305. [[PubMed](#)]
27. Fantozzi, A.; Christofori, G. Mouse models of breast cancer metastasis. *Breast Cancer Res. BCR* **2006**, *8*, 212. [[CrossRef](#)]
28. Bugge, T.H.; Lund, L.R.; Kombrinck, K.K.; Nielsen, B.S.; Holmbäck, K.; Drew, A.F.; Flick, M.J.; Witte, D.P.; Danø, K.; Degen, J.L. Reduced metastasis of Polyoma virus middle T antigen-induced mammary cancer in plasminogen-deficient mice. *Oncogene* **1998**, *16*, 3097–3104. [[CrossRef](#)]

29. Almholt, K.; Lærum, O.D.; Nielsen, B.S.; Lund, I.K.; Lund, L.R.; Rømer, J.; Jögi, A. Spontaneous lung and lymph node metastasis in transgenic breast cancer is independent of the urokinase receptor uPAR. *Clin. Exp. Metastasis* **2015**, *32*, 543–554. [[CrossRef](#)]
30. Almholt, K.; Lund, L.R.; Rygaard, J.; Nielsen, B.S.; Danø, K.; Rømer, J.; Johnsen, M. Reduced metastasis of transgenic mammary cancer in urokinase-deficient mice. *Int. J. Cancer* **2004**, *113*, 525–532. [[CrossRef](#)]
31. Almholt, K.; Juncker-Jensen, A.; Laerum, O.D.; Danø, K.; Johnsen, M.; Lund, L.R.; Rømer, J. Metastasis is strongly reduced by the matrix metalloproteinase inhibitor Galardin in the MMTV-PymT transgenic breast cancer model. *Mol. Cancer Ther.* **2008**, *7*, 2758–2767. [[CrossRef](#)] [[PubMed](#)]
32. Juncker-Jensen, A.; Rømer, J.; Pennington, C.J.; Lund, L.R.; Almholt, K. Spontaneous metastasis in matrix metalloproteinase 3-deficient mice. *Mol. Carcinog.* **2009**, *48*, 618–625. [[CrossRef](#)] [[PubMed](#)]
33. Sevenich, L.; Werner, F.W.; Gajda, M.; Schurigt, U.; Sieber, C.; Muller, S.C.; Follo, M.Y.; Peters, C.; Reinheckel, T. Transgenic expression of human cathepsin B promotes progression and metastasis of polyoma-middle-T-induced breast cancer in mice. *Oncogene* **2011**, *30*, 54–64. [[CrossRef](#)] [[PubMed](#)]
34. Vasiljeva, O.; Korovin, M.; Gajda, M.; Brodoefel, H.; Bojic̆, L.; Krüger, A.; Schurigt, U.; Sevenich, L.; Turk, B.; Peters, C.; et al. Reduced tumour cell proliferation and delayed development of high-grade mammary carcinomas in cathepsin B-deficient mice. *Oncogene* **2008**, *27*, 4191–4199. [[CrossRef](#)]
35. Ricciardelli, C.; Frewin, K.M.; Tan, I.D.A.; Williams, E.D.; Opeskin, K.; Pritchard, M.A.; Ingman, W.V.; Russell, D. The ADAMTS1 Protease Gene Is Required for Mammary Tumor Growth and Metastasis. *Am. J. Pathol.* **2011**, *179*, 3075–3085. [[CrossRef](#)]
36. Wyckoff, J.; Wang, W.; Lin, E.Y.; Wang, Y.; Pixley, F.; Stanley, E.R.; Graf, T.; Pollard, J.W.; Segall, J.; Condeelis, J. A Paracrine Loop between Tumor Cells and Macrophages Is Required for Tumor Cell Migration in Mammary Tumors. *Cancer Res.* **2004**, *64*, 7022–7029. [[CrossRef](#)]
37. Lin, E.Y.; Nguyen, A.V.; Russell, R.G.; Pollard, J.W. Colony-stimulating factor 1 promotes progression of mammary tumors to malignancy. *J. Exp. Med.* **2001**, *193*, 727–740. [[CrossRef](#)]
38. Scholzen, T.; Gerdes, J. The Ki-67 protein: From the known and the unknown. *J. Cell Physiol.* **2000**, *182*, 311–322. [[CrossRef](#)]
39. Hüsemann, Y.; Geigl, J.B.; Schubert, F.; Musiani, P.; Meyer, M.; Burghart, E.; Forni, G.; Eils, R.; Fehm, T.; Riethmüller, G.; et al. Systemic spread is an early step in breast cancer. *Cancer Cell.* **2008**, *13*, 58–68. [[CrossRef](#)]
40. Weng, D.; Penzner, J.H.; Song, B.; Koido, S.; Calderwood, S.K.; Gong, J. Metastasis is an early event in mouse mammary carcinomas and is associated with cells bearing stem cell markers. *Breast Cancer Res. BCR* **2012**, *14*, R18. [[CrossRef](#)]
41. Pollard, J.W. Macrophages define the invasive microenvironment in breast cancer. *J. Leukoc. Biol.* **2008**, *84*, 623–630. [[CrossRef](#)] [[PubMed](#)]
42. Pollard, J.W. Tumour-educated macrophages promote tumour progression and metastasis. *Nat. Rev. Cancer.* **2004**, *4*, 71–78. [[CrossRef](#)] [[PubMed](#)]
43. Rumney, R.M.H.; Coffelt, S.B.; Neale, T.A.; Dhayade, S.; Tozer, G.M.; Miller, G. PyMT-MaCLOW: A novel, inducible, murine model for determining the role of CD68 positive cells in breast tumor development. *PLoS ONE* **2017**, *12*, e0188591. [[CrossRef](#)] [[PubMed](#)]
44. Madureira, P.A.; Bharadwaj, A.G.; Bydoun, M.; Garant, K.; O’Connell, P.; Lee, P.; Waisman, D.M. Cell surface protease activation during RAS transformation: Critical role of the plasminogen receptor, S100A10. *Oncotarget* **2016**, *7*, 47720–47737. [[CrossRef](#)]
45. Das, R.; Burke, T.; Plow, E.F. Histone H2B as a functionally important plasminogen receptor on macrophages. *Blood* **2007**, *110*, 3763–3772. [[CrossRef](#)]
46. Miles, L.A.; Lighvani, S.; Baik, N.; Khaldoyanidi, S.; Mueller, B.M.; Parmer, R.J. New Insights into the Role of Plg-RKT in Macrophage Recruitment. *Int. Rev. Cell Mol. Biol.* **2014**, *309*, 259–302.
47. Ichaso, N.; Dilworth, S.M. Cell transformation by the middle T-antigen of polyoma virus. *Oncogene* **2001**, *20*, 7908–7916. [[CrossRef](#)]
48. Denis, D.; Rouleau, C.; Schaffhausen, B.S. A Transformation-Defective Polyomavirus Middle T Antigen with a Novel Defect in PI3 Kinase Signaling. *J. Virol.* **2017**, *91*. [[CrossRef](#)]
49. Riedl, A.; Schleder, M.; Pudelko, K.; Stadler, M.; Walter, S.; Unterleuthner, D.; Unger, D.; Kramer, N.; Hengstschläger, M.; Kenner, L.; et al. Comparison of cancer cells in 2D vs 3D culture reveals differences in AKT-mTOR-S6K signaling and drug responses. *J. Cell Sci.* **2017**, *130*, 203–218. [[CrossRef](#)]

50. Weigelt, B.; Lo, A.T.; Park, C.C.; Gray, J.W.; Bissell, M.J. HER2 signaling pathway activation and response of breast cancer cells to HER2-targeting agents is dependent strongly on the 3D microenvironment. *Breast Cancer Res. Treat.* **2010**, *122*, 35–43. [[CrossRef](#)]
51. Van Nguyen, A.; Pollard, J.W. Colony stimulating factor-1 is required to recruit macrophages into the mammary gland to facilitate mammary ductal outgrowth. *Dev. Biol.* **2002**, *247*, 11–25. [[CrossRef](#)] [[PubMed](#)]
52. Miles, L.A.; Baik, N.; Bai, H.; Makarenkova, H.P.; Kiesses, W.B.; Krajewski, S.; Castellino, F.J.; Valenzuela, A.; Varki, N.M.; Mueller, B.M.; et al. The plasminogen receptor, Plg-RKT, is essential for mammary lobuloalveolar development and lactation. *J. Thromb. Haemost.* **2018**, *16*, 919–932. [[CrossRef](#)] [[PubMed](#)]
53. McBryan, J.; Howlin, J.; Napoletano, S.; Martin, F. Amphiregulin: Role in mammary gland development and breast cancer. *J. Mammary Gland Biol. Neoplasia* **2008**, *13*, 159–169. [[CrossRef](#)] [[PubMed](#)]
54. Nath, S.; Mukherjee, P. MUC1: A multifaceted oncoprotein with a key role in cancer progression. *Trends Mol. Med.* **2014**, *20*, 332–342. [[CrossRef](#)] [[PubMed](#)]
55. Lim, S.Y.; Yuzhalin, A.E.; Gordon-Weeks, A.N.; Muschel, R.J. Tumor-infiltrating monocytes/macrophages promote tumor invasion and migration by upregulating S100A8 and S100A9 expression in cancer cells. *Oncogene* **2016**, *35*, 5735–5745. [[CrossRef](#)] [[PubMed](#)]
56. Méndez-García, L.A.; Nava-Castro, K.E.; Ochoa-Mercado, T.D.L.; Palacios-Arreola, M.I.; Ruiz-Manzano, R.A.; Segovia-Mendoza, M.; Solleiro-Villavicencio, H.; Cázares-Martínez, C.; Montor, J.M. Breast Cancer Metastasis: Are Cytokines Important Players During Its Development and Progression? *J. Interface Cytokine Res.* **2019**, *39*, 39–55. [[CrossRef](#)]
57. Zhang, S.; Wang, Z.; Liu, W.; Lei, R.; Shan, J.; Li, L.; Wang, X. Distinct prognostic values of S100 mRNA expression in breast cancer. *Sci. Rep.* **2017**, *7*, 39786. [[CrossRef](#)]
58. Liu, R.-Z.; Graham, K.; Glubrecht, D.D.; Germain, D.R.; Mackey, J.R.; Godbout, R. Association of FABP5 expression with poor survival in triple-negative breast cancer: Implication for retinoic acid therapy. *Am. J. Pathol.* **2011**, *178*, 997–1008. [[CrossRef](#)]
59. Holloway, R.W.; Thomas, M.L.; Cohen, A.M.; Bharadwaj, A.G.; Rahman, M.; Marcato, P.; Marignani, P.A.; Waisman, D.M. Regulation of cell surface protease receptor S100A10 by retinoic acid therapy in acute promyelocytic leukemia (APL). *Cell Death Dis.* **2018**, *9*, 920. [[CrossRef](#)]







Publisher’s Note: MDPI stays neutral with regard to jurisdictional claims in published maps and institutional affiliations.



© 2020 by the authors. Licensee MDPI, Basel, Switzerland. This article is an open access article distributed under the terms and conditions of the Creative Commons Attribution (CC BY) license (<http://creativecommons.org/licenses/by/4.0/>).

Article

Investigating Radiotherapy Response in a Novel Syngeneic Model of Prostate Cancer

Charles M. Haughey ^{1,2,†}, Debayan Mukherjee ^{3,†} , Rebecca E. Steele ^{1,4} , Amy Popple ³,
Lara Dura-Perez ¹, Adam Pickard ^{1,5} , Mehjabin Patel ³, Suneil Jain ¹, Paul B. Mullan ¹,
Rich Williams ¹, Pedro Oliveira ⁶, Niamh E. Buckley ^{1,7}, Jamie Honeychurch ³,
Simon S. McDade ¹ , Timothy Illidge ^{3,6,*}, Ian G. Mills ^{1,2,*}  and Sharon L. Eddie ^{1,*} 

- ¹ Patrick G Johnston Centre for Cancer Research, Queen's University, Belfast BT9 7AE, UK; charles.haughey@nds.ox.ac.uk (C.M.H.); rebecca.steele@icr.ac.uk (R.E.S.); laraduraperez@gmail.com (L.D.-P.); adam.pickard@manchester.ac.uk (A.P.); s.jain@qub.ac.uk (S.J.); P.Mullan@qub.ac.uk (P.B.M.); rich.williams@qub.ac.uk (R.W.); n.obrien@qub.ac.uk (N.E.B.); S.McDade@qub.ac.uk (S.S.M.)
- ² Nuffield Department of Surgical Sciences, John Radcliffe Hospital, University of Oxford, Oxford OX3 9DU, UK
- ³ Targeted Therapy Group, Division of Cancer Sciences, Faculty of Biology Medicine and Health, The University of Manchester, Manchester M13 9PL, UK; debayan.mukherjee@manchester.ac.uk (D.M.); apopple@microbiotica.com (A.P.); mehjabinpatel94@hotmail.com (M.P.); Jamie.Honeychurch@manchester.ac.uk (J.H.)
- ⁴ The Breast Cancer Now Toby Robins Breast Cancer Research Centre, The Institute of Cancer Research, London SM2 5NG, UK
- ⁵ Wellcome Centre for Cell Matrix Research, University of Manchester, Manchester M13 9PL, UK
- ⁶ The Christie Hospital Foundation Trust, Manchester M20 4BX, UK; Pedro.Oliveira@christie.nhs.uk
- ⁷ School of Pharmacy, Queen's University Belfast, Belfast BT9 7BL, UK
- * Correspondence: tim.illidge@manchester.ac.uk (T.I.); ian.mills@nds.ox.ac.uk (I.G.M.); s.eddie@qub.ac.uk (S.L.E.)
- † Joint first authorship—These authors contributed equally to this work.

Received: 17 August 2020; Accepted: 24 September 2020; Published: 29 September 2020



Simple Summary: Pre-clinical models are required to develop new therapeutics to improve patient care. In the prostate cancer field, significant progress has been made in the development of in vivo models but with a predominant focus on transgenics, which are time and cost prohibitive. Conversely, other available models do not closely resemble patient disease and tumour immune microenvironment. In this study, a new graft-based model is described, using a cell-line derived from a transgenic: the DVL3 model. Grafts using the DVL3 cells retain the pathological and immunological features of localized clinical disease, whilst genetically the model is sustained by poor prognosis drivers of disease progression. Irradiating tumours post-engraftment leads to remodeling of the tumour immune microenvironment and increased expression of genes associated with nucleic acid sensing pathways and the type I interferon response. This paper establishes this model as resource for the pre-clinical characterization of new prostate cancer therapies and biological responses to treatment.

Abstract: The prostate cancer (PCa) field lacks clinically relevant, syngeneic mouse models which retain the tumour microenvironment observed in PCa patients. This study establishes a cell line from prostate tumour tissue derived from the *Pten*^{-/-}/*trp53*^{-/-} mouse, termed DVL3 which when subcutaneously implanted in immunocompetent C57BL/6 mice, forms tumours with distinct glandular morphology, strong cytokeratin 8 and androgen receptor expression, recapitulating high-risk localised human PCa. Compared to the commonly used TRAMP C1 model, generated with SV40 large T-antigen, DVL3 tumours are immunologically cold, with a lower proportion of CD8⁺ T-cells, and high proportion of immunosuppressive myeloid derived suppressor cells (MDSCs), thus resembling high-risk PCa. Furthermore, DVL3 tumours are responsive to fractionated RT, a standard treatment for localised and

metastatic PCa, compared to the TRAMP C1 model. RNA-sequencing of irradiated DVL3 tumours identified upregulation of type-1 interferon and STING pathways, as well as transcripts associated with MDSCs. Upregulation of STING expression in tumour epithelium and the recruitment of MDSCs following irradiation was confirmed by immunohistochemistry. The DVL3 syngeneic model represents substantial progress in preclinical PCa modelling, displaying pathological, micro-environmental and treatment responses observed in molecular high-risk disease. Our study supports using this model for development and validation of treatments targeting PCa, especially novel immune therapeutic agents.

Keywords: tumour microenvironment; syngeneic model; prostate cancer; radiotherapy; preclinical modelling; myeloid-derived suppressor cells

1. Introduction

Prostate cancer (PCa) is the most common cancer in men and the fifth leading cause of cancer deaths [1]. It is estimated that 1.3 million new cases of PCa were diagnosed worldwide in 2018 alone [1]. The vast majority of PCa (91%) is localised disease at diagnosis [2], and can be treated with a range of therapeutic modalities including surgery, androgen-deprivation therapy (ADT) and radiotherapy (RT). Unfortunately, roughly 30% of high-risk localised PCa will develop into aggressive metastatic disease [3], with limited treatment options. The current standard of care for these patients is ADT, but this has many adverse side effects and has a median relapse rate of only 11 months [4].

As a result, efforts have focused on the use of RT, as it can be utilised to treat both localised and metastatic disease, with comparable patient outcomes to radical prostatectomy [5]. However, one major challenge in enhancing RT response, by combining this modality with other treatments, is the paucity of appropriate preclinical PCa models in which to test these combinations. Immune compromised mice are required for xenograft models, thus failing to recapitulate the patient tumour microenvironment (TME) and the critical role the immune component plays in both therapeutic response and relapse of disease.

The most commonly used immune-competent model is the TRAMP C1 murine cell line, which can be syngeneically, subcutaneously grafted to generate more uniform, accessible prostate tumours [6]. The TRAMP C1 model was generated by engineered expression of viral SV40 large T-antigen. Unfortunately, TRAMP C1 allografts develop neuroendocrine tumours which are rare clinically, rather than adenocarcinomas which are most often seen in PCa patients [7].

Consequently, novel PCa models that more accurately recapitulate human tumours and the surrounding TME are urgently required, in order to continue to develop and improve PCa treatment. *PTEN* deletion occurs in ~20% of localized PCa, and is implicated in RT failure [8,9], however, an engraftable mouse syngeneic model with *Pten* deletion, which can be utilised to investigate host response to radiotherapy has long been lacking. In this study we have developed a syngenic model from the *Pten*^{-/-}/*trp53*^{-/-} transgenic mouse tumour [10]; the DVL3 cell line (derived from tumour formed from the dorsal, ventral and lateral prostate lobes. These lobes are most similar to the peripheral zone of the human prostate where 75–85% of adenocarcinomas originate [11]; whereas, the anterior lobe of the mouse prostate is considered analogous to the central zone which rarely develops cancer in the human prostate [12].

DVL3 cells develop tumours in immune competent, C57BL/6 mice that retain morphological, lineage and immune characteristics of localised, high-risk PCa. These tumours respond to RT, retain androgen receptor (AR) expression and sensitivity to androgens, and display an immune ‘cold’ phenotype with tumours being poorly infiltrated by T-cells, and heavily infiltrated with myeloid cells, which is primarily driven by *Pten* loss [13]. Clinically, human prostate cancers are broadly classified as non-T-cell inflamed/ ‘cold’ tumours [14], and PTEN deficiency is associated with an immunosuppressive TME [15]. The DVL3 model accurately mimics both patient disease and TME and

is therefore ideal for future pre-clinical evaluation of novel treatment combinations including immune therapeutic agents.

2. Results

2.1. DVL3 Cell Engraftment in Immunocompetent Mice Results in Tumour Formation, which Accurately Models Human Prostate Adenocarcinoma

Murine cell lines were generated via spontaneous immortalisation of normal prostate epithelium (mPECs) and prostate tumours (DVL3) (Supplementary Figure S1). To establish tumorigenic potential, both mPEC and the DVL3 cells were subcutaneously implanted into wild-type C57BL/6 male mice, as all cell lines were originally generated from the C57BL/6 strain. Engrafted tumour growth rate was compared to the established TRAMP C1 model. Mice engrafted with mPEC cells did not develop any sign of disease after 12 weeks (data not shown), consistent with their status as untransformed, but spontaneously immortalised wild-type prostate epithelial cells. DVL3 tumours grew at a similar rate to the TRAMP C1 model, with measurable tumour established after 4 weeks post-inoculation (Figure 1A). DVL3 tumours displayed heterogeneous pathology with neoplastic, glandular structures akin to human acinar adenocarcinoma (Figure 1B, Supplementary Figure S2A). Some regions of adenocarcinoma were observed in larger, terminal endpoint tumours as previously reported arising from *Pten*^{-/-}/*trp53*^{-/-} Pb-Cre4 mice [10]. In contrast, TRAMP C1 tumours were uniformly undifferentiated and lacked glandular morphology (Figure 1B).

PCa arises from glandular epithelium of the prostate, and retains expression of classical prostate markers including cytokeratins 5 and 8 (CK5 and CK8, basal and luminal epithelial markers respectively) [16]. Immunohistochemical staining revealed that the DVL3 tumours highly expressed CK8 throughout the entire tumour, particularly in the cells surrounding the lumen of glandular structures (representative images in Figure 1B,C with further images in Supplementary Figure S3). DVL3 tumours also had regions of CK5 positivity, with varied expression between the tumours. In comparison the TRAMP C1 tumours lacked the expression of both CK8 and CK5 (Figure 1B,C).

Androgen receptor (AR) was present in the nucleus of cells throughout DVL3 tumours but was most abundant in clustered regions lining the lumen of glandular structures. Conversely, TRAMP C1 tumours had notably less AR staining likely due to fewer glandular structures, with some tumours lacking AR expression entirely (Figure 1B,C, Supplementary Figures S2 and S3). To investigate if AR within the tumours was active, a downstream target of the AR, NKX3.1 expression was evaluated. NKX3.1 is prostate-specific protein, and thus used to identify PCa metastatic disease and is also known to be lost in castrate-resistant PCa [17,18]. Both the DVL3 and the TRAMP C1 tumours were positive for NKX3.1 throughout the tumour section (Supplementary Figures S2B and S3). Expression of CD34, which highlights endothelial cells, was also investigated, with no notable differences observed in staining intensity between the models (Supplementary Figure S2B).

Characterisation of mPEC and DVL3 cell lines was also performed to establish expression in serially passaged cell lines in vitro. qRT-PCR revealed significantly higher mRNA expression of CK5 and CK8 in mPEC and DVL3 cells compared to the TRAMP C1 cells (Figure 1D). Protein expression of CK8 was also notably higher in mPEC and DVL3 cells compared to TRAMP C1 and the DVL3 cells did not express *Pten*, in keeping with their origin (Figure 1E, densitometry provided in Supplementary Figure S4). All models expressed AR at both the mRNA and protein level (Supplementary Figures S2C,D and S4). Although expression of AR was higher in TRAMP C1 cells, DVL3 responded similarly to the AR antagonist (enzalutamide), as demonstrated in vitro using cell viability assay (Supplementary Figure S2E). The expression of CK8 and AR was also validated using immunofluorescence staining (Figure 1F). Interestingly, CK5 protein expression was not detectable in any of the prostate cell models when examined via immunocytochemistry (Figure 1F).

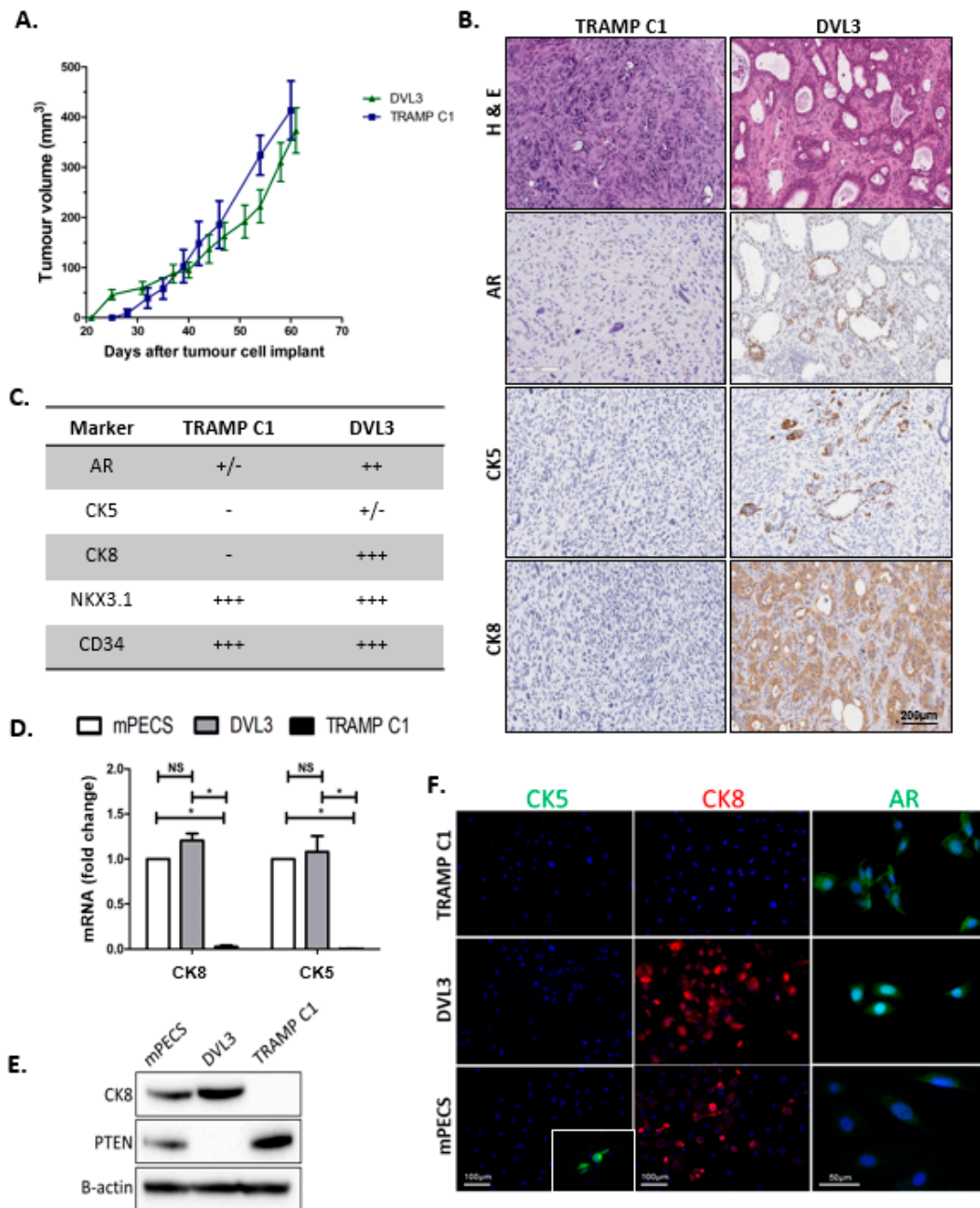


Figure 1. DVL3 syngeneic tumours replicate patient disease. (A) DVL3 tumour growth (Green) is comparable to TRAMP C1 (Blue), $n = 5-8$ mice per group. Both models take ~4 weeks to generate substantial tumours. The mPEC model of normal prostate epithelium did not generate tumours (data not shown) (B) DVL3 tumours develop heterogeneous glandular morphology graded at Gleason 7, whereas TRAMP C1 tumours were undifferentiated with neuroendocrine features (H&E). DVL3 also expressed clinical prostate cancer markers; androgen receptor (AR), cytokeratin 5 (CK5) and cytokeratin 8 (CK8). TRAMP C1 expressed no CK8 or CK5 and less AR than DVL3 tumours, with complete absence of AR noted in some tumours. (C) Summary of histological evaluation of prostate specific markers in DVL3 and TRAMP C1 prostate tumours (- indicates absence, +/- presence in only some of tumour samples, and + indicates the level of positive expression). Both DVL3 and TRAMP C1 express NKX3.1 and CD34 (Supplementary Figure S2). (D) Both novel cell models (mPEC and DVL3) express CK5 and CK8 mRNA at significantly higher levels than TRAMP C1 cells, as analysed via qRT-PCR ($n = 3$ biological replicates per cell type). mRNA expression was normalised to β -actin expression and shown as a fold change relative to

mPECs transcript levels. (E) Expression of CK8 (luminal marker, 60 kDa) was also evident at the protein level. Importantly, DVL3 cells demonstrate loss of the clinically relevant tumour suppressor, Pten (55 kDa). B-actin provided as a loading control (47 kDa). (F) Immunocytochemical staining was consistent with qRT-PCR and western blotting results for CK8 (Red) and AR (Green). CK5 protein (Green) was not detectable in any of the models (MCF7 cells provided as a positive control, inset). Dapi (Blue) used as a counterstain. Data represents mean \pm SEM. * denotes $p \leq 0.05$, NS denotes non-significant, as determined by Student's *t*-test. Immunohistochemistry and western blotting are representative of $n = 3$ biological replicates.

2.2. DVL3 Tumours Have Immunosuppressive Microenvironment Similar to Human Prostate Adenocarcinomas

Human prostate cancers are broadly classified as non-T-cell inflamed/‘cold’ tumours with dysfunctional or suppressed tumour infiltrating lymphocytes (TILs) [14]. Pten deficient prostate cancers are also associated with an immunosuppressive TME [15]. Having established that DVL3 tumours (*Pten*^{-/-}/*trp53*^{-/-}) retained expression of several key markers of human disease, the immunological characteristic of the TME were assessed compared to the TRAMP-C1. Flow cytometry was performed for T cells (CD4+, CD8+), macrophages (F4/80), and myeloid-derived suppressor cells (MDSC), identified as dual (Gr1+/CD11b+) cells in dissociated DVL3 and TRAMP C1 (gating strategy demonstrated in Supplementary Figure S5), at similar size/ tumor volume for baseline immune profiling (Supplementary Figure S6A). The DVL3 tumours have a lower proportion of both cytotoxic CD8 + T-cells (0.187% vs. 2.05%, $p = 0.01$) and CD4 + T-cells (0.36% vs. 4.31%, $p = 0.01$) compared to the TRAMP C1 tumours (Figure 2A,B). In contrast, both tumour lines have comparable level of macrophage (F4/80+) cells (Figure 2C). The DVL3 tumours have a higher proportion of MDSCs (CD11b+/ Gr1+), compared to the TRAMP C1 tumour (16.90% vs 6.61%, $p = 0.04$, Figure 2D).

Interestingly, the DVL3 tumours have higher proportion of MDSCs (CD11b+/Gr1+ cells) compared to other syngeneic mouse models, such as 4T1 (breast cancer) CT26 (colorectal cancer) and 4434 (BRAF^{V600E} melanoma) models ($p = 0.003$, 0.01, and 0.01 respectively, Supplementary Figure S6B,C). Comparison to other syngeneic models was performed using tumours that had reached terminal endpoint and thus were larger in volume. Notably, these data suggest that in the DVL3 model, irrespective of the tumour size, the relative ratio of (CD11b +/Gr1 +) cells within the leukocyte compartment is significantly higher and increases over time or as the tumour develops.

We also evaluated the CD8+ T cell using immunohistochemistry in DVL3 tumours compared to the 4434 melanoma model, which are immunologically active, ‘hot’ tumours [19] (Figure 2E). In agreement with the flow cytometry data (Figure 2A), immunohistochemistry demonstrates the DVL3 tumours are immunologically ‘cold’ having very few basal CD8+ T cells, that were sparsely distributed primarily around the tumour edge, but absent in the centre or around the tumour epithelium/ glandular structures.

In comparison the syngeneic murine melanoma 4434 (BRAF^{V600E}) model had a greater proportion of CD8 + T-cells ($p < 0.001$), which were uniformly distributed, including in the central region of the tumour (Figure 2E,F). These data demonstrate that murine DVL3 prostate tumours have immunologically inactive/ non-inflamed phenotype, with the TME primarily compromising of myeloid cells, but, lacking TILs population similar to the advanced human disease.

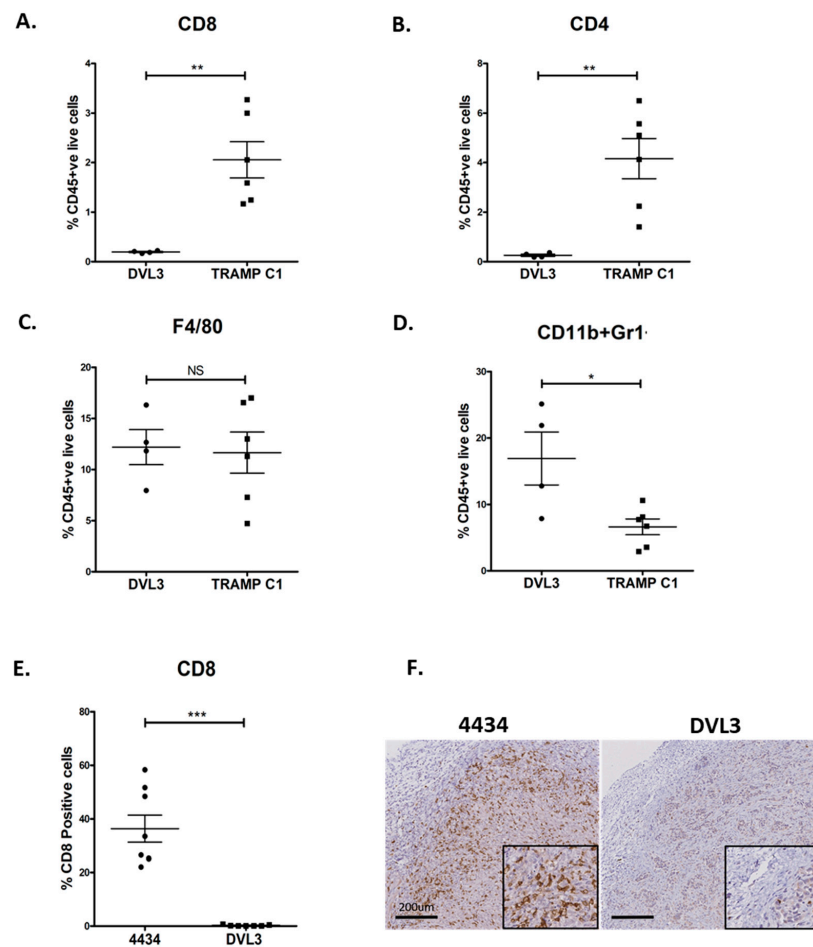


Figure 2. The DVL3 model generates immunosuppressive, ‘cold’ tumours similar to the TME seen clinically in prostate cancer. Flow cytometry was performed on DVL3 and TRAMP-C1 subcutaneous, syngeneic tumours taken 4–6 weeks post engraftment or when they reached the treatment size (100–200 mm³). DVL3 tumours had significantly fewer (A) cytotoxic (CD8+) and (B) helper T cells (CD4+) when compared with the TRAMP-C1 model. (C) There was no difference in the proportion of macrophages (F4/80) between the two models. (D) However, the population of myeloid derived suppressor cells (MDSCs, CD11b+Gr1+) was significantly increased in the DVL3 compared to TRAMP-C1 tumours. (E) Quantification of immunohistochemical staining for CD8+ T-cells in inflamed syngeneic murine (4434 Braf^{4006E}) melanoma model compared to the non-immunogenic DVL3 murine prostate cancer model shown as a percentage of total cells as quantified by haematoxylin. (F) Representative IHC staining comparing 4434 (Braf^{4006E}) melanoma vs DVL3 prostate tumour demonstrating lack of CD8+ T-cells within the tumour microenvironment in the DVL3 tumours. In 4434 (Braf^{4006E}) melanoma model CD8+ T-cells are uniformly distributed, including the central of the tumour. Data represents mean ± SEM of $n = 4–9$ independent murine tumors as indicated by points on each graph. * denotes $p \leq 0.05$, ** denotes $p \leq 0.01$, *** denotes $p < 0.001$ as determined by Mann-Whitney, non-parametric testing.

2.3. Fractionated Radiotherapy Leads to Marginal Growth Delay and Alters the Local Tumour Immune Microenvironment

RT is a radical primary treatment administered to patients with high-risk localised PCa, and also to patients with metastatic PCa. Therefore, therapeutic response to RT was evaluated in the DVL3 model and compared to the TRAMP C1 model. Established tumours (100–200 mm³) were assigned to treatment groups. The mice received either a single high dose of 8 Gy, which is often prescribed to treat PCa patients with metastatic disease; or conventional fractionated RT of 2 Gy administered over 5-consecutive days, which is similar to that used to treat localised disease (Figure 3A). Both single

high dose (8 Gy) and fractionated RT (5 × 2 Gy) exhibited a growth delay compared to non-treated controls (0 Gy, $p = 0.02$, Figure 3B) and this improved survival of mice with engrafted DVL3 tumour cells ($p = 0.03$ and 0.02 respectively, Figure 3C). Conversely, neither the TRAMP C1 tumour size nor survival was significantly affected by either RT regime (Figure 3D,E). This demonstrates DVL3 allograft tumours are responsive to RT, including fractionated RT, whilst TRAMP C1 do not, as previously described (summarized in Figure 3F) [20].

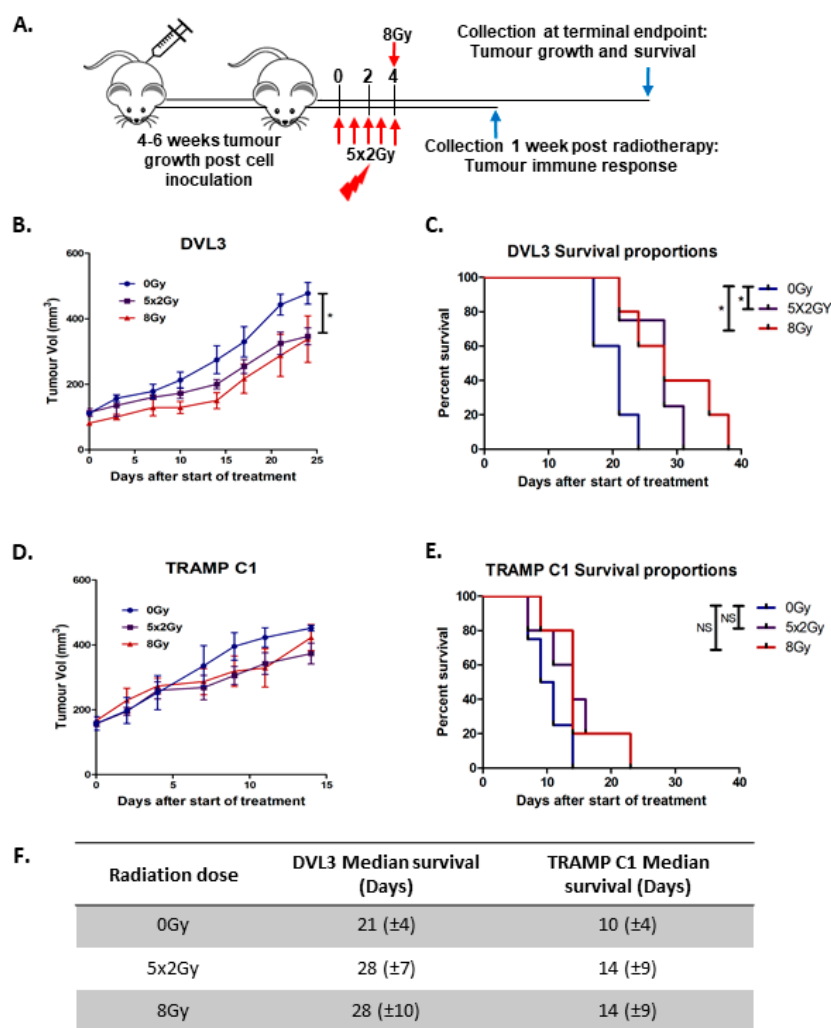


Figure 3. DVL3 tumours respond and are more sensitive to radiotherapy than the resistant TRAMP C1 model. (A) DVL3 or TRAMP C1 cells were engrafted into immune competent mice and allowed to reach a tumour volume of 100–200 mm³. Mice were randomly assigned to no treatment (0 Gy) (Blue), fractionated dose (5 × 2 Gy) (Purple) or single high dose (8 Gy) (Red) radiotherapy (RT) group. A cohort of mice were sacrificed one week after radiotherapy to examine immune response and a further cohort was left to terminal endpoint to examine tumour growth (Figure 1A) and survival. (B) DVL3 tumours were sensitive to fractionated RT but no difference was seen with single high dose RT. (C) Kaplan Meier curves showing survival in mice engrafted with DVL3 tumour cells was improved for both treatment regimens (5 × 2 Gy and 8 Gy) compared to for mice treated with 0 Gy (5 × 2 Gy $p = 0.0255$ and 8 Gy $p = 0.0386$). (D) TRAMP C1 tumours did not respond to radiotherapy. (E) There was no change in survival with radiation in the mice engrafted with TRAMP C1 cells treated with RT. (F) Summary of timeline for DVL3 and TRAMP C1 tumours treated with RT, demonstrating DVL3 tumours are more radiosensitive. Data represents mean ± SEM of $n = 5–8$ mice per treatment group. * denotes $p \leq 0.05$, NS denotes non-significant, as determined by Student’s t -test or log Mantel-cox tests on Kaplan-Meier plots.

2.4. Fractionated Radiotherapy Differentially Upregulated Genes Associated with STING/Type-1 Interferon Signalling and Myeloid Signatures

RT induces immunological changes in tumour cells and can re-calibrate the immune contexture of the tumour microenvironment [21]. In order to establish how fractionated (5×2 Gy) RT altered the tumour immune microenvironment, RNA sequencing analysis was performed on DVL3 tumours excised a week after final dose of RT (Figure 3A). Interestingly, ENRICHR pathway analysis on differentially expressed genes highlighted an enrichment for pathways involved in interferon alpha/beta (IFN- β) signalling ($p < 0.001$), IRF3 mediated activation of type-1 Interferon (IFN) pathway ($p = 0.02$), regulation of innate immune responses to cytosolic DNA ($p < 0.05$), and stimulator of interferon genes (STING) mediated immune response ($p < 0.05$, Figure 4A). RT also led to significant downregulation of pathways involved in extra cellular matrix remodelling, collagen degradation and activation of matrix metalloproteinases (Supplementary Figure S7A).

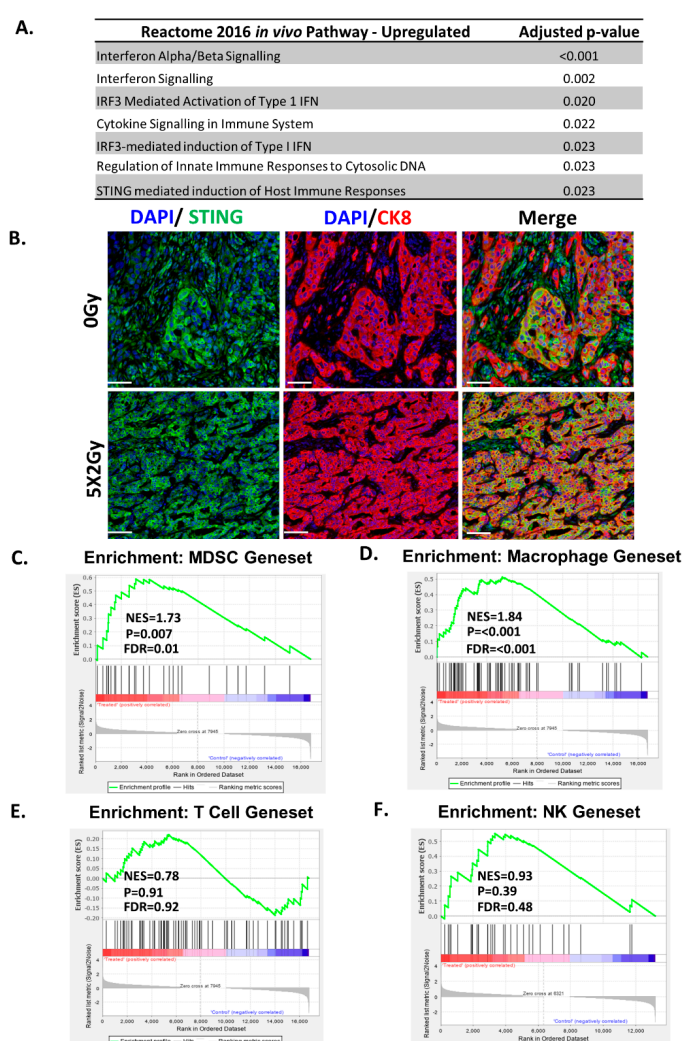


Figure 4. DVL3 immunosuppressive microenvironment enhanced by radiotherapy treatment. (A) Pathway enrichment analysis was performed using the online software Enricher for differential gene expression comparing the fractionated (5×2 Gy) syngeneic tumours to non-irradiated control ($n = 3$ samples per group). Upregulated pathways enrichment in the Reactome 2016 for transcripts with a significance of greater than 0.05 and fold increase of ≥ 1 . Upregulated pathways include interferon signalling and immune response. (B) In keeping with RNA sequencing analysis, STING immunohistochemical analysis (Green) revealed a significant upregulation of expression in response to

RT primarily within glandular epithelium as demonstrated via co-localisation with CK8 (Red). DAPI nuclear counterstain shown in blue. Scale bar equals 50 μm . Image representative of $n = 3$ independent tumour samples. GSEA enrichment analysis of tumours treated with fractionated (5×2 Gy) radiotherapy demonstrates an upregulation of (C) MDSC and (D) macrophage and signatures, but no enrichment of (E) T-cell or (F) NK cell signatures when compared with non-irradiated tumours. NES: normalized enrichment score, FDR: false discovery rate.

In order to establish phenotypic significance of the activation of type-1 IFN-pathway, the expression of STING was evaluated via immunohistochemistry in the irradiated DVL3 tumours. Fractionated RT led to a substantial, but non-significant increase in STING expression compared to non-treated controls (Supplementary Figure S7B). The increase in STING expression was primarily expressed by tumour epithelium in glandular structures. This was confirmed by multiplex immunohistochemistry, demonstrating STING co-localisation primarily in CK8+ tumour cells (Figure 4B, Supplementary Figure S8). Although STING expression was highest in tumour epithelium, this was not exclusive, as STING was also observed in the stromal and other cellular compartments (defined here as CK8 negative areas). Taken together with the RNA seq analysis, our data indicates towards a global upregulation of STING, and associated pathways within the tumour.

STING-dependent cytosolic DNA sensing promotes type-1 interferon response which is critical for activation and influx of MDSC population after radiation [22], and it is well documented that it can also enhance both T-and NK cell activation [23,24]. Therefore, Gene Set Enrichment Analysis (GSEA) was performed using the published gene set for MDSCs signature [25]. In the irradiated DVL3 tumours there was enrichment of the MDSC gene signature (Figure 4C; $p = 0.007$). We also performed GSEA analysis for gene signatures associated with activated macrophages, T-cells and NK cells, however, interestingly our data showed only upregulation of transcripts associated with activated macrophages (Figure 4D; $p < 0.001$), but not the cytotoxic T-cells (CD8) nor the natural killer T-cells or any other associated pathways (Figure 4E,F).

2.5. Fractionated Radiotherapy Resulted in an Increase in Infiltration of Myeloid Cells, but no Changes Were Observed in T-Cell Infiltrates

In order to establish how RT induces phenotypic changes in the immune cell infiltrates in our novel syngeneic tumour model, immunohistochemical staining was performed for T cells and myeloid cells. A marginal increase in natural killer T cells was observed in a portion of irradiated tumours, which predominantly localised around the necrotic areas, defined by morphological assessment and cleaved caspase-3 staining (NKp46, Figure 5A,C, Supplementary Figure S9A). Fractionated RT did not result in a significant change to the macrophage population (F4/80, Figure 5A,D).

Using multiplex immunohistochemistry, T-cell (CD4, CD8) and myeloid cell (CD11b) expression were investigated in excised tumours (Figure 5B). RT did not result in an increase in either CD8+ or CD4+ T cells (Figure 5E,F). However, RT lead to an increase in myeloid cell infiltration (CD11b+) in the irradiated tumours compared to non-treated tumours (23.32% vs. 15.15%, $p = 0.04$, Figure 5G). As the F4/80 macrophage numbers showed no difference after administration of fractionated RT, the increase in CD11b myeloid cells could be due to an increase in either granulocytic and/or monocytic MDSCs.

Next, the expression of program cell-death ligand 1 (PD-L1) was investigated in the irradiated DVL3 tumours [26]. We have previously demonstrated that IFN- γ produced by CD8+ T-cells can cause adaptive upregulation of PD-L1 on tumour cells after delivery of low dose fractionated radiotherapy [27]. RT can also lead to increase in expression of PD-L1 on MDSCs and macrophages as demonstrated previously in a range of tumour models at higher doses [24]. Interestingly, in the DVL3 tumours, fractionated RT had no impact on PD-L1 expression measured as median fluorescence intensity on the surface of tumour cells, MDSCs cell or the macrophages (Supplementary Figure S9B–D).

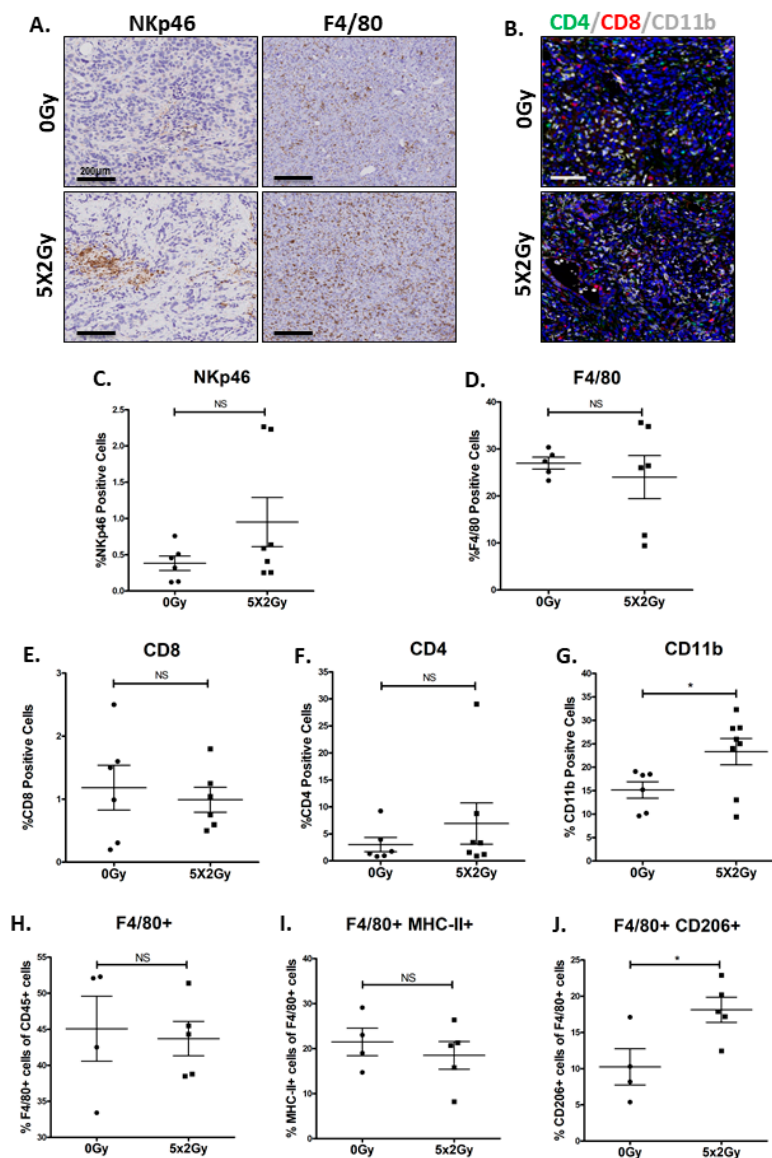


Figure 5. Radiotherapy resulted in an increase in immunosuppressive myeloid cells infiltrates and macrophages acquiring an M2 phenotype in the DVL3 tumours. (A) Representative immunohistochemical staining for natural killer T-cells (Nkp46) and macrophages (F/480) in DVL3 tumours. Nkp46 staining was sparse and mainly localised around the necrotic areas within the tumour. (B). Representative multiplex staining images for CD4 (green), CD8 (red) and CD11b (white) in the DVL3 tumours revealing an increase in CD11b staining in the irradiated tumours. Quantification of immunohistochemical staining comparing untreated (0 Gy) and tumours treated with fractionated radiotherapy (5 × 2 Gy) showed no significant difference in (C) NK-T-cells (Nkp46), (D) macrophages (F4/80), (E) cytotoxic T cells (CD8), or (F) helper T cells (CD4). (G) However, radiotherapy treatment did induce a significant increase in myeloid cells (CD11b+) in the irradiated tumour. (H) Flow cytometry analysis for macrophages (gated as CD45+/F480+) cells showing no significant increase in proportion of cells in the irradiated tumours. (I) Flow cytometry analysis for MHC-II+ cells (M1 marker) on macrophages gated as (CD45+/F480+/ MHC-II+) in the irradiated tumours (J) Flow cytometry analysis for CD206 (Mannose receptor, an M2 marker) on macrophages gated as (CD45+/F480+/CD206+) revealing a significant increase in CD206+ staining in the irradiated tumours (gating strategy in Supplementary Figure S5). Data represents mean ± SEM of $n = 4-8$ independent murine tumours as indicated by points on each graph. * denotes $p \leq 0.05$, NS denotes non-significant, as determined by Student's *t*-test (immunohistochemistry) or Mann-Whitney, nonparametric testing (flow cytometry).

We also investigated whether RT had an impact on macrophage reprogramming from M2 to M1 phenotype. Using flow cytometric analysis, we demonstrate that although there was no significant difference in either the macrophage numbers (Figure 5H) or in the proportion of macrophages expressing MHC-II (an M1 marker) in the irradiated tumour (Figure 5I). However, the macrophages were skewed towards an immunosuppressive M2 phenotype, defined as (F480+/CD206+) cells ($p = 0.03$; Figure 5J). These findings taken together with RNA sequencing data suggest that the activation of type-1 signaling in the irradiated DVL3 tumours could be due to influx of MDSCs and activation of myeloid innate immune response pathway, and not driven by T cells.

3. Discussion

Whilst significant progress has been made in the treatment of metastatic, castration-resistant prostate cancer (CRPC), the majority of these cancers remain incurable. In order to have greater impact, it is important to understand the involvement of the TME in PCa evolution and treatment resistance, so that more effective treatment combinations can be developed for molecular high risk disease. RT remains an important treatment for primary localized PCa, and is increasingly used for treatment for metastatic disease [28–32]. Although both *Pten* and *p53* loss have been implicated in treatment failure, the narrow range of PCa pre-clinical models limits therapeutic development. This study has developed two novel murine cell models; mPECs, which model normal prostate epithelium and the tumorigenic DVL3 cell line derived with genetically relevant drivers (*Pten*^{-/-}/*trp53*^{-/-}) which has been extensively characterized for sensitivity to RT and TME response. Additionally, the mPEC model serves as a normal epithelial control, but also provides a key model for further genetic manipulation to examine pathways thought to be important in tumour development or immune response in a syngeneic environment.

Transgenic tumours from which the DVL3 cells were generated, were derived via deletion of *Pten* and *trp53*, genes that are frequently mutated in human PCa and are implicated in aggressive forms of the disease [10]; thus, avoiding the introduction of tumorigenic viral proteins such as SV40 large T-antigen, which was used to generate the TRAMP C1 cell line [6]. Although the TRAMP C1 cell line has contributed significantly to PCa research, recent evidence indicates it generates neuroendocrine tumours, which clinically equates to only 0.5–2% of all PCa cases [7]. Furthermore, although other syngeneic PCa models exist [33,34] (e.g. MyC-CaP and Pten-CaP8), they have not been well characterized for their similarity to human disease, and immune microenvironment. The DVL3 cell line develops tumours that represent an adenocarcinoma phenotype much more akin to the majority of human PCa, and displays a similar TME to patient disease. The DVL3 model also sets itself apart, as it can be easily generated via subcutaneous allograft into immune-competent mice. As such, not only is it both time and cost beneficial compared with conventional GEM models, the tumours are easily accessible for therapeutic intervention, such as local delivery of RT and tumour assessment.

Transgenic models of PCa, and subsequent cell lines, generated from the *Pten*^{-/-}/*trp53*^{-/-} model generate heterogeneous tumours, forming distinct glandular structures [10]. Arguably, heterogeneity is one of the greatest benefits of this model, as most cell-based models are thought to be clonally selected due to genetic drift. As PCa is a multifocal heterogeneous disease, the derivation of a bulk DVL3 population allows for research into PCa evolution and response to treatment [35]. Tumours formed by the DVL3 model maintained the heterogeneous CK8+/CK5+ glandular structures and regions of AR positivity, similar to the tumours from which they were derived. Additionally, unlike other *Pten*^{-/-}/*trp53*^{-/-} murine cell lines, previously described in the literature, the DVL3 cells can be implanted in immune competent C57BL/6 mice, presenting with immunological cold tumour immune microenvironment, mirroring observations seen clinically [10,36].

Development of immune therapies as a method of harnessing the immune system's anti-tumour effects has recently gained traction [36]. Immune checkpoint inhibitors (ICI) have been used successfully to treat melanoma and lung cancers; however, their impact on PCa is more limited [37]. Unlike melanoma and lung cancer, PCa has low levels of infiltrating CD8+ T cells, high proportion of

MDSCs and tumour promoting M2 macrophages, therefore ICI are unlikely to work in majority of PCa patients [36,37]. Furthermore, variations in the PCa tumour microenvironment have been reported to correlate with PTEN-loss, defects in DNA repair pathways, low levels of tumour-associated antigens and differences in the immune function of patients [37]. PTEN loss occurs in 20% of primary PCa patients and has been associated with poorer overall survival [9,10,37]. Additionally, melanoma patients with PTEN loss also have lower levels of tumour infiltrating lymphocytes (TIL) [37]. We have confirmed that this is also true in the tumours resulting from DVL3 syngeneic engraftment, underscoring the more immuno-suppressed microenvironment of these tumours compared to the TRAMP C1 tumours.

Comparing the DVL3 allografts to published transgenic models driven by *Pten* deletion highlights other similarities and opportunities for future studies. For example *Pten* deletion is known to lead to the expansion and immunosuppressive activities of Gr1⁺/CD11b⁺ myeloid derived suppressor cells (MDSC) [13]. High numbers of MDSCs in a *Pten*^{-/-} setting provide a protective effect on PCa cells from senescence, therefore sustaining tumour growth [13,38]. Mechanistically this has been observed to occur in CRPC patients and in transgenic prostate cancer models through the activation of AR signalling due to paracrine IL-23 secretion by MDSCs [39]. Furthermore, influx of tumour MDSCs has been detected following RT, an observation which has been previously associated with the RT-induced up-regulation of STING expression in tumour cells [22,40,41]. Targeting MDSC, through IL-23 inhibition, in combination with RT and ADT could therefore provide a survival benefit for PCa patients.

STING mediated type-1 IFN production can be an effective approach to cancer therapy, due to its role in T-cell priming and dendritic cell activation. Counterintuitively, STING activation can also be immunosuppressive as previously reported [24]. In the DVL3 model, RT mediated STING activation does not result in enrichment of T- or NK cell gene signatures, nor did it result in a significant increase in the proportion of T- or NK cells, suggesting dominant immunosuppressive effects in the TME. However, we did note aggregation of NK-cells in and around necrotic areas after RT [42]. Further studies using the DVL3 model are necessary to clarify the role of NK-cell mediated cell killing, which may have potential therapeutic implications. Interestingly, in spite of the IFN-type-1 pathway activation, no significant change in PD-L1 expression was observed either in the tumor or macrophages after RT. It has been demonstrated that the kinetics of PD-L1 expression can be transient, time, and radiation dose-dependent [27,43]. In this study, we investigated the expression of PD-L1 at a single time point (a week after RT), and after administration of low dose fractionated RT (5 × 2 Gy). As such, further investigations are required with high radiation dose and observation and differing time points to establish the kinetics of PD-L1 upregulation on tumour cells and macrophages. Furthermore, PD-L1 expression on MDSCs can be activated by type-1 IFN in an autocrine manner, which is partially controlled by IFNAR1 expression on MDSCs [44]. Our gene expression analysis demonstrated no significant change in the expression of IFNAR1 with RT (data not shown). This may partly explain our findings, however, we cannot fully rule out other environmental factors.

Overall, the DVL3 model recapitulates clinically relevant immune microenvironment features that have been previously observed in PCa transgenic models following RT or androgen deprivation therapy, such as influx of MDSC, M2 tumour promoting macrophages, and lack of cytotoxic T-cell priming [13,39,41]. Although similar models have previously been published upon [10,45,46], to our knowledge this is the first report of a model which has been proven to be syngeneically engraftable and is driven by relevant genetic drivers to prostate cancer (*Pten* and *trp53*), and mirrors clinical response. The genetic status of the model, resultant histological Gleason score, and immunological features suggest the DVL3 model is currently poised for extensive future work as a model of molecular high-risk localized disease, which is benefited by its cost and time effectiveness compared with other models, ease of accessibility and tumour tracking, and its accurate recapitulation of PCa patient disease. However, further characterization of the model is required to examine if it is also suitable as a model of metastatic disease via orthotopic engraftment to the prostate or bone.

4. Materials and Methods

4.1. Cell Line Derivation and Maintenance

Mouse prostate epithelial cells (mPEC) were generated from normal dorsal, ventral and lateral lobes of the prostate from Probasin Cre^{-/-} (Pb-Cre4) mice. Murine prostate cancer cells (DVL3) were generated from tumours derived from the dorsal, ventral and lateral prostate lobes of a *Pten*^{-/-}/*trp53*^{-/-} Pb-Cre4 mouse [10]. These lobes were specifically utilised for both models as they are morphologically more similar to the peripheral zone in the human prostate gland which generates adenocarcinoma [11] and these lobes are also those which generate adenocarcinoma in the *Pten*^{-/-}/*trp53*^{-/-} Pb-Cre4 murine model. mPEC and DVL3 cell line generation is summarised in Supplemental Figure S1. Briefly, tissue fragments were collected in PBS and manually dissociated into 1 mm³ fragments using a scalpel. The sample was centrifuged at 2000 rpm to remove extraneous blood and fat, and remaining tissue digested in 1 mg/mL collagenase/dispase in PBS for 30 min at 37 °C, after digestion the tissue was further disrupted via serological pipetting. The supernatant containing prostate cells was collected, and the collagenase/dispase inactivated with EDTA. The digestion process was repeated twice with remaining tissue fragments. Supernatant from the digestions was pooled and centrifuged at 2000 rpm and prostate cells were re-suspended in RPMI supplemented with 10% FBS, 1× penicillin/streptomycin, 100 nM DHT and 10 µmol/L ROCK inhibitor (Y-27632, Sigma, Gillingham, UK). These cells were then incubated for 10 min at 37 °C to allow for prostate fibroblasts to adhere to the tissue culture plastic. Remaining cell suspension, enriched for prostate epithelium was transferred to a new culture flask. This process of differential plating, allowing for initial adherence of fibroblasts and removal and retention of less adherent epithelial cells, was repeated for 10 passages, at which time use of the ROCK inhibitor (Y-27632, Sigma) was stopped and the population was characterised as epithelial. After isolation and initial 10 passages to reach a homogenous epithelial population, the mPEC and DVL3 cell lines were maintained in RPMI-media supplemented with 10% FBS, L-glutamine and 100 nM DHT.

The TRAMP C1 murine prostate carcinoma cells were purchased from ATCC (Manassas, VA, USA) and maintained in DMEM high glucose medium, supplemented with 4 mM L-glutamine, 5% FBS, 5% Nu Serum (Corning, Bedford, MA, USA), 0.005 mg/mL of bovine insulin, and 10 nM dehydroisoandrosterone (Sigma). CT26 murine colon carcinoma cells (ATCC) and 4434 cells isolated from BRAFV600E p16^{-/-} mice (Richard Marias, Cancer Research UK Manchester Institute, Manchester, UK) were maintained in DMEM, and 4T1 triple-negative breast cancers (ATCC) maintained in RPMI-media supplemented with 10% FCS, 1% L-glutamine (Invitrogen, Paisley, UK).

4.2. Syngeneic Modelling

C57BL/6 and BALB/C male mice (8-weeks old) were obtained from Harlan (Derby, UK). All animal experiments were performed under United Kingdom Home Office Licenses held at Queen's University Belfast or the CRUK Manchester Institute, University of Manchester (PPL2775; PCC943F76 respectively). Prior to each in vivo experiment, cells were screened for mycoplasma contamination and mouse hepatitis virus (MHV). Mice were housed on a 12/12 light/dark cycle and were given filtered water and fed *ad libitum*. C57BL/6 male mice were inoculated subcutaneously with either 5 × 10⁶ TRAMP C1, 1 × 10⁶ DVL3 cells, 1 × 10⁶ mPEC cells or 5 × 10⁶ 4434 cells; BALB/C mice were inoculated with 5 × 10⁵ CT26 cells, 1 × 10⁵ 4T1 cells under light general anaesthetic using Isoflurane and oxygen gaseous mix in accordance with project license and home office regulations. Tumour volume was measured using calipers as length × (width)²/2.

4.3. Sample Preparation

Tumour bearing mice were sacrificed at the indicated time points using standard schedule-1 procedure, and in accordance with current UK home office legislation. Tumour samples were cut into half and either fixed in 4% buffered formalin (Sigma Aldrich) for 24 h or collected in media for tumour

disaggregation. The formalin fixed tumour samples were transferred to 70% ethanol and processed to FFPE blocks at the CRUK Manchester histology core facility. H&E slides obtained were evaluated by a dedicated uropathologist (PO) with the aim to compare with morphological features of human prostate cancer as well as estimate a Gleason pattern and score.

4.4. Immunohistochemistry

Briefly, the slides were deparaffinised in xylene followed by rehydration in ethanol. Antigen retrieval was performed using pH 6 citrate buffer, followed by 3% H₂O₂ block. Slides were incubated with 10% serum, prior to incubation with primary antibody overnight at 4° (Table S1). Primary antibody was detected with either HRP detection kit or biotinylated secondary antibody followed by ABC detection kit (Vector Labs, Burlingame, CA, USA). Slides were briefly incubated in DAB substrate (Vector Labs), washed in water, and counter-stained using haematoxylin. STING and cleaved Caspase-3 staining was performed on the BOND Rx automation system (Leica, Microsystems, Milton Keynes, UK) using standard protocol. For multiplex staining of mouse FFPE tumour sections, the opal TSA detection system (Opal 520[®], 570[®] and 650[®]) were applied to sections following manufacturer's instruction and run on Leica BOND Rx automated system. The slides were counterstained with DAPI. Chromagen slides were scanned digitally using Leica SCN 4000 slide scanner (Leica Microsystems) VS-200 slide scanner (Olympus, Essex, UK), and the multiplex slides were scanned using Versa Slide scanner (Leica Microsystems) and VS-120 slide scanner (Olympus). Image analysis and quantification was performed using Definiens[®] Tissue Phenomics Software (Munich, Germany) or Halo[®] image analysis (Indica Labs, Albuquerque, NM, USA). Quantification of the percentage of positive cells was determined using either hematoxylin or DAPI staining to identify total cell count. Scoring of positive staining of chromogen slides (summarized in Figure 1C) was performed in a blinded fashion by two independent researchers. For quantification of co-localisation using Halo[®]; High plex FL Ver 3.1.0 module was used.

4.5. Immunocytochemistry

Cells were seeded onto glass slides pre-coated with collagen type II (BD Biosciences, San Jose, CA, USA) and left to adhere for 24 h before fixation with 4% paraformaldehyde at RT. Cells were permeabilised with 0.1% Triton X and blocked with 3% FBS-PBS. Primary antibody was added to slides and incubated for 1 h at RT followed by incubation in secondary antibody for 1 h at RT (Table S1). Coverslips were mounted onto glass slides using Mounting media (Invitrogen) containing Dapi and imaged.

4.6. RNA Isolation and cDNA Synthesis

Total RNA from cells was isolated using TriPure Isolation reagent (Roche, Mannheim, Germany) and phenol-chloroform extraction and cDNA synthesised using first strand cDNA (Roche) according to the respective manufacturer's instructions.

4.7. qRT-PCR

mRNA levels were determined by RT-PCR and measured on Roche LightCycler[®]480 II with SYBR Green I Master (Roche). All primers were obtained from Eurofins (Ebersberg, Germany) and sequences are detailed in (Table S2). mRNA expression was evaluated using β -actin and GAPDH housekeeping genes and is shown normalized to β -actin as a fold change relative to mPECs transcript levels.

4.8. Western Blotting

Cells were lysed with RIPA buffer (Sigma) supplemented with Protease Inhibitor Cocktail (Roche), centrifuged and supernatant containing protein analysed by SDS Page (Invitrogen). Proteins were transferred onto a nitrocellulose membrane, blocked for 1 h in 5% milk TBS-T prior to incubation

with primary antibody at 4 °C overnight, concentrations are detailed in (Table S2). Complementary secondary antibodies were used at 1:3000. Membranes were visualised via chemiluminescence on a Syngene G:Box imager using reagent (Merck, Cambridge, UK).

4.9. Flow Cytometry on Cell Lines

Cells were incubated with primary antibody conjugated fluorophore for 30 min at 4 °C, washed with PBS and analysed on the Introducing the BD Accuri™ C6 Plus according to the manufacturer's instructions.

4.10. Radiotherapy

Upon tumour establishment (4–6 weeks post inoculation), mice were randomised to treatment groups. Irradiation was performed when the tumours were between (100–200 mm³). The tumour bearing mice were placed in a lead jig with an opening for the tumour and shielding for the rest of the body. Radiotherapy was delivered using an AGO cell X-Ray unit and XSTRAHL (CIX3) in vivo irradiator at a dose rate of 2.086 Gy/min. Tumour bearing mice received either single dose of 8 Gy irradiation, or 5 fractions of 2 Gy delivered over 5 consecutive days (as shown in Figure 3A).

4.11. RNA Extraction for RNA Seq Analysis

RNA from FFPE mouse tumour tissue was extracted. Briefly, 2–4 (10 µM) sections were transferred into RNAase free microcentrifuge tube. The paraffin was removed by incubating in xylene and ethanol. For lysate and total RNA purification, digestion buffer and proteinase-K was added to the samples as per manufacturer's instructions (Norgen Kit, Ontario, Canada). The samples were spun briefly followed by transferring the supernatant to a new RNAase free microcentrifuge tube. The RNA containing tubes were incubated for 15 min at 80 °C. The lysates were then passed through RNA purification microcolumn and centrifuged for 1 min at 14,000 RPM. The microcolumns were washed according to manufacturer's instructions and the RNA eluted using the Elution solution (Norgen Kit).

4.12. RNA Library Preparation, Sequencing and Analysis

RNA libraries preparations were generated using the Quant-seq 3' mRNA-Seq FWD kit (PART NO k15.96, Lexogen, Vienna, Austria) according to manufacturer's instructions, with 500ng input RNA. FFPE-derived RNA was prepared using the suggested manufacturer's instructions. Libraries were pooled and sequenced on the NextSeq 500 using the Queen's University Genomics Core Technology Unit, yielding an average of 10 million reads per sample. FASTQ files were aligned to the mm10 genomic reference using STAR aligner [47] and counts quantified at a gene level with HTseq-Counts [48] to yield 5–8M mapped reads per sample. Differential gene expression was performed between the irradiated and un-irradiated samples using the DESEQ 2. Differentially expressed genes were filtered; FDR adjusted—*p* Value < 0.05 and Log2 Fold-Change ≥1 (up-regulated) or ≤−1 (down-regulated). Pathway analysis was performed on filtered genelists using the Reactome database [49] in Enrichr [50,51]. To identify enrichment of immune populations with the RT tumours vs untreated, enrichment analysis was performed using the open assess tool gene set enrichment analysis (GSEA) [52,53] with 1000 gene label permutations. Immune cell gene signatures for macrophages, NK cells, T-cells and MDSC were taken from previous published studies [25,54,55].

4.13. Flow Cytometry on Tumour Tissue

To obtain single cell suspensions, tumours were processed using a gentleMacs dissociator and a murine dissociation kit (Miltenyi Biotec, Surrey, UK). For staining of cells, non-specific binding was blocked with rat anti-CD16/CD32 Fc block on ice. Cells were incubated with Gr-1-FITC, CD11b-APC (eBioscience, Leicestershire, UK), washed in 1% FCS/PBS. For analysis, live cells were gated using vital

dye exclusion (Invitrogen) and population phenotyped on FACs Canto (BD Bioscience) and analyzed using Flow Jo software. An example of the gating strategy employed is provided in Figure S5.

4.14. Statistical Analysis

Results were analysed using GraphPad Prism (v7.03, San Diego, CA, USA). Data was analysed via a Shapiro-Wilk normality test was first used to confirm that groups were distributed normally. When comparing two groups, if the data was normally distributed it was analysed by Student's *t*-test. Nonparametric data was analysed via Mann-Whitney testing. When comparing more than two groups a one-way analysis of variance (ANOVA) followed by a Tukey's multiple comparisons test was used to detect significant differences between means. The limit for significance was set at $p \leq 0.05$. Data are described with standard error of the mean (SEM). To compare survival curves from in vivo experiments, Log-Rank Mantel–Cox tests were performed on Kaplan–Meier plots.

5. Conclusions

This study highlights that the DVL3 model represents substantial progress in preclinical PCA modelling displaying similar molecular, histological, and microenvironmental features compared to alternative models. Furthermore, the DVL3 cells and subsequent tumours can be generated quickly and inexpensively compared to standard transgenic models, and tumours are readily accessible for therapeutic intervention. Importantly, DVL3 cells can be syngeneically engrafted into immune component hosts and respond to standard of care RT, with a similar immune influx, thus enabling future validation of novel therapeutics for PCA including immunomodulatory agents targeting MDSC, macrophages and agents that can prime T-cell responses either alone or in combination with standard of care RT or ADTs.

Supplementary Materials: The following are available online at <http://www.mdpi.com/2072-6694/12/10/2804/s1>, All antibodies utilised for immunohistochemistry, immunocytochemistry, western blotting and flow cytometry can be found in Supplementary Table S1. Further, all primers utilised for qRT-PCR can be found in Supplementary Table S2. RNA-seq files have been deposited on the Gene Expression Omnibus (GEO) database. GSE number—GSE146790. Figure S1: Summary schematic of DVL3 and mPEC cell model isolation, Figure S2: Further characterization of the DVL3 model compared with TRAMP C1 with focus on AR signaling, Figure S3: Additional high and low magnification immunohistochemical staining of DVL3 tumours, Figure S4: Whole blot images and densitometry for western blot experiments, Figure S5: Gating strategies for flow cytometry, Figure S6: Comparison of DVL3 to other commonly used syngeneic models, Figure S7: Reactome analysis of RNA sequencing revealing downregulated pathways and evidence of STING response, Figure S8: Additional STING analysis and quantification, Figure S9: Nkp46 expression around necrotic tissues and PDL1 expression, Table S1: List of antibodies utilised for immunohistochemistry, western blotting, immunocytochemistry and flow cytometry, Table S2: List of qRT-PCR primers.

Author Contributions: Conceptualization, C.M.H., D.M., R.E.S., L.D.-P., A.P. (Adam Pickard), S.J., J.H., S.S.M., T.I., I.G.M., S.L.E.; Methodology, D.M., C.M.H., R.E.S., A.P. (Amy Popple), L.D.-P., A.P. (Adam Pickard), M.P., P.O., N.E.B., S.L.E.; Formal analysis, C.M.H., D.M., A.P. (Amy Popple), M.P., S.L.E.; Writing—original draft, C.M.H., D.M., S.L.E., I.G.M.; Writing—review/editing, C.M.H., D.M., R.E.S., A.P. (Amy Popple), L.D.-P., A.P. (Adam Pickard), S.J., P.O., N.E.B., P.B.M., R.W., J.H., S.S.M., T.I., I.G.M., S.L.E.; Funding acquisition, I.G.M., S.J., P.B.M., R.W., S.S.M., T.I. All authors have read and agreed to the published version of the manuscript.

Funding: C.M.H. was funded by the Gracey Foundation. D.M., R.E.S., L.D.-P., A.P. (Adam Pickard), S.J., S.S.M., T.I., and I.G.M. were supported by the Belfast-Manchester Movember Centre of Excellence (MA-CE018-002), funded in partnership with Prostate Cancer UK. S.L.E., P.B.M. and R.W. were funded by Prostate Cancer UK (PCUK PG13-021). I.G.M. was also supported by the Norwegian Research Council (230559) and is supported by the John Black Charitable Foundation. N.B. funded by Breast Cancer Now (2012MAYSF122). T.I. supported by CRUK programme grant (C431/A28280). A.P. (Amy Popple) and J.H. were funded by Cancer Research UK Programme grant (A17737).

Acknowledgments: We acknowledge the generous gift of mouse prostate tissue from the David Waugh laboratory from which the mPEC and DVL3 cell lines were generated. The authors thank the members of the Cancer Research UK Manchester Institute BRU core facility, Caron Behan and Garry Ashton from the Histology Core Facility for the technical expertise and help with staining, MBCF, Flow Cytometry Core Facilities and Alex Baker from Imaging Core facility for image analysis.

Conflicts of Interest: The authors declare no conflict of interest.

Ethical Approval: All procedures were performed in accordance with the Animal Scientific Procedures Act of 1986 (UK) (Project Licence Number PL2775 and PCC943F76) which was issued by the home office. Protocols were approved by the animal welfare and ethical review body at both Queen’s University Belfast and the Cancer Research UK Manchester Institute. Animals were housed in individually ventilated cages on a 12:12 light: dark cycle and ad libitum access to food and filtered water. Prior to each in vivo experiment, cells were screened for mycoplasma and MHV contamination.

References

1. Bray, F.; Ferlay, J.; Soerjomataram, I.; Siegel, R.L.; Torre, L.A.; Jemal, A. Global cancer statistics 2018: GLOBOCAN estimates of incidence and mortality worldwide for 36 cancers in 185 countries. *CA A Cancer J. Clin.* **2018**, *68*, 394–424. [[CrossRef](#)]
2. Siegel, R.L.; Miller, K.D.; Jemal, A. Cancer statistics, 2018. *CA Cancer J Clin.* **2018**, *68*, 7–30. [[CrossRef](#)]
3. Jemal, A.; Siegel, R.; Xu, J.; Ward, E. Cancer statistics, 2010. *CA Cancer J Clin.* **2010**, *60*, 277–300. [[CrossRef](#)]
4. James, N.D.; Spears, M.R.; Clarke, N.W.; Dearnaley, D.P.; De Bono, J.S.; Gale, J.; Hetherington, J.; Hoskin, P.J.; Jones, R.; Laing, R.; et al. Survival with Newly Diagnosed Metastatic Prostate Cancer in the “Docetaxel Era”: Data from 917 Patients in the Control Arm of the STAMPEDE Trial (MRC PR08, CRUK/06/019). *Eur. Urol.* **2015**, *67*, 1028–1038. [[CrossRef](#)]
5. Donovan, J.L.; Hamdy, F.C.; Lane, J.A.; Mason, M.; Metcalfe, C.; Walsh, E.; Blazeby, J.; Peters, T.J.; Holding, P.; Bonnington, S.; et al. Patient-Reported Outcomes after Monitoring, Surgery, or Radiotherapy for Prostate Cancer. *N. Engl. J. Med.* **2016**, *375*, 1425–1437. [[CrossRef](#)]
6. Foster, B.A.; Gingrich, J.R.; Kwon, E.D.; Madias, C.; Greenberg, N.M. Characterization of prostatic epithelial cell lines derived from transgenic adenocarcinoma of the mouse prostate (TRAMP) model. *Cancer Res.* **1997**, *57*, 3325–3330. [[PubMed](#)]
7. Berman-Booty, L.D.; Knudsen, K.E. Models of neuroendocrine prostate cancer. *Endocr.-Relat. Cancer* **2014**, *22*, R33–R49. [[CrossRef](#)] [[PubMed](#)]
8. Zafarana, G.; Ishkanian, A.S.; Malloff, C.A.; Locke, J.A.; Sykes, J.; Thoms, J.; Lam, W.L.; Squire, J.A.; Yoshimoto, M.; Ramnarine, V.R.; et al. Copy number alterations of c-MYC and PTEN are prognostic factors for relapse after prostate cancer radiotherapy. *Cancer* **2012**, *118*, 4053–4062. [[CrossRef](#)] [[PubMed](#)]
9. Geybels, M.S.; Fang, M.; Wright, J.L.; Qu, X.; Bibikova, M.; Klotzle, B.; Fan, J.-B.; Feng, Z.; Ostrander, E.A.; Nelson, P.S.; et al. PTEN loss is associated with prostate cancer recurrence and alterations in tumor DNA methylation profiles. *Oncotarget* **2017**, *8*, 84338–84348. [[CrossRef](#)]
10. Martin, P.; Liu, Y.-N.; Pierce, R.; Abou-Kheir, W.; Casey, O.; Seng, V.; Camacho, D.; Simpson, R.M.; Kelly, K. Prostate Epithelial Pten/TP53 Loss Leads to Transformation of Multipotential Progenitors and Epithelial to Mesenchymal Transition. *Am. J. Pathol.* **2011**, *179*, 422–435. [[CrossRef](#)]
11. Oliveira, D.S.M.; Dzinic, S.; Bonfil, A.I.; Saliganan, A.D.; Sheng, S.; Bonfil, R.D. The mouse prostate: A basic anatomical and histological guideline. *Bosn. J. Basic Med. Sci.* **2016**, *16*, 8–13. [[CrossRef](#)] [[PubMed](#)]
12. Roy-Burman, P.; Wu, H.; Powell, W.C.; Hagenkord, J.; Cohen, M.B. Genetically defined mouse models that mimic natural aspects of human prostate cancer development. *Endocr.-Relat. Cancer* **2004**, *11*, 225–254. [[CrossRef](#)] [[PubMed](#)]
13. Garcia, A.J.; Ruscetti, M.; Arenzana, T.L.; Tran, L.M.; Bianci-Frias, D.; Sybert, E.; Priceman, S.J.; Wu, L.; Nelson, P.S.; Smale, S.T.; et al. Pten Null Prostate Epithelium Promotes Localized Myeloid-Derived Suppressor Cell Expansion and Immune Suppression during Tumor Initiation and Progression. *Mol. Cell. Biol.* **2014**, *34*, 2017–2028. [[CrossRef](#)] [[PubMed](#)]
14. Sharma, P.; Hu-Lieskovan, S.; Wargo, J.A.; Ribas, A. Primary, Adaptive, and Acquired Resistance to Cancer Immunotherapy. *Cell* **2017**, *168*, 707–723. [[CrossRef](#)] [[PubMed](#)]
15. Vidotto, T.; Saggiaro, F.P.; Jamaspishvili, T.; Chesca, D.L.; De Albuquerque, C.G.P.; Reis, R.B.; Graham, C.H.; Berman, D.M.; Siemens, D.R.; Squire, J.A.; et al. PTEN-deficient prostate cancer is associated with an immunosuppressive tumor microenvironment mediated by increased expression of IDO1 and infiltrating FoxP3+ T regulatory cells. *Prostate* **2019**, *79*, 969–979. [[CrossRef](#)]
16. Wang, Y.; Hayward, S.W.; Cao, M.; Thayer, K.A.; Cunha, G.R. Cell differentiation lineage in the prostate. *Differentiation* **2001**, *68*, 270–279. [[CrossRef](#)]

17. Bhatia-Gaur, R.; Donjacour, A.A.; Scivolino, P.J.; Kim, M.; Desai, N.; Young, P.; Norton, C.R.; Gridley, T.; Cardiff, R.D.; Cunha, G.R.; et al. Roles for Nkx3.1 in prostate development and cancer. *Genes Dev.* **1999**, *13*, 966–977. [[CrossRef](#)]
18. Gurel, B.; Ali, T.Z.; Montgomery, E.A.; Begum, S.; Hicks, J.; Goggins, M.; Eberhart, C.G.; Clark, D.P.; Bieberich, C.J.; Epstein, J.I.; et al. NKX3.1 as a Marker of Prostatic Origin in Metastatic Tumors. *Am. J. Surg. Pathol.* **2010**, *34*, 1097–1105. [[CrossRef](#)]
19. Young, H.L.; Rowling, E.J.; Bugatti, M.; Giurisato, E.; Luheshi, N.; Arozarena, I.; Acosta, J.C.; Kamarashev, J.; Frederick, D.T.; Cooper, Z.; et al. An adaptive signaling network in melanoma inflammatory niches confers tolerance to MAPK signaling inhibition. *J. Exp. Med.* **2017**, *214*, 1691–1710. [[CrossRef](#)]
20. Chen, F.-H.; Chiang, C.-S.; Wang, C.-C.; Tsai, C.-S.; Jung, S.-M.; Lee, C.-C.; McBride, W.H.; Hong, J.-H. Radiotherapy decreases vascular density and causes hypoxia with macrophage aggregation in TRAMP-C1 prostate tumors. *Clin. Cancer Res.* **2009**, *15*, 1721–1729. [[CrossRef](#)]
21. Walshaw, R.C.; Honeychurch, J.; Illidge, T.; Choudhury, A. The anti-PD-1 era—An opportunity to enhance radiotherapy for patients with bladder cancer. *Nat. Rev. Urol.* **2017**, *15*, 251–259. [[CrossRef](#)] [[PubMed](#)]
22. Liang, H.; Deng, L.; Hou, Y.; Meng, X.; Huang, X.; Rao, E.; Zheng, W.; Mauceri, H.; Mack, M.; Xu, M.; et al. Host STING-dependent MDSC mobilization drives extrinsic radiation resistance. *Nat. Commun.* **2017**, *8*, 1736. [[CrossRef](#)] [[PubMed](#)]
23. Woo, S.-R.; Fuertes, M.B.; Corrales, L.; Spranger, S.; Furdyna, M.J.; Leung, M.Y.; Duggan, R.; Wang, Y.; Barber, G.N.; Fitzgerald, K.A.; et al. STING-dependent cytosolic DNA sensing mediates innate immune recognition of immunogenic tumors. *Immunity* **2014**, *41*, 830–842. [[CrossRef](#)] [[PubMed](#)]
24. Deng, L.; Liang, H.; Burnette, B.; Beckett, M.; Darga, T.; Weichselbaum, R.R.; Fu, Y.-X. Irradiation and anti-PD-L1 treatment synergistically promote antitumor immunity in mice. *J. Clin. Investig.* **2014**, *124*, 687–695. [[CrossRef](#)] [[PubMed](#)]
25. Wang, G.; Lü, X.; Dey, P.; Deng, P.; Wu, C.C.; Jiang, S.; Fang, Z.; Zhao, K.; Konaparthi, R.; Hua, S.; et al. Targeting YAP-Dependent MDSC Infiltration Impairs Tumor Progression. *Cancer Discov.* **2015**, *6*, 80–95. [[CrossRef](#)]
26. Ko, E.C.; Formenti, S.C. Radiotherapy and checkpoint inhibitors: A winning new combination? *Ther. Adv. Med. Oncol.* **2018**, *10*. [[CrossRef](#)]
27. Dovedi, S.J.; Adlard, A.; Lipowska-Bhalla, G.; McKenna, C.; Jones, S.; Cheadle, E.J.; Stratford, I.J.; Poon, E.; Morrow, M.; Stewart, R.; et al. Acquired Resistance to Fractionated Radiotherapy Can Be Overcome by Concurrent PD-L1 Blockade. *Cancer Res.* **2014**, *74*, 5458–5468. [[CrossRef](#)]
28. Brand, D.H.; Tree, A.C.; Ostler, P.; Van Der Voet, H.; Loblaw, A.; Chu, W.; Ford, D.; Tolan, S.; Jain, S.; Martin, A.; et al. Intensity-modulated fractionated radiotherapy versus stereotactic body radiotherapy for prostate cancer (PACE-B): Acute toxicity findings from an international, randomised, open-label, phase 3, non-inferiority trial. *Lancet Oncol.* **2019**, *20*, 1531–1543. [[CrossRef](#)]
29. Dearnaley, D.P.; Syndikus, I.; Mossop, H.; Khoo, V.; Birtle, A.; Bloomfield, D.; Graham, J.D.; Kirkbride, P.; Logue, J.; Malik, Z.; et al. Conventional versus hypofractionated high-dose intensity-modulated radiotherapy for prostate cancer: 5-year outcomes of the randomised, non-inferiority, phase 3 CHHiP trial. *Lancet Oncol.* **2016**, *17*, 1047–1060. [[CrossRef](#)]
30. Payne, H.; Mason, M. Androgen deprivation therapy as adjuvant/neoadjuvant to radiotherapy for high-risk localised and locally advanced prostate cancer: Recent developments. *Br. J. Cancer* **2011**, *105*, 1628–1634. [[CrossRef](#)]
31. Parker, C.; James, N.D.; Brawley, C.D.; Clarke, N.W.; Hoyle, A.P.; Ali, A.; Ritchie, A.W.S.; Attard, G.; Chowdhury, S.; Cross, W.; et al. Radiotherapy to the primary tumour for newly diagnosed, metastatic prostate cancer (STAMPEDE): A randomised controlled phase 3 trial. *Lancet* **2018**, *392*, 2353–2366. [[CrossRef](#)]
32. Weichselbaum, R.R. The 46th David A. Karnofsky Memorial Award Lecture: Oligometastasis—From Conception to Treatment. *J. Clin. Oncol.* **2018**, *36*, 3240–3250. [[CrossRef](#)] [[PubMed](#)]
33. Watson, P.A.; Ellwood-Yen, K.; King, J.C.; Wongvipat, J.; Lebeau, M.M.; Sawyers, C.L. Context-Dependent Hormone-Refractory Progression Revealed through Characterization of a Novel Murine Prostate Cancer Cell Line. *Cancer Res.* **2005**, *65*, 11565–11571. [[CrossRef](#)] [[PubMed](#)]
34. Jiao, J.; Wang, S.; Qiao, R.; Vivanco, I.; Watson, P.A.; Sawyers, C.L.; Wu, H. Murine Cell Lines Derived from Pten Null Prostate Cancer Show the Critical Role of PTEN in Hormone Refractory Prostate Cancer Development. *Cancer Res.* **2007**, *67*, 6083–6091. [[CrossRef](#)]

35. Carm, K.T.; Hoff, A.M.; Bakken, A.C.; Axcrone, U.; Axcrone, K.; Lothe, R.A.; Skotheim, R.I.; Løvf, M. Interfocal heterogeneity challenges the clinical usefulness of molecular classification of primary prostate cancer. *Sci. Rep.* **2019**, *9*, 13579–13586. [[CrossRef](#)]
36. Bilusic, M.; Madan, R.A.; Gulley, J.L. Immunotherapy of Prostate Cancer: Facts and Hopes. *Clin. Cancer Res.* **2017**, *23*, 6764–6770. [[CrossRef](#)]
37. Vitkin, N.; Nersesian, S.; Siemens, D.R.; Koti, M. The Tumor Immune Contexture of Prostate Cancer. *Front. Immunol.* **2019**, *10*. [[CrossRef](#)]
38. Di Mitri, D.; Toso, A.; Chen, J.; Sarti, M.; Pinton, S.; Jost, T.R.; D’Antuono, R.; Montani, E.; García-Escudero, R.; Guccini, I.; et al. Tumour-infiltrating Gr-1+ myeloid cells antagonize senescence in cancer. *Nature* **2014**, *515*, 134–137. [[CrossRef](#)]
39. Calcinotto, A.; Spataro, C.; Zagato, E.; Di Mitri, D.; Gil, V.; Crespo, M.; De Bernardis, G.; Losa, M.; Miranda, M.; Pasquini, E.; et al. IL-23 secreted by myeloid cells drives castration-resistant prostate cancer. *Nature* **2018**, *559*, 363–369. [[CrossRef](#)]
40. Ostrand-Rosenberg, S.; Horn, L.A.; Ciavattone, N.G. Radiotherapy Both Promotes and Inhibits Myeloid-Derived Suppressor Cell Function: Novel Strategies for Preventing the Tumor-Protective Effects of Radiotherapy. *Front. Oncol.* **2019**, *9*. [[CrossRef](#)]
41. Vatner, R.E.; Formenti, S.C. Myeloid-Derived Cells in Tumors: Effects of Radiation. *Semin. Radiat. Oncol.* **2015**, *25*, 18–27. [[CrossRef](#)] [[PubMed](#)]
42. Pasero, C.; Gravis, G.; Guérin, M.; Granjeaud, S.; Piana, J.T.; Rocchi, P.; Paciencia-Gros, M.; Poizat, F.; Bentobji, M.; Azario-Cheillan, F.; et al. Inherent and Tumor-Driven Immune Tolerance in the Prostate Microenvironment Impairs Natural Killer Cell Antitumor Activity. *Cancer Res.* **2016**, *76*, 2153–2165. [[CrossRef](#)] [[PubMed](#)]
43. Vanpouille-Box, C.; Formenti, S.C.; Demaria, S. Toward precision radiotherapy for use with immune checkpoint blockers. *Clin. Cancer Res.* **2018**, *24*, 259–265. [[CrossRef](#)] [[PubMed](#)]
44. Xiao, W.; Klement, J.D.; Lu, C.; Ibrahim, M.L.; Liu, K. IFNAR1 Controls Autocrine Type I IFN Regulation of PD-L1 Expression in Myeloid-Derived Suppressor Cells. *J. Immunol.* **2018**, *201*, 264–277. [[CrossRef](#)]
45. Grabowska, M.M.; DeGraff, D.J.; Yu, X.; Jin, R.J.; Chen, Z.; Borowsky, A.D.; Matusik, R.J. Mouse models of prostate cancer: Picking the best model for the question. *Cancer Metastasis Rev.* **2014**, *33*, 377–397. [[CrossRef](#)] [[PubMed](#)]
46. Ittmann, M.M.; Huang, J.; Radaelli, E.; Martin, P.; Signoretti, S.; Sullivan, R.; Simons, B.W.; Ward, J.M.; Robinson, B.D.; Chu, G.C.; et al. Animal Models of Human Prostate Cancer: The Consensus Report of the New York Meeting of the Mouse Models of Human Cancers Consortium Prostate Pathology Committee. *Cancer Res.* **2013**, *73*, 2718–2736. [[CrossRef](#)]
47. Dobin, A.; Davis, C.A.; Schlesinger, F.; Drenkow, J.; Zaleski, C.; Jha, S.; Batut, P.; Chaisson, M.; Gingeras, T.R. STAR: Ultrafast universal RNA-seq aligner. *Bioinformatics* **2012**, *29*, 15–21. [[CrossRef](#)]
48. Anders, S.; Pyl, P.T.; Huber, W. HTSeq—A Python framework to work with high-throughput sequencing data. *Bioinformatics* **2014**, *31*, 166–169. [[CrossRef](#)]
49. Fabregat, A.; Jupe, S.; Matthews, L.; Sidiropoulos, K.; Gillespie, M.; Garapati, P.; Haw, R.; Jassal, B.; Korninger, F.; May, B.; et al. The Reactome Pathway Knowledgebase. *Nucleic Acids Res.* **2018**, *46*, D649–D655. [[CrossRef](#)]
50. Chen, E.Y.; Tan, C.M.; Kou, Y.; Duan, Q.; Wang, Z.; Meirelles, G.V.; Clark, N.R.; Ma’Ayan, A. Enrichr: Interactive and collaborative HTML5 gene list enrichment analysis tool. *BMC Bioinform.* **2013**, *14*, 128. [[CrossRef](#)]
51. Kuleshov, M.V.; Jones, M.R.; Rouillard, A.D.; Fernandez, N.F.; Duan, Q.; Wang, Z.; Koplev, S.; Jenkins, S.L.; Jagodnik, K.M.; Lachmann, A.; et al. Enrichr: A comprehensive gene set enrichment analysis web server 2016 update. *Nucleic Acids Res.* **2016**, *44*. [[CrossRef](#)] [[PubMed](#)]
52. Mootha, V.K.; Lindgren, C.M.; Eriksson, K.F.; Subramanian, A.; Sihag, S.; Lehar, J.; Puigserver, P.; Carlsson, E.; Laurila, E.; Tamayo, P.; et al. PGC-1 α -responsive genes involved in oxidative phosphorylation are coordinately downregulated in human diabetes. *Nat Genet.* **2003**, *34*, 267–273. [[CrossRef](#)]
53. Subramanian, A.; Tamayo, P.; Mootha, V.K.; Mukherjee, S.; Ebert, B.L.; Gillette, M.A.; Paulovich, A.; Pomeroy, S.L.; Golub, T.R.; Lander, E.S.; et al. Gene set enrichment analysis: A knowledge-based approach for interpreting genome-wide expression profiles. *Proc. Natl. Acad. Sci. USA* **2005**, *102*. [[CrossRef](#)] [[PubMed](#)]

54. Nirmal, A.J.; Regan, T.; Shih, B.B.; Hume, D.A.; Sims, A.H.; Freeman, T. Immune Cell Gene Signatures for Profiling the Microenvironment of Solid Tumors. *Cancer Immunol. Res.* **2018**, *6*, 1388–1400. [[CrossRef](#)] [[PubMed](#)]
55. Cursons, J.; Souza-Fonseca-Guimaraes, F.; Foroutan, M.; Anderson, A.; Hollande, F.; Hediya-Zadeh, S.; Behren, A.; Huntington, N.; Davis, M.J. A gene signature predicting natural killer infiltration and improved survival in melanoma patients. *Cancer Immunol. Res.* 2019. [[CrossRef](#)]



© 2020 by the authors. Licensee MDPI, Basel, Switzerland. This article is an open access article distributed under the terms and conditions of the Creative Commons Attribution (CC BY) license (<http://creativecommons.org/licenses/by/4.0/>).

Review

Cancer Acidity and Hypertonicity Contribute to Dysfunction of Tumor-Associated Dendritic Cells: Potential Impact on Antigen Cross-Presentation Machinery

Sven Burgdorf ^{1,†}, Stefan Porubsky ^{2,3,†}, Alexander Marx ³ and Zoran V. Popovic ^{3,*}

¹ Department of Cellular Immunology, LIMES Institute, University of Bonn, 53115 Bonn, Germany; burgdorf@uni-bonn.de

² Institute of Pathology, University Hospital, Johannes-Gutenberg University Mainz, 55131 Mainz, Germany; Stefan.Porubsky@unimedizin-mainz.de

³ Institute of Pathology, University Hospital Mannheim, University of Heidelberg, 68167 Mannheim, Germany; Alexander.Marx@umm.de

* Correspondence: Zoran.Popovic@umm.de; Tel.: +49-(0)621-383-1114

† Authors contribute equally.

Received: 3 July 2020; Accepted: 16 August 2020; Published: 24 August 2020



Abstract: Macrophages (M Φ) and dendritic cells (DC), major players of the mononuclear phagocyte system (MoPh), are potent antigen presenting cells that steadily sense and respond to signals from the surrounding microenvironment, leading to either immunogenic or tolerogenic outcomes. Next to classical MHC-I/MHC-II antigen-presentation pathways described in the vast majority of cell types, a subset of MoPh (CD8⁺, XCR1⁺, CLEC9A⁺, BDCA3⁺ conventional DCs in human) is endowed with a high competence to cross-present external (engulfed) antigens on MHC-I molecules to CD8⁺ T-cells. This exceptional DC function is thought to be a crucial crossroad in cytotoxic antitumor immunity and has been extensively studied in the past decades. Biophysical and biochemical fingerprints of tumor micromilieus show significant spatiotemporal differences in comparison to non-neoplastic tissue. In tumors, low pH (mainly due to extracellular lactate accumulation via the Warburg effect and via glutaminolysis) and high oncotic and osmotic pressure (resulting from tumor debris, increased extracellular matrix components but in part also triggered by nutritive aspects) are—despite fluctuations and difficulties in measurement—likely the most constant general hallmarks of tumor microenvironment. Here, we focus on the influence of acidic and hypertonic micromilieu on the capacity of DCs to cross-present tumor-specific antigens. We discuss complex and in part controversial scientific data on the interference of these factors with to date reported mechanisms of antigen uptake, processing and cross-presentation, and we highlight their potential role in cancer immune escape and poor clinical response to DC vaccines.

Keywords: cancer acidity; hyperosmolarity; tumor microenvironment; cross-presentation

1. The Role of Mononuclear Phagocytes in the Tumor Microenvironment

The mononuclear phagocyte system (MoPh) with its most important and most broadly explored players—macrophages (M Φ) and dendritic cells (DC)—comprises a major population of immune cells that migrate to and infiltrate tumor tissue. Crucial influence of continuous, highly plastic interaction between MoPh, tumor cells and surrounding milieu has been well-documented in the past decades [1]. The opposing role of different M Φ /DC subsets to this regard has highlighted the need to define (from a quantitative point of view) more and more ‘smaller’ genotypic, phenotypic and functional

MoPh subgroups in order to decipher their possible role in antitumor immunity. The former strict differentiation between MΦ- and DC-expression profiles has meanwhile been updated and replaced by current concept based on the understanding that an expression signature and functional specialization of MoPh cells represents a rather unstable momentum that depends on interplay between cellular and molecular microenvironmental factors [2,3]. Due to an extraordinary instability and fluctuations in tumor microenvironment (TME), the categorization of tumor-associated MoPh profiles thus remains a challenging task. A number of scientific reports and excellent up-to-date reviews have addressed the question of receptor expression profiling of tumor-associated MΦ and DC in order to classify them functionally [4–6]. Thus, we do not intend to address MoPh classification algorithms; instead, we focus in this review on the cross-presentation by a subtype of tumor-associated DCs as an important functional link in triggering the cytotoxic antitumor response, and highlight the influence of low pH and high osmolarity of the TME on the cross-presenting capacities of these cells.

2. Modules of Efficient Antigen Presentation by MHC Molecules

Classical antigen-presentation pathways are not limited to professional phagocytes and imply two well-described antigen-presentation modules: (1) engulfment and processing of exogenous antigens for endosomal digestion and surface presentation in the complex with MHC-II-molecules to CD4⁺ T cells—an unspecific mechanism present in a vast majority of cell types; and (2) processing and presentation of endogenous (intracellular) antigens on MHC-I molecules in order to activate CD8⁺ T cell and induce their proliferation and cytotoxic response.

A third, special form of antigen-presentation can be seen (not exclusively, but most prominently) in a subset of DC: it is termed cross-presentation and is characterized as the capacity to present an external, phagocytosed antigen in the complex with MHC-I molecules to CD8⁺ T cells [7], thereby sensing the tumor- (or virus-) specific antigens and exposing them to induce an effective cytotoxic antitumor response [8].

2.1. Cross-Presenting Capacity of DC Subsets

Generally, DCs are categorized into conventional DCs (cDCs with previously defined cDC1 and cDC2 categories) and plasmacytoid DCs (pDCs), as reviewed elsewhere [9,10]. cDC2 (BDCA1⁺) have—especially in humans—at least a minor capacity to cross-present, even though there is evidence that cDC2 prefer classical MHC-II antigen presentation module [5,11]. By contrast, the role of cross-presentation by pDC is controversial: there are experiments showing intact clearance of viral antigens in a pDC-depleted system [12], indicating that pDCs likely do not have a major role in cross-presentation.

The cDC1 subtype seems to be the most potent cross-presenting DC population. The development of cDC1 has been reported to depend on IRF8- and Batf3- transcription factors and is characterized in humans by expression of the chemokine receptor XCR1, efficient uptake of apoptotic particles via CLEC9A (DNGR1) or necrotic debris via BDCA3 (CD141), prominent TLR3-reactivity with high IL-12 output, high intraendosomal reactive oxygen species and low acidification of endosomes [8,13,14]. In several animal models, the failure of cDC1-deficient mice to reject transplanted immunogenic tumors (for example, using Batf3^{-/-} mice) underscores the importance of these cells in cross-presentation and consecutive CD8⁺ T cell priming [5,15]. Next, high expression of MHC-I pathway related genes has been reported as a hallmark of the cDC1 subset [16]. These cells also show enhanced expression of NADPH-oxidase 2 (NOX2), which has been linked to ROS production and active alkalization of endosomes, together with synchronous, low-level expression of the c-type lectin, Siglec-G (a potent NOX2-inhibitor). Both features are required for efficient cross-presentation and are critically responsible for the enhanced cross-presentation capacities of cDC1 cells [14,17].

Of relevance, compared to other intratumoral/peritumoral leukocytes, the cDC1 population is generally small in tumor tissue. Additionally, in contrast to the immunosuppressive role of tumor-associated macrophages (TAM), a high cDC1-load in malignant tumors has been shown to

have a positive prognostic and predictive value [5,18]. Accordingly, if augmentation of the cytotoxic antitumor response through attraction of cDC1 to the cancer site and prolongation of their retention there is a therapeutic goal, induction of specific chemokine secretion by tumor cells and other immune cells (CCL4, CCL5, XCL1) might be the appropriate strategy [19,20]. Especially tumor-associated NK cells might be a key factor in this regard. Next to the aforementioned chemokines, NK cells secrete fms-like tyrosine kinase 3 ligand (FLT3-L) as well, which is regarded as a factor that prolongs cDC1 viability [5,21].

2.2. Subcellular Pathways of Cross-Presentation

On a subcellular level, two general cross-presentation pathways are described to date: the vacuolar pathway and the endosome-to-cytosol pathway [22,23]. In the vacuolar pathway, internalized antigens are degraded within endosomal compartments by lysosomal proteases and loaded onto MHC-I molecules there [24,25]. In the endosome-to-cytosol pathway, internalized antigens need to be translocated from endosomes into the cytosol, where they are degraded by the proteasome [26,27]. Afterwards, antigen-derived peptides are retranslocated by the transporter associated with antigen processing (TAP) into the ER or into endosomes for loading onto MHC-I [28–30]. Although both cross-presentation pathways have been well-documented in the past [31,32], most of the published data point to the endosome-to-cytosol pathway as a dominant mechanism of cross-presentation. The proteosomal antigen degradation seems to be a step of crucial importance for an efficient activation of CD8⁺ T cells to recognize and kill the target tumor cells or virus-carrying cells (reviewed in [8]). A recent study pointed out that proteasomes might also be present in antigen-containing endosomes and hence, proteasomal degradation might also play a role in the vacuolar cross-presentation pathway [33]. However, the physiological relevance of endosomal proteasomes still needs to be determined. In addition to the vacuolar and the endosome-to-cytosol pathway, ‘alternative’, endocytosis-independent mechanisms of cross-presentation have been suggested, such as the transfer of preprocessed antigens via a gap junction-mediated contact between a ‘donor cell’ and a DC [34] or ‘cross-dressing’, which assumes the acquisition of a peptide-loaded MHC-I molecule via membrane transfer [35]. Yet, the *in vivo* relevance of such models in the tumor setting remains unclear and needs further investigation.

3. Acidity and Hypertonicity as Biophysical Hallmarks of the TME

In addition to varying biochemical and cellular parameters, physical stress plays an important role in tumor spreading and therapy response [36]. The typical microenvironment of solid tumors is characterized by hypoxia (mainly due to insufficient blood perfusion), low extracellular pH and high intratumoral pressure (Figure 1).

3.1. Mechanisms of TME Acidification

Acidity of the TME has been traditionally linked to hypoxia, as both phenomena are synchronous hallmarks of the TME. Briefly, normal human cells under aerobic conditions produce required amounts of ATP molecules from energy-rich glucose via cellular respiration process down to CO₂ molecules resulting in the production of 32 molecules of ATP from one molecule of glucose. In normal cells under anaerobic conditions—but constitutively also in many tumors due to the Warburg effect (i.e., aerobic glycolysis; first described by Otto Warburg and his team in the 1923)—NADH is re-oxidized, leading to a reduction of pyruvate into lactate, the production of only two ATP molecules per molecule of glucose and resulting in local accumulation of lactate (reviewed in [37]). Thereby, even though the synthesis of lactate is not necessarily associated with hypoxic conditions, excessive lactate production and accumulation inside many tumors is responsible for their well described acidic TME. Specifically, melanomas, squamous cell carcinomas, breast cancer and many other adenocarcinomas as well as brain tumors show low pH values in their milieu, ranging from pH 5.8 to pH 7.4, as reviewed by Diaz et al. [38]. Other substrates next to glucose may also result in tumor-associated lactate production:

for example, glutaminolysis pathway via citric acid cycle may be even a major source of lactate in cancer microenvironment [39]. Functionally, acidosis of the tumor interstitium has been shown to be a crucial factor of tumor survival, local progression and metastasis [40].

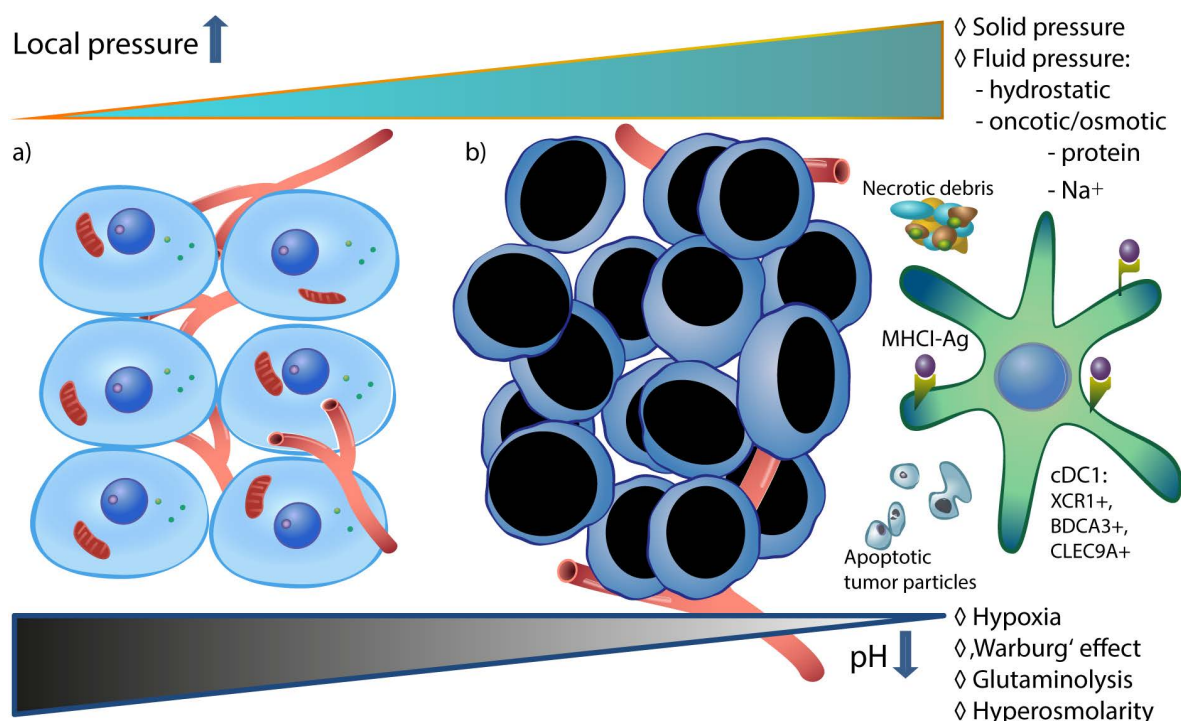


Figure 1. Typical microenvironment of tumor-associated cDC1 is acidic and hypertonic. In comparison to physiologic conditions (a), malignant neoplastic tissue (b) is characterized by lactate-induced decrease of pH value via hypoxia, aerobic glycolysis and glutaminolysis. On the other hand, increased (fluid and solid) pressure of tumor interstitium depends on biophysical characteristics of tumor mass, tumor cell death rate, abnormal blood supply but also nutritive aspects, like high-salt diet. Increased extracellular Na⁺ may further enhance lactate accumulation via supporting aerobic glycolysis.

3.2. Elevated TME Pressure—Biophysical Prediction Models

On the other hand, very few reports are available on the role of high pressure in tumor micromilieus. It has been reported and reviewed that many solid tumors demonstrate an elevated interstitial pressure [1], forming a physical barrier to transcapillary transport and thereby affecting the antitumor therapy. Still, as a result of technical difficulties to directly measure intratumoral pressure in different tissue compartments, its relevance for tumor progression (involving immune escape mechanisms) has remained largely unexplored to date. In general, pressure-induced stress in tumors can be divided into two categories: fluid-phase and solid-phase stress. Further, fluid-phase stress can be roughly categorized into hydrostatic fluid pressure of the tumor interstitium and osmotic/oncotic pressure [41]. Increased osmotic pressure results from increased ionic and protein load of distinct etiologies. Limited available data in this regard demonstrate a general hypertonicity of some TMEs (for instance, in a pancreatic adenocarcinoma murine subcutaneous tumor graft model) [42–44]. In the absence of direct in vivo measurement techniques, a compelling biomechanical approach to predict an intratumoral osmotic pressure has been proposed [42]. In this approach, based on previously published data on increased hyaluron (and other glycosaminoglycan) content in melanomas, sarcomas and adenocarcinomas, the authors developed a triphasic mathematical and biomechanical model that takes into account solid and fluid tumor pressure together with transport of anions and cations. Interestingly, the authors suggest that increased hydraulic conductivity of the tumor-associated blood vessels

(defined as interstitial fluid flow through the interstitial compartment [45]) elevates the intratumoral concentration of free ions and thereby osmotic pressure [42].

3.3. Potential Contribution of Increased Na^+ Uptake to Hypertonicity of TME

Regulation of tissue osmolarity in regard to interstitial Na^+ concentration has been extensively explored in the past decade. In order to understand and discuss a plausible Na^+ accumulation in the tumor interstitium, it is necessary to understand recent updates and challenges concerning the (patho)physiology of 'central' (renal) and peripheral regulation of Na^+ metabolism:

First, historically, despite the documentation of interstitial storage of chloride in preclinical studies (observed already 1909 by Padtberg; reviewed in [46]) more than a century ago, for a long time it was assumed that the regulatory function of kidney in regard to Na^+ keeps osmolarity of interstitium including peripheral tissue in a tight range, similar to that of plasma (290–300 mOsm/L). The concept of constant Na^+ concentration of extracellular tissue has been challenged in the past years and pointed at alternative pathways of Na^+ regulation, especially nonosmotic Na storage pools via electrolytic binding to sulfated glucosaminoglycans, i.e., important constituents of extracellular matrix. It has been proposed that this mechanism prevents water loss and buffers sodium concentration by balancing between free and stored (bound) Na^+ [47]. In concordance with these observations, a recently developed MRI-based approach (Na-MRI) enabled precise detection of extracellular Na^+ -fluctuations in time and space and revealed that peripheral tissue indeed does not maintain steady-state extracellular Na^+ concentration [48]. As detected in subcutaneous tissue, patients with autoimmune disease, arterial hypertension, or renal failure show higher Na^+ concentrations in skin in comparison to healthy counterparts [49,50].

Second, as mainly demonstrated in experimental animal models, a shift of nutritional habits towards high salt uptake may provoke a markedly increased Na^+ content in peripheral tissues, independent on a putative preexisting pathologic condition [51,52].

4. Cross-Presentation Cascade in Acidic and Hypertonic Milieu: Current Data and Possible Implications

A successful cross-presentation of tumor antigen requires efficient binding and processing of engulfed material. The cascade of antigen processing (starting with antigen uptake, delayed degradation, translocation into the cytosol, transport and loading on MHC-I molecules and transport of endoplasmatic reticulum components to endosome) has been recently reviewed [8]. Therefore, we focus here on the scarce currently available data on pH- and Na^+ -dependent modifications of the cross-presentation pathway.

4.1. Cross-Presentation in Low Extracellular pH

4.1.1. The Influence of Low pH on Antigen Uptake

DCs in the tumor micromilieu screen and bind soluble and particular antigens via a wide range of surface receptors. The abundancy and type of endocytic receptor in combination with the presented antigen likely have a significant influence on efficacy of cross-presentation per se. It is reasonable to assume, that binding and processing of apoptotic and necrotic tumor material via binding to different receptors like e.g., DEC205 will be a dominant mechanism of uptake in apoptotic particles-rich or necrotic tumors. DEC205, a member of mannose receptor family typically expressed on cross-presenting dendritic cells and on thymic epithelial cells [53,54], is a well-characterized endocytic receptor that may induce either tolerance or immunity, depending on external signals [55]. An *in vitro* study has shown a pH-dependent recognition of apoptotic particles and necrotic tumor cells by DEC205 via formation of a double-ringed receptor conformation in the acidic microenvironment, implying enhanced engulfment of tumor-associated material in acidic TME [53].

In dendritic cells, mannose receptor (MR) is another effective endocytic carbohydrate-binding damage-associated-molecular-pattern (DAMP) receptor with a variety of ligands (endogenous and microbial) [56]. MR has been reported to target the endocytosed material via pH-dependent steps for cross-presentation [57]. At physiological pH, the MR acquires an extended conformation. A decrease in pH (6–7, corresponding to early endosomes or pH 5–6 in late endosomes), results in a continuous conformational change of the receptor, which mediates ligand release [58]. Based on these data, it can be hypothesized that tumor-associated extracellular low pH decreases the capacity of MR to form stable receptor-antigen complexes and thus can be responsible for reduced cross-presentation in acidic micromilieu. Indeed, it has been shown that antigenic targeting of the human MR is capable of inducing antitumor immunity [59].

Of note, although both DEC205 and MR belong to the mannose receptor family, their pathways after antigen internalization seem to diverge. Whereas MR-mediated antigen engulfment in human DCs leads to its routing into early endosomes, delayed degradation and potent cross-presentation, internalization via the DEC205-pathway favors antigen-processing in lysosomes and rather poor cross-presentation [60]. Thus, summarizing these data, it can be discussed that an acidic cancer milieu may abrogate successful antigen internalization and processing within tumor-associated dendritic cell by favorizing less efficient DEC205-dependent cross-presentation model (Figure 2).

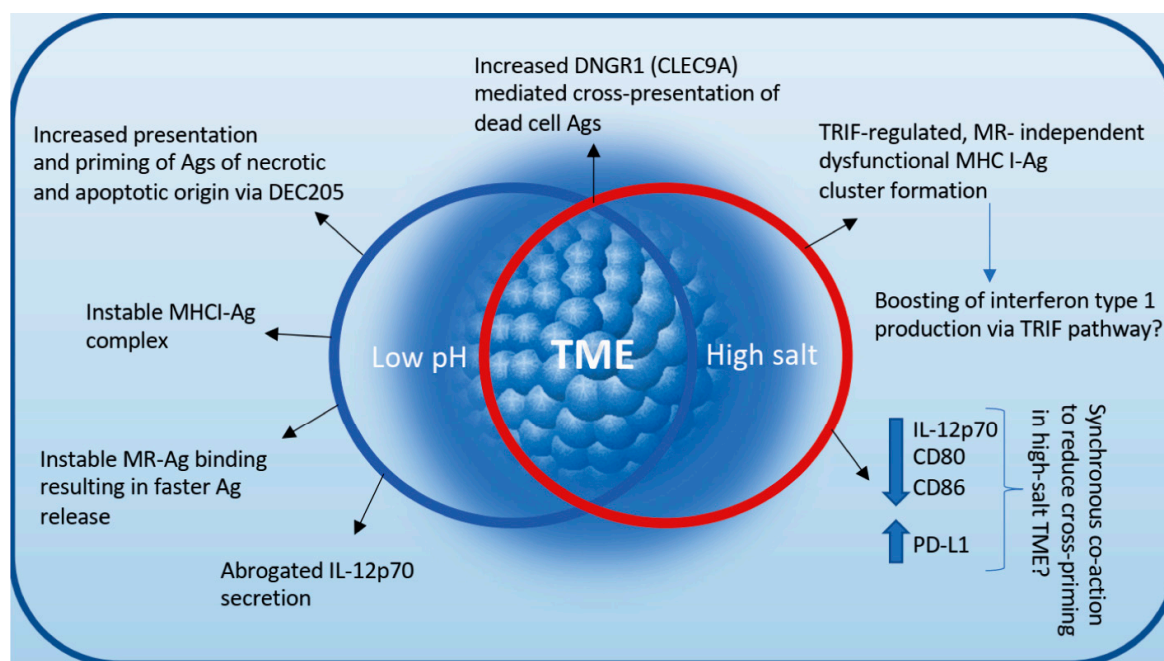


Figure 2. Impact of acidic and hyperosmolar tumor microenvironment (TME) on cross-presentation and cross-priming cascade is dynamic and complex. Interplay of low pH- and high Na^+ - triggered phenomena likely decides the fate and efficacy of cross-presentation. Also here can be postulated that tumor nature and viability (in regard to apoptotic and necrotic rate) partially shape the receptor-antigen binding signature and thus contribute to the response of cDC1 to biophysical TME stresses.

It is evident that low pH influences other DC receptors as well, not necessarily leading to a similar outcome, adding to the complexity of the phenomenon. An example is the pH- and ionic load- dependent alteration of another marker of type 1 classical DCs, DNGR1 [61]. DNGR1 (synonym: CLEC9A) is a DAMP-receptor typically expressed on cross-presenting DCs, facilitating cross-presentation of dead-cell-associated antigens. Hanc et al. have convincingly shown that low pH and increased ionic content of the microenvironment lead to a conformational change of the neck region and induction of so-called reduction-sensitive receptor dimers to trigger more efficient cross-presentation and cross-priming [61]. The detailed role of DNGR1 in regulation of the necrotic-cargo intracellular compartment [62] via directing the necrotic antigen material to

nonlysosomal, rather alkaline, nondegradative niche, thereby facilitating CD8⁺ T cell activation [63] has been reviewed by Cueto et al. [64].

4.1.2. The Influence of Low pH on Antigen-MHC-I Stability and Costimulatory Signals

Supporting the theory of damaged cross-presentation at low pH, older studies have documented that peptide-MHC-I complexes are more stable at neutral than at acidic pH [65]; still, no recent data are available to this regard. In addition, lactate has been reported to modulate cytokine secretion by monocyte-derived DCs. Lactic acid has triggered a significant reduction of IL-12p70 in tumor associated dendritic cells, hence blocking an important stimulatory signal in the cross-priming cascade [66,67]. In the same experimental setting no significant impact on secretion of 'anti-inflammatory' IL-10 could be seen.

Interestingly, both high salt and acidic milieu have been shown to trigger IL-1 β secretion via activation of inflammasome pathway ([68]; also recent publication from Pitzer et al., FASEB, April 2020). Although recently published ovalbumine-based in vitro models suggest that NLRP3 inflammasome activation may trigger (MHC-I- and MHC-II- dependent) antigen presentation in general [69], its role in an efficient cross-presentation remains to be further investigated.

4.2. Cross-Presentation in Hyperosmolar Micromilieu

4.2.1. Lessons from Murine Kidney and Cell Culture Models

The influence of hyperosmolarity via increased Na⁺ in the microenvironment of MoPh in inflammatory, non-neoplastic settings has been the subject of extensive studies in the past years [46,70–77]. Focusing on dendritic cells, our initial data from a murine kidney transplantation model have demonstrated a strong abrogation of cross-presentation pathway associated genes in the hypertonic renal medullary compartment [71]. Linking these results to function of DCs in hypertonic microenvironment that may reflect the osmolarity range of TME, our in vitro model of cross-presentation showed a significant reduction of cross-priming capacity in bone marrow derived dendritic cells (BMDCs) developed in hyperosmolarity [78]. Notably, the decreased cross-priming effect occurred despite increased uptake, processing and presentation of OVA-derived antigen in high salt conditions. In our experiments, blockade of cross-priming was a result of a TRIF-mediated (yet toll-like receptor-independent) dysfunctional MHC-I-peptide complex cluster formation. Having on mind the link between Interferon type 1 and TRIF signaling, as discussed by Jantsch et al. [46], it is possible that the Na⁺ induced, TRIF-mediated excessive expression of interferon type 1 reduces the cross-priming by DCs [79]. This hypothesis still requires further examination.

To our surprise, Na⁺-induced dysregulation of co-stimulatory and co-inhibitory molecules (including reduction of IL-12 secretion as well as upregulation of PD-L1 and inhibition of both CD80 and CD86 expression upon exposure to high salt) was not responsible for the reduction of cross-priming—at least not in a 'single-parameter'-dependent manner. Nevertheless, we cannot exclude a coaction of the abovementioned regulatory molecules in high-salt induced blockade of cross-priming [78]. Intriguingly, the salt-induced cross-presentation phenotype was in this experimental setting independent of MR, suggesting that also the hypertonic TME may redirect MR-mediated antigen uptake towards other, in the light of cross-presentation less efficient DAMP receptors [78].

4.2.2. Linking TME Hyperosmolarity to Lactate-Induced Acidosis

High salt content of TME may also modify cancer metabolism towards supporting aerobic glycolysis and consequent accumulation of lactate, highlighting the complexity of metabolic tumor surveillance [80]. It has been suggested that hypertonic extracellular stress induces the Warburg effect by enhancing glucose transport and lactic acidosis in tumor cells [81]; these results were concordant with older observations from breast cancer and liver tumor mouse models [82].

Taken together, limited and in part discordant published data indicate that interplay between acidic and hypertonic stress results in modification of cancer cell metabolism and dendritic cell function towards blockade of efficient cross-presentation and cross-priming (Figure 2).

5. Conclusions

Dendritic cells (specifically cDC1) are the most efficient antigen-presenting cells. Their unique cross-presentation capacity has been extensively explored in attempts to boost cytotoxic tumor immunity via DC vaccine strategies, albeit with rather poor clinical results to date. We reviewed here focused, limited and to some extent discordant data on the role of hypertonicity and acidity on DC function that largely go in line with other published observations regarding a general suppression of antitumor immunity via tumor metabolites [67,83,84].

In general, available evidence on the effects of low pH and hypertonicity on dendritic cells is (a) mainly focused on single steps of antigen uptake and presentation per se (to our knowledge without available data on subcellular antigen processing cascade) and thus poorly explored to date; (b) mostly related to in vitro or animal models, hence not automatically applicable to clinical situation and (c) in part based on older scientific studies that do not necessarily follow the current state of immunological knowledge. Specifically, methodological issues in measurement of pH and osmolarity of extracellular microenvironment in situ—in time and space—represent to our opinion the major obstacle to be addressed to this regard.

It must be pointed out that—independent of subcellular pathways—the effect of TME on immune cell activation should be finally observed in the context of tumor survival as the most relevant clinical endpoint. Clearly, antitumor immunity is a result of coaction of all parts of immune system at the tumor site and in regional draining lymph nodes and cannot be determined via observation of single components alone. Indeed, opposing data from two in vivo mouse tumor models based on subcutaneous injection of murine melanoma and lung carcinoma cells reported significant reduction of tumor growth upon high-salt intake via depletion of myeloid-derived suppressor cells [85]. On the other hand, in humans, highly malignant nature of tumors rising in hypertonic organ compartments (like collecting duct carcinoma of kidney and medullary renal cell cancer) with an extraordinary metastatic potential speak in favor of high salt-induced immune escape mechanisms. In the same line, a large set of epidemiologic data clearly indicates that high salt diet (independent on *Helicobacter pylori* infection) represents an independent high-risk factor for the development and progression of gastric cancer [86]. Nonetheless, mechanisms underlying the development and progression of potentially salt-induced malignancies remain unclear.

Finally, further interdisciplinary investigations of molecular and physical mechanisms of pH- and Na⁺-mediated modulation of DC function together with appreciation of dynamic, complex, species-, tissue- and tumor-type-specific relationships between immune system compartments and tumor microenvironments are necessary for a better understanding of and fighting against the immune escape of cancer.

Author Contributions: Z.V.P. designed and took the lead in writing the manuscript with critical input from S.B. and S.P. A.M. contributed to the design and aided in interpreting literature data. All authors provided feedback and contributed to the final manuscript. All authors have read and agreed to the published version of the manuscript.

Funding: This manuscript received no external funding.

Conflicts of Interest: The authors declare no conflict of interest.

References

1. Heldin, C.H.; Rubin, K.; Pietras, K.; Ostman, A. High interstitial fluid pressure—an obstacle in cancer therapy. *Nat. Rev. Cancer* **2004**, *4*, 806–813. [[CrossRef](#)] [[PubMed](#)]
2. Laviron, M.; Boissonnas, A. Ontogeny of Tumor-Associated Macrophages. *Front. Immunol.* **2019**, *10*, 1799. [[CrossRef](#)] [[PubMed](#)]

3. Murray, P.J.; Allen, J.E.; Biswas, S.K.; Fisher, E.A.; Gilroy, D.W.; Goerdt, S.; Gordon, S.; Hamilton, J.A.; Ivashkiv, L.B.; Lawrence, T.; et al. Macrophage activation and polarization: Nomenclature and experimental guidelines. *Immunity* **2014**, *41*, 14–20. [[CrossRef](#)] [[PubMed](#)]
4. Blander, J.M. Regulation of the Cell Biology of Antigen Cross-Presentation. *Annu. Rev. Immunol.* **2018**, *36*, 717–753. [[CrossRef](#)] [[PubMed](#)]
5. Bottcher, J.P.; Reis e Sousa, C. The Role of Type 1 Conventional Dendritic Cells in Cancer Immunity. *Trends. Cancer* **2018**, *4*, 784–792. [[CrossRef](#)] [[PubMed](#)]
6. Olingy, C.E.; Dinh, H.Q.; Hedrick, C.C. Monocyte heterogeneity and functions in cancer. *J. Leukoc. Biol.* **2019**, *106*, 309–322. [[CrossRef](#)]
7. Huang, A.Y.; Golumbek, P.; Ahmadzadeh, M.; Jaffee, E.; Pardoll, D.; Levitsky, H. Role of bone marrow-derived cells in presenting MHC class I-restricted tumor antigens. *Science* **1994**, *264*, 961–965. [[CrossRef](#)]
8. Embgenbroich, M.; Burgdorf, S. Current Concepts of Antigen Cross-Presentation. *Front. Immunol.* **2018**, *9*, 1643. [[CrossRef](#)]
9. Guilliams, M.; Ginhoux, F.; Jakubzick, C.; Naik, S.H.; Onai, N.; Schraml, B.U.; Segura, E.; Tussiwand, R.; Yona, S. Dendritic cells, monocytes and macrophages: A unified nomenclature based on ontogeny. *Nat. Rev. Immunol.* **2014**, *14*, 571–578. [[CrossRef](#)]
10. Guilliams, M.; Malissen, B. A Death Notice for In-Vitro-Generated GM-CSF Dendritic Cells? *Immunity* **2015**, *42*, 988–990. [[CrossRef](#)]
11. Savina, A.; Jancic, C.; Hugues, S.; Guermonprez, P.; Vargas, P.; Moura, I.C.; Lennon-Dumenil, A.M.; Seabra, M.C.; Raposo, G.; Amigorena, S. NOX2 controls phagosomal pH to regulate antigen processing during crosspresentation by dendritic cells. *Cell* **2006**, *126*, 205–218. [[CrossRef](#)] [[PubMed](#)]
12. Savina, A.; Peres, A.; Cebrian, I.; Carmo, N.; Moita, C.; Hacohen, N.; Moita, L.F.; Amigorena, S. The small GTPase Rac2 controls phagosomal alkalinization and antigen crosspresentation selectively in CD8(+) dendritic cells. *Immunity* **2009**, *30*, 544–555. [[CrossRef](#)] [[PubMed](#)]
13. Spranger, S.; Dai, D.; Horton, B.; Gajewski, T.F. Tumor-Residing Batf3 Dendritic Cells Are Required for Effector T Cell Trafficking and Adoptive T Cell Therapy. *Cancer Cell* **2017**, *31*, 711–723. [[CrossRef](#)] [[PubMed](#)]
14. Dudziak, D.; Kamphorst, A.O.; Heidkamp, G.F.; Buchholz, V.R.; Trumpfheller, C.; Yamazaki, S.; Cheong, C.; Liu, K.; Lee, H.W.; Park, C.G.; et al. Differential antigen processing by dendritic cell subsets in vivo. *Science* **2007**, *315*, 107–111. [[CrossRef](#)] [[PubMed](#)]
15. Ding, Y.; Guo, Z.; Liu, Y.; Li, X.; Zhang, Q.; Xu, X.; Gu, Y.; Zhang, Y.; Zhao, D.; Cao, X. The lectin Siglec-G inhibits dendritic cell cross-presentation by impairing MHC class I-peptide complex formation. *Nat. Immunol.* **2016**, *17*, 1167–1175. [[CrossRef](#)] [[PubMed](#)]
16. Merad, M.; Sathe, P.; Helft, J.; Miller, J.; Mortha, A. The dendritic cell lineage: Ontogeny and function of dendritic cells and their subsets in the steady state and the inflamed setting. *Annu. Rev. Immunol.* **2013**, *31*, 563–604. [[CrossRef](#)]
17. GeurtsvanKessel, C.H.; Willart, M.A.; van Rijt, L.S.; Muskens, F.; Kool, M.; Baas, C.; Thielemans, K.; Bennett, C.; Clausen, B.E.; Hoogsteden, H.C.; et al. Clearance of influenza virus from the lung depends on migratory langerin+CD11b- but not plasmacytoid dendritic cells. *J. Exp. Med.* **2008**, *205*, 1621–1634. [[CrossRef](#)]
18. Ma, Y.; Shurin, G.V.; Peiyuan, Z.; Shurin, M.R. Dendritic cells in the cancer microenvironment. *J. Cancer* **2013**, *4*, 36–44. [[CrossRef](#)]
19. Halama, N.; Zoernig, I.; Berthel, A.; Kahlert, C.; Klupp, F.; Suarez-Carmona, M.; Suetterlin, T.; Brand, K.; Krauss, J.; Lasitschka, F.; et al. Tumoral Immune Cell Exploitation in Colorectal Cancer Metastases Can Be Targeted Effectively by Anti-CCR5 Therapy in Cancer Patients. *Cancer Cell* **2016**, *29*, 587–601. [[CrossRef](#)]
20. Tan, M.C.; Goedegebuure, P.S.; Belt, B.A.; Flaherty, B.; Sankpal, N.; Gillanders, W.E.; Eberlein, T.J.; Hsieh, C.S.; Linehan, D.C. Disruption of CCR5-dependent homing of regulatory T cells inhibits tumor growth in a murine model of pancreatic cancer. *J. Immunol.* **2009**, *182*, 1746–1755. [[CrossRef](#)]
21. Barry, K.C.; Hsu, J.; Broz, M.L.; Cueto, F.J.; Binnewies, M.; Combes, A.J.; Nelson, A.E.; Loo, K.; Kumar, R.; Rosenblum, M.D.; et al. A natural killer-dendritic cell axis defines checkpoint therapy-responsive tumor microenvironments. *Nat. Med.* **2018**, *24*, 1178–1191. [[CrossRef](#)] [[PubMed](#)]
22. Burgdorf, S.; Kurts, C. Endocytosis mechanisms and the cell biology of antigen presentation. *Curr. Opin. Immunol.* **2008**, *20*, 89–95. [[CrossRef](#)] [[PubMed](#)]

23. Burgdorf, S.; Scholz, C.; Kautz, A.; Tampe, R.; Kurts, C. Spatial and mechanistic separation of cross-presentation and endogenous antigen presentation. *Nat. Immunol.* **2008**, *9*, 558–566. [[CrossRef](#)] [[PubMed](#)]
24. Bertholet, S.; Goldszmid, R.; Morrot, A.; Debrabant, A.; Afrin, F.; Collazo-Custodio, C.; Houde, M.; Desjardins, M.; Sher, A.; Sacks, D. Leishmania antigens are presented to CD8+ T cells by a transporter associated with antigen processing-independent pathway in vitro and in vivo. *J. Immunol.* **2006**, *177*, 3525–3533. [[CrossRef](#)] [[PubMed](#)]
25. Shen, L.; Sigal, L.J.; Boes, M.; Rock, K.L. Important role of cathepsin S in generating peptides for TAP-independent MHC class I crosspresentation in vivo. *Immunity* **2004**, *21*, 155–165. [[CrossRef](#)]
26. Ackerman, A.L.; Kyritsis, C.; Tampe, R.; Cresswell, P. Early phagosomes in dendritic cells form a cellular compartment sufficient for cross presentation of exogenous antigens. *Proc. Natl. Acad. Sci. USA* **2003**, *100*, 12889–12894. [[CrossRef](#)]
27. Kovacovics-Bankowski, M.; Rock, K.L. Presentation of exogenous antigens by macrophages: Analysis of major histocompatibility complex class I and II presentation and regulation by cytokines. *Eur. J. Immunol.* **1994**, *24*, 2421–2428. [[CrossRef](#)]
28. Ackerman, A.L.; Giodini, A.; Cresswell, P. A role for the endoplasmic reticulum protein retrotranslocation machinery during crosspresentation by dendritic cells. *Immunity* **2006**, *25*, 607–617. [[CrossRef](#)]
29. Guermonprez, P.; Saveanu, L.; Kleijmeer, M.; Davoust, J.; Van Endert, P.; Amigorena, S. ER-phagosome fusion defines an MHC class I cross-presentation compartment in dendritic cells. *Nature* **2003**, *425*, 397–402. [[CrossRef](#)]
30. Houde, M.; Bertholet, S.; Gagnon, E.; Brunet, S.; Goyette, G.; Laplante, A.; Princiotta, M.F.; Thibault, P.; Sacks, D.; Desjardins, M. Phagosomes are competent organelles for antigen cross-presentation. *Nature* **2003**, *425*, 402–406. [[CrossRef](#)]
31. Liu, T.; Zhou, X.; Abdel-Motal, U.M.; Ljunggren, H.G.; Jondal, M. MHC class I presentation of live and heat-inactivated Sendai virus antigen in T2Kb cells depends on an intracellular compartment with endosomal characteristics. *Scand. J. Immunol.* **1997**, *45*, 527–533. [[CrossRef](#)]
32. Pfeifer, J.D.; Wick, M.J.; Roberts, R.L.; Findlay, K.; Normark, S.J.; Harding, C.V. Phagocytic processing of bacterial antigens for class I MHC presentation to T cells. *Nature* **1993**, *361*, 359–362. [[CrossRef](#)] [[PubMed](#)]
33. Sengupta, D.; Graham, M.; Liu, X.; Cresswell, P. Proteasomal degradation within endocytic organelles mediates antigen cross-presentation. *EMBO J.* **2019**, *38*, e99266. [[CrossRef](#)] [[PubMed](#)]
34. Neijssen, J.; Herberts, C.; Drijfhout, J.W.; Reits, E.; Janssen, L.; Neefjes, J. Cross-presentation by intercellular peptide transfer through gap junctions. *Nature* **2005**, *434*, 83–88. [[CrossRef](#)] [[PubMed](#)]
35. Dolan, B.P.; Gibbs, K.D., Jr.; Ostrand-Rosenberg, S. Dendritic cells cross-dressed with peptide MHC class I complexes prime CD8+ T cells. *J. Immunol.* **2006**, *177*, 6018–6024. [[CrossRef](#)]
36. Jain, R.K.; Martin, J.D.; Stylianopoulos, T. The role of mechanical forces in tumor growth and therapy. *Annu. Rev. Biomed. Eng.* **2014**, *16*, 321–346. [[CrossRef](#)]
37. Liberti, M.V.; Locasale, J.W. The Warburg Effect: How Does it Benefit Cancer Cells? *Trends. Biochem. Sci.* **2016**, *41*, 211–218. [[CrossRef](#)]
38. Erra Diaz, F.; Dantas, E.; Geffner, J. Unravelling the Interplay between Extracellular Acidosis and Immune Cells. *Mediat. Inflamm.* **2018**, *2018*, 1218297. [[CrossRef](#)]
39. DeBerardinis, R.J.; Mancuso, A.; Daikhin, E.; Nissim, I.; Yudkoff, M.; Wehrli, S.; Thompson, C.B. Beyond aerobic glycolysis: Transformed cells can engage in glutamine metabolism that exceeds the requirement for protein and nucleotide synthesis. *Proc. Natl. Acad. Sci. USA* **2007**, *104*, 19345–19350. [[CrossRef](#)]
40. Corbet, C.; Feron, O. Tumour acidosis: From the passenger to the driver's seat. *Nat. Rev. Cancer* **2017**, *17*, 577–593. [[CrossRef](#)]
41. Stylianopoulos, T.; Martin, J.D.; Snuderl, M.; Mpekris, F.; Jain, S.R.; Jain, R.K. Coevolution of solid stress and interstitial fluid pressure in tumors during progression: Implications for vascular collapse. *Cancer Res.* **2013**, *73*, 3833–3841. [[CrossRef](#)] [[PubMed](#)]
42. Voutouri, C.; Stylianopoulos, T. Evolution of osmotic pressure in solid tumors. *J. Biomech.* **2014**, *47*, 3441–3447. [[CrossRef](#)] [[PubMed](#)]

43. DuFort, C.C.; DelGiorno, K.E.; Carlson, M.A.; Osgood, R.J.; Zhao, C.; Huang, Z.; Thompson, C.B.; Connor, R.J.; Thanos, C.D.; Scott Brockenbrough, J.; et al. Interstitial Pressure in Pancreatic Ductal Adenocarcinoma Is Dominated by a Gel-Fluid Phase. *Biophys. J.* **2016**, *110*, 2106–2119. [[CrossRef](#)] [[PubMed](#)]
44. DuFort, C.C.; DelGiorno, K.E.; Hingorani, S.R. Mounting Pressure in the Microenvironment: Fluids, Solids, and Cells in Pancreatic Ductal Adenocarcinoma. *Gastroenterology* **2016**, *150*, 1545–1557. [[CrossRef](#)] [[PubMed](#)]
45. Stylianopoulos, T.; Munn, L.L.; Jain, R.K. Reengineering the Physical Microenvironment of Tumors to Improve Drug Delivery and Efficacy: From Mathematical Modeling to Bench to Bedside. *Trends. Cancer* **2018**, *4*, 292–319. [[CrossRef](#)] [[PubMed](#)]
46. Neubert, P.; Schroder, A.; Muller, D.N.; Jantsch, J. Interplay of Na(+) Balance and Immunobiology of Dendritic Cells. *Front. Immunol.* **2019**, *10*, 599. [[CrossRef](#)]
47. Titze, J.; Shakibaei, M.; Schaffhuber, M.; Schulze-Tanzil, G.; Porst, M.; Schwind, K.H.; Dietsch, P.; Hilgers, K.F. Glycosaminoglycan polymerization may enable osmotically inactive Na⁺ storage in the skin. *Am. J. Physiol. Heart Circ. Physiol.* **2004**, *287*, H203–H208. [[CrossRef](#)]
48. Linz, P.; Santoro, D.; Renz, W.; Rieger, J.; Ruehle, A.; Ruff, J.; Deimling, M.; Rakova, N.; Muller, D.N.; Luft, F.C.; et al. Skin sodium measured with (2)(3)Na MRI at 7.0 T. *NMR Biomed.* **2015**, *28*, 54–62. [[CrossRef](#)]
49. Jantsch, J.; Schatz, V.; Friedrich, D.; Schroder, A.; Kopp, C.; Siegert, I.; Maronna, A.; Wendelborn, D.; Linz, P.; Binger, K.J.; et al. Cutaneous Na⁺ storage strengthens the antimicrobial barrier function of the skin and boosts macrophage-driven host defense. *Cell Metab.* **2015**, *21*, 493–501. [[CrossRef](#)]
50. Kopp, C.; Beyer, C.; Linz, P.; Dahlmann, A.; Hammon, M.; Jantsch, J.; Neubert, P.; Rosenhauer, D.; Muller, D.N.; Cavallaro, A.; et al. Na⁺ deposition in the fibrotic skin of systemic sclerosis patients detected by ²³Na-magnetic resonance imaging. *Rheumatology* **2017**, *56*, 556–560. [[CrossRef](#)]
51. Titze, J.; Lang, R.; Ilies, C.; Schwind, K.H.; Kirsch, K.A.; Dietsch, P.; Luft, F.C.; Hilgers, K.F. Osmotically inactive skin Na⁺ storage in rats. *Am. J. Physiol. Renal. Physiol.* **2003**, *285*, F1108–F1117. [[CrossRef](#)] [[PubMed](#)]
52. Wiig, H.; Schroder, A.; Neuhofer, W.; Jantsch, J.; Kopp, C.; Karlsen, T.V.; Boschmann, M.; Goss, J.; Bry, M.; Rakova, N.; et al. Immune cells control skin lymphatic electrolyte homeostasis and blood pressure. *J. Clin. Investig.* **2013**, *123*, 2803–2815. [[CrossRef](#)] [[PubMed](#)]
53. Cao, L.; Shi, X.; Chang, H.; Zhang, Q.; He, Y. pH-Dependent recognition of apoptotic and necrotic cells by the human dendritic cell receptor DEC205. *Proc. Natl. Acad. Sci. USA* **2015**, *112*, 7237–7242. [[CrossRef](#)] [[PubMed](#)]
54. Jiang, W.; Swiggard, W.J.; Heufler, C.; Peng, M.; Mirza, A.; Steinman, R.M.; Nussenzweig, M.C. The receptor DEC-205 expressed by dendritic cells and thymic epithelial cells is involved in antigen processing. *Nature* **1995**, *375*, 151–155. [[CrossRef](#)] [[PubMed](#)]
55. Hawiger, D.; Inaba, K.; Dorsett, Y.; Guo, M.; Mahnke, K.; Rivera, M.; Ravetch, J.V.; Steinman, R.M.; Nussenzweig, M.C. Dendritic cells induce peripheral T cell unresponsiveness under steady state conditions in vivo. *J. Exp. Med.* **2001**, *194*, 769–779. [[CrossRef](#)]
56. Martinez-Pomares, L. The mannose receptor. *J. Leukoc. Biol.* **2012**, *92*, 1177–1186. [[CrossRef](#)]
57. Burgdorf, S.; Lukacs-Kornek, V.; Kurts, C. The mannose receptor mediates uptake of soluble but not of cell-associated antigen for cross-presentation. *J. Immunol.* **2006**, *176*, 6770–6776. [[CrossRef](#)]
58. Hu, Z.; Shi, X.; Yu, B.; Li, N.; Huang, Y.; He, Y. Structural Insights into the pH-Dependent Conformational Change and Collagen Recognition of the Human Mannose Receptor. *Structure* **2018**, *26*, 60–71. [[CrossRef](#)]
59. He, L.Z.; Crocker, A.; Lee, J.; Mendoza-Ramirez, J.; Wang, X.T.; Vitale, L.A.; O'Neill, T.; Petromilli, C.; Zhang, H.F.; Lopez, J.; et al. Antigenic targeting of the human mannose receptor induces tumor immunity. *J. Immunol.* **2007**, *178*, 6259–6267. [[CrossRef](#)]
60. Chatterjee, B.; Smed-Sorensen, A.; Cohn, L.; Chalouni, C.; Vandlen, R.; Lee, B.C.; Widger, J.; Keler, T.; Delamarre, L.; Mellman, I. Internalization and endosomal degradation of receptor-bound antigens regulate the efficiency of cross presentation by human dendritic cells. *Blood* **2012**, *120*, 2011–2020. [[CrossRef](#)]
61. Hanc, P.; Schulz, O.; Fischbach, H.; Martin, S.R.; Kjaer, S.; Reis e Sousa, C. A pH- and ionic strength-dependent conformational change in the neck region regulates DNGR-1 function in dendritic cells. *EMBO J.* **2016**, *35*, 2484–2497. [[CrossRef](#)] [[PubMed](#)]
62. Zelenay, S.; Keller, A.M.; Whitney, P.G.; Schraml, B.U.; Deddouche, S.; Rogers, N.C.; Schulz, O.; Sancho, D.; Reis e Sousa, C. The dendritic cell receptor DNGR-1 controls endocytic handling of necrotic cell antigens to favor cross-priming of CTLs in virus-infected mice. *J. Clin. Investig.* **2012**, *122*, 1615–1627. [[CrossRef](#)] [[PubMed](#)]

63. Burgdorf, S.; Kautz, A.; Bohnert, V.; Knolle, P.A.; Kurts, C. Distinct pathways of antigen uptake and intracellular routing in CD4 and CD8 T cell activation. *Science* **2007**, *316*, 612–616. [[CrossRef](#)] [[PubMed](#)]
64. Cueto, F.J.; Del Fresno, C.; Sancho, D. DNGR-1, a Dendritic Cell-Specific Sensor of Tissue Damage That Dually Modulates Immunity and Inflammation. *Front. Immunol.* **2019**, *10*, 3146. [[CrossRef](#)]
65. Stryhn, A.; Pedersen, L.O.; Romme, T.; Olsen, A.C.; Nissen, M.H.; Thorpe, C.J.; Buus, S. pH dependence of MHC class I-restricted peptide presentation. *J. Immunol.* **1996**, *156*, 4191–4197.
66. Gottfried, E.; Kunz-Schughart, L.A.; Ebner, S.; Mueller-Klieser, W.; Hoves, S.; Andreesen, R.; Mackensen, A.; Kreutz, M. Tumor-derived lactic acid modulates dendritic cell activation and antigen expression. *Blood* **2006**, *107*, 2013–2021. [[CrossRef](#)] [[PubMed](#)]
67. Romero-Garcia, S.; Moreno-Altamirano, M.M.; Prado-Garcia, H.; Sanchez-Garcia, F.J. Lactate Contribution to the Tumor Microenvironment: Mechanisms, Effects on Immune Cells and Therapeutic Relevance. *Front. Immunol.* **2016**, *7*, 52. [[CrossRef](#)] [[PubMed](#)]
68. Rajamaki, K.; Nordstrom, T.; Nurmi, K.; Akerman, K.E.; Kovanen, P.T.; Oorni, K.; Eklund, K.K. Extracellular acidosis is a novel danger signal alerting innate immunity via the NLRP3 inflammasome. *J. Biol. Chem.* **2013**, *288*, 13410–13419. [[CrossRef](#)] [[PubMed](#)]
69. Li, T.; Zehner, M.; He, J.; Prochnicki, T.; Horvath, G.; Latz, E.; Burgdorf, S.; Takeoka, S. NLRP3 inflammasome-activating arginine-based liposomes promote antigen presentations in dendritic cells. *Int. J. Nanomed.* **2019**, *14*, 3503–3516. [[CrossRef](#)]
70. Chessa, F.; Hielscher, T.; Mathow, D.; Grone, H.J.; Popovic, Z.V. Transcriptional profiling of dendritic cells matured in different osmolarities. *Genom. Data* **2016**, *7*, 64–66. [[CrossRef](#)] [[PubMed](#)]
71. Chessa, F.; Mathow, D.; Wang, S.; Hielscher, T.; Atzberger, A.; Porubsky, S.; Gretz, N.; Burgdorf, S.; Grone, H.J.; Popovic, Z.V. The renal microenvironment modifies dendritic cell phenotype. *Kidney Int.* **2016**, *89*, 82–94. [[CrossRef](#)] [[PubMed](#)]
72. Machnik, A.; Neuhofer, W.; Jantsch, J.; Dahlmann, A.; Tammela, T.; Machura, K.; Park, J.K.; Beck, F.X.; Muller, D.N.; Derer, W.; et al. Macrophages regulate salt-dependent volume and blood pressure by a vascular endothelial growth factor-C-dependent buffering mechanism. *Nat. Med.* **2009**, *15*, 545–552. [[CrossRef](#)]
73. Muller, D.N.; Wilck, N.; Haase, S.; Kleinewietfeld, M.; Linker, R.A. Sodium in the microenvironment regulates immune responses and tissue homeostasis. *Nat. Rev. Immunol.* **2019**, *19*, 243–254. [[CrossRef](#)]
74. Schatz, V.; Neubert, P.; Schroder, A.; Binger, K.; Gebhard, M.; Muller, D.N.; Luft, F.C.; Titze, J.; Jantsch, J. Elementary immunology: Na(+) as a regulator of immunity. *Pediatr. Nephrol.* **2017**, *32*, 201–210. [[CrossRef](#)] [[PubMed](#)]
75. Titze, J. Interstitial fluid homeostasis and pressure: News from the black box. *Kidney Int.* **2013**, *84*, 869–871. [[CrossRef](#)]
76. Titze, J.; Dahlmann, A.; Lerchl, K.; Kopp, C.; Rakova, N.; Schroder, A.; Luft, F.C. Spooky sodium balance. *Kidney Int.* **2014**, *85*, 759–767. [[CrossRef](#)] [[PubMed](#)]
77. Wiig, H.; Luft, F.C.; Titze, J.M. The interstitium conducts extrarenal storage of sodium and represents a third compartment essential for extracellular volume and blood pressure homeostasis. *Acta Physiol.* **2018**, *222*, e13006. [[CrossRef](#)]
78. Popovic, Z.V.; Embgenbroich, M.; Chessa, F.; Nordstrom, V.; Bonrouhi, M.; Hielscher, T.; Gretz, N.; Wang, S.; Mathow, D.; Quast, T.; et al. Hyperosmolarity impedes the cross-priming competence of dendritic cells in a TRIF-dependent manner. *Sci. Rep.* **2017**, *7*, 311. [[CrossRef](#)]
79. Pfaender, S.; Grabski, E.; Detje, C.N.; Riebesehl, N.; Lienenklaus, S.; Steinmann, E.; Kalinke, U.; Pietschmann, T. Hepatitis C Virus Stimulates Murine CD8alpha-Like Dendritic Cells to Produce Type I Interferon in a TRIF-Dependent Manner. *PLoS Pathog.* **2016**, *12*, e1005736. [[CrossRef](#)]
80. Amara, S.; Tiriveedhi, V. Inflammatory role of high salt level in tumor microenvironment (Review). *Int. J. Oncol.* **2017**, *50*, 1477–1481. [[CrossRef](#)]
81. Epstein, T.; Xu, L.; Gillies, R.J.; Gatenby, R.A. Separation of metabolic supply and demand: Aerobic glycolysis as a normal physiological response to fluctuating energetic demands in the membrane. *Cancer Metab.* **2014**, *2*, 7. [[CrossRef](#)] [[PubMed](#)]
82. Sparks, R.L.; Pool, T.B.; Smith, N.K.; Cameron, I.L. Effects of amiloride on tumor growth and intracellular element content of tumor cells in vivo. *Cancer Res.* **1983**, *43*, 73–77. [[PubMed](#)]



83. Huber, V.; Camisaschi, C.; Berzi, A.; Ferro, S.; Lugini, L.; Triulzi, T.; Tuccitto, A.; Tagliabue, E.; Castelli, C.; Rivoltini, L. Cancer acidity: An ultimate frontier of tumor immune escape and a novel target of immunomodulation. *Semin. Cancer Biol.* **2017**, *43*, 74–89. [[CrossRef](#)]
84. Lee, J.H.; Choi, S.Y.; Jung, N.C.; Song, J.Y.; Seo, H.G.; Lee, H.S.; Lim, D.S. The Effect of the Tumor Microenvironment and Tumor-Derived Metabolites on Dendritic Cell Function. *J. Cancer* **2020**, *11*, 769–775. [[CrossRef](#)] [[PubMed](#)]
85. Willebrand, R.; Hamad, I.; Van Zeebroeck, L.; Kiss, M.; Bruderek, K.; Geuzens, A.; Swinnen, D.; Corte-Real, B.F.; Marko, L.; Lebegge, E.; et al. High Salt Inhibits Tumor Growth by Enhancing Anti-tumor Immunity. *Front. Immunol.* **2019**, *10*, 1141. [[CrossRef](#)]
86. Peleteiro, B.; Lopes, C.; Figueiredo, C.; Lunet, N. Salt intake and gastric cancer risk according to Helicobacter pylori infection, smoking, tumour site and histological type. *Br. J. Cancer* **2011**, *104*, 198–207. [[CrossRef](#)]



© 2020 by the authors. Licensee MDPI, Basel, Switzerland. This article is an open access article distributed under the terms and conditions of the Creative Commons Attribution (CC BY) license (<http://creativecommons.org/licenses/by/4.0/>).

Review

Histone Demethylase KDM5B as a Therapeutic Target for Cancer Therapy

Anmi Jose ¹, Gautham G. Shenoy ², Gabriel Sunil Rodrigues ³, Naveena A. N. Kumar ⁴ , Murali Munisamy ¹, Levin Thomas ¹, Jill Kolesar ⁵ , Ganesh Rai ⁶, Praveen P. N. Rao ⁷  and Mahadev Rao ^{1,*}

- ¹ Department of Pharmacy Practice, Manipal College of Pharmaceutical Sciences, Manipal Academy of Higher Education, Manipal, Karnataka 576104, India; anmi.jose@learner.manipal.edu (A.J.); murali.m@manipal.edu (M.M.); levin.thomas@learner.manipal.edu (L.T.)
- ² Department of Pharmaceutical Chemistry, Manipal College of Pharmaceutical Sciences, Manipal Academy of Higher Education, Manipal, Karnataka 576104, India; gautham.gs@manipal.edu
- ³ Department of Surgery, Kasturba Medical College, Manipal Academy of Higher Education, Manipal, Karnataka 576104, India; gaby.rodrigues@manipal.edu
- ⁴ Department of Surgical Oncology, Kasturba Medical College, Manipal Academy of Higher Education, Manipal, Karnataka 576104, India; naveenkumar.an@manipal.edu
- ⁵ Department of Pharmacy Practice & Science, 567 TODD Building, 789 South Limestone Street, Lexington, KY 40539-0596, USA; jill.kolesar@uky.edu
- ⁶ National Center for Advancing Translational Sciences, National Institutes of Health, 9800 Medical Center Drive, MSC 3370, Bethesda, MD 20892, USA; bantukallug@mail.nih.gov
- ⁷ School of Pharmacy, Health Sciences Campus, 200 University Avenue West, University of Waterloo, Waterloo, ON N2L 3G1, Canada; praopera@uwaterloo.ca
- * Correspondence: mahadev.rao@manipal.edu; Tel.: +91-820-2922454

Received: 26 June 2020; Accepted: 26 July 2020; Published: 31 July 2020



Abstract: Lysine-specific demethylase 5B (KDM5B/PLU1/JARID1B) is found to be overexpressed in numerous malignancies, including breast, lung, skin, liver, and prostate cancer. Identification of molecules targeting the KDM5B enzyme could be a potential lead in cancer research. Although many KDM5B inhibitors with promising outcomes have been developed so far, its further application in clinical practice is limited due to toxicity and lack of target specificity. Here, we summarize the significance of targeting KDM5B in anticancer therapy and report the molecular docking studies of some known anti-viral agents, decitabine, entecavir, abacavir, penciclovir, and 3-deazaneplanocin A in the catalytic domain JmjC of KDM5B. These studies show the repurposing potential of identified anti-viral agents in cancer therapy.

Keywords: cancer; histone modification; inhibitor; KDM5B; molecular docking; repurposing

1. Introduction

Studies over the past few decades and ongoing research reveal that, along with genetic alterations, epigenetic aberrations play a vital part in the evolution and progress of numerous diseases, including several types of cancers [1]. Epigenetic changes, including DNA methylation and histone modifications, cause altered gene expression without changing the DNA sequence [2,3].

Histone, being the functional protein, not only actively takes part in gene expression, but also acts as a spool for DNA to wind around. Any modification on histone molecules via methylation, acetylation, phosphorylation, ubiquitylation, or sumoylation alters the compact chromatin architecture, leading to abnormal gene expression [4]. Histone methylation on arginine or lysine, which are

abundantly present on N- and C- terminal tails of histones, can either turn on or off transcription based on the degree and location of methylation [5].

Lysine-specific demethylation is finely tuned by two enzyme categories, called lysine-specific demethylase (KDM1/LSD1) and the JumonjiC (JmjC) domain, encompassing histone demethylases (KDMs). JmjC, being the largest among two families, displays high substrate specificity, with demethylase activity targeting histones H3 and H4 [6]. In mammals, around thirty KDMs have been identified and grouped as phylogenetically distinct subfamilies from KDM2-8 with numerous subcategories [7].

The KDM5/JARID1 subfamily consists of four interrelated histone demethylase enzymes—KDM5A, KDM5B, KDM5C and KDM5D—involved in several human biological processes, including hormonal response, stem cell regeneration, genomic stability, cellular proliferation, and differentiation [8,9]. KDM5B (also known as PLU1 or JARID1B), demethylates lysine 4 of histone 3 (H3K4), and acts as a transcriptional repressor on certain tumor suppressor genes, thus converting it into the transcriptionally inactive state [10]. The deregulated expression of KDM5B has been implicated in numerous cancer types, including breast, lung, skin, prostate, testis, and liver [11]. Figure 1 depicts the top ten cancers, with high KDM5B mRNA expression data extracted from cBioPortal for cancer genomics—TCGA, PanCancer Atlas study [12–14]. Thus, KDM5B could be considered as a potential therapeutic target in precision oncology. Hence, drugs that can selectively inhibit KDM5B could be of substantial importance as a therapeutic intervention for such cancer types. This review attempts to comprehend, as thoroughly as possible, the oncogenic role of KDM5B in major cancer types and the drug repurposing potential of some known small molecules by targeting KDM5B’s catalytic domain through molecular docking studies.

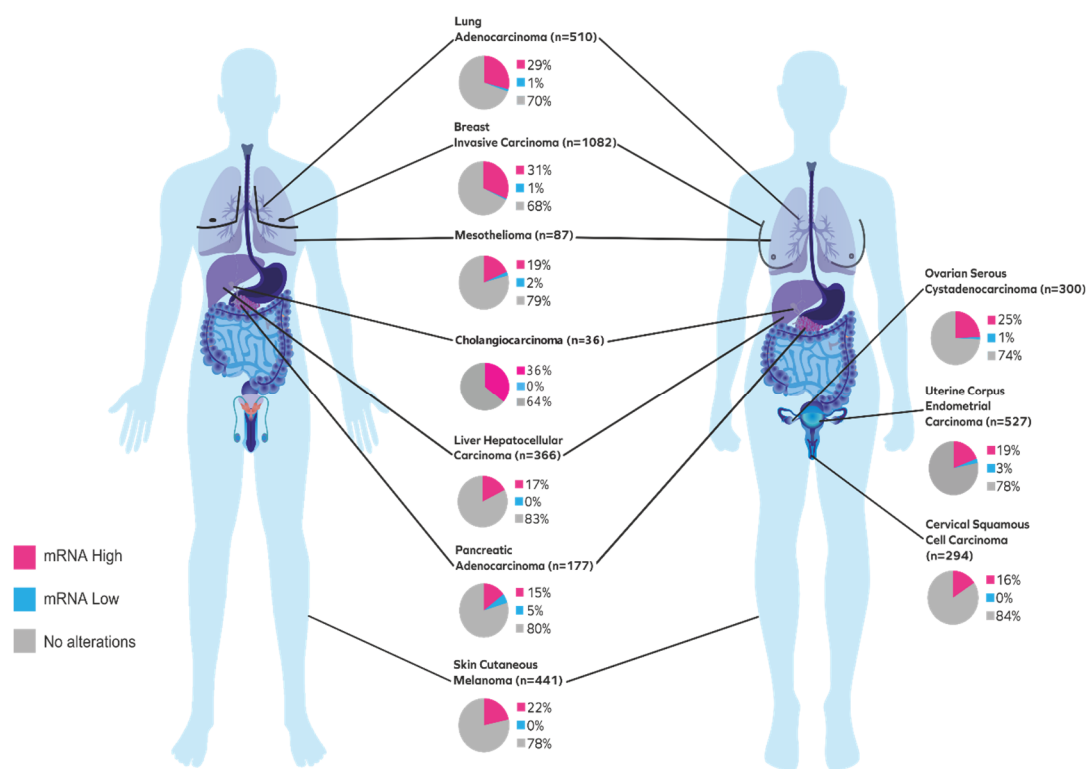


Figure 1. Pictorial representation of the top ten cancers with high KDM5B mRNA expression. Data extracted from the cBioPortal for cancer genomics—TCGA, PanCancer Atlas (*n* = number of patients).

2. Structure and Enzymatic Function of KDM5B

The JmjC family is reliant on Fe (II) and α -ketoglutarate co-factors for its demethylating activity. KDM5B gene consists of 4632 bases, positioned on chromosome 1, in the cytogenetic band of 1q32.1 with a molecular mass of 175 kilodaltons. It encodes a protein of 1544 amino acids [15] comprising an N-terminal Jumonji (JmjN) domain, a catalytic JmjC domain, an AT-rich domain (ARID), a C5HC2 zinc finger domain, a PLU1 motif and three plant homeobox domain (PHD1, PHD2, and PHD3). The domain architecture of KDM5B is highly conserved and homologous from yeast to humans. JmjN and JmjC are vital domains required for enzymatic activity, whereas AT-rich domain binds to GC rich DNA sequences. PHD domains contribute to substrate recognition in which it prevents reverse reaction [16–21]. ARID and PHD domains have very less influence, whereas JmjN and JmjC along with C5HC2 zinc finger domain have more impact on the KDM5B's catalytic activity. The overall catalytic core is composed of three conserved domains consisting of: (i) the JmjN, JmjC, and ARID domains (residues 31–72, 375–602 and 94–100, respectively); (ii) a C-terminal helical domain (residues 604–671 and 737–753); (iii) a β -sheet composed of three β -strands (residues 673–734) that harbored a C5HC2 zinc finger motif [20].

3. Significance of KDM5B in Various Cancers

3.1. Breast Cancer

Although the consistent expression of KDM5B in breast cancer was established by Lu P.J. et al. [22] in 1999, Yamane K. et al. in 2007 revealed the salient role of KDM5B in breast cancer cell proliferation via the transcriptional repression of tumor suppressor genes, including BRCA1 [19]. Subsequent studies both in vitro and in vivo, involving gene expression and KDM5B knockdown, confirmed its putative role in breast tumorigenesis [19,23–25]. One of the proposed mechanisms of KDM5B-mediated tumor cell proliferation was by repressing tumor suppressor miRNA let-7e [26]. Besides, the TFAP2C-Myc-KDM5B complex can repress p21, leading to tumorigenesis and therapy failure [27]. A recent study showed that estrogen receptor-positive (ER⁺) tumors, with KDM5B overexpression, had poor clinical outcomes and resistance to hormonal therapy [25]. Moreover, KDM5B expression was found to be negatively correlated with p16 protein expression [28]. Significantly, microRNA hsa-miR-448 can suppress KDM5B expression through MALAT1 and can prevent triple-negative breast cancer (TNBC) progression [29]. The downregulation of KDM5B led to 3'UTR lengthening of the cyclin D1 (CCND1) oncogene and lengthening of a tumor suppressor gene, DICER1, suggesting KDM5B as a novel target for 3'UTR processing [30]. KDM5B inhibition promoted the re-expression of tumor suppressor protein HEXIM1, and upregulated HEXIM1 aided in the inhibition of breast cancer cell proliferation using KDM5B inhibitors [31]. Recently, Paroni G. et al. showed that HER2-positive breast cancer cells were sensitive to KDM5 inhibition and KDM5 inhibitors exhibited a synergistic effect with HER2 targeting drugs, trastuzumab and lapatinib [32]. Similarly, numerous studies have reported the oncogenic role of KDM5B, where gene expression levels were related with poor prognosis, cancer cell proliferation, and metastasis [33–35]. Figure 2 shows the KDM5B mRNA overexpression in breast cancer from various studies retrieved from the cBioPortal for cancer genomics [12–14,36–38].

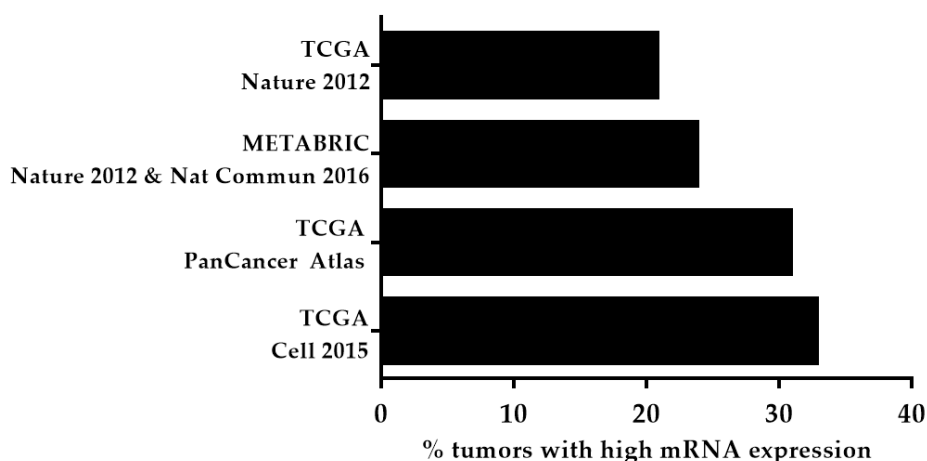


Figure 2. A graphical representation of the high KDM5B mRNA expression among breast cancer patients. Data extracted from the cBioPortal for cancer genomics.

3.2. Lung Cancer

KDM5B expression rate was found to be highly elevated in neoplastic tissues, in contrast to normal tissues, irrespective of lung carcinoma histology [39–41]. The suppression of KDM5B expression showed a significant reduction in cancer cell growth via the E2F/RB1 pathway [40]. Han L. et al. reported in 2013 that KDM5B positively regulates brain metastasis in NSCLC [42]. Moreover, KDM5B aids in the proliferation, invasion, and metastasis activities of lung cancer cells through downregulated p53 [39]. Besides, Shen X. et al. reported that KDM5B overexpression positively correlated with size and stage of the tumor, lymph node metastasis, and reduced survival rate [39]. A recent study by Lu Y. et al. established that KDM5B plays crucial roles in hypoxia-induced gefitinib (EGFR TKI) resistance and epithelial–mesenchymal transition (EMT) [43].

3.3. Melanoma

The role of KDM5B in melanoma is still controversial. Roesch A. et al., in their studies, showed that KDM5B promoted tumor cell maintenance and metastasis, and its knockdown led to the exhaustion of melanoma cells [44]. However, KDM5B has also been suggested as a tumor-suppressive agent in melanocytic cells through the regulation of activities of the retinoblastoma protein [45,46]. Interestingly, it is evident that, in melanoma cells, KDM5B expression is dynamically regulated. However, KDM5B was overexpressed in certain benign tumors, whereas downregulated in aggressive and metastatic melanomas [47]. The relevance of KDM5B in chemo-resistance was confirmed when KDM5B depletion led to the increased sensitivity of melanocytes to anti-melanoma treatment [48].

3.4. Hepatocellular Carcinoma

KDM5B was often upregulated in hepatocellular carcinoma (HCC) samples, compared to corresponding non-neoplastic tissues. Besides, the gene expression level was associated with tumor properties and stages of cancer. HCC patients with KDM5B overexpression had more tumor metastasis, poor prognosis, and significantly shorter overall survival [49–52]. KDM5B exerts its oncogenic function by inactivating PTEN transcription [49] and by silencing KDM5B, which, remarkably, hinders cancer cell proliferation through p15 and p27 up-regulation [50].

3.5. Gastric Cancer

The aberrant expression of KDM5B mRNA was detected in gastric tumor specimens and cell lines in comparison with normal tissues. The expression rate also correlated with TNM stage and depth of invasion [53]. Various studies confirm the contribution of KDM5B in various signaling pathways for tumor cell development and migration [53,54]. Bao J. et al. reported that miR-194,

which obstructs gastric cancer cell growth and invasion, directly targets and negatively regulates KDM5B [55]. These findings revealed the potential role of KDM5B, as a tumor promoter in gastric cancer. A recent study by Xu W. et al. described that increased KDM5B expression, associated with cisplatin resistance in gastric cancer cell lines and targeting KDM5B, reversed the phenotype [56].

3.6. Colorectal Cancer

The functional significance of KDM5B in colorectal cancer (CRC) stem cells was confirmed through *in vitro* and *in vivo* studies. KDM5B knockdown was found to surge H3K4 trimethylation at the p16/INK4A tumor suppressor's promoter region, which subsequently induced cellular senescence [57]. Besides, KDM5B was found to be overexpressed in CRC tumor tissue compared with normal colon samples and this overexpression positively correlated with cancer progression [58].

3.7. Bladder Cancer

Knockdown and apoptosis studies demonstrated the close link of KDM5B, in cell cycle regulation and cancer cell maintenance, in bladder cancer cell lines. Overexpression of KDM5B was noted in the early and advanced stages of bladder cancer, irrespective of cancer grade [40]. A potential inverse connection between KDM5B and connexin 26 (CX26) in the progression of bladder cancer was reported, where KDM5B was found to be upregulated in contrast to CX26 [59].

3.8. Prostate Cancer

KDM5B was found to be overexpressed in prostate cancer tissues, compared to benign tissues, and has been suggested as a potential therapeutic target [15,60]. Various studies evaluated the role of microRNAs in regulating KDM5B. The forced miR-29a expression inhibited proliferation, and induced apoptosis in prostate cancer cells, by repressing KDM5B expression, whereas, by KDM5B targeting, miR-137 aided as a tumor suppressor in prostate carcinogenesis [61,62].

3.9. KDM5B in Other Cancers

KDM5B showed significantly high expression levels in patients with B-cell precursor acute lymphoblastic leukemia (B-ALL), compared to normal bone marrow [63]. The suppression of KDM5B hindered metastasis and the invasion of human oral squamous cell carcinoma and sensitized radiation therapy [64]. KDM5B overexpression was significantly associated with tumor cell proliferation in head and neck cancer, and KDM5B silencing caused cell growth suppression both *in vitro* and *in vivo* [65]. Similar studies supporting the oncogenic role of KDM5B were observed in other malignancies, such as esophageal squamous cell carcinoma [66], cervical cancer [67], renal cell carcinoma [68], epithelial ovarian cancer [69] and neuroblastoma [70].

3.10. KDM5B as a Therapeutic Target

Apart from the oncogenic and tumorigenic role, KDM5B is also considered as a cancer-testis antigen (CTA), where gene expression is restricted in normal tissues except adult testes [22,71]. Therefore, abnormal overexpression of KDM5B in any neoplastic tissue, in comparison with corresponding non-neoplastic tissues, makes it an ideal therapeutic target. Furthermore, CTA properties suggest that targeting KDM5B may be associated with reduced toxicity. Therefore, the development of specific KDM5B inhibitors will offer a deeper insight into the therapeutic potential for many types of cancers.

As Fe (II) and α -ketoglutarate are the two vital co-factors of KDM5B in demethylation, studies are focusing on the development of compounds that mimic α -ketoglutarate or compounds that chelate with Fe (II). Over the years, many KDM5B inhibitors have been developed (Figure 3) and have provided promising outcomes [72]. The 2,4-pyridinedicarboxylic acid (2,4-PDCA) inhibits KDM5B *in vitro* with an IC_{50} value of $3 \pm 1 \mu M$ [5], whereas GSK-J1 with an IC_{50} of $0.55 \mu M$ [20,73]. GSK467 displayed an inhibitory concentration of $0.026 \mu M$. The crystalline structure of KDM5B with GSK467 provides a

possible template for the development of selective KDM5B inhibitors [20,74]. Compounds 54j and 54k are potent, cell permeable dual inhibitors of the KDM4 and KDM5 subfamilies. Compounds 54j and 54k inhibit KDM5B with IC_{50} values 0.014 μ M and 0.023 μ M, respectively, and have shown adequate cellular permeability [75]. CPI-455 with IC_{50} of 0.003 μ M, was identified as a pan-KDM5 inhibitor that competitively binds to the two cofactor binding sites [76]. KDM5-C49, a 2,4-PDCA analogue, and further modified KDOAM-25 have shown acceptable inhibitory potency on KDM5B, in which KDOAM-25 exhibited good stability, high selectivity and low cytotoxicity [20,77]. An orally available, potent inhibitor of KDM5B, named compound 33, was identified through structure activity relationship exploration and presented promising selectivity compared to early inhibitors [78]. Recently, a pyrazole derivative, compound 27ab, was discovered, which inhibited MKN45 cell proliferation, wound healing and migration [79]. All these inhibitors are in their initial stage of development and have not made it to the clinics yet.

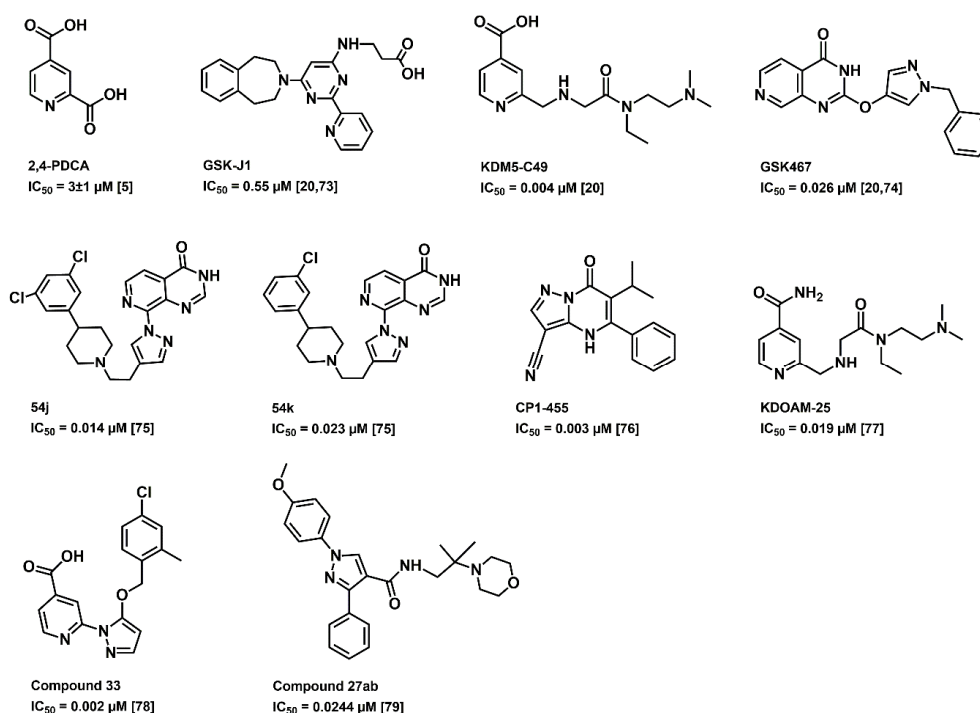


Figure 3. Previously reported KDM5B inhibitors (IC_{50} : half maximal inhibitory concentration).

4. Molecular Docking Studies

The JmjC domain of native KDM5B, which is involved in histone demethylation, contains Fe (II) ion and α -ketoglutarate as cofactors. This site is an attractive target to develop KDM5B inhibitors. One of the solved crystal structures of KDM5B, with an inhibitor GSK467 in the JmjC domain, contains Mn (II) instead of Fe (II) [20]. This structure provides an excellent starting point to develop novel KDM5B inhibitors using computational tools. Accordingly, we used computational modeling to explore the potential of known drugs to inhibit KDM5B. Drug repurposing is an approach where new therapeutic indications for already marketed drugs are discovered. This approach aims to lessen the price and time involved in drug discovery process [80,81]. On this note, we considered the drug repurposing potential of nucleoside derivatives, which are well known as antiviral agents [82]. Several studies in the past have shown that nucleoside derivatives, with monocyclic or bicyclic ring systems, exhibit anticancer properties [83–85]. We investigated the drug repurposing potential of known compounds, such as decitabine, entecavir, abacavir, penciclovir, and 3-deazaneplanocin A (DZNep) (Figure 4), which are all nucleoside derivatives, as inhibitors of KDM5B, by conducting molecular docking experiments. In addition, we compared the binding modes of previously reported KDM5B inhibitors containing planar bicyclic rings, such as GSK467, 54j, and CPI-455, with penciclovir and DZNep, to determine

their interactions in the JmjC domain of KDM5B. It should be noted that decitabine (Dacogen[®]) is currently used to treat myelodysplastic syndrome (MDS), entecavir (Baraclude[®]) is used as an anti-hepatitis B agent, abacavir (Ziagen[®]) is used to treat HIV infections and penciclovir (Denavir[®]) is a known drug used in the treatment of herpes infections. The carbocyclic adenosine derivative DZNep, is a known inhibitor of histone methyltransferase EZH2 and is a promising compound in cancer immunotherapy [86]. Molecular docking studies were carried out using the computational software, Discovery Studio (DS) Structure-Based-Design (BIOVIA Inc, Dassault Systemes, USA). Moreover, previous studies have shown that nucleoside derivatives with either a monocyclic or bicyclic ring exhibit anticancer property. The ligands decitabine, entecavir, abacavir, penciclovir, and DZNep were built in 3D, using the Small Molecules module in DS using CHARMM force field. The X-ray crystal structure of human KDM5B was obtained from PDB (pdb id: 5FUN) [20]. This KDM5B structure contains a pyridopyrimidine ligand GSK467 and the catalytic site contains Mn²⁺ ion. All the water molecules were removed and a 10 Å binding site sphere was defined by selecting the bound ligand GSK467, after which it was deleted. The KDM5B protein was prepared using the Macromolecules module in DS using CHARMM force field. Docking was carried out using the LibDock algorithm by employing 100 hotspots, a docking tolerance of 0.25 Å, and an implicit solvent model, with a distance-dependent dielectric constant and CHARMM force field. The binding poses obtained, were further energy minimized using Smart minimizer (1000 steps and an RMS gradient of 0.001 kcal/mol) and ranked using the LibDock scoring function. The ligand-binding interactions were further studied by considering the polar and nonpolar contacts in the KDM5B binding site. The general computational methods applied were as per our previously reported method [87].

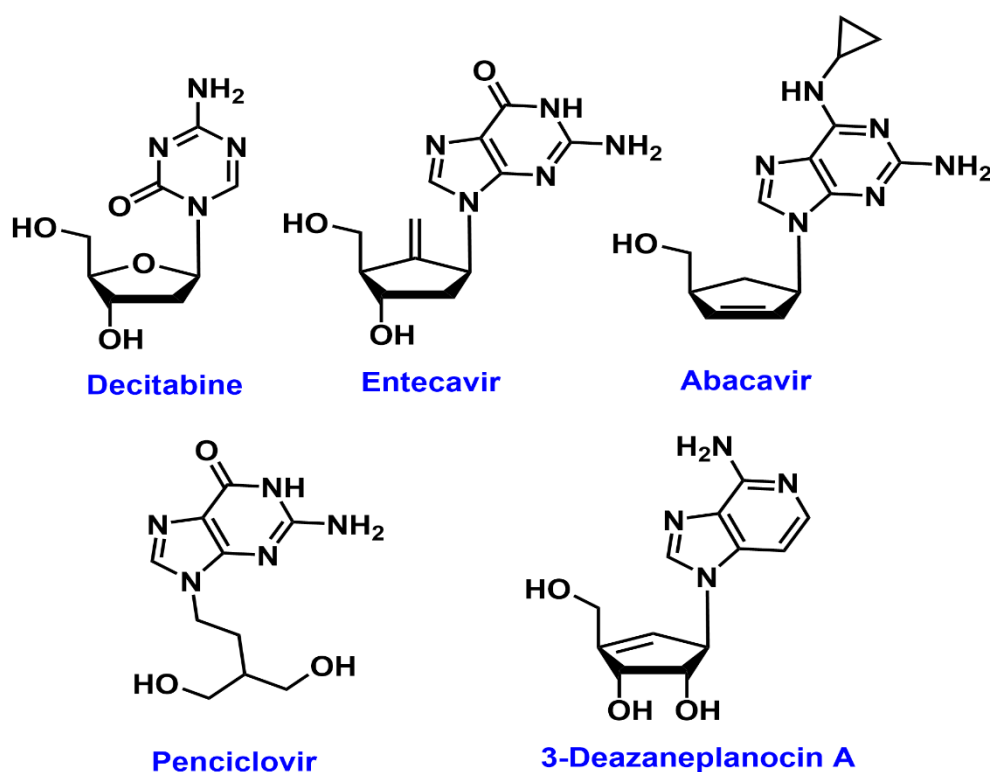


Figure 4. Selected antiviral drugs targeting KDM5B.

Docking the nucleoside decitabine in the KDM5B catalytic site shows that the 6-member azacytidine ring was in the α -ketoglutarate binding pocket and underwent π - π stacked hydrophobic interactions with aromatic rings of Tyr488 and Phe496, respectively (distance < 4.1 Å). The azacytidine N3 was not forming any metal-ligand bonding with Mn²⁺ center (distance \approx 5.0 Å, Figure 5, Panel A). The deoxy sugar moiety was in a region comprised of Tyr425, Gly426, and Ser495. The hydroxy and

the hydroxymethyl groups were in contact with Ser495 and Gly426 backbones, via hydrogen bonding interaction (distance < 1.9 Å, Figure 5, Panel A). These studies suggest that decitabine can undergo favorable interactions with KDM5B.

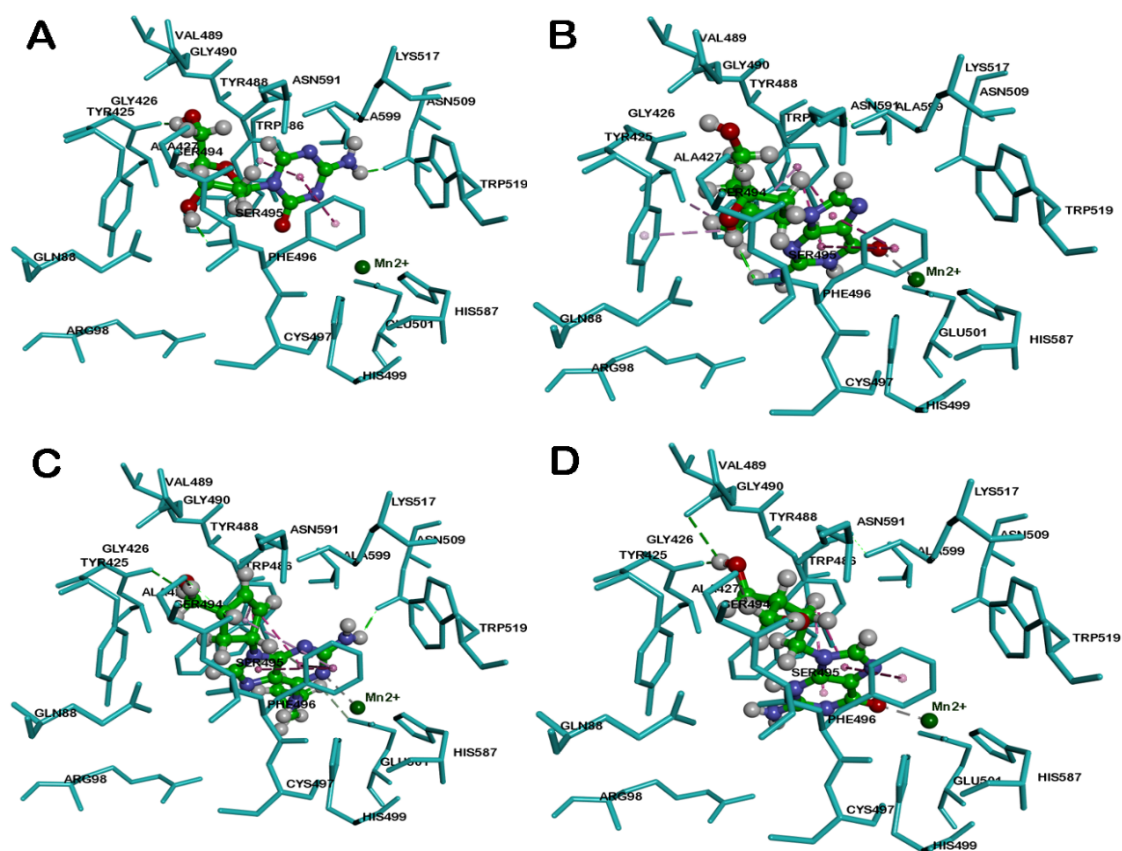


Figure 5. The binding modes of decitabine (A), entecavir (B), abacavir (C) and penciclovir (D) in ball and stick cartoon within the JmjC domain of human KDM5B (pdb id: 5FUN). Mn²⁺ ion is shown as a green circle. Hydrogen atoms are removed to enhance clarity. Polar and nonpolar interactions are color-coded.

Docking entecavir in KDM5B shows that the bicyclic guanosine ring was oriented in the α -ketoglutarate binding pocket, where it underwent some favorable interactions. The pyrimidine and imidazole rings were in contact with Tyr488 and Phe496 via four π - π stacked hydrophobic interactions (distance < 4.5 Å, Figure 5, Panel B). Interestingly, the guanosine C6 ketone (C = O) underwent metal-ligand bonding with the Mn²⁺ center (distance = 2.6 Å). The exocyclic alkene was in contact with Tyr425, Ala427, and Tyr488 (distance < 5.0 Å), whereas the hydroxy group of the cyclopentenyl ring formed a hydrogen bond with the backbone of Ser495 (distance < 2.0 Å, Figure 5, Panel B). In general, entecavir exhibited better binding interactions with KDM5B compared to decitabine. This can be attributed to the presence of a planar bicyclic guanosine ring in entecavir, and the metal-ligand bond with the guanosine ketone.

Docking the anti-HIV agent abacavir with KDM5B shows that it was buried in the α -ketoglutarate binding pocket closer to the metal center similar to entecavir, and the purine ring underwent π - π stacking interactions with aromatic rings of Tyr488 and Phe496 (distance < 4.8 Å) and the N1 of purine ring was in contact with Mn²⁺ (distance = 2.6 Å). Furthermore, the C2 amino substituent underwent hydrogen bonding interaction with the backbone of Asn509 (distance < 1.9 Å, Figure 5, Panel C). The cyclopentenyl ring was in contact with Tyr488 and Phe496 via hydrophobic interactions (distance < 4.8 Å).

Docking another purine-based drug penciclovir, which contains a guanosine ring similar to entecavir in the KDM5B, shows that it was exhibiting a similar binding mode as entecavir, and the guanosine ring was in hydrophobic contact with Tyr488 and Phe496 by forming several π - π stacking interactions (distance < 4.4 Å, Figure 5, Panel D). The guanosine ketone forms a metal–ligand interaction with Mn^{2+} (distance = 2.4 Å). The acyclic sugar moiety was closer to a polar region comprised of Gly426, Ser494, Val489, and Asn591. The hydroxy and hydroxymethyl substituents form hydrogen-bonding interactions with Gly429, Ser494, and Val489 backbones (distance < 2.8 Å, Figure 5, Panel D). These studies show that drugs containing a bicyclic purine template exhibit favorable binding in KDM5B.

Docking DZNep, an investigational drug molecule, which also contains a planar bicyclic imidazo[4,5-c]pyridine ring template (Figure 4), and a cyclopentenyl moiety, shows that the bicyclic imidazo[4,5-c]pyridine ring, forms a π - π stacking interaction with Tyr488 and Phe496 (distance < 4.3 Å). Interestingly, the pyridine nitrogen, chelated with Mn^{2+} (distance = 2.8 Å, Figure 6A) and C2 amino substituents formed a hydrogen bond interaction with backbone of Asn509. The cyclopentenyl hydroxyl and hydroxymethyl substituents also underwent hydrogen bonding interactions with Gly426 and Ser495 (distance < 2.0 Å).

Among these compounds, DZNep exhibited the most favorable binding interaction with KDM5B. The binding interaction was measured by calculating the LibDock scores for the best binding poses. The ranking order was DZNep (LibDock score = 131.60) $>$ penciclovir (LibDock score = 129.84) $>$ entecavir (LibDock score = 121.26) $>$ abacavir (LibDock score = 118.10) $>$ decitabine (LibDock score = 109.55). Molecular docking studies of known KDM5B inhibitor, 54j (Figure 6B), shows that its bicyclic pyridopyrimidine ring underwent van der Waal's contact with Tyr488 and Phe496 (π - π stacked interactions, distance < 5 Å) and the pyrimidinone ketone formed a hydrogen bond with the side chain of Lys517 (distance = 1.55 Å). Interestingly, the nitrogen of pyrazole and pyrimidinone rings was close to the metal center, indicating the ability of 54j to form metal–ligand interactions (Figure 6B). The piperidine benzene with 3,5-dichloro substituents, was oriented in a hydrophobic pocket made up of Ile500, Val553 and Tyr586. Furthermore, 54j is a much larger molecule (molecular volume = 345.7 Å³) compared to GSK467, CPI-455, decitabine, entecavir, abacavir, penciclovir, and DZNep (molecular volume range ~ 168.7 –231.5 Å³). Therefore, 54j is able to bind in the entire span of the JmjC domain (Figure 6B), which is not possible for the antivirals investigated in this study, as they are smaller. This is also supported by a superior LibDock score obtained for 54j (LibDock score = 145.08). However, similar to 54j, all the bicyclic ring-containing agents, entecavir, abacavir, penciclovir, and DZNep, are able to undergo metal–ligand interaction (Figures 5 and 6), which is a common feature observed.

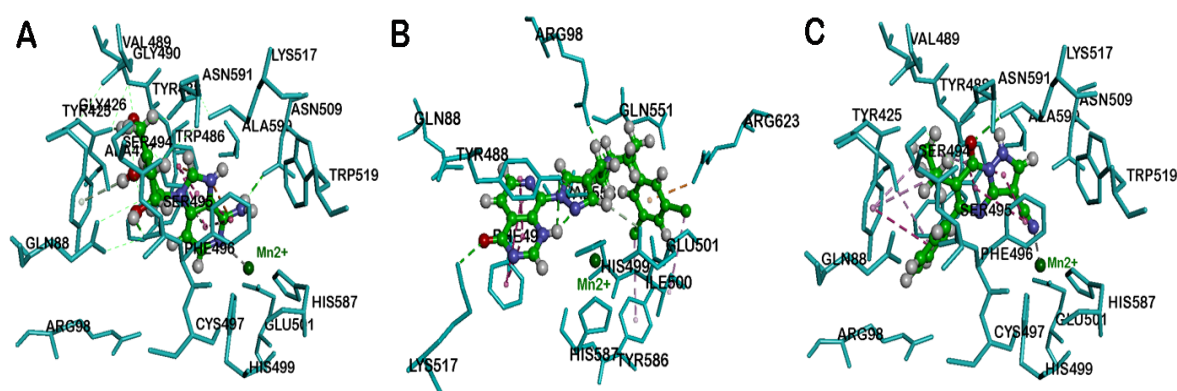


Figure 6. The binding mode of DZNep (A), 54j (B) and CPI-455 (C) (ball and stick cartoon) within JmjC domain of human KDM5B (pdb id: 5FUN). Mn^{2+} ion is shown as a green circle. Hydrogen atoms are removed to enhance clarity. Polar and nonpolar interactions are color-coded.

Molecular docking studies of the known KDM5B inhibitor, CPI-455 (Figure 6C), shows that it was oriented in a similar region compared to molecules containing the planar bicyclic ring investigated in this study. The bicyclic pyrazolopyrimidinone ring of CPI-455 was in van der Waal's contact with Tyr488 and Phe496 (distance < 5 Å), and the pyrimidinone ketone underwent a hydrogen-bonding interaction with the Lys517 side chain (distance = 2.48 Å). The C6 isopropyl substituent was in a hydrophobic pocket and underwent multiple interactions with Tyr425 and Ala427 (distance < 5 Å), whereas the C5 phenyl ring underwent π - π stacking interactions with Tyr425 (distance < 5 Å). Interestingly, the C3 nitrile substituent was able to chelate with the metal center (distance = 2.6 Å, Figure 6C) which shows the significance of a nitrile substituent in KDM5B binding (LibDock score = 120.19). These molecular docking studies also show that bicyclic ring-containing agents (e.g., 54j, CPI-455, entecavir, abacavir, penciclovir, and DZNep), exhibit better binding in the JmjC domain of KDM5B, compared to monocyclic ring-containing decitabine, which is also reflected in a lower LibDock score (109.55) obtained for decitabine compared to other molecules.

The binding modes of DZNep and penciclovir, which exhibited superior LibDock scores, were compared with the known X-ray structure of GSK467 (Figure 3), bound to KDM5B. This investigation shows that, similar to GSK467, the planar bicyclic rings of DZNep and penciclovir were oriented in the α -ketoglutarate binding pocket, and more significantly, the pyridine nitrogen of DZNep and guanosine ketone of penciclovir were in contact with the metal center Mn^{2+} (Figure 7). These observations were similar to the binding mode of GSK467 in the JmjC domain of human KDM5B, where the pyridopyrimidine nitrogen interacts with the metal center (Figure 7) [20].

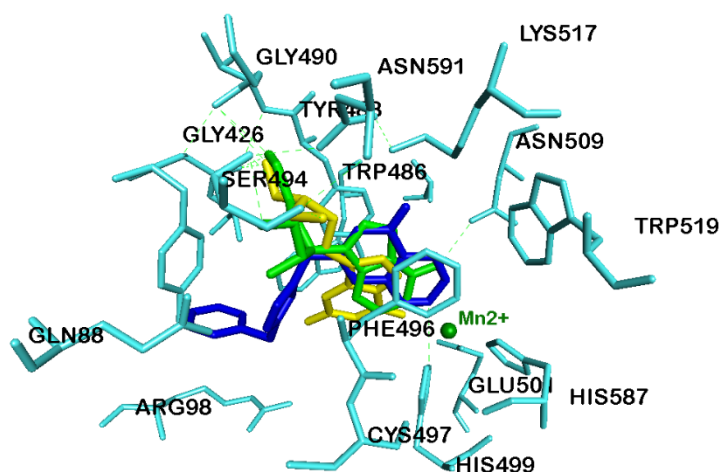


Figure 7. Comparison of binding modes of GSK467 (blue stick cartoon), penciclovir (yellow stick cartoon) and DZNep (green stick cartoon) in the JmjC domain of human KDM5B (pdb id: 5FUN). Mn^{2+} ion is shown as a green circle. Hydrogen atoms are removed to enhance clarity.

These results also show that small molecules, which possess planar bicyclic heterocyclic rings, exhibit favorable binding toward the JmjC domain of human KDM5B. This is due to their ability to undergo interactions with the catalytic site metal ion, which is an important criterion in KDM5 inhibition and is consistent with previous studies [20,77,88]. Our molecular docking investigations show that decitabine, entecavir, abacavir, penciclovir, and DZNep have the potential to be repurposed as KDM5B inhibitors to treat various types of cancers.

5. Conclusions

The leading role of KDM5B oncogene in tumorigenesis and cancer progression is well established in various malignancies and is therefore, considered as a potential therapeutic target. Although many small molecule inhibitors of KDM5B have been identified so far, their possible clinical application in cancer treatment is a work in progress. This study provides a rationale on how repurposing antiviral

drugs could contribute to the discovery and development of KDM5B inhibitors. We anticipate that these studies will stimulate further research in considering drug repurposing approaches to target KDM5B, and to discover novel therapies for various cancers.

Author Contributions: Conceptualization, M.R., P.P.N.R., and A.J.; writing—original draft preparation, A.J., P.P.N.R., and M.R.; writing—review and editing, A.J., M.R., P.P.N.R., G.R., G.G.S., J.K., N.A.N.K., G.S.R., M.M., and L.T. All authors have read and agreed to the published version of the manuscript.

Funding: This review received no external funding.

Acknowledgments: A.J. and L.T. are thankful for the TMA Pai PhD Scholarship from Manipal Academy of Higher Education, Manipal, India.

Conflicts of Interest: The authors declare no conflict of interest.

References

1. Sharma, S.; Kelly, T.K.; Jones, P.A. Epigenetics in cancer. *Carcinogenesis* **2010**, *31*, 27–36. [[CrossRef](#)] [[PubMed](#)]
2. Feinberg, A.P.; Tycko, B. The history of cancer epigenetics. *Nat. Rev. Cancer* **2004**, *4*, 143–153. [[CrossRef](#)] [[PubMed](#)]
3. Dupont, C.; Armant, D.R.; Brenner, C.A. Epigenetics: Definition, mechanisms and clinical perspective. *Semin. Reprod. Med.* **2009**, *27*, 351–357. [[CrossRef](#)] [[PubMed](#)]
4. Wang, G.G.; Allis, C.D.; Chi, P. Chromatin remodeling and cancer, Part I: Covalent histone modifications. *Trends Mol. Med.* **2007**, *13*, 363–372. [[CrossRef](#)] [[PubMed](#)]
5. Kristensen, L.H.; Nielsen, A.L.; Helgstrand, C.; Lees, M.; Cloos, P.; Kastrup, J.S.; Helin, K.; Olsen, L.; Gajhede, M. Studies of H3K4me3 demethylation by KDM5B/Jarid1B/PLU1 reveals strong substrate recognition in vitro and identifies 2, 4-pyridine-dicarboxylic acid as an in vitro and in cell inhibitor. *FEBS J.* **2012**, *279*, 1905–1914. [[CrossRef](#)]
6. Agger, K.; Christensen, J.; Cloos, P.A.; Helin, K. The emerging functions of histone demethylases. *Curr. Opin. Genet. Dev.* **2008**, *18*, 159–168. [[CrossRef](#)]
7. Allis, C.D.; Berger, S.L.; Cote, J.; Dent, S.; Jenuwien, T.; Kouzarides, T.; Pillus, L.; Reinberg, D.; Shi, Y.; Shiekhhattar, R. New nomenclature for chromatin-modifying enzymes. *Cell* **2007**, *131*, 633–636. [[CrossRef](#)]
8. Shi, Y.; Whetstine, J.R. Dynamic regulation of histone lysine methylation by demethylases. *Mol. Cell.* **2007**, *25*, 1–14. [[CrossRef](#)]
9. Harmeyer, K.M.; Facompre, N.D.; Herlyn, M.; Basu, D. JARID1 histone demethylases: Emerging targets in cancer. *Trends Cancer* **2017**, *3*, 713–725. [[CrossRef](#)]
10. Benevolenskaya, E.V. Histone H3K4 demethylases are essential in development and differentiation. *Biochem. Cell Biol.* **2007**, *85*, 435–443. [[CrossRef](#)]
11. Rotili, D.; Mai, A. Targeting histone demethylases: A new avenue for the fight against cancer. *Genes Cancer* **2011**, *2*, 663–679. [[CrossRef](#)] [[PubMed](#)]
12. Cerami, E.; Gao, J.; Dogrusoz, U.; Gross, B.E.; Sumer, S.O.; Aksoy, B.A.; Jacobsen, A.; Byrne, C.J.; Heuer, M.L.; Larsson, E. The cBio cancer genomics portal: An open platform for exploring multidimensional cancer genomics data. *AACR* **2012**, 401–404. [[CrossRef](#)] [[PubMed](#)]
13. Gao, J.; Aksoy, B.A.; Dogrusoz, U.; Dresdner, G.; Gross, B.; Sumer, S.O.; Sun, Y.; Jacobsen, A.; Sinha, R.; Larsson, E. Integrative analysis of complex cancer genomics and clinical profiles using the cBioPortal. *Sci. Signal.* **2013**, *6*, p11. [[CrossRef](#)]
14. Hoadley, K.A.; Yau, C.; Hinoue, T.; Wolf, D.M.; Lazar, A.J.; Drill, E.; Shen, R.; Taylor, A.M.; Cherniack, A.D.; Thorsson, V. Cell-of-origin patterns dominate the molecular classification of 10,000 tumors from 33 types of cancer. *Cell* **2018**, *173*, 291–304.e6. [[CrossRef](#)] [[PubMed](#)]
15. Xiang, Y.; Zhu, Z.; Han, G.; Ye, X.; Xu, B.; Peng, Z.; Ma, Y.; Yu, Y.; Lin, H.; Chen, A.P. JARID1B is a histone H3 lysine 4 demethylase up-regulated in prostate cancer. *Proc. Natl. Acad. Sci. USA.* **2007**, *104*, 19226–19231. [[CrossRef](#)] [[PubMed](#)]
16. Wilsker, D.; Probst, L.; Wain, H.M.; Maltais, L.; Tucker, P.W.; Moran, E. Nomenclature of the ARID family of DNA-binding proteins. *Genomics* **2005**, *86*, 242–251. [[CrossRef](#)] [[PubMed](#)]

17. Wysocka, J.; Swigut, T.; Xiao, H.; Milne, T.A.; Kwon, S.Y.; Landry, J.; Kauer, M.; Tackett, A.J.; Chait, B.T.; Badenhorst, P. A PHD finger of NURF couples histone H3 lysine 4 trimethylation with chromatin remodelling. *Nature* **2006**, *442*, 86–90. [[CrossRef](#)] [[PubMed](#)]
18. Pilka, E.S.; James, T.; Lisztwan, J.H. Structural definitions of Jumonji family demethylase selectivity. *Drug Discov. Today*. **2015**, *20*, 743–749. [[CrossRef](#)]
19. Yamane, K.; Tateishi, K.; Klose, R.J.; Fang, J.; Fabrizio, L.A.; Erdjument-Bromage, H.; Taylor-Papadimitriou, J.; Tempst, P.; Zhang, Y. PLU-1 is an H3K4 demethylase involved in transcriptional repression and breast cancer cell proliferation. *Mol. Cell* **2007**, *25*, 801–812. [[CrossRef](#)]
20. Johansson, C.; Velupillai, S.; Tumber, A.; Szykowska, A.; Hookway, E.S.; Nowak, R.P.; Strain-Damerell, C.; Gileadi, C.; Philpott, M.; Burgess-Brown, N. Structural analysis of human KDM5B guides histone demethylase inhibitor development. *Nat. Chem. Biol.* **2016**, *12*, 539–545. [[CrossRef](#)]
21. Dorosz, J.; Kristensen, L.H.; Aduri, N.G.; Mirza, O.; Lousen, R.; Bucciarelli, S.; Mehta, V.; Sellés-Baiget, S.; Solbak, S.M.Ø.; Bach, A. Molecular architecture of the Jumonji C family histone demethylase KDM5B. *Sci. Rep.* **2019**, *9*, 4019. [[CrossRef](#)]
22. Lu, P.J.; Sundquist, K.; Baeckstrom, D.; Poulsom, R.; Hanby, A.; Meier-Ewert, S.; Jones, T.; Mitchell, M.; Pitha-Rowe, P.; Freemont, P. A novel gene (PLU-1) containing highly conserved putative DNA/chromatin binding motifs is specifically up-regulated in breast cancer. *J. Biol. Chem.* **1999**, *274*, 15633–15645. [[CrossRef](#)] [[PubMed](#)]
23. Scibetta, A.G.; Santangelo, S.; Coleman, J.; Hall, D.; Chaplin, T.; Copier, J.; Catchpole, S.; Burchell, J.; Taylor-Papadimitriou, J. Functional analysis of the transcription repressor PLU-1/JARID1B. *Mol. Cell Biol.* **2007**, *27*, 7220–7235. [[CrossRef](#)] [[PubMed](#)]
24. Catchpole, S.; Spencer-Dene, B.; Hall, D.; Santangelo, S.; Rosewell, I.; Guenatri, M.; Beatson, R.; Scibetta, A.G.; Burchell, J.M.; Taylor-Papadimitriou, J. PLU-1/JARID1B/KDM5B is required for embryonic survival and contributes to cell proliferation in the mammary gland and in ER+ breast cancer cells. *Int. J. Oncol.* **2011**, *38*, 1267–1277. [[CrossRef](#)] [[PubMed](#)]
25. Yamamoto, S.; Wu, Z.; Russnes, H.G.; Takagi, S.; Peluffo, G.; Vaske, C.; Zhao, X.; Volland, H.K.M.; Maruyama, R.; Ekram, M.B. JARID1B is a luminal lineage-driving oncogene in breast cancer. *Cancer Cell* **2014**, *25*, 762–777. [[CrossRef](#)]
26. Mitra, D.; Das, P.M.; Huynh, F.C.; Jones, F.E. Jumonji/ARID1 B (JARID1B) protein promotes breast tumor cell cycle progression through epigenetic repression of microRNA let-7e. *J. Biol. Chem.* **2011**, *286*, 40531–40535. [[CrossRef](#)] [[PubMed](#)]
27. Wong, P.-P.; Miranda, F.; Chan, K.V.; Berlato, C.; Hurst, H.C.; Scibetta, A.G. Histone demethylase KDM5B collaborates with TFAP2C and Myc to repress the cell cycle inhibitor p21cip (CDKN1A). *Mol. Cell. Biol.* **2012**, *32*, 1633–1644. [[CrossRef](#)]
28. Zhao, L.; Liu, H. Immunohistochemical detection and clinicopathological significance of JARID1B/KDM5B and P16 expression in invasive ductal carcinoma of the breast. *Genet. Mol. Res.* **2015**, *14*, 5417–5426. [[CrossRef](#)]
29. Bamodu, O.A.; Huang, W.-C.; Lee, W.-H.; Wu, A.; Wang, L.S.; Hsiao, M.; Yeh, C.-T.; Chao, T.-Y. Aberrant KDM5B expression promotes aggressive breast cancer through MALAT1 overexpression and downregulation of hsa-miR-448. *BMC Cancer* **2016**, *16*, 160. [[CrossRef](#)]
30. Blair, L.P.; Liu, Z.; Labitigan, R.L.D.; Wu, L.; Zheng, D.; Xia, Z.; Pearson, E.L.; Nazeer, F.I.; Cao, J.; Lang, S.M. KDM5 lysine demethylases are involved in maintenance of 3' UTR length. *Sci. Adv.* **2016**, *2*, e1501662. [[CrossRef](#)]
31. Montano, M.M.; Yeh, I.J.; Chen, Y.; Hernandez, C.; Kiselar, J.G.; de la Fuente, M.; Lawes, A.M.; Nieman, M.T.; Kiser, P.D.; Jacobberger, J.; et al. Inhibition of the histone demethylase, KDM5B, directly induces re-expression of tumor suppressor protein HEXIM1 in cancer cells. *Breast Cancer Res.* **2019**, *21*, 138. [[CrossRef](#)]
32. Paroni, G.; Bolis, M.; Zanetti, A.; Ubezio, P.; Helin, K.; Staller, P.; Gerlach, L.O.; Fratelli, M.; Neve, R.M.; Terao, M. HER2-positive breast-cancer cell lines are sensitive to KDM5 inhibition: Definition of a gene-expression model for the selection of sensitive cases. *Oncogene* **2019**, *38*, 2675–2689. [[CrossRef](#)]
33. Hinohara, K.; Wu, H.-J.; Vigneau, S.; McDonald, T.O.; Igarashi, K.J.; Yamamoto, K.N.; Madsen, T.; Fassl, A.; Egri, S.B.; Papanastasiou, M. KDM5 histone demethylase activity links cellular transcriptomic heterogeneity to therapeutic resistance. *Cancer Cell* **2018**, *34*, 939–953.e9. [[CrossRef](#)]

34. Tang, D.; Zhao, X.; Zhang, L.; Wang, Z.; Wang, C. Identification of hub genes to regulate breast cancer metastasis to brain by bioinformatics analyses. *J. Cell. Biochem.* **2019**, *120*, 9522–9531. [[CrossRef](#)] [[PubMed](#)]
35. Zhang, Z.-G.; Zhang, H.-S.; Sun, H.-L.; Liu, H.-Y.; Liu, M.-Y.; Zhou, Z. KDM5B promotes breast cancer cell proliferation and migration via AMPK-mediated lipid metabolism reprogramming. *Exp. Cell Res.* **2019**, *379*, 182–190. [[CrossRef](#)] [[PubMed](#)]
36. Ciriello, G.; Gatza, M.L.; Beck, A.H.; Wilkerson, M.D.; Rhie, S.K.; Pastore, A.; Zhang, H.; McLellan, M.; Yau, C.; Kandoth, C. Comprehensive molecular portraits of invasive lobular breast cancer. *Cell* **2015**, *163*, 506–519. [[CrossRef](#)] [[PubMed](#)]
37. Cancer Genome Atlas Network. Comprehensive molecular portraits of human breast tumours. *Nature* **2012**, *490*, 61–70. [[CrossRef](#)]
38. Pereira, B.; Chin, S.-F.; Rueda, O.M.; Vollan, H.-K.M.; Provenzano, E.; Bardwell, H.A.; Pugh, M.; Jones, L.; Russell, R.; Sammut, S.-J. The somatic mutation profiles of 2433 breast cancers refine their genomic and transcriptomic landscapes. *Nat. Commun.* **2016**, *7*, 11479. [[CrossRef](#)]
39. Shen, X.; Zhuang, Z.; Zhang, Y.; Chen, Z.; Shen, L.; Pu, W.; Chen, L.; Xu, Z. JARID1B modulates lung cancer cell proliferation and invasion by regulating p53 expression. *Tumor Biol.* **2015**, *36*, 7133–7142. [[CrossRef](#)]
40. Hayami, S.; Yoshimatsu, M.; Veerakumarasivam, A.; Unoki, M.; Iwai, Y.; Tsunoda, T.; Field, H.I.; Kelly, J.D.; Neal, D.E.; Yamaue, H. Overexpression of the JmJc histone demethylase KDM5B in human carcinogenesis: Involvement in the proliferation of cancer cells through the E2F/RB pathway. *Mol. Cancer* **2010**, *9*, 59. [[CrossRef](#)]
41. Kuo, K.-T.; Huang, W.-C.; Bamodu, O.A.; Lee, W.-H.; Wang, C.-H.; Hsiao, M.; Wang, L.-S.; Yeh, C.-T. Histone demethylase JARID1B/KDM5B promotes aggressiveness of non-small cell lung cancer and serves as a good prognostic predictor. *Clin. Epigenetics.* **2018**, *10*, 107. [[CrossRef](#)] [[PubMed](#)]
42. Han, L.; Liang, X.-H.; Chen, L.-X.; Bao, S.-M.; Yan, Z.-Q. SIRT1 is highly expressed in brain metastasis tissues of non-small cell lung cancer (NSCLC) and in positive regulation of NSCLC cell migration. *Int. J. Clin. Exp. Pathol.* **2013**, *6*, 2357–2365. [[PubMed](#)]
43. Lu, Y.; Liu, Y.; Oeck, S.; Glazer, P.M. Hypoxia promotes resistance to EGFR inhibition in NSCLC cells via the histone demethylases, LSD1 and PLU-1. *Mol. Cancer Res.* **2018**, *16*, 1458–1469. [[CrossRef](#)] [[PubMed](#)]
44. Roesch, A.; Fukunaga-Kalabis, M.; Schmidt, E.C.; Zabierowski, S.E.; Brafford, P.A.; Vultur, A.; Basu, D.; Gimotty, P.; Vogt, T.; Herlyn, M. A temporarily distinct subpopulation of slow-cycling melanoma cells is required for continuous tumor growth. *Cell* **2010**, *141*, 583–594. [[CrossRef](#)] [[PubMed](#)]
45. Roesch, A.; Mueller, A.M.; Stempf, T.; Moehle, C.; Landthaler, M.; Vogt, T. RBP2-H1/JARID1B is a transcriptional regulator with a tumor suppressive potential in melanoma cells. *Int. J. Cancer* **2008**, *122*, 1047–1057. [[CrossRef](#)] [[PubMed](#)]
46. Roesch, A.; Becker, B.; Schneider-Brachert, W.; Hagen, I.; Landthaler, M.; Vogt, T. Re-expression of the retinoblastoma-binding protein 2-homolog 1 reveals tumor-suppressive functions in highly metastatic melanoma cells. *J. Invest. Dermatol.* **2006**, *126*, 1850–1859. [[CrossRef](#)]
47. Roesch, A.; Becker, B.; Meyer, S.; Wild, P.; Hafner, C.; Landthaler, M.; Vogt, T. Retinoblastoma-binding protein 2-homolog 1: A retinoblastoma-binding protein downregulated in malignant melanomas. *Mod. Pathol.* **2005**, *18*, 1249–1257. [[CrossRef](#)]
48. Roesch, A.; Vultur, A.; Bogeski, I.; Wang, H.; Zimmermann, K.M.; Speicher, D.; Körbel, C.; Laschke, M.W.; Gimotty, P.A.; Philipp, S.E. Overcoming intrinsic multidrug resistance in melanoma by blocking the mitochondrial respiratory chain of slow-cycling JARID1B(high) cells. *Cancer Cell* **2013**, *23*, 811–825. [[CrossRef](#)]
49. Tang, B.; Qi, G.; Tang, F.; Yuan, S.; Wang, Z.; Liang, X.; Li, B.; Yu, S.; Liu, J.; Huang, Q. JARID1B promotes metastasis and epithelial-mesenchymal transition via PTEN/AKT signaling in hepatocellular carcinoma cells. *Oncotarget* **2015**, *6*, 12723–12739. [[CrossRef](#)]
50. Wang, D.; Han, S.; Peng, R.; Jiao, C.; Wang, X.; Yang, X.; Yang, R.; Li, X. Depletion of histone demethylase KDM5B inhibits cell proliferation of hepatocellular carcinoma by regulation of cell cycle checkpoint proteins p15 and p27. *J. Exp. Clin. Cancer Res.* **2016**, *35*, 37. [[CrossRef](#)]
51. Shigekawa, Y.; Hayami, S.; Ueno, M.; Miyamoto, A.; Suzaki, N.; Kawai, M.; Hirono, S.; Okada, K.-I.; Hamamoto, R.; Yamaue, H. Overexpression of KDM5B/JARID1B is associated with poor prognosis in hepatocellular carcinoma. *Oncotarget* **2018**, *9*, 34320–34335. [[CrossRef](#)] [[PubMed](#)]

52. Gong, J.; Yan, S.; Yu, H.; Zhang, W.; Zhang, D. Increased Expression of Lysine-Specific Demethylase 5B (KDM5B) Promotes Tumor Cell Growth in Hep3B Cells and is an Independent Prognostic Factor in Patients with Hepatocellular Carcinoma. *Med. Sci. Monit.* **2018**, *24*, 7586–7594. [[CrossRef](#)] [[PubMed](#)]
53. Wang, Z.; Tang, F.; Qi, G.; Yuan, S.; Zhang, G.; Tang, B.; He, S. KDM5B is overexpressed in gastric cancer and is required for gastric cancer cell proliferation and metastasis. *Am. J. Cancer Res.* **2015**, *5*, 87–100. [[PubMed](#)]
54. Li, Y.; Chen, L.; Feng, L.; Zhu, M.; Shen, Q.; Fang, Y.; Liu, X.; Zhang, X. NEK2 promotes proliferation, migration and tumor growth of gastric cancer cells via regulating KDM5B/H3K4me3. *Am. J. Cancer Res.* **2019**, *9*, 2364–2378.
55. Bao, J.; Zou, J.; Li, C.; Zheng, G. miR-194 inhibits gastric cancer cell proliferation and tumorigenesis by targeting KDM5B. *Eur. Rev. Med. Pharmacol. Sci.* **2016**, *20*, 4487–4493.
56. Xu, W.; Zhou, B.; Zhao, X.; Zhu, L.; Xu, J.; Jiang, Z.; Chen, D.; Wei, Q.; Han, M.; Feng, L. KDM5B demethylates H3K4 to recruit XRCC1 and promote chemoresistance. *Int. J. Biol. Sci.* **2018**, *14*, 1122–1132. [[CrossRef](#)]
57. Ohta, K.; Haraguchi, N.; Kano, Y.; Kagawa, Y.; Konno, M.; Nishikawa, S.; Hamabe, A.; Hasegawa, S.; Ogawa, H.; Fukusumi, T. Depletion of JARID1B induces cellular senescence in human colorectal cancer. *Int. J. Oncol.* **2013**, *42*, 1212–1218. [[CrossRef](#)]
58. Tarnowski, M.; Czerewaty, M.; Deskur, A.; Safranow, K.; Marlicz, W.; Urańska, E.; Ratajczak, M.Z.; Starzyńska, T. Expression of cancer testis antigens in colorectal cancer: New prognostic and therapeutic implications. *Dis. Markers* **2016**, *2016*, 1987505. [[CrossRef](#)]
59. Li, X.; Su, Y.; Pan, J.; Zhou, Z.; Song, B.; Xiong, E.; Chen, Z. Connexin 26 is down-regulated by KDM5B in the progression of bladder cancer. *Int. J. Mol. Sci.* **2013**, *14*, 7866–7879. [[CrossRef](#)]
60. Lu, W.; Liu, S.; Li, B.; Xie, Y.; Adhiambo, C.; Yang, Q.; Ballard, B.R.; Nakayama, K.I.; Matusik, R.J.; Chen, Z. SKP2 inactivation suppresses prostate tumorigenesis by mediating JARID1B ubiquitination. *Oncotarget* **2015**, *6*, 771–788. [[CrossRef](#)]
61. Li, J.; Wan, X.; Qiang, W.; Li, T.; Huang, W.; Huang, S.; Wu, D.; Li, Y. MiR-29a suppresses prostate cell proliferation and induces apoptosis via KDM5B protein regulation. *Int. J. Clin. Exp. Med.* **2015**, *8*, 5329–5339. [[PubMed](#)]
62. Nilsson, E.M.; Laursen, K.B.; Whitchurch, J.; McWilliam, A.; Ødum, N.; Persson, J.L.; Heery, D.M.; Gudas, L.J.; Mongan, N.P. MiR137 is an androgen regulated repressor of an extended network of transcriptional coregulators. *Oncotarget* **2015**, *6*, 35710–35725. [[CrossRef](#)] [[PubMed](#)]
63. Wang, H.; Song, C.; Ding, Y.; Pan, X.; Ge, Z.; Tan, B.-H.; Gowda, C.; Sachdev, M.; Muthusami, S.; Ouyang, H. Transcriptional regulation of JARID1B/KDM5B histone demethylase by ikaros, histone deacetylase 1 (HDAC1), and casein kinase 2 (CK2) in B-cell acute lymphoblastic leukemia. *J. Biol.* **2016**, *291*, 4004–4018. [[CrossRef](#)]
64. Lin, C.-S.; Lin, Y.-C.; Adebayo, B.O.; Wu, A.; Chen, J.-H.; Peng, Y.-J.; Cheng, M.-F.; Lee, W.-H.; Hsiao, M.; Chao, T.-Y. Silencing JARID1B suppresses oncogenicity, stemness and increases radiation sensitivity in human oral carcinoma. *Cancer Lett.* **2015**, *368*, 36–45. [[CrossRef](#)] [[PubMed](#)]
65. Cui, Z.; Song, L.; Hou, Z.; Han, Y.; Hu, Y.; Wu, Y.; Chen, W.; Mao, L. PLU-1/JARID1B overexpression predicts proliferation properties in head and neck squamous cell carcinoma. *Oncol. Rep.* **2015**, *33*, 2454–2460. [[CrossRef](#)] [[PubMed](#)]
66. Kano, Y.; Konno, M.; Ohta, K.; Haraguchi, N.; Nishikawa, S.; Kagawa, Y.; Hamabe, A.; Hasegawa, S.; Ogawa, H.; Fukusumi, T. Jumonji/Arid1b (Jarid1b) protein modulates human esophageal cancer cell growth. *Mol. Clin. Oncol.* **2013**, *1*, 753–757. [[CrossRef](#)]
67. Zhou, Y.; An, Q.; Guo, R.-X.; Qiao, Y.-H.; Li, L.-X.; Zhang, X.-Y.; Zhao, X.-L. miR424-5p functions as an anti-oncogene in cervical cancer cell growth by targeting KDM5B via the Notch signaling pathway. *Life Sci.* **2017**, *171*, 9–15. [[CrossRef](#)]
68. Kumar, A.; Kumari, N.; Nallabelli, N.; Sharma, U.; Rai, A.; Singh, S.K.; Kakkar, N.; Prasad, R. Expression profile of H3K4 demethylases with their clinical and pathological correlation in patients with clear cell renal cell carcinoma. *Gene* **2020**, *739*, 144498. [[CrossRef](#)]
69. Wang, L.; Mao, Y.; Du, G.; He, C.; Han, S. Overexpression of JARID1B is associated with poor prognosis and chemotherapy resistance in epithelial ovarian cancer. *Tumor Biol.* **2015**, *36*, 2465–2472. [[CrossRef](#)]

70. Kuo, Y.-T.; Liu, Y.-L.; Adebayo, B.O.; Shih, P.-H.; Lee, W.-H.; Wang, L.-S.; Liao, Y.-F.; Hsu, W.-M.; Yeh, C.-T.; Lin, C.-M. JARID1B expression plays a critical role in chemoresistance and stem cell-like phenotype of neuroblastoma cells. *PLoS ONE* **2015**, *10*, e0125343. [[CrossRef](#)]
71. Barrett, A.; Madsen, B.; Copier, J.; Lu, P.J.; Cooper, L.; Scibetta, A.G.; Burchell, J.; Taylor-Papadimitriou, J. PLU-1 nuclear protein, which is upregulated in breast cancer, shows restricted expression in normal human adult tissues: A new cancer/testis antigen? *Int. J. Cancer* **2002**, *101*, 581–588. [[CrossRef](#)] [[PubMed](#)]
72. Zheng, Y.-C.; Chang, J.; Wang, L.-C.; Ren, H.-M.; Pang, J.-R.; Liu, H.-M. Lysine demethylase 5B (KDM5B): A potential anti-cancer drug target. *Eur. J. Med. Chem.* **2019**, *161*, 131–140. [[CrossRef](#)] [[PubMed](#)]
73. Heinemann, B.; Nielsen, J.M.; Hudlebusch, H.R.; Lees, M.J.; Larsen, D.V.; Boesen, T.; Labelle, M.; Gerlach, L.-O.; Birk, P.; Helin, K. Inhibition of demethylases by GSK-J1/J4. *Nature* **2014**, *514*, E1–E2. [[CrossRef](#)] [[PubMed](#)]
74. Westaway, S.M.; Preston, A.G.; Barker, M.D.; Brown, F.; Brown, J.A.; Campbell, M.; Chung, C.-W.; Drewes, G.; Eagle, R.; Garton, N. Cell penetrant inhibitors of the KDM4 and KDM5 families of histone lysine demethylases. 2. Pyrido [3-d] pyrimidin-4 (3 H)-one derivatives. *J. Med. Chem.* **2016**, *59*, 1370–1387. [[CrossRef](#)]
75. Bavetsias, V.; Lanigan, R.M.; Ruda, G.F.; Atrash, B.; McLaughlin, M.G.; Tumber, A.; Mok, N.Y.; Le Bihan, Y.-V.; Dempster, S.; Boxall, K.J. 8-Substituted Pyrido [3, 4-d] pyrimidin-4 (3 H)-one Derivatives as Potent, Cell Permeable, KDM4 (JMJD2) and KDM5 (JARID1) Histone Lysine Demethylase Inhibitors. *J. Med. Chem.* **2016**, *59*, 1388–1409. [[CrossRef](#)]
76. Vinogradova, M.; Gehling, V.S.; Gustafson, A.; Arora, S.; Tindell, C.A.; Wilson, C.; Williamson, K.E.; Guler, G.D.; Gangurde, P.; Manieri, W. An inhibitor of KDM5 demethylases reduces survival of drug-tolerant cancer cells. *Nat. Chem. Biol.* **2016**, *12*, 531–538. [[CrossRef](#)]
77. Tumber, A.; Nuzzi, A.; Hookway, E.S.; Hatch, S.B.; Velupillai, S.; Johansson, C.; Kawamura, A.; Savitsky, P.; Yapp, C.; Szykowska, A. Potent and selective KDM5 inhibitor stops cellular demethylation of H3K4me3 at transcription start sites and proliferation of MM1S myeloma cells. *Cell Chem. Biology* **2017**, *24*, 371–380. [[CrossRef](#)]
78. Nie, Z.; Shi, L.; Lai, C.; O’Connell, S.M.; Xu, J.; Stansfield, R.K.; Hosfield, D.J.; Veal, J.M.; Stafford, J.A. Structure-based design and discovery of potent and selective KDM5 inhibitors. *Bioorg. Med. Chem. Lett.* **2018**, *28*, 1490–1494. [[CrossRef](#)]
79. Zhao, B.; Liang, Q.; Ren, H.; Zhang, X.; Wu, Y.; Zhang, K.; Ma, L.-Y.; Zheng, Y.-C.; Liu, H.-M. Discovery of pyrazole derivatives as cellular active inhibitors of histone lysine specific demethylase 5B (KDM5B/JARID1B). *Eur. J. Med. Chem.* **2020**, *192*, 112161. [[CrossRef](#)]
80. Pushpakom, S.; Iorio, F.; Eyers, P.A.; Escott, K.J.; Hopper, S.; Wells, A.; Doig, A.; Guilliams, T.; Latimer, J.; McNamee, C. Drug repurposing: Progress, challenges and recommendations. *Nat. Rev. Drug Discov.* **2019**, *18*, 41–58. [[CrossRef](#)]
81. Sleire, L.; Førde, H.E.; Netland, I.A.; Leiss, L.; Skeie, B.S.; Enger, P.Ø. Drug repurposing in cancer. *Pharmacol. Res.* **2017**, *124*, 74–91. [[CrossRef](#)] [[PubMed](#)]
82. Eyer, L.; Nencka, R.; De Clercq, E.; Seley-Radtke, K.; Růžek, D. Nucleoside analogs as a rich source of antiviral agents active against arthropod-borne flaviviruses. *Antivir. Chem. Chemother.* **2018**, *26*, 2040206618761299. [[CrossRef](#)] [[PubMed](#)]
83. Damaraju, V.L.; Damaraju, S.; Young, J.D.; Baldwin, S.A.; Mackey, J.; Sawyer, M.B.; Cass, C.E. Nucleoside anticancer drugs: The role of nucleoside transporters in resistance to cancer chemotherapy. *Oncogene* **2003**, *22*, 7524–7536. [[CrossRef](#)] [[PubMed](#)]
84. Tănase, C.I.; Drăghici, C.; Cojocaru, A.; Galochkina, A.V.; Orshanskaya, J.R.; Zarubaev, V.V.; Shova, S.; Enache, C.; Maganu, M. New carbocyclic N6-substituted adenine and pyrimidine nucleoside analogues with a bicyclo [2.2. 1] heptane fragment as sugar moiety; synthesis, antiviral, anticancer activity and X-ray crystallography. *Bioorg. Med. Chem.* **2015**, *23*, 6346–6354. [[CrossRef](#)] [[PubMed](#)]
85. Guinan, M.; Benckendorff, C.; Smith, M.; Miller, G.J. Recent Advances in the Chemical Synthesis and Evaluation of Anticancer Nucleoside Analogues. *Molecules* **2020**, *25*, E2050. [[CrossRef](#)]
86. Rao, M.; Chinnasamy, N.; Hong, J.A.; Zhang, Y.; Zhang, M.; Xi, S.; Liu, F.; Marquez, V.E.; Morgan, R.A.; Schrupp, D.S. Inhibition of histone lysine methylation enhances cancer–testis antigen expression in lung cancer cells: Implications for adoptive immunotherapy of cancer. *Cancer Res.* **2011**, *71*, 4192–4204. [[CrossRef](#)]

87. Mohamed, T.; Rao, P.P. 2, 4-Disubstituted quinazolines as amyloid- β aggregation inhibitors with dual cholinesterase inhibition and antioxidant properties: Development and structure-activity relationship (SAR) studies. *Eur. J. Med. Chem.* **2017**, *126*, 823–843. [[CrossRef](#)]
88. Horton, J.R.; Liu, X.; Gale, M.; Wu, L.; Shanks, J.R.; Zhang, X.; Webber, P.J.; Bell, J.S.; Kales, S.C.; Mott, B.T. Structural basis for KDM5A histone lysine demethylase inhibition by diverse compounds. *Cell Chem. Biol.* **2016**, *23*, 769–781. [[CrossRef](#)]



© 2020 by the authors. Licensee MDPI, Basel, Switzerland. This article is an open access article distributed under the terms and conditions of the Creative Commons Attribution (CC BY) license (<http://creativecommons.org/licenses/by/4.0/>).

Article

Serum PD-1/PD-L1 Levels, Tumor Expression and PD-L1 Somatic Mutations in HER2-Positive and Triple Negative Normal-Like Feline Mammary Carcinoma Subtypes

Catarina Nascimento ¹, Ana Catarina Urbano ¹, Andreia Gameiro ¹, João Ferreira ², Jorge Correia ¹ and Fernando Ferreira ^{1,*}

¹ CIISA—Centro de Investigação Interdisciplinar em Sanidade Animal, Faculdade de Medicina Veterinária, Universidade de Lisboa, Avenida da Universidade Técnica, Lisboa 1300-477, Portugal; catnasc@fmv.ulisboa.pt (C.N.); curbano.ms@gmail.com (A.C.U.); agameiro@fmv.ulisboa.pt (A.G.); jcorreia@fmv.ulisboa.pt (J.C.)

² Instituto de Medicina Molecular, Faculdade de Medicina, Universidade de Lisboa, Lisboa 1649-028, Portugal; hjoao@medicina.ulisboa.pt

* Correspondence: fernandof@fmv.ulisboa.pt; Tel.: (+351)-21-365-2800 (ext. 431234)

Received: 16 April 2020; Accepted: 26 May 2020; Published: 28 May 2020



Abstract: Tumor microenvironment has gained great relevance due to its ability to regulate distinct checkpoints mediators, orchestrating tumor progression. Serum programmed cell death protein-1 (PD-1) and programmed death ligand-1 (PD-L1) levels were compared with healthy controls and with serum cytotoxic T-lymphocyte-associated antigen 4 (CTLA-4) and tumor necrosis factor-alpha (TNF- α) levels in order to understand the role of PD-1/PD-L1 axis in cats with mammary carcinoma. PD-1 and PD-L1 expression was evaluated in tumor-infiltrating lymphocytes (TILs) and cancer cells, as the presence of somatic mutations. Results showed that serum PD-1 and PD-L1 levels were significantly higher in cats with HER2-positive ($p = 0.017$; $p = 0.032$) and triple negative (TN) normal-like mammary carcinomas ($p = 0.004$; $p = 0.015$), showing a strong positive correlation between serum CTLA-4 and TNF- α levels. In tumors, PD-L1 expression in cancer cells was significantly higher in HER2-positive samples than in TN normal-like tumors ($p = 0.010$), as the percentage of PD-L1-positive TILs ($p = 0.037$). *PD-L1* gene sequencing identified two heterozygous mutations in exon 4 (A245T; V252M) and one in exon 5 (T267S). In summary, results support the use of spontaneous feline mammary carcinoma as a model for human breast cancer and suggest that the development of monoclonal antibodies may be a therapeutic strategy.

Keywords: feline mammary carcinoma; PD-1; PD-L1; CTLA-4; TNF- α ; biomarkers; immunotherapy

1. Introduction

Breast cancer is the most diagnosed tumor among women [1] and feline mammary carcinoma (FMC) is the third most common tumor in the cat. At the molecular level, there are distinct subtypes of breast cancer: Luminal A, Luminal B, HER2-positive and triple-negative (normal-like and basal-like) [2]. The HER2-positive subtype is characterized by a HER2 overexpression and a lack of hormone receptors (estrogen receptor (ER) and/or progesterone receptor (PR)), while the triple negative tumors are defined by the absence of ER, PR and HER2 expression, each representing 15–20% of all breast cancer cases [1,3]. As in human breast cancer [4], FMC presents an aggressive and infiltrative behavior [5,6], with both HER2-positive and triple negative (TN) subtypes showing worse prognosis than luminal A and B subtypes. Furthermore, a surgical approach is often necessary for the treatment of FMC,

as the adjuvant chemotherapy (cyclophosphamide, vincristine, doxorubicin) is not useful in some cases [7]. Thus, the identification of novel diagnostic biomarkers and therapeutic targets is needed, not only to improve the clinical outcome of cats with mammary carcinoma but also because FMC shares clinicopathological, histopathological and epidemiological features, as well as the molecular classification with human breast cancer [4,8–10]. Moreover, the use of animal models has been increasing, allowing researchers to understand the mechanisms underlying tumorigenesis; mouse species are the most used due to their small size and short gestation period. Nevertheless, laboratory rodents have several limitations, such as a lack of genetic heterogeneity and discrepancies to the human tumor development [11], while pets that spontaneously develop malignant tumors provide natural models, making them excellent for the study of human breast cancer [12].

In humans, the role of the PD-1/PD-L1 axis is being investigated in different tumor types, with the programmed death ligand-1 (PD-L1) expressed by tumor cells regulating T cell activity, promoting immune suppression and tumor escape [13–15]. This immune checkpoint molecule can be expressed by cancer cells and immune cells, as T and B lymphocytes, macrophages and dendritic cells, being its expression on tumor-infiltrating lymphocytes (TILs) correlated with clinical response to anti-PD-L1-targeted immunotherapy (atezolizumab) [16]. Accordingly, a monoclonal antibody that blocks PD-L1 binding to the programmed cell death protein-1 (PD-1) receptor on T cells was recently approved by the Food and Drug Administration (FDA) to treat different tumor types and also PD-L1 positive unresectable locally advanced and metastatic TN breast cancer [17,18], since, several studies showed that PD-1 and PD-L1 are overexpressed in the most aggressive cancer subtypes (HER2-positive and triple negative) [19–22].

The less studied serum PD-1 (sPD-1) and PD-L1 (sPD-L1) levels may also play an important role in anti-tumor immune responses. Studies in patients with breast cancer, lung cancer, metastatic melanoma and renal cell carcinoma reported higher sPD-1 or sPD-L1 levels than in healthy controls, suggesting that elevated serum PD-1 and PD-L1 levels may promote immunosuppression and are therefore to be considered adverse prognostic factors [23–25]. Furthermore, cytotoxic T-lymphocyte-associated antigen 4 (CTLA-4) is another immune mediator that inhibits T-cell immune function, being also targeted in breast cancer. Accordingly, serum CTLA-4 levels are increased in cats with mammary carcinoma, as well as in human malignant tumors [10]. Some trials are evaluating the combination of anti-PD-1/PD-L1 antibodies with CTLA-4 inhibitors [17,26]. In humans, CTLA-4 regulates T-cell proliferation at the initial stage of immune responses, primarily in lymph nodes, whereas PD-1 suppresses T cells in later stages, typically in peripheral tissues. Additionally, it has been described that certain pro-inflammatory cytokines, such as tumor necrosis factor-alpha (TNF- α), can up-regulate PD-L1 expression in cancer cells, contributing to create an immunosuppressive tumor microenvironment [27,28]. Furthermore, TNF- α is described to be elevated in cats with mammary carcinoma, being positively correlated with serum CTLA-4 levels, as in humans [10].

The *PD-L1* gene encodes for a transmembrane glycoprotein with 290 amino acid residues [29], presenting two extracellular immunoglobulin domains, a cytoplasmic domain and shows a sequence homology of 74.5% with feline *PD-L1* gene (UniProt, accession numbers: *Felis catus*—M3WAP8, *Homo sapiens*—Q9NZQ7).

Considering the above evidences and the lack of knowledge on the role of the PD-1/PD-L1 signaling pathway in tumor progression in the cat, this study aimed to: (i) quantify and compare the sPD-1 and sPD-L1 levels in animals with different mammary carcinoma subtypes and healthy controls; (ii) evaluate the PD-1 and PD-L1 expression in tumor-infiltrating lymphocytes (TILs) and cancer cells; (iii) test for statistical associations between serum PD-1, PD-L1, CTLA-4 and TNF- α levels; (iv) identify genomic mutations in the *PD-L1* gene to validate future checkpoint-blocking therapies.

2. Results

2.1. Cats with HER2-Positive or TN Normal-Like Mammary Carcinoma Showed Higher Serum PD-1 and PD-L1 Levels

Serum PD-1 and PD-L1 levels were measured in cats with mammary carcinoma, grouped according to their tumor subtype and compared with serum levels detected in the healthy control group (Tables 1 and 2).

Table 1. Serum programmed cell death protein-1 (PD-1) levels in healthy cats and queens grouped according to their mammary carcinoma molecular subtype.

Group	<i>n</i>	sPD-1 (pg/mL) Median ± SD	sPD-1 (pg/mL) Mean ± SEM
Control	12	534.0 ± 253.2	459.0 ± 73.1
Luminal A	7	708.8 ± 2165.2	1826.5 ± 818.8
Luminal B	15	590.3 ± 1776.8	1386.3 ± 458.8
HER2-positive	11	1148.9 ± 3386.0	3129.6 ± 1020.9
TN Normal-Like	7	3655.1 ± 31,478.1	21,637.3 ± 11,897.6
TN Basal-Like	6	513.3 ± 145.0	519.3 ± 59.2

Table 2. Serum programmed death ligand-1 (PD-L1) levels detected in healthy cats and queens stratified by their mammary carcinoma molecular subtype.

Group	<i>n</i>	sPD-L1 (pg/mL) Median ± SD	sPD-L1 (pg/mL) Mean ± SEM
Control	13	1835.5 ± 545.6	1762.5 ± 151.3
Luminal A	7	1789.6 ± 941.6	2121.5 ± 355.9
Luminal B	15	1628.0 ± 773.4	1877.6 ± 199.7
HER2-positive	9	5490.4 ± 3789.6	5672.6 ± 1263.2
TN Normal-Like	7	4377.5 ± 8819.4	8313.0 ± 3333.4
TN Basal-Like	6	1436.3 ± 425.6	1534.2 ± 173.8

Results from the Kruskal–Wallis test found significant differences between the mean ranks of at least one pair of groups ($p = 0.044$ for PD-1; $p = 0.006$ for PD-L1). Indeed, cats showing HER2-positive or TN normal-like mammary carcinoma displayed higher serum PD-1 levels than healthy group (1148.9 pg/mL vs. 534.0 pg/mL, $p = 0.017$; 3655.1 pg/mL vs. 534.0 pg/mL, $p = 0.004$, Figure 1A), as well as serum PD-L1 levels (5490.4 pg/mL vs. 1835.5 pg/mL, $p = 0.032$; 3641.4 pg/mL vs. 1835.5 pg/mL, $p = 0.015$, Figure 1B). Furthermore, the optimal cut-off value of serum PD-1 levels was 801.6 pg/mL in cats with HER2-positive mammary carcinoma (AUC = 0.765 ± 0.104 , 95% CI: 0.562–0.968, $p = 0.031$; sensitivity = 54.5%; specificity = 91.7%; Figure 1C) and 801.6 pg/mL in cats with TN normal-like mammary carcinoma (AUC = 0.857 ± 0.092 , 95% CI: 0.676–1.000, $p = 0.011$; sensitivity = 57.1%; specificity = 91.7%; Figure 1D). Regarding the serum PD-L1 levels, the optimal cut-off value in cats with HER2-positive mammary carcinoma was 2545.0 pg/mL (AUC = 0.778 ± 0.117 , 95% CI: 0.548–1.000, $p = 0.030$; sensitivity = 66.7%; specificity = 92.3%; Figure 1E) and 2519.0 pg/mL in cats with TN normal-like tumor subtype (AUC = 0.857 ± 0.123 , 95% CI: 0.617–1.000, $p = 0.010$; sensitivity = 85.7%; specificity = 92.3%; Figure 1F). No significant differences were found in serum PD-1 and PD-L1 levels between cats with mammary carcinoma of other molecular subtypes and the control group.

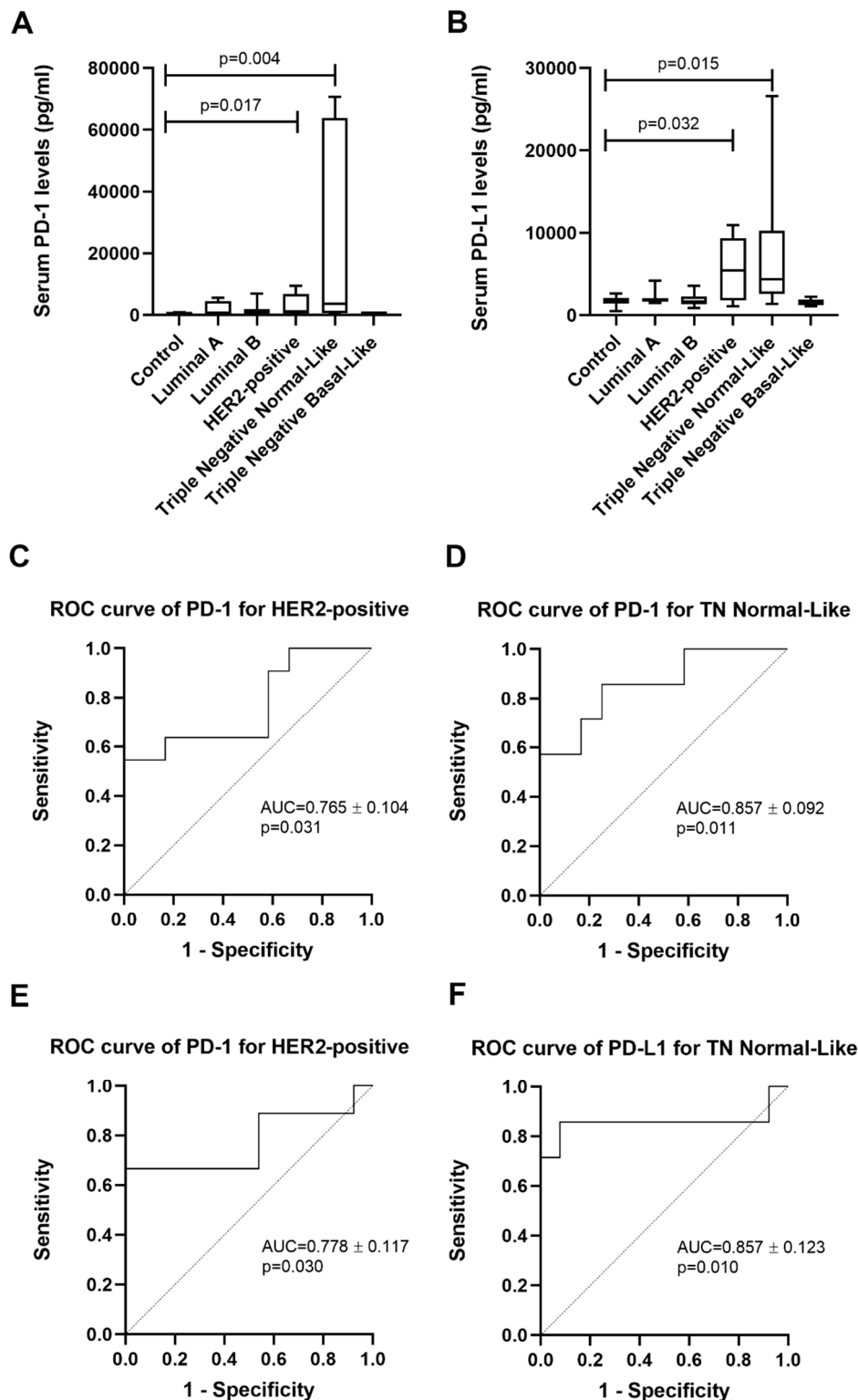


Figure 1. Serum programmed cell death protein-1 (PD-1) and programmed death ligand-1 (PD-L1) levels in cats with HER2-positive and triple negative (TN) normal-like mammary carcinoma. (A) Box plot analysis showing the range of serum PD-1 and (B) PD-L1 levels in control group and cats with mammary carcinoma stratified according to their molecular subtype. (C) Receiver Operating Characteristic (ROC) curve analysis for the identification of the optimal cut-off value of sPD-1 levels for cats with HER2-positive mammary carcinoma and (D) for cats with TN normal-like mammary carcinoma. (E) ROC curve analysis of PD-L1 for cats showing HER2-positive mammary carcinoma and (F) TN normal-like carcinoma.

The data obtained also revealed a positive correlation between serum PD-1 and PD-L1 levels in cats with mammary carcinoma ($r = 0.780$, $p < 0.0001$, Figure 2A), particularly in those exhibiting HER2-positive ($r = 0.786$, $p = 0.03$, Figure 2B) or TN normal-like tumor subtypes ($r = 0.857$, $p = 0.03$, Figure 2C).

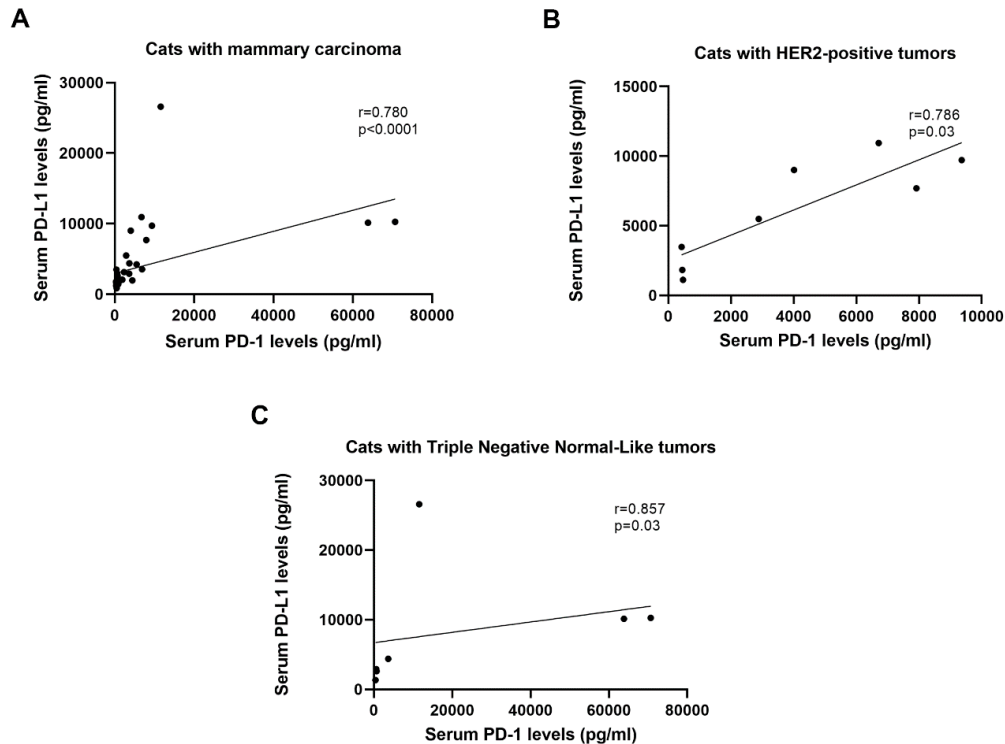


Figure 2. Serum programmed cell death protein-1 (PD-1) and programmed death ligand-1 (PD-L1) levels are strongly correlated in cats with HER2-positive and TN normal-like mammary carcinoma. (A) Correlation between sPD-1 and sPD-L1 levels in cats with mammary carcinoma (B) and in cats with HER2-positive and (C) triple negative (TN) normal-like carcinoma subtypes.

2.2. Serum CTLA-4 and TNF- α Levels are Positively Correlated with Serum PD-1/PD-L1 Levels in Cats with HER2-Positive and TN Normal-Like Tumors

A strong positive correlation was found in cats with HER2-positive mammary carcinomas between the serum PD-1 levels and serum PD-L1 ($r = 0.923$), CTLA-4 ($r = 0.975$) and TNF- α ($r = 0.968$) levels (Table 3). The queens with TN normal-like carcinomas also showed a strong positive correlation between serum PD-1 levels and serum PD-L1 ($r = 0.857$), CTLA-4 ($r = 0.927$) and TNF- α ($r = 0.893$) levels (Table 3).

2.3. TN normal-like Mammary Carcinomas Showed Lower PD-L1 Expression than HER2-Positive Tumors

Considering the high serum PD-L1 levels presented by cats with HER2-positive or TN normal-like mammary carcinomas, we further evaluated the percentage and staining intensity of PD-L1 expression in tumor-infiltrating lymphocytes (TILs) and in cancer cells, by immunostaining of tumor samples. Results showed a higher score of PD-L1-positive TILs in HER2-positive tumors than in TN normal-like ones ($p = 0.037$, Figures 3A and 4A,B,E,F). Besides, the PD-L1 score on cancer cells was significantly higher in HER2-positive tumors than in TN normal-like mammary carcinomas ($p = 0.010$, Figures 3B and 4C–F).

Table 3. Spearman’s correlation between serum programmed cell death protein-1 (PD-1), programmed death ligand-1 (PD-L1), cytotoxic T-lymphocyte-associated antigen 4 (CTLA-4) and tumor necrosis factor-alpha (TNF- α) levels in cats with HER2-positive and triple negative (TN) normal-like mammary carcinomas.

HER2-Positive	PD-1	PD-L1	CTLA-4	TNF- α
PD-1	–	0.923**	0.975**	0.968**
PD-L1	0.923**	–	0.947**	0.922**
CTLA-4	0.975**	0.947**	–	0.947**
TNF- α	0.968**	0.922**	0.947**	–
TN Normal-Like	PD-1	PD-L1	CTLA-4	TNF- α
PD-1	–	0.857*	0.927**	0.893**
PD-L1	0.857*	–	0.815*	0.857*
CTLA-4	0.927**	0.815*	–	0.927**
TNF- α	0.893**	0.857*	0.927**	–

* indicates $p < 0.05$, ** indicates $p < 0.01$.

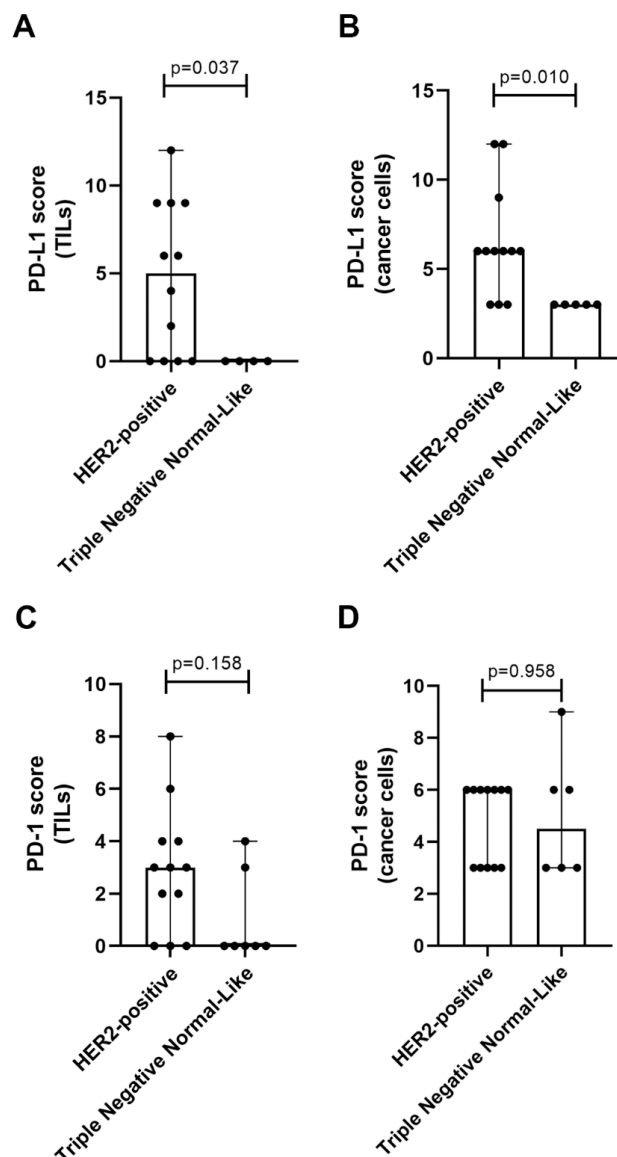


Figure 3. Programmed death ligand-1 (PD-L1) and programmed cell death protein-1 (PD-1) staining analysis of tumor-infiltrating lymphocytes (TILs) and cancer cells in HER2-positive and triple negative (TN) normal-like tumor samples (range values). (A) The score of PD-L1-positive TILs (B) and cancer cells

in HER2-positive mammary carcinomas in comparison to TN normal-like tumors. (C) The score of PD-1-positive TILs between HER2-positive tumors and TN normal-like mammary carcinomas and (D) cancer cells.

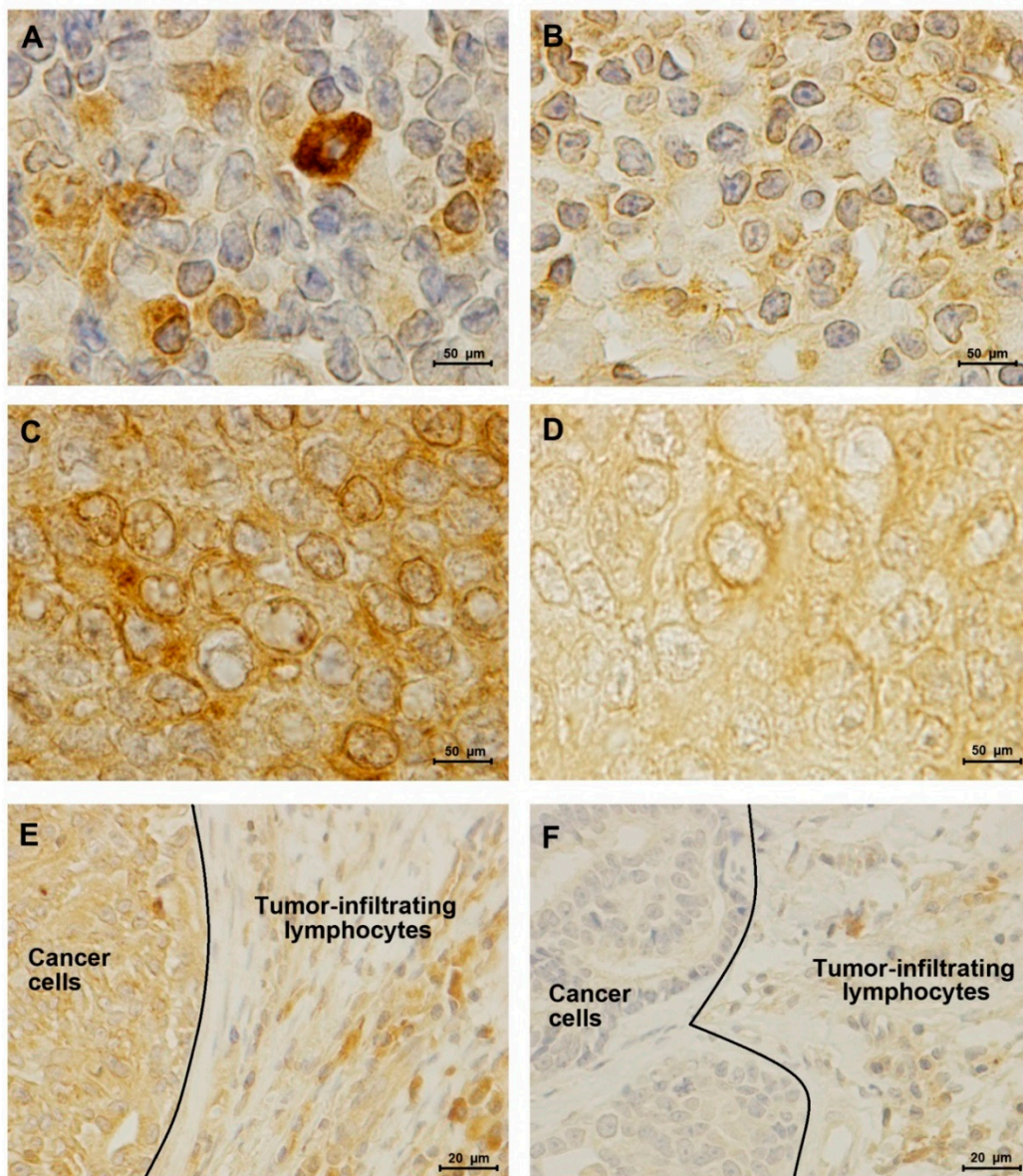


Figure 4. Programmed death ligand-1 (PD-L1) expression in tumor-infiltrating lymphocytes (TILs) and cancer cells of HER2-positive mammary carcinomas and triple negative (TN) normal-like tumors. (A) Representative PD-L1 immunostaining of tumor infiltrating lymphocytes in a HER2-positive (B) and in a TN normal-like mammary carcinoma (100× objective). (C) PD-L1 score intensity 4+ in HER2-positive cancer cells (D) and score 1+ in TN normal-like cancer cells (100× objective). Furthermore, in TILs, PD-L1 is localized to the cell membrane and cytoplasm, while in cancer cells it is mainly distributed to cytoplasmic and nuclear membranes. (E) Immunohistochemical staining of PD-L1 in a HER2-positive solid carcinoma (F) and in a TN normal-like tubulopapillary carcinoma (40× objective).

Regarding PD-1 expression in TILs and cancer cells, no significant differences were found between HER2-positive tumors and TN normal-like mammary carcinomas ($p = 0.158$, Figure 3C; $p = 0.958$, Figure 3D).

2.4. Elevated Serum PD-1/PD-L1 Levels Showed A Higher Concordance with IHC for PD-1 and PD-L1 in Cancer Cells than in TILs

Our results revealed that elevated serum PD-1 levels, PD-1-positive TILs and PD-1-positive cancer cells were found in 61.5%, 41.7% and 100% of cats with HER2-positive mammary carcinoma and in 57.1%, 33.3% and 100% of cats with triple-negative normal-like mammary tumors. In parallel, elevated serum PD-L1 levels, PD-L1-positive TILs and PD-L1-positive cancer cells were detected in 76.9%, 66.7% and 100% of cats with HER2-positive tumors and in 85.7%, 20% and 100% of cats with a triple-negative normal-like tumor subtype (Table 4). Thus, these results demonstrated that serum analysis could provide differential information when compared with the expression of the two immune checkpoint molecules in TILs and cancer cells.

Table 4. Concordance between the animals with elevated serum PD-1/PD-L1 levels (sPD-1, sPD-L1), PD-1/PD-L1-positive TILs infiltration and PD-1/PD-L1-positive cancer cells.

Tumor subtype	sPD-1	TILs	Concordance	sPD-1	Cancer cells	Concordance
HER2-positive	61.5%	41.7%	58.3%	61.5%	100%	66.7%
Triple Negative Normal-Like	57.1%	33.3%	0%	57.1%	100%	66.7%
Tumor subtype	sPD-L1	TILs	Concordance	sPD-L1	Cancer cells	Concordance
HER2-positive	76.9%	66.7%	41.7%	76.9%	100%	75%
Triple Negative Normal-Like	85.7%	20%	20%	85.7%	100%	100%

2.5. Three Non-Redundant Mutations Were Detected in Feline PD-L1 gene

Results from DNA sequencing allowed us to identify three heterozygous mutations in the feline *PD-L1* gene (Figure 5). Two were found in exon 4 (c.16.756G > A; c.16.777G > A), one changing a neutral nonpolar amino acid (alanine-245) to a neutral polar residue (threonine) in 3.8% of the studied population (1/26). The second mutation converted a methionine to a valine (p.V252M), both neutral nonpolar amino acids, in 42.3% of the animals evaluated (11/26). A third mutation was identified in exon 5 (c.18.526A > C), replacing a neutral polar threonine by a neutral polar serine at residue number 267, in 3.8% of the DNA samples (1/26).

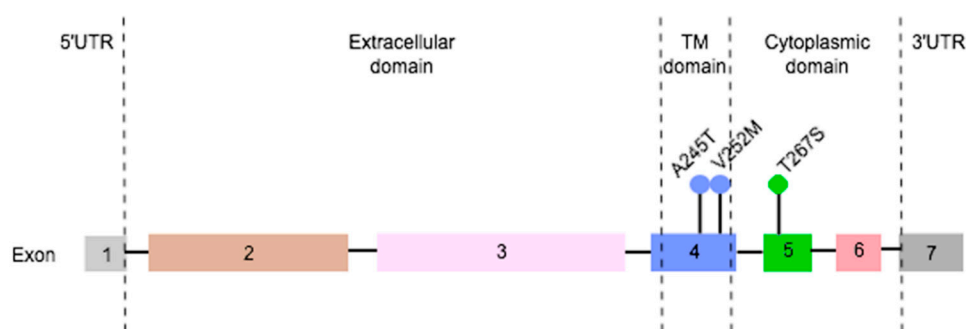


Figure 5. Three heterozygous and non-redundant somatic mutations were found in feline programmed death ligand-1 (*PD-L1*) gene.

3. Discussion

In order to escape the immune system, cancer cells can develop mechanisms to downregulate immune responses. For example, by overexpression of distinct immune checkpoint molecules such as PD-L1. In humans, the interaction between PD-L1 and its receptor has been revealed as an important step in the maintenance of an immunosuppressive tumor microenvironment [30]. Thus, a better understanding of the PD-1/PD-L1 pathway may also contribute to the development of new diagnostic tools and molecular therapies targeting PD-L1 in pets.

The results obtained showed that cats presenting mammary carcinoma subtypes associated with more aggressive features and poor prognosis [31] (HER2-positive and TN normal-like) displayed

significantly increased serum PD-1 and PD-L1 levels, as reported in humans with HER2-positive metastatic breast cancer [32], TN breast cancer [23], renal cell carcinoma [25], esophageal cancer [33], gastric cancer [24], advanced pancreatic cancer [34], lung cancer [35] and metastatic melanoma [36] correlated to shorter overall survival and tumor-free survival times [23,25,32,33,35], suggesting a conserved role of the PD-1/PD-L1 axis in both species. Moreover, as reported in humans, our findings uncovered a positive correlation between serum PD-1 and PD-L1 levels, suggesting that both molecules are co-regulated [23,34]. Furthermore, cats with HER2-positive or TN normal-like tumors showed a strong positive correlation between serum PD-1, PD-L1, CTLA-4 and TNF- α levels, which are immune-inhibitory molecules that downregulate T-cell immune responses, suggesting that these animals were immunosuppressed. CTLA-4 is another immune molecule located on the surface of T cells and expressed by regulatory T cells (Tregs), which triggers an inhibitory signal to immune cells [37], also being targeted in breast cancer treatment [26]. Additionally, the higher serum levels of the pro-inflammatory cytokine TNF- α may contribute to the increased tumor cell survival and PD-L1 stabilization on breast tumor cells, playing a critical role for tumor escape from immune surveillance [28]. Accordingly, a previous study also reported elevated serum CTLA-4 levels in cats with mammary carcinoma, being associated with HER2-positive status and TNF- α levels, in accordance with our findings.

Results from the immunostaining analysis revealed that PD-L1 expression in TILs and cancer cells was higher in HER2-positive mammary carcinoma, as reported in humans [2,3,16,20,22], contrasting with TN mammary carcinoma tumor samples. In spite of our findings, previous studies in human breast cancer showed that PD-1 and PD-L1 positive TILs and cancer cells overexpressing PD-L1 were frequently found in triple negative breast cancer subtype [16,23,38–41]. These controversial results may be due to the fact that serum PD-1 levels were higher in cats with TN normal-like carcinomas compared with animals presenting HER2-positive carcinomas, indicating that sPD-1 can bind to PD-L1 attached to the cell membrane of dendritic cells, inhibiting T cell function and proliferation, as previously described [42]. Additionally, recent studies described the presence of tumor-derived exosomes that carry PD-L1, suggesting an effective paracrine mechanism that cancer cells use to communicate and reprogram immune cells and consequently suppress T-cell activation [43–45]. These findings support that HER2-positive cancer cells lead to a local immunosuppressive microenvironment, strengthening the systemic immunosuppression found in cats with this tumor subtype. Moreover, our results revealed PD-L1 expression in cell membrane and cytoplasm of TILs, while in cancer cells the immunostaining was distributed to cytoplasmic and nuclear membranes. Accordingly, in human breast cancer different approaches were used to evaluate the PD-L1 expression, with some studies described only membranous staining and others, in agreement with our findings, registered both membranous and cytoplasmic staining [46,47]. In addition, Ghebeh et al. showed a predominant staining in the cytoplasm near to the nuclear membrane, probably the endoplasmic reticulum, and an expression of PD-L1 in the nucleus, as we described [48]. Additionally, our results showed that elevated serum PD-1/PD-L1 levels were detected more frequently than PD-1/PD-L1 overexpression in TILs of HER2-positive and triple-negative normal-like feline mammary carcinomas. Notably, a high concordance rate was found between elevated serum PD-1/PD-L1 levels and PD-1/PD-L1 overexpression in cancer cells of the same FMC subtypes, suggesting that the serum analysis can be a non-invasive tool for the real-time assessment of these immune checkpoints molecules in feline mammary carcinoma, as reported for breast cancer [49].

Lastly, three non-redundant heterozygous mutations were found in the feline *PD-L1* gene, with none of them located at the PD-L1 extracellular domain, which is recognized by the recent and promising monoclonal antibody approved for the treatment of human metastatic TN breast cancer [29]. This shall not compromise the future development of checkpoint-blocking therapies targeting PD-L1 for FMC treatment. According to the Catalogue of Somatic Mutations in Cancer (COSMIC), six mutations were reported with very low frequency in human breast cancer patients (148/47,194; 0.3%), all different from the ones that we detected.

4. Material and Methods

4.1. Animal Population

Tumor and serum samples were collected from 53 queens with mammary carcinoma that underwent mastectomy and 15 healthy queens presenting for elective ovariohysterectomy at the Small Animal Hospital of the Veterinary Medicine Faculty, University of Lisbon. All mammary lesions were embedded in paraffin after fixation in 10% buffered formalin (pH 7.2) during 24–48 h. Serum was separated from clotted blood by centrifugation (1500× g, 10 min, 4 °C) and stored at −80 °C until further use. All samples that showed hemolysis were discarded, as recommended for humans [50].

For each animal enrolled in the study, the following clinicopathological characteristics were recorded: age, breed, reproductive status, contraceptive administration, treatment performed (none, surgery or surgery plus chemotherapy), number, location and size of tumor lesions, histopathological classification, malignancy grade, presence of tumor necrosis, lymphatic invasion, lymphocytic infiltration, cutaneous ulceration, regional lymph node involvement, stage of the disease (TNM system), disease free-survival (DFS) and overall survival (OS) [31]. Table 5 summarizes the collected clinical data. Briefly, the mean age at diagnosis was 11.8 years (range 6.5–18 years), while the mean size of the primary lesions was 2.6 cm (range 0.3–7 cm). The DFS was 9.2 ± 7.8 months ($n = 49$; 95% CI: 7.3–11.7 months) and the OS was 15.0 ± 9.8 months ($n = 51$; 95% CI: 12.2–17.7 months).

Table 5. Clinicopathological features of the 53 female cats with mammary carcinoma enrolled in this study.

Clinicopathological Feature	Number of Animals (%)	Clinicopathological Feature	Number of Animals (%)
Age		Tumor size	
<8 years old	3 (5.7%)	<2 cm	19 (35.8%)
≥ 8 years old	50 (94.3%)	≥ 2 cm	34 (64.2%)
Breed		HP classification	
Not determined	39 (73.6%)	Tubulopapillary carcinoma	21 (39.6%)
Siamese	5 (9.4%)	Solid carcinoma	6 (11.3%)
Persian	6 (11.3%)	Cribriiform carcinoma	5 (9.4%)
Norwegian Forest Cat	2 (3.8%)	Papillary-cystic carcinoma	1 (1.9%)
Blue Russian	1 (1.9%)	Tubular carcinoma	12 (22.6%)
Spayed		Mucinous carcinoma	8 (15.2%)
No	28 (52.8%)	Tumor malignancy grade	
Yes	24 (45.3%)	I	3 (5.7%)
Unknown	1 (1.9%)	II	7 (13.2%)
Contraceptive administration		III	43 (81.1%)
No	19 (35.9%)	Tumor necrosis	
Yes	28 (52.8%)	No	13 (24.5%)
Unknown	6 (11.3%)	Yes	40 (75.5%)
Treatment		Tumor lymphatic invasion	
None	1 (1.9%)	No	48 (90.5%)
Mastectomy	48 (90.6%)	Yes	5 (9.5%)
Mastectomy + Chemo	4 (7.5%)	Lymphocytic infiltration	
Multiple tumors		No	17 (32.0%)
No	19 (35.8%)	Yes	34 (64.2%)
Yes	34 (64.2%)	Unknown	2 (3.8%)
Lymph node status		Tumor ulceration	
Negative	32 (60.4%)	No	46 (86.8%)
Positive	17 (32.1%)	Yes	7 (13.2%)
Unknown	4 (7.5%)	Ki-67 index	
TNM classification		Low (<14%)	36 (67.9%)
I	13 (24.5%)	High (>14%)	17 (32.1%)
II	6 (11.3%)	Progesterone status	
III	29 (54.7%)	Negative	28 (52.8%)
IV	5 (9.5%)	Positive	25 (47.2%)
Tumor localization		Estrogen status	
M1	8 (15.1%)	Negative	37 (69.8%)

Table 5. Cont.

Clinicopathological Feature	Number of Animals (%)	Clinicopathological Feature	Number of Animals (%)
M2	10 (18.9%)	Positive	16 (30.2%)
M3	20 (37.7%)	HER2 status	
M4	15 (28.3%)	Negative	41 (77.4%)
		Positive	12 (22.6%)

TNM—Tumor, Node, Metastasis; HP—Histopathological.

4.2. Quantification of Serum PD-1, PD-L1, CTLA-4 and TNF- α Levels

Serum PD-1, PD-L1, CTLA-4 and TNF- α levels were quantified by using the commercially available immunoassay kits from R&D systems (Minneapolis, MN, USA) and following the manufacturer's recommendations. PD-1 levels were measured with the PD-1 DuoSet ELISA kit (DY1086); PD-L1 levels with the PD-L1/B7-H1 DuoSet ELISA kit (DY156); CTLA-4 levels with the CTLA-4 DuoSet ELISA kit (DY476); and the TNF- α levels with the TNF- α DuoSet ELISA kit (DY2586), all based on a solid-phase sandwich enzyme-linked immunosorbent assay (ELISA) technique. The concentration levels of the above molecules were calculated using appropriate standard curves, by making serial dilutions from a stock solution of recombinant PD-1, PD-L1, CTLA-4 and TNF- α (9, 18, 36, 78, 156, 312.5, 625, 1250, 2500, 5000 and 10,000 pg/mL). Serum PD-1 and PD-L1 levels (pg/mL) were calculated using a quadratic regression ($y = ax^2 + bx + c$, $r^2 = 0.99$ for PD-1 and $r^2 = 0.96$ for PD-L1) and serum CTLA-4 and TNF- α concentrations were determined using a curve-fitting equation ($y = mx + c$, $r^2 > 0.99$) [10].

Briefly, quantification of the abovementioned molecules was performed in 96-well microplates incubated overnight with the corresponding capture antibodies (100 μ L/well), at room temperature (RT). On the next day, plates were washed three times with 400 μ L/well of PBS-Tween 0.05% and incubated with 300 μ L/well of PBS/BSA blocking agent (1%, *w/v*), at RT for 60 min. Then, plates were washed three times with 400 μ L/well PBS-Tween 0.05% and incubated with 100 μ L/well of each dilution, in duplicate. For determination of serum PD-1, PD-L1, CTLA-4 and TNF- α levels, serum samples were diluted 20 times in PBS/BSA 1% and 100 μ L of each sample was added to the wells. The plates were thereafter sealed and incubated for 2 hours at RT. After another washing step (3 \times 400 μ L/well PBS-Tween 0.05%), 100 μ L/well of detection antibodies was added and incubated for 2 hours at RT. Later and after three washes with 400 μ L/well of PBS-Tween 0.05%, 100 μ L/well of streptavidin-HRP was added and incubated for 20 min at RT, avoiding placing the microplate in direct light. Afterwards a further washing step (3 \times 400 μ L/well PBS-Tween 0.05%), 100 μ L/well of substrate solution (1:1 mixture of H₂O₂ and tetramethylbenzidine) was added and incubated for 20 min at RT in the dark. Finally, the reaction was stopped by adding 50 μ L/well of 2 N H₂SO₄ and gently shaking the plate. The absorbance was measured by a spectrophotometer (Fluostar Optima Microplate Reader, BMG, Ortenberg, Germany), following the manufacturer's recommendations.

4.3. Immunohistochemical Staining and Analysis

To analyze PD-1 and PD-L1 expression, two sections of formalin-fixed paraffin-embedded tissues of FMC with 3 μ m thickness (Microtome Leica RM2135, Newcastle, UK) were prepared, mounted on adhesive glass slides (SuperFrost Plus, Thermo Fisher Scientific, MA, USA) and placed at 64 $^{\circ}$ C for 60 min and then at 37 $^{\circ}$ C overnight. Then deparaffinization, rehydration and epitope retrieval were performed using a PT-Link module (Dako, Agilent, Santa Clara, CA, USA), by immersing glass slides in Antigen Target Retrieval Solution pH 9 from Dako during 40 min at 95 $^{\circ}$ C. Thereafter, slides were cooled for 30 min at RT and rinsed twice for 5 min in distilled water. The endogenous peroxidase activity was blocked by an incubation period of 20 min with Peroxidase Block Novocastra Solution (Novocastra, Leica Biosystems, Newcastle, UK), and after two washing steps with PBS the nonspecific binding of immunoglobulins was prevented by incubating the tissue slices with the Protein Block Novocastra Solution (Leica Biosystems) for 60 min. Then, before two PBS washes (2 \times 5 min), tissue slides were incubated with an anti-PD-1 monoclonal antibody (1:25 dilution, clone J116, Abcam, Cambridge, UK)

or with an anti-PD-L1 monoclonal antibody (1:100 dilution, clone 28-8, Abcam), at 4 °C overnight. After two washes with PBS for 5 min, each tissue section was incubated at RT with the Novolink Polymer (Leica Biosystems) for 30 min. Subsequently and after an additional wash in PBS, the staining was performed using the DAB Chromogen Solution (Leica Biosystems) diluted in Novolink DAB Substrate Buffer (Leica Biosystems, 1:20, 5 min). Finally, tissue sections were counterstained with hematoxylin (Leica Biosystems) for 1 min, dehydrated in a graded ethanol series and mounted.

The analyses of PD-1 and PD-L1 immunostaining was scored following the recommendations of the International TILs Working Group 2014, established for breast cancer [52]. Briefly, the area occupied by positive lymphocytes in the stromal compartment was evaluated in whole tumor sections, excluding the TILs outside of the tumor border or in tumor zones with artifacts or necrosis, with 200–400× magnification. In addition, to identify the TILs the pathologists observed their characteristic morphology, as a scarce cytoplasm, a round and small nucleus and the presence of a dense chromatin. The scores of percentages of positive cells were recorded as: 0 (<1%), 1 (1–5%), 2 (6–30%) or 3 (>30%) [10]. The intensity scores were as follows: 0 (negative), 1+ (weak), 2+ (moderate), 3+ (strong) and 4+ (very strong). The percentage of positive cells and intensity scores were then multiplied to obtain a final IHC score. To explore the concordance between the serum PD-1/PD-L1 levels and the PD-1/PD-L1 overexpression in TILs and cancer cells, the cut-off values used were $\geq 5\%$ and $\geq 1\%$ for TILs overexpressing PD-1 [41,53] and PD-L1 [18], and $\geq 1\%$ for cancer cells overexpressing PD-1 or PD-L1 [54,55]. Human placenta and feline lymph node tissues were used as positive controls, whereas sections of healthy mammary tissues were used as negative controls and feline lymph nodes as internal controls. All slides were independently subjected to blind scoring by two independent pathologists.

4.4. DNA Extraction, Amplification and Sequence Analysis of Feline PD-L1 Gene

Genomic DNA extraction was performed in 26 primary mammary tumors using a QIAamp FFPE kit (Qiagen, Dusseldorf, Germany) following the manufacturer's recommendations. Initially, tumor samples were homogenized with Tissue Lyser II (Qiagen) and digested with protease K in a concentration of 20 mg/mL (Qiagen). After several washing steps, the genomic DNA was eluted from the extraction columns and its quantity and quality were measured by NanoDrop ND-100 Spectrophotometer (Thermo Fischer Scientific). Then, the exons of interest in *PD-L1* gene were amplified by using specific primers (Table 6) with a PCR thermal cycler (VWR Thermocycler, Leicestershire, England). PCR procedures were performed with a standard reaction mixture (4 μ L/sample of Phusion GC Buffer (Thermo Fischer Scientific), 0.4 μ L/sample of dNTPs (Grisp, Porto, Portugal), 0.1 μ L/sample of each forward and reverse primers and 0.2 μ L/sample of DNA Polymerase (Thermo Fischer Scientific)). In all samples, PCR-grade water and DNA were added to maintain a concentration of 4 ng/mL. For amplification of exons 3 and 6, PCR reactions were performed as follows: denaturation at 98 °C for 30 s, followed by 35 cycles at 98 °C for 10 s, 56 °C for 30 s, 72 °C for 10 s, plus one extension step of 72 °C for 10 min. For exons 2, 4 and 5, the melting temperature was 60 °C. After confirmation of the expected size for each amplified fragment in an agarose gel (2.5%, Sigma-Aldrich, Darmstadt, Germany), DNA fragments were purified and sequenced by Sanger technique (StabVida, Almada, Portugal).

Table 6. Sequence of the primers used for PCR amplification of exons of feline *programmed death ligand-1 (PD-L1)* gene.

Exons	Forward 5'–3'	Reverse 5'–3'
2	TTTGGGGACAGCAGCTTGTT	TGAACAGACTGACACCGTGG
3	TCTGAGAACCAGCCAGAATTGA	ACTGGAACATAGGGCGTGTT
4	GTCGAAGGCATCTCGCTGT	AGAGCCACTGTGACAACAACA
5	AATTGACCTCAGGGGTTGGAA	GAGGTAAGGAGGAGCCCCGTT
6	TACTGCAGAGGTAAGTGGACA	GGCCTCTCACATCCGACATC

The identification of PD-L1 exons was performed using BLAST software (Basic Local Alignment Search Tool, NCBI) by comparing the sequence of feline *PD-L1* gene (NC_018735.3) with its transcript

(Ensembl, ENSFCAT00000078517.1). Sequenced fragments were aligned using the ClustalW tool (Bioedit software), while protein mutations and SNP loci were identified by using the Expert Protein Analysis System's (ExPASy) translate tool (XM_006939039).

4.5. Statistical Analysis

The Kruskal–Wallis test and Dunn's multiple comparisons post-test were applied to compare the serum PD-1 and PD-L1 levels between cats with different mammary carcinoma subtypes and healthy controls. Animals that had serum PD-1 or PD-L1 levels that fell more than three standard deviations from the mean were considered outliers and removed from further analysis. The optimal cut-off values were determined using the Youden index and the area under the receiver operating characteristic (ROC) curve values were calculated. Significant differences on the PD-1 and PD-L1 staining of tumor infiltrating lymphocytes and on the staining intensity of cancer cells were evaluated by using the Mann–Whitney test. Spearman's coefficient was used to assess the correlations between serum PD-1, PD-L1, CTLA-4 and TNF- α levels.

Statistical analysis was conducted in SPSS software version 25.0 (IBM, Armonk, NY, USA) and the two-sided p -value < 0.05 was considered statistically significant. Results were presented as median values. GraphPad Prism version 8.1.2 (GraphPad Software, CA, USA) and Microsoft Excel for MacOS (version 16.30, Microsoft Corporation, Redmond, WA, USA) were used to plot the graphs.

5. Conclusions

In conclusion, our data demonstrated that serum PD-1 and PD-L1 levels were elevated in cats with HER2-positive and TN normal-like mammary carcinomas. The strong positive correlations detected between serum PD-1, PD-L1, CTLA-4 and TNF- α levels also suggest a systemic immunosuppression in cats presenting these tumor subtypes. Additionally, the microenvironment of HER2-positive tumors was revealed to be locally immunosuppressed by overexpressing PD-L1, contrasting with the human breast cancer studies that showed a higher PD-1 and PD-L1 expression in triple negative molecular subtype. Altogether, our results indicate that cats presenting HER2-positive or TN normal-like tumors could benefit from immunostimulatory therapies (e.g., anti-PD-L1, anti-CTLA-4) and provide support to the use of spontaneous feline mammary carcinoma as a model for human breast cancer.

Author Contributions: Conceptualization, C.N. and F.F.; Methodology, C.N. and F.F.; Formal analysis, C.N. and A.C.U. and F.F.; Investigation, C.N., A.C.U., A.G., J.F., J.C. and F.F.; Supervision, F.F.; Funding acquisition, F.F.; Project administration, F.F.; Writing—original draft preparation, C.N. and F.F.; Writing—review and editing, C.N., A.C.U., A.G., J.F., J.C., and F.F. All authors have read and agreed to the published version of the manuscript.

Funding: This research was funded by Fundação para a Ciência e a Tecnologia (Portugal) through the projects PTDC/CVT-EPI/3638/2014 and CIISA-UIDP/CVT/00276/2020. C.N. is receipt of a PhD fellowship from University of Lisbon (ref.C00191r) and A.G. is receipt of a PhD fellowship from Fundação para a Ciência e a Tecnologia (ref. SFRH/BD/132260/2017).

Acknowledgments: The authors would like to thank Dra. Maria Soares for the clinical samples and database.

Conflicts of Interest: The authors declare no conflict of interest. The funders had no role in the design of the study; in the collection, analyses, or interpretation of data; in the writing of the manuscript, or in the decision to publish the results.

References

1. Soare, G.R.; Soare, C.A. Immunotherapy for Breast Cancer: First FDA Approved Regimen. *Discoveries* **2019**, *7*, 4–6. [[CrossRef](#)]
2. Solinas, C.; Carbognin, L.; De Silva, P.; Criscitiello, C.; Lambertini, M. Tumor-infiltrating lymphocytes in breast cancer according to tumor subtype: Current state of the art. *Breast* **2017**, *35*, 142–150. [[CrossRef](#)] [[PubMed](#)]
3. Padmanabhan, R.; Kheraldine, H.S.; Meskin, N.; Vranic, S.; Al Moustafa, A.E. Crosstalk between HER2 and PD-1/PD-L1 in Breast Cancer: From Clinical Applications to Mathematical Models. *Cancers* **2020**, *12*, 636. [[CrossRef](#)] [[PubMed](#)]

4. Cannon, C. Cats, Cancer and Comparative Oncology. *Vet. Sci.* **2015**, *2*, 111–126. [[CrossRef](#)]
5. Adegá, F.; Borges, A.; Chaves, R. Cat Mammary Tumors: Genetic Models for the Human Counterpart. *Vet. Sci.* **2016**, *3*, 17. [[CrossRef](#)]
6. Hassan, B.B.; Elshafae, S.M.; Supsavhad, W.; Simmons, J.K.; Dirksen, W.P.; Sokkar, S.M.; Rosol, T.J. Feline Mammary Cancer: Novel Nude Mouse Model and Molecular Characterization of Invasion and Metastasis Genes. *Vet. Pathol.* **2017**, *54*, 32–43. [[CrossRef](#)] [[PubMed](#)]
7. Michishita, M.; Ohtsuka, A.; Nakahira, R.; Tajima, T.; Nakagawa, T.; Sasaki, N.; Arai, T.; Takahashi, K. Anti-tumor effect of bevacizumab on a xenograft model of feline mammary carcinoma. *J. Vet. Med. Sci.* **2016**, *78*, 685–689. [[CrossRef](#)] [[PubMed](#)]
8. Soares, M.; Ribeiro, R.; Najmudin, S.; Gameiro, A.; Rodrigues, R.; Cardoso, F.; Ferreira, F. Serum HER2 levels are increased in cats with mammary carcinomas and predict tissue HER2 status. *Oncotarget* **2016**, *7*. [[CrossRef](#)] [[PubMed](#)]
9. Ferreira, D.; Soares, M.; Correia, J.; Adegá, F.; Ferreira, F.; Chaves, R. Assessment of ERBB2 and TOP2 α gene status and expression profile in feline mammary tumors: Findings and guidelines. *Aging* **2019**, *11*. [[CrossRef](#)]
10. Urbano, A.C.; Nascimento, C.; Soares, M.; Correia, J.; Ferreira, F. Clinical Relevance of the serum CTLA-4 in Cats with Mammary Carcinoma. *Sci. Rep.* **2020**, *10*, 3822. [[CrossRef](#)]
11. Bürtin, F.; Mullins, C.S.; Linnebacher, M. Mouse models of colorectal cancer: Past, present and future perspectives. *World J. Gastroenterol.* **2020**, *26*, 1394–1426. [[CrossRef](#)] [[PubMed](#)]
12. Soares, M.; Correia, J.; Adegá, F.; Ferreira, D. Gene expression association study in feline mammary carcinomas. *PLoS ONE* **2019**, *14*. [[CrossRef](#)]
13. Gatalica, Z.; Snyder, C.; Maney, T.; Ghazalpour, A.; Holterman, D.A.; Xiao, N.; Overberg, P.; Rose, I.; Basu, G.D.; Vranic, S.; et al. Programmed cell death 1 (PD-1) and its ligand (PD-L1) in common cancers and their correlation with molecular cancer type. *Cancer Epidemiol. Biomark. Prev.* **2014**, *23*, 2965–2970. [[CrossRef](#)]
14. Kim, A.; Lee, S.J.; Kim, Y.K.; Park, W.Y.; Park, D.Y.; Kim, J.Y.; Lee, C.H.; Gong, G.; Huh, G.Y.; Choi, K.U. Programmed death-ligand 1 (PD-L1) expression in tumour cell and tumour infiltrating lymphocytes of HER2-positive breast cancer and its prognostic value. *Sci. Rep.* **2017**, *7*, 11671. [[CrossRef](#)] [[PubMed](#)]
15. Baptista, M.Z.; Sarian, L.O.; Derchain, S.F.M.; Pinto, G.A.; Vassallo, J. Prognostic significance of PD-L1 and PD-L2 in breast cancer. *Hum. Pathol.* **2016**, *47*, 78–84. [[CrossRef](#)]
16. Cimino-Mathews, A.; Thompson, E.; Taube, J.M.; Ye, X.; Lu, Y.; Meeker, A.; Xu, H.; Sharma, R.; Lecksel, K.; Cornish, T.C.; et al. PD-L1 (B7-H1) expression and the immune tumor microenvironment in primary and metastatic breast carcinomas. *Hum. Pathol.* **2016**, *47*, 52–63. [[CrossRef](#)]
17. Gu, D.; Ao, X.; Yang, Y.; Chen, Z.; Xu, X. Soluble immune checkpoints in cancer: Production, function and biological significance. *J. Immunother. Cancer* **2018**, *6*, 1–14. [[CrossRef](#)]
18. U.S. Food & Drug FDA Approves Atezolizumab for PD-L1 Positive Unresectable Locally Advanced or Metastatic Triple-Negative Breast Cancer. Available online: <https://www.fda.gov/drugs/drug-approvals-and-databases/fda-approves-atezolizumab-pd-l1-positive-unresectable-locally-advanced-or-metastatic-triple-negative> (accessed on 15 April 2019).
19. Wimberly, H.; Brown, J.R.; Schalper, K.; Haack, H.; Silver, M.R.; Nixon, C.; Bossuyt, V.; Pusztai, L.; Lannin, D.R.; Rimm, D.L. PD-L1 expression correlates with tumor-infiltrating lymphocytes and response to neoadjuvant chemotherapy in breast cancer. *Cancer Immunol. Res.* **2015**, *3*, 326–332. [[CrossRef](#)]
20. Solinas, C.; Garaud, S.; De Silva, P.; Boisson, A.; Van den Eynden, G.; de Wind, A.; Risso, P.; Vitória, J.R.; Richard, F.; Migliori, E.; et al. Immune checkpoint molecules on tumor-infiltrating lymphocytes and their association with tertiary lymphoid structures in human breast cancer. *Front. Immunol.* **2017**, *8*, 1412. [[CrossRef](#)]
21. Noske, A.; Möbus, V.; Weber, K.; Schmatloch, S.; Weichert, W.; Köhne, C.H.; Solbach, C.; Ingold Heppner, B.; Steiger, K.; Müller, V.; et al. Relevance of tumour-infiltrating lymphocytes, PD-1 and PD-L1 in patients with high-risk, nodal-metastasised breast cancer of the German Adjuvant Intergroup Node-positive study. *Eur. J. Cancer* **2019**, *114*, 76–88. [[CrossRef](#)]
22. Vranic, S.; Cyprian, F.S.; Gatalica, Z.; Palazzo, J. PD-L1 status in breast cancer: Current view and perspectives. *Semin. Cancer Biol.* **2019**. [[CrossRef](#)] [[PubMed](#)]









23. Li, Y.; Cui, X.; Yang, Y.J.; Chen, Q.Q.; Zhong, L.; Zhang, T.; Cai, R.L.; Miao, J.Y.; Yu, S.C.; Zhang, F. Serum sPD-1 and sPD-L1 as biomarkers for evaluating the efficacy of neo-adjuvant chemotherapy in triple-negative breast cancer patients. *Clin. Breast Cancer* **2019**, 326–332. [[CrossRef](#)]
24. Zheng, Z.; Bu, Z.; Liu, X.; Zhang, L.; Li, Z.; Wu, A.; Wu, X.; Cheng, X.; Xing, X.; Du, H.; et al. Level of circulating PD-L1 expression in patients with advanced gastric cancer and its clinical implications. *Chin. J. Cancer Res.* **2014**, 26, 104–111. [[CrossRef](#)]
25. Frigola, X.; Inman, B.A.; Lohse, C.M.; Krco, C.J.; Cheville, J.C.; Thompson, R.H.; Leibovich, B.; Blute, M.L.; Dong, H.; Kwon, E.D. Identification of a soluble form of B7-H1 that retains immunosuppressive activity and is associated with aggressive renal cell carcinoma. *Clin. Cancer Res.* **2011**, 17, 1915–1923. [[CrossRef](#)] [[PubMed](#)]
26. Makhoul, I.; Atiq, M.; Alwbari, A.; Kieber-Emmons, T. Breast Cancer Immunotherapy: An Update. *Breast Cancer Basic Clin. Res.* **2018**, 12. [[CrossRef](#)] [[PubMed](#)]
27. Wang, X.; Yang, L.; Huang, F.; Zhang, Q.; Liu, S.; Ma, L.; You, Z. Inflammatory cytokines IL-17 and TNF- α up-regulated PD-L1 expression in human prostate and colon cancer cells. *Physiol. Behav.* **2016**, 176, 139–148. [[CrossRef](#)]
28. Lim, S.O.; Li, C.W.; Xia, W.; Cha, J.H.; Chan, L.C.; Wu, Y.; Chang, S.S.; Lin, W.C.; Hsu, J.M.; Hsu, Y.H.; et al. Deubiquitination and Stabilization of PD-L1 by CSN5. *Cancer Cell* **2016**, 30, 925–939. [[CrossRef](#)]
29. Lawson, N.L.; Dix, C.I.; Scorer, P.W.; Stubbs, C.J.; Wong, E.; Hutchinson, L.; McCall, E.J.; Schimpl, M.; DeVries, E.; Walker, J.; et al. Mapping the binding sites of antibodies utilized in programmed cell death ligand-1 predictive immunohistochemical assays for use with immuno-oncology therapies. *Mod. Pathol.* **2019**. [[CrossRef](#)]
30. Li, S.; Chen, L.; Jiang, J. Role of programmed cell death ligand-1 expression on prognostic and overall survival of breast cancer: A systematic review and meta-analysis. *Medicine* **2019**, 98. [[CrossRef](#)]
31. Soares, M.; Madeira, S.; Correia, J.; Peleteiro, M.; Cardoso, F.; Ferreira, F. Molecular based subtyping of feline mammary carcinomas and clinicopathological characterization. *Breast* **2016**, 27, 44–51. [[CrossRef](#)]
32. Leitzel, K.; Ali, S.M.; Shepherd, L.E.; Parulekar, W.R.; Zhu, L.; Virk, S.; Nomikos, D.; Aparicio, S.; Gelmon, K.A.; Drabick, J.J.; et al. Serum PD-L1 and outcomes in CCTG MA.31 phase 3 trial of anti-HER2 therapy in first-line HER2+ metastatic breast cancer patients (trastuzumab arm only). *J. Clin. Oncol.* **2018**, 36, 1031. [[CrossRef](#)]
33. Ito, M.; Yajima, S.; Suzuki, T.; Oshima, Y.; Nanami, T.; Sumazaki, M.; Shiratori, F.; Funahashi, K.; Tochigi, N.; Shimada, H. High serum PD-L1 level is a poor prognostic biomarker in surgically treated esophageal cancer. *Cancer Med.* **2019**, 1321–1327. [[CrossRef](#)] [[PubMed](#)]
34. Kruger, S.; Legenstein, M.L.; Rösgen, V.; Haas, M.; Modest, D.P.; Westphalen, C.B.; Ormanns, S.; Kirchner, T.; Heinemann, V.; Holdenrieder, S.; et al. Serum levels of soluble programmed death protein 1 (sPD-1) and soluble programmed death ligand 1 (sPD-L1) in advanced pancreatic cancer. *Oncoimmunology* **2017**, 6, e1310358. [[CrossRef](#)]
35. Abu Hejleh, T.; Furqan, M.; Ballas, Z.; Clamon, G. The clinical significance of soluble PD-1 and PD-L1 in lung cancer. *Crit. Rev. Oncol. Hematol.* **2019**, 143, 148–152. [[CrossRef](#)]
36. Ugurel, S.; Schadendorf, D.; Horny, K.; Sucker, A.; Schramm, S.; Utikal, J.; Pföhler, C.; Herbst, R.; Schilling, B.; Blank, C.; et al. Elevated baseline serum PD-1 or PD-L1 predicts poor outcome of PD-1 inhibition therapy in metastatic melanoma. *Ann. Oncol. Off. J. Eur. Soc. Med. Oncol.* **2020**, 31, 144–152. [[CrossRef](#)] [[PubMed](#)]
37. Ward, F.J.; Dahal, L.N.; Wijesekera, S.K.; Abdul-Jawad, S.K.; Kaewarpai, T.; Xu, H.; Vickers, M.A.; Barker, R.N. The soluble isoform of CTLA-4 as a regulator of T-cell responses. *Eur. J. Immunol.* **2013**, 43, 1274–1285. [[CrossRef](#)]
38. Buisseret, L.; Garaud, S.; De Wind, A.; Van Den Eynden, G.; Boisson, A.; Solinas, C. Tumor-infiltrating lymphocyte composition, organization and PD-1 / PD-L1 expression are linked in breast cancer. *Oncoimmunology* **2017**, 6. [[CrossRef](#)]
39. Mittendorf, E.A.; Philips, A.V.; Meric-Bernstam, F.; Qiao, N.; Wu, Y.; Harrington, S.; Su, X.; Wang, Y.; Gonzalez-Angulo, A.M.; Akcakanat, A.; et al. PD-L1 expression in triple-negative breast cancer. *Cancer Immunol. Res.* **2014**, 2, 361–370. [[CrossRef](#)]
40. Polónia, A.; Pinto, R.; Cameselle-Teijeiro, J.F.; Schmitt, F.C.; Paredes, J. Prognostic value of stromal tumour infiltrating lymphocytes and programmed cell death-ligand 1 expression in breast cancer. *J. Clin. Pathol.* **2017**, 70, 860–867. [[CrossRef](#)]

41. Bottai, G.; Raschioni, C.; Losurdo, A.; Di Tommaso, L.; Tinterri, C.; Torrisi, R.; Reis-Filho, J.S.; Roncalli, M.; Sotiriou, C.; Santoro, A.; et al. An immune stratification reveals a subset of PD-1/LAG-3 double-positive triple-negative breast cancers. *Breast Cancer Res.* **2016**, *18*, 121. [[CrossRef](#)]
42. Kuipers, H.; Muskens, F.; Willart, M.; Hijdra, D.; van Assema, F.B.J.; Coyle, A.J.; Hoogsteden, H.C.; Lambrecht, B.N. Contribution of the PD-1 ligands/PD-1 signaling pathway to dendritic cell-mediated CD4+ cell activation. *Eur. J. Immunol.* **2006**, *36*, 2472–2482. [[CrossRef](#)]
43. Theodoraki, M.N.; Whiteside, T.L.; Gooding, W.E.; Yerneni, S.S.; Hoffmann, T.K. Clinical Significance of PD-L1 + Exosomes in Plasma of Head and Neck Cancer Patients. *Clin. Cancer Res.* **2017**, *24*, 896–905. [[CrossRef](#)] [[PubMed](#)]
44. Ludwig, S.; Floros, T.; Theodoraki, M.N.; Hong, C.S.; Jackson, E.K.; Lang, S.; Whiteside, T.L. Suppression of lymphocyte functions by plasma exosomes correlates with disease activity in patients with head and neck cancer. *Clin. Cancer Res.* **2017**, *23*, 4843–4854. [[CrossRef](#)] [[PubMed](#)]
45. Chen, G.; Huang, A.C.; Zhang, W.; Zhang, G.; Wu, M.; Xu, W.; Yu, Z.; Yang, J.; Wang, B.; Sun, H.; et al. Exosomal PD-L1 contributes to immunosuppression and is associated with anti-PD-1 response. *Nature* **2018**, *560*, 382–386. [[CrossRef](#)] [[PubMed](#)]
46. Stovgaard, E.S.; Dyhl-Polk, A.; Roslind, A.; Balslev, E.; Nielsen, D. PD-L1 expression in breast cancer: Expression in subtypes and prognostic significance: A systematic review. *Breast Cancer Res. Treat.* **2019**, *174*, 571–584. [[CrossRef](#)]
47. Beckers, R.K.; Selinger, C.I.; Vilain, R.; Madore, J.; Wilmott, J.S.; Harvey, K.; Holliday, A.; Cooper, C.L.; Robbins, E.; Gillett, D.; et al. Programmed death ligand 1 expression in triple-negative breast cancer is associated with tumour-infiltrating lymphocytes and improved outcome. *Histopathology* **2016**, *69*, 25–34. [[CrossRef](#)]
48. Ghebeh, H.; Lehe, C.; Barhoush, E.; Al-Romaih, K.; Tulbah, A.; Al-Alwan, M.; Hendrayani, S.F.; Manogaran, P.; Alaiya, A.; Al-Tweigeri, T.; et al. Doxorubicin downregulates cell surface B7-H1 expression and upregulates its nuclear expression in breast cancer cells: Role of B7-H1 as an anti-apoptotic molecule. *Breast Cancer Res.* **2010**, *12*. [[CrossRef](#)]
49. Papadaki, M.A.; Koutsopoulos, A.V.; Tsoulfas, P.G.; Lagoudaki, E.; Aggouraki, D.; Monastirioti, A.; Koutoulaki, C.; Apostolopoulou, C.A.; Merodoulaki, A.C.; Papadaki, C.; et al. Clinical relevance of immune checkpoints on circulating tumor cells in breast cancer. *Cancers* **2020**, *12*, 376. [[CrossRef](#)]
50. Lippi, G.; Avanzini, P.; Zoppi, V.; Ippolito, L. Influence of mechanical hemolysis of blood on two D-dimer immunoassays. *Blood Coagul. Fibrinolysis* **2012**, *23*, 461–463. [[CrossRef](#)]
51. Soares, M.; Correia, J.; Peleteiro, M.C.; Ferreira, F. St Gallen molecular subtypes in feline mammary carcinoma and paired metastases—Disease progression and clinical implications from a 3-year follow-up study. *Tumor Biol.* **2016**, *37*, 4053–4064. [[CrossRef](#)]
52. Salgado, R.; Denkert, C.; Demaria, S.; Sirtaine, N.; Klauschen, F.; Pruneri, G.; Wienert, S.; Van den Eynden, G.; Baehner, F.L.; Penault-Llorca, F.; et al. The evaluation of tumor-infiltrating lymphocytes (TILS) in breast cancer: Recommendations by an International TILS Working Group 2014. *Ann. Oncol.* **2015**, *26*, 259–271. [[CrossRef](#)] [[PubMed](#)]
53. Wang, Y.; Dong, T.; Xuan, Q.; Zhao, H.; Qin, L.; Zhang, Q. Lymphocyte-Activation Gene-3 Expression and Prognostic Value in Neoadjuvant-Treated Triple-Negative Breast Cancer. *J. Breast Cancer* **2018**, *21*, 124. [[CrossRef](#)] [[PubMed](#)]
54. Sun, W.Y.; Lee, Y.K.; Koo, J.S. Expression of PD-L1 in triple-negative breast cancer based on different immunohistochemical antibodies. *J. Transl. Med.* **2016**, *14*, 173. [[CrossRef](#)] [[PubMed](#)]
55. Ács, B.; Madaras, L.; Tóké, A.M.; Kovács, A.K.; Kovács, E.; Oszvári-Vidákovich, M.; Karászi, Á.; Birtalan, E.; Dank, M.; Szász, A.M.; et al. PD-1, PD-L1 and CTLA-4 in pregnancy-related and in early-onset breast cancer: A comparative study. *Breast* **2017**, *35*, 69–77. [[CrossRef](#)] [[PubMed](#)]



Article

Hypoxia and Macrophages Act in Concert Towards a Beneficial Outcome in Colon Cancer

Flávia Martins ^{1,2,3,4,†} , Rosa Oliveira ^{1,2,†}, Bruno Cavadas ^{1,3}, Filipe Pinto ^{1,3} , Ana Patrícia Cardoso ^{1,2} , Flávia Castro ^{1,2,5} , Bárbara Sousa ^{1,3} , Marta Laranjeiro Pinto ^{1,2,6} , Ana João Silva ^{1,2}, Diogo Adão ^{1,2}, José Pedro Loureiro ^{1,7} , Nicole Pedro ^{1,3}, Rui Manuel Reis ^{8,9,10} , Luísa Pereira ^{1,3,4}, Maria José Oliveira ^{1,2,4,5} and Angela Margarida Costa ^{1,2,*}

¹ i3S-Institute for Research and Innovation in Health, University of Porto, 4200-135 Porto, Portugal

² INEB-Institute of Biomedical Engineering, University of Porto, 4200-135 Porto, Portugal

³ IPATIMUP-Institute of Molecular Pathology and Immunology, University of Porto, 4200-135 Porto, Portugal

⁴ Department of Pathology and Oncology, Faculty of Medicine, University of Porto, 4200-319 Porto, Portugal

⁵ ICBAS-Institute of Biomedical Sciences Abel Salazar, University of Porto, 4050-313 Porto, Portugal

⁶ CNC-Center for Neuroscience and Cell Biology, University of Coimbra, 3004-517 Coimbra, Portugal

⁷ IBMC-Institute of Molecular and Cellular Biology, University of Porto, 4200-135 Porto, Portugal

⁸ Molecular Oncology Research Center, Barretos Cancer Hospital, 14.784-400 Barretos-SP, Brazil

⁹ Life and Health Sciences Research Institute (ICVS), School of Medicine, University of Minho, 4710-057 Braga, Portugal

¹⁰ ICVS/3B's-PT Government Associate Laboratory, 4710-057 Braga, Portugal

* Correspondence: angela.amorimcosta@ineb.up.pt

† These authors contributed equally to this paper.

Received: 5 March 2020; Accepted: 24 March 2020; Published: 28 March 2020



Abstract: In colon cancer, the prognostic value of macrophages is controversial, and it is still unknown how hypoxia modulates macrophage–cancer cell crosstalk. To unravel this, co-cultures of human primary macrophages and colon cancer cells were performed at 20% and 1% O₂, followed by characterization of both cellular components. Different colon cancer patient cohorts were analyzed for hypoxia and immune markers, and their association with patient overall survival was established. A positive correlation between *HIF1A* and *CD68* in colon cancer patients was identified but, unexpectedly, in cases with higher macrophage infiltration, *HIF1A* expression was associated with a better prognosis, in contrast to breast, gastric, and lung cancers. Under hypoxia, co-cultures' secretome indicated a shift towards a pro-inflammatory phenotype. These alterations occurred along with increased macrophage phagocytic activity and decreased SIRP α expression. Cancer cells were more invasive and exhibited higher CD47 expression. We hypothesize that the better prognosis associated with *HIF1A*^{High}*CD68*^{High} tumors could occur due to macrophagic pro-inflammatory pressure. Indeed, we found that tumors *HIF1A*^{High}*CD68*^{High} expressed increased levels of *CD8A*, which is positively correlated with *HIF1A*. In conclusion, we show that in colon cancer, hypoxia drives macrophages into a pro-inflammatory phenotype, concomitant with increased infiltration of anti-tumor immune cells, favoring better disease outcome.

Keywords: hypoxia; macrophages; colon cancer; tumor microenvironment; immune cell infiltration; prognosis

1. Introduction

It is recognized that the non-malignant component of the tumor microenvironment (TM) has a pivotal role in both tumorigenesis and tumor progression. To improve cancer therapy, it is crucial to better understand cancer cell behavior and the associated molecular mechanisms, which cannot be

achieved without knowing how the different TM components influence each other's behavior, driving disease outcomes. As an ecosystem, the TM is composed of different entities besides cancer cells, namely, immune cells, fibroblasts, adipocytes, and the extracellular matrix (ECM), which communicate and modulate each other's activities [1].

Macrophages are abundant in the TM, and their high infiltration is associated, in several malignancies, with poor prognosis and therapy resistance [2]. Due to their plasticity, macrophages can polarize into pro-inflammatory and anti-tumor or into anti-inflammatory and pro-tumor [3], being, therefore, interesting therapeutic targets. In fact, it is known that a pro-inflammatory environment is a driving force for the tumorigenic process, driving mutagenesis, while in the context of an established tumor, the pro-inflammatory environment could favor the elimination of already-transformed cells [4].

In colon cancer, the role of macrophages is controversial, with some authors claiming that a high infiltration is associated with better prognosis, while others report that their presence is associated with increased tumor progression-associated activities [5]. Our group has previously evidenced that macrophages induce gastric and colon cancer cell invasion, in a process partially mediated by secreted factors, and that the secretome of macrophages differs from that of macrophages co-cultured with cancer cells [6].

Due to aberrant cancer cell growth and abnormal vascularization, the TM is generally hypoxic. This condition leads to reactive oxygen species accumulation and acidosis, both associated with enhanced invasion, metastasis, and therapy resistance [7], hypoxia being an independent prognostic factor in several types of cancer [8]. Nevertheless, the mechanisms through which hypoxia interferes with the non-malignant components of TM are still a matter of study.

It has been reported that macrophages preferentially accumulate within tumor hypoxic regions, and that hypoxia leads to the genetic reprogramming of both cancer cells and macrophages, mainly through hypoxia inducible factor (HIF) transcription factors. HIF1 α , the most important of them, is constitutively expressed and is targeted to degradation at normal oxygen tension, but stabilized under hypoxia [9,10]. The activation of HIF downstream targets leads to cellular adjustments such as metabolic alterations and expression of ECM-remodeling enzymes [11]. It is also known that HIF can affect the immunogenicity of hypoxic breast cancer by inducing the expression of CD47, a cell surface receptor that impairs macrophage pro-phagocytic signaling [12]. Due to its importance, HIF-inhibitors are under consideration as anti-cancer agents [13]. However, the experiments studying the colon cancer cells–macrophages interplay were not performed under hypoxia, nor were the studies about hypoxia focused on this crosstalk, resulting in an incomplete understanding of the role of hypoxia in the colon cancer microenvironment. Giving the controversial role of macrophages in colon cancer, the study of this interplay will provide a deeper understanding of the colon cancer microenvironment complexity.

In the present study, we characterize the effect of low oxygen levels on macrophage behavior and the modulation of macrophages and cancer cells crosstalk. The influence of hypoxia and macrophages is also analyzed in different cohorts of colon cancer patients. The data gathered in this work increases the insight on colon TM specificity and provides information that can result in the development of novel and more efficient therapeutic strategies.

2. Results

2.1. CD68 and HIF1A Are Positively Correlated in Colon Cancer Patients, and the Population

CD68^{High}HIF1A^{High} Presents Better Prognosis

To understand the relevance of hypoxia on the modulation of macrophage behavior in colon cancer patients, we took advantage of TCGA and Oncomine databases. Therefore, the expression levels of CD68, a macrophage lineage marker, and of HIF1A, a master hypoxia regulator, in which slight mRNA changes can cause significant alterations in its activity and protein levels, were analyzed [14]. Since TCGA compiles expression data from normal and cancer colon tissues, we focused our analysis in HIF1A in CD68^{High} and CD68^{Low} populations, in both tissues, assuming that CD68^{High} population has a higher

degree of macrophagic infiltration. As normal colon tissue could have some endogenous degree of inflammation, the threshold used to subdivide the population between $CD68^{High}$ and $CD68^{Low}$ was defined based on the median $CD68$ expression in the normal tissue. Moreover, we found that $HIF1A$ expression was significantly higher in tumors from patients with elevated macrophage infiltration ($CD68^{High}$) and that $CD68$ expression positively correlated with $HIF1A$ expression (Figure 1A). It is described that colon carcinomas exhibit increased nuclear expression of HIF1- α [15]. However, as it may be rapidly targeted to degradation, we evaluated the expression levels of HIF1- α downstream targets that are upregulated under hypoxia conditions, specifically $CA9$ and LOX (Figure 1B). Using the previous approach, we found a significant increase in $CA9$ and LOX expression in tumor tissue, which was significantly more pronounced in $CD68^{High}$ patients (Figure 1B). Due to the present focus on the role of macrophages on the TM, we particularly evaluated the $CD68^{High}$ population. By dividing this population between $HIF1A^{High}$ and $HIF1A^{Low}$, we found that $CA9$ and LOX expression levels are significantly higher in the $HIF1A^{High}$ population (Figure 1C). The positive correlation between $CD68$ and $HIF1A$, and the increased $CA9$ and LOX expression in $CD68^{High}HIF1A^{High}$ patients were validated on the Oncomine database (colon cancer Bittner cohort, with the highest number of patients) (Figure 1D). $CA9$ or LOX were not used in further analysis as hypoxic markers due to statistical constraints when the number of patients needed to be sub-divided into $CD68^{High}$ and $CD68^{Low}$, and $HIF1A^{High}$ and $HIF1A^{Low}$.

A major point of interest was to investigate whether the association between high macrophage infiltration and enhanced expression of hypoxic markers had any impact on patient prognosis. Surprisingly, we found that the $CD68^{High}HIF1A^{High}$ population presented a significantly better prognosis than the $CD68^{High}HIF1A^{Low}$ population (Figure 1E). To check whether this was a common feature in cancers where macrophagic infiltration was associated with prognosis, we used the same TCGA approach to analyze gastric, breast, and lung cancer patients. Despite the low number of patients in some populations, this specific association only occur in colon cancer (Figure 1F). The same analysis was not performed in the Oncomine cohort since survival data is not available.

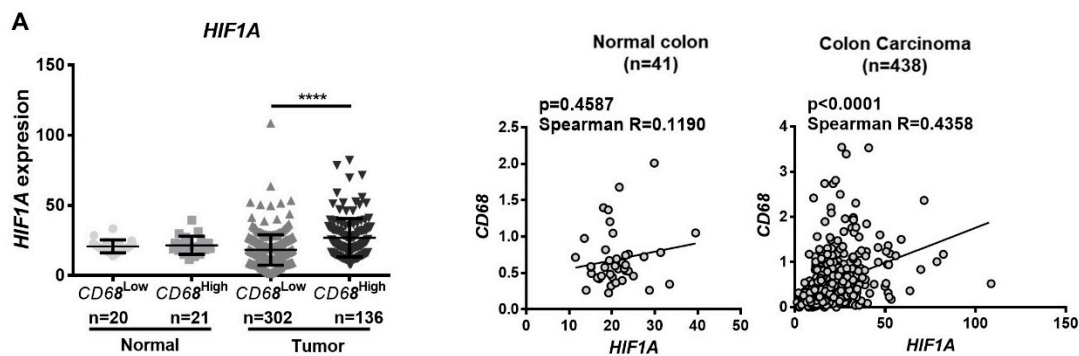


Figure 1. Cont.

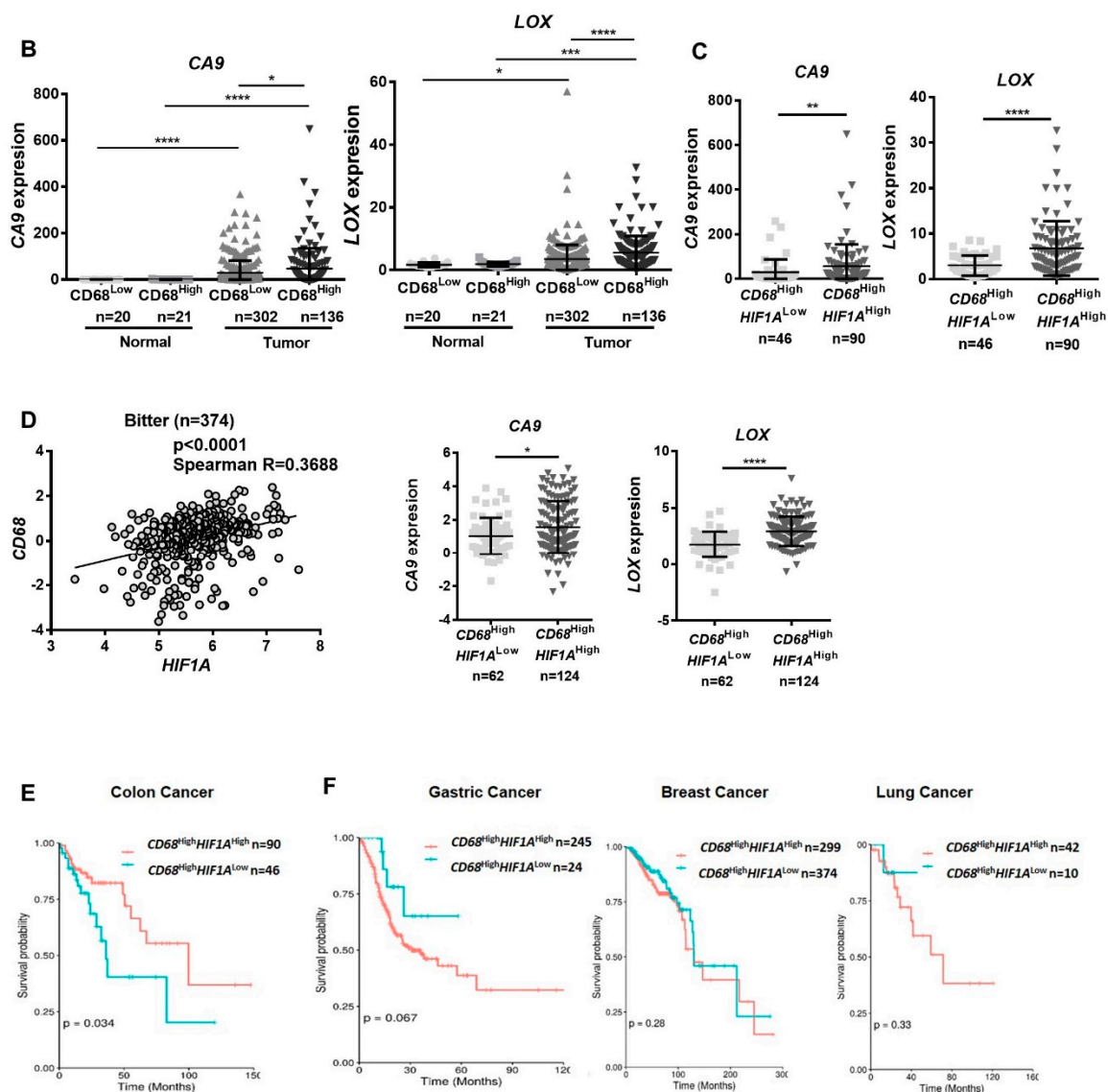


Figure 1. CD68 and HIF1A are positively correlated in colon cancer, and CD68^{High}HIF1A^{High} tumors present better prognosis. Microarray and RNASeq expression data were downloaded from The Cancer Genome Atlas (TCGA) (A–C, E–F) and from Oncomine databases (D). (A–C) Normal and tumor samples were divided into CD68^{Low} and CD68^{High}, according to the median levels of CD68 expression in normal samples. In each group, the expression of the hypoxic marker HIF1A (A), CA9 and LOX (B,C) genes, known to be regulated by HIF1α in hypoxic conditions, was evaluated. (A) The correlation between CD68 and HIF1A was assessed. (B,C) The expression of CA9 and LOX was evaluated in both normal and tumor samples, in CD68^{High} and CD68^{Low} populations, and within the CD68^{High} population, the expression levels of both genes were compared between HIF1A^{Low} and HIF1A^{High}, according to the median levels of HIF1A expression in normal samples. (D) Correlations between CD68 and HIF1A, and LOX and CA9 expression in CD68^{High}HIF1A^{High} patients were confirmed on Bitter’s colon cancer cohort from Oncomine. (E,F) Kaplan–Meier curves were made with patients’ survival data, comparing the populations CD68^{High}HIF1A^{High} and CD68^{High}HIF1A^{Low}. The division high/low expression was made according to the median expression of the selected genes in normal tissue (A–C; E–F), or by the median expression of tumor (D). Data from colon (E), gastric, breast, and lung (F) cancer patients were analyzed. Kruskal–Wallis, Mann–Whitney, or unpaired *t*-test were used to compare gene expression among groups. Spearman’s statistical test was used to assess correlation, which was considered moderate positive when Spearman Rs were between 0.2500 and 0.3500, and strong positive when Spearman R > 0.3500. Long-rank (Mantel–Cox) test was performed in the analysis of the survival curves. **** *p* < 0.0001; *** *p* < 0.001; ** *p* < 0.01; * *p* < 0.05.

2.2. Hypoxia Impacts Macrophage Antigen-Presentation Associated Molecules

In order to understand the impact of the hypoxic microenvironment on macrophage–colon cancer cell crosstalk, and particularly on macrophage function, indirect co-cultures of macrophages with cancer cells were established at both 20% and 1% O₂ (Figure S1A). The significant increase in cancer cell CA9 expression at 1% O₂ validates the cellular sensing of the hypoxic stimulus, to which both cells were simultaneously exposed to (Figure S1B), without affecting cellular viability between the conditions (Figure S1C). This indirect co-culture system enables the analysis of differences induced by exchanged secreted factors, but in conditions that allow the full recovery of both cellular populations for further independent studies. The selection of primary macrophages instead of the widely used and modified human monocytic cell line, THP-1, added variability to our equation, being more representative of the existent individual differences. Besides more closely mimicking the TM, human macrophages were preferred in relation to their murine counterparts, given the described interspecies variability regarding polarization markers and activation programs [16].

Macrophages are professional antigen-presenting cells, and immune evasion of cancer cells is a major cancer hallmark. To analyze whether hypoxia can trigger some alterations in the expression of key molecules involved in antigen presentation, macrophage major histocompatibility complexes (MHC) class I (HLA-ABC) and class II (HLA-DR) molecules, and of the co-stimulatory receptor CD86, were investigated by flow cytometry (gating strategy described in Figure S2A). Our results at 1% O₂ evidenced a slight reduction in the percentage of macrophages expressing HLA-ABC ($p < 0.0533$) and CD86 ($p < 0.0938$) (Figure 2A,B,D), with a significant decrease in the percentage of cells expressing HLA-DR (Figure 2A,C) and in the intensity of CD86 expressed by each cell (Figure 2A,D).

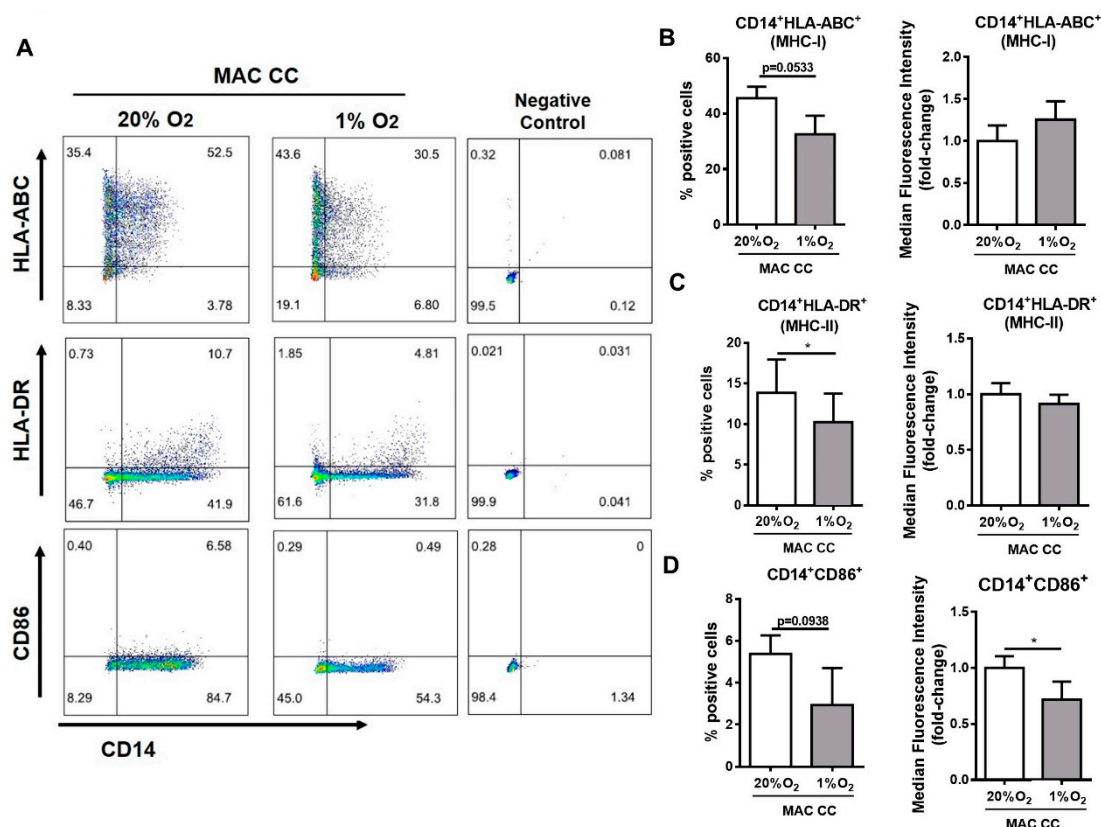


Figure 2. Hypoxia impacts macrophage antigen-presentation associated molecules. Macrophages were indirectly co-cultured with colon cancer cells RKO (MAC CC), at 20% or 1% O₂ for 72 h. Expression of the monocyte/macrophage lineage marker CD14, HLA-ABC (MHC-I), HLA-DR (MHC-II), and CD86 was determined by flow cytometry. (A) Pseudo-color plots display the gating strategy for flow cytometry created with FlowJo. (B–D) Graphs represent the percentage and median fluorescence

intensity, which is presented as fold-change relatively to 20% O₂ condition of (B) CD14+HLA-ABC+, (C) CD14+HLA-DR+, or (D) CD14+CD86+ cells. Graphs represent the mean values with standard deviations, and are representative of *n* = 7 (HLA-ABC); *n* = 10 (HLA-DR); *n* = 6 (CD86) independent experiments. The statistical tests Wilcoxon or paired *t*-test were used; * *p* < 0.05. The *p*-values between 0.05 and 0.1 were presented and considered a tendency.

2.3. Hypoxia Modulates Macrophage Phagocytic Activity and SIRP α Expression, and CD47 Expression on Cancer Cells

One of the major functions of macrophages is to phagocytose foreign or self-cellular components targeted to degradation. This is particularly important in the context of macrophage defensive functions against pathogens, their role in regeneration, and also in anti-tumor activities. Noteworthy, it is known that cancer cells express “don’t eat me” signals, as the CD47 receptor, which will bind to SIRP α in macrophages, and impairs phagocytosis.

In the present study, we exploited whether hypoxia alters macrophage phagocytic activity, in a similar process already described in breast cancer [12], using hypoxic cancer cells as a phagocytic stimulus. Accordingly, macrophages were co-cultured with cancer cells for 72 h at 20% or 1% O₂ (Figure S1A). Then, cancer cells were removed, and macrophages were directly stimulated with CFSE (Carboxyfluorescein Diacetate Succinimidyl Ester)-labeled cancer cells, previously cultured at 1% O₂ for 72 h. Although no differences were observed in the percentage of phagocytic macrophages, the amount of phagocytosed CFSE-labeled cancer cells almost doubled on macrophages pre-conditioned by hypoxia and cancer cells (Figure 3A and Figure S2A,B). Afterwards, we explored alterations in SIRP α levels in the phagocytic macrophages, those engulfing CFSE+ cancer cells (CD14+CFSE+). Interestingly, we found a significant decrease in the percentage of phagocytic macrophages expressing SIRP α , when previously maintained at 1% O₂ in comparison to those at 20% O₂ (Figure 3B and Figure S2A,B). Based on these results, we further analyzed the SIRP α expression in macrophages and CD47 in cancer cells from the indirect co-cultures, maintained for 72 h at 20% or 1% O₂, before the direct contact with the CFSE-labeled cancer cells. Notably, we found that the co-cultures were already sufficient to trigger a decrease in macrophage SIRP α (Figure 3C), and an increase in cancer cells CD47 (Figure 3D).

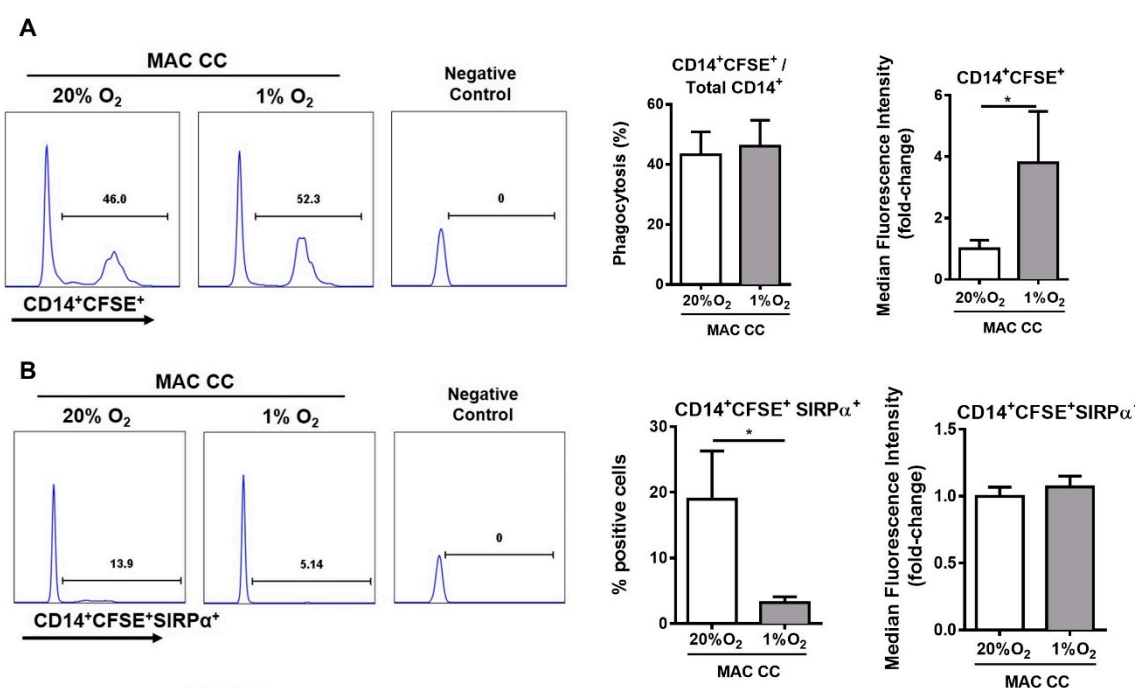


Figure 3. Cont.

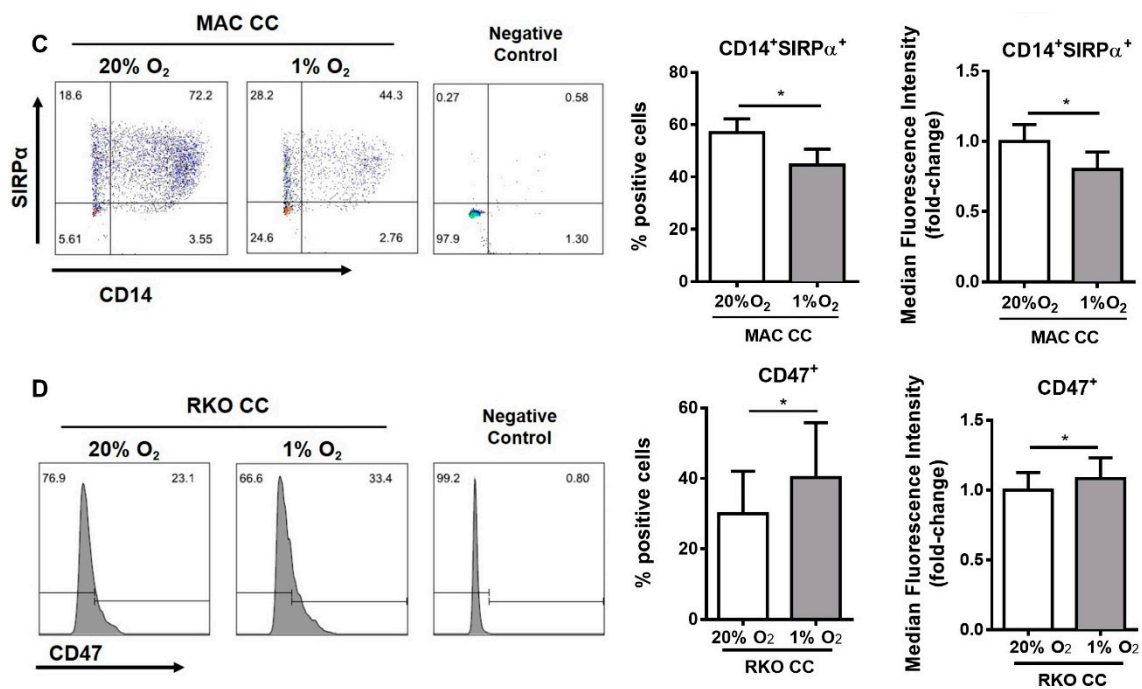


Figure 3. Hypoxia modulates macrophage phagocytic activity and SIRP α expression and CD47 expression on cancer cells. (A,B) Macrophages that were indirectly co-cultured with RKO (MAC CC) cells, at 20% or 1% O₂ for 72 h, were posteriorly directly stimulated with CFSE-labeled RKO cells for 2 h. Macrophages were analyzed by flow cytometry. Histograms display the gating strategy for flow cytometry created with FlowJo. (A) Phagocytic activity was calculated as the ratio of CD14+CFSE+ cells/Total CD14+ cells. (B) Graphs represent the percentage of CD14+CFSE+SIRP α + cells, and the median fluorescence intensity, which is presented as fold-change relatively to 20% O₂ condition. (C,D) Macrophages were indirectly co-cultured with RKO, at 20% or 1% O₂ for 72 h. Expression of the monocyte/macrophage lineage marker CD14 and SIRP α was evaluated on macrophages (C) and of CD47 on cancer cells (D) by flow cytometry. Pseudo-color plots (C) and histograms (D) display the gating strategy for flow cytometry. Graphs represent the percentage and median fluorescence intensity, which is presented as fold-change relatively to 20% O₂ condition of (C) CD14+SIRP α +, or (D) CD47 cells. Graphs represent the mean values with standard deviations, and are representative of $n = 11$ (phagocytosis); $n = 7$ (CFSE+SIRP α +); $n = 10$ (SIRP α); $n = 11$ (CD47) independent experiments. The statistical tests Wilcoxon or paired t -test were used; * $p < 0.05$.

2.4. Hypoxia Decreases the Anti-Inflammatory Pressure and Increases IL-1 β Secretion

It is described that, depending on the stimulation, macrophages may polarize as pro- or anti-inflammatory, sustaining thereafter anti- or pro-tumor activities, respectively [3]. Therefore, we investigated the impact of hypoxia on the polarization profile of macrophages co-cultured with cancer cells, analyzing the expression of a panel of pro- and anti-inflammatory markers [17] by flow cytometry and ELISA. Despite the fact that hypoxia is usually associated with a worse prognosis and with cellular features related to tumor progression, we found that 1% O₂ treatment resulted in a mixed macrophage phenotype, with alterations in both pro and anti-inflammatory markers. However, the clear decrease in anti-inflammatory markers CD163, TGF β , CCL18, and IL-10 (Figure 4A,B), along with the increased expression of the pro-inflammatory cytokine IL-1 β (Figure 4B), which seems to sustain a hypoxia-induced pro-inflammatory effect, is relevant. Nevertheless, we also observed a significant decrease in pro-inflammatory marker CCR7 (Figure 4A).

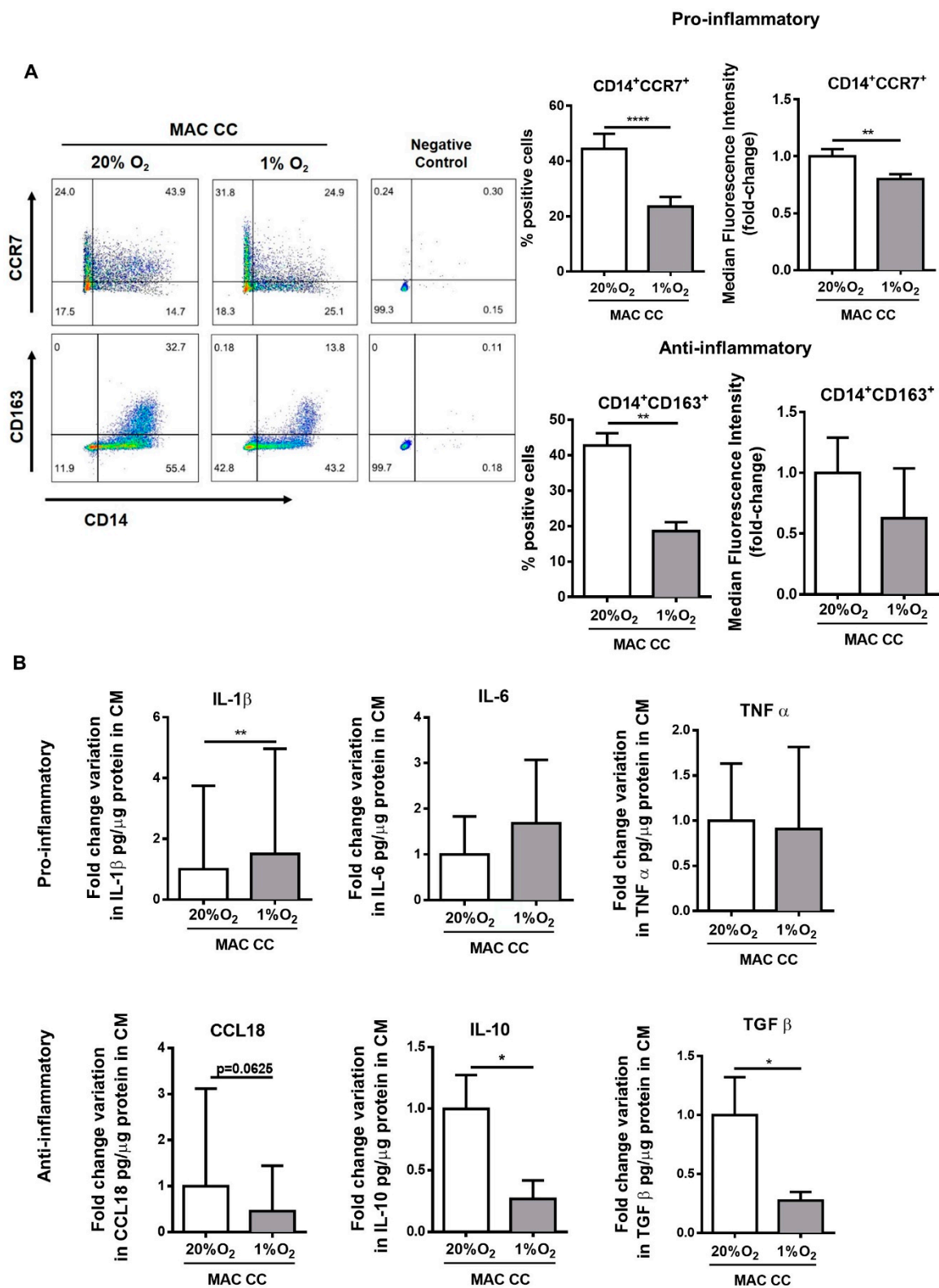


Figure 4. Hypoxia decreases the anti-inflammatory pressure and increases IL-1 β secretion. Macrophages were indirectly co-cultured with RKO (MAC CC), at 20% or 1% O₂ for 72 h. (A) Expression of CD14 and of the polarization markers CCR7 and CD163 was evaluated on macrophages by flow cytometry. Pseudo-color plots display the gating strategy for flow cytometry. Graphs represent the percentage and median fluorescence intensity, which is presented as fold-change relatively to 20% O₂ condition.

(B) Concentration of secreted molecules was measured by ELISA, and normalized to conditioned media (CM) protein levels. Graphs represent cytokine concentration of pro- and anti-inflammatory markers, as a fold change variation to macrophages cultured at 20% O₂. Graphs display the mean values with standard deviations, and are representative of *n* = 12 (CCR7); *n* = 5 (CD163); *n* = 10 (IL-1β); *n* = 8 (IL-6); *n* = 5 (TNF-α); *n* = 5 (CCL18); *n* = 5 (IL-10); *n* = 7 (TGF-β) independent experiments. The statistical tests Wilcox or paired *t*-test were used **** *p* < 0.0001; ** *p* < 0.01; * *p* < 0.05. The *p*-values between 0.05 and 0.1 were presented and considered a tendency.

2.5. Hypoxia Impacts Colon Cancer Cell Behavior, Increasing Invasion and Glucose Consumption

Given the alterations in macrophage behavior induced by the hypoxic environment, as well as differences regarding a patient’s overall survival, we decided to assess whether hypoxia and macrophages influence cancer cell behavior.

No differences were observed in both cell proliferation and cell death in cancer cells when co-cultured with macrophages at 20% or 1% O₂ (Figure 5A,B).

As it is well reported that hypoxia can modulate cancer cell metabolism favoring glycolysis, we evaluated the levels of glucose consumption, lactate production, and pH in indirect co-cultures media, established at 20% and 1% O₂. It is important to note that the glucose and lactate levels in co-cultures conditioned media (CM) results from both macrophages and cancer cells, being impossible to discriminate the specific contribution of each cellular population. To obtain additional information, cancer cell expression levels of *SLC2A1*, the gene that codifies the glucose transporter GLUT-1, and of *LDHA*, the gene that codifies an enzyme involved in lactate production were also analyzed. Interestingly, at 1% O₂, we found a significant increase in glucose consumption, which was accompanied by enhanced expression of the glucose-transporter codifying gene (*SLC2A1*) (Figure 5C). Nevertheless, no differences in lactate production were observed, despite the increase in *LDHA* expression, as well as a significant decrease in pH levels (Figure 5C). Noteworthy, all the differences found resulted from the combination of both macrophages and hypoxia.

When we looked into the invasive capacity of cancer cells, we observed that macrophages and hypoxia alone were sufficient to promote cancer cell invasion and, most importantly, this is potentiated when both factors are combined (Figure 5D).

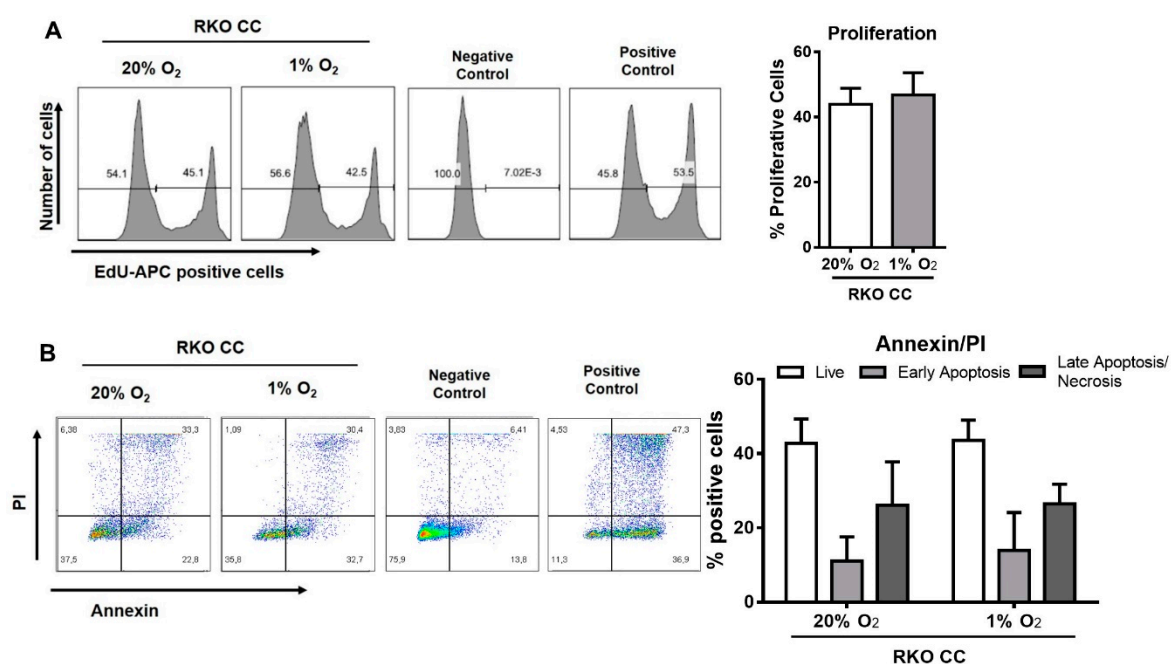


Figure 5. Cont.

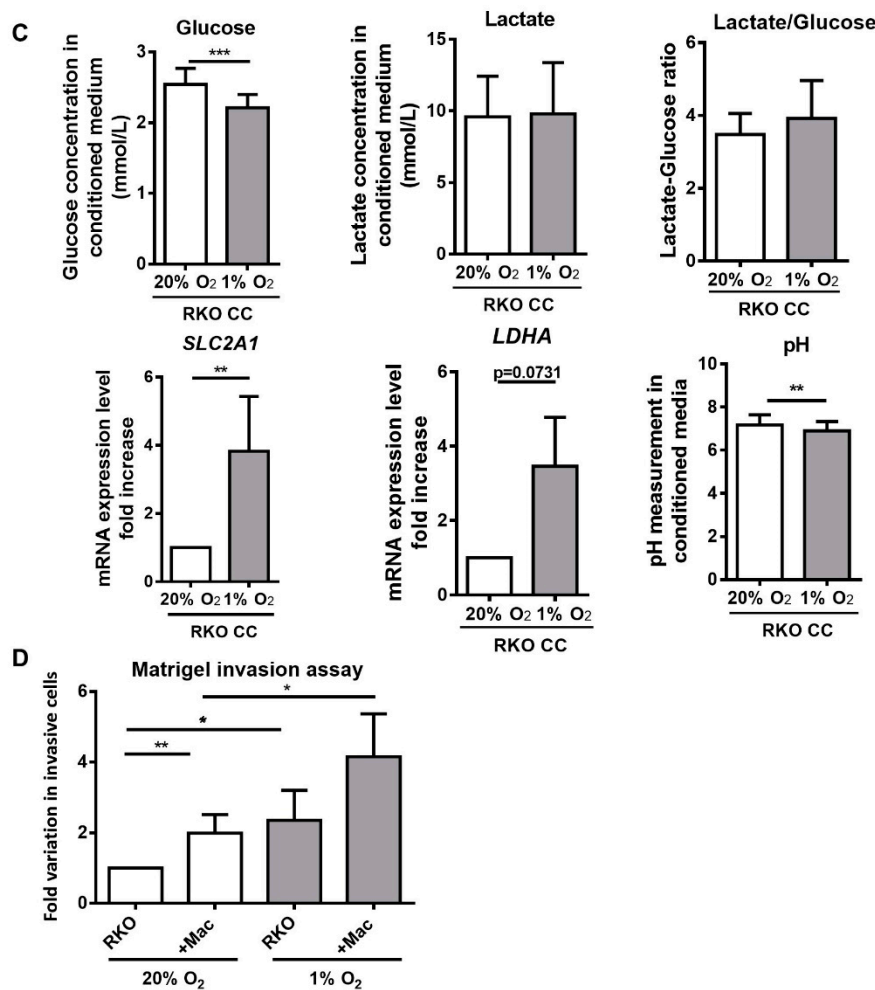


Figure 5. Hypoxia impacts colon cancer cell behavior, increasing invasion and glucose consumption. (A–C) Macrophages were indirectly co-cultured with RKO, at 20% or 1% O₂ for 72 h, and (A) proliferation of cancer cells was assessed for that period. Data are presented as percentage of proliferative cells. (B) AnnexinV/PI assay was used to quantify the percentage of viable (AnnexinV/PI negative), early apoptotic (AnnexinV positive/PI negative), and late apoptotic/necrotic (Annexin V/PI positive) cells. (C) Lactate production, glucose consumption, and pH measurements were made on co-cultures CM. Lactate/glucose ratio was calculated with the glucose and lactate concentration values of the same experiments. Cancer cells *SLC2A1* and *LDHA* mRNA levels were measured by qRT-PCR. Relative expression changes are presented as fold variation *SLC2A1/ACTB* and *LDHA/ACTB* relatively to 20% O₂ condition. (D) Cells maintained at 20% or 1% O₂, and stimulated or not with macrophages previously maintained at 20% or 1% O₂ were cultured for 24 h on Matrigel coated filters, at 20% or 1% O₂. Data are presented as fold variation in the number of invasive cells relative to RKO cells cultured at 20% O₂ without any stimulation with macrophages. Graphs represent the mean values with standard deviations, and are representative of $n = 5$ (proliferation assay); $n = 6$ (Annexin V/PI assay); $n = 10$ (glucose quantification); $n = 11$ (lactate quantification); $n = 6$ (*SLC2A1*); $n = 5$ (*LDHA*); $n = 9$ (pH); $n = 10$ (invasion assay) independent experiments. The statistical tests Friedman, RM one-way ANOVA, Wilcox or paired *t*-test were used *** $p < 0.001$; ** $p < 0.01$; * $p < 0.05$. The p -values between 0.05 and 0.1 were presented and considered a tendency.

2.6. Colon Cancer Patients with CD68^{High} HIF1A^{High} Phenotype Present Increased Expression of Pro-Inflammatory Cytokines and Increased Infiltration of Cytotoxic T-Cells

While the *in vitro* results indicated that hypoxia was associated with features related both with worse prognosis (increased invasion, decreased expression of macrophage antigen-presenting

molecules) and good prognosis (increase in phagocytosis and secretion of pro-inflammatory cytokines), the colon cancer patient’s survival data evidenced that the $CD68^{High}HIF1A^{High}$ population correlates with better prognosis. These led us to hypothesize that the in vitro cellular features associated with better prognosis may prevail in vivo, particularly the secretion of pro-inflammatory cytokines, which could lead to the recruitment of other anti-tumor immune cells.

Initially, the expression of the three pro-inflammatory cytokines previously analyzed, IL-1 β , IL-6, and TNF- α , were compared between $CD68^{High}HIF1A^{High}$ and $CD68^{High}HIF1A^{Low}$ patients, using the TCGA and Oncomine databases. A significantly increased expression of the three cytokines was confirmed in $CD68^{High}HIF1A^{High}$ tumors (Figure 6A). Moreover, in $CD68^{High}$ tumors, a positive correlation between $HIF1A$ and the expression of the three pro-inflammatory cytokines was found (Figure 6B). These results corroborate our in vitro findings, in which the analysis of the total lysates of macrophages or cancer cells exposed to 20% or 1% O₂ for 72 h evidenced that the main contributor to the pro-inflammatory IL-1 β cytokine, detected in co-cultures CM, is indeed the macrophages and not the cancer cells (Figure 6C and Figure S4). Since it is known that a pro-inflammatory pressure can contribute to the recruitment and activation of anti-tumor immune cells [18–20], we assessed whether $CD68^{High}HIF1A^{High}$ enriched tumors presented an increased expression of markers of natural killer (NK) cells ($NCAM1$, within the $CD3D^{Low}$ population), cytotoxic T-cells ($CD8A$, within the $GZMB^{High}$ population), and Th1 cells ($TBX21$, within the $IFNG^{High}$ population). Our results confirmed a significant increase in the expression of $NCAM1$ and $CD8A$, and an increase, although not statistically significant, of $TBX21$ (Figure 6D). Nevertheless, of the two markers that presented significant differences, only $CD8A$ evidenced a positive correlation with $HIF1A$ expression on the $CD68^{High}$ tumors (Figure 6E).

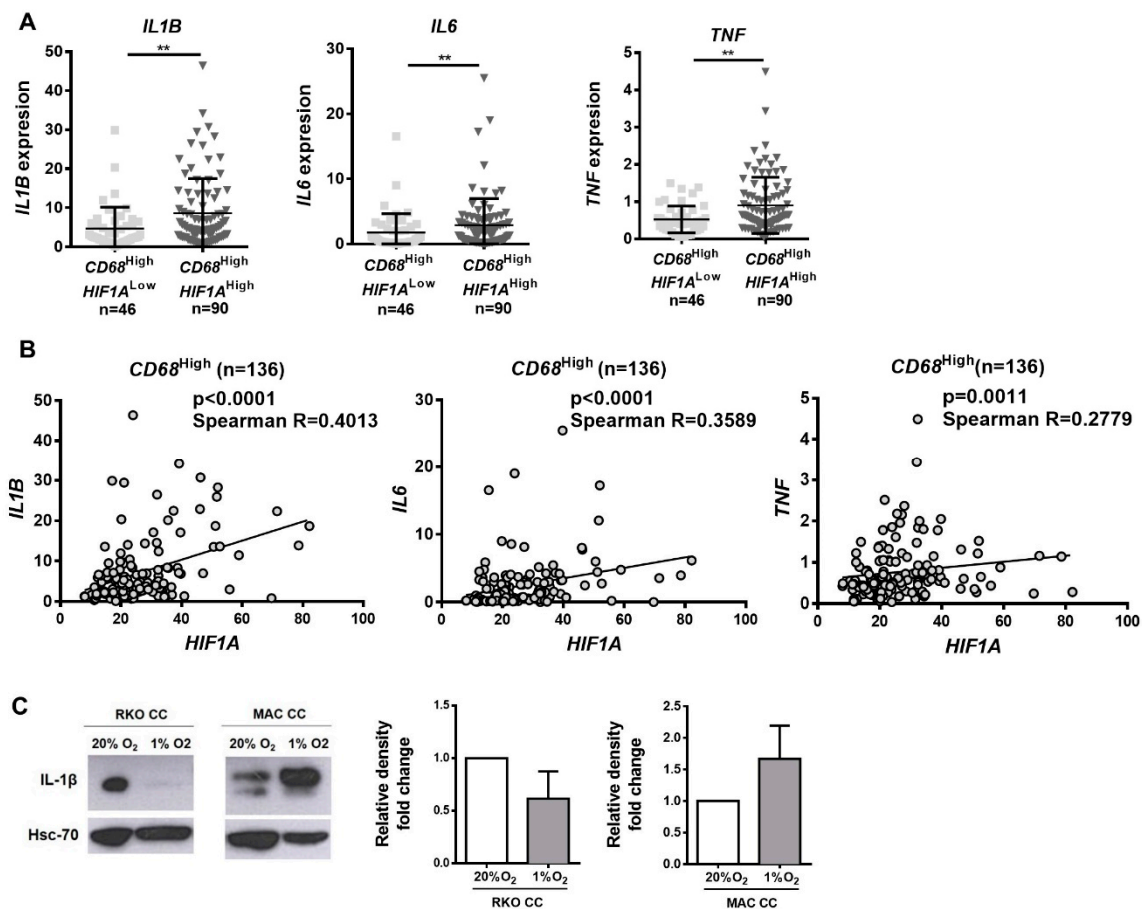


Figure 6. Cont.

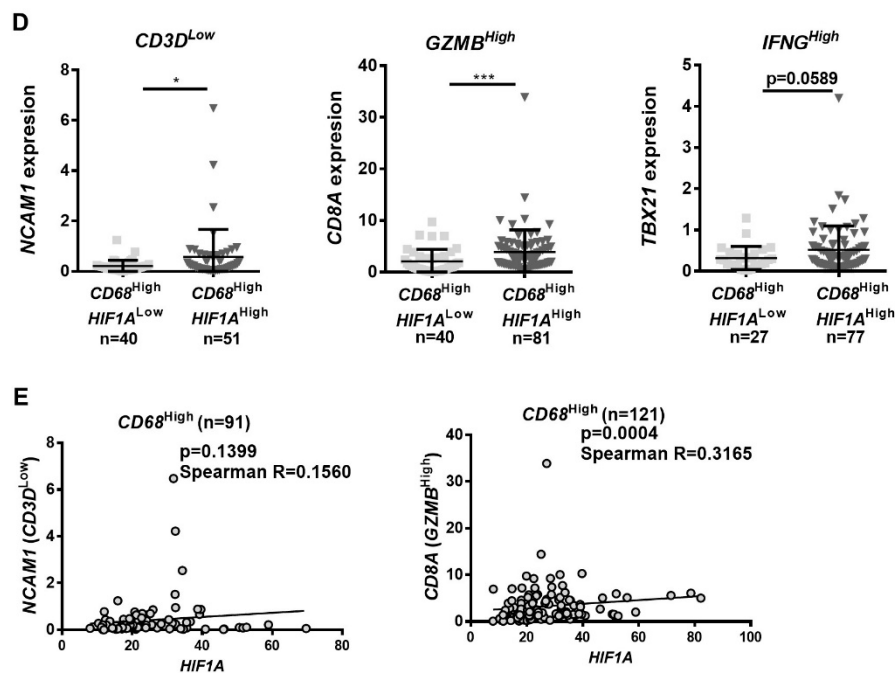


Figure 6. $CD68^{High} HIF1A^{High}$ tumors present increased expression of pro-inflammatory cytokines and increased infiltration of cytotoxic T-cells. RNASeq expression data were downloaded from TCGA. (A) The expression of *IL1B*, *IL6*, and *TNF* was evaluated within the $CD68^{High}$ population, between $HIF1A^{Low}$ and $HIF1A^{High}$, according to the median levels of *CD68* and *HIF1A* expression in normal samples. (B) The correlation between *IL1B*, *IL6*, *TNF*, and *HIF1A* was assessed within the $CD68^{High}$ population. (C) IL-1 β protein levels were evaluated in total lysates from co-cultured RKO cells (RKO CC) and macrophages (MAC CC), by Western blot, and band densitometry quantification presented. Hsc70 was used as loading control, and the figure is representative of 3 independent experiments. (D) The expressions of *NCAM1*, *CD8A*, and *TBX21* were evaluated within the $CD68^{High}$ population, between $HIF1A^{Low}$ and $HIF1A^{High}$ subpopulations, according to the median levels of *CD68* and *HIF1A* expression in normal samples. *NCAM1* levels were evaluated within the $CD3D^{Low}$ population, *CD8A* levels were evaluated within the $GZMB^{High}$ population, and *TBX21* levels were evaluated within the $IFNG^{High}$ population. $CD3D^{Low}$, $GZMB^{High}$, and $IFNG^{High}$ populations were established according to the median levels of each marker expression in normal samples. (E) Correlations between *NCAM1*($CD3D^{Low}$), *CD8A*($GZMB^{High}$), and *HIF1A* were assessed within the $CD68^{High}$ population. Mann–Whitney statistical test was used to compare expression between groups. Spearman statistical test was used to assess correlation, which was considered moderate positive when Spearman Rs were between 0.2500 and 0.3500, and strong positive when Spearman R > 0.3500. **** $p < 0.0001$; *** $p < 0.001$; ** $p < 0.01$; * $p < 0.05$. The p -values between 0.05 and 0.1 were presented and considered a tendency.

The results from the TCGA data analysis were confirmed using the Oncomine Bittner colon cancer cohort (Figure S3). Of note, since this cohort does not include data regarding *IFNG* expression, only the levels of *TBX21*, a Th1 cell-specific transcription factor which controls the expression of the hallmark Th1 cytokine IFN- γ was used.

2.7. The Pressure of Hypoxia on Macrophages at the CMS1-MSI-Immune Colon Cancer Type

We anticipated that the observed phenotype might be more relevant in the consensus molecular subtype 1–microsatellite instable (CMS1–MSI)-immune colon cancer subtype [21], due to the increased immune infiltration. To test our hypothesis, we compared the *HIF1A* expression in distal and proximal colon, within the tumors expressing $CD68^{High}$, as the proximal colon is associated with the aforementioned colon cancer subtype. Accordingly, we found that *HIF1A* expression is significantly higher in the proximal than on the distal colon (Figure 7A). In addition, the correlation

between *CD68* and *HIF1A* was only observed in proximal tumors (Figure 7B), supporting our hypothesis. Despite no significant differences being found on the survival rates of patients harboring $CD68^{High}HIF1A^{High}$ and $CD68^{High}HIF1A^{Low}$ proximal and distal colon tumors, it is possible to observe that the pattern between the two locations is clearly different, suggesting that $CD68^{High}HIF1A^{High}$ patients might have a better prognosis than $CD68^{High}HIF1A^{Low}$ patients (Figure 7C). This question should be clarified by increasing the sample size. Since the CMS1–MSI-immune colon cancer subtype is also characterized by high MSI, high levels of *BRAF* mutations, and low levels *KRAS* mutations, we decided to explore whether $CD68^{High}$ tumors presented differences in *HIF1A* expression comparing MSI/MSS, and *BRAF* and *KRAS* wild-type versus mutated. Despite the low number of cases available at TCGA with the characterization of the MSI status and *BRAF* and *KRAS* mutations, our analysis showed that, in $CD68^{High}$ tumors, the *HIF1A* expression is significantly higher in MSI and *BRAF* mutated cases (Figure 7D). Given these differences, we also looked to *HIF1A* expression in tumors with and without loss of mismatch repair proteins, but no significant difference was found (Figure 7E).

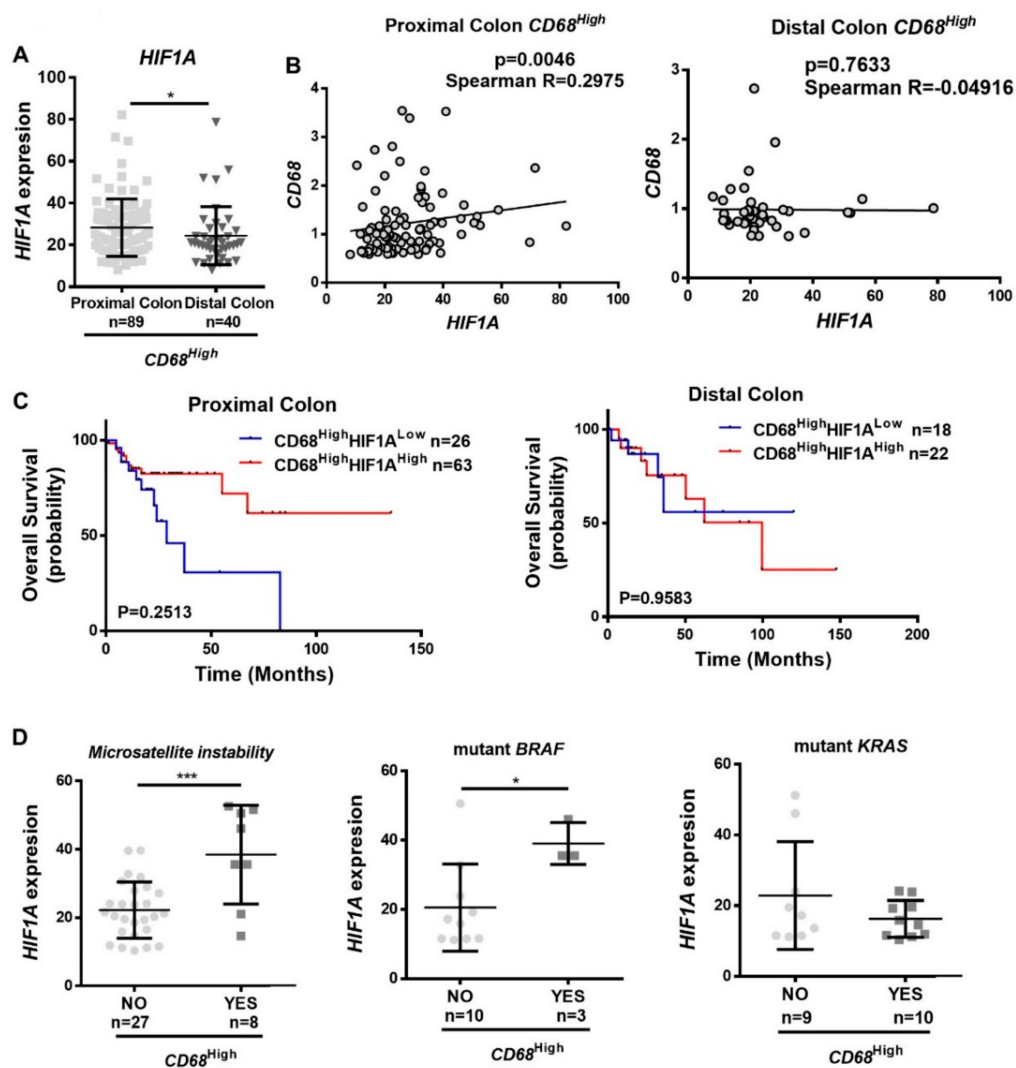


Figure 7. Cont.

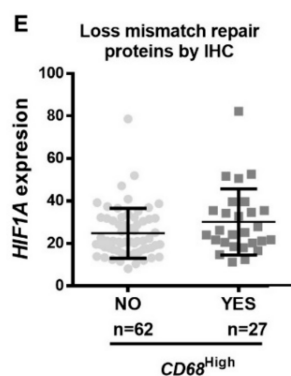


Figure 7. The pressure of hypoxia on macrophages at the consensus molecular subtype 1–microsatellite instable (CMS1–MSI)-immune colon cancer type. Microarray and RNASeq expression data were downloaded from TCGA. **(A)** *HIF1A* expression was evaluated between patients with tumors in proximal colon (cecum, ascending colon, hepatic flexure, and transverse colon) and in distal colon (splenic flexure, descending colon, and sigmoid colon), within the $CD68^{High}$ population. **(B)** The correlation between *CD68* and *HIF1A* was assessed in proximal and distal colon population. **(C)** Kaplan–Meier curves were made with patients’ survival data, comparing the populations $CD68^{High}HIF1A^{High}$ with the population $CD68^{High}HIF1A^{Low}$, on distal and proximal colon patients. **(D)** *HIF1A* expression was evaluated, within the $CD68^{High}$ population, between patients with or without microsatellite instability, BRAF and KRAS mutations. **(E)** *HIF1A* expression was evaluated, within the $CD68^{High}$ population, between patients with or without loss of mismatch repair proteins, evaluated by immunohistochemistry. The division high/low expression was made according the median expression of the genes in normal tissue. Mann–Whitney statistical test was used to compare expression between groups. Spearman statistical test was used to assess correlation, which was considered moderate positive when Spearman R_s were between 0.2500 and 0.3500, and strong positive when Spearman $R > 0.3500$. Long-rank (Mantel–Cox) test to the analysis of the survival curves. ** $p < 0.01$; * $p < 0.05$.

3. Discussion

The full understanding of the interactions established among the distinct TM components is crucial for the development of novel and more efficient anti-tumor therapies. The case of colon cancer is particularly relevant due to the high incidence and mortality, and because several studies have described a very particular behavior of colon cancer cells, in comparison with other tissues, underlying the importance of the colon cancer microenvironment.

In this work, we focused our attention on the crosstalk established between macrophages and colon cancer cells, and on its modulation by hypoxia. Hypoxia is a key feature of solid tumors that has been reported to critically influence cancer cell behavior and is often disregarded. In fact, most of the studies focusing on the role of hypoxia at the tumor microenvironment explored cancer cell metabolic changes [8], while its influence in the non-tumor compartment is still poorly explored. Therefore, the present work brings pioneer information concerning the study of hypoxia on the modulation of macrophage and colon cancer cell interactions.

When exploring tumor databases, we demonstrated that colon tumors exhibit distinct levels of macrophage infiltration, where the most infiltrated tumors are also the most hypoxic ones, presenting higher levels of *HIF1A*, *CA9*, and *LOX* expression. Although the novelty of these findings in colon cancer, these results are not unexpected since it has been previously reported, in other tumors, that hypoxic areas are the ones with enhanced inflammatory infiltration [9]. Notably, this association was accompanied by improved survival rates, clearly evident in $CD68^{High}$ tumors, which could reinforce the idea of a protective anti-tumor and pro-inflammatory effect of the recruited macrophages. Indeed, it was previously reported that chemotactic HIF is essential for myeloid cell infiltration and activation through a VEGF-independent mechanism [22]. Here, we assume that *HIF1A* is produced by both tumor and non-tumor cells at the microenvironment, contributing to this immune cell recruitment,

but it will be important to determine which population is the main contributor to pursue possible therapeutic applications. It will also be interesting to evaluate the role of HIF2 α in this process, as it was reported that HIF1 α and HIF2 α have opposing roles [23]. In contrast to our results, previous reports in colon cancer described that HIF1 α had no association [24], or was associated with worse prognosis [25]. However, none of these studies took the immune component of the microenvironment into consideration.

Importantly, the macrophage infiltration considered in the tumor databases is mainly derived from the tumor core, which is generally the most hypoxic area. It is possible that, depending on localization, macrophage might function in different ways. As our group and others reported, the macrophage inflammatory profile varies according to their location: adjacent tissue, invasive front or intratumor region [2,26]. It will therefore be interesting to assess in patients' samples whether hypoxia influences other macrophage populations besides the ones from the core of the tumor, which is the main region represented in the TCGA patients' samples.

Paradoxically, we found that in vitro hypoxia decreases the expression of macrophage antigen-presenting molecules, namely, HLA-ABC and HLA-DR, and of the co-stimulatory receptor CD86. These results are in line with other reports conducted with macrophage monocultures under hypoxia [27]. Nevertheless, antigen-presentation may still occur at the expense of other immune cells, such as dendritic cells.

This is the first study demonstrating that, although not affecting the percentage of phagocytic macrophages, colon cancer cells and hypoxia enhance macrophage phagocytic capacity. This characteristic might be important in vivo given the increase in necrosis, resulting in enhanced cell debris to collect. In addition, at the molecular level, this finding may suggest the inexistence of a functional anti-phagocytic SIRP α /CD47 system. In line with previous reports in other tumors, we found that hypoxic stimulation leads to an increase of CD47 levels on cancer cells [12,28]. In our system, the enhanced expression of this "don't eat me" signal is counteracted by a decrease in macrophage SIRP α expression. In fact, it seems that less SIRP α expression is associated with increased phagocytosis. In agreement, we found that the percentage of SIRP α + phagocytic macrophages significantly decreases at 1% O₂, explaining the increased macrophage phagocytic capacity. Accordingly, other authors have described that silencing or blocking of SIRP α in RAW264.7 macrophages promoted the phagocytosis of osteosarcoma cancer cells [29]. Our findings regarding phagocytosis are divergent from previously reported work on breast cancer [12] but are in line with other results showing that macrophagic HIF1 α enhances phagocytosis [30], suggesting that this might be a feature dependent on the cancer type. For the first time, we described that, in colon cancer, hypoxia impacts the SIRP α /CD47 axis through the decrease of macrophage SIRP α expression, which may favor their phagocytic capacity. Importantly, the molecular mechanisms associated with this apparent impairment of the SIRP α /CD47 axis need further elucidation.

Regarding the impact of macrophages and hypoxia on cancer cells, we found that despite the increased levels of glucose consumption and *SLC2A1* expression, there was no increase of lactate production, despite the increase in *LDHA* expression and acidosis. Previous reports have stated that lactate polarizes macrophages into an anti-inflammatory phenotype [31]. In our model, where no major alterations on lactate secretion were detected, we also did not find a clear-cut shift on macrophage phenotype. We found that hypoxia potentiated the already described ability of macrophage to induce cancer cell invasion [6]. The maintenance of this pro-tumor feature, despite the secretion of pro-inflammatory cytokines, had already been reported by our group, when macrophage and colon cancer cell co-cultures were treated with ionizing radiation [32].

Some authors have claimed that hypoxia leads to macrophage recruitment and polarization into an anti-inflammatory phenotype [33], while others have reported that hypoxia is not a major driver of macrophage polarization, but instead only triggers fine-tuning of metabolic genes in anti-inflammatory macrophages [34]. Others have described that *HIF1A* depleted macrophages exhibit increased anti-inflammatory markers [35]. In our model, we found alterations in both anti- and pro-inflammatory

markers, and, at the secretome level, a shift into a pro-inflammatory phenotype is suggested. For the first time, we demonstrated that macrophages under the influence of colon cancer cells and hypoxia significantly decreased CCR7 expression, in line with other reports of macrophages monocultures [27]. Nevertheless, no impact in the pro-inflammatory markers IL-6 and TNF- α was observed. Interestingly, it has been recently described that HIF and IL-6 expression is increased in colorectal tumors, being both markers positively correlated [36]. In fact, we observed a slight increase in IL-6 secretion levels at 1% O₂, although without statistical significance. In line with our findings, THP-1 macrophages under hypoxia exhibit decreased CD163 mRNA levels [37]; also being reported is that there is a decrease in CCL18 and IL-10 and an increase in IL-1 β secretion in macrophages monocultures [27,38]. Accordingly, in our work, the analysis of CM of co-cultures combined with the total lysates of macrophages and cancer cells, evidenced that macrophages are the main producers of secreted IL-1 β . While in macrophages, hypoxia is triggering increased IL-1 β expression, on cancer cells, the opposite was observed. Overall, our results suggest that hypoxia triggers a decrease in macrophage anti-inflammatory pressure.

Importantly, we found that in CD68^{High} tumors, hypoxia is associated with the expression of pro-inflammatory cytokines, such as *IL1B*, *IL6*, and *TNF*, previously associated with the recruitment of other anti-tumor immune cells [18–20], suggesting the establishment of a pro-inflammatory TM. Interestingly, some authors described that hypoxia-associated anti-inflammatory macrophages repress T-cell activity [9], while others reported that (1) macrophages without HIF had less capacity to stimulate CD8 T-cell proliferation [39]; (2) hypoxia protected activated T-cells from death [40]; (3) CD8 T-cells with constitutive HIF expression delayed T-cell differentiation into effector cells but increased their cytotoxic function, through increased expression of granzyme B [41]. Notably, the CD68^{High} HIF1A^{High} tumors are those presenting higher levels of infiltrated NK and cytotoxic T-cells, which could be related to the improved survival rate observed in these patients. In fact, these findings are in accordance with other reports demonstrating that colon tumors with higher T-cell infiltration are the ones associated with improved survival [42].

We hypothesize that the results described in this work might be particularly important in the CMS1 MSI-immune tumors, those characterized by an immune infiltrate mainly composed of Th1, NK, and cytotoxic T-cells, and with upregulation of proteins involved in immune response pathways [21,43]. Also, it was described that the number of tumors infiltrating macrophages is higher in MSI colon tumors, those associated with better prognosis [44]. Those tumors are generally associated with the proximal colon, and we confirmed that *HIF1A* was significantly upregulated in this region. Interestingly, it was only in those tumors located in the proximal colon that we found a positive correlation between *CD68* and *HIF1A*, and, furthermore, the survival curves associated with these two colon regions were clearly different from each other. It will be important to validate these results in bigger series of colon cancers, comparing distal and proximal tumors. Moreover, it is known that HIF1 α represses DNA repair genes [45], which could account for an increased mutation burden and tumor immunogenicity. However, in our analysis, *HIF1A* expression could not be associated with mismatch repair protein expression. Interestingly, it is also known that mutant *BRAF*, a common event on CMS1 tumors, regulates HIF-1 α expression in melanoma, affecting cell survival under hypoxic conditions [46]. Indeed, the colon cancer cases with *BRAF* mutation presented a significantly higher expression of *HIF1A*, while no differences were found on *KRAS* mutated cases. It will be interesting to further explore these associations among hypoxia, *BRAF* mutation and MSI status, and macrophage infiltration on colon tumors. In addition, given the documented relevance of the microbiome in cancer progression, the knowledge that there is a particular microbiota organization in proximal colon [47], and that colon bacterial products modulate HIF1- α expression and activation [48,49], it may also be important to explore the impact of the microbiome on macrophage–colon cancer cell crosstalk, within an hypoxic environment.

Despite the well documented influence of hypoxia in triggering different hallmarks of cancer, this work highlights that, depending on the component of the microenvironment, the tumor origin, and even on its localization, hypoxia can play a beneficial role in the combat against the tumor.

4. Materials and Methods

4.1. Bioinformatic Analysis

TCGA

The Cancer Genome Atlas (TCGA; <https://cancergenome.nih.gov/>) dataset of colon carcinomas was analyzed, and for comparison purposes, gastric, breast ductal, and lung adenocarcinoma datasets were used. Survival plots were performed in R using survival and survminer packages. Median values were calculated in normal tissue and used as threshold to define “high” and “low” expression levels in cancer patients. The expression of genes was quantified as FPKM (fragments per kilobase million), which are provided by TCGA consortium. The number of individuals with information simultaneously on gene expression and survival were 136 for colon, 269 for gastric, 673 for breast ductal, and 52 for lung adenocarcinoma. Clinical and somatic mutation metadata were also provided by the TCGA consortium at <https://gdc.cancer.gov/>.

4.2. Oncomine

CD68, *HIF1A*, *CA9*, *LOX*, *IL1B*, *IL6*, *TNF*, *CD3D*, *NCAM*, *GZMB*, *CD8A*, and *TBX21* mRNA expression was assessed in the Bittner colon cancer dataset from Oncomine database (<https://www.oncomine.org>), encompassing a total of 374 cases. Categorization of patient samples was assigned into low (lowest 50%) and high (highest 50%) subgroups according to the log₂ median-centered intensity levels of mRNA expression.

4.3. Ethics Statement

The buffy coats used for monocyte isolation are highly leukocyte-enriched waste-products that results from a whole blood donation of healthy blood donors. The isolation of immune cells from healthy blood donors was approved by the Centro Hospitalar Universitário São João Ethics Committee (protocol 90/19) after collecting each donor’s informed consent.

4.4. Human Monocyte Isolation and Macrophage Differentiation

Human monocytes were isolated from buffy coats from healthy blood donors, as previously described (6). Isolated cells were resuspended in RPMI1640 supplemented with 10% fetal bovine serum (FBS, Biowest, Nuaille, France) and 100 U/mL penicillin and 100 µg/mL streptomycin (PS, Invitrogen, Carlsbad, CA, USA). Then, 1.2×10^6 monocytes were plated per 6-well culture plates and differentiated into macrophages for 10 days. In the first 7 days, macrophages were supplemented with M-CSF (50 ng/mL, ImmunoTools, Friesoythe, Germany). Cells were maintained at 37 °C and 5% CO₂ humidified atmosphere.

4.5. Cancer Cell Culture

RKO colon cancer cell line, from American Type Culture Collection (ATCC), was cultured in RPMI1640 (Invitrogen), supplemented with 10% FBS and 1% PS, and maintained at 37 °C and 5% CO₂ humidified atmosphere.

4.6. Macrophage and Cancer Cell Indirect Co-Cultures

For co-cultures, 1×10^5 RKO cells were seeded into 6-well-plate permeable transwell inserts (PET inserts with 1-µm pore, Corning, Corning, NY, USA) positioned on top of a macrophage culture, 10 days after monocyte isolation. Co-cultures between macrophages and cancer cells were maintained in complete RPMI medium for 72 h at 37 °C, at 20% O₂ or 1% O₂ (94% N₂), 5% CO₂ humidified atmosphere.

4.7. RNA Extraction, cDNA Preparation, and Quantitative Real-Time PCR Analysis

Total RNA was extracted using TRIzol reagent (Invitrogen), according to the manufacturer's instructions. cDNA was synthesized using 1 µg of RNA, using NZY M-MuLV Reverse Transcriptase enzyme (NZYTech, Lisboa, Portugal), according to the manufacturer's instructions. Quantitative real-time PCR (qRT-PCR) was performed with Kapa Probe Fast qPCR Master Mix (Kapa Biosystems, Roche, Basel, Switzerland) using the probes to *ACTB* (Hs01060665), *CA9* (Hs00154208), *LDHA* (Hs.PT.58.22929122), and *SLC2A1* (Hs.PT.58.25872862) (Applied Biosystems, Foster City, CA, USA). Relative mRNA expression of the target genes was normalized to the levels of the housekeeping gene, using the comparative $\Delta\Delta C_t$ method. *ACTB* was used as a housekeeping gene to RKO cells.

4.8. Viability Assay

Macrophage and cancer cell viability was measured by resazurin reduction assay. After 3 days of co-culture, resazurin redox dye (0.01 mg/mL, Sigma-Aldrich, St.Louis, MO, USA) was added (1/10 of the total volume of culture medium) to cell culture, incubated for 4 h at 37 °C and 5% CO₂, and the fluorescence intensity was measured at 530/590 nm in a Synergy Mx fluorometer.

4.9. Flow Cytometry

Macrophages and cancer cells were incubated with accutase (eBioscience, Affymetrix, Santa Clara, CA, USA) at 37 °C for 30 min and harvested by gently scraping. Cells were washed and resuspended in FACS buffer (PBS, 2% FBS (Biowest), 0.01% sodium azide) containing appropriate conjugated antibodies, and stained in the dark for 40 min at 4 °C. Macrophages were immunostained with the following antibodies: anti-human CD14-APC (clone MEM-12), CD14-PE/FITC (clone 18D11), CD14-PerCP/Cy5.5 (clone OFC14D), CD86-FITC (clone BU63), HLA-ABC-PE (clone W6/32), HLA-DR-PE/FITC (clone MEM-12) (Immunotools), CCR7-PerCP/Cy5.5 (G043H7), SIRP α -APC (clone SE5A5) (Biolegend, San Diego, CA, USA), CD163-PE (clone GHI/61) (BD Bioscience, Franklin Lakes, NJ, USA). Cancer cells were stained with anti-human CD47-FITC (clone MEM-122) (Immunotools). Unstained cells and single stained with antibodies or with the respective isotype IgGs were used as control. After additional washing steps, cell fluorescence was acquired on a FACS Canto Flow Cytometer (BD Biosciences) using FACS Diva Software. Data analysis was performed with FlowJo software.

4.10. Phagocytosis Assay

Colon cancer cells were grown for 72 h at 1% O₂, and after this period, suspension of 1×10^7 cells/mL was stained with 2.5 µM CellTrace™ CFSE (Invitrogen), according to the manufacturer's protocol. Macrophages that were previously indirectly co-cultured with cancer cells, for 72 h, were incubated in serum-free medium for 2 h before adding 2.4×10^6 CFSE-labeled cancer cells (1 macrophage:2 cancer cells). After coculture for 2 h at 37 °C, macrophages were harvested and evaluated by flow cytometry, with anti-CD14 and anti-SIRP α antibodies. Phagocytosis was calculated as the percentage of CD14+CFSE+ cells among total CD14+.

4.11. Enzyme-Linked Immunosorbent Assay (ELISA)

Cytokine levels were measured in the CM of mono and co-cultures by ELISA to TGF- β , TNF- α , IL-10, IL-1 β , IL-6 (Biolegend), and CCL18 (Abcam, Cambridge, UK) according to the manufacturer's instructions. Concentrations were normalized to the CM total protein concentration, which was measured using the DCProtein assay kit (BioRad, Hercules, CA, USA), following the manufacturer's instructions.

4.12. Proliferation Assay

Cell proliferation was determined through the use of the Click-iTTM Plus EdU Flow Cytometry Assay Kit (Invitrogen), according to the manufacturer's instructions. RKO cells cultured in 6-well plates without EdU treatment were used as a negative control, while RKO treated with EdU was used as a positive control.

4.13. Cell Death Quantification Assay

Cell death was measured using the FITC Annexin V Apoptosis Detection kit (BD Pharmingen, BD Bioscience, Franklin Lakes, NJ, USA) according to the manufacturer's instructions. Untreated RKO cells cultured in a 6-well plate were used as a negative control, and cells treated with H₂O₂ were used as a positive control.

4.14. Glucose Quantification Assay

Glucose levels were measured in the CM of the co-cultures using the enzymatic colorimetric kit, Glucose Assay Kit (Roche), following the manufacturer's instructions. The standard curve for glucose quantification was done using serial dilutions of RPMI, with known glucose concentration.

4.15. Lactate Quantification Assay

An enzymatic colorimetric kit (Spinreact, Girona, Spain) was used to determine lactate concentration in co-cultures CM, according to the manufacturer's instructions.

4.16. pH Measurement

The CM pH was measured using the Electro Kinetic Analyzer (EKA) (Anton Paar, Graz, Austria).

4.17. Matrigel Invasion Assay

Invasion was measured using Matrigel-coated invasion inserts of 8µm pore (Corning), according to the manufacturer's instructions. In the upper compartment, 2.5×10^4 RKO cells were cultured at 20% O₂ or 1% O₂ conditions, either alone or stimulated with macrophages cultured at 20% O₂ or 1% O₂ at the lower compartment. Cells were allowed to invade for 24 h at 37 °C, at 20% O₂ or 1% O₂, respectively. After this period, the inserts were washed with PBS and fixed in 4% PFA for 20 min at RT, and the non-invading cells in the upper compartment of the inserts were removed. The filters were mounted in Vectashield Mounting Medium with DAPI (Vector Laboratories, Burlingame, CA, USA), and the invading cells were visualized and counted with a Leica DM2000 fluorescence microscope (Leica Microsystems, Wetzlar, Germany).

4.18. Western Blot

Cell lysates were prepared with Rippa buffer (50 mM Tris HCl pH = 7.5; 1% NonidetP (NP)-40; 150 mM NaCl and 2 mM EDTA) with proteases/phosphatases inhibitors cocktails (Sigma-Aldrich). Protein concentration was determined using the DCProtein assay kit (BioRad) and 20 µg of protein were loaded and run in a 12.5% SDS-polyacrylamide gel. Afterwards, gels were transferred to nitrocellulose membranes (GE Healthcare, Chicago, IL, USA), blocked with 5% non-fat powder milk in PBS + 0.1% Tween-20 (PBS-T 0.1%) for 30 min, and incubated overnight with primary antibodies rabbit anti-IL-1β (GeneTex, Irvine, CA, USA), and mouse anti-Hsc-70 (Santa Cruz, Dallas, TX, USA). HRP-conjugated anti-mouse and anti-rabbit (GE Healthcare, Chicago, IL, USA) were used as secondaries antibodies. Membranes were incubated with Clarity Western ECL Substrate (BioRad) for signal detection. Bands intensity measurements were performed with ImageJ.

4.19. Statistical Analysis

Data were expressed as the mean with standard deviation (SD), and collected from at least three independent experiments with macrophages from different donors. The normality of the distribution was evaluated using the Kolmogorov–Smirnov test. For comparison between two independent groups, *t*-test (paired, Wilcoxon, and Mann–Whitney) was used. For comparison among four independent groups, one-way ANOVA (RM one-way ANOVA, Friedman, and Kruskal–Wallis), with Dunn’s multiple comparison was used. Correlations were tested with the Spearman test and considered moderate positive when Spearman *R*s were between 0.2500 and 0.3500, and strong positive when Spearman *R* > 0.3500. Survival curves were analyzed with the log-rank (Mantel–Cox) test. Statistical tests were performed in GraphPad Prism 8. Differences were considered significant at *p* < 0.05.

5. Conclusions

Our results demonstrate the importance of considering hypoxia as a major player on the tumor microenvironment modulation. In particular, we found that in colon tumors with high macrophage infiltration, hypoxia is associated with better prognosis, possibly due to the pro-inflammatory pressure induced by macrophages, which could potentiate the recruitment of other anti-cancer immune cells. This phenomenon appears to be tissue-specific and even dependent on tumor localization within the colon.

Altogether, these data underlie the need to consider the specificities of each tumor microenvironment, since the particular context in which cancer cells are enclosed can have a major impact in disease prognosis and the selection of therapeutic options.

Supplementary Materials: The following supplementary figures are available online at <http://www.mdpi.com/2072-6694/12/4/818/s1>, Figure S1: Experimental setup and confirmation of cellular response to hypoxia; Figure S2: Gating strategy for flow cytometry analysis; Figure S3: The *CD68^{High}HIF1A^{High}* population is associated with increased recruitment of cytotoxic T-cells; Figure S4: Western blot.

Author Contributions: Conceptualization, A.M.C. and B.S.; Data curation, A.M.C., F.M., R.O., B.C., F.P., F.C., and B.S.; Formal analysis, A.M.C., F.M., R.O., B.C., F.P., A.P.C., F.C., R.M.R., L.P., and M.J.O.; Funding acquisition, M.J.O.; Investigation, A.M.C., F.M., R.O., A.P.C., M.L.P., A.J.S., D.A., and J.P.L.; Methodology, A.M.C., A.P.C., F.C., B.S., M.L.P., A.J.S., D.A., and J.P.L.; Software, B.C., F.P., R.M.R., and L.P.; Supervision, A.M.C.; Validation, A.M.C.; Writing—original draft, A.M.C.; Writing—review and editing, A.M.C., N.P., and M.J.O. All authors have read and agreed to the published version of the manuscript.

Funding: This work was supported by Portuguese Foundation for Science and Technology (FCT) project POCI-01-0145-FEDER-031859 (MAGICIAM). This work was supported by Portuguese Foundation for Science and Technology (FCT) project POCI-01-0145-FEDER-031859 (MAGICIAM). A.M.C. (DL 57/2016/CP1360/CT0009) and A.P.C. (POCI-01-0145-FEDER-031859) are junior researchers, F.M. (SFRH/BD/143669/2019) is a PhD FCT fellow, F.P. is a post-doc FCT fellow (SFRH/BPD/115730/2016), and F.C. (POCI-01-0145-FEDER-016390) is a research fellow.

Acknowledgments: We acknowledge Sérgio Velho’s team for the scientific discussion, Cecília Durães and Tânia Cruz for the help with statistics. We acknowledge all the help from i3S Scientifics Platforms technicians: Catarina Meireles and Emília Cardoso from the Translational Cytometry Unit, Dalila Pedro and Ricardo Vidal from the Biointerfaces and Nanotechnology Unit, Mafalda Rocha and Rob Mensink from the Genomics Unit. The authors would like to thank Serviço de Imunohemoterapia of Centro Hospitalar Universitário de São João (CHUSJ), for kindly donating Buffy Coats.

Conflicts of Interest: The authors declare no conflict of interest.

References

- Colangelo, T.; Polcaro, G.; Muccillo, L.; D’Agostino, G.; Rosato, V.; Ziccardi, P.; Lupo, A.; Mazzocchi, G.; Sabatino, L.; Colantuoni, V. Friend or foe? The tumour microenvironment dilemma in colorectal cancer. *Biochim. Biophys. Acta* **2017**, *1867*, 1–18. [[CrossRef](#)]
- Yang, M.; McKay, D.; Pollard, J.W.; Lewis, C.E. Diverse Functions of Macrophages in Different Tumor Microenvironments. *Cancer Res.* **2018**, *78*, 5492–5503. [[CrossRef](#)] [[PubMed](#)]
- Mosser, D.M.; Edwards, J.P. Exploring the full spectrum of macrophage activation. *Nature reviews. Immunology* **2008**, *8*, 958–969. [[CrossRef](#)] [[PubMed](#)]

4. Crusz, S.M.; Balkwill, F.R. Inflammation and cancer: Advances and new agents. *Nat. Rev. Clin. Oncol.* **2015**, *12*, 584–596. [[CrossRef](#)] [[PubMed](#)]
5. Zhong, X.; Chen, B.; Yang, Z. The Role of Tumor-Associated Macrophages in Colorectal Carcinoma Progression. *Cell. Physiol. Biochem.* **2018**, *45*, 356–365. [[CrossRef](#)]
6. Cardoso, A.P.; Pinto, M.L.; Pinto, A.T.; Oliveira, M.I.; Pinto, M.T.; Goncalves, R.; Relvas, J.B.; Figueiredo, C.; Seruca, R.; Mantovani, A.; et al. Macrophages stimulate gastric and colorectal cancer invasion through EGFR Y(1086), c-Src, Erk1/2 and Akt phosphorylation and smallGTPase activity. *Oncogene* **2014**, *33*, 2123–2133. [[CrossRef](#)]
7. Semenza, G.L. The hypoxic tumor microenvironment: A driving force for breast cancer progression. *Biochim. Biophys. Acta* **2016**, *1863*, 382–391. [[CrossRef](#)]
8. Vaupel, P.; Mayer, A. Hypoxia in cancer: Significance and impact on clinical outcome. *Cancer Metastasis Rev.* **2007**, *26*, 225–239. [[CrossRef](#)]
9. Henze, A.T.; Mazzone, M. The impact of hypoxia on tumor-associated macrophages. *J. Clin. Investig.* **2016**, *126*, 3672–3679. [[CrossRef](#)]
10. Palazon, A.; Goldrath, A.W.; Nizet, V.; Johnson, R.S. HIF Transcription Factors, Inflammation, and Immunity. *Immunity* **2014**, *41*, 518–528. [[CrossRef](#)]
11. Semenza, G.L. Targeting HIF-1 for cancer therapy. *Nat. Rev. Cancer* **2003**, *3*, 721–732. [[CrossRef](#)] [[PubMed](#)]
12. Zhang, H.; Lu, H.; Xiang, L.; Bullen, J.W.; Zhang, C.; Samanta, D.; Gilkes, D.M.; He, J.; Semenza, G.L. HIF-1 regulates CD47 expression in breast cancer cells to promote evasion of phagocytosis and maintenance of cancer stem cells. *Proc. Natl. Acad. Sci. USA* **2015**, *112*, E6215–E6223. [[CrossRef](#)] [[PubMed](#)]
13. Onnis, B.; Rapisarda, A.; Melillo, G. Development of HIF-1 inhibitors for cancer therapy. *J. Cell. Mol. Med.* **2009**, *13*, 2780–2786. [[CrossRef](#)] [[PubMed](#)]
14. Kenneth, N.S.; Mudie, S.; van Uden, P.; Rocha, S. SWI/SNF Regulates the Cellular Response to Hypoxia. *J. Biol. Chem.* **2009**, *284*, 4123–4131. [[CrossRef](#)] [[PubMed](#)]
15. Simiantonaki, N.; Taxeidis, M.; Jayasinghe, C.; Kurzik-Dumke, U.; Kirkpatrick, C.J. Hypoxia-inducible factor 1 alpha expression increases during colorectal carcinogenesis and tumor progression. *BMC Cancer* **2008**, *8*, 320. [[CrossRef](#)]
16. Martinez, F.O.; Helming, L.; Milde, R.; Varin, A.; Melgert, B.N.; Draijer, C.; Thomas, B.; Fabbri, M.; Crawshaw, A.; Ho, L.P.; et al. Genetic programs expressed in resting and IL-4 alternatively activated mouse and human macrophages: Similarities and differences. *Blood* **2013**, *121*, E57–E69. [[CrossRef](#)]
17. Dalton, H.J.; Armaiz-Pena, G.N.; Gonzalez-Villasana, V.; Lopez-Berestein, G.; Bar-Eli, M.; Sood, A.K. Monocyte subpopulations in angiogenesis. *Cancer Res.* **2014**, *74*, 1287–1293. [[CrossRef](#)]
18. Okada, M.; Kitahara, M.; Kishimoto, S.; Matsuda, T.; Hirano, T.; Kishimoto, T. Il-6 Bsf-2 Functions as a Killer Helper Factor in the Invitro Induction of Cyto-Toxic T-Cells. *J. Immunol.* **1988**, *141*, 1543–1549.
19. Ben-Sasson, S.Z.; Hogg, A.; Hu-Li, J.; Wingfield, P.; Chen, X.; Crank, M.; Caucheteux, S.; Ratner-Hurevich, M.; Berzofsky, J.A.; Nir-Paz, R.; et al. IL-1 enhances expansion, effector function, tissue localization, and memory response of antigen-specific CD8 T cells. *J. Exp. Med.* **2013**, *210*, 491–502. [[CrossRef](#)]
20. Turner, M.D.; Nedjai, B.; Hurst, T.; Pennington, D.J. Cytokines and chemokines: At the crossroads of cell signalling and inflammatory disease. *Biochim. Biophys. Acta* **2014**, *1843*, 2563–2582. [[CrossRef](#)]
21. Guinney, J.; Dienstmann, R.; Wang, X.; de Reynies, A.; Schlicker, A.; Sonesson, C.; Marisa, L.; Roepman, P.; Nyamundanda, G.; Angelino, P.; et al. The consensus molecular subtypes of colorectal cancer. *Nat. Med.* **2015**, *21*, 1350–1356. [[CrossRef](#)] [[PubMed](#)]
22. Cramer, T.; Yamanishi, Y.; Clausen, B.E.; Forster, I.; Pawlinski, R.; Mackman, N.; Haase, V.H.; Jaenisch, R.; Corr, M.; Nizet, V.; et al. HIF-1alpha is essential for myeloid cell-mediated inflammation. *Cell* **2003**, *112*, 645–657. [[CrossRef](#)]
23. Keith, B.; Johnson, R.S.; Simon, M.C. HIF1 alpha and HIF2 alpha: Sibling rivalry in hypoxic tumour growth and progression. *Nat. Rev. Cancer* **2012**, *12*, 9–22. [[CrossRef](#)] [[PubMed](#)]
24. Jubb, A.M.; Turley, H.; Moeller, H.C.; Steers, G.; Han, C.; Li, J.L.; Leek, R.; Tan, E.Y.; Singh, B.; Mortensen, N.J.; et al. Expression of delta-like ligand 4 (Dll4) and markers of hypoxia in colon cancer. *Br. J. Cancer* **2009**, *101*, 1749–1757. [[CrossRef](#)]
25. Baba, Y.; Noshio, K.; Shima, K.; Irahara, N.; Chan, A.T.; Meyerhardt, J.A.; Chung, D.C.; Giovannucci, E.L.; Fuchs, C.S.; Ogino, S. HIF1A overexpression is associated with poor prognosis in a cohort of 731 colorectal cancers. *Am. J. Pathol.* **2010**, *176*, 2292–2301. [[CrossRef](#)]

26. Pinto, M.L.; Rios, E.; Doraes, C.; Ribeiro, R.; Machado, J.C.; Mantovani, A.; Barbosa, M.A.; Carneiro, F.; Oliveira, M.J. The Two Faces of Tumor-Associated Macrophages and Their Clinical Significance in Colorectal Cancer. *Front. Immunol.* **2019**, *10*. [[CrossRef](#)]
27. Raggi, F.; Pelassa, S.; Pierobon, D.; Penco, F.; Gattorno, M.; Novelli, F.; Eva, A.; Varesio, L.; Giovarelli, M.; Bosco, M.C. Regulation of Human Macrophage M1-M2 Polarization Balance by Hypoxia and the Triggering Receptor Expressed on Myeloid Cells-1. *Front. Immunol.* **2017**, *8*, 1097. [[CrossRef](#)]
28. Romano, E.; Rufo, N.; Korf, H.; Mathieu, C.; Garg, A.D.; Agostinis, P. BNIP3 modulates the interface between B16-F10 melanoma cells and immune cells. *Oncotarget* **2018**, *9*, 17631–17644. [[CrossRef](#)]
29. Ray, M.; Lee, Y.W.; Hardie, J.; Mout, R.; Yesilbag Tonga, G.; Farkas, M.E.; Rotello, V.M. CRISPRed Macrophages for Cell-Based Cancer Immunotherapy. *Bioconj. Chem.* **2018**, *29*, 445–450. [[CrossRef](#)]
30. Anand, R.J.; Gribar, S.C.; Li, J.; Kohler, J.W.; Branca, M.F.; Dubowski, T.; Sodhi, C.P.; Hackam, D.J. Hypoxia causes an increase in phagocytosis by macrophages in a HIF-1 alpha-dependent manner. *J. Leukoc. Biol.* **2007**, *82*, 1257–1265. [[CrossRef](#)]
31. Colegio, O.R.; Chu, N.Q.; Szabo, A.L.; Chu, T.; Rhebergen, A.M.; Jairam, V.; Cyrus, N.; Brokowski, C.E.; Eisenbarth, S.C.; Phillips, G.M.; et al. Functional polarization of tumour-associated macrophages by tumour-derived lactic acid. *Nature* **2014**, *513*, 559–563. [[CrossRef](#)]
32. Pinto, A.T.; Pinto, M.L.; Cardoso, A.P.; Monteiro, C.; Pinto, M.T.; Maia, A.F.; Castro, P.; Figueira, R.; Monteiro, A.; Marques, M.; et al. Ionizing radiation modulates human macrophages towards a pro-inflammatory phenotype preserving their pro-invasive and pro-angiogenic capacities. *Sci. Rep.* **2016**, *6*. [[CrossRef](#)]
33. Leblond, M.M.; Gerault, A.N.; Corroyer-Dulmont, A.; MacKenzie, E.T.; Petit, E.; Bernaudin, M.; Valable, S. Hypoxia induces macrophage polarization and re-education toward an M2 phenotype in U87 and U251 glioblastoma models. *Oncoimmunology* **2016**, *5*, e1056442. [[CrossRef](#)]
34. Laoui, D.; Van Overmeire, E.; Di Conza, G.; Aldeni, C.; Keirse, J.; Morias, Y.; Movahedi, K.; Houbracken, I.; Schouppe, E.; Elkrim, Y.; et al. Tumor hypoxia does not drive differentiation of tumor-associated macrophages but rather fine-tunes the M2-like macrophage population. *Cancer Res.* **2014**, *74*, 24–30. [[CrossRef](#)] [[PubMed](#)]
35. Kumar, V.; Gabrilovich, D.I. Hypoxia-inducible factors in regulation of immune responses in tumour microenvironment. *Immunology* **2014**, *143*, 512–519. [[CrossRef](#)] [[PubMed](#)]
36. Xu, K.; Zhan, Y.; Yuan, Z.; Qiu, Y.; Wang, H.; Fan, G.; Wang, J.; Li, W.; Cao, Y.; Shen, X.; et al. Hypoxia Induces Drug Resistance in Colorectal Cancer through the HIF-1 α /miR-338-5p/IL-6 Feedback Loop. *Mol. Ther.* **2019**. [[CrossRef](#)] [[PubMed](#)]
37. Ye, X.J.; Zhang, J.; Lu, R.; Zhou, G. Signal regulatory protein a associated with the progression of oral leukoplakia and oral squamous cell carcinoma regulates phenotype switch of macrophages. *Oncotarget* **2016**, *7*, 81305–81321. [[CrossRef](#)] [[PubMed](#)]
38. Song, J.; Cheon, S.Y.; Jung, W.; Lee, W.T.; Lee, J.E. Resveratrol induces the expression of interleukin-10 and brain-derived neurotrophic factor in BV2 microglia under hypoxia. *Int. J. Mol. Sci.* **2014**, *15*, 15512–15529. [[CrossRef](#)]
39. Bhandari, T.; Olson, J.; Johnson, R.S.; Nizet, V. HIF-1 alpha influences myeloid cell antigen presentation and response to subcutaneous OVA vaccination. *J. Mol. Med.* **2013**, *91*, 1199–1205. [[CrossRef](#)]
40. Makino, Y.; Nakamura, H.; Ikeda, E.; Ohnuma, K.; Yamauchi, K.; Yabe, Y.; Poellinger, L.; Okada, Y.; Morimoto, C.; Tanaka, H. Hypoxia-inducible factor regulates survival of antigen receptor-driven T cells. *J. Immunol.* **2003**, *171*, 6534–6540. [[CrossRef](#)]
41. Doedens, A.L.; Phan, A.T.; Stradner, M.H.; Fujimoto, J.K.; Nguyen, J.V.; Yang, E.; Johnson, R.S.; Goldrath, A.W. Hypoxia-inducible factors enhance the effector responses of CD8(+) T cells to persistent antigen. *Nat. Immunol.* **2013**, *14*, 1173–1182. [[CrossRef](#)] [[PubMed](#)]
42. Galon, J.; Costes, A.; Sanchez-Cabo, F.; Kirilovsky, A.; Mlecnik, B.; Lagorce-Pages, C.; Tosolini, M.; Camus, M.; Berger, A.; Wind, P.; et al. Type, density, and location of immune cells within human colorectal tumors predict clinical outcome. *Science* **2006**, *313*, 1960–1964. [[CrossRef](#)]
43. Vasaikar, S.; Huang, C.; Wang, X.; Petyuk, V.A.; Savage, S.R.; Wen, B.; Dou, Y.C.; Zhang, Y.; Shi, Z.A.; Arshad, O.A.; et al. Proteogenomic Analysis of Human Colon Cancer Reveals New Therapeutic Opportunities. *Cell* **2019**, *177*, 1035–1049.e19. [[CrossRef](#)]
44. Bauer, K.; Michel, S.; Reuschenbach, M.; Nelius, N.; Doeberitz, M.V.; Kloor, M. Dendritic cell and macrophage infiltration in microsatellite-unstable and microsatellite-stable colorectal cancer. *Fam. Cancer* **2011**, *10*, 557–565. [[CrossRef](#)] [[PubMed](#)]

45. Yoo, Y.G.; Hayashi, M.; Christensen, J.; Huang, L.E. An Essential Role of the HIF-1 alpha-c-Myc Axis in Malignant Progression. *Ann. N. Y. Acad. Sci.* **2009**, *1177*, 198–204. [[CrossRef](#)] [[PubMed](#)]
46. Kumar, S.M.; Yu, H.; Edwards, R.; Chen, L.; Kazianis, S.; Brafford, P.; Acs, G.; Herlyn, M.; Xu, X. Mutant V600E BRAF increases hypoxia inducible factor-1alpha expression in melanoma. *Cancer Res.* **2007**, *67*, 3177–3184. [[CrossRef](#)]
47. Dejea, C.M.; Wick, E.C.; Hechenbleikner, E.M.; White, J.R.; Welch, J.L.M.; Rossetti, B.J.; Peterson, S.N.; Snesrud, E.C.; Borisy, G.G.; Lazarev, M.; et al. Microbiota organization is a distinct feature of proximal colorectal cancers. *Proc. Natl. Acad. Sci. USA* **2014**, *111*, 18321–18326. [[CrossRef](#)]
48. Zgouras, D.; Wächtershauser, A.; Frings, D.; Stein, J. Butyrate impairs intestinal tumor cell-induced angiogenesis by inhibiting HIF-1alpha nuclear translocation. *Biochem. Biophys. Res. Commun.* **2003**, *300*, 832–838. [[CrossRef](#)]
49. Koury, J.; Deitch, E.A.; Homma, H.; Abungu, B.; Gangurde, P.; Condon, M.R.; Lu, Q.; Xu, D.Z.; Feinman, R. Persistent HIF-1alpha activation in gut ischemia/reperfusion injury: Potential role of bacteria and lipopolysaccharide. *Shock* **2004**, *22*, 270–277. [[CrossRef](#)]



© 2020 by the authors. Licensee MDPI, Basel, Switzerland. This article is an open access article distributed under the terms and conditions of the Creative Commons Attribution (CC BY) license (<http://creativecommons.org/licenses/by/4.0/>).

MDPI
St. Alban-Anlage 66
4052 Basel
Switzerland
Tel. +41 61 683 77 34
Fax +41 61 302 89 18
www.mdpi.com

Cancers Editorial Office
E-mail: cancers@mdpi.com
www.mdpi.com/journal/cancers



MDPI
St. Alban-Anlage 66
4052 Basel
Switzerland

Tel: +41 61 683 77 34
Fax: +41 61 302 89 18

www.mdpi.com



ISBN 978-3-0365-1607-3